february 1960

the institute of radio engineers

Proceedings of the IRE

in this issue

Wideband Balun Transformer: Page 156

VOLUME 48, NUMBER 2

February, 1960

published monthly by The Institute of Radio Engineers, Inc.

Proceedings of the IRE®

contents

COVER

By spreading one conductor of a two-wire transmission line so that it gradually encircles the other conductor, engineers at the Collins Radio Company have developed a very-broad-band balun transformer for matching a two-wire line to a coaxial line over a 100-to-1 frequency range. Shown is an artist's conception of the device, which is described on page 156.

FEBRUARY

published monthly by The Institute of Radio Engineers, Inc.

Proceedings of the IRE

continued

PROCEEDINGS OF THE IRE, published monthly by The Institute of Radio Engineers, Inc. at 1 East 79 Street, New York 21, N. Y. Manuscripts should be submitted in triplicate to the Editorial Department. Responsibility for contents of papers published rests upon the authors, and not the IRE or its members. All republication rights, including translations, are reserved by the IRE and granted only on request. Abstracting is permitted with mention of source.

Thirty days advance notice is required for change of address. Price per copy: members of the Institute of Radio Engineers, one additional copy $1.25; non-members $2.25. Yearly subscription price: to members $9.00, one additional subscription $13.50; to non-members in United States, Canada, and U. S. Possessions $18.00; to non-members in foreign countries $19.00. Second-class postage paid at Menasha, Wisconsin under the act of March 3, 1879. Acceptance for mailing at a special rate of postage is provided for in the act of February 28, 1925, embodied in Paragraph 4, Section 412, P. L. and R., authorized October 26, 1927. Printed in U.S.A.

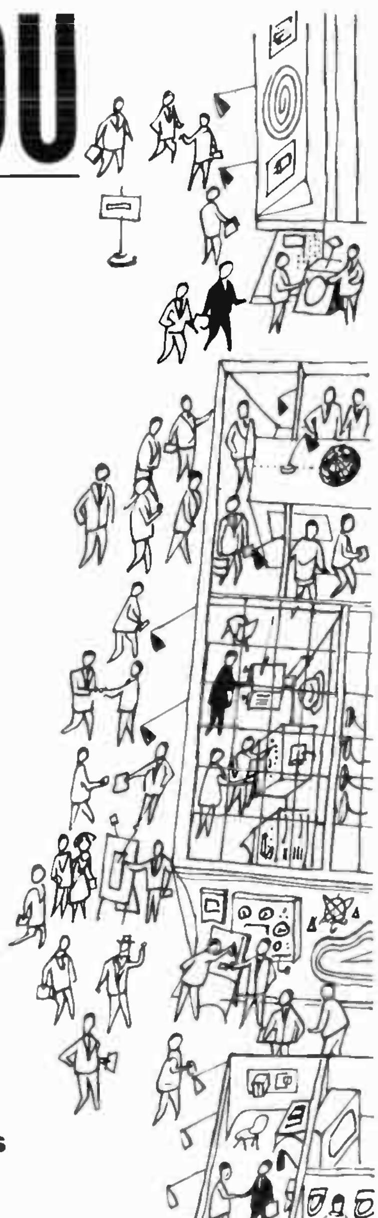

ON DISPLAY FOR YOU

NEW IDEAS in RADIO-ELECTRONICS . . . 1960!

Year after year, the IRE NATIONAL CONVENTION AND RADIO ENGINEERING SHOW gets bigger! That's because you and your gigantic radio-electronics industry are surging ahead with NEW IDEAS and remarkable speed to make the Space Age the most exciting time in which to live.

That's why it takes all *4 floors* of New York's great Coliseum to show what your industry is doing. Takes 950 exhibitors...takes over 200 papers...takes over 60,000 of your co-workers to view the impressive sight.

If you're not at the IRE CONVENTION AND SHOW this year you'll miss a once-a-year opportunity unequalled in your industry to see progress in action. Plan to be at the Coliseum to see...to hear about...the NEW IDEAS IN RADIO-ELECTRONICS, 1960!

The IRE NATIONAL CONVENTION
Waldorf-Astoria Hotel
and The RADIO ENGINEERING SHOW
Coliseum, New York City

MARCH 21, 22, 23, 24

The Institute of Radio Engineers
1 East 79th St., New York 21, N. Y.

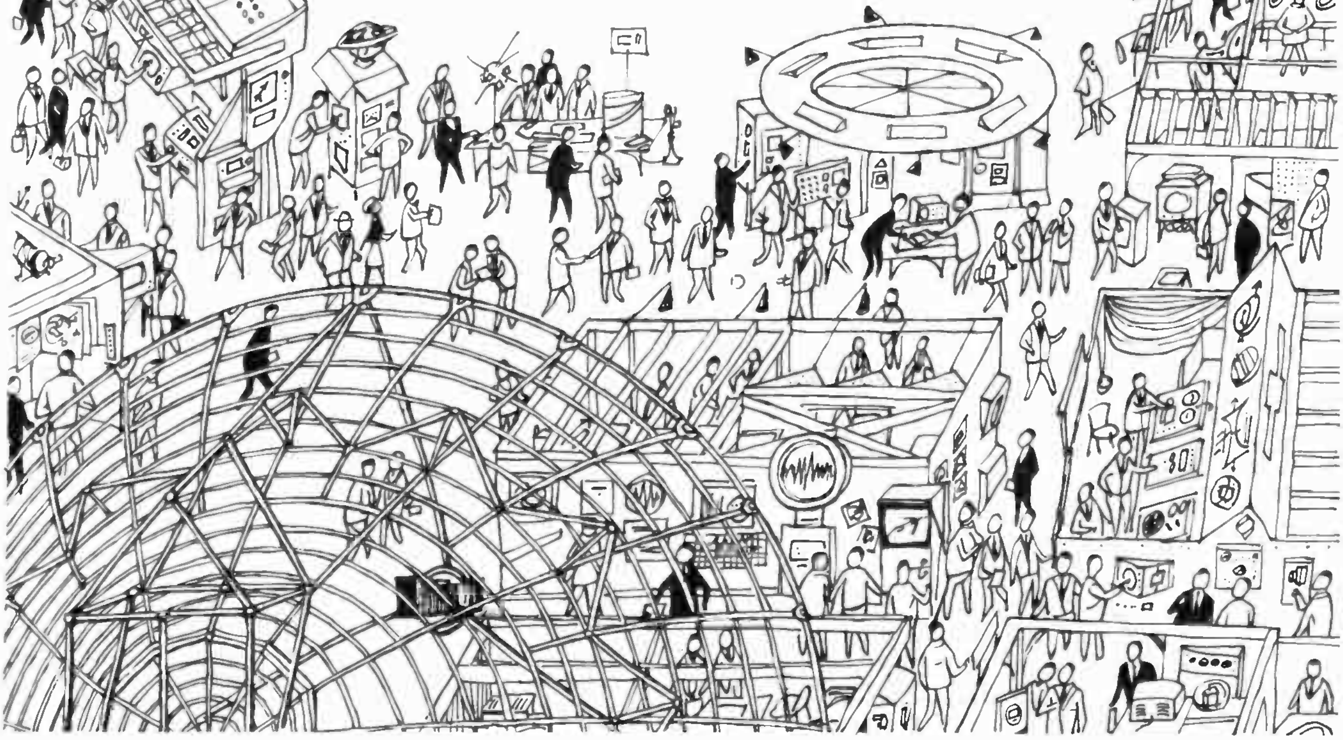

Recently, dispersive networks in which the time delay is a linear function of frequency have assumed considerable importance in certain electronic applications. In their patents, Cauer[1] and Darlington[2] show how these networks make it possible for a long pulse of low peak power to do the work of a shorter pulse having much higher peak power. When we are limited in the peak power we can produce, the advantage of these networks is obvious. This month Warren White, Consultant in our Research and Engineering Division, discusses another application of these networks in which the advantage gained has nothing to do with peak power limitations.

RAPID-FREQUENCY SCANS

Consider a conventional panoramic receiver. Assume that the rate of change of frequency of the sweeping oscillator will be fixed by the requirement that we must cover a certain band n times per second. We now ask ourselves, "What should the IF bandwidth be to obtain the best resolution?" If the IF band is very narrow, the output pulse is essentially just the transient response of the IF amplifier, and its duration will be inversely proportional to the bandwidth. We find that, in this region, the resolution improves as we widen the band. On the other hand, if the band is very wide, the output pulse is simply a trace of the pass-band characteristic, and its duration is proportional to the bandwidth. In this region, the resolution deteriorates as we widen the bandwidth. Clearly there is an optimum bandwidth between these extremes. Figure 1 illustrates the case for a Gaussian-shaped pass band. For other types of pass band, the details will be different, but the general shape of the curve will be the same.

The curve of Figure 1 was plotted for a sweep rate $\dot{f} = 1$ Mc/μsec and shows that optimum resolution occurs when the IF bandwidth is about 0.664 Mc (3 db) and that the resolution obtainable is about 0.94 Mc. What happens if this resolution is not good enough? What can we do if the problem requires a resolution of, say, 0.25 Mc? In the past, the only answer has been that we must slow down the sweep rate—accepting either a lower rate of scan or a smaller coverage. In the example just cited, to improve the available resolution to 0.25 Mc would require the sweep rate to be slowed down by a factor of about 14 : 1, meaning that we must either scan 1/14 as often or cover only 1/14 of the band with one receiver.

The anomalous part of this situation is the fact that, in the right-hand region of Figure 1, the output pulse duration increases as we increase the bandwidth. As we increase the bandwidth, we should be able to increase the output data rate—but in fact the reverse is true. Let's see how this situation can be corrected. In Figure 2, a time vs frequency diagram, the signal coming out of the mixer is represented as an oblique straight line (frequency varying linearly with time). Roughly speaking, the output pulse duration is from the instant the signal frequency enters the IF pass band until the instant it leaves. The wider the bandwidth, the wider the output pulse will be. Suppose, however, that we introduce a network having a dispersive time delay. The network is arranged so that signals at the low end of the band are delayed τ_1 seconds, and the signals at the high end of the band are delayed τ_2 seconds. The result is that the low-frequency

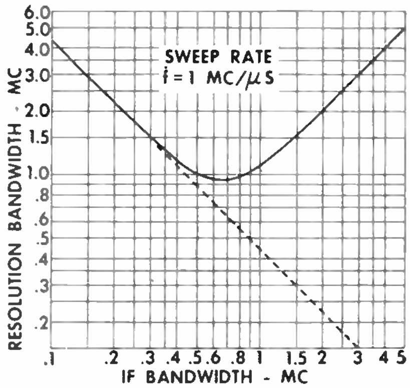

Figure 1

part of the signal emerges from the network simultaneously with the high-frequency part. The spectrum of the output now has the shape of the IF pass band, and the phase is a linear function of frequency corresponding to a uniform time delay. In consequence, the resolution continues to improve as the bandwidth is widened, as indicated by the dotted line of Figure 1.

The improvement in resolution obtained in this way is not obtained without paying a price—the complexity of the network required. This complexity is a function of the "compression ratio" or the ratio of uncorrected resolution bandwidth to corrected resolution bandwidth. To achieve 0.25-Mc resolution at 1 Mc/μsec sweep rate, we need a bandwidth of 1.765 Mc; at this bandwidth, the uncorrected resolution is 1.783 Mc. The required compression ratio is then 1.783/0.25 or 7.132. This is a fairly modest requirement as such networks go. Depending on the tolerance specifications, the requirement can be met by a lumped-constant network having 18 or 20 all-pass sections. The cost of this network is to be compared with the cost of 14 receivers to cover the same band.

Figure 3 is a scope photograph showing results obtained with a breadboard setup. The dispessive network consisted of 24 all-pass sections and was designed to provide a compression factor of about 10 : 1 for signals sweeping at a rate of 1 Mc/μsec. No particular pains were taken to adjust

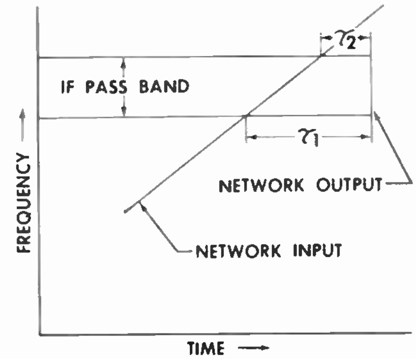

Figure 2

the network precisely, and its performance is far from optimum. The top line is a 2-Mc sine wave, which serves as a timing reference; the second line is the IF signal at the input to the network; the third line is the network output signal. The signal being analyzed is amplitude-modulated at 0.5 Mc. The sidebands are clearly resolved at the output of the network. The signal is being overmodulated somewhat, as evidenced by the fact that the carrier amplitude is roughly equal to that of the sidebands, and higher-order sidebands are visible. For this sweep speed, the optimum resolution without the network would be about 1 Mc whereas the resolution actually achieved appears to be about 0.25 Mc.

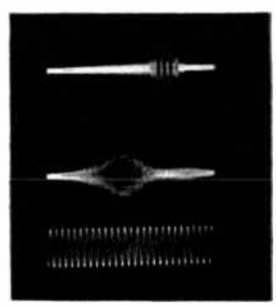

1. 2 Mc timing wave
2. Input to network
3. Output from network

Figure 3

References

1. Wilhelm Adolph Eduard Cauer, German Patent #892772.
2. S. Darlington, U.S. Patent #2,678,997.

A complete bound set of our third series of articles is available on request. Write to Harold Hechtman at AIL for your set.

Airborne Instruments Laboratory
A DIVISION OF CUTLER-HAMMER, INC.
DEER PARK, LONG ISLAND, N. Y.
Phone MYrtle 2-6100

2N393

2 x actual size

2N1122

HIGH-SPEED, HIGH-GAIN MICRO-ALLOY TRANSISTORS for modern computer circuitry

Types 2N393 and 2N1122 Micro-Alloy Transistors combine high gain with excellent high frequency response to meet demands of high-speed computer switching applications in the megacycle range. Low saturation resistance, low hole storage, and exceptionally good life characteristics make these micro-alloy transistors top performers in general high frequency applications and computer circuits.

Made by electrochemical manufacturing techniques, Sprague Micro-Alloy Transistors are uniformly reliable, as well as reasonably priced for transistors with such excellent operating parameters.

All Sprague transistors—micro-alloy, micro-alloy diffused base, and surface barrier types—are now produced in Sprague's completely new spotless semiconductor facility.

For engineering data sheets on the types in which you are interested, write Technical Literature Section, Sprague Electric Company, 235 Marshall Street, North Adams, Massachusetts.

Sprague micro-alloy, micro-alloy diffused base, and surface barrier transistors are fully licensed under Philco patents. All Sprague and Philco transistors having the same type numbers are manufactured to the same specifications and are fully interchangeable. You have two sources of supply when you use micro-alloy and surface barrier transistors!

Other popular SPRAGUE transistors

2N128
SB MIL GENERAL PURPOSE
(MIL-T-19500/9)

2N240
FOR COMPUTER SWITCHING

2N344/SB101
FOR MEDIUM GAIN AMPLIFIERS

2N345/SB102
FOR HIGH GAIN AMPLIFIERS

2N346/SB103
FOR HIGH FREQUENCY OSCILLATORS

2N501
MADT FOR ULTRA-HIGH SPEED SWITCHING

SPRAGUE COMPONENTS:

TRANSISTORS • RESISTORS • MAGNETIC COMPONENTS • CAPACITORS • INTERFERENCE FILTERS • PULSE NETWORKS • HIGH TEMPERATURE MAGNET WIRE • CERAMIC-BASE PRINTED NETWORKS • PACKAGED COMPONENT ASSEMBLIES

SPRAGUE®
THE MARK OF RELIABILITY

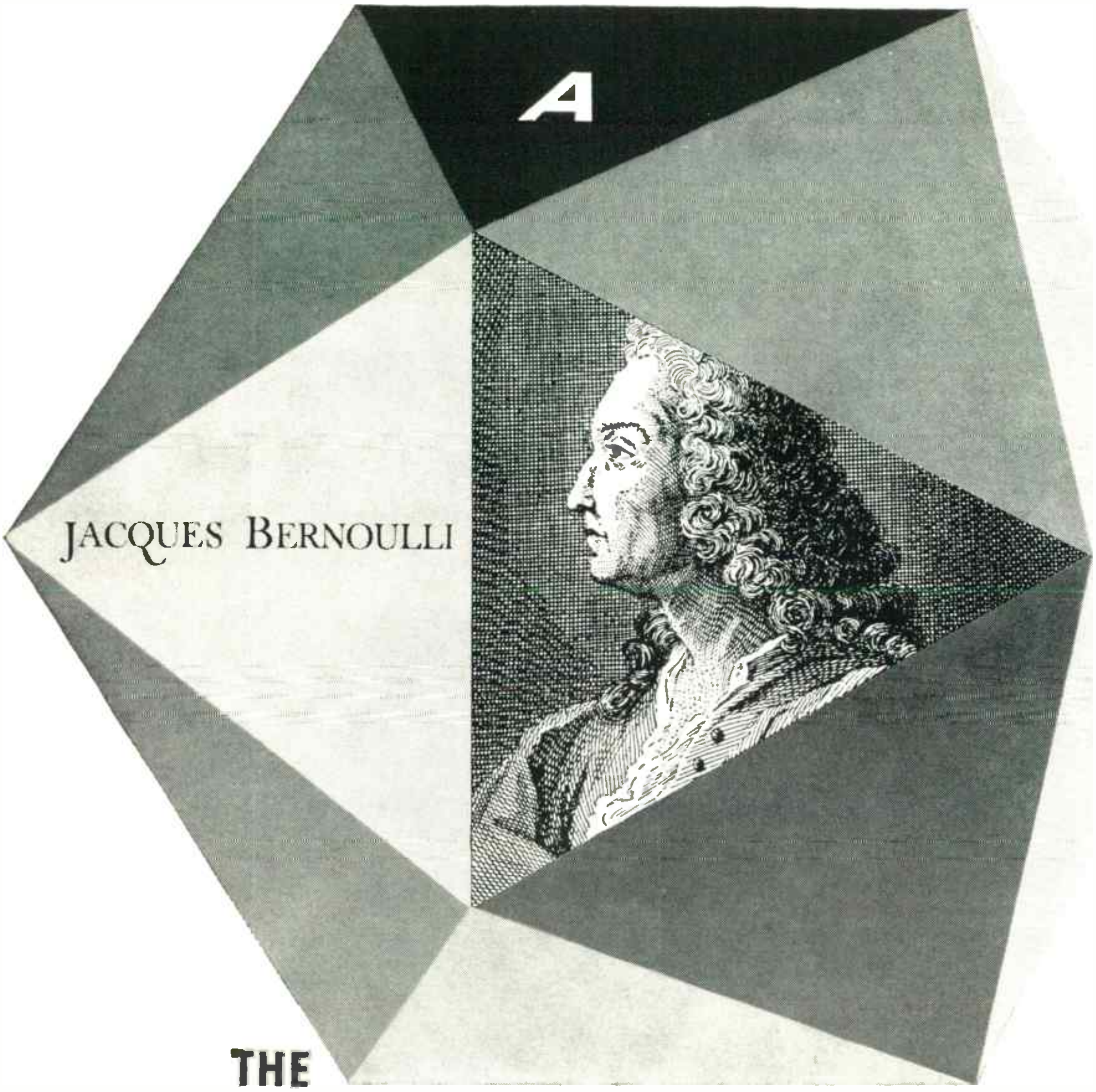

THE WIZARD OF ODDS *He solved a telephone traffic problem two centuries ago*

Jacques Bernoulli, the great Swiss mathematician, pondered a question early in the 18th century. Can you mathematically predict what will happen when events of chance take place, as in throwing dice?

His answer was the classical Bernoulli binomial distribution—a basic formula in the mathematics of probability (published in 1713). The laws of probability say, for instance, that if you roll 150 icosahedrons (the 20-faced solid shown above), 15 or more of them will come to rest with side "A" on top only about once in a hundred times.

Identical laws of probability govern the calls coming into your local Bell Telephone exchange. Suppose you are one of a group of 150 telephone subscribers, each of whom makes a three-minute call during the busiest hour of the day. Since three minutes is one-twentieth of an hour, the probability that you or any other subscriber will be busy is 1 in 20, the same as the probability that side "A" of an icosahedron will be on top. The odds against 15 or more of you talking at once are again about 100 to 1. Thus it would be extravagant to supply your group with 150 trunk circuits when 15 are sufficient for good service.

Telephone engineers discovered at the turn of the century that telephone users obey Bernoulli's formula. At Bell Telephone Laboratories, mathematicians have developed the mathematics of probability into a tool of tremendous economic value. All over the Bell System, the mathematical approach helps provide the world's finest telephone service using the least possible equipment. The achievements of these mathematicians again illustrate how Bell Laboratories works to improve your telephone service.

BELL TELEPHONE LABORATORIES

World center of communications research and development

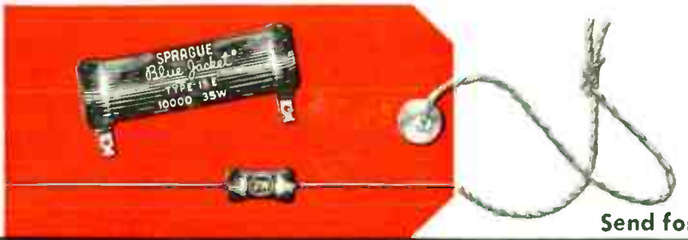

BLUE JACKET®

VITREOUS ENAMEL-PROTECTED,
POWER WIREWOUND RESISTORS.

Send for Bulletins: 7410-A (Axial Lead), 7400-A (Tab Type)

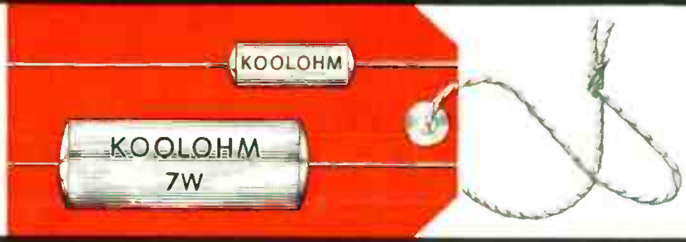

KOOLOHM®

CERAMIC INSULATED-SHELL,
POWER WIREWOUND RESISTORS.

Send for Engineering Bulletin: 7300-A

PERMASEAL®

CAST EPOXY HOUSING,
PRECISION WIREWOUND RESISTORS.

Send for Engineering Bulletin: 7500

SPRAGUE RESISTORS

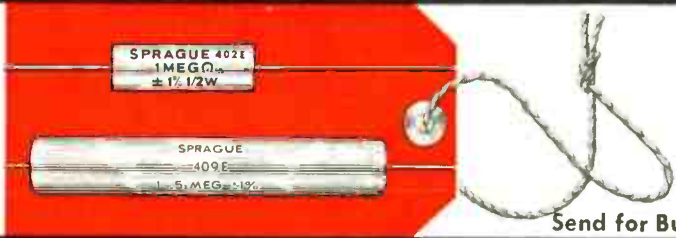

FILMISTOR®

PRECISION CARBON FILM RESISTORS.

Send for Bulletins: 7000 (Molded shell), 7010-B (Ceramic shell)

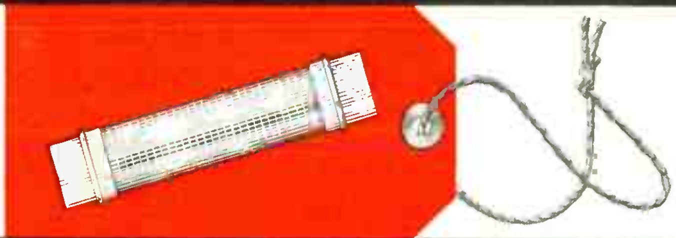

MEG-O-MAX®

GLASS-JACKETED HIGH VOLTAGE,
HIGH POWER RESISTORS.

Send for Engineering Bulletin: 7200-A

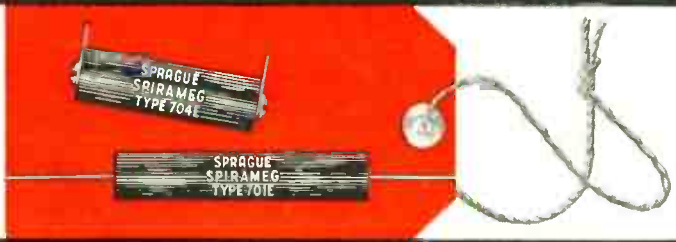

SPIRAMEG®

HIGH-RESISTANCE SPIRAL ELEMENT
RESISTORS.

Send for Engineering Bulletin: 7100

SPRAGUE ELECTRIC COMPANY 235 Marshall Street North Adams, Mass.

SPRAGUE COMPONENTS: RESISTORS • CAPACITORS • MAGNETIC COMPONENTS • TRANSISTORS
INTERFERENCE FILTERS • PULSE NETWORKS • HIGH TEMPERATURE MAGNET WIRE • PRINTED CIRCUITS

Meetings with Exhibits

As a service both to Members and the industry, we will endeavor to record in this column each month those meetings of IRE, its sections and professional groups which include exhibits.

March 21-24, 1960

IRE 1960 International Convention and Engineering Show, Waldorf-Astoria Hotel and New York Coliseum, New York, N.Y.

Exhibits: Mr. William C. Copp, Institute of Radio Engineers, 72 West 45th St., New York 36, N.Y.

April 3-8, 1960

Sixth Nuclear Congress, New York Coliseum, New York, N.Y.

Exhibits: Mr. F. M. Howell, c/o EJC, 29 W. 39th St., New York 18, N.Y.

April 20-22, 1960

SWIRECO, Southwestern IRE Regional Conference & Electronics Show, Shamrock-Hilton Hotel, Houston, Texas.

Exhibits: Mr. A. D. Seixas, SWIRECO, P.O. Box 22331, Houston, Texas.

May 2-4, 1960

National Aeronautical Electronics Conference, Dayton Biltmore Hotel, Dayton, Ohio.

Exhibits: Mr. Edward M. Lisowski, General Precision Lab., Inc., Suite 452, 333 West First St., Dayton 2, Ohio.

May 2-6, 1960

Western Joint Computer Conference, Fairmont Hotel, San Francisco, Calif.

Exhibits: Mr. H. K. Farrar, Pacific Tel. & Tel. Co., 140 New Montgomery St., San Francisco 5, Calif.

May 24-26, 1960

Seventh Regional Technical Conference & Trade Show, Olympic Hotel, Seattle, Wash.

Exhibits: Mr. Rush Drake, 1806 Bush Place, Seattle 44, Wash.

May 24-26, 1960

Armed Forces Communications & Electronics Association Convention and Exhibit, Sheraton-Park Hotel, Washington, D.C.

Exhibits: Mr. William C. Copp, 72 West 45th St., New York 36, N.Y.

June 27-29, 1960

National Convention on Military Electronics, Sheraton-Park Hotel, Washington, D.C.

Exhibits: Mr. L. David Whitelock, BuShips, Electronics Div., Dept. of Navy, Washington, D.C.

August 23-26, 1960

WESCON, Western Electronic Show and Convention, Ambassador Hotel & Memorial Sports Arena, Los Angeles, Calif.

Exhibits: Mr. Don Larson, WESCON, 1435 LaCienega Blvd., Los Angeles, Calif.

(Continued on page 10A)

Meetings with Exhibits

(Continued from page 8A)

September 19-21, 1960

National Symposium on Space Electronics & Telemetry, Shoreham Hotel, Washington, D.C.

Exhibits: John Leslie Whitlock Associates, 6044 Ninth St., North, Arlington 5, Va.

October 3-5, 1960

Sixth National Communications Symposium, Hotel Utica & Utica Memorial Auditorium, Utica, N.Y.

Exhibits: Mr. W. R. Roberts, 102 Fort Stanwix Park N., Rome, N.Y.

October 10-12, 1960

National Electronics Conference, Hotel Sherman, Chicago, Ill.

Exhibits: Mr. Arthur H. Streich, National Electronics Conference, 184 E. Randolph St., Chicago, Ill.

October 24-26, 1960

East Coast Aeronautical & Navigational Electronics Conference, Lord Baltimore Hotel & 7th Regiment Armory, Baltimore, Md.

Exhibits: Mr. R. L. Pigeon, Westinghouse Electric Corp., Air Arm Div., P.O. Box 746, Baltimore, Md.

Oct. 31-Nov. 2, 1960

13th Annual Conference on Electrical Techniques in Medicine & Biology, Sheraton-Park Hotel, Washington, D.C.

Exhibits: Mr. Lewis Winner, 152 West 42nd St., New York 36, N.Y.

November 14-16, 1960

Mid-America Electronics Convention (MAECON), Municipal Auditorium, Kansas City, Mo.

Exhibits: Mr. John V. Parks, Bendix Aviation Corp., P.O. Box 1159, Kansas City 41, Mo.

November 15-17, 1960

Northeast Electronics Research & Engineering Meeting (NEREM), Boston Commonwealth Armory, Boston, Mass.

Exhibits: Miss Shirley Whitcher, IRE Boston Office, 73 Tremont St., Boston, Mass.

December 1-2, 1960

PGVC Annual Meeting, Sheraton Hotel, Philadelphia, Pa.

Exhibits: Mr. E. B. Dunn, Atlantic Refining Co., 260 S. Broad St., Philadelphia 1, Pa.

Δ

Note on Professional Group Meetings: Some of the Professional Groups conduct meetings at which there are exhibits. Working committeemen on these groups are asked to send advance data to this column for publicity information. You may address these notices to the Advertising Department and of course listings are free to IRE Professional Groups.

WHAT HAS THE **7182 S BAND MAGNETRON** IN COMMON WITH THIS CAT?

A good question! According to legend, a cat has nine lives—something that has yet to be proved. The 7182, on the other hand, has a *proved* life 8 to 10 times greater than any similar S-Band magnetron.

The 7182 retains its remarkable stability and reliability during a life of 10,000 hours, and is one of a series of magnetrons now in production providing peak powers of 5 MW. These magnetrons operate at voltages and current densities usually associated with magnetrons rated at a fraction of the power output.

A parallel development in L-Band ensures that attainments in this field equal the phenomenal successes already achieved with S-Band magnetrons.

'ENGLISH ELECTRIC'

Agents throughout the World

ENGLISH ELECTRIC VALVE CO. LTD.

CHELMSFORD, ENGLAND
Telephone: Chelmsford 3491

AP 134

IRE News and Radio Notes

Calendar of Coming Events and Authors' Deadlines*

1960

PGMIL Winter Mtg., Biltmore Hotel, Los Angeles, Calif., Feb. 3–5.

Cleveland Electronics Conf., Cleveland Engrg. and Sci. Center, Cleveland, Ohio, Feb. 10–12.

1960 Solid State Circuits, Conf., Sheraton Hotel, Philadelphia, Pa., Feb. 10–12.

IRE National Conv., N. Y. Coliseum and Waldorf-Astoria Hotel, New York, N. Y., Mar. 21–24.

First Natl. Symp. on Human Factors in Electronics, BTL Aud., New York, N. Y., Mar. 24–25.

Scintillation Counter Symp., Washington, D.C., Mar.

6th Nuclear Congress, N. Y. Coliseum. New York, N. Y., Apr. 4–8.

14th Spring Tech. Conf., Cincinnati, Ohio, Apr. 12–13.

Conf. on Automatic Tech., Sheraton-Cleveland Hotel, Cleveland, Ohio, Apr. 18–19.

Int'l Symp. on Active Networks and Feedback Systems, Engrg. Soc. Bldg. Auditorium, New York, N. Y., Apr. 19–21. (DL*: Jan. 15, H. J. Carlin, 55 Johnson St., Brooklyn, N. Y.)

Int'l Symp. on Active Networks and Feedback Systems, Polytechnic Inst. of Brooklyn, Brooklyn, N. Y., Apr. 19–21.

1960 SWIRECO (Southwestern IRE Regional Conf. and Electronics Show), simultaneously with the Nat'l. PGME Conf., Houston, Texas, Apr. 20–22.

Natl. Aeronautical Electronics Conf., Biltmore and Miami-Pick Hotels, Dayton, Ohio, May 2–4. URSI-IRE Spring Mtg., Sheraton Hotel, Washington, D.C., May 2–5.

Western Joint Computer Conf., San Francisco, Calif, May 2–6.

PGMTT Natl. Symp., San Diego, Calif., May 9–11.

Electronic Components Conf., Hotel Washington, Washington, D. C., May 10–12.

7th Reg. Tech. Conf. & Trade Show, Olympic Hotel, Seattle, Wash., May 24–26.

6th Radar Symp., Ann Arbor, Mich., June 1–3.

Conf. on Standards and Electronic Measurements, NBS Boulder Labs., Boulder, Colo., June 22–24. (DL*: Feb. 15, G. E. Shafer, NBS, Boulder, Colo.)

Natl. Conv. on Mil. Elec., Sheraton Park Hotel, Washington, D. C., June 27–29.

* DL = Deadline for submitting abstracts.

(Continued on page 15A)

IRE Cumulative Index for 1954–1958 Now Available

A new cumulative index covering all technical papers and letters which have appeared in IRE publications during 1954 through 1958 is now available from the Institute of Radio Engineers, 1 East 79 St., New York 21, N. Y., at the following prices: IRE Members, $2.50; libraries, $4.80; nonmembers, $6.00.

The index covers the Proceedings of the IRE, IRE Transactions of the Professional Groups, IRE National Convention Record, IRE Wescon Convention Record, and the IRE Student Quarterly.

Cumulative indexes for years prior to 1954 are also available as follows:

	1913–1942	1943–1947	1948–1953
Members	$1.25	$1.25	$1.25
Libraries	1.65	1.65	2.40
Nonmembers	2.25	2.25	3.00

Armstrong Medal Presented to J. H. Bose

The Armstrong Medal of the Radio Club of America was presented to John H. Bose (S'33–A'36–VA'39–M'55–SM'58), associate professor of Engineering at Columbia University, New York, N. Y., at the Club's golden anniversary dinner December 4, 1959 at the Hotel Plaza, New York, N. Y.

The award will mark the eleventh presentation of the medal since it was established December 19, 1935, in recognition of the discovery of radio frequency modulation by Major Edwin H. Armstrong, professor of Electrical Engineering at Columbia and a prominent member of the Club.

Major Armstrong, who died in 1954 at the age of 63, invented numerous improvements in radio transmission and reception. One of his accomplishments, announced the year before he died, was the perfection of a system of multiplex radio transmission that enables FM broadcasting stations to transmit two or more different programs simultaneously.

The presentation of the medal was made by Walter Knoop, president of the Club, who also presented Professor Bose with a citation which reads:

"The award of the Armstrong Medal of the Radio Club of America to John Henry Bose is in recognition of his pioneering contributions to the art of radio communications and particularly frequency modulation.

"He was closely associated with Edwin Howard Armstrong and has contributed especially to the development of FM multiplexing systems, phase shift frequency modulation, and CW radar.

"As inventor, teacher and true scientist, much is still expected from John Bose in the continuing advance of radio communication techniques. A comparatively young man, with years of productive and creative future ahead, he is an outstanding first of radio's second generation."

The principal speaker at the dinner was Dr. Alfred N. Goldsmith, cofounder and editor emeritus of the IRE.

Professor Bose was born March 26, 1912. He received the B.S. degree from Columbia in 1934, and the E.E. degree from Columbia in 1935. From the time he received his engineering degree he was associated with Professor Armstrong and collaborated with Armstrong in the development of the FM multiplexing system of transmission, as well as many other classified projects for the government.

Professor Bose is a founding member and a director of the Armstrong Memorial Research Foundation and a former president of the Radio Club of America.

Attendance Limited At PGHFE Symposium

Attendance at the first Annual Symposium on Human Factors in Electronics, March 24–25, 1960, will be limited. Those interested in attending the Symposium, which will be held in New York, N. Y., are urged to send $2.00 (PGHFE members) or $3.00 (all others) for preregistration to J. E. Karlin, Chairman, Meetings Committee, % Bell Telephone Labs., Murray Hill, N. J. Anyone interested in obtaining further information about the Symposium should also contact Mr. Karlin.

At the press conference held during the 12th Annual Conference on Electrical Techniques in Medicine and Biology at the Sheraton Hotel, Philadelphia, Pa., *left to right:* Dr. J. Schultz, session chairman; Dr. R. L. Bowman, conference vice-chairman; Dr. H. P. Schwan, conference chairman; L. E. Flory, program chairman for conference; Dr. E. Hendler, session chairman; and Carl Berkley, publicity-exhibits conference chairman.

Eleventh Annual MAECON Held in Kansas City

Paul C. Constant, Jr., Conference General Chairman, opened the 11th Annual Mid-America Electronics Conference (MAECON) in Kansas City, Missouri, November 3, 1959. Dr. Ernst Weber, the principal speaker at the opening session, gave an address on "Radio Engineers of the Future."

Speakers at the conference included Dr. John D. Ryder (IRE Past President, 1955), Dr. Benjamin E. Shackelford (IRE Past President, 1948), Dr. R. L. McFarlan, T. C. Combs, Yudell Luke, Dr. John S. McNown, Dr. Castruccio, Philip E. Ohmart, D. R. Hull, Dr. H. Unz, Delmer C. Ports, Dr. Clyde M. Hyde, J. F. Tormey, Robert L. Francisco, Dr. W. W. Hohenner, Dr. Joseph C. Shipman, Gerald O. Hayman, Dr. John N. Warfield.

The seventeen technical sessions covered the following areas: Engineering Education, Engineering Management, Simulation and Computers, Technical Writing, Broadcasting Equipment, Components, Guidance and Communications, Transmission and Control Systems, Adaptive Servos and Other Nonlinear Devices, Wave Propagation, Medical Electronics, and Airborne Electronics.

More than 1350 MAECON registrants, (from more than 40 different states) attended the technical sessions, exhibits and social activities at MAECON. A few of the highlights were the 11th Annual Banquet, the Ladies Program, and the reunion of Past National Presidents of the IRE.

Mr. R. L. Hull, President of the Electronics Industries Association and Vice-President of Raytheon Company, was the principal speaker at the banquet. He spoke on "The National and Political Problems of the Electronics Industry."

On November 4 the past presidents of the IRE were honored. The reunion began with a testimonial luncheon at the Hotel Muehlebach at which Dr. John S. McNown, Dean of the School of Engineering of the University of Kansas spoke on "Why Research is Important in the Education of Engineers." This was followed by a ceremony in which the past presidents were presented with MAECON Chairman's Emblem, and given the title of Honorary Chairman of MAECON. They were given a certificate and a MAECON pin. Arthur F. Van Dyck, IRE president, 1942, and a charter member of the IRE, spoke for all the Past Presidents at the annual banquet Wednesday evening. Those honored and who became honorary Chairmen of MAECON were Dr. Haraden Pratt (President, 1938), Arthur F. Van Dyck (President, 1942), Dr. Benjamin E. Shackelford (President, 1948), Dr. John D. Ryder (President, 1955) and Dr. Ernst Weber (President, 1959).

Other reunion activities for the past national presidents included a tour of Midwest Research Institute and Linda Hall Library, and a social hour which preceded the annual banquet.

1960 NAECON Conference Plans Near Completion

Plans are being completed for the NAECON Conference in Dayton, Ohio, on May 2–4, 1960. This year's Twelfth Annual National Aeronautical Electronics Conference theme is "Electronics Probes the Universe."

Jointly sponsored by the professional group on Aeronautical and Navigational Electronics and the Dayton Section of the IRE, with participation by the Institute of Aeronautical Sciences, this year's NAECON will offer a program of value to everyone interested in electronics. The program will consist of technical papers, a forum, exhibits, ladies program, banquet and a ball. The following are a few selected subjects which have been suggested as session topics: Radio Astronomy, Safety in Space flight, Space Systems Integration, Bionics, Solid State Devices, Navigation In the Universe and other similar topics.

For additional information, on hotel and motel accommodations and rates in Dayton, write to:

NAECON Housing Chairman
P.O. Box 621
Far Hills Br.
Dayton 19, Ohio.

Distinguished guests at MAECON and the testimonial luncheon for the IRE Past Presidents. First row (*left to right*): Dr. John D. Ryder (President, 1955), Dr. Benjamin E. Shackelford (President, 1942), Dr. Ernst Weber (President, 1959), Arthur F. Van Dyck (President, 1942), and Dr. Haraden Pratt (President, 1938). Second Row (*left to right*): Paul C. Constant, Jr. (MAECON General Chairman), David R. Hull (principal speaker at MAECON's Annual Banquet), R. L. McFarlan (IRE President-elect), Noble Vilander (Chairman, Kansas City IRE Section), Charles E. Harp (Director Region 6, IRE).

Calendar of Coming Events and Authors' Deadlines*

(Continued from page 14A)

Cong. Intl. Federation of Automatic Control, Moscow, USSR, June 25–July 9.

Int'l Conf. on Electrical Engrg. Education, Sagamore Conf. Center, Syracuse Univ., Syracuse, N. Y., Jul.

WESCON, Los Angeles Mem. Sports Arena, Los Angeles, Calif., Aug. 23–26, (DL*: May 1, R. G. Leitner, WESCON Bus. Office, 1435 So. La Cugna Blvd., Los Angeles 35, Calif.)

Space Electronics and Telemetry Conv. and Symp., Shoreham Hotel, Washington, D.C., Sept. 19–22.

Industrial Elec. Symp., Sept. 21–22.

Sixth Natl. Communications Symp., Hotel Utica and Utica Municipal Aud., Utica, N. Y., Oct. 3–5. (DL*: June 1, B. H. Baldridge, 25 Bolton Rd., New Hartford, N. Y.)

Natl. Elec. Conf., Chicago, Ill., Oct. 10–12.

Symp. on Space Navigation, Deshler-Hilton Hotel, Columbus, Ohio, Oct. 19–21.

East Coast Conf. on Aero & Nav. Elec., Baltimore, Md., Oct. 24–26.

Electron Devices Mtg., Hotel Shoreham, Washington, D. C., Oct. 27–29.

13th Ann. Conf. on Elec. Tech. in Med. and Bio., Sheraton Park Hotel, Washington, D. C., Oct. 31, Nov. 1–2.

Radio Fall Mtg., Hotel Syracuse, Syracuse, N. Y., Oct. 31, Nov. 1–2.

Mid-Amer. Elec. Conv., Kansas City, Mo., Nov. 14–16.

1960 NEREM (Northeast Electronics Res. & Engrg. Mtg.), Boston, Mass., Nov. 15–17.

PGVC Ann. Mtg., Sheraton Hotel, Philadelphia, Pa., Dec. 1–2.

Eastern Joint Computer Conf., New Yorker Hotel, New York, N.Y., Dec.

1961

7th Natl. Symp. on Reliability and Quality Control, Bellevue-Strafford Hotel, Philadelphia, Pa., Jan. 9–11. (DL*: May 9, 1960, W. T. Summerlin, Philco Corp., 4700 Wissahickon Ave., Philadelphia 44, Pa.)

IRE National Conv., N.Y. Coliseum and Waldorf-Astoria Hotel, New York, N.Y., Mar. 20–23.

5th Midwest Symp. on Circuit Theory, Univ. of Illinois, Urbana, May 7–8. (DL*: Oct. 1, M. E. Van Valkenberg, Dept. of E.E. Univ. of Ill., Urbana.)

Electronic Computer Conf., West Coast, May 9–11.

WESCON, San Francisco, Calif., Aug. 22–25.

Natl. Symp. on Space Elec. and Telemetry, Sept.

* DL = Deadline for submitting abstracts.

Major General Clyde H. Mitchell, left, Commander, Rome Air Materiel Area, receiving the citation from the IRE. The citation was presented by Mr. William J. Kuehl, center, Chairman of the Rome-Utica Section of the IRE and Manager of Communications and Navigational Engineers at General Electric. Mr. Richard C. Benoit, right, General Chairman, 6th National IRE Symposium and Chief, Directional and Telecommunications Branch, Directorate of Communications at Rome Air Development Center, and Mr. Michael P. Forte, background, Vice-Chairman of Rome-Utica Section of IRE and Chief, Instrumentation Branch of General Engineering Laboratory at Rome Air Development Center, were also present to congratulate the General.

IRE Presents Citation to Major Gen. C. H. Mitchell

A citation was presented to Major General Clyde H. Mitchell, Commander, Rome Air Materiel Area at Griffiss Air Force Base, N. Y., for his outstanding support and contributions to The Institute of Radio Engineers' activities.

The citation read in part: "Major General Clyde H. Mitchell has contributed significantly to the growth and welfare of the Rome-Utica Section. Outstanding in leadership and in devotion to the aims, ideals, and purposes of the Institute, it is our judgment that he has served us well.

"In recognition thereof, and in token of our appreciation, the officers and executive committee hereby unanimously declare him to be a patron of the Rome-Utica Section entitled to the accolade of distinguished fine fellowship among all members at all times and places."

Technical Writers' and Medical Writers' Institutes To Be Held at Rensselaer

Technical writing as a tool for industry and the government services will feature the Eighth Annual Technical Writers' Institute scheduled from June 13–17, 1960 at Rensselaer Polytechnic Institute, Troy, N. Y. The week-long Institute, directed by Professor Jay R. Gould, will present key lectures by industrial speakers on editing; writing reports, manuals and instruction books, technical promotion, articles, and government publications; technical illustration; and supervision of publications.

Lecturers in the specialized fields will be S. J. Goodman, Manager of Technical Publications, Aircraft Radio Corp.; Ralph V. Rice, Supervisor of Publication Production, Bell Telephone Labs.; Lt. Col. Herbert Herman, Research Studies Institute, Maxwell Air Force Base; Willard E. Roberts, Manager of Technical Publications, Ordnance Department, General Electric Co.; Richard W. Ford, Supervisor of Sales Promotion, Data Processing Division, IBM; M. M. Matthews, Managing Editor, Westinghouse *Engineer;* and Stuart P. Hall, President, Hall Industrial Publicity.

Basic instruction will be given by Professors S. P. Olmsted, Wentworth K. Brown, and Douglas H. Washburn, coauthors of the communications text *The Uses of Language;* Professor Robert A. Sencer, consultant to business, in charge of Rensselaer's Special Communications Program; and Professor Gould, coauthor of the writing texts *Technical Reporting* and *Exposition: Technical and Popular.*

Rensselaer's pioneer Institute was founded in 1953 to provide a forum and workshop for technical writers and editors. During the past seven years over 500 representatives from 250 large industrial companies government agencies, and technical publishing companies have taken advantage of the intensive Monday through Friday seminar.

The third Medical Writers' Institute will be held at the same time as the Technical Writers' Institute. It will be coordinated by Dr. Joseph F. Montague, New York surgeon and writer. Although lectures on fundamentals will be shared with the technical writing group, the medical writers will attend sessions presided over by these speakers from the pharmaceutical firms and medicine: Dr. W. D. Snively, Medical Director, Mead, Johnson and Co.; Dr. Raymond C. Pogge, Director of Medical Research, the Wm. S. Merrell Co., and editor of the AMWA *Bulletin;* Col. John B. Coates, Director, Historical Unit—Medical Corps, USA; Dr. John H. Beckley, Medical Director, Warwick and Legler, advertising consultants; Dr. Otto L. Bettmann, Director, Bettmann Archive; Dr. Eric W. Martin, Editor, *Spectrum,* Pfizer and Co.; and Dr. Granville W. Larimore, Deputy Commissioner, New York State Department of Health.

Inquiries about both Writers' Institutes should be sent to Professor Jay R. Gould, Director, Technical Writers' Institute, Troy, N. Y.

4th National MIL-E-CON Plans Being Finalized

Dr. T. Keith Glennan, Administrator, National Aeronautics and Space Administration, heads a list of civilians and military officers who will serve as advisors for the Fourth National Convention on Military Electronics—1960 (MIL-E-CON), to be held at the Sheraton-Park Hotel in Washington, D. C., June 27–29, 1960. The meeting is sponsored by the IRE Professional Group on Military Electronics.

Other advisors, as announced by R. H. Cranshaw, MIL-E-CON President and Manager, Advanced Space Products, General Electric Co., Utica, N. Y., are Dr. H. F. York, Director of Defense Res. and Engrg., Dept. of Defense; Admiral A. Burke, USN, Chief of Naval Operations; Lieutenant General A. G. Trudeau, USA, Chief of Res. and Dev., Dept. of the Army; Lieutenant General R. C. Wilson, USAF, Deputy Chief of Staff, Development, U. S. Air Force; Vice Admiral J. T. Hayward, USN, Deputy Chief of Naval Operations (Development); Lieutenant General B. A. Schriever, USAF, Commander, Hq., Air Res. and Dev. Command; Lieutenant General W. E. Kepner, USAF (Ret.), Chairman of the Board, Radiation, Inc., Orlando, Fla., H. Randall, Chairman, PGIL; Office of Electronics, Office of the Director of Defense Res. and Engrg.; J. E. Durkovic, Chairman, Washington, D. C., Section of The IRE and Corporate Secretary, Aeronautical Radio, Inc., Washington, D. C.

Dr. C. M. Crenshaw, Chief Scientist, Office of the Chief Signal Officer, Dept. of Defense (Army), is chairman of the Technical Program Committee, which has set a deadline of February 1, 1960 for technical papers on the various fields of military electronics. Exhibits Chairman is L. D. Whitelock, 5614 Greentree Road, Bethesda 14, Md.

More than 4000 engineers, scientists, and executives from industry, Government agencies and laboratories, the Armed Forces, universities and embassies listened to more than 100 technical papers and looked at over 100 exhibits of new developments in military electronics at the 1959 MIL-E-CON. This branch of electronics includes such topics as space electronics, space navigation, guidance and control systems, electronic propulsion, reconnaissance systems simulation, and communications systems.

WESCON Papers Deadline Set for May 1, 1960

Authors wishing to present papers at the 1960 Western Electronic Show and Convention technical sessions to be held August 23–26 should register their interest by May 1. Required are 100-200 words abstracts, together with complete texts or detailed summaries. They should be sent to the Chairman of the Technical Program, Richard G Leitner, WESCON Business Office, 1435 South La Cienega Blvd., Los Angeles 35, Calif.

Selection of papers for the program will be made before June 1; authors will be advised of acceptance or rejection by that date.

There will again be an IRE-WESCON Convention Record published in advance of WESCON by the National Headquarters of the IRE.

RADAR AND REVOLUTION

One sweltering July afternoon in 1789, a tattered raggedy mob appeared outside the gates of the Bastille, the formidable prison of Paris, and demanded entrance.

"Go away," the guard shouted, "or we'll have to arrest you."

"That's exactly the idea!" a voice came back. "We're starving to death. All we want is a little of that moldy bread and canal water you feed your prisoners!"

Word was passed to the prison commandant, one Maurice Antoinette. "If they want their just desserts," he smiled, "let them eat cake!"

It was this remark that sparked the Revolution. The mob grew ugly. "Force the gate!" shouted a sickle-wielding daughter of France named Brigitte Sourdough. A radar controlled battering ram, appropriated from the local armory, swung into play. In moments, the Bastille gate had been hammered into shambles, and the unfortunate Maurice Antoinette was at the mercy of the mob.

"Observe the instrument of your defeat!" sneered Brigitte Sourdough, pointing at the radar.

"Pfui," the commandant replied, calm and disdainful. "No Beaumac (French for Bomac) tubes."*

Brigitte was furious. "The commandant wants 'Beaumac'? He shall have Beaumac!"

With that, Antoinette was led to a second instrument of the people — a device consisting of a heavy blade, poised between grooved uprights. It had no tubes at all.

"This is your Beaumac?" the commandant asked.

"Oui, monsieur," Brigitte Sourdough leered. "This is Beau Mac — the knife!"

No sooner had Maurice Antoinette heard these words than his icy calm vanished.

Matter of fact, he lost his head completely.

No. 18 of a series . . . **BOMAC LOOKS AT RADAR THROUGH THE AGES**

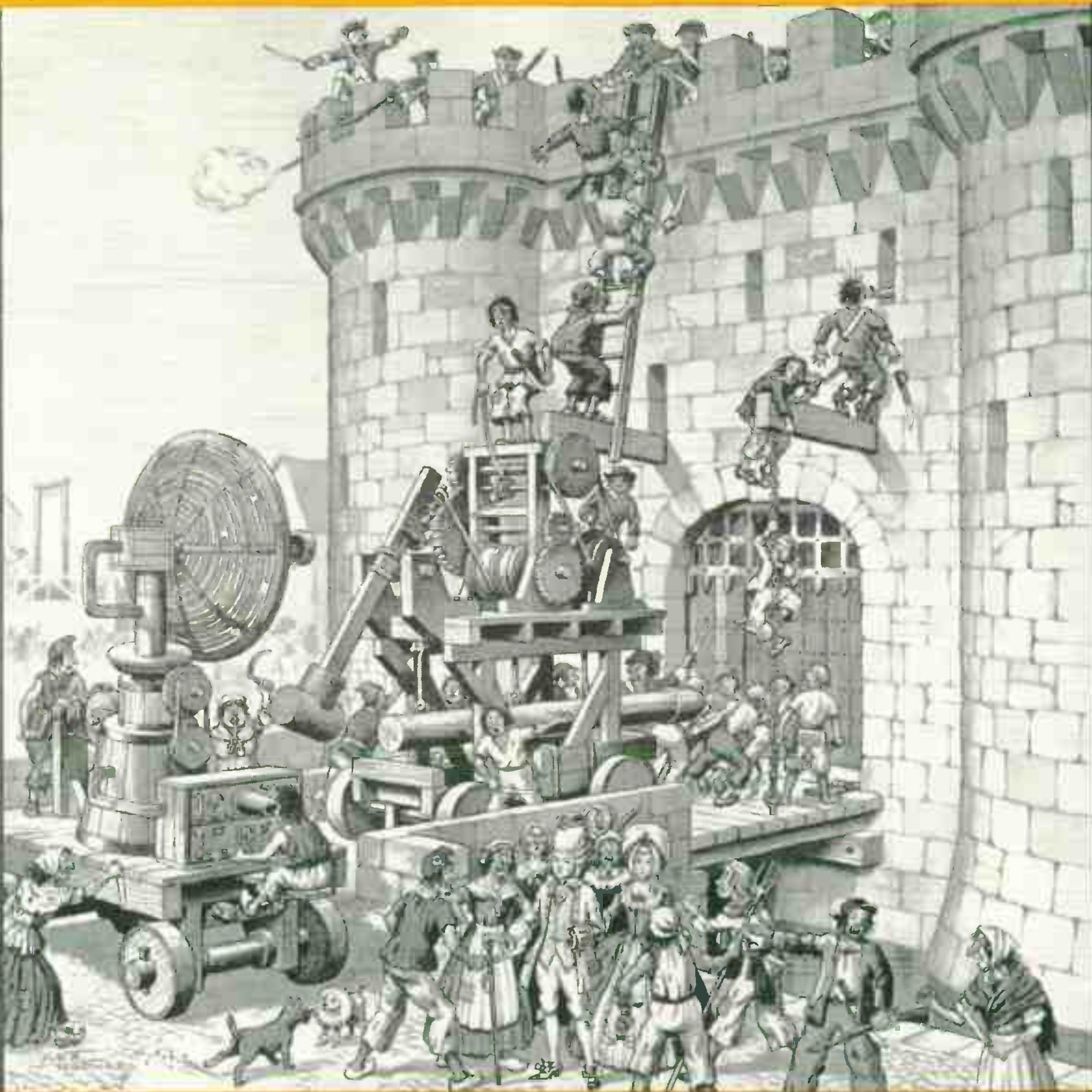

* *Bomac makes the finest microwave tubes and components since the storming of the Bastille*

BOMAC laboratories, inc.

SALEM ROAD • BEVERLY, MASSACHUSETTS

Leaders in the design, development and manufacture of TR, ATR, Pre-TR tubes; shutters; reference cavities; crystal protectors; silicon diodes; magnetrons; klystrons; duplexers; pressurizing windows; noise source tubes; high frequency triode oscillators; surge protectors.

Offices in major cities— Chicago • Kansas City • Los Angeles • Dallas • Dayton • Washington • Seattle • San Francisco • Canada: R-O-R Associates Limited, 1470 Don Mills Road, Don Mills, Ontario • Export: Maurice I. Parisier, 741-745 Washington St., N. Y. C. 14, N. Y.

URSI Toronto Symposium Proceedings Available

The IRE Professional Group on Antennas and Propagation has published the *Proceedings of the URSI International Symposium on Electromagnetic Theory*, held at the University of Toronto, Canada, June 15–20, 1959. The volume consists of invited papers by fifty-four of the world's leading authorities; subjects covered include Diffraction and Scattering Theory, Radio Telescopes, Surface Waves, Boundary Value Problems, Propagation of Waves, and Antennas. The complete program can be found on pages 18A of the June, 1959 issue of the Proceedings of the IRE.

Those who registered at the Toronto Symposium will automatically receive one copy as a part of their symposium registration fee. All others interested in ordering the Proceedings should turn to page 106A of this issue for further information.

International Conference on Medical Electronics To Be Held in London

The Electronics and Communications Section of The Institution of Electrical Engineers, in association with the International Federation for Medical Electronics, are organizing the Third International Conference on Medical Electronics which will be held at Olympia, London, England, July 21–27, 1960.

The Conference is planned to bring together members of the medical and electrical engineering professions so that each will gain a better understanding of the problems of the other; besides sessions for experts, there will also be less specialized meetings to enable those who have no deep insight of the subject to increase their background knowledge. With the many recent advances both in electronics and medicine, it is generally recognized by members of both professions that discussions on medical electronics can do much to stimulate progress.

The scope of the Conference is indicated by the following preliminary subject list: Instrumentation for Medicine and Biology, Medical Electronics in Space Research, Isotopes and Radiology, Ultrasonics and Microwave Radiation, The Respiratory System, Digestive System, Metabolism and Biochemistry, The Circulatory System, Electronic Aspects of Sight, Hearing and Locomotion, and The Motor and Nervous Systems.

In view of the International nature of the Conference it is planned to provide simultaneous translation facilities.

In conjunction with the Conference, The Institution is promoting an International Scientific Exhibition which will be held at Olympia at the same time as the Conference, and where the research organizations, universities, hospitals and industrial organizations from all over the world who are working in this important field can display their latest developments. The Exhibition is being organized by Industrial Exhibitions Ltd., 9 Argyll Street, London, W.1 (GERRARD 1622); enquiries from those interested should be addressed to this organization.

The Institution is now inviting the submission of papers for consideration. The following are the broad classes which are acceptable:

- *Survey papers* giving an account, in part descriptive, of developments in a particular part of the field.
- *Integrating papers* which present a critical review of the developments which have led to the present practice in a particular part of one of the branches of the science.
- *Papers recording the results of research or advanced development.*
- *Papers on medical electronics engineering practice and achievements* which present details of some new project or achievement with which the author has been concerned.
- *Short papers* dealing with practical problems or with limited aspects of a wider subject will also be welcome.

Short papers should be of between 1000–2500 words; other papers should not exceed 8000 words.

The Conference will be open to all interested persons, and those who would like to have registration forms and further information, or who are interested in submitting a paper should write to the Program Coordinator for the United States: Lee B. Lusted, M.D., Dept. of Radiology, Univ. of Rochester School of Medicine, Rochester 20, N. Y.

First Army MARS Technical Net Celebrates 2nd Anniversary

On January 6, 1960, The First U. S. Army MARS SSB Technical Net celebrated its second anniversary. During two years of operation, the net has presented sixty-three talks and forums by electronic scientists and engineers from many parts of the country.

In order to expand the activities of the net in the Boston area, Colonel Clinton W. Janes, W4KS/1, of Acton, Mass., was appointed an associate net director for the section. Colonel Janes, who is the U. S. Army Signal Corps liaison officer at the M.I.T. Lincoln Laboratory, will make arrangements for scheduling a speaker each month from this section.

The speakers scheduled for February are:

February 3—"Application of Quartz Crystals in SSB Filters," W. E. Benton, Division Chief, Manufacturing Engineering, Western Electric Co., Andover, Mass.

February 10—"Design Philosophy of a Modern SSB Transceiver," C. Carney, Manager Amateur Equipment Sales, Collins Radio Co., Cedar Rapids, Iowa.

February 17—"Harmonic and Intermodulation Distortion in High Fidelity Amplifiers," M. Snitzer, Technical Editor, Electronics World, New York, N. Y.

February 24—"High Power Transmitter Stations," H. C. Hawkins, Project Engineer, Long Range Radio Branch, U. S. Army Signal Development Lab., Fort Monmouth, N. J.

7th Scintillation Counter Symposium To Be Held

The Seventh Scintillation Counter Symposium will be held February 25–26, 1960 at the Hotel Shoreham in Washington, D. C. It is sponsored by the American Institute of Electrical Engineers, Atomic Energy Commission, Institute of Radio Engineers and National Bureau of Standards.

This is one of the series of Symposia which have been held biennially since 1948. They have served to bring together those interested in scintillation counters for the purpose of exchanging information on advanced techniques, recent equipment developments and new components. The meetings are on a high technical level and treat both the theoretical and practical aspects of the field.

The Seventh Scintillation Counter Symposium will consist of four sessions of a half-day each treating the following topics:

Session I—Scintillators
Session II—Photomultipliers and Associated Electronics
Session III—Scintillation Track Imaging
Session IV—Astrophysical and Space Applications of Scintillation Counters.

A dinner and evening session will be held February 25. The evening session will be an open group discussion of some of the important current problems in scintillation counting. The program includes invited papers by U. S. and foreign scientists and contributed papers by workers in the field. Further information can be obtained from G. A. Morton, Chairman, Scintillation Counter Symposium Committee, RCA Laboratories, Princeton, N. J.

Publish Bimonthly Journal on Mathematical Physics

A bimonthly *Journal of Mathematical Physics*, devoted to new mathematical methods for the solution of physical problems as well as original research in physics furthered by such methods, is being published by the American Institute of Physics. The scope of the magazine includes mathematical aspects of quantum field theory, statistical mechanics of interacting particles, new approaches to eigenvalue and scattering problems, theory of stochastic processes, novel variational methods, theory of graphs, and review papers on mathematical topics for physicists.

Subscription rates for the journal will be \$10.00 in the United States and Canada and \$11.00 elsewhere. Orders and inquiries should be addressed to the American Institute of Physics, 335 E 45 St., New York 17, N. Y.

Professional Group News

The following Chapters were approved by the IRE Executive Committee on November 16th and December 15, respectively: PG on Medical Electronics—North Carolina Chapter, PG on Medical Electronics—Portland Chapter.

Air Force MARS Eastern Net Schedules February Program

The February program of the Air Force MARS Eastern Technical Net, which can be heard from 2 to 4 P.M. EST Sundays, at 3295 kc SSB, 7540 and 15,715 kc AM, is as follows:

February 7—"Principles of Infra-red," Staff discussion, Rome Air Dev. Center.
February 14—"UHF Radiotelephone Systems," J. Longly, Eng'r., New York Telephone Co.
February 21—"Oscillator Circuit Considerations," R. Gunderson, Editor, Braille Technical Press.
February 28—"Quality Control Techniques," A. Stein, Eng'r., Riverside Plastics Corp.
March 6—"The IRE National Convention," G. Bailey, Chairman of the Convention.

Ninth Annual SSB Dinner To Be Held March 22

The SSB Amateur Radio Association will sponsor the Ninth Annual SSB Dinner and Hamfest on Tuesday, March 22, 1960, at the Hotel Statler-Hilton, New York, N. Y. All amateurs and their friends are invited. This dinner, held during the week of the IRE Convention, attracts many outstanding radio amateurs and communications men from all parts of the world.

Equipment displays open at 10 A.M. and the dinner starts at 7:30 P.M. Bill Leonard, W2SKE, will be the master of ceremonies. Tickets purchased in advance are $8.50 a piece; those purchased at the door are $9.50.

Checks for reservations should be sent to
SSBARA
c/o Mike Le Vine, WA2BLH
33 Allen Road
Rockville Centre, L. I., N. Y.

NSF Announces Deadline, Policy on Research Grants

The National Science Foundation announces that the next closing date for receipt of proposals for support of renovation and/or construction of graduate level (doctoral) research laboratories is March 1, 1960. Proposals received prior to that date will be reviewed during late spring and early summer. Disposition of approved proposals will be made during late summer, 1960. Proposals received after the closing date in March will be reviewed following the next closing date, which is expected to be September 1, 1960.

This program will continue to require at least 50 per cent participation by the institution with funds derived from non-Federal sources. Proposals may be submitted for modernization or construction of research laboratories, including laboratory furnishings but not including apparatus or equipment, in any field of the natural sciences. For the present, this program is restricted to those departments which have an on-going program leading to the Ph.D. degree. Support of facilities to be used primarily for instructional purposes will not be considered. It is suggested that preliminary inquiry be made to either the Division of Biological and Medical Sciences or the Division of Mathematical, Physical, and Engineering Sciences, National Science Foundation, Washington 25, D. C. Information concerning the Program and instructions for preparation of proposals may be obtained upon request.

Also, the NSF announces that effective January 1, 1960, pending completion of a study of the entire problem of indirect costs, it will permit institutions to request up to 20 per cent of total direct costs as the allowance for indirect costs in research proposals. In no event, however, may such indirect costs exceed the last "audited" or "negotiated" rate approved for the institution by a Federal agency for purposes of Government-sponsored research and development. An institution with an "audited" or "negotiated" indirect cost rate so approved may claim such rate provided it does not exceed 20 per cent of the total direct costs.

Cleveland Conference Includes IRE Panel

The seventh annual Cleveland Electronics Conference will take place on February 10-12, 1960, at the Cleveland Engineering and Scientific Center. Allen S. Nace (A'39–SM'46) is conference chairman. The conference program includes presentation of ten technical papers and three evening seminars.

The IRE will sponsor a panel discussion on silicone controlled rectifiers on Thursday evening, February 11, at 7:30. The moderator will be John Flick, and three participating panelists will be E. E. Von Zastrow, Robert McKenna (S'58–M'59) and Eric Johnson.

The six groups which annually sponsor this conference are the Instrument Society of America, the Institute of Radio Engineers, the American Institute of Electrical Engineers, the Cleveland Physics Society, Case Institute of Technology, and Western Reserve University.

Cincinnati Section to Hold Spring Technical Conference

The Fourteenth Annual Spring Technical Conference will be held by the Cincinnati Section of the IRE and the Southern Ohio Section of the American Rocket Society in Cincinnati, Ohio, April 12 and 13, 1960.

This year the conference committee has planned expanded technical sessions, featuring papers on Space Electronics and Data Processing; expanded exhibit areas, including displays from major concerns in the electronics and missile fields; a conference ball, featuring a keynote speaker of national interest; and a luncheon program, at which several prominent personalities in the rocket and electronics fields will be presented. The conference will have a double theme of Space Technology and Electronic Data Processing.

A registration fee of $3.00 in advance or $3.50 at or during the conference has been established. There will be an additional charge of $1.00 for each bound copy of the technical papers.

OBITUARY

John Robinson Binns (A'26–VA'39–SM'54), honorary chairman of the board of Hazeltine Corp., died recently at the age of 75.

J. R. Binns

One of the pioneers in the electronics industry, he won fame in 1909 for his lifesaving role as a wireless operator during the first sea rescue by radio. He sent the distress signal and then guided the rescue ships following the collision of the steamships *Republic* and *Florida* at sea off Nantucket.

Born in Lincolnshire, England in 1884, he became interested in electrical sciences as a boy. He attended the technical school of Great Eastern Railway, where he received a thorough grounding in electricity and learned the Morse telegraphic code. In 1905, he joined the Marconi Company as a wireless operator.

On January 23, 1909, the *USS Republic*, en route to Egypt with 1600 passengers on board was rammed in the fog off Nantucket by the *Flordia*, an Italian ship with almost 2000 passengers bound for New York. As wireless operator on the *Republic*, Mr. Binns stayed in his flooded radio shack and contacted the Siasconsett Station on Nantucket Island. It was the first time that S.O.S. (C.Q.D.) had been used successfully.

Mr. Binns worked as a wireless operator for Marconi Wireless until 1912. He then joined the staff of the *New York American* as a reporter and following World War I, became Radio and Aviation Editor of the *New York Tribune*. During the war, he was a flying and radio instructor for the Canadian Flying Corps.

In 1924, he became associated with Hazeltine Corp., when it was formed to develop and license radio patents. He was made assistant treasurer in 1925, treasurer in 1926 and a director in 1927. He was elected vice president in 1935, president in 1942 and chairman of the board in 1952. In 1957, he was elected first honorary chairman of the firm.

Mr. Binns was a member of the Radio Club of America, Society of Naval Engineers, Armed Forces Communications and Electronics Association and Society of the Silurians, a newspaper men's group.

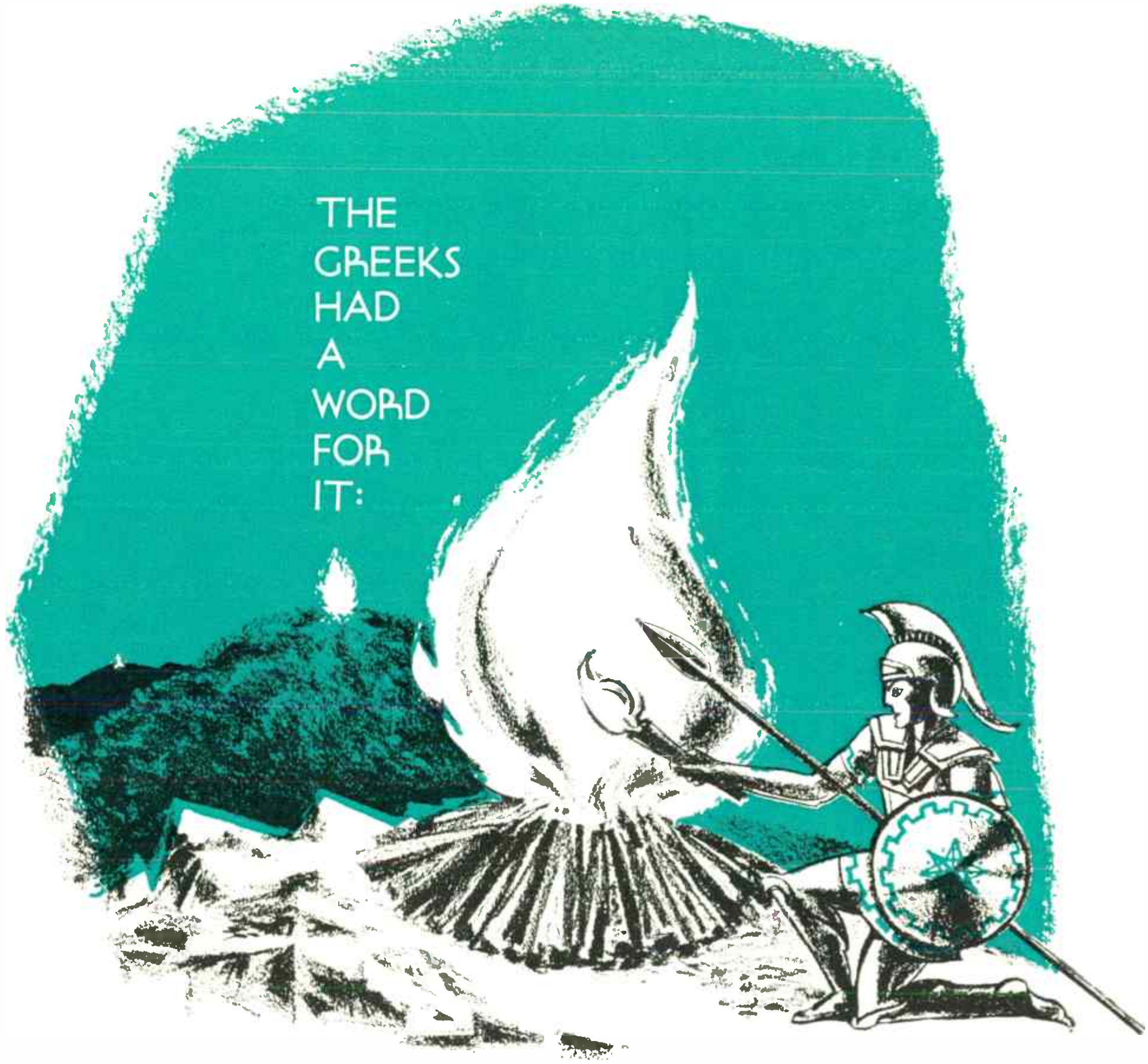

TELECOMMUNICATIONS

Signal fires flaming across a network of some nine stations over a distance of sixty miles flashed the news of the fall of Troy to Agamemnon's palace at Mycenae. *Tele* in Greek means distance, and this—in 1194 B.C.—was *telecommunications*.

The newest and most advanced technique in telecommunications is the tropospheric scatter method using ultra high frequency signals which travel beyond the horizon, leap-frogging mountains, oceans, and other geographical barriers.

Pioneering in the development of tropo scatter communications has been Radio Engineering Laboratories, which is responsible for the design and construction of the radio equipment for eight out of nine of the major tropo networks.

REL welcomes the opportunity to use this experience in solving your commercial and military telecommunications problems.

REL

Radio Engineering Laboratories · Inc

A subsidiary of Dynamics Corporation of America

Dept. I · 29-01 Borden Ave · Long Island City 1, NY

Creative careers at REL await a few exceptional engineers. Address résumés to James W. Kelly, Personnel Director.

1959 IRE NATIONAL AND WESCON CONVENTION RECORDS

All Parts of the 1959 IRE National Convention Record and the 1959 IRE Wescon Convention Record are now available. Because of the large number of requests received for both Records, several parts had been completely sold out, but they are now being reprinted.

The following important changes have been made in 1959 with regard to the Records:

1) Prices have been reduced by more than 50 per cent.
2) A special reduced rate has been established for members of IRE Professional Groups.
3) The practice of distributing free copies to Professional Group members has been discontinued.

Professional Group members and Affiliates are entitled to purchase the Part sponsored by the Professional Group to which they belong at the special PG rate indicated below. Other Parts may be purchased at the IRE Member rate.

IRE members may purchase any Part at the IRE Member rate indicated. However, if a member applies for membership in the appropriate Professional Group at the time he places his order, he will be entitled to the PG rate.

Nonmembers and libraries may place orders at the Nonmember and the Library rates, respectively. Individuals who apply for IRE membership at the time they place their orders are entitled to the IRE member rates.

Subscription agencies are entitled to purchase any of the Record Parts at the Library rate.

Clip out the order form on the opposite page, and return it, with remittance, to the Institute of Radio Engineers, Inc., 1 East 79 Street, New York 21, N. Y. In ordering, be sure to refer to the proper columns for subjects and prices.

1959 IRE NATIONAL CONVENTION RECORD

Part	Sessions	Subject and Sponsoring IRE Professional Group	Prices for Members of Sponsoring Professional Group (PG), IRE Members (M), Libraries (L), and Nonmembers (NM)			
			PG	M	L	NM
1	38, 46, 53	Antennas & Propagation	$0.70	$1.05	$2.80	$3.50
2	34, 41, 49	Circuit Theory	0.70	1.05	2.80	3.50
3	8, 16, 23, 32, 39	Electron Devices Microwave Theory & Techniques	1.00	1.50	4.00	5.00
4	1, 9, 17, 25, 33, 40, 48	Automatic Control Electronic Computers Information Theory	1.20	1.80	4.80	6.00
5	7, 15, 24, 28, 36, 43, 51	Aeronautical & Navigational Electronics Military Electronics Space Electronics & Telemetry	1.20	1.80	4.80	6.00
6	6, 22, 27, 31, 35, 42, 44, 50	Component Parts Industrial Electronics Production Techniques Reliability & Quality Control Ultrasonics Engineering	1.40	2.10	5.60	7.00
7	11, 12, 19, 20, 26, 52	Audio Broadcast & TV Receivers Broadcasting	1.00	1.50	4.00	5.00
8	2, 4, 30, 37	Communications Systems Radio Frequency Interference Vehicular Communication	0.80	1.20	3.20	4.00
9	10, 14, 18, 21, 45, 47, 54	Human Factors in Electronics Instrumentation Medical Electronics Nuclear Science	1.20	1.80	4.80	6.00
10	3, 5, 13, 29	Education Engineering Management Engineering Writing & Speech	0.80	1.20	3.20	4.00
		Complete Set (10 Parts)	$10.00	$15.00	$40.00	$50.00

ORDER FORM

1959 IRE National and Wescon Convention Records

National Convention Record

Part	1	2	3	4	5	6	7	8	9	10	Complete Set
Number of Copies											
Amount Paid											

Total Remittance

Wescon Convention Record

Part	1	2	3	4	5	6	7	8	Complete Set
Number of Copies									
Amount Paid									

Total Remittance

Total Remittance for both Records ________

Name (Please Print): ________________________

Shipping Address: ________________________

____

1959 IRE WESCON CONVENTION RECORD

Part	Sessions	Subject and Sponsoring IRE Professional Group	Prices for Members of Sponsoring Professional Group (PG), IRE Members (M), Libraries and Sub. Agencies (L), and Nonmembers (NM)			
			PG	M	L	NM
1	3, 8, 13, 31, 37, 42	Antennas & Propagation Microwave Theory & Techniques	$1.00	$1.50	$4.00	$5.00
2	11, 17, 24, 29	Circuit Theory	.80	1.20	3.20	4.00
3	5, 10, 14, 15, 19	Electron Devices	.90	1.35	3.60	4.50
4	4, 9, 22, 27, 30, 36, 41	Automatic Control Electronic Computers Information Theory	1.20	1.80	4.80	6.00
5	20, 25, 26, 28, 34	Aeronautical & Navigational Electronics Human Factors in Electronics Military Electronics Space Electronics & Telemetry	.90	1.35	3.60	4.50
6	1, 2, 12, 16, 18, 33, 40	Component Parts Industrial Electronics Production Techniques Reliability & Quality Control Ultrasonics Engineering	1.20	1.80	4.80	6.00
7	6, 23, 39	Audio Broadcast & Television Receivers Broadcasting Communications Systems	.70	1.05	2.80	3.50
8	7, 32, 35, 38	Instrumentation Medical Electronics Nuclear Science Engineering Management	.80	1.20	3.20	4.00
		Complete Set (8 Parts)	$7.50	$11.25	$30.00	$37.50

IRE People

Raymond F. Guy (A'25–M'31–F'39), Senior Staff Engineer of the National Broadcasting Company, has been elected President of the De Forest Pioneers, a society consisting of former associates of Dr. Lee De Forest, the distinguished scientist and inventor.

Mr. Guy is a pioneer in radio, television and short wave broadcasting. He was a combined announcer and engineer and a well-known air personality in the earliest days of broadcasting in the New York area. For nearly 30 years he was responsible for the planning and construction of all NBC transmitting facilities, which included a leading part in the creation of the pioneering Empire State Building TV tower which is shared by all New York stations.

He is a Fellow of the American Institute of Electrical Engineers, a Past President of the Broadcast Pioneers, newly elected President of the De Forest Pioneers and First Vice President of the Veteran Wireless Operators Association, an organization of prominent industry veterans of the very early days of wireless. He is Chairman of the Engineering Committee of the Voice of America, for many years was Chairman of the Engineering Committee of the Television Broadcasting Association and the Engineering Advisory Committee of the National Association of Broadcasters, and is active in many other organizations, several of which have honored him with medals of achievement and special citations.

❖

Frank A. Comerci (SM'55) has joined Audio Devices, Inc., New York, N. Y., manufacturer of magnetic recording tape, as senior project engineer at the Stamford, Conn., laboratory.

F. A. Comerci

For the past twelve years he has been in charge of the Communication and Acoustics Section at the New York Naval Shipyard in Brooklyn, N. Y. In this capacity he supervised electronic scientists in applied research development and acted as consultant to The Bureau of Ships.

Mr. Comerci is a member of the Audio Engineering Society, the Acoustical Society of America and the Research Society of America and has published many papers in the audio communications field. He is also active on the standards committees of all these societies as well as chairman of the Sound Committee of the Society of Motion Picture and Television Engineers.

❖

The appointment of **Dr. J. R. McCaughna** (M'53) to direct electronics research and development at Broadview Research Corporation has been announced by Richard De Lancie, president.

Dr. McCaughna's initial activities will be devoted to expansion of Broadview's electronics activity into the microwave and solid state areas. In addition he will act in a senior consulting capacity on projects currently under way.

He comes to Broadview after ten years of consulting in electronics to many military and industrial organizations. He holds numerous patents, including basic patents on processes for the commercial refining of germanium.

A native of San Francisco, he had his early schooling in Burlingame. After graduation from Burlingame High School he attended the University of California at Berkeley, where he received the B.S., M.S. and Ph.D. degrees in chemistry.

Upon completion of his graduate work and prior to embarking on his career as a consultant, Dr. McCaughna studied electrical engineering, worked in Mexico for Mexican Industries, Ltd., and was chief engineer for Pacific Electronics Corporation.

❖

United Research Inc., Cambridge, Mass., has announced the appointment of **Dr. A. B. Van Rennes** (S'42–A'48–M'50–SM'56) as vice-president in charge of its Technical Division. Among his responsibilities will be the direction of fundamental research and development programs in instrumentation, including programs for the measurement of meteorological variables and fuel contamination.

A. B. Van Rennes

He was formerly associated with the Research Laboratories Division of Bendix Aviation Corporation. At Bendix he was supervisor of the Nuclear Technology Group, with activities embracing design and fabrication of nuclear instrumentation systems using solid state components, kinetic analysis of reactors and reactor systems, development of control systems for rocket reactors, and airborne radiation detection systems. Prior to 1956 he was a faculty member at the Massachusetts Institute of Technology, holding the position of Associate Professor of Electrical Engineering.

A graduate of M.I.T., he served in the United States Naval Reserve during World War II. He participated in the 1946 atom bomb tests conducted at Bikini by Joint

(*Continued on page 26A*)

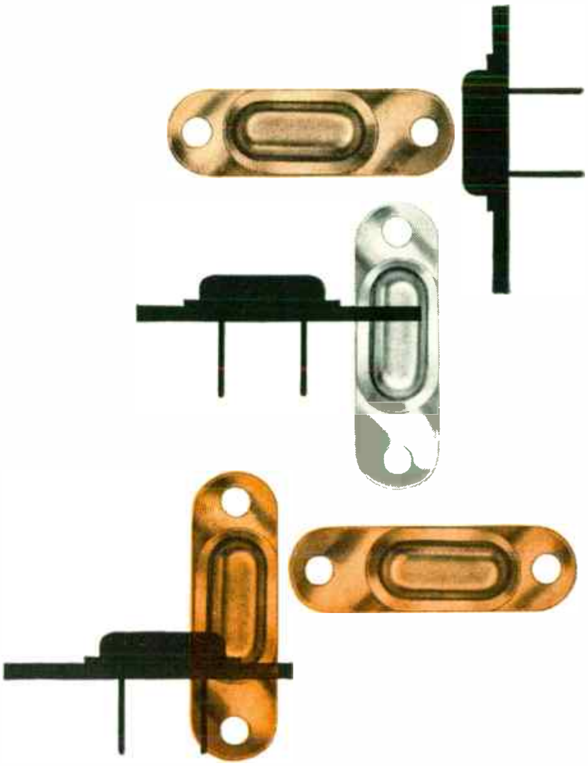

CLEVITE'S NEW
SPACESAVER
TRANSISTOR

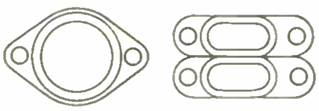

½ actual size

THREE AMPERE SWITCHING TYPES

TEST	CTP 1728	CTP 1735	CTP 1729	CTP 1730	CTP 1731	CTP 1736	CTP 1737	CTP 1733
Min BVcbo @ 2 ma (volts)	40	60	80	100	40	60	80	100
Min BVceo @ 500 ma (volts)	25	40	55	65	25	40	55	65
Min BVces @ 300 ma (volts)	35	50	65	75	35	50	65	75
Max Icbo @ 90°C @ Max Vcb (ma)	10	10	10	10	10	10	10	10
Max Icbo @ 2 V (μa)	50	50	50	50	50	50	50	50
D. C. Current Gain @ 0.5A	30-75	30-75	30-75	30-75	60-150	60-150	60-150	60-150
Max Veb @ 3.0 A (volts)	1.5	1.5	1.5	1.5	1.5	1.5	1.5	1.5
Max Vce (sat) @ 3.0A, 300 ma (volts)	1.0	1.0	1.0	1.0	0.8	0.8	0.8	0.8
Min fae @ 3.0 A (kc)	20	20	20	20	15	15	15	15
Max Thermal Resistance (°c/w)	2.5	2.5	2.5	2.5	2.5	2.5	2.5	2.5

Compared with present power transistors of similar ratings, the new Clevite *Spacesaver* gives you important new advantages.

Better Switching — Its low base resistance gives lower input impedance for the same power gain and lower saturation resistance, resulting in lower "switched on" voltage drop. Its lower cut off current means better temperature stability in direct coupled circuits (such as regulated power supplies) and a higher "switched off" impedance.

Better Amplifying — Improved frequency response leads to higher audio fidelity, faster switching and improved performance in regulated power supply applications.

Better Mounting — The *Spacesaver's* simple rectangular configuration and low silhouette make it adaptable to a wide variety of mounting requirements where space is at a premium. In aircraft and missile applications, its low mass (half present type) improves shock and vibration resistance of lightweight assemblies.

Phone for data and prices.

A DIVISION OF CLEVITE CORPORATION

CLEVITE TRANSISTOR

254 Crescent Street Waltham 54, Mass. Tel: TWinbrook 4-9330

(Continued from page 24A)

Task Force One, and received for this effort a citation by Admiral W. H. Blandy. Following the war he returned to M.I.T. to join the faculty and complete his graduate study.

During the past eight years, Dr. Van Rennes has been a consultant to various industrial and Government groups, and has published a variety of papers on nuclear instrumentation techniques and on nuclear reactor kinetics, control and instrumentation. He is currently chairman of the IRE Professional Group on Nuclear Science, and a member of standards committees of the American Nuclear Society and of the American Standards Association. Other affiliations include the American Society for Engineering Education and the honorary societies, Tau Beta Pi, Eta Kappa Nu, and Sigma Xi.

❖

Rear Admiral **Richard S. Mandelkorn (USN, Ret.),** (SM'57), who has held a number of the Navy's highest engineering-scientific posts, has joined General Instrument Corp. as Executive Vice-President of its Harris Transducer Corp. subsidiary. Harris Transducer, a key unit in General Instrument's six-plant Defense and Engineering Products Group, develops and produces electronic-acoustical devices in the Sonar and anti-submarine warfare fields. He will be in complete charge of operations and planning at the Harris Transducer, Woodbury, Conn. plant, under direction of Dr. Wilbur T. Harris, president of the General Instrument subsidiary.

R. S. Mandelkorn

Immediately prior to joining General Instrument, he had been Operations Manager and Director of Planning for Philco Corporation's Lansdale Tube Division since 1957, when he retired from the Navy. In the Navy his career included the posts of: Commanding Officer and Director of U. S. Naval Radiological Defense laboratory (1956–57); Comptroller, Bureau of Ships (1955); Director of Value Engineering, Bureau of Ships (1954); Shipbuilding Superintendent, Portsmouth Naval Shipyard, in charge of submarine design and construction (1951–53); Deputy Director of Research, Armed Forces Special (nuclear) Weapons Project, Sandia Base, Albuquerque, N. M.; Weapons Division, Los Alamos Scientific Laboratories (1947–48); Coordinator of Guided Missiles, Bureau of Ships (1945–1947).

He received the B.S. degree in '32 "with distinction" from the U. S. Naval Academy, Annapolis, Md., and the M.S. degree in 1937 from the Massachusetts Institute of Technology. He served in the Pacific

(Continued on page 28A)

IRE People

(Continued from page 26A)

during World War II. He is a member of Sigma Xi and Tau Beta Pi professional engineering societies, the American Society of Naval Engineers, and the Society of Naval Architects and Marine Engineers, and is Chairman of the Value Engineering Committee of the Electronics Industries Association.

❖

The Teleregister Corp. has appointed **Edward Rathje, Jr.,** (A'48–M'55) to the post of Manager of the Development Section.

He has been with Sanders Associates Inc. of Nashua, N. H. for the past five years in various positions, including Assistant to the Vice President of Engineering and Project Manager. During this time he was concerned with technical and administrative direction of counter-measures and missile guidance projects and development of the related analogue and digital devices. Previously he was with Daystrom Instrument Co. and Stavid Engineering Inc., in design, development, and research capacities.

A member of the AIEE, Mr. Rathje received the B.S. degree in Electrical Engineering, and has done graduate study at Northeastern University, Boston.

❖

Eugene F. Brosseau (M'56) has been appointed manager, Employment of Advanced Professional Personnel, for the International Business Machines Corporation. He reports to the manager of Corporate Employment at the IBM World Headquarters in New York City.

E. F. Brosseau

At his office at the IBM, Poughkeepsie, N. Y., research laboratory, he is responsible for Ph.D. recruiting at 32 key colleges and universities and maintaining liaison with some 30 other schools throughout the country. His responsibilities also include maintaining communication with department managers as to their needs for professional people of particular background, and hiring newly graduated and experienced Ph.Ds. to fill these needs.

He joined IBM in July, 1954 as a technical engineer assisting in the design and construction of automatic ferrite core evaluation equipment. Subsequently he held positions of associate engineer, project engineer, and research engineer.

His assignments have included work on magnetic core measurements, setting up equipment for thin film preparation and evaluation; he has been group leader of the magnetic materials and devices group,

(Continued on page 30A)

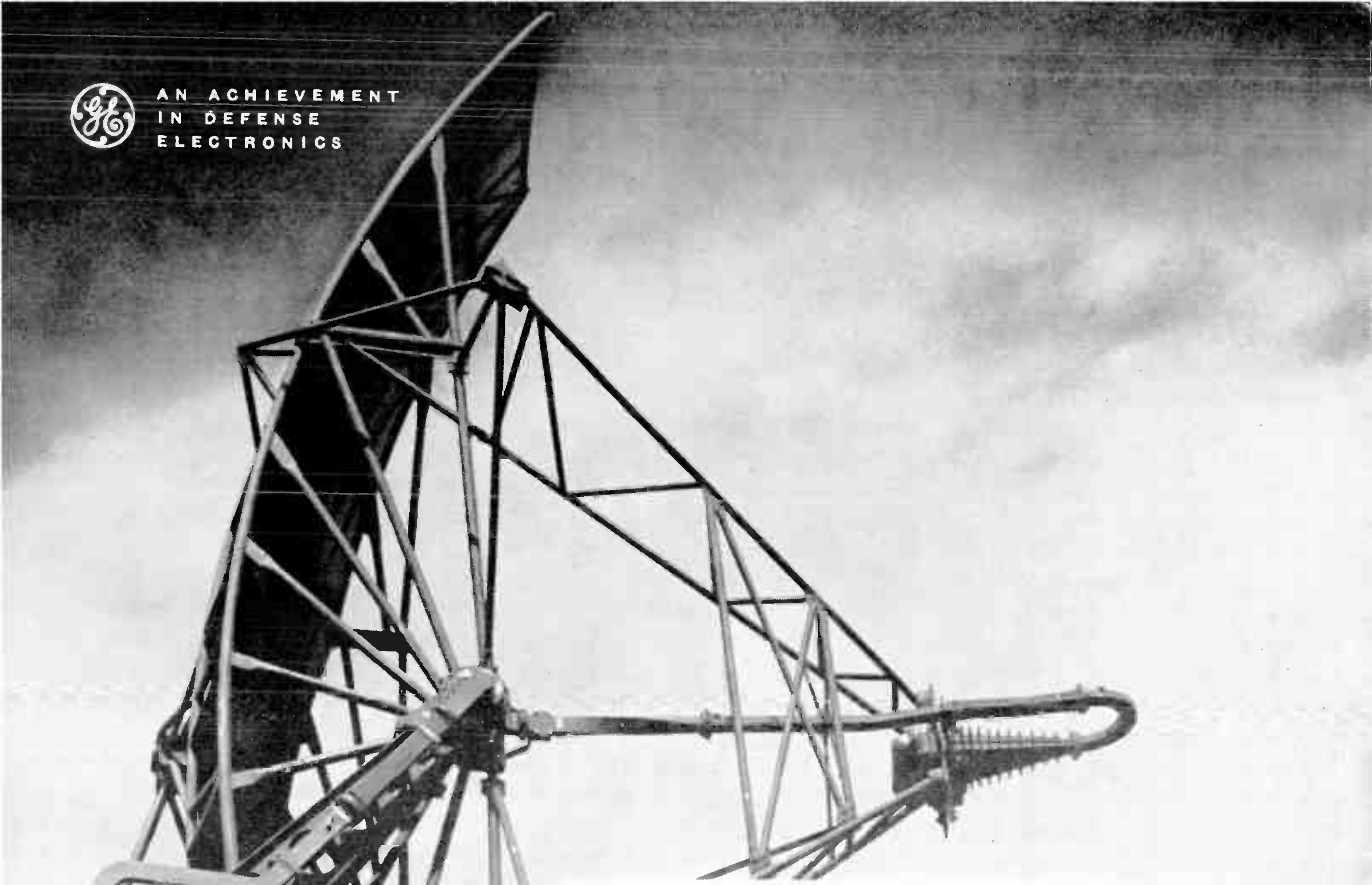

HOW A 6-YEAR-OLD RADAR STAYS YOUNG

A six-year operational veteran, the FPS-6 is still the principal height-finder for air defense. Fundamentally sound design and built-in capacity for improvement enable General Electric to keep this radar "young."

Contrasted with earlier versions, today's FPS-6 features height line display as a full-time trace. Indicator calibration, sector scan, performance monitoring and azimuth blanking are automatic. The nod angle, formerly fixed, has been made variable to attain more hits per target. A new ferrite isolator increases magnetron life and stability. Noise figure has been improved by nearly 1.5 db.

The sustained effectiveness of this radar at operational sites during six years of a rapidly changing air defense environment is truly an achievement in defense electronics. 227-4

Progress Is Our Most Important Product

GENERAL ELECTRIC

DEFENSE ELECTRONICS DIVISION
HEAVY MILITARY ELECTRONICS DEPARTMENT

IRE People

(Continued from page 28A)

group leader of the magnetic film group and technical assistant to the resident manager of the Poughkeepsie research laboratory.

Mr. Brosseau is a graduate of the University of Colorado, having received the B.S. degree in electrical engineering.

❖

Anthony G. Schifino (M'48), who has resigned as vice president and general manager of Stromberg-Carlson's Special Products Division, is joining Rochester Radio Supply Company, Inc., as executive vice president. This move is being made to implement plans of the company for extensive expansion in the Western New York area.

A. G. Schifino

He will continue to serve as a consultant to Stromberg-Carlson in the sound equipment field for an indefinite period.

He was born in Retsof, N. Y., and has been active in Rochester business since 1929, when he joined Stromberg-Carlson's telephone laboratory after graduation from Ohio Northern University with a degree in electrical engineering. Subsequently he left Stromberg-Carlson to establish and operate Rochester Radio Supply Company for several years, returning to Stromberg-Carlson in 1940 as chief sound equipment engineer.

Mr Schifino is currently serving on the Board of Directors of the Rochester Sales Executives Club, and as chairman of the Amplifier and Sound Equipment Section of the Electronic Industries Association. He also is a member of the American Institute of Electrical Engineers.

❖

Frederick J. Seufert (S'49–A'50–SM'57) has been named section manager of the newly established Systems Development Section of Hoffman Laboratories Division, Hoffman Electronics Corporation, it was announced by Richard A. Maher, vice-president-engineering for the division. He previously was operations director for Hoffman's ULD-1 "Tall Tom" program.

The new Systems Development Section is being established to further Hoffman Laboratories' capabilities in advanced systems programs. The section will consist of a neucleus of highly trained systems engineers who will anticipate future requirements for advanced military systems, and conduct studies and analyses of these requirements. This group will form the core for any future systems programs Hoffman undertakes.

Mr. Seufert, who joined Hoffman four

(Continued on page 32A)

Publisher's Price, $8.00
Club Price, $6.80

Transistor Circuits and Applications by J. M. Carroll. Detailed information to aid in circuit design.

Publisher's Price, $12.50
Club Price, $10.65

Pulse and Digital Circuits by J. Millman and H. Taub. Explains circuits for effective system design.

Publisher's Price, $9.50
Club Price, $8.10

Sampled-data Control Systems by J. R. Ragazzini and G. F. Franklin. Covers both analysis and design.

Publisher's Price, $7.00
Club Price, $5.95

Operational Mathematics by R. V. Churchill. Theory and applications of Laplace and other transforms.

Publisher's Price, $12.00
Club Price, $10.25

Electronic Measurements by F. E. Terman and J. M. Pettit. Techniques for use in many electronic fields.

Publisher's Price, $9.00
Club Price, $7.65

Modern Physics for the Engineer by L. N. Ridenour. Physical science on which modern engineering is based.

Publisher's Price, $7.00
Club Price, $5.95

Mathematics for Electronics with Applications by H. M. Nodelman and F. W. Smith. For solving practical problems.

Publisher's Price, $7.50
Club Price, $6.40

Electronic Analog Computers by G. A. and T. M. Korn. How to design and set up problems for computers.

Publisher's Price, $8.75
Club Price, $7.45

Handbook of Industrial Electronic Control Circuits by J. Markus and V. Zeluff. Over 300 tested circuits.

To new members of the
ELECTRONICS AND CONTROL ENGINEERS' BOOK CLUB

Special Introductory Offer

ANY ONE FREE

YOURS WITH A CHARTER MEMBERSHIP AND SENT WITH YOUR FIRST SELECTION

Values from $7.00 to $12.50

Select one AS A GIFT! Choose from *Electronic Measurements, Operational Mathematics, Pulse and Digital Circuits,* and six other valuable books . . . your introduction to membership in the *Electronics and Control Engineers' Book Club.*

If you're missing out on important technical literature—if today's high cost of reading curbs the growth of your library—here's the solution to your problem. *The Electronics and Control Engineers' Book Club was organized for you,* to provide an economical technical reading program that cannot fail to be of value to you.

All books are chosen by qualified editors and consultants. Their thoroughgoing understanding of the standards and values of the literature in your field guarantees the authoritativeness of the selections.

How the Club operates. Every second month you receive free of charge *The Electronics and Control Engineers' Book Bulletin* (issued six times a year). This gives complete advance notice of the next main selection, as well as a number of alternate selections. If you want the main selection you do nothing; the book will be mailed to you. If you want an alternate selection . . . or if you want no book at all for that two-month period . . . notify the Club by returning the form and postage-paid envelope enclosed with your *Bulletin.*

We ask you to agree only to the purchase of three books in a year. Certainly out of the large number of books in your field offered in any twelve months there will be at least three you would buy anyway. By joining the Club you save yourself the bother of searching and shopping and save in cost about 15 per cent from publishers' prices.

Send no money now. Just check any two books you want—one FREE and one as your first Club selection—in the coupon below. Take advantage of this offer *now,* and get two books for less than the regular price of one.

THIS COUPON IS WORTH UP TO $12.50

The Electronics and Control Engineers' Book Club
330 West 42nd Street, New York 36, N. Y., Dept. IRE-2

Please enroll me as a member of the Electronics and Control Engineers' Book Club. I am to receive my FREE book along with my first selection, both checked at the right. You will bill me for my first selection only at the special club price, plus a few additional cents for postage and handling. (The Club assumes this charge on prepaid orders.) Forthcoming selections will be described to me in advance and I may decline any book. I need take only 3 selections or alternates in 12 months of membership. (This offer good in U. S. only.)

PLEASE PRINT

Name ....

Address ....

City .... Zone...... State..........

Company ....

NO RISK GUARANTEE: If not completely satisfied, you may return your first shipment within 10 days and your membership will be cancelled.

Check 2 books: We will send the higher priced book as your FREE book:

- ☐ Transistor Circuits and Applications, $6.80
- ☐ Pulse and Digital Circuits, $10.65
- ☐ Sampled-data Control Systems, $8.10
- ☐ Operational Mathematics, $5.95
- ☐ Electronic Measurements, $10.25
- ☐ Modern Physics for the Engineer, $7.65
- ☐ Mathematics for Electronics with Applications, $5.95
- ☐ Electronic Analog Computers, $6.40
- ☐ Handbook of Industrial Electronic Control Circuits, $7.45

IRE-2

IRE People

(Continued from page 30A)

years ago, was previously with the Santa Barbara Research Center. Prior to that he served with Hughes Aircraft Co. and the Brookhaven National Laboratory. He is a member of the Institute of Aeronautical Science.

❖

Dr. Euyen Gott (S'50–A'52–SM'58) has been appointed associate professor of Electrical Engineering of the University of Hawaii, Honolulu.

E. Gott

Born in Kweilin, Kwangsi, China, he received the B.S. degree from the National Kwangsi University, the M.A. and the Engineer degrees from Stanford University, Stanford, Calif., and the degree of Dr. Eng. from Johns Hopkins University, Baltimore, Md.

Before joining the University of Hawaii, he was a research associate at the Radiation Laboratory of Johns Hopkins University for six years, doing research in signal analysis and transistor circuitry. He also had nine years of design and development experience in circuit analysis and electronics when he was associated with the Radio Corporation of America, in Lancaster, Pa., the Sierra Electronic Corporation in San Carlos, Calif., and the Yee-Chong Electric Manufacturing Company in Kweilin, China. He taught at the National Kwangsi University for three years.

Dr. Gott has published several technical papers on computer and transistor circuitry. He is a member of Sigma Xi.

❖

The Bavarian Academy of Sciences in Germany has honored **Dr. Ronald W. P. King** (A'30–SM'43–F'53) of Harvard University. Dr. King, who is Gordon Mackay Professor of Applied Physics, has been appointed a Corresponding Member of the Academy's Department of the Mathematical and Natural Sciences.

Among his colleagues, he is well known for his work on electromagnetic radiation and on antennas. He is a Fellow of the American Academy of Arts and Sciences and the American Physical Society.

A native of Williamstown, Mass., he received the B.A. and M.S. degrees from the University of Rochester and the Ph.D. degree from the University of Wisconsin. He has been at Harvard since 1938.

❖

(Continued on page 38A)

Use your IRE DIRECTORY! It's valuable!

STACKPOLE Coldite 70+®

fixed composition **RESISTORS**

1/2-, 1- and 2-watt sizes

The resistors that are setting today's higher performance standards! Unmatched for load life and moisture resistance—and, with performance that exceeds MIL-R-11 requirements. And now, for the first time, you can get such resistors in a *complete* line of RC-42 (2-watt); RC-32 (1-watt) and RC-20 (1/2-watt) types from stock from leading distributors!

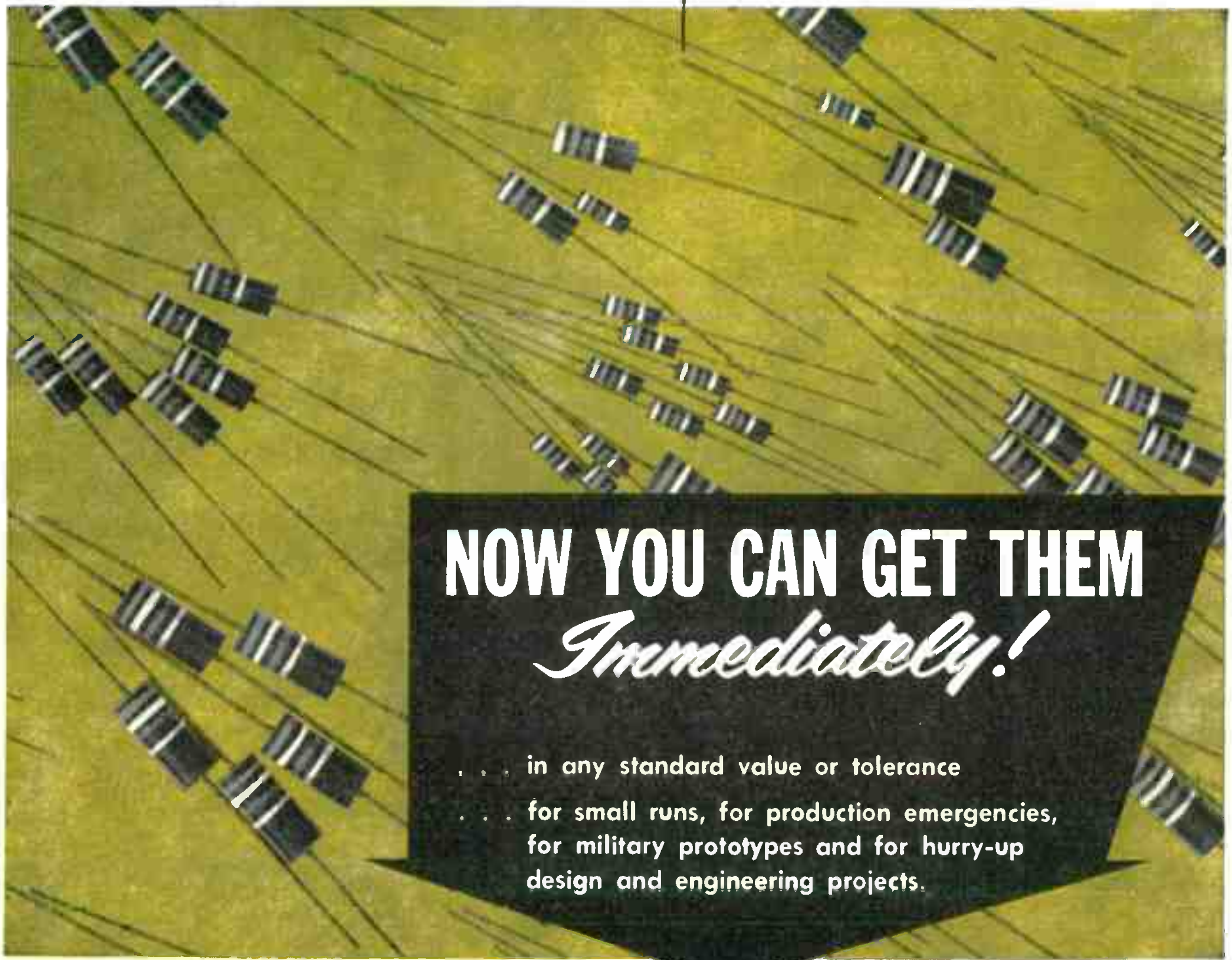

FROM STOCK . . . from these selected STACKPOLE distributors:

BALTIMORE, MD.
Kann-Ellert Electronics, Inc.

BATTLE CREEK, MICH.
Electronic Supply Corp.

BIRMINGHAM, ALA.
MG Electrical Supply Co.

BOSTON, MASS.
Sager Electrical Supply

BROOKLYN, N. Y.
Electronic Equipment Corp.

CLEVELAND, OHIO
Pioneer Electronic Supply Co.

DALLAS, TEXAS
Wholesale Electronics Supply Co.

DAYTON, OHIO
Srepco, Inc.

DENVER, COLO.
Denver Electronics Supply Co.

GLENDALE, CALIF.
R. V. Weatherford Company

INDIANAPOLIS, INDIANA
Radio Distg. Co.

KANSAS CITY, MO.
Burstein-Applebee Co.

MELBOURNE, FLORIDA
Electronic Supply

MIAMI, FLORIDA
Electronic Supply

NEW YORK, N. Y.
Harvey Radio Co.

PHILADELPHIA, PA.
Almo Radio Co.

SAN DIEGO, CALIF.
Radio Parts Co.

SCRANTON, PA.
Fred P. Pursell

SEATTLE, WASH.
C & G Radio Supply Co.

ST. LOUIS, MO.
Interstate Supply Co.

SYRACUSE, N. Y.
Morris Electronics of Syracuse

TACOMA, WASH.
C & G Radio Supply Co.

WASHINGTON, D. C.
Electronic Wholesalers, Inc.

WATERBURY, CONN.
Bond Radio Supply Co. Inc.

WEST PALM BEACH, FLA.
Goddard Distributors, Inc.

WICHITA, KANSAS
Interstate Electronic Sup. Corp.

WILBRAHAM, MASS.
Industrial Components Corp.

WINSTON-SALEM, N. C.
Dalton-Hege Radio Supply

. . . and G-C/STACKPOLE, TOO!

Attractively packaged by G-C Electronics for service replacement uses, Coloite 70+ Resistors are also available through over 800 G-C distributors.

NEWS New Products

These manufacturers have invited PROCEEDINGS readers to write for literature and further technical information. Please mention your IRE affiliation.

Meteorological Telemeter

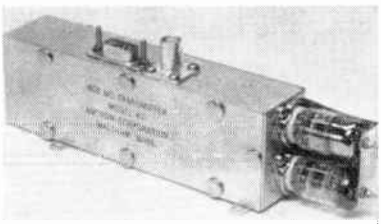

Amtron Corp., 17 Felton St., Waltham, Mass., has recently developed an FM telemetry radio link designed to operate in the 400 to 406 mc radiosonde band. The transmitter, Model KT, is a low cost, small 6 ounce package, capable of 2 watts RF output. A semiconductor modulator provides 125 kc deviation for a 1.0 volt RMS modulation level. The linearity of the modulation system is such that a number of IRIG FM subcarriers can be transmitted simultaneously. Antenna output is 50 ohm coaxial. Power input requirements are 6 to 12 volts ac or dc at 2.8 watts and 150 volts dc at 55 ma.

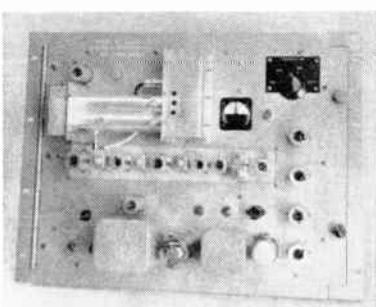

The companion receiver, designated Model KR, is a high quality FM receiver featuring a 6280/416A grounded grid low noise RF stage and a very effective automatic frequency control. The AFC hold-in range is over 10 mc which permits the received signal to drift over the entire turning range of the receiver without detuning effects being noticeable. AFC time constant is fast, 3 milliseconds, capable of correcting for not only thermal drift, but also frequency changes due to G loading which may be encountered by the transmitter. The semiconductor AFC control also permits signal-seeking, panoramic and remote tuning features if they are desired.

The receiver operates on 115 volts, 60 cps ac and is built on a hinged rack panel 19″ wide, allowing rear access from the front of the equipment rack. An airborne version is also available power by 115 volts 400 cps ac.

FM Signal Generator

A new FM signal generator covering the frequency range of 1300 to 2500 mc in one band is now available from **Sierra Electronic Corp., a division of Philco Corp.,** 3885 Bohannon Dr., Menlo Park, Calif.

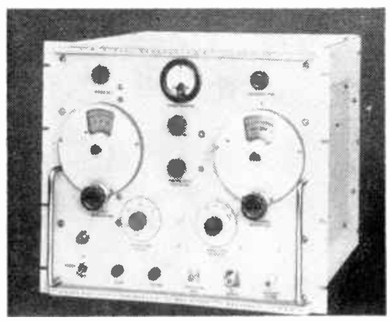

The Model 201B, is specifically designed for telemetry and data transmission applications in the 1.3 to 2.5 kmc range. Featuring a 1% deviation linearity, the instrument can be frequency modulated by applications of external signals having modulation bandwidths up to 500 kc. A nominal deviation of 2 mc peak is produced by external modulation signals having an amplitude of 1.0 volts peak to peak. Model 201B also provides good CW characteristics by virtue of the low value of residual FM.

The instrument's RF output is continuously variable from 0 dbm to −110 by means of a precision calibrated piston attenuator. Model 201B also provides direct reading, single dial tuning and high stability.

Sierra has also announced the availability of a wide deviation FM signal generator, Model 202B. This instrument, covering the frequency range 2200 to 2300 mc, also provides excellent FM characteristics with large deviation for use in wide band applications. Its modulation amplifier response is flat within the limits of 0 db to −6 db from 10 cps to 10 mc.

Pulse Delay Module

The NAVCOR Model 304 Pulse Delay module, designed by **Navigation Computer Corp.,** 1621 Snyder Ave., Philadelphia 45, Pa., contains five independent, all semiconductor, delay circuits. Each section provides (1) a delayed pulse output, and (2) a square wave output for the delay duration.

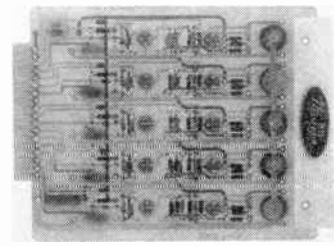

Each delay circuit includes a high gain regenerative delay stage, a dc pulse amplifier which provides a square-wave for the delay duration, and a differentiating circuit which provides a negative spike at the end of the delay interval.

The Model 304 is a 5″×6″ glass-epoxy printed circuit card, $\frac{1}{16}$″ thick, and is for use with an 18 pin PC receptacle.

The delay range, of each delay section, is adjustable from 3 to 30 μsec. The delayed pulse output is a negative differentiated pulse, −3 volts unloaded, 1 ma loading capability. The square-wave output for the delay duration is −12 volts switching to 0.2 volts. Rise and fall times of 0.3 μsec remain constant for full range of pulse width adjustments.

Spectra Electronics Corporation

Due to a clerical error in the statistical department, the name of **Spectra Electronics Corp., div. of Douglas Microwave Corp.,** 250 E. Third St., Mount Vernon, N. Y., was omitted from the 1960 IRE Directory.

This firm was included in the infrared section of the book, however this one product section does not cover the full line of activities in which this firm participates. These people are specialists in the ultraviolet, visible, and infrared systems for geophysical and meteorological applications. Their record of creative performance also includes the following fields of endeavor: communications, telemetry, antennas, radar instrumentation, countermeasures, security systems, display and storage systems, and information systems.

Just before the close of the year this firm announced the appointment of Richard A. Bolz as director of research. Bolz will assume the full responsibility for the technical direction of the scientific and engineering effort. Daniel B. Ventre was appointed project leader. Systems project development is Ventre's responsibility. Edward J. Warner, president of the firm, was appointed to the board of directors of the Corporation.

(Continued on page 92A)

Creative Microwave Technology

Published by MICROWAVE AND POWER TUBE DIVISION, RAYTHEON COMPANY, WALTHAM 54, MASS., Vol. 1, No. 9

NEW RAYTHEON MAGNETRONS FOR A WIDE RANGE OF APPLICATIONS

Designed for C-band systems requiring tunability, the RK-7156 magnetron has a minimum peak power output rating of 250 kilowatts over a frequency range of 5,450 to 5,825 megacycles. Applications include a flight-tested, revolutionary airborne weather radar system. The RK-7156 is in quantity production.

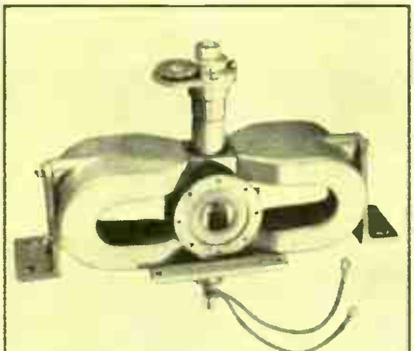

RK-7156

* * *

X-band magnetron for airborne search radar provides one megawatt minimum peak power and 875 watts average power within a frequency range of 9,340 to 9,440 Mc. Designated QK-624, this pulsed-type tube is liquid cooled and should give at least 1,000 hours of reliable service.

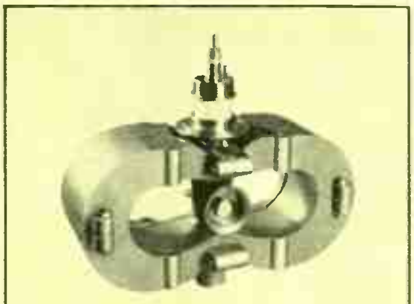

QK-624

* * *

For ground-based and airborne radar systems, the RK-7529 magnetron provides a 2.0 microsecond pulse of 3.5 megawatts minimum peak power over 2,700 to 2,850 Mc. This liquid-cooled tube is interchangeable with other fixed-frequency S-band tubes operating at similar power levels.

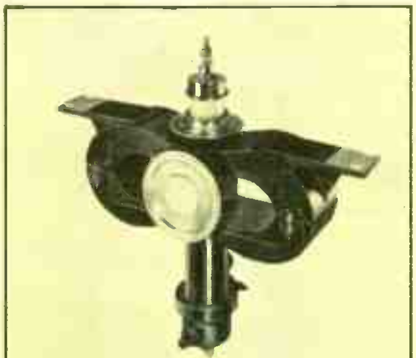

RK-7529

* * *

A one kilowatt beacon magnetron, the RK-7578 weighs only 14 ozs., yet will withstand vibrations of 15 G's at 20 to 2,000 cycles and shock up to 100 G's. It is mechanically tunable and covers the 5,400 to 5,900 Mc range.

RK-7578

* * *

Developed to withstand extreme environmental conditions, the RK-7449 magnetron is a lightweight, compact tube with a minimum peak power output of 45 kilowatts at the operating frequency of 24 kmc. The RK-7449 is required to withstand repeated shocks of 50G. Stable operation is guaranteed at vibration frequencies up to 2,000 c.p.s. with 30G applied.

RK-7449

IRE People

(Continued from page 32A)

Two new assistant directors in electronics research have been named at Armour Research Foundation of Illinois Institute of Technology. The appointments were made by Virgil H. Disney, director of electronics research.

Named to the post in charge of computer development and controls systems, electrical machinery, components, and measurements was **George T. Jacobi** (J'41–A'42–SM'55), formerly of General Electric Company, Phoenix, Ariz.

Harold H. Kantner (M'52), with the Foundation since 1951, was named assistant in charge of computer applications and operations research.

Mr. Jacobi, educated in Lausanne, Switzerland, and Ohio State University, spent 11 years with General Electric, the last ten of which were in close association with the computer art and development. He was manager of special computer engineering before joining ARF.

Mr. Kantner was supervisor of computer applications and operations research at the Foundation before receiving his new appointment.

He was educated at Reed College and did graduate work at the University of Chicago. Since 1951, when he joined ARF, Kantner has worked with control systems in the areas of missile guidance, flight simulation, and electromedical measurements. He has been supervisor of computer applications and operations research since 1955.

❖

David A. Hill (M'51–SM'57) has been named manager of the semiconductor division of the Hughes Aircraft Co. Products Group, Culver City, Calif. He formerly held the Santa Barbara, Calif., Research managership for Hughes.

❖

S. Merrill Skeist (A'51–M'53) has been named director of marketing for the systems division of Consolidated Avionics Corp., a subsidiary of Consolidated Diesel Electric Corp.

S. M. Skeist

In his new post, he will be responsible for market planning and sales activity for the company's electronic data handling and automatic testing systems.

Immediately prior to joining Consolidated Avionics, he was connected with Bradley Associates, a New York electronics manufacturers' representative firm. Previously he had been vice president, sales, for Budd-Stanley Corp., vice president, contracts, for Polarad Electronics Corp., and vice-president, contracts, W. L. Maxson Corp.

(Continued on page 40A)

For original equipment, direct replacement

NEC tubes with new doped-nickel cathode

Both tube series described here use NEC's new doped-nickel cathode core material. This 10-year development increases emission without raising operating temperature. Oxide evaporation rate is lower than any known core material. Operating data show tube life is extended up to 50%.

6R-P10

6R-R8

WIDE-BAND AMPLIFIER TUBES: Development began seven years ago with the 6R-R8, which was used in Japan's first microwave link. A modification, 6R-R8C, with very low distortion factor, is used in coaxial amplifiers. 6R-P10 Power Amplifier Pentode, with high mutual conductance and small capacitance, is designed for larger power output.

Type	Name	Cathode Rating		Screen and Plate Supply Voltage Eb (V) Ec2 (V)	Plate Current Ib (mA)	Trans-conductance Gm ([illegible])	Capacitances		Interchangeable Tubes
		Volts Ef (V)	Amp If (A)				Input F	Output F	
6R-R8	Sharp-Cutoff Pentode	6.3	0.3	150	13	12,500	7.8	3.2	with WE 404A
6R-R8C	Sharp-Cutoff Pentode	6.3	0.3	150	13	12,500	7.3	3.2	with WE 404A
6R-P10	Power Amplifier Pentode	6.3	0.5	150	36	13,500	10.5	2.7	——

2C40

2C39B

Type	Use	Cathode Rating		Maximum Plate Voltage Ev (V)	Maximum Plate Dissipation Pp (W)	Power Po (W)	Maximum Frequency f (MC)
		Voltage Ef (V)	Current If (A)				
2B22	Detector	6.3	0.75	150	—	—	1200
2C39A	Amplifier Oscillator (Continuous)	6.3	1.0	1000	100	15	2500
2C40	Amplifier Oscillator (Continuous)	6.3	0.75	500	4	0.75	3370
2C43	Amplifier Oscillator (Continuous & Pulse)	6.3	0.9	3500*	12	1.0	3370
5861	Amplifier Oscillator (Continuous)	6.3	0.4	350	10	0.5	3700

* Pulse plate Voltage (eb)

DISC-SEALED TRIODES: NEC designed the first disc-sealed tube in 1939, giving NEC many years of experience in the design and manufacture of this type of microwave tube. Each is a direct replacement under all circumstances for the corresponding type. The NEC tube will give longer life, an especially important advantage in repeater stations.

Please write for specification sheets.

NEC *Nippon Electric Company Ltd.* Tokyo, Japan

COMPONENTS / SYSTEMS

IRE People

(Continued from page 38A)

His appointment is part of a plan for increased activity in the use of digital data handling techniques to solve reliability problems in test and ground support equipment.

A mechanical engineering graduate of Worcester Polytechnic Institute, Mr. Skeist is a member of the Air Force Association, the American Institute of Management, American Ordnance Association, American Rocket Society, Armed Forces Communications and Electronics Association, Sales Executives Club and Society of Automotive Engineers.

❖

The study of underwater phenomena will be the primary interest of the newly formed Underwater Systems, Inc., in

M. S. WEINSTEIN

R. W. VAN HOESEN

Wheaton, Md., promising applications for anti-submarine warfare and basic oceanographic study.

According to the organization's founders and senior scientists, **Dr. Marvin S. Weinstein** (S'48–A'50–M'55) and **Richard W. Van Hoesen** (A'54) Underwater Systems, Inc., will undertake research and development in acoustics and other promising underwater influences. The firm will seek military contracts and also provide consultation services to industries in allied fields.

Through broad applications of underwater instrumentation techniques, Mr. Van Hoesen, president of the new firm, foresees development of many devices useful to other technologies. These include new audio concepts useful to the television and radio industry, noise control devices, meteorological instruments, and self calibrating microphone systems.

Dr. Weinstein, formerly of the U. S. Naval Ordnance Laboratory, was awarded the Ph.D. degree in physics by the University of Maryland in 1956. His studies in underwater acoustics, hydrodynamics and ultrasonics led to increased efficiency in data gathering, electronic design, instrumentation and ordnance systems evaluation.

Mr. Van Hoesen is noted for his design and direction of naval data recording programs, both here and abroad, while with the U. S. Naval Ordnance Laboratory. He holds the B.S. degree in physics from Union College, Schenectady, N. Y.

❖

(Continued on page 48A)

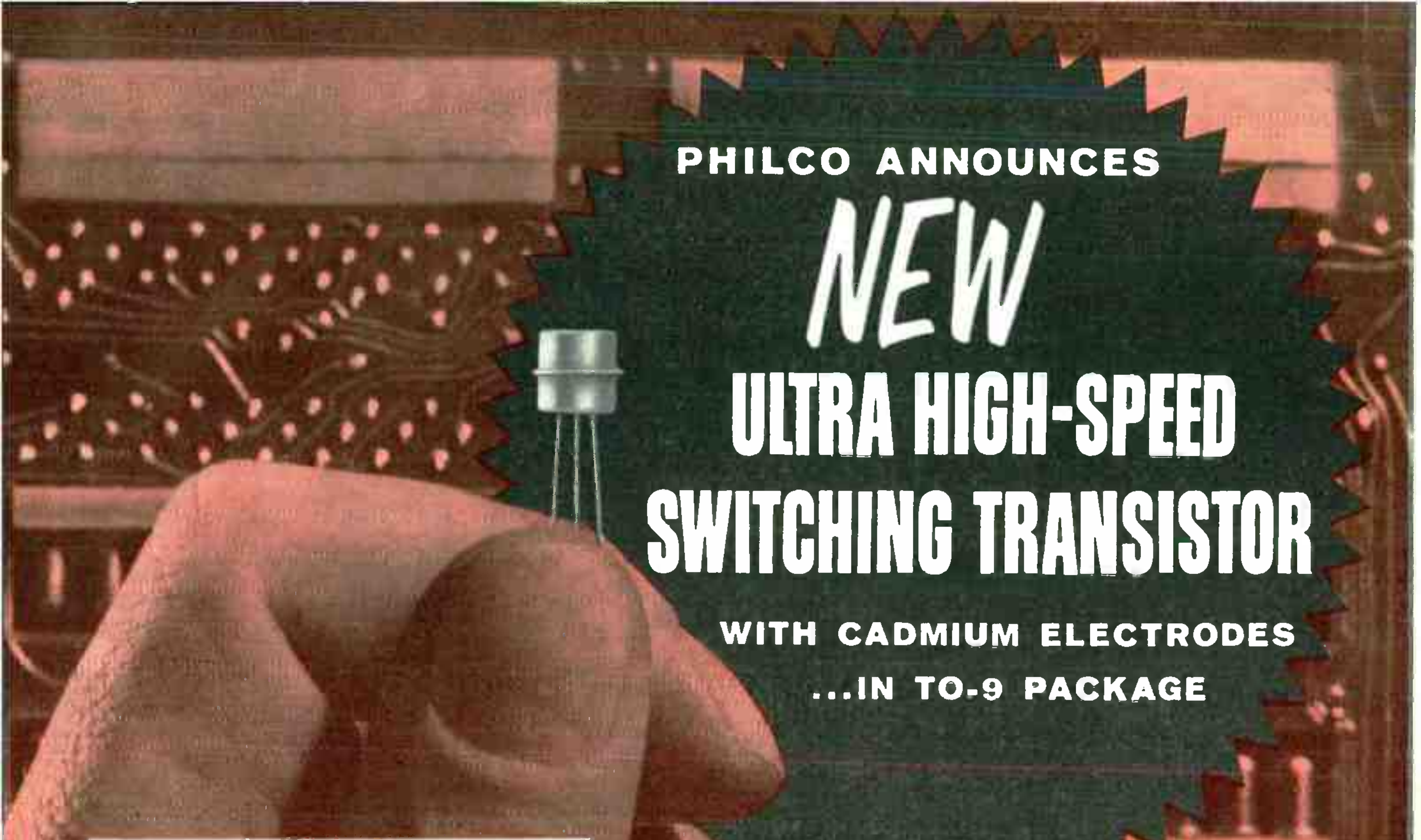

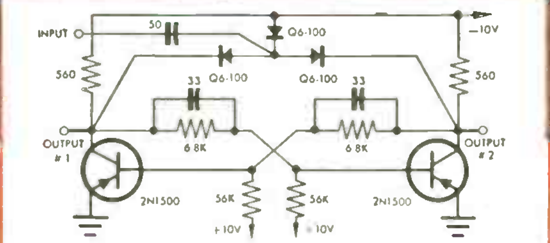

SIMPLE 20MC BINARY STAGE

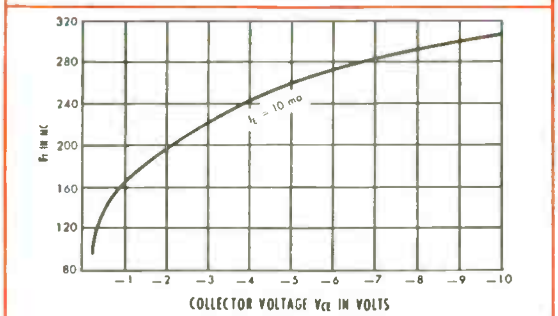

TYPICAL GAIN-BANDWIDTH PRODUCT, f_T VS. COLLECTOR VOLTAGE

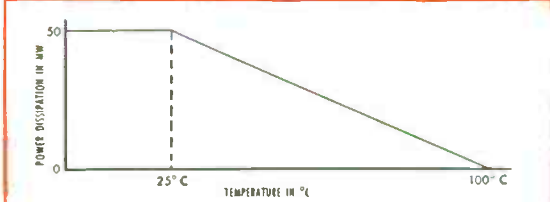

DERATING CURVE

*MADT . . . TRADEMARK PHILCO CORPORATION for Micro Alloy Diffused-base Transistor.

New MADT* 2N1500 Provides Increased Power Dissipation

Here is another Philco "break-through" in the design and manufacture of high frequency, ultra high-speed switching transistors! This new Micro Alloy Diffused-base Transistor (MADT*) uses cadmium electrodes in place of indium. The higher thermal conductivity of cadmium insures cooler-running junctions for any given power dissipation and provides an extra margin of safety as added assurance of reliable performance.

The new 2N1500 offers the designer these important advantages:

- 100° C maximum junction temperature
- low collector capacitance
- low saturation voltage
- high Beta and excellent Beta linearity with temperature and current
- low hole storage time (Typical: 7 mμsec)

In electrical characteristics, the 2N1500 is similar to 2N501, which has been thoroughly field-proven in many military and industrial computer applications. It is manufactured on Philco's exclusive fully-automated production lines to the highest standards of uniformity. For complete specifications and applications data, write Dept. **IR-260.**

Max. Ratings		Typical Parameters				
T_{STG} °C	V_{CB} volts	t_r mμsec	t_s mμsec	t_f mμsec	h_{FE}	$V_{CE}(SAT)$ volts
100	—15	12	7	4	35	—0.1

AVAILABLE IN PRODUCTION QUANTITIES . . . and in quantities 1-99 from your Philco Industrial Semiconductor Distributor.

PHILCO®

LANSDALE DIVISION / LANSDALE, PENNSYLVANIA

TRANSISTOR CENTER U.S.A.

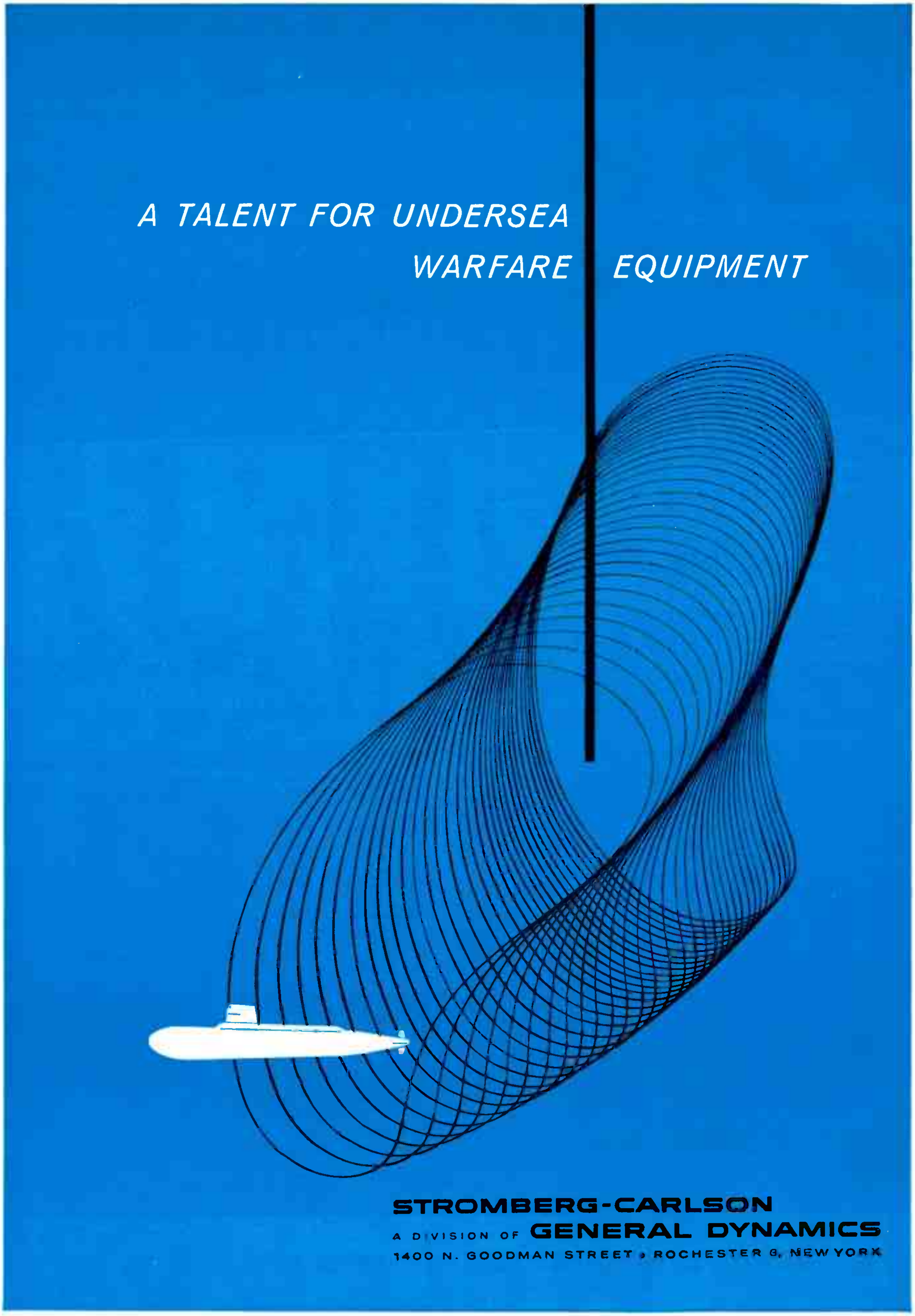
A TALENT FOR UNDERSEA
WARFARE EQUIPMENT
STROMBERG-CARLSON
A DIVISION OF GENERAL DYNAMICS
1400 N. GOODMAN STREET • ROCHESTER 3, NEW YORK

IRE People

(*Continued from page 40A*)

Cozzens & Cudahy, Inc., Electronics Manufacturers Representatives, with offices at the Old Orchard Shopping Center in Skokie, Ill., has announced plans for the reorganization of their firm to include **Robert E. Bard** (S'44–M'47–SM'52), former executive of General Radio Company. The firm name will be changed to Cozzens, Cudahy & Bard, Inc., in the early spring of 1960.

R. E. Bard

Mr. Bard, a former Associate Professor of Electrical Engineering at the Illinois Institute of Technology, joins the company with a vast experience in precision components and laboratory instruments. He has been with the Chicago office of General Radio Company of West Concord, Mass., since the year 1952, and is currently the Chairman of the Chicago Section of the IRE. He has also recently been a member of the Board of Directors of the National Electronics Conference, as well as Editor and President of Scanfax, Inc.

❖

Appointment of **Lynn C. Holmes** (M'44–SM'49–F'49), formerly director of research for the Stromberg-Carlson Division of General Dynamics Corp., as director of engineering operations for the same company, has been announced by Dr. Royal Weller, vice-president of engineering.

L. C. Holmes

In this new position he will be concerned with plans for engineering staffing and for the evaluation of engineering projects in keeping with long range plans for expansion of the division's engineering functions.

He has been with Stromberg-Carlson since 1943, when he joined the company as senior engineer in charge of sound recording research. In 1950 he became associate director of research, and, later that same year, director of research.

He is currently serving as vice president of the Empire District No. 1 of the American Institute of Electrical Engineers, of which he is a fellow, and he has, at various times, held all the offices of the Rochester Section of the A.I.E.E. He is also a member of the Acoustical Society of America, a member of the Rochester Engineering Society, and a member of Sigma Xi and the Scientific Research Society of America. He

(*Continued on page 44A*)

IRE People

(*Continued from page 13A*)

is the Stromberg-Carlson representative in the American Society for Engineering Education and in the Industrial Research Institute, and in 1955 he served as chairman of the Institute's Awards Committee.

Mr. Holmes was born in Brookfield, N. Y., and received the bachelor's and master's degrees in electrical engineering from Rensselaer Polytechnic Institute. From 1925 until he joined Stromberg-Carlson in 1943 he was a member of the engineering faculty at Rensselaer, first as an instructor, and later as assistant professor of electrical engineering. He holds a New York State professional engineer's license.

❖

Adam M. Wilczenski (A'58) has been appointed Manager, Technical Services of the Specialty Blower Division, The Torrington Manufacturing Company, Torrington, Conn. He will direct all Specialty Blower engineering and sales services in the field and technical service personnel at the Torrington plant. The Specialty Blower Division was organized in January, 1959, to design and manufacture complete blower assemblies for cooling electronic, missile, airborne and ground support equipment, largely for military use.

A. M. Wilczenski

He joined Torrington Manufacturing in early 1955 and spent three years in the Design Engineering Section working on specialized mechanical development. He was transferred in January, 1958, as Project Engineer in the Air Impeller Division Sales Department. He returned to the Engineering Department earlier this year when the Specialty Blower Division was activated under C. A. Hathaway, Director of Engineering, Air Impeller Division.

Before joining Torrington Manufacturing, he was a field engineer for the Navy Department, concerned primarily with evaluating the capacities of potential prime contractors. For three years prior to that, he was a Mechanical Engineer at the Haydon Division of General Time Corporation, where his major responsibility was the design of electro-mechanical timing devices.

He is a native of Torrington and was educated at local schools. While serving in the Air Force in World War II, he attended George Washington University, Washington, D. C., and Union University, Jackson, Tenn., during aviation cadet training. After his discharge in 1945, he studied mechanical engineering at Indiana Technical College, Fort Wayne, Ind.

Mr. Wilczenski is a member of the American Society of Mechanical Engineers and several other professional organizations.

❖

(*Continued on page 46A*)

IRE People

(Continued from page 44A)

Vinton D. Carver (SM'59) has been named assistant general manager of Litton Industries Electron Tube Division, San Carlos, Calif. As assistant general manager, he will be in charge of all Electron Tube Division operations.


V. D. Carver

Since 1957 he has been manager of the Salt Lake City, Utah, plant of the Electron Tube Division.

Prior to joining Litton, he was vice president and general manager of the Pacific Division of Farnsworth Electronics Company, which post followed association with Farnsworth for several years in Fort Wayne, Ind.

Other key positions held in earlier years by Mr. Carver were with Argonne National Laboratory, Tennessee Eastman Corporation, and Boeing Airplane Company.

Professional Group Meetings

Aeronautical and Navigational Electronics

Boston—November 2

"Integration of Air Traffic Control and Air Defense," D. R. Israel, Mitre Corp.

Philadelphia—November 18

"Attitude Control of an Orbital Vehicle," R. Whealan, General Electric Co.

Antennas and Propagation

Akron—November 17

"A New Radio Interferometer Tracking System for Satellites," C. H. Grace, Smith Electronics, Inc.

San Francisco—November 10

"The Argus Experiment," N. C. Christofilos, Univ. of Calif.

Audio

Baltimore—October 20

"Report of the New York Hi-Fi Show and AES Convention," L. R. Mills, Recordings Inc.

(Continued on page 48A)

Professional Group Meetings

(Continued from page 46A)

Milwaukee—November 17

"The High Fidelity System," K. Kramer, Jensen Mfg. Co.

Automatic Control

Philadelphia—October 20

"The Compensation of a Digital Type II Servo," R. P. Cheetham, RCA.

Communication Systems

Los Angeles—October 22

"Active Communication Satellites," D. E. Miller, Hughes Communications.
"Passive Communication Satellites," D. O. Muhleman, Jet Propulsion Lab.

Washington, D. C.—November 4

"Space Communications," W. R. Donsbach, Westinghouse Elec. Co.

Component Parts

Los Angeles—November 9

"Technical Theory of Controlled Rectifiers," C. Smith, Texas Instruments, Inc.
"Applications of Controlled Rectifiers," Panel: W. Gutzwiller, General Electric, R. McKenna, Texas Instruments, Inc., L. Dixon, Solid State Products, A. DeVenuti, Transitron, F. Parrish, International Rectifier.

Philadelphia—November 11

"Specification of Component Part Reliability," D. I. Troxel, RCA.

Component Parts/Production Techniques

Washington—November 9

"Thin Film Circuit Functions Techniques," J. J. Bohrer, International Resistance Co.

Electron Devices

Los Angeles—October, 19

"Design of High Energy Particle Accelerators," R. V. Langmuir, Calif. Institute of Tech.

Los Angeles—November 9

"Technical Theory of Controlled Rectifiers," C. Smith, Texas Instruments, Inc.
"Applications of Controlled Rectifiers," Panel: M. Clark, PSI Co.; R. G. McKenna, Texas Instruments, Inc.; A. L. DiVenuti, Transitron; W. Gutzwiller, General Electric; F. W. Parrish, International Rectifier.

San Francisco—November 16

"One Hundred Years of Progress in Parametric Devices," G. Wade, Electronics Res. Lab., Stanford Univ.

(Continued on page 52A)

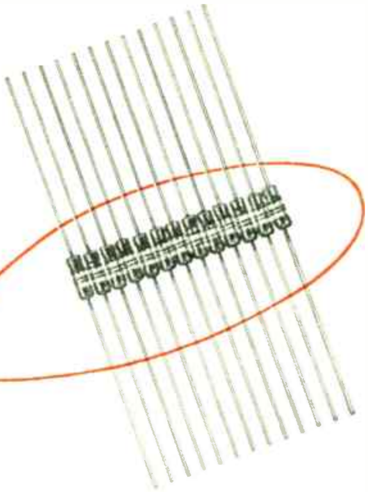

Now available in commercial quantities!

Sylvania D-1820 germanium High-Speed Switching Diode

4 mμSECS

GUARANTEED MAXIMUM RECOVERY TIME!

SYLVANIA D-1820 is the forerunner of an outstanding family of diodes, designed, produced and controlled specifically for logic circuitry. The cost of this new SYLVANIA diode is low enough to make it especially attractive for use in quantity-produced electronic computers. SYLVANIA D-1820, and the circuits designed around this diode, feature:

high-speed operation — with recommended circuits, all units are guaranteed to provide a maximum recovery time of 4 millimicroseconds. However, recovery times of 2.5 millimicroseconds are typical.

long-life performance — proved in 1000-hours operating and 7000-hours storage life tests.

high reliability — basic point-contact structure has been field-proved for more than a decade. Withstands environmental conditions of shock and vibration.

exceptional uniformity of electrical characteristics—assures complete interchangeability within the type—result of modern automated-production techniques employed in the manufacture of SYLVANIA D-1820.

economy — SYLVANIA pioneered the field of germanium point-contact diode manufacture, has "know-how" of superior-quality, large-quantity economical production. SYLVANIA is able to pass these savings on to you.

simplicity—diode-logic circuitry is relatively uncomplicated, requires few components. It reduces computer construction costs. It adds to equipment reliability.

compactness—SYLVANIA D-1820 "package" is miniature all-glass.

availability—units can be supplied immediately through your local Sylvania Semiconductor Distributor or through your local Sylvania Field Office.

Complete sales information on quantity prices, delivery and sampling for your own evaluation is available from your local Sylvania Semiconductor Distributor or Field Office. For engineering data sheets on the new Sylvania D-1820 High-Speed Switching Diode or on any Sylvania Semiconductor Device, write Sylvania Semiconductor Division, Dept. 43-2, Woburn, Mass.

ELECTRICAL CHARACTERISTICS— SYLVANIA D-1820

Absolute Maximum Ratings*	Typical Operating Conditions*
Fwd. Volt ....1.3 V†	Fwd. Volt..............0.9 V
Fwd. Curr. ....50 mA	Fwd. Curr. ....2.0 μA
Back Volt ....20 V	Rev. Recovery........2.5 mμs
Pwr. Diss. ....80 mW	

†at 10 mA *at 20° C.

SYLVANIA

Subsidiary of **GENERAL TELEPHONE & ELECTRONICS**

GENERAL SYSTEM

Professional Group Meetings

(Continued from page 48A)

Electronic Computers

Detroit—October 5

"Learning Machines," Dr. Holland, Univ. of Michigan.

San Francisco—October 27

"Micro-Miniature Circuits," J. Last, Fairchild Semiconductor Corp.

Washington, D. C.—November 11

"Ultra High Speed Computers Utilizing Microwave Phase Locked Oscillators," G. B. Herzog, RCA Labs.

Engineering Management

Syracuse—November 17

"Selection and Development of Engineering Managers," Panel discussion, Moderator: R. A. Galbraith, Syracuse Univ.; Speakers: E. F. Herzog, General Electric; J. A. Basher, The Murray Corp. of America; C. H. Northrup, Crouse Hinds Co.; M. H. Pratt, Niagara Mohawk Power Corp.; L. Macrow, Carrier Corp.

Washington, D. C.—October 19

"Evaluation and Control of R&D Expenses," F. X. Lamb, Weston Instrument Div. of Daystrom, Inc.

Washington, D. C.—November 2

"Men, Money, and Management," Rear Admiral R. Bennett, USN.

Industrial Electronics

Cleveland—November 19

"Instrumentation for Steel Mill Coil Classification," W. C. George, Designers for Industry, Inc.

Instrumentation

Los Angeles—November 4

"Extrasensory Perception Instrumentation," Dr. A. Puharich.

Washington, D. C.—November 16

"Design of an RC Filter for use at Very Low Frequencies," W. S. Campbell, David Taylor Model Basin.

"A Telemetering Torque and Horsepower Meter," M. W. Wilson, David Taylor Model Basin.

Medical Electronics

Boston—November 4

"Measuring Mental Stability in Space," J. H. Mendelson, Boston Naval Hosp.

Los Angeles—November 19

Informal Seminar in Medical Electronic Problems.

(Continued on page 54A)

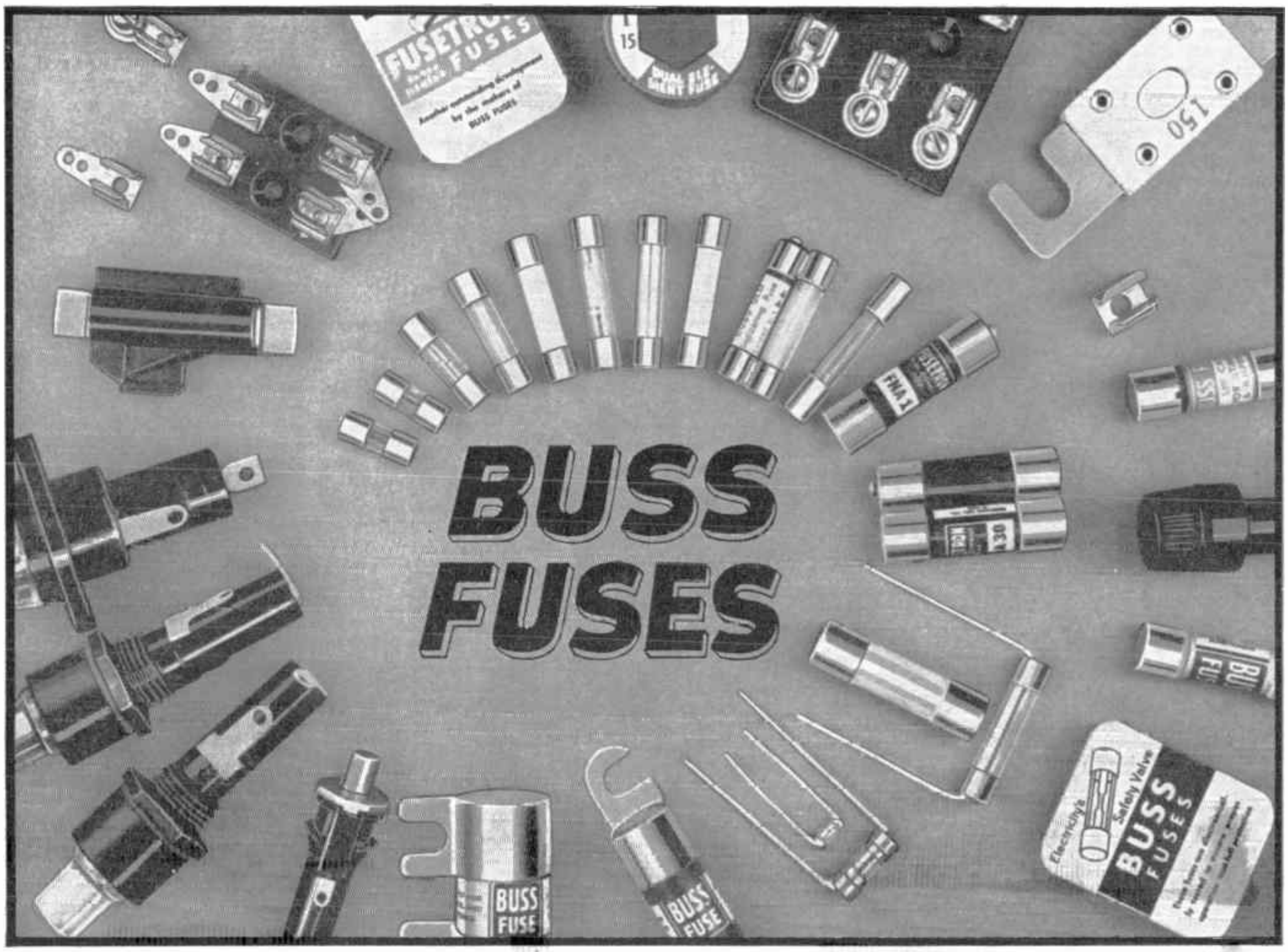

TWO-WAY PROTECTION

Dependable BUSS Fuses safeguard both your product . . . and helps enhance its reputation for quality

When you specify BUSS or FUSETRON fuses for the products you manufacture, you not only provide the finest electrical protection possible — but you also help protect your company's reputation for quality products.

Remember: No matter how good your product is, a poor quality fuse that opens needlessly deprives a customer of the use of your device, — or a fuse that does not protect may permit costly damage to occur. In either case you may lose a customer's goodwill and future business.

Why take the risk when you know you can depend on BUSS and FUSETRON fuses?

Every fuse is tested in a sensitive electronic device that automatically rejects any fuse not correctly calibrated, properly constructed and right in all physical dimensions.

BUSS — the one source for all your fuse needs . . .

To meet all your fuse needs, the BUSS line is most complete, — including a companion group of fuse clips, blocks and holders.

To help you on special problems in electrical protection . . .

BUSS places at your service the facilities of the world's largest fuse research laboratory and its engineering staff. If possible, our engineers will help you select a fuse readily available in local wholesalers' stocks so that your products can be easily serviced.

For more information on BUSS and FUSETRON Small Dimension fuses and fuseholders, write for bulletin SFB.

BUSSMANN MFG. DIVISION,
McGrow-Edison Co.
University at Jefferson, St. Louis 7, Mo.

260

BUSS fuses are made to protect - not to blow, needlessly.

BUSS makes a complete line of fuses for home, farm, commercial, electronic, electrical, automotive and industrial use.

FUSETRON TRUSTWORTHY NAMES IN ELECTRICAL PROTECTION BUSS

McGRAW EDISON

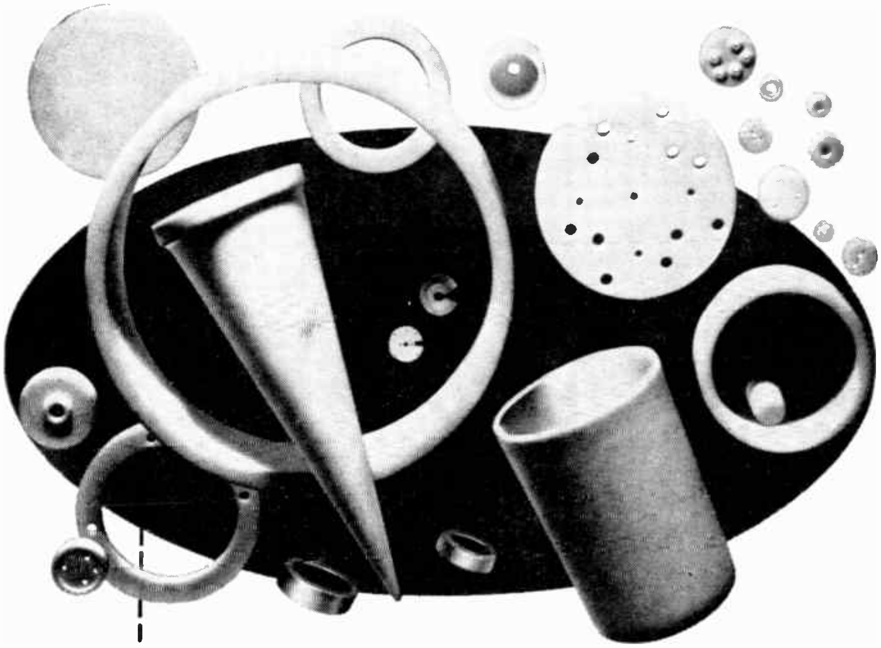

Only Wesgo AL-300 Ceramics assure the superior performance you want from alumina

Material alone does not assure a reliable alumina part . . . the exceptional performance characteristics associated with alumina are directly related to manufacturing knowledge and techniques. Since 1948, Wesgo has perfected the precise controls over composition and manufacturing techniques that alone impart a uniform quality to alumina parts. Quality can only be superficially specified . . . knowledge of alumina ceramics plus quality consciousness are the important extras offered by Wesgo. Alumina is a premium ceramic material . . . but with many cost saving advantages. Be assured of these advantages . . . use Wesgo AL-300 ceramics in shapes to your specifications.

PURE WHITE AND TRANSLUCENT. 97.6% Al_2O_3. Visibly free from impurities. Vacuum tight.

HIGH STRENGTH. 46000 PSI Flexural, 285000 PSI in compression.

UNIFORM IN COMPOSITION AND PROPERTIES from lot to lot.

HIGH DIELECTRIC STRENGTH AND RESISTIVITY.

VERY LOW LOSS FACTOR.

For details on properties, write for illustrated brochure

WESTERN GOLD AND PLATINUM COMPANY

Manufacturers of Wesgo Brazing Alloys

BELMONT, CALIFORNIA

Professional Group Meetings

(*Continued from page 52A*)

Microwave Theory and Techniques

Baltimore—November 12

"Some Aspects of Solid State Phenomena in the Microwave Region," P. Pan, Westinghouse Air Arm Div.

No. New Jersey—September 30

A. G. Clavier, ITT Labs., reviewed his early experiments in microwave transmission.

No. New Jersey—October 28

"A New High Capacity Microwave Relay System," R. F. Privett, RCA.

Washington, D. C.—November 10

"Atomic Stabilized Oscillators," R. T. Daly, Tech. Research Group.

Microwave Theory and Techniques/Antennas and Propagation

Syracuse—October 13

"Radar Exploration of Nearby Space," W. E. Gordon, Cornell Univ.

Military Electronics

Philadelphia—November 19

"Automatic Checkout," O. T. Carver, RCA.

Nuclear Science

Atlanta—November 19

"Wind Tunnel Instrumentation," W. T. Earheart, Jr., A.R.O.

"Transistorized Galvanometer Current Limiter," P. Clemens, A.R.O.

Production Techniques

Philadelphia—November 12

"Future Printed Circuits—Military Application," R. Geisler, U. S. Army Signal Corps.

"Future Printed Circuits—Commercial Application," A. Ansley, Ansley Man. Co.

San Francisco—October 27

"Electroplating," G. Dodge, Tepco Co.

"Organic Finishes," S. Simon, Rhino Tech. Co. and Technical Coating Corp.

"Water Dispersed Coating," a film with comments by R. Koren, Doidge-Koren Co.

Space Electronics and Telemetry

Philadelphia—November 18

"Attitude Control of Orbiting Vehicles," R. Whealan, General Electric Co.

(*Continued on page 56A*)

How to design 250 mw at 140 mc transistorized power amplifiers

2N715—2N716 140 Megacycle Power Amplifier

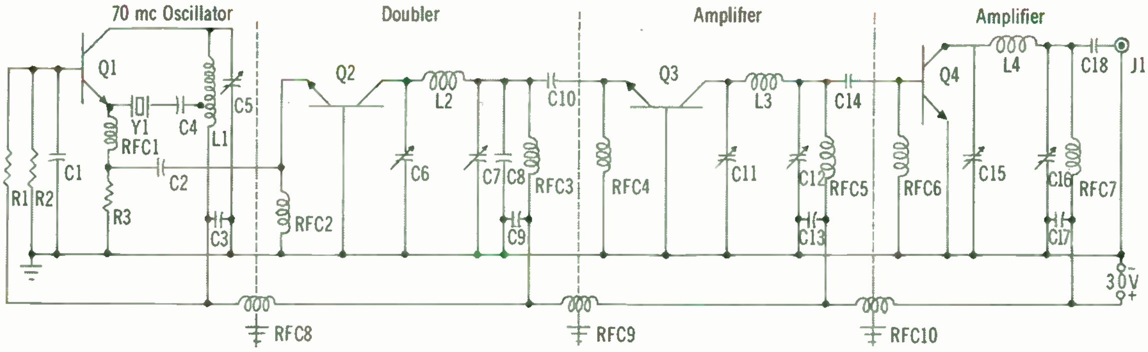

C1, C2, C3—.001 μf disc ceramic
C4,—20 $\mu\mu f$ tubular ceramic
C5, C6, C7, C11, C15—1.8-13 $\mu\mu f$
C8,—47 $\mu\mu f$ silver mica
C9, C10, C13, C14, C17, C18—500 $\mu\mu f$ disc ceramic
C12,—7—45 $\mu\mu f$ mica trimmer
C16,—3.2—50 $\mu\mu f$
L1,—8 turns #408 Airdux, tapped 2 turns from ground
L2,—4 turns #12 magnet wire, ½" D, ¾" L
L3,—3 turns #12 magnet wire, ½" D, ⁷⁄₁₆" L
L4,—3 turns #12 magnet wire ½" D, ⅜" L
Q1, Q2, Q3, Q4,—TI 2N716
R1—5100 ohms, ½ watt
R2—680 ohms, ½ watt
R3—200 ohms, ½ watt
RFC1—.47 μh
RFC2—4.7 μf
RFC3 through RFC10
1.2 μh
Y1—70 mc crystal

ACTUAL SIZE

...with NEW TI 2N716 silicon mesa transistors

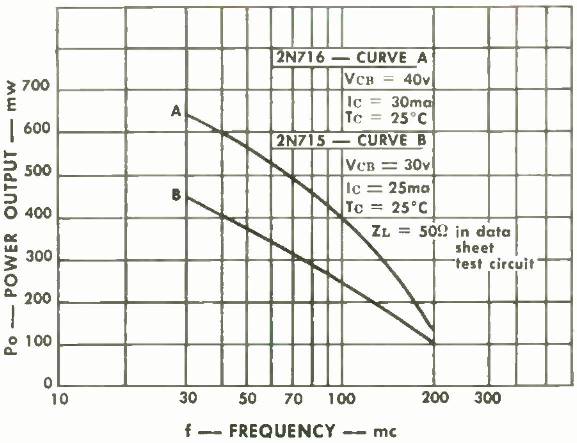

OSCILLATOR POWER OUTPUT vs. FREQUENCY

Now . . . silicon high frequency transistors *specifically* designed for your VHF power circuits . . . another addition to the industry's broadest line of silicon mesa transistors (now 16 TI types!).

TI 2N715 and TI 2N716 *guarantee 500-mw amplifier output at 70 mc* and provide *100-mw typical power output at 200 mc.*

These subminiature (TO-18) silicon units feature . . . 1.2-w dissipation at 25°C case temperature . . . 10-50 beta spread . . . collector reverse voltages of 50 and 70v . . . maximum collector reverse currents of 1.0 μa (25°C) and 100 μa (150°C).

Check the guaranteed specs below and take immediate advantage of advanced performance in your designs. Both units are ready for your orders in every TI distributor's stocks today, and in quantities of 1,000 and up from your nearest TI sales office.

Tentative Specifications 2N715 - 2N716

1 P_C T_C = 25°C watt	T_{stg} °C	2 V_{CB} v dc	2 V_{EB} v dc	3 V_{CE} v dc
1.2	−65 to + 175	+70 (2N716) +50 (2N715)	+5	+40 (2N716) +35 (2N715)

Parameter	Test Condition	2N715 Min	2N715 Typ	2N715 Max	2N716 Min	2N716 Typ	2N716 Max	Units
**BV_{EBO}	I_{EBO} = 100 μ a, I_C = 0	5			5			v dc
***BV_{CBO}	I_{CBO} = 10 μ a dc, I_E = 0	50			70			v dc
*h_{FE}	V_{CE} = 10 v dc, I_C = 15ma dc	10		50	10		50	
*V_{CE}(sat)	I_C = 15ma, I_B = 3ma	1 2			1 2			v dc
C_{ob}	V_{CB} = 5 v dc, I_E = 0, F = 1 mc		3	6		3	6	$\mu\mu f$
Amplifier Power Output and	(V_{CB} = 40 v dc, (I_C = 30 ma dc, (P (AC) — 500 mw, (F = 70 mc				500 4	600 7.5		mw db
Transducer gain	(V_{CB} = 30 v dc, (I_C = 25 ma dc, (P (AC) = 300 mw, (F = 70 mc	300 4	400 8					mw db

1 This power rating for 1000 hours expected life at a case temperature of 25°C derated linearly to +175° case temperature at the rate of .125°C per mw.
2 Maximum voltage ratings at an ambient temperature of +25°C.
3 BV_{CEO}: This is the voltage at which h_{FB} approaches one when the emitter-base diode is open circuited. This value may be exceeded in applications where the dc circuit resistance (R_{BE}) between base and emitter is a finite value.
When the emitter-base diode has a reverse voltage applied, peak collector to emitter voltage equal to BV_{CBO} minus V_{EB} may be allowed. Such conditions may be encountered in class B or C amplifiers and oscillators.
*Pulse Measurement
**Specify I_{EBO} on commercial data sheet
***Specify I_{CBO} on commercial data sheet

TEXAS INSTRUMENTS INCORPORATED

the first silicon transistor manufacturer

SEMICONDUCTOR-COMPONENTS DIVISION
13500 N. CENTRAL EXPRESSWAY
POST OFFICE BOX 312 · DALLAS, TEXAS

Professional Group Meetings

(Continued from page 54A)

Vehicular Communications

Los Angeles—September 17

"Commercial Consideration and Basic Engineering Techniques on Audio 'Special Service' Circuits, Working with Vehicular Communications Systems," O. E. Wiedman and P. L. Cunningham, Pac. Tel. & Tel.

Los Angeles—October 15

"Single Position Control for Radio Dispatching and Telephone Answering," R. C. Crabb, Mobilephone of L. A.

"Plug-in Transistorized Microphone and Line Amplifiers," J. Fellis, Los Angeles Fire Dept.

Washington, D. C.—November 18

"A Transmission Line and Antenna Measuring Technique for Mobile Systems," W. F. Biggerstaff, U. S. Dept. of Agriculture.

Industrial Engineering Notes

Industry Marketing Data

The EIA Marketing Data Department estimated that of the $7.5 billion funding for the Federal Aviation Agency through fiscal year 1970, $1.6 billion, or about 16 per cent, will be devoted to electronics. Funding for FAA will rise from the present level of $500 million annually to nearly $750 million by 1970, the Association estimates, and the electronics portion is expected to increase from about 15 to 25 per cent during this period. The EIA report states that two elements comprise the aviation electronics market: 1) the elements of the control system funded by FAA, and 2) the equipment carried in aircraft which permits them to fly safely within or without the system. **EIA figures just released show a drop in radio-TV production in October from the September level.** On all counts, though, the figures show an increase over October, 1958 and cumulatively this year compared with the first ten months last year. TV output in October totaled 706,583 compared with 808,337 televisions made in September and 495,617 TV's produced in October 1958. This figure

(Continued on page 60A)

* The data on which these NOTES are based were selected by permission from *Weekly Reports*, issues of November 30 and December 7 published by the Electronic Industries Association whose helpfulness is gratefully acknowledged.

10 Mc COUNTER

does everything without plug-ins

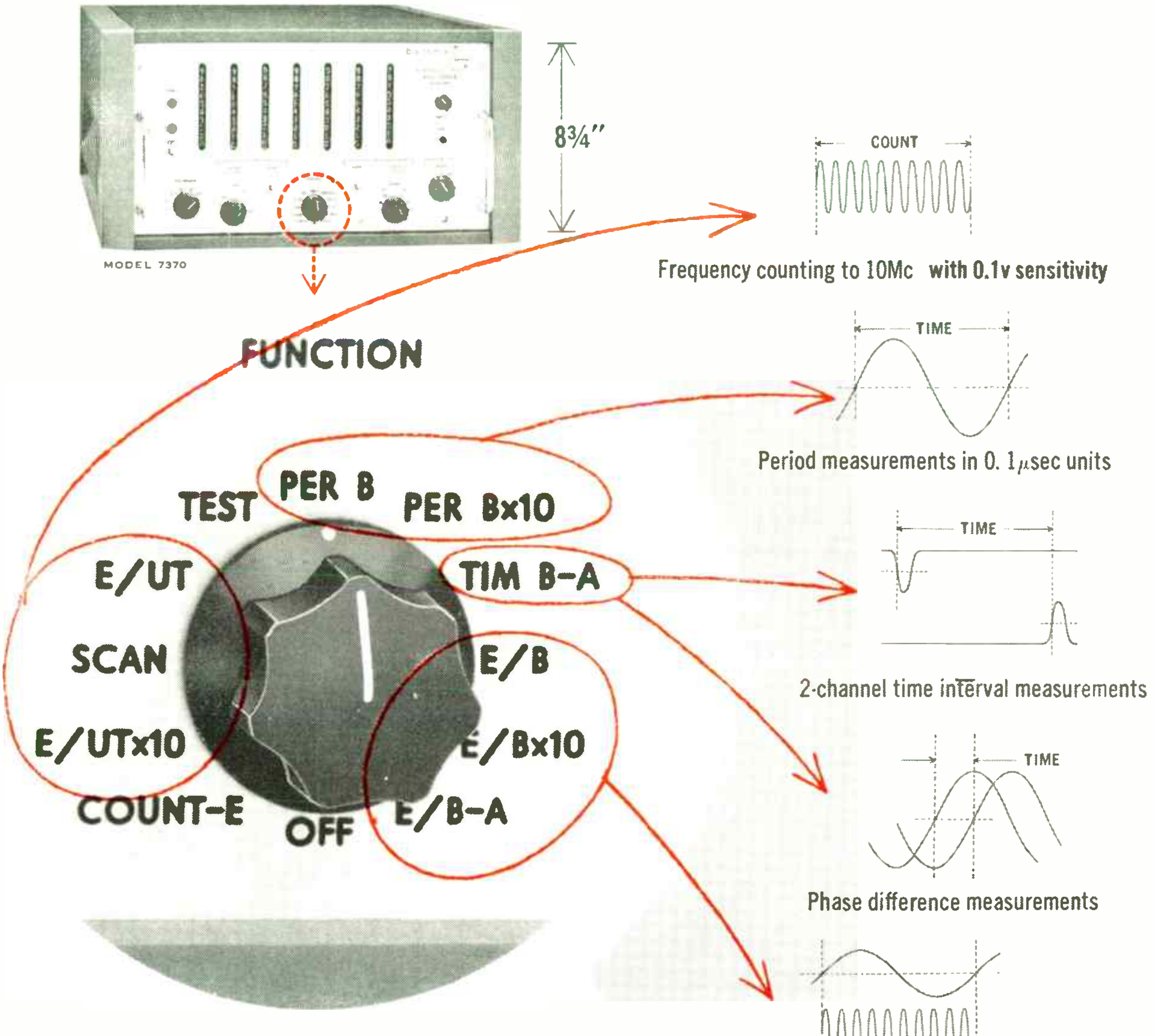

Add this heterodyne unit (Model 7570 Series) to measure frequencies up to 1000Mc.

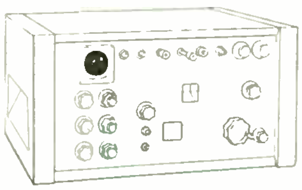

Or add this computing transfer oscillator (Model 7580) to get a counter display of frequencies up to 15,000Mc.

Complete specifications on Models 7370, 7570 and 7580 will be sent on request.

Beckman | *Berkeley Division*
2200 Wright Avenue, Richmond 8, California
a division of Beckman Instruments, Inc.

T21

Announcing . . .

SILICON RECTIFIERS

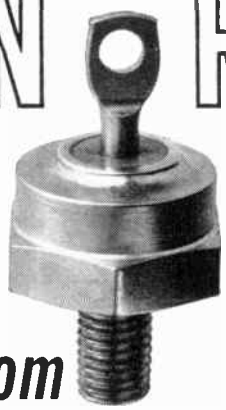

from

DELCO RADIO

High Quality

High Performance

Extreme Reliability

From the leading manufacturer of power transistors, new Silicon Power Rectifiers to meet your most exacting requirements. Even under conditions of extreme temperatures, humidity and mechanical shock, these diffused junction rectifiers continue to function at maximum capacity! Thoroughly dependable, completely reliable—new Delco Rectifiers are an important addition to Delco Radio's high quality semiconductor line.

Conservatively rated at 40 and 22 amperes for continuous duty up to case temperatures of 150°C.

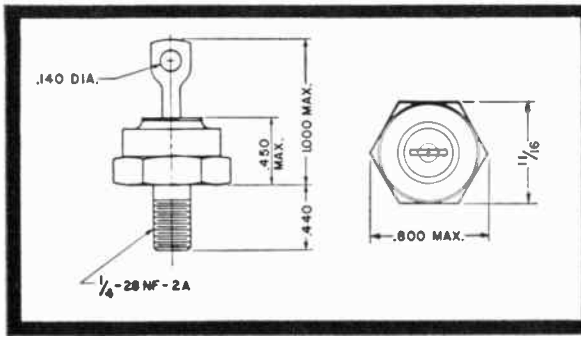

TYPE	AVG. DC CURRENT	PIV	NORMAL MAX. TEMP.	MAX. FORWARD DROP	MAX. REVERSE CURRENT
1N1191A	22A	50V	150°C	1.2V at 60 amps.	5.0 MA
1N1192A	22A	100V	150°C	1.2V at 60 amps.	5.0 MA
1N1193A	22A	150V	150°C	1.2V at 60 amps.	5.0 MA
1N1194A	22A	200V	150°C	1.2V at 60 amps.	5.0 MA
1N1183A	40A	50V	150°C	1.1V at 100 amps.	5.0 MA
1N1184A	40A	100V	150°C	1.1V at 100 amps.	5.0 MA
1N1185A	40A	150V	150°C	1.1V at 100 amps.	5.0 MA
1N1186A	40A	200V	150°C	1.1V at 100 amps.	5.0 MA at 150° C case temperature and rated PIV

For full information and applications assistance, contact your Delco Radio representative.

Newark, New Jersey
1180 Raymond Boulevard
Tel: Mitchell 2-6165

Chicago, Illinois
5750 West 51st Street
Tel: Portsmouth 7-3500

Santa Monica, California
726 Santa Monica Boulevard
Tel: Exbrook 3-1465

Division of General Motors • Kokomo, Indiana

DELCO RADIO

To assure a new order of reliability

MICRO-MODULE

EQUIPMENT

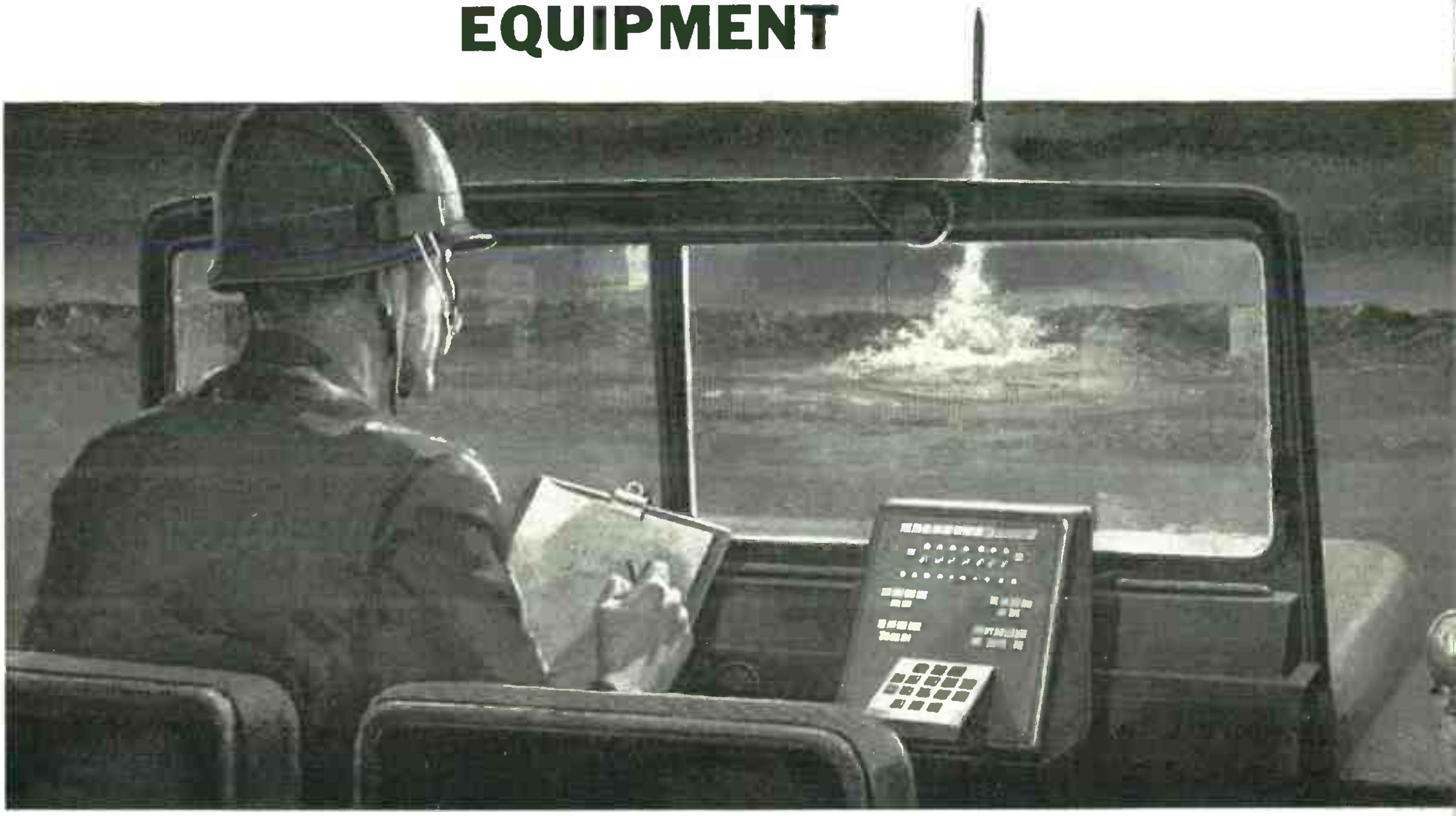

The micro-module is a new dimension in military electronics. It offers answers to the urgent and growing need for equipment which is smaller, lighter, more reliable and easier to maintain. Large scale automatic assembly will bring down the high cost of complex, military electronic equipment. Looking into the immediate future, we see a tactical digital computer occupying a space of less than two cubic feet. It will be capable of translating range, wind velocity, target position, barometric pressure, and other data into information for surface to surface missile firings. The soldier-technician monitoring the exchange of computer data will have modularized communications with the other elements of his tactical organization. RCA is the leader contractor of this important United States Army Signal Corps program and is working in close harmony with the electronic components industry.

RCA

Tmk(s) ®

RADIO CORPORATION of AMERICA

DEFENSE ELECTRONIC PRODUCTS

CAMDEN, NEW JERSEY

Industrial Engineering Notes

(Continued from page 56A)

includes 55,113 sets capable of receiving UHF signals as against the 51,555 such sets made in September and 42,171 UHF receivers made in October last year. Cumulative UHF output during the first ten months of this year totaled 340,980 compared with 353,980 such sets made at this time last year. Year-to-date TV output totaled 5,195,440 compared with 4,067,606 televisions made during the like January–October period last year. The number of radios produced in October totaled 1,795,718 including 531,116 automobile receivers, compared with 1,981,208 radios made in September including 717,501 auto receivers, and 1,218,575 radios made in October last year which included 296,067 auto sets. The number of FM radios made in October totaled 62,959 compared with 76,942 made in September and 59,586 FM receivers made in October in 1958. Cumulative FM output during the 10 month period this year totaled 430,763 compared with 235,647 such receivers made at this time last year. Cumulative over-all radio output during the first 10 months of this year totaled 12,722,970, including 4,682,962 automobile receivers, compared with the 8,904,772 radios made during the like 1958 period which included 2,679,618 automobile receivers. **Factory sales of transistors in September set a new all-time monthly record, EIA figures show.** Sales during September alone were more than double the number of units sold during calendar year 1955. Cumulative sales during the first nine months of 1959 exceeded the total number of transistors sold during calendar year 1958. Total factory sales of transistors in 1958 amounted to 47,051,000 units valued at $112,730,000.

Military Electronics

The Department of Defense released for the consideration of the electronic industries early in January, 1960 the preliminary recommendations of its Ad Hoc Study Group on Parts Specification Management for Reliability—a DOD appointed producer-user-Government group that for the past year has been working to establish guidelines for increased reliability in electronic parts and tubes. The office of Perkins McGuire, Assistant Secretary of Defense (Supply and Logistics) said that the group's expanded program affecting the procurement of electronic parts and tubes is part of the over-all DOD effort to increase the reliability of complex weapon systems.

The group, headed by Dr. P. S. Darnell, of Bell Telephone Laboratories, Whippany, N. J. expects to submit its preliminary recommendations to Dr. Herbert F. York, Director of R&E, and to Mr. McGuire following its January 5 meeting. Mr. McGuire's office said that the group's recommendations will be released for study to the electronic industries before they are acted upon by the DOD.

(Continued on page 62A)

Industrial Engineering Notes

(Continued from page 60A)

Concerning the nature of the group's recommendations, Mr. McGuire's office said it is expected to urge uniform criteria for use by the military Services in specifying desired reliability levels in equipment, including specific reliability parameters for various selected types of components. The group also is said to be considering changes in the QPL procedure that would require producers to furnish considerably more reliability data for qualification, and the possible use of incentives in procurement to encourage parts producers to develop components with a higher degree of reliability. The DOD's Ad Hoc Study Group is described as a subgroup of the Advisory Group on Electronic Parts, located at the University of Pennsylvania, Engineering Bldg., Philadelphia.

Publication of quarterly supplements to its electronics reliability design handbook, temporarily suspended in January, 1959, has been resumed by the Navy's BuShips. The supplements are sold by the Office of Technical Services, Dept. of Commerce, Washington 25, D. C., on subscription at \$2.25 a year or individually at 75 cents a copy.

The handbook is intended as a source of information on ways of achieving greater simplicity, economy, and reliability in electronics equipment for the Navy.

OTS still maintains stock of previous issuances. The basic handbook (PB 121839) sells for \$1. Six previous supplements, PB 121839-S1 through PB 121839-S6, October, 1957 through January, 1959, are 75 cents each.

Section Meetings

ALAMOGORDO-HOLLOMAN

"Solar Disturbances and Their Effect on Radio Transmission Phenomena," Dr. John Evans, Cambridge Research Center. 11/16/59.

ALBUQUERQUE-LOS ALAMOS

Annual Christmas Social Party. 12/5/59.

ANCHORAGE

"Reliability and Maintainability," Myron Bakst, Federal Electric Corp. 10/5/59.

"History of GEEIA," Charles Parker, GEEIA Organization. 11/2/59.

"Engineering Calculations with Digital Computers," Dr. J. G. Tryon, University of Alaska. 12/7/59.

ATLANTA

"Electronics in the Space Age," Dr. Ernst Weber, IRE President. 11/30/59.

BEAUMONT-PORT ARTHUR

"Off-Shore Gas-Condensate Production by Electronics," J. R. Scroggs, Pure Oil Co.; "Prob-

(Continued on page 64A)

Section Meetings

(*Continued from page 62A*)

lems of Broadcasting" (Technical Brief), Ben Hughes, KTRM-AM Broadcasting Co. 9/22/59.

"What is a Good Capacitor" "How to Reduce Your Capacitor Cost!" D. E. Harris, H & M Research & Development Co.; "Microwave Communications for Power Utilities," W. Haack, Gulf States Utilities Co. 10/20/59.

"Computers for Engineering," Lloyd Hubbard, IBM; "Ampex VR-1000B Video Tape Recorder," Harold Bartlett, KFDM-TV. 11/17/59.

BUENOS AIRES

"Microwave Spectroscopy," Dr. Gunnar Erlandsson. 7/2/59.

"Stereophonic Systems," L. M. Radrizzani Goni. 7/16/59.

"Biological Risks in the Radiations," Dr. Dan Beninson. 8/6/59.

"TV Relay Systems," L. J. Leibson, A.I.R.E. 8/20/59.

"Digital Computing Machines of Associative Words," F. R. Tanco. 9/17/59.

"Some Applications of the Radioisotopes in the Argentine Industry," C. C. Papadopulos. 10/1/59.

Visit to Electronic Argentine Navy Laboratories. 10/8/59.

"Possibilities of Astronautics in Argentine," Teofilo Tabanera. 10/15/59.

"Contribution of the IGY to the Development of Telecommunications," J. A. Rodriguez. 11/5/59.

BUFFALO-NIAGARA

"The How, What and Why of the Ampere," J. H. Miller, Daystrom-Weston. 11/18/59.

CENTRAL PENNSYLVANIA

"The Generalized Machine," R. A. Strand, Pennsylvania State Univ. 10/20/59.

CINCINNATI

"Data Handling Systems," W. C. Nash, Minneapolis-Honeywell Regulator Co.; "Planning for Central City Industry," H. W. Stevens, City of Cincinnati Planning Div. 11/17/59.

COLUMBUS

"Dew Line Radar," Alfred Ruppel, Bell Telephone Labs. 11/24/59.

"Thermoelectricity," Dr. S. Angello, Westinghouse. 12/15/59.

DALLAS

Panel Discussion "Trans-horizon Communications," R. M. Mitchell, J. H. Bistrup, H. D. Hern, A. J. Svien, Collins Radio Co. 12/15/59.

EGYPT

"Some Aspects of TV Transmitter and Studio Equipment," Mr. Tokunoh, Shibaura Electric Co., Ltd., Japan. 11/4/59.

EMPORIUM

"Infrared Radiation," F. C. Bennett, Jr. Kodak. 11/17/59

EVANSVILLE-OWENSBORO

"Inertial Guidance," W. G. Wing, Sperry Gyroscope Co. 12/9/59.

FLORIDA WEST COAST

"Communications on a Strategic Air Command Base," Maj. W. E. Smith, MacDill AFB 11/18/59.

(*Continued on page 70A*)

ABSOLUTE MAXIMUM RATINGS AT 25°C

Forward Current	I_f	50 mA
Minimum Breakover Voltage	V_{bo}	TSW-30 30V TSW-60 60V
Reverse Breakdown Voltage	V_r	TSW-30 30V TSW-60 60V
Storage Temperature		−65°C to 150°C
Ambient Temperature Range		−55°C to +125°C

SPECIFICATIONS AND TYPICAL CHARACTERISTICS
(At 25°C Unless Otherwise Stated)

		Typical	Max.	Test Conditions	
Saturation Voltage	V_S	1.0	1.5	Volts	$I_C = 50$ mA
Forward Leakage Current	I_F	0.1	10	μA	$V_C = 30V$
Reverse Leakage Current	I_R	0.1	10	μA	$V_C = -30V$
Forward Leakage Current	I_F	20.	50.	μA	at 125°C
Reverse Leakage Current	I_R	20.	50.	μA	at 125°C
Gate Voltage to Switch "ON"	V_g On	0.7	1.0	Volts	$R_L = 1K$
Gate Current to Switch "ON"	I_g On	0.1	1.0	mA	$R_L = 1K$
Gate Voltage to Switch "OFF"	V_g Off	1.2	4.0	Volts	$I_C = 50$ mA
Gate Current to Switch "OFF"	I_g Off	7.0	10.	mA	$I_C = 50$ mA
Holding Current	I_H	2.0	5.0	mA	$R_L = 1K$

SPECIALLY DESIGNED FOR:

- Miniaturized Memory Circuits
- Ring Counters
- Shift Registers
- Controlled Rectifier Driver
- Flip-Flop Equivalent
- Simplified Information Storage
- 0.3 m second Switching

Transitron

announces a NEW computer element for: Greater Reliability • Circuit Simplicity

THE TRANSWITCH

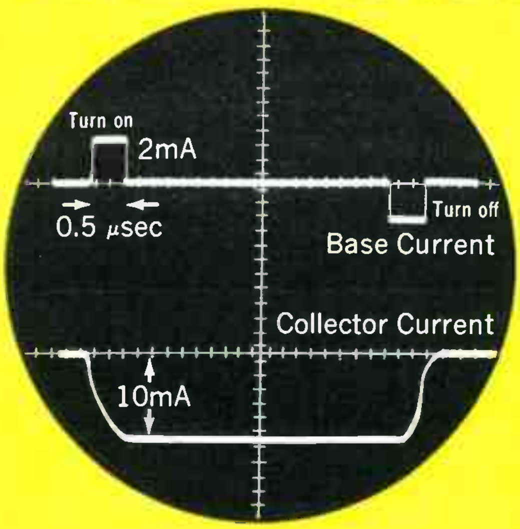

The TRANSWITCH is a new bistable silicon device that can be TURNED OFF with gate current.

This PNPN latching device "remembers" its last gate signal. High current gain, both turn-on and turn-off, leads to greater circuit simplicity and inherent reliability. Excellent linearity of electrical parameters over a wide current range fulfills both low logic level and medium power needs.

Here is a unique device that replaces TWO transistors plus resistors in most bistable circuits and permits increased component density.

Furthermore, the transwitch is FAST . . . requiring only 0.3 microseconds to turn ON or OFF!

The TRANSWITCH is now available from TRANSITRON in the popular JEDEC TO-5 package, ready to solve your switch-on-switch-off requirements.

For further information, write for Bulletin TE-1357A

Transitron
electronic corporation • wakefield, massachusetts

"Leadership in Semiconductors" SEE YOUR LOCAL AUTHORIZED TRANSITRON DISTRIBUTOR FOR QUANTITIES FROM 1-999.

NEW UNIVERSAL SPECTRUM ANALYZER

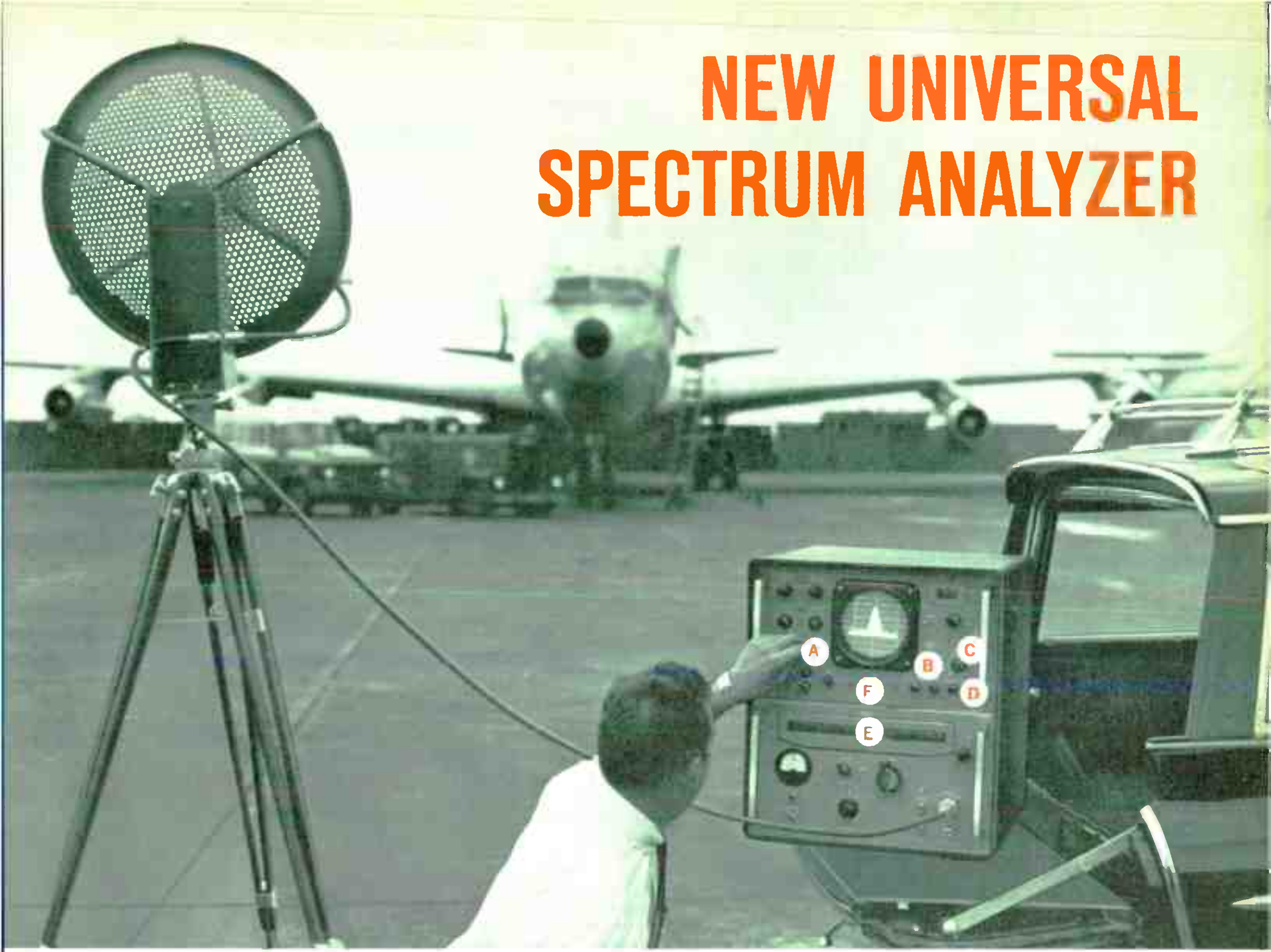

Polarad Model SA-84W being used to make pulse analysis of radar aboard a Pan American Boeing 707, Jet Clipper®

MODEL SA-84W 10 to 44,000 MC in a single unit

FEATURES:

- **Over 80 mc dispersion**
  1 mc to over 80 mc for narrow pulse analysis.
  100 kc to 7 mc for wide pulse analysis.
- **Dual Resolution**
  7 kc or 50 kc automatically set by dispersion control.
- **Crystal controlled markers from 10 to 44,000 mc.**
- **Provision for use with a multi-pulse spectrum decoder (Polarad Model SD-1)**
- **Log-linear amplifiers**
- **Expanded, direct-reading, slide rule dial.**
- **Accurately calibrated IF attenuator**

The Polarad Model SA-84W is the most accurate universal microwave analyzer to measure nearly all parameters — Pulse, CW, FM, VSWR, antenna patterns, bandwidths and filter characteristics.

FREE LIFETIME SERVICE ON ALL POLARAD INSTRUMENTS

MAIL THIS CARD for specifications. Ask your nearest Polarad representative (in the Yellow Pages) for a copy of "Notes on Microwave Measurements."

POLARAD ELECTRONICS CORPORATION

43-20 34th Street, Long Island City 1, N. Y.
Representatives in principal cities.

POLARAD ELECTRONICS CORPORATION:

MEP

POLARAD

Please send me information and specifications on:

☐ Model SA-84W Universal Spectrum Analyzer
☐ Model SD-1 Multi-Pulse Spectrum Selector (see reverse side of page)

My application is__________

Name__________

Title__________ Dept.__________

Company__________

Address__________

City__________ Zone_____ State______

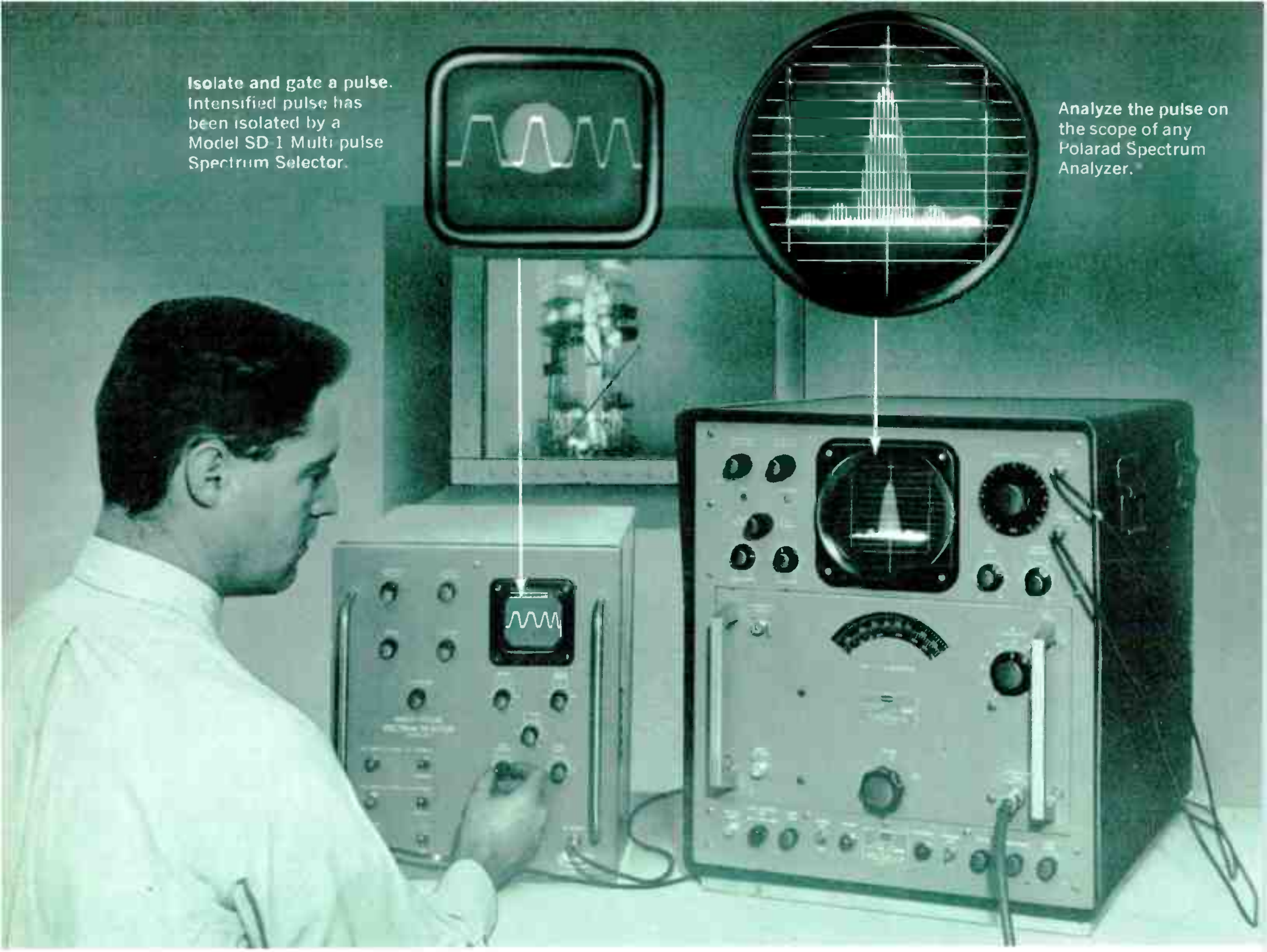

COMPLEX SPECTRUM DECODING

10 to 44,000 mc.

Signal Analysis for Missiles, Telemetry, IFF, Beacons and Radar

The Polarad spectrum selector permits spectrum analysis and decoding of any selected pulse within a multiple pulse train. Sweep, gate width and position can be controlled. Model SD-1 permits the selection and gating of a group of pulses up to 180 μsec. in length (Model SD-IX permits 350 μsec.)

Works with POLARAD Models TSA, TSA-S, TSA-W, SA-84 and SA-84W spectrum analyzers.

Postage Will be Paid by Addressee

No Postage Stamp Necessary If Mailed in the United States.

BUSINESS REPLY CARD
First Class Permit No. 18, Long Island City 1, N.Y.

POLARAD ELECTRONICS CORP
43-20 34th St., Long Island City 1, N. Y.

POLARAD

MAIL THIS CARD for specifications. Ask your nearest Polarad representative (in the Yellow Pages) for a copy of "Notes on Microwave Measurements."

FREE LIFETIME SERVICE ON ALL POLARAD INSTRUMENTS

POLARAD ELECTRONICS CORPORATION

43-20 34th Street, Long Island City 1, N. Y.
Representatives in principal cities.

ultimate

FREEDOM

from amplifier **NOISE**

✓ **WITHOUT THE NEED FOR COSTLY CORRELATION TECHNIQUES**

✓ **AVAILABLE IN MILLIVAC'S VS-64A HUSHED TRANSISTOR AMPLIFIER**

Check these specifications in the light of your own amplifier requirements . . .

NOISE VOLTAGE, REFERRED TO SHORTED INPUT: 10^{-9} V RMS

Bandpass	E Noise
20 cps–300 cps	50×10^{-9} V
20 cps–14 kc	155×10^{-9} V
20 cps–90 kc	445×10^{-9} V
20 cps–180 kc	615×10^{-9} V

SELECTION OF INPUT IMPEDANCES:

10K, low noise (as above) and 100K, approximately 50% higher noise.

BANDPASS SELECTOR SWITCHES:

Upper Frequency Limiting Switch, 11 positions, 300 cps to 180 kc; Lower Frequency Limiting Switch, 11 positions, 2 cps to 120 kc.

GAIN:

Selectable in 8 steps, 10 db to 80 db.

EXTENDED FREQUENCY RANGE AND HIGHER INPUT IMPEDANCE AVAILABLE IN SPECIAL DESIGNS TO MEET SPECIFIC REQUIREMENTS.

MEMORANDUM

From the desk of Walter K. Volkers

Attention: Ad Dept.

Please note, we can also combine 'correlation techniques with the VS-64A design. This gives us new low-noise levels which "out-hush" the world's most noise-free transistor-amplifier!

W.K.V.

tomorrow is our yesterday

MILLIVAC

A DIVISION OF

COHU

ELECTRONICS, INC.

Box 997 Schenectady, New York

Section Meetings

(Continued from page 64A)

FORT HUACHUCA

"Silicon Capacitors," J. G. Hammerslag, Hughes Aircraft Co. 11/23/59.

FORT WAYNE

"Communication by a Polar Orbit Satellite Relay," W. K. Hagan, Magnavox Co. 11/5/59.

GAINESVILLE

"Formation and Destruction of Negative Ions in Dielectrics," Dr. E. E. Muschlitz, Jr., University of Florida. 12/10/59.

HAMILTON

"The What, When, How and Why of the Ampere," J. H. Miller, Weston Instruments. 11/18/59.

HOUSTON

"A New Analog Multiplier," Dr. P. E. Pfeiffer, Rice Institute. 11/17/59.

INDIANAPOLIS

"Operation of a Television Studio," Norman Nixon, WLW-I TV Studio. 12/4/59.

LONG ISLAND

"High Speed Binary Arithmetic Components," R. W. Merwin, IBM Lab.; Movie—"Metropolis in Motion." 11/10/59.

LOS ANGELES

"Communication at Vandenberg AFB," Col. N. Gaynos, VAFB. 11/10/59.

LUBBOCK

"SAC Communication Systems," Capt. Phillips, Dyess AFB. 11/23/59.

MIAMI

"Doppler Radar Navigation System," C. K. Hartwiegen; Election of Officers. 12/10/59.

"New Developments and Things to Come in Telephony," W. D. Bullock, Bell Telephone Labs. 12/14/59.

MONTREAL

"Engineering in Medicine," J. A. Hopps, National Research Council. 11/25/59.

NEWFOUNDLAND

Social Meeting. 10/29/59.

"Air Traffic Control," Mr. Dorsett, Ottawa Dept. of Transport. 11/20/59.

NEW ORLEANS

"New Aspects of Stereophonic Audio Reproduction," P. W. Klipsch, Klipsch Associates. 10/27/59.

"New Tube Developments For Use With Single Sideband," H. Vance, RCA. 11/13/59.

"Interplanetary Guidance of Space Vehicles," R. N. Hutson, Chance-Vought Aircraft, Inc. 11/25/59.

NORTH CAROLINA

"Space Communications," Dr. D. P. Ling, Bell Telephone Labs. 12/4/59.

NORTHERN ALBERTA

"Electronics at Work," C. N. Hoyler, RCA; Election of Officers. 10/15/59.

(Continued on page 72A)

Section Meetings

(Continued from page 70A)

Northern New Jersey

"Guidance of Lunar Probes," Dr. S. Darlington, Bell Telephone Labs. 11/18/59.

Omaha-Lincoln

"The Changing Challenges of Electronics Training," LaVon Peterson, Omaha Radio Engineering Institute. 11/20/59.

Ottawa

"Combat Surveillance," Maj. L. H. Wylie, Army HQ, Ottawa; "Army Field Communications and Field Equipment" "Radiac Equipment for Military Use," Capt. J. T. Bradley and Capt. W. R. Smale, Army HQ, Ottawa. 12/3/59.

Philadelphia

"New Developments in Low Noise Amplifiers—A Review of Low Noise Amplifiers," Dr. Henry Lewis, RCA; "New Developments in Low Noise Amplifiers—Variable Capacitance Parametric Amplifier," Dr. E. Reed, Bell Laboratories. 12/2/59.

Phoenix

"Magnetic Amplifiers—Circuits and Applications," H. Patton, Aeromag, Inc. 11/18/59.

Portland

"Industrial Development in Oregon Past, Present and Future," C. L. Sauvie, Oregon State Planning & Development Dept. 11/23/59.
Organization meeting. 11/28/59.

Princeton

"Random Functions and Non-linear Processes in Engineering," Dr. Norbert Wiener, MIT. 11/12/59.

Quebec

"Experimental Methods in the Study of Aerodynamics," Dr. J. Bonneville, Laval University. 11/24/59.

"Inertial Platforms and Inertial Navigation," J. F. Smith, Pratt & Whitney. 12/1/59.

Rio De Janeiro

"Plano Bandeirante," Dr. J. A. Wiltgen, Companhia Telefonica Brasileira. 12/2/59.

Rome-Utica

Panel Discussion—"How to Achieve Reliability," M. M. Tall, RCA; E. J. Nucci, DOD; H. Benjamin, GE; J. Naresky, RADC. 11/24/59.

San Diego

"New Developments in Radio Astronomy," Dr. W. C. Erickson, Convair Research Laboratory. 11/4/59.

Shreveport

"The Application of Electromagnetic Radiation to Geophysical Prospecting," H. A. Morriss, USAF. 11/3/59.

"Processing and Rebuilding TV Picture Tubes," B. Bernstein, Imperial Electronics, Inc. Tour of Imperial Electronics Factory. 12/1/59.

South Carolina

"Capacitor Design and Development," Ray Lane, Pyramid Electric Co. 11/21/59.

"Being Prepared," Dr. Ernst Weber, IRE President. 12/2/59.

Toledo

"Human Survival in Space," Renato Contini, New York University. 11/19/59.

(Continued on page 74A)

RELIABLE SILICON TRANSISTOR SWITCHING

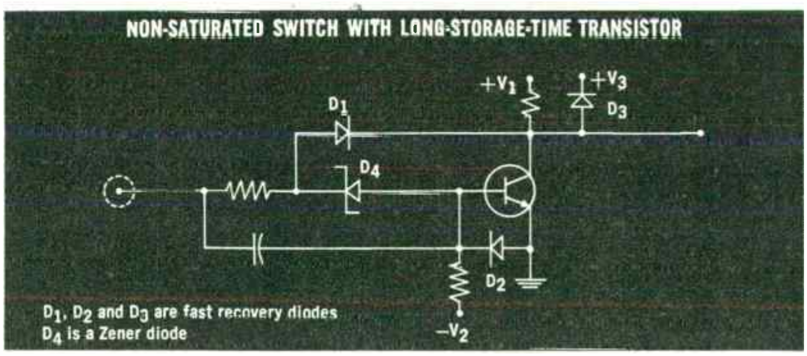

9 COMPONENTS REPLACED BY 4

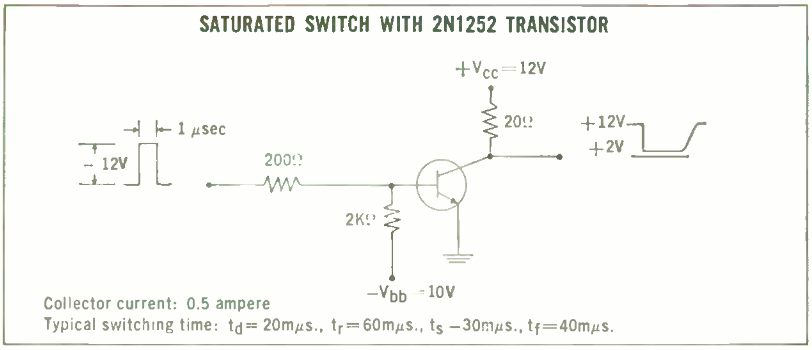

HOW? – By using Fairchild's 2N1252 or 2N1253 **lowstorage** silicon mesa transistors. The guaranteed low storage characteristic permits a simple saturating circuit to achieve switching speeds that previously required complex non-saturating circuits.

WHY? – Improved reliability and reduced cost – one semiconductor instead of five and fewer soldered connections. Power dissipation is only 1/3rd to 1/5th as great, making possible much higher component densities in packaging. Cost and reliability are improved all the way from development through volume production.

WHERE? – Switching circuits in general. The 2N1252 and 2N1253 are ideally suited to high-speed high-current switching applications such as magnetic-core drivers, drum and tape write drivers, high-current pulse generators and clock amplifiers. In addition, the transistors are applicable to medium-speed saturated logic circuits.

FAIRCHILD 2N1252 and 2N1253

Symbol	Characteristic	Rating	Min	Typ	Max	Test Conditions	
h_{FE}	D.C. pulse current gain 2N1252 2N1253		15 30	35 45	45 90	$I_C = 150mA$	$V_C = 10V$
P_C	Total dissipation at 25°C case temperature	2 watts					
$V_{BE\ SAT.}$	Base saturation voltage			0.9V	1.3V	$I_C = 150mA$	$I_B = 15mA$
$V_{CE\ SAT.}$	Collector saturation voltage			0.6V	1.5V	$I_C = 150mA$	$I_B = 15mA$
h_{fe}	Small signal current gain at f=20mc 2N1252 2N1253		2 2.5	4 5.5		$I_C = 50mA$	$V_C = 10V$
I_{CBO}	Collector cutoff current			0.1μA 100μA	10μA 600μA	$V_C = 20V$ $V_C = 20V$	T=25°C T=150°C
$t_s + t_f$	Turn off time			75mμs	150mμs	$I_C = 150mA$ $I_{B2} = 5mA$ Pulse width=10ms	$I_{B1} = 15mA$ $R_L = 40Ω$

For full specifications, write Dept. E-2

FAIRCHILD SEMICONDUCTOR CORPORATION

545 WHISMAN ROAD • MOUNTAIN VIEW, CALIFORNIA • YORKSHIRE 8-8161 • TWX: MOUNTAIN VIEW CAL 122

New York Area: Pioneer 1-4770 • **Syracuse:** GRanite 2-3391 • **Philadelphia Area:** TUrner 6-6623
Washington D.C.: NAtional 8-7770 • **Chicago:** BRowning 9-5680 • **Los Angeles:** OLeander 5-6058

Section Meetings

(*Continued from page 72A*)

TUCSON

"Magnetic Amplifiers," Henry Patton, Detroit. 11/19/59.

VIRGINIA

"Radio Astronomy and the National Radio Astronomy Observatory," Dr. J. W. Findlay, National Radio Astronomy Observatory. 11/13/59.

"Tunnel Diodes," Dr. R. Hall, GE Co. 12/4/59.

WILLIAMSPORT

"Glass Processing," Dr. W. Shaver, Corning Glass Works. 11/18/59.

SUBSECTIONS

EASTERN NORTH CAROLINA

"The Federal Aviation Agency—Electronic Guardian of the Airways," J. Mears and T. R. Hight, FAA. 11/13/59.

KITCHENER-WATERLOO

"Noise, Its Effects on Communications," Dr. K. K. Neely, Defense Research Medical Labs. 11/7/59.

LAS CRUCES-WHITE SANDS

"Infra-Red Physics," Dr. H. A. Daw, New Mexico State University; Election of Officers. 11/24/59.

LEHIGH VALLEY

"BMEWS—Ballistic Missile Early Warning System," H. F. Baker, RCA. 10/28/59.

MEMPHIS

"Satellites and Their Scientific Import," Dr. Carol Ijams, Memphis State Univ. 12/9/59.

MERRIMACK VALLEY

"Instrumentation of Atlantic Missile Test Range," J. A. Luceri, AVCO. 11/23/59.

MID-HUDSON

"Cablevision (Wide Band Video Distribution)," H. J. Giest, Giest-Hietz, Inc. 10/15/59.

"Control of the Machine By the Spoken Word," H. W. Dudley, Bell Telephone Labs. 10/20/59.

"Radio Interference Testing of Large Scale Computing Systems—Theory and Practice," Norman Taylor, IBM. 11/12/59.

MONMOUTH

"Parametric Amplifiers: Historical Background and Recent Results With UHF Travelling Wave Amplifiers Using Diodes," W. W. Mumford and R. S. Engelbrecht, Bell Telephone Labs. 10/21/59.

"Exploration of the Earth's Outer Atmosphere," Dr. S. J. Bauer, U. S. Army Lab. 11/18/59.

NEW HAMPSHIRE

"Radio Astronomy," Dr. Harold Ewen, Ewen-Knight Corp. 12/10/59.

PANAMA CITY

"Theory and Application of Instrumentation Magnetic Tape Recording," W. Craig, Ampex Corp. 12/15/59.

SAN FERNANDO VALLEY

"Color TV Behind the Scenes," NBC tour of Studio. 10/20/59.

"X-15," Q. C. Harvey, North American Aviation. 11/11/59.

(*Continued on page 76A*)

NEWEST way to write performance . . .

servo/riter*

SELF-BALANCING POTENTIOMETRIC RECORDER

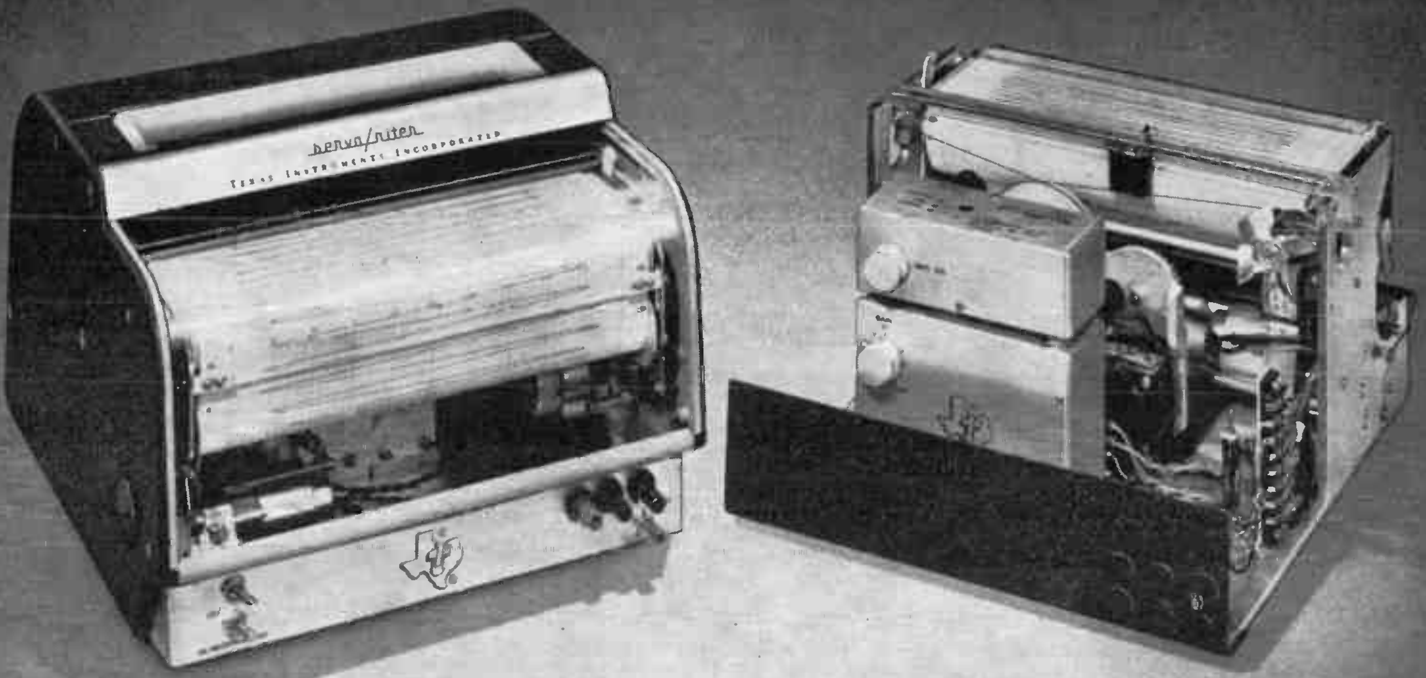

NO OTHER RECORDER OFFERS YOU AS MANY HIGH PERFORMANCE FEATURES...at any price!

The old cliché, "You can pay more but you can't buy better" was never more applicable than in the new "servo/riter" recorder. Texas Instruments has developed a self-balancing potentiometric recorder that incorporates *premium* engineering refinements, sensitivity, reliability and quality construction as *standard* equipment.

High-Sensitivity — Standard electrical span of 2.5 millivolt d-c with off-balance input resistance of 4 megohms gives a power sensitivity of better than 10^{-17} watts.

Fast Pen Speed — Span step response is less than 0.5 second.

High Interference Rejection — Good filtering provides high orders of rejection to common-mode d-c and all types of 60 cps interference. Guard shields permit making full-accuracy measurements at hundreds of volts above ground.

Long-Term Reliability — Tube life is prolonged by heat-dissipating shields. Amplifier gain is stabilized by partial negative feedback. Non-lash, non-wearing, toothed belt drive gives long consistent performance.

Superior Operating Conveniences — Recorder function is easily changed by plug-in input units. Presently standard are 2.5, 5, or 10 millivolt d-c electrical spans . . . special applications and ranges are easily accommodated. "Micrometer" control for zero adjustment and main amplifier gain control are readily accessible as are all other adjustments, connections, and controls. The popular 10-speed chart gears and the high-capacity, easy-prime ink handling system proved on the "recti/riter"® recorder are standard equipment on the "servo/riter" recorder.

There are four "servo/riter" recorder models to choose from . . . *Single Channel, Narrow Grid; Single Channel, Wide Grid; Dual Channel, Narrow Grids; and Dual Channel (overlapping pens), Wide Grid.* Write for technical literature and TI engineering assistance in your specific end or OEM use.

TEXAS INSTRUMENTS
INCORPORATED
GEOSCIENCES & INSTRUMENTATION DIVISION
3609 BUFFALO SPEEDWAY • HOUSTON 6, TEXAS • CABLE: TEXINS

The new "servo/riter" recorder is a companion to the proved "recti/riter" recorder.

*"servo/riter" is a trademark of Texas Instruments

Section Meetings

(*Continued from page 74A*)

SANTA ANA

"The Electron, Research and the Navy," Rear Adm. R. Bennett, Dept. of Navy—Washington 11/17/59.

SANTA BARBARA

"Economics in Electronics," Burgess Dempster, Electronic Engineering Co. of Calif. 11/17/59.

WESTERN NORTH CAROLINA

Conducted Tour of NIKE Plant, Douglas Aircraft Co. 11/19/59.

Membership

The following transfers and admissions have been approved and are now effective:

Transfer to Senior Member

Becker, L., Brooklyn, N. Y.
Bekkering, D. H., The Hague, Holland
Benham, E. E., Hollywood, Calif
Bouchier, P., Brussels, Belgium
Catanzarite, F. J., Dayton, Ohio
Cullen, A. L., Sheffield, England
Desirant, M. C., Charleroi, Belgium
Detwiler, S. P., New Hyde Park, N. Y.
Eckstein, G., Glen Burnie, Md.
Forster, M. C., Santa Barbara, Calif.
Guyton, R. D., Starkville, Miss.
Harmengnies, P. A., Mons, Belgium
Hines, W. S., Eau Gallie, Fla.
Hoffmann, J. A., Brussels, Belgium
Howell, J. F., Milwaukee, Wis.
Marique, J., Uccle-Brussels, Belgium
Matthews, E. W., Jr. Moorestown, N. J.
Mushiake, Y., Sendai, Japan
Overby, H. S., Oslo, Norway
Rosenblith, W. A., Cambridge, Mass.
Schneider, S., New York, N. Y.
Seals, R. B., Irving, Tex.
Sellers, J. D., Melbourne, Fla.
Sharpe, G., Murray Hill, N. J.
Silvey, J. O., Fort Wayne, Ind.
Stoklas, F. P. Eau Gallie, Fla.
Sundaram, V. R., Geneva, Switzerland
Swartz, E. E., Utica, Mich.
Talbot, R. V., Corona, Calif.
Thompson, D. G., College Park, Md.
van Wijngaarden, A., Amsterdam, Oost, The Netherlands
Waller, S. L., Arlington, Va.
Watson, S. E., Jr., University City, Mo.
Weston, B. J., Albuquerque, N. M.
Wever, L. R., Cocoa Beach, Fla.
Wolf, F. A., Columbus, Ohio
Woodbury, H. L., Orland Park, Ill.

Admission to Senior Member

Benjamin, R. B., Newport Beach, Calif.
Bosenberg, W. A., Somerville, N. J.
Boudreaux, F. J., Lafayette, La.
Cardwell, L. R., Orlando, Fla.
Doherty, R. H., Boulder, Colo.
Garrow, H. J., San Mateo, Calif.
Graham, G. E., Stratford, Conn.
Heaton, A. R., The Hague, Netherlands
Herrlin, R. C., Dayton, Ohio
Lefkov, S., Washington, D. C.

(*Continued on page 78A*)

Membership

(Continued from page 76A)

Metzelaar, W., The Hague, Netherlands
Pace, N. C., Washington, D. C.
Pollard, B. W., Pasadena, Calif.
Rogers, T. W., Washington, D. C.
Rooney, W. R., Fulton, Md.
Shockley, W. L., Richardson, Tex.
Tani, K., Tokyo, Ohta-ku, Japan
van Hall, J. N., Hilversum, Holland
Wheeler, C. R., Harrison, N. J.

Transfer to Member

Adams, R. R., Upton, L. I., N. Y.
Albert, B., Belmont, Mass.
Albon, R., Jr., Lynwood, Calif.
Amort, D. L., Corvallis, Ore.
Austin, R. C., Camp Hill, Pa.
Ayers, D. C., Cedar Rapids, Iowa
Baiamonte, F. L., Greeley, Colo.
Bain, T. D., Columbus, Ohio
Barbour, R. E., Richfield, Minn.
Bartol, T. J., Milwaukee, Wis.
Bauer, R. L., Riverside, Calif.
Behrendt, R. T., Billings, Mont.
Bein, G. E., Norfolk, Va.
Bennett, W. F., Reading, Pa.
Bertelsen, B. I., Vestal, N. Y.
Boesch, P. W., Washington, D. C.
Bookwalter, E. C., Sante Fe, N. M.
Boys, H. N., Levittown, Pa.
Bradley, K. M., New Haven, Conn.
Brandes, N. J., Nutley, N. J.
Breckenridge, W. G., Jr., Altadena, Calif.
Brown, C. R., Houston, Tex.
Buchanan, K. J., St. Paul, Minn.
Buchfeller, J. E., Riverside, Calif.
Budell, L. A., Marcellus, N. Y.
Burhans, R. W., Cleveland, Ohio
Brunhart, W., Norwalk, Conn.
Carreon, D. G., Newark, N. J.
Case, S. W., Plainview, L. I., N. Y.
Catenaro, R. D., Seaford, L. I., N. Y.
Chambers, D. R., Ft. Wayne, Ind.
Clarke, E. L., Kansas City, Mo.
Cockerham, F. E., Eau Gallie, Fla.
Cohen, K. J., King of Prussia, Pa.
Cole, D. A., Burlington, N. J.
Cole, J. E., Tucson, Ariz.
Coleman, H. R., Garland, Tex.
Collier, A. F., Rochester, Mich.
Copithorne, A. R., Marblehead, Mass.
Cox, G. C., Northbridge, Calif.
Cross, A. H., W. Somerville, Mass.
Crouch, M. B., Ottawa., Canada
Dalton, M. M., Los Angeles, Calif.
Dargue, F. B., Roselle Park, N. J.
Di Napoli, G. W., Reno, Nev.
Dobbs, W., Vandenberg A.F.B., Calif.
Dodge, J. E., Arlington, Va.
Donovan, C., Bedford, Mass.
Dubbel, W. C., St. Paul, Minn.
Dunn, J. G., Upper Montclair, N. J.
Dunning, R. A., Memphis, Tenn.
Dvoracek, F. H., Oxnard, Calif.
Elhoff, W. C., Constantia, N. Y.
Faber, D. C., Timonium, Md.
Fedotin, L. S., Dayton, Ohio
Fleishman, G., Long Island City, N. Y.
Greenberg, S. A., Malden, Mass.
Greis, W. F., Sao Paulo, Brazil
Heizer, L. E., Ft. Worth, Tex.
Held, G., Seattle, Wash.
Hendrickson, H. S., Bloomfield, Conn.
Heyer, E. M., Mt. Holly, N. J.
Hodgin, R. M., Jr., Liverpool, N. Y.
Holly, C. M., El Cajon, Calit.
Howard, D. V., Jr., Camden, N. J.
Hughes, A. M., Boston, Mass.
Hughey, A. H., Hollywood, Calif.

(Continued on page 80A)

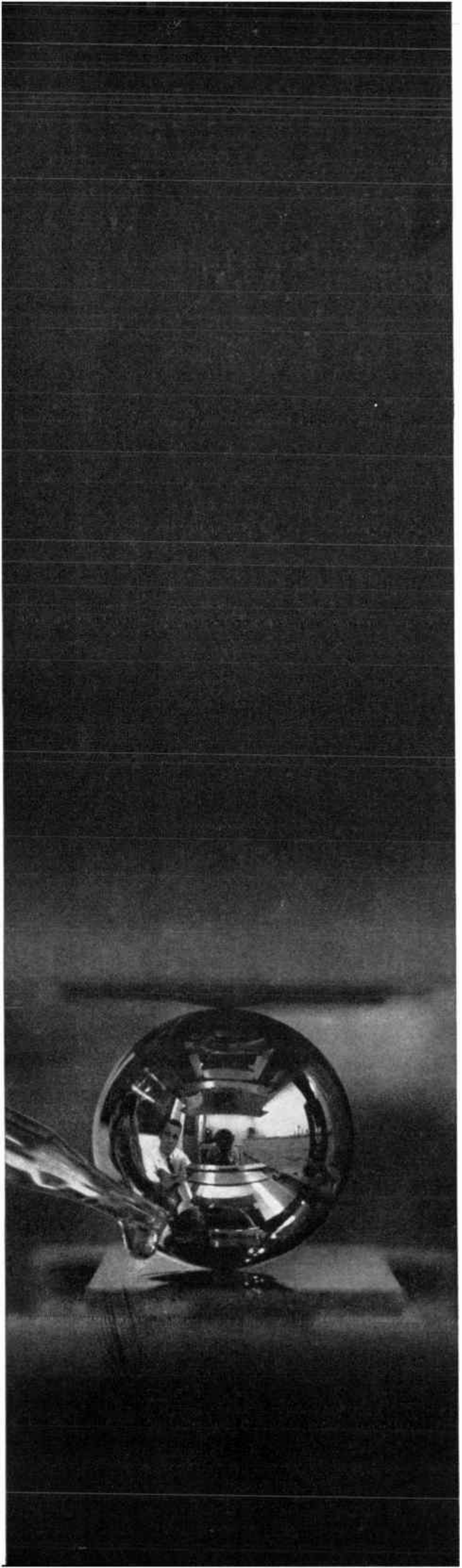

One of a series

On the riddle of rolling friction

It doesn't take much to roll a hard ball across a hard, smooth, level surface — actually only about 0.00001 times the normal force acting vertically on the ball. But by careful measurement of this tiny rolling force, scientists at the General Motors Research Laboratories are helping to unravel the riddle of rolling friction.

An important relationship recently uncovered in this fundamental study: the rolling force is proportional to the volume of material that is stressed above a certain level. As a result, a GM Research group have not only confirmed the hypothesis of *how* a rolling ball loses energy (Answer: elastic hysteresis) but also have learned *where* this lost energy is dissipated (Answer: in the interior of the material, not on the surface). Mathematical analyses have indicated the exact shape of the elastically stressed volume in which all the significant frictional loss takes place.

The purpose of friction research at the GM Research Laboratories is to learn more about the elastic and inelastic behavior of materials. This knowledge — of academic interest now — will eventually give GM engineers greater control of energy lost through friction. This is but one more example of how General Motors lives up to its promise of "More and better things for more people."

General Motors Research Laboratories

Warren, Michigan

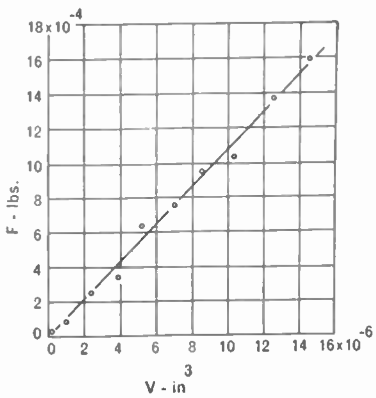

Relationship of rolling force to elastically stressed volume.

Membership

(*Continued from page 78A*)

Hunting, R. A., Liverpool, N. Y.
Ingrao, H. C., Bedford, Mass.
Johns, M. W., Tipp City, Ohio
Kaneko, G. S., Los Angeles, Calif.
Katz, S., New York, N. Y.
Keenan, O. B., Inglewood, Calif.
Kennedy, J. D., Rumson, N. J.
Knight, J. P., Melbourne, Fla.
Krakauer, S. M., Palo Alto, Calif.
Kramer, A. G., Culver City, Calif.
Kromhout, O. M., Tallahassee, Fla.
Kushner, E. E., Bala-Cynwyd, Pa.
Landreman, G. R., Dayton, Ohio
Lappi, U. T., Fullerton, Calif.
Lerner, D., Smithtown, L. I., N. Y.
Lesperance, B. J., Montreal, Que., Canada
Lillibridge, E. H., Woodland Hills, Calif.
Lipton, M. H., West Long Branch, N. J.
Mannel, W. M., Asbury Park, N. J.
Mapes, T. J., Hamden, Conn.
Markes, R. T., No. Syracuse, N. Y.
McCormick, G. C., Ottawa, Ont., Canada
McCotter, J. D., Jr., Lansdale, Pa.
McLaughlin, W. E., Wyomissing, Pa.
Melloh, C. L., Mitchellville, Iowa
Metchmann, C. Owensboro, Ky.
Metzger, J. A., Dayton, Ohio
Molina, R. E., Winston-Salem, N. C.
Molnar, S., San Diego, Calif.
Moshier, L. S., Jr., Kitchener, Ont., Canada
Munushian, J., Culver City, Calif.
Neidenberger, T. A., Kansas City, Mo.
Newhouse, P. D., Linthicum Heights, Md.
Nossen, E. J., Haddonfield, N. J.
O'Brien, W. C., San Pedro, Calif.
O'Connor, R. J., Wappingers Falls, N. Y.
Olson, D. S., Seattle, Wash.
Oppenheimer, H. N., New York, N. Y.
Park, K. L., Alexandria, Va.
Pearce, C. R., Redondo Beach, Calif.
Perry, G. W., Cincinnati, Ohio
Pierson, L. L., Santa Maria, Calif.
Potts, R., Binghamton, N. Y.
Rawley, J. W., Scarborough, Ont., Canada
Reiner, R. L., Verona, N. J.
Reynolds, R. J., Palo Alto, Calif.
Rogers, J. M., South Gate, Calif.
Rouse, R. E., Washington, D. C.
Sagan, E. A., Chatham, N. J.
Samuels, D. S., Mt. Vernon, N. Y.
Schmidt, E. J., Norristown, Pa.
Skov, R. A., Poughkeepsie, N. Y.
Stack, J. F., Syracuse, N. Y.
Stewart, T. W. W., London, Ont., Canada
Stickle, R. L., Murray Hill, N. J.
Stout, C. D., Livonia, Mich.
Striegel, M. E., Milwaukee, Wis.
Stutz, T. O. J., Zollikerberg, Switzerland
Than, M. P., Rangoon, Burma
Toepel, W. A., West Caldwell, N. J.
Torres, H. S., Albuquerque, N. M.
Townsend, W. H., Jr., Plainfield, N. J.
Tracey, B. P., Playa Del Rey, Calif.
Vecchiarelli, N., Newburgh, N. Y.
Webster, K. R., Silver Spring, Md.
Willner, W. H., Crownsville, Md.
Wilson, P. B., Jr., Lexington, Mass.
Wood, G. C., Owensboro, Ky.
Wood, G. K., Ft. Worth, Tex.
Yeager, D. L., Garland, Tex.

Admission to Member

Abernathy, W. J., Rochester, N. Y.
Abrams, G. L., Wantagh, L. I., N. Y.
Afifi, M. S., Cairo, Guiza, U. A. R.
Agarwal, R. K., Hawthorne, Calif.
Anderson, C. E., San Carlos, Calif.

(*Continued on page 82A*)

Membership

(Continued from page 80A)

Andreasen, M. G., Palo Alto, Calif.
Appelt, O. H., San Salvador, El Salvador, C. A.
Arbuckle, C. E., St. Petersburg, Fla.
Ashley, A. C., Redwood City, Calif.
Azary, Z. P., Ann Arbor, Mich.
Baker, J. L., Norwood, Mass.
Barnes, J. M., Lynchburg, Va.
Barnes, W. H., Palo Alto, Calif.
Barnhart, W., Palo Alto, Calif.
Berkin, G. M., Poughkeepsie, N. Y.
Blank, C. A., Huntington Station, N. Y.
Borek, R. W., Edwards, Calif.
Breetand, G. L., Lubbock, Tex.
Broderick, R. F., Melrose, Mass.
Brooks, W. D., South Plainfield, N.J.
Brown, D. M., San Francisco, Calif.
Brown, E. W., Jr., Falls Church, Va.
Brown, R. P., Endicott, N. Y.
Bruni, D. J., Boston, Mass.
Bnoymaster, N. W., Glen Burnie, Md.
Calpena, L., Syosset, L. I., N. Y.
Carbin, R. A., Melrose, Mass.
Cenacchi, C. M. A., Monza, Italy
Cermignani, D. J., Huntington Station, L. I., N. Y.
Chapin, J. W., Natick, Mass.
Chernack, G., Teaneck, N. J.
Clark, B. H., Lynchburg, Va.
Clarke, M. L., Antigonish, Nova Scotia, Canada
Connor, W. E., Kokomo, Ind.
Cooper, R. E., San Antonio, Tex.
Corelli, G. J., Elmhurst, L. I., N. Y.
Corgan, W. G., Allentown, Pa.
Coyle, D. J., Haddonfield, N. J.
Craig, J. B., Littleton, Colo.
Dallargine, G., Milano, Italy.
Harter, C. U., Phoenix, Ariz.
De Polo, N., Milano, Italy
Di Marino, A., Bradford, Pa.
Dinter, E., Philadelphia, Pa.
Dong, P., Los Angeles, Calif.
Drucker, S., Glendale, Calif.
Duffy, F. P., Madison, N. J.
Dunlap, J. L., Oak Ridge, Tenn.
Ehrlich, E., St. Petersburg, Fla.
Elfenbein, L., Brooklyn, N. Y.
Elliot, R. R., Pointe Claire, Que., Canada
Elwood, F. P., Jr., Philadelphia, Pa.
Erdman, R. C., Rochester, N. Y.
Estersohn, N., Los Angeles, Calif.
Fates, E. M., Jr., Tucson, Ariz.
Farrelly, R. J., Levittown, Pa.
Ferri, A. J., Jr., Bedford, Mass.
Fischer, W., Silver Spring, Md.
Fitch, T. L., Indianapolis, Ind.
Friebertshauser, R. E., St. Petersburg, Fla.
Fyfe, S. B., Jr., Garden City, L. I., N. Y.
Gardiner, D. J., Cobham, Surrey, England
Genet, A. T., Santa Monica, Calif.
Gentry, B. F., Fort Worth, Tex.
Gilfert, J. C., Columbus, Ohio
Glaser, E. R., Philadelphia, Pa.
Glazer, S., Los Angeles, Calif.
Goldsmith, B. P., Walpole, Mass.
Gower, D. E., Binghamton, N. Y.
Grant, R. D., Remsen, N. Y.
Gray, B. C., Buena Park, Calif.
Haback, D. H., Roslyn, N. Y.
Haggard, T. Y., Lexington, Ky.
Hamilton, D. T., Buffalo, N. Y.
Haney, B. M., Indialantic, Fla.
Hanfan, D. T., Burbank, Calif.
Havstad, J. W., Watertown, Mass.
Heckman, D. E., Montreal, P. Q., Canada
Henker, J. W., Mishawaka, Ind.
Herskowitz, G. J., Fresh Meadow, L. I., N. Y.
Hertz, D., Brighton, Mass.
Hoyle, J., Granada Hills, Calif.
Hundley, J. G., Jr., Winston-Salem, N. C.

(Continued on page 84A)

0.5 0.4 0.3 µsec

Fastest recovery yet...

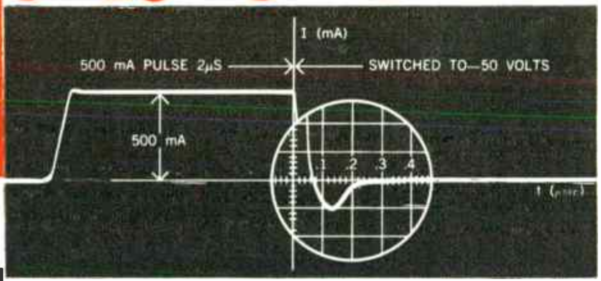

½ AMPERE SILICON SWITCHING DIODES

. . . in a high-current silicon switching diode. The 1N920-1N923 series is the latest result of Sperry Semiconductor's unique developments for the computer field.

The most advanced addition to the industry's most complete line of high conduction fast recovery diodes, this series meets the severe requirements of high current pulse circuits for high speed computer switching, pulse clamping, gating, blocking, and diode logic circuits.

Designed for high temperature operation (to 175° C), the 1N920 series features high forward conductance (500mA at 1.0V.) and low leakage (50µA at 150° C). Peak dissipation is 800 mw.

All units feature a maximum recovery time of 0.3 microseconds to return to 10K ohms when switched from a forward current 2 microsecond pulse of 500mA to a reverse voltage of —50 volts (—30 V for 1N920), with a loop impedance of 1K ohms. Faster switching speeds are obtained at lower currents.

TENTATIVE DATA

Type	Working Inv. DC Voltage (Volts)	Max. Forward Voltage Drop at 25°C (V.)	Max. Inverse Current (µA) 25°C	Max. Inverse Current (µA) 150°C	Min. Saturation Voltage at 100µA 25°C	Max.* Recovery Time µsec.
1N920	36	1.0 at 500mA	.25	50 @ 30V.	40	0.3
1N921	70	1.0 at 500mA	.25	50 @ 60V.	80	0.3
1N922	100	1.0 at 500mA	.25	50 @ 90V.	120	0.3
1N923	130	1.0 at 500mA	.25	50 @ 120V.	150	0.3

*Refer to Sperry Bulletin No. 2103

SPECIAL SAMPLE OFFER

Order a sample lot for your own application at the special price of only $50 for a lot of 10 1N921 diodes. Direct your order to the So. Norwalk plant or the nearest Sperry sales office as listed below.

SPERRY

SPERRY SEMICONDUCTOR DIVISION, *SPERRY RAND CORPORATION, SOUTH NORWALK, CONN.*

Call or write: *Sperry Semiconductor, Wilson Avenue. SOUTH NORWALK, Conn., VOlunteer 6-1641; in NEW YORK PLaza 2-0885; 3555 W. Peterson Ave., CHICAGO 45, Ill., KEystone 9-1776; 2200 East Imperial Highway, EL SEGUNDO, Calif., ORegon 8-6226.*

Membership

(Continued from page 82A)

Hunt, D. P., Las Vegas, Nev.
Hurst, A. H., Erie, Pa.
Jacobs, E. C., Valley Stream, L. I., N. Y.
Jacobs, R., Wakefield, Mass.
Janone, V., White Plains, N. Y.
Jansen, J. J., Washington, D. C.
Johnson, J. E., Detroit, Mich.
Julian, C. E., Sacramento, Calif.
Julinsburger, H. Y., Ossining, N. Y.
Kahn, A. G., Colonia Del Vale, D. F., Mex.
Karp, D., Wayland, Mass.
Kazmierczak, B., Schenectady, N. Y.
Kelly, D. A., Saugerties, N. Y.
Kelly, J. D., Concord, Masss.
Kelly, R. J., Baltimore, Md.
Kidder, R. W., Medford, N. J.
Kohn, D., Great Neck, L. I., N. Y.
Lachmann, G. E. G., Brookline, Mass.
Lasch, K. B., Wakefield, Mass.
Lassetter, T. A., Lexington, Ky.
Ledgerwood, F. A., Melbourne, Fla.
Lee, A., Florissant, Mo.
Leonard, P. F., St. Paul, Minn.
Levine, G., Silver Spring, Md.
Levy, I., Milano, Italy
Ligis, T., Elizabeth, N. J.
Lilley, C. M., Denver, Colo.
Loaec, G. L., Huntington Station, L. I., N. Y.
Lovely, C., Akron, Ohio
Lovely, H. E., San Antonio, Tex.
Lynch, J. F., Downey, Calif.
MacKenzie, M. V., Winchester, Mass.
Mackson, D. J., Lanesboro, Mass.
Macleod, W. A., Norwich, Norfolk, England
Mahant, M. C., London, England
Marsh, J. L., Jr., Isle of Palms, S. C.
Martin, J. B., Roslyn Heights, N. Y.
Martinez, P. J., Buenos Aires, Argentina
Mastalli, P., Milano, Italy
May, P. J., Webster, N. Y.
McCarthy, W. A., Wayland, Mass.
McConnell, W. E., Granada Hills, Calif.
McGihon, R. S., Charleston, S. C.
McGunigle, R. D., Garfield Heights, Ohio
Mead, D. C., Jr., Ridgewood, N. J.
Meloff, M., Philadelphia, Pa.
Meltzer, M. I., Newton Centre, Mass.
Mener, J. M., Seattle, Wash.
Meyer, R. J., Cedar Rapids, Iowa
Migneault, G. B., Pont-Vian, Montreal, Que., Canada
Mild, L. M., Annapolis, Md.
Miller, M. S., Holliston, Mass.
Monteiro, R., Norristown, Pa.
Moore, J. H., Havertown, Pa.
Moore, T. H., Torrance, Calif.
Morrison, R. G., Las Vegas, Nev.
Motes, J. H., Owego, N. Y.
Murphy, W. V., Jackson Heights, L. I., N. Y.
Myers, G. A., Palo Alto, Calif.
Myhre, R. W., San Bruno, Calif.
Myrberg, J. E., Salt Lake City, Utah
Nakamura, F. T., Charlotte, N. C.
Narendra, K. S., Cambridge, Mass.
Nippe, L. O., Poughkeepsie, N. Y.
Nowick, W., Bowie, Md.
Olson, H. H., Glenolden, Pa.
Orsino, R. J., Washington, D. C.
Osborn, T. F., Jr., North Hollywood, Calif.
Pal, G. L., Hamilton, Ont., Canada
Parish, R., Winston-Salem, N. C.
Pavell, P. J., Falls Church, Va.
Payne, R. R., Los Altos, Calif.
Peltzer, K. E., Adelphi, Md.
Perez-Belisario, H., Caracas, Venezuela
Pipher, M. D., West Hollywood, Calif.
Polhamus, J. R., Fort Wayne, Indiana
Ponce de Leao, H. B., Rio De Janeiro, Brazil
Quam, W. M., Las Vegas, Nev.
Raggi, F., Milano, Italy

(Continued on page 88A)

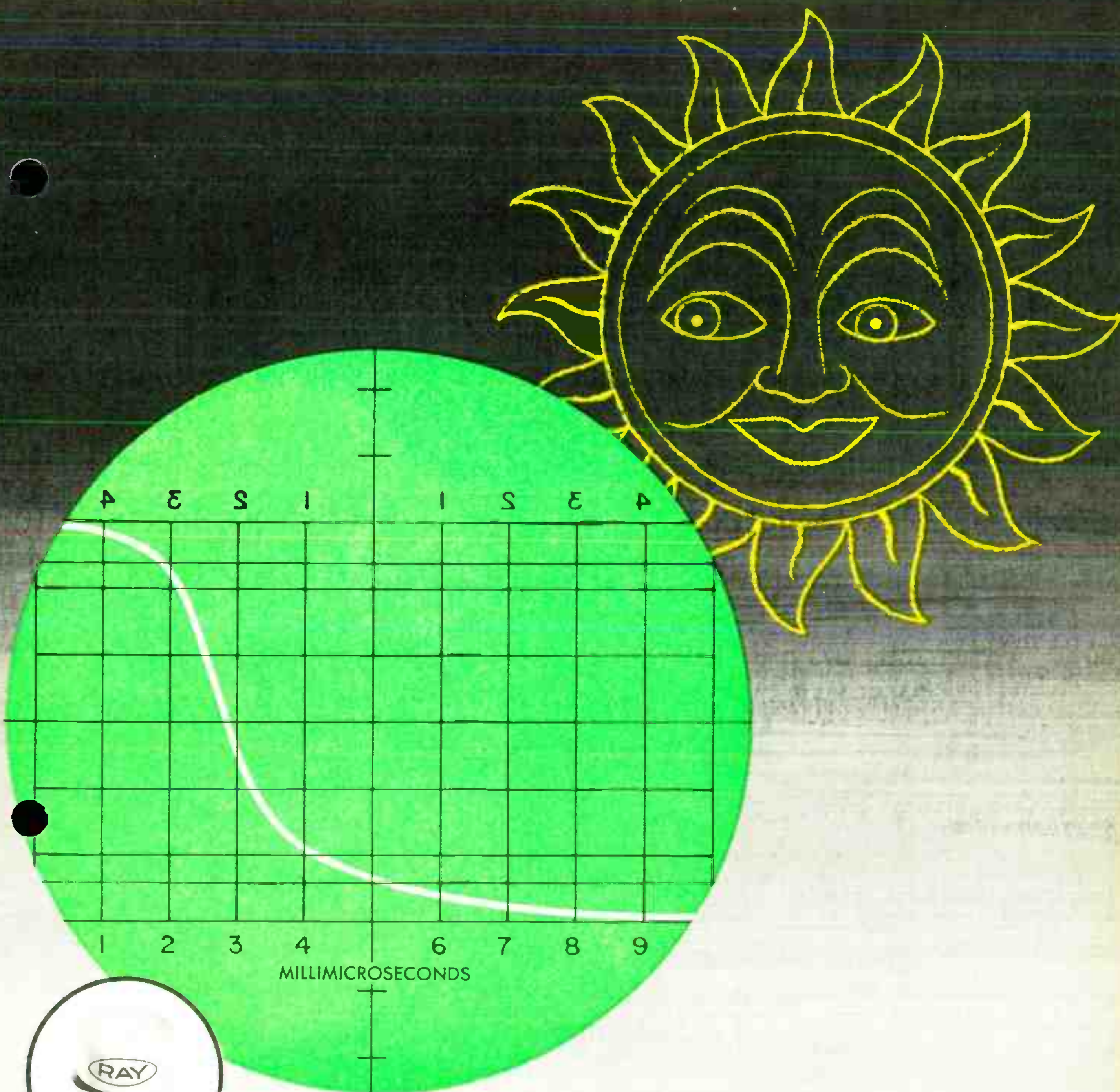
1 2 3 4 6 7 8 9
MILLIMICROSECONDS
RAY

NOTABLE ACHIEVEMENTS AT JPL...

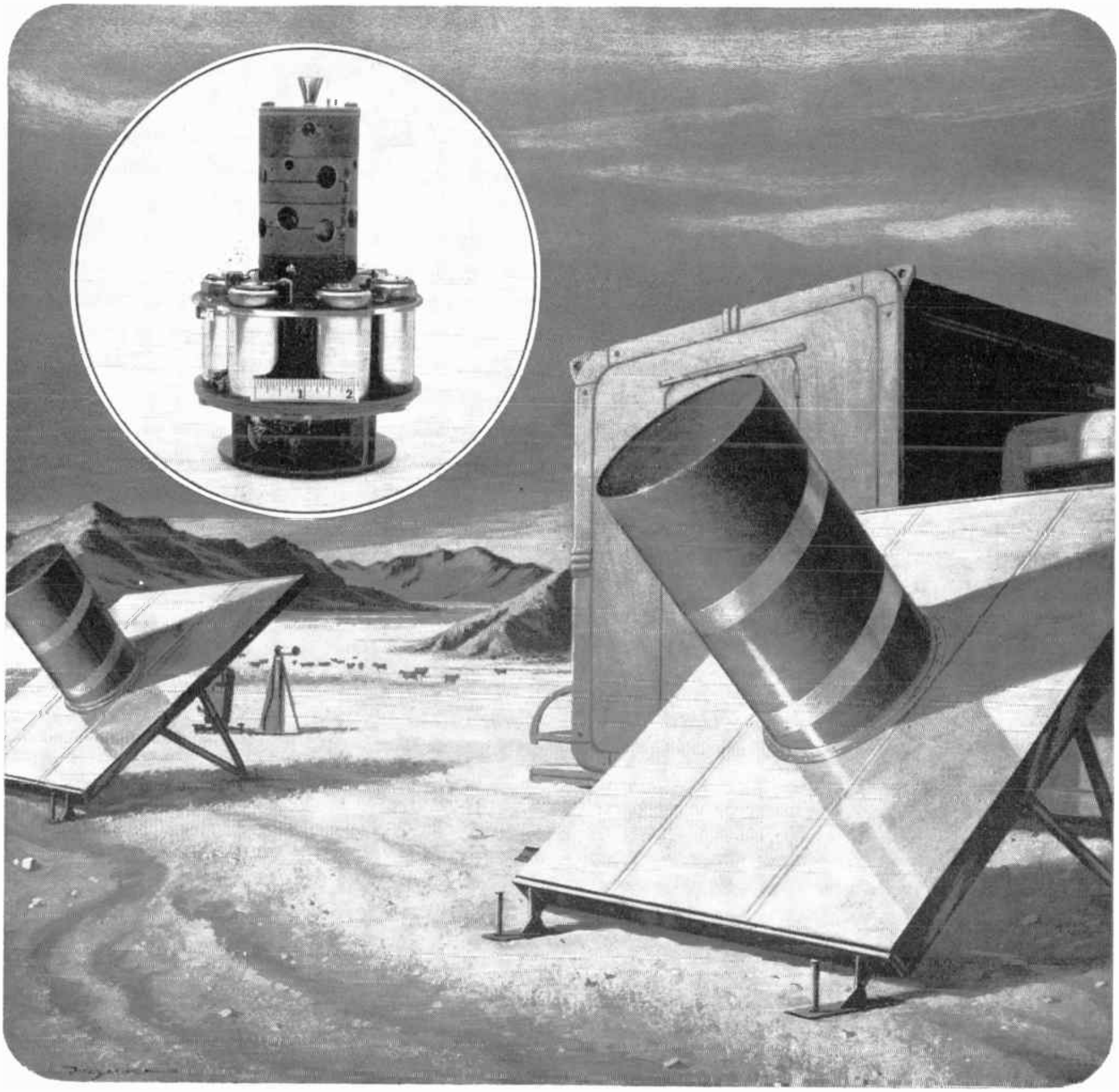

From MICROLOCK to microlock

One of the most interesting and useful scientific activities at JPL has been the development of MICROLOCK, a radio tracking and communication system for satellites.

Microlock is designed to transmit information over extreme ranges of space with a minimal amount of transmitter power and weight. The objective was achieved by sophisticated design of the ground receiving equipment. The design utilizes basic electronic circuits and techniques carefully combined in a novel manner to provide superior performance and sensitivity.

The satellite transmitter consists of a radio-frequency oscillator, phase-modulated by telemetering signals, and radiates a power of 3 mW. It is capable of operating for several months on a battery weighing one pound.

Used successfully in previous space vehicles, microlock remains a useful and expandable instrument for continuing space exploration. It is a prime example of JPL's activity on the space frontier.

CALIFORNIA INSTITUTE OF TECHNOLOGY
JET PROPULSION LABORATORY
A Research Facility operated for the National Aeronautics and Space Administration
PASADENA, CALIFORNIA

Employment opportunities for Engineers and Scientists interested in basic and applied research in these fields:

INFRA-RED • OPTICS • MICROWAVE • SERVOMECHANISMS • COMPUTERS • LIQUID AND SOLID PROPULSION • STRUCTURES • CHEMISTRY • INSTRUMENTATION • MATHEMATICS • AND SOLID STATE PHYSICS •

Send professional resume, with full qualifications and experience, for our immediate consideration

Membership

(Continued from page 84A)

Rainbird, K. V. K., Raleigh, N. C.
Rakonitz, J. G., San Francisco, Calif.
Randig, G. W., West Acton, Mass
Rapoza, E. J., Westmont, N. J.
Rapp, F. J., Ottawa, Ont., Canada
Ray, H., Washington, D. C.
Reynolds, R. E., Cocoa, Fla.
Roberts, B. C., Los Altos, Calif.
Roberts, H. L., Englewood, Colo.
Roig, R. W., Wright-Patterson AFB, Ohio
Rosa, J., Smithtown, L. I., N. Y.
Rosellini, G. R., Milano, Italy
Rossi, R., Bologna, Italy
Russell, H. L., New York, N. Y.
Sanders, H. L., Albuquerque, N. M.
Sarabacha, H., Oxnard, Calif.
Sasaki, T., Kobe, Japan
Saunders, I. H., Roslindale, Mass.
Schneider, L. J., Woodhaven, N. Y.
Schreiber, S., Wayne, N. J.
Schumacher, R. B. F., Basking Ridge, N. J.
Scott, R. J., San Diego, Calif.
Seltzer, A. D., Glen Oaks, N. Y.
Sharko, N., Morris Plains, N. J.
Sinclair, J. C., Oak Park, Ill.
Sippel, R. J., Poughkeepsie, N. Y.
Skinner, A. L., Ft. Huachuca, Ariz.
Smith, J. F., Philadelphia, Pa.
Sobel, R. L., Evanston, Ill.
Sondik, H., Brooklyn, N. Y.
Spiess, E. R., Las Vegas, Nev.
Sprague, J. L., North Adams, Mass.
Spruth, W. G., Poughkeepsie, N. Y.
Stalberg, N. G., Goteborg, Sweden
Steinsto, O., Oslo, Kjelsas, Norway
Stern, A. J., Peabody, Mass.
Sturman, J. C., Cleveland, Ohio
Subrahmanyam, V., Bangalore, India
Suchannek, R. G., Elmira, N. Y.
Swamy, A., Aachen, Germany
Tabusso, G., Milano, Italy
Taylor, W. V., Winter Park, Fla.
Thomas, P. S., Seattle, Wash.
Thomas, P. R., Downend, Bristol, England
Thornton, H. L. H., Seattle, Wash.
Tinkle, T. M., Albuquerque, N. M.
Touw, C. L., North Highlands, Calif.
Tucker, C. K., Seattle, Wash.
Turner, V. D., Andover, Mass.
Urseny, W. G., Carmichael, Calif.
Vacca, R., Rome, Italy
Verdooren, H. W., Wakefield, Mass.
Watanabe, H., Kawasaki, Kanagawa, Japan
Watson, H. L., Washington, D. C.
Watson, J. P., Weston, Ont., Canada
Weaver, C. B., Jr., Chevy Chase, Md.
Webb, D. O., Wichita, Kansas
Weeks, R. F., Los Angeles, Calif.
Weiss, D. W., Bayshore, L. I., N. Y.
Whiteside, R. B., Maple Shade, N. J.
Wilbur, W. C., Jr., Torrance, Calif.
Wilkins, D. R., Winston-Salem, N. C.
Wilmanns, I. G., Sierra Madre, Calif.
Witham, R. G., St. Paul, Indiana
Woodruff, J. G., Jr., Whitesboro, N. Y.
Woodward, R. M., Jr., Eatontown, N. J.
Yonge, P. K., Sunnyvale, Calif.

Admission to Associate

Abell, D. P., Falls Church, Va.
Aivazian, S. G., Jackson Heights, L. I., N. Y.
Albert, C. C., McClellan AFB, Calif.
Anders, B. J., Moorpark, Calif.
Andersen, E. C., Omaha, Nebr.
Atkinson, M. H., Rome, N. Y.
Auerbach, S. S., Levittown, Pa.
Ayer, H. G., San Diego, Calif.
Bengtson, C. N., Alamogordo, N. M.
Blank, G. F., Cleveland, Ohio

(Continued on page 90A)

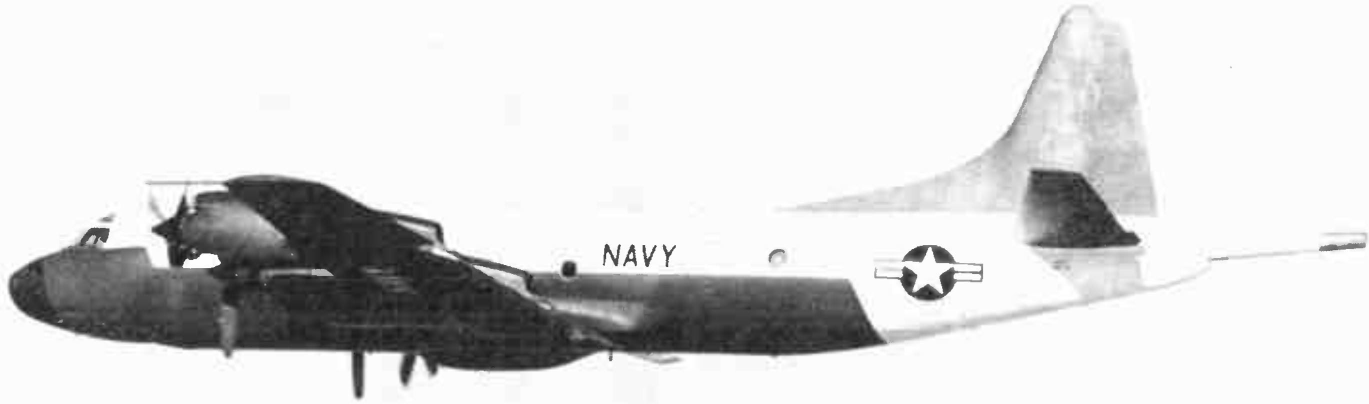

Lockheed P3V

AIRBORNE SUB-HUNTERS USE TI ASW SYSTEMS

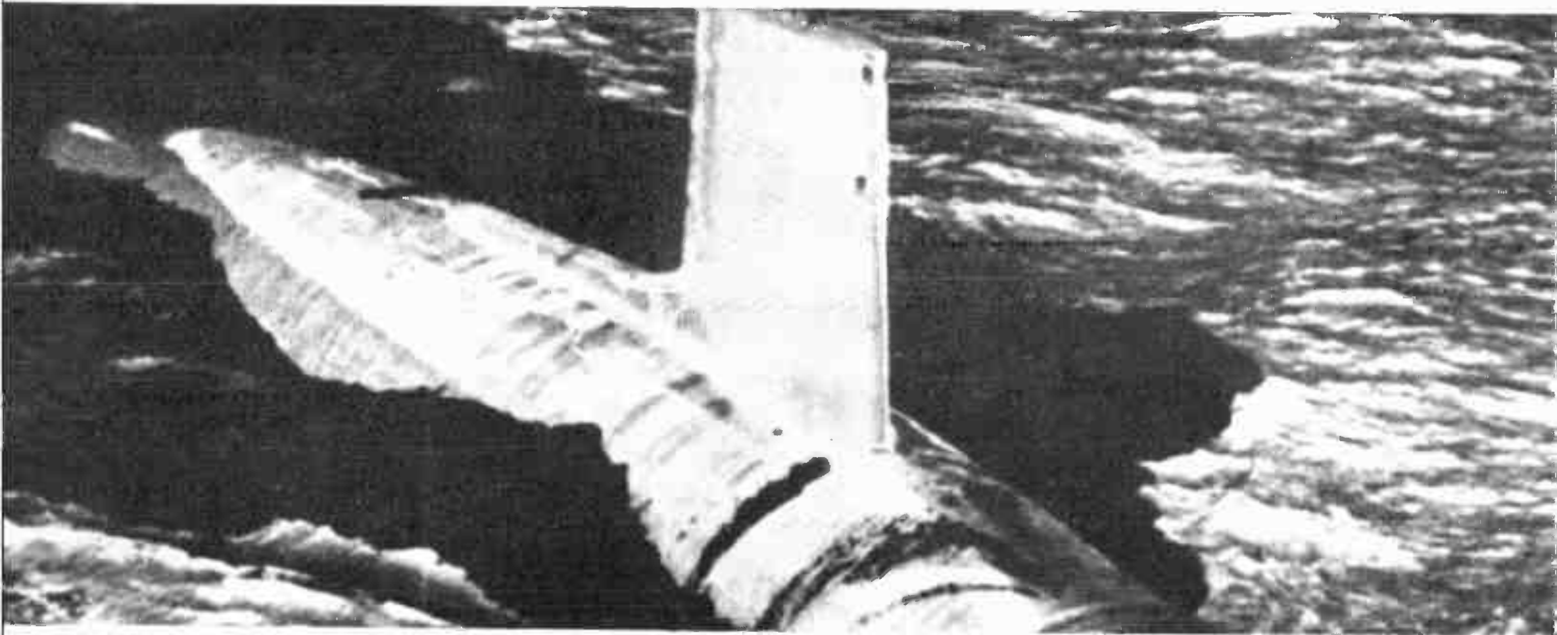

Five major ASW aircraft today use antisubmarine warfare systems supplied by Texas Instruments. These include radar, sonar, magnetic anomaly detection, interval computers, intercom, and advanced detection systems.

Now, TI is applying its 14-years' antisubmarine experience to newer and better methods for detecting, localizing, classifying and positively identifying both conventional and nuclear-powered submarines.

For detailed information about these special activities, properly cleared personnel with a need to know are invited to contact SERVICE ENGINEERING:

Sikorsky HSS-1N

Martin P5M-2

Lockheed P2V

Grumman S2F-1

TEXAS INSTRUMENTS
INCORPORATED

APPARATUS DIVISION

6000 LEMMON AVENUE
DALLAS 9, TEXAS

Membership

(Continued from page 88A)

Bosler, R. B., Boston, Mass.
Bycroft, E. E., Panama City, Fla.
Caligiuri, G. P., Rome, Italy
Carrara, A. S., Bayside, L. I., N. Y.
Ceretta, B. J., Chicago, Ill.
Chehab, E. R. C., Beirut, Lebanon
Christo, V. S., Jamaica Plain, Mass.
Clark, K., Hampton, Middlesex, England
Colello, A., Milano, Italy
Cory, C. W., Palo Alto, Calif.
Costamagna, G. G. A., Milano, Italy
Crawford, F. L., Milwaukee, Wis.
Diger, J. E., Minneapolis, Minn.
Draper, J. D., Prince Albert, Sask., Canada
Ehret, F. W., Burlington, Iowa
Eisler, C. J., St. John's, Newfoundland, Canada
Ellner, D. M., New York, N. Y.
Erney, D. W., Omaha, Nebr.
Feigenbaum, M. L., Buffalo, N. Y.
Forlani, F., Monza, Milano, Italy
Friedlander, M. O., Bethpage, L. I., N. Y.
Fritz, G. L., Fremont, Nebr.
Gahagan, J. W., Danvers, Mass.
Giles, J. R., Midland, Tex.
Giusti, A., Somerville, Mass.
Guth, R. U., Lynchburg, Va.
Haizlip, J. H., Hawthorne, Calif.
Harley, R. L., North Bay, Ont., Canada
Haynes, F. H., Florissant, Mo.
Hinz, H. E., Huntington, L. I., N. Y.
Hodde, R. L., Florissant, Mo.
Holtzer, H., Brooklyn, N. Y.
Hrubes, W. R., Cleveland, Ohio
Humphrie, S-T., Ottawa, Ont., Canada
Hunter, O. E., Anaheim, Calif.
Jayson, R. M., Wright-Patterson AFB, Ohio
Johnson, S. E., Jr., Fort Worth, Tex.
Johnson, D. H., Center Valley, Pa.
Jones, B. L., Ottawa, Ont., Canada
Katz, J., Granada Hills, Calif.
Kelley, F. L., Concord, Mass.
Kline, L., Buenos Aires, Argentina
Lander, B., San Diego, Calif.
Lannan, K. E., Philadelphia, Pa.
Lea, R. H., Danville, Va.
Leach, R. E., Oakland, Calif.
Lebovitz, S., Haddonfield, N. J.
Lenz, E. L., New York, N. Y.
Lodl, J. J., Oxnard, Calif.
Logan, S., Madras, India
Lyon, C. C., Hightstown, N. J.
Magiera, L. E., Lansing, Mich.
Marino, J., Nesconset, L. I., N. Y.
Mathiesen, M., Copenhagen, Denmark
May, F. G., Millis, Mass.
McClure, H. W., Toledo, Ore.
McDermott, H. R., Warrington, Lancashire, England
McDougall, A., Far Hills, N. J.
McFarland, T. O., Moline, Mich.
Mescall, J. J., Santa Barbara, Calif.
Morganti, F., Milano, Italy
Morris, W. T., Middletown, Ohio
Nadarajah, S. S., London, England
Niquette, R., Jr., Los Angeles, Calif.
Nisbett, J. R., Rome, N. Y.
Noll, R. A., North Little Rock, Ark.
Norling, A. E., Mansfield Depot, Conn.
Oswald, J. R., Versailles, France
Owens, J. N., Seattle, Wash.
Patterson, A. D., Albuquerque, N. M.
Pazera, J. A., Hudson, N. Y.
Pennington, F. J., Jr., Somerville, Mass.
Perry, F. G., Barrington, R. I.
Prette, M., Milano, Italy
Ray, R., Zurich, Switzerland
Repchuk, J. S., Poughkeepsie, N. Y.

(Continued on page 92A)

Membership

(Continued from page 90A)

Richardson, C. E., Silver Spring, Md.
Richer, P. J., Huachuca City, Ariz.
Rider, P. M., New York, N. Y.
Ruffman, S. H., Jamaica, L. I., N. Y.
Schmitt, M. J., Towson, Md.
Schwelb, O., Montreal, Que, Canada
Shelton, W. D., Pittsburgh, Pa.
Siahatgar, S., Hyattsville, Md.
Simon, S. S., Stamford, Conn.
Suzuki, C. K., Honolulu, Hawaii
Svete, D. L., Anchorage, Alaska
Terada, H., Tokyo, Japan
Tiedt, M. C., Parma, Ohio
Titterington, E. J., Socorro, N. M.
Trevisan, S., Milano, Italy
Troth, B. J., Columbia, Mo.
Vachha, R. P., Bombay, India
Wall, C. K., Montclair, N. J.
Wareham, W. S., Fort Knox, Ky.
Warner, C. E., Hialeah, Fla.
Watts, M. A., Edmonton, Alta, Canada
White, E. F., Florissant, Mo.
Whyte, J. D., Anzac, Alta., Canada
Wood, R. A., Los Altos, Calif.
Zalter, R., Omaha, Nebr.

NEWS New Products

These manufacturers have invited PROCEEDINGS readers to write for literature and further technical information. Please mention your IRE affiliation.

(Continued from page 56A)

Counter-Timers

Three new all solid-state dc to 10 megacycle counting, timing, and frequency measuring instruments—the first successful high frequency application of transistors to high speed circuitry equipment—have been developed by **Computer-Measurements Co.**, 12920 Bradley Ave., Sylmar, Calif.

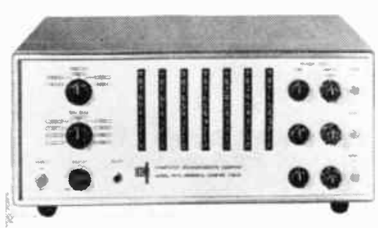

The firm offers these instruments with two year free service warranties.

These 10 megacycle units: the Model 727A Transistor Universal Counter-Timer, the Model 707A Transistor frequency-Period Meter, and the Model 757A Transistor Time Interval Meter are now in production.

The Model 727A combines the functions of a counter, time interval meter, and frequency/period meter. It performs five basic functions selectable by a front panel switch. Input circuitry has been designed to exploit the desirability of remote operation and switching without special regard to cable lengths, type of cable, impedance

(Continued on page 94A)

Subminiature ...
Proven Reliability

ACTUAL SIZE

TRIMPOT® MODEL 220

As many as 17 of these compact units can be mounted in a space of just one cubic inch. Designed for printed circuits and modular assemblies, Trimpot Model 220 measures less than 3/16" x 5/16" x 1". Power rating is 1 watt and maximum operating temperature is 175°C. This Potentiometer meets or exceeds Mil-Specs for humidity, salt spray, fungus, sand and dust, as well as acceleration, vibration and shock. Self-locking 15-turn shaft insures sharp, stable settings...exclusive Silverweld® fused-bond termination and ceramic mandrel provide extreme temperature stability. The Model 220 is available in a wide variety of resistance ranges and a choice of two terminal types—gold-plated Copperweld wire or insulated stranded leads.

Stocked by leading electronic distributors across the nation, these units are ready for immediate delivery. **Write for complete technical data and list of stocking distributors.** AVAILABLE AS PANEL MOUNT UNIT (illustrated at right) with same specifications.

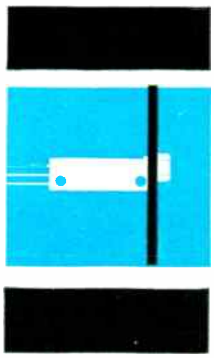

BOURNS

Bourns, Inc., Trimpot Division
6135 Magnolia Ave., Riverside, Calif.
Plants: Riverside, California
and Ames, Iowa

Exclusive manufacturers of Trimpot®, Trimit®. Pioneers in potentiometer transducers for position, pressure and acceleration.

NEWS New Products

(Continued from page 92A)

matching, etc. All functions are brought to the rear. This flexibility makes the instrument useful for automatic programming of the control functions.

The Universal Counter-Timer consists of three input channels, a special decade countdown time base, time which eliminates the need for divider adjustment, and a series of plugin, transistorized decade counting units. Output information from each DCU will operate digital printers, punches, inline readouts and other data processing equipment. Readout is available in either the standard vertical numeral panels as shown or in the inline Nixie version.

The Universal Counter-Timer's measurement ranges are dc to 10 mc for frequency; 0.1 μsec to 10^7 second for time interval; 0.1 μsec for period. Frequency converters are available for higher frequencies.

Accuracy is ± 1 count $\pm$oscillator stability. Sensitivity is 0.25 volt rms; input impedance is 25 K ohms per volt.

Prices of the three instruments are: Model 727A Universal Counter-Timer, $3,500; Model 707A Frequency Period Meter, $2,700; Model 757A Time Interval Meter, $2,500.

For complete information, write to the firm.

Kaminski Heads New Clare Firm

C. P. Clare Transistor Corp., Glen Head, N. Y., announces the election of Amos Kaminski, former chief research scientist of General Transistor Corporation, as president. The new company is a sister company to C. P. Clare & Co., Chicago manufacturer of relays and allied electronic components. C. P. Clare, president of the Chicago company, and executive vice president of Universal Controls, is chairman of the board of the new company.

The new Clare transistors are of the alloyed junction type and are custom-built to meet the specific design requirements of computers and other high speed devices. Four major classifications include Germanium PNP, Germanium NPN, Silicon PNP, and Silicon NPN. All are of low and medium power dissipation ratings (up to 250 mw). Frequency cutoff is between 3 and 30 mc, varying from type to type.

The new transistors will be sold through all C. P. Clare & Co. sales offices. A projected ultra-modern plant specially designed for the manufacture of semiconductor circuit components is expected to greatly increase production facilities next year (Continued on page 98A)

STABILITY & HEAT BARRIER BROKEN

with Metal-Ceramic Variable Resistor

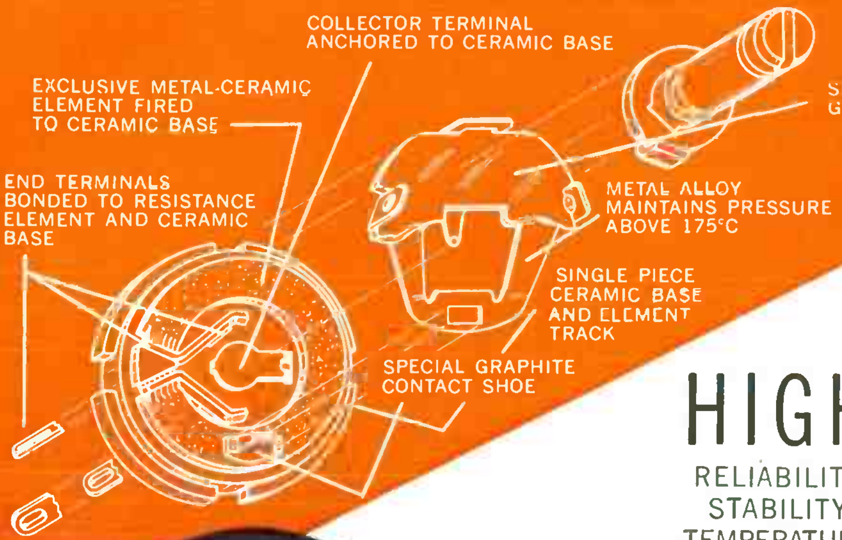

HIGH
RELIABILITY
STABILITY
TEMPERATURE

Miniature
CeraTrolS
with new metal-ceramic element

CeraTrolS' rugged, hard-surfaced metal-ceramic element, having been fired at temperatures exceeding 600°C, meets temperatures up to 500°C with high safety factors at ratings listed below.

New Series 600 Characteristics:

- Infinite resolution.
- 100 ohms thru 5 meghoms (linear taper) resistance range.
- ½" diameter; interchangeable with Style RV6 MIL-R-94B.
- Power ratings: ¾ watt @ 85°C, ½ watt @ 125°C, zero load @ 175°C.

CTS ®

COMPARATIVE TEST DATA: No carbonaceous variable resistors (either film or molded) can equal Series 600 performance. Ideal for critical applications requiring high stability and reliability. Far exceeds MIL-R-94B.

Tests	MIL-R-94B (Style RV6, Char. Y) Requirement	Series 600 CTS Maximum	Series 600 CTS Average
Load life 1000 hrs.			
½ watt @ 125°C, 350 V max.	±10% @ 70°C	±7% @ 125°C	±4% @ 125°C
¾ watt @ 85°C			
Thermal Stability (1000 hrs. @ 175°C no load)	No test in MIL-R-94B	±5%	±3%
Temperature Co-eff.* (Room to −63°C; room to +175°C)	No test in MIL-R-94B		
25K and over		±250 PPM/°C	±150 PPM/°C
under 25K		±500 PPM/°C	±300 PPM/°C
Moisture Resistance	± 6% avg. ±10% max.	± 2% avg. ± 4% max.	±1.3%
Low Temp. Storage	±2%	±1%	±.5%
Low Temp. Operation	±3%	±2%	±1%
Thermal Cycling	±6%	±3%	±2%
Voltage Co-efficient	No test in MIL-R-94B	±.01%/volt	±.005%/volt
Rotational Life	±10% (after 25,000 cycles)	±10%	±7.5%
Acceleration	±3%	±2%	±1%
High Freq. Vibration	±2%	±2%	±1%
Shock	±2%	±2%	±1%

* Lower temperature coefficient can be developed for specific applications.

Newly developed 500°C Metal-Ceramic Resistance Element is separately available for other applications than variable resistors. Because the element is very stable to 500°C, it is extremely reliable at the elevated temperatures currently demanded and anticipated in military requirements. Ceramic bases can be made in a wide variety of shapes and sizes; the metal resistance film can be made to cover an entire surface or an accurately defined pattern. Consult CTS engineers on your requirements.

Note Exceptional Stability. Note extent that MIL-R-94B is exceeded.

Complete Series 600 CeraTrolS electrical and mechanical specs and dimensional drawings will be sent upon request.
CTS manufactures a complete line of composition and wirewound variable resistors for military, industrial and commercial applications. CTS specialists are willing to help solve your variable resistor problems. Contact your nearest CTS office today.

Founded CTS 1896

Factories in Elkhart & Berne, Indiana, South Pasadena, California, Asheville, No. Carolina and Streetsville, Ontario. Sales Offices and Representatives conveniently located throughout the world.

CHICAGO TELEPHONE SUPPLY
Corporation
ELKHART • INDIANA

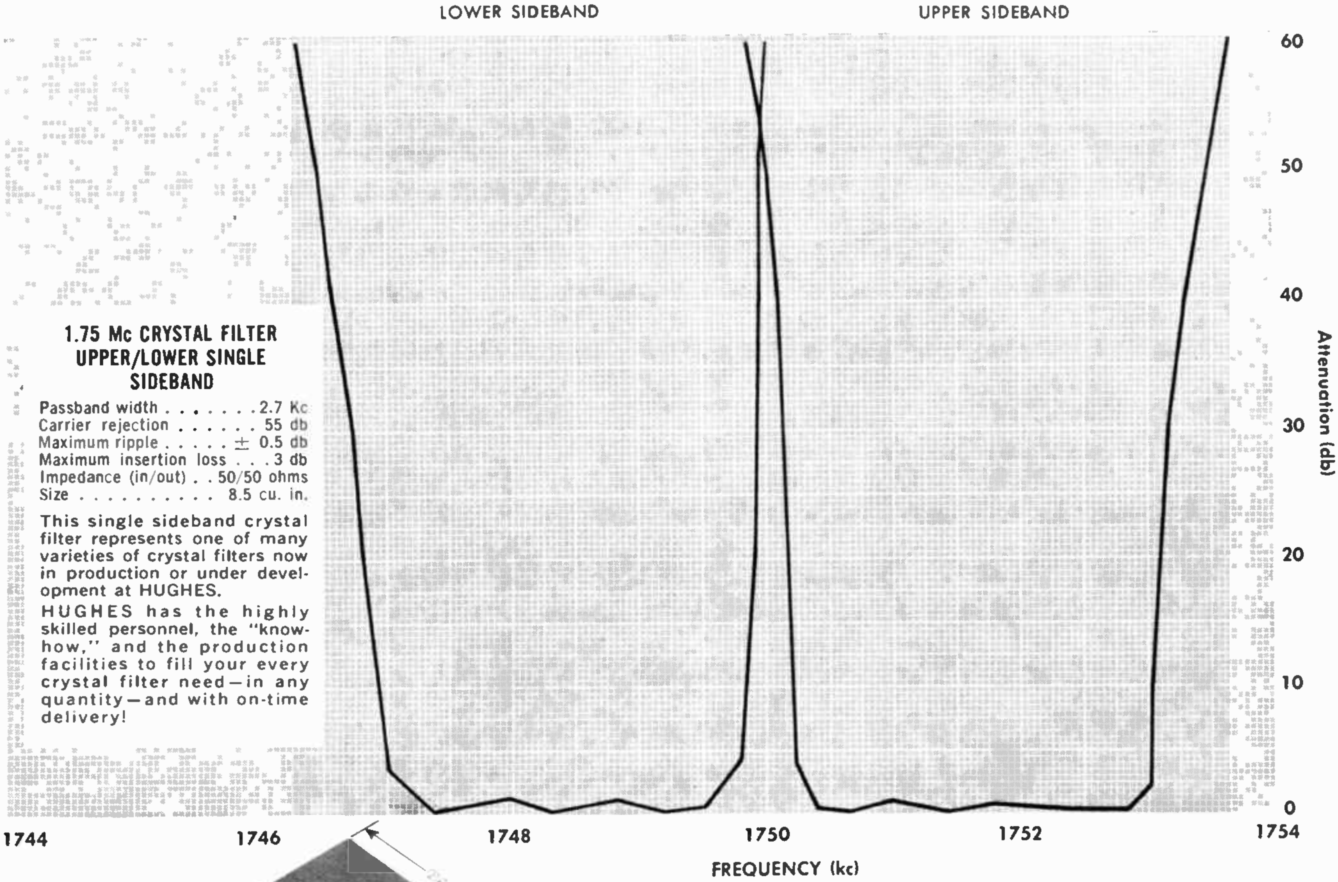

1.75 Mc CRYSTAL FILTER UPPER/LOWER SINGLE SIDEBAND

Passband width . . . . 2.7 Kc
Carrier rejection . . . . . . 55 db
Maximum ripple . . . . . ± 0.5 db
Maximum insertion loss . . . 3 db
Impedance (in/out) . . 50/50 ohms
Size . . . . 8.5 cu. in.

This single sideband crystal filter represents one of many varieties of crystal filters now in production or under development at HUGHES.

HUGHES has the highly skilled personnel, the "know-how," and the production facilities to fill your every crystal filter need—in any quantity—and with on-time delivery!

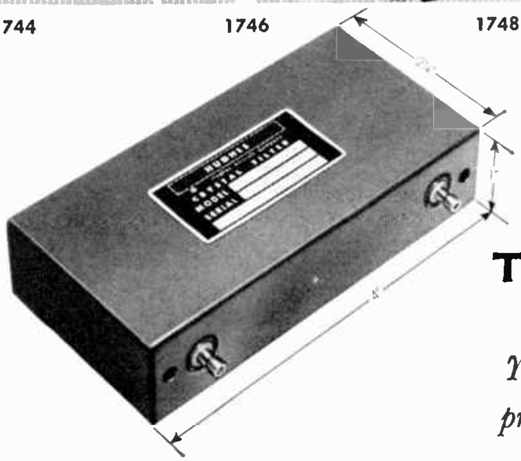

TIGHTEN YOUR "SPECS" WITH HUGHES CRYSTAL FILTERS

Your difficult filtering problems solved with high-performance, precision crystal filters custom-designed and produced for you!

Do you face tough filtering problems in: Single Sideband, Doppler Systems, Missile Guidance, Radio Communications, Radar and Navigation, Spectrum Analyzers, Carrier and Multiplexing, Frequency Shift, High Selectivity Amplifiers?

Check these advantages of Hughes precision crystal filters: Small size, light weight, low insertion loss, low passband ripple, precise selectivity, high frequency filtering, wide temperature stability, high reliability, rugged resistance to shock/vibration, quick delivery in quantity.

Experienced Hughes Application Engineers are available to work with you on your filtering problems. For additional information on crystal filters with center frequencies of 30 kc to 52 mc, and fractional bandwidths of 0.01%-6.0%, write: HUGHES, *Industrial Systems Division, International Airport Station, Los Angeles 45, California.*

For export information, write: Hughes International, *Culver City, California.*

Creating a new world with ELECTRONICS

HUGHES

INDUSTRIAL SYSTEMS DIVISION

Microwave Component News from SYLVANIA

Tee Circulator—FD-TC531—typical of Sylvania's tee circulator and isolator line is this model, which operates at 24 KMC, weighs only three ounces and is 1½" x 1½" x ¾". It is less expensive than conventional phase shift circulators. The line covers from 5.4 to 26 KMC.

22 TYPES OF FERRITE DEVICES NOW IN FULL PRODUCTION AT SYLVANIA

COMPETITIVELY PRICED

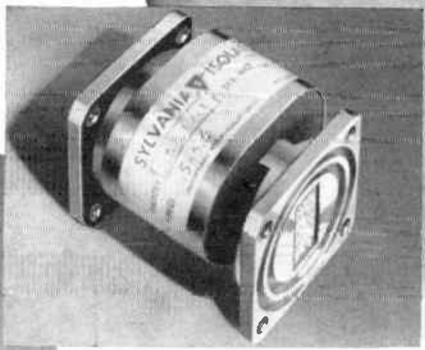

Waveguide Isolator—FD-5213A—this miniature X-band isolator is representative of Sylvania's success in miniaturizing these important components. Units from 2.6 to 26 KMC are available.

Coaxial Isolator—FD-151P—representative of Sylvania's coaxial line, it gives octave coverage. The units in this line exhibit unequalled electrical performance and cover the range from 1 through 11 KMC.

EXPANDED facilities now make it possible for Sylvania to offer 22 different ferrite devices as full production items at competitive prices. These production units represent over one-third of the types now in Sylvania's growing line of ferrite devices.

Modifications of Sylvania ferrite devices can be provided within three weeks. In addition, new types developed to meet your special requirements can be delivered in as little as 60 days, and we can be in full production on these new items within 60 days after design approval.

All ferrite devices in the line are made to Sylvania's recognized high standards and have these characteristics:

FREQUENCIES from 1 to 26 KMC
ISOLATION up to 80 db
INSERTION Loss as low as 0.2 db

SYLVANIA GENERAL SYSTEM
Subsidiary of
GENERAL TELEPHONE & ELECTRONICS

Sylvania Electric Products Inc.
Special Tube Operations
500 Evelyn Ave., Mountain View, Calif.

New Catalog—Get this new ferrite catalog free from your Sylvania sales office, or by writing to the address below.

NEWS New Products

These manufacturers have invited PROCEEDINGS readers to write for literature and further technical information. Please mention your IRE affiliation.

(Continued from page 94A)

Delay Lines Bulletin

Bulletin DL1159, released by **Valor Instruments, Inc.**, 13214 Crenshaw Blvd., Gardena, Calif., describes a standard line of miniature lumped constant delay lines. Data are provided on the electrical specifications, packaging and the construction techniques which enable a high degree of miniaturization. Design factors that should be considered when establishing specifications for special delay lines are also explained.

Multi-Channel Transducer Supply

Up to six transistor-regulated isolated power supplies can be relay-rack mounted on a standard 3½-inch panel using the new MA603A Panel Mounting Assembly now offered by **Elcor, Inc.**, 1225 W. Broad St., Falls Church, Va. Designed for supplying multiple strain gage or other transducer systems, the six small isolated power supplies (ISOPLYS) that are employed in this ensemble are individually isolated from ground and individually adjustable in output voltage. The two or three units may be employed initially in this assembly and other units added later as the system is expanded. All units are easily removable for replacement, repair or testing.

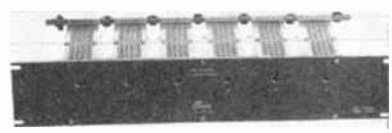

Sixteen models of power supplies covering from five to fifty volts dc output make this mounting assembly useful with diverse transducer systems. Each of the six channels may have its regulated output voltage adjusted from the front panel over a range of about 15%. Special features of the power supplies include 40 $\mu\mu$f shunt capacitance between output and ground, less than 10 microvolts of hum and noise per kilohm impedance to ground, temperature coefficient for output voltage less than 0.02% per degree F, and leakage resistance to ground greater than 100,000 megohms.

Computer Training Course

An industrial training course in analog computers is offered for technicians, engineers and management by **EBEX Technical Institute, Inc.**, Orem, Utah. The course is entirely conducted by correspondence with a certificate of completion given. No prerequisites are required. Theory, practical applications, case histories and illustrated equipment evaluation are given. Write to ETI, industrial training Dept., EBEX Sales Inc., Orem, Utah.

(Continued on page 106A)

FREQUENCY STANDARDS

*3⅛" high
400 - 1000 cy.

PRECISION FORK UNIT
TYPE 50

Size 1" dia. x 3¾" H. Wght., 4 oz.*

Frequencies: 240 to 1000 cycles
Accuracies:—
Type 50 (±.02% at —65° to 85°C)
Type R50 (±.002% at 15° to 35°C)
Double triode and 5 pigtail parts required
Input, Tube heater voltage and B voltage
Output, approx. 5V into 200,000 ohms

FREQUENCY STANDARD
TYPE 50L

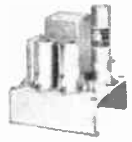

Size 3¾" x 4½" x 5½" High
Weight, 2 lbs.

Frequencies: 50, 60, 75 or 100 cycles
Accuracies:—
Type 50L (±.02% at —65° to 85°C)
Type R50L (±.002% at 15° to 35°C)
Output, 3V into 200,000 ohms
Input, 150 to 300V, B (6V at .6 amps.)

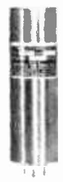

*3½" high
400 to 500 cy.
optional

PRECISION FORK UNIT
TYPE 2003

Size 1½" dia. x 4⅛" H. Wght. 8 oz.*

Frequencies: 200 to 4000 cycles
Accuracies:—
Type 2003 (±.02% at —65° to 85°C)
Type R2003 (±.002% at 15° to 35°C)
Type W2003 (±.005% at —65° to 85°C)
Double triode and 5 pigtail parts required
Input and output same as Type 50, above

FREQUENCY STANDARD
TYPE 2005

Size, 8" x 8" x 7¼" High
Weight, 14 lbs.

Frequencies: 50 to 400 cycles
(Specify)
Accuracy: ±.001% from 20° to 30°C
Output, 10 Watts at 115 Volts
Input, 115V. (50 to 400 cycles)

FREQUENCY STANDARD
TYPE 2007-6 **NEW**

TRANSISTORIZED, Silicon Type
Size 1½" dia. x 3½" H. Wght. 7 ozs.

Frequencies: 400 — 500 or 1000 cycles
Accuracies:
2007–6 (± .02% at —50° to +85°C)
R2007–6 (±.002% at +15° to +35°C)
W2007–6 (±.005% at —65° to +125°C)
Input: 10 to 30 Volts, D. C., at 6 ma.
Output: Multitap, 75 to 100,000 ohms

FREQUENCY STANDARD
TYPE 2121A

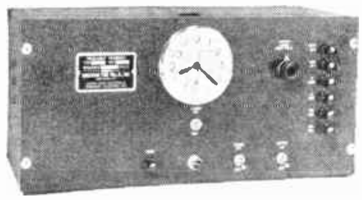

Size
8¾" x 19" panel
Weight, 25 lbs.

Output: 115V
60 cycles, 10 Watt
Accuracy:
±.001% from 20° to 30°C
Input, 115V (50 to 400 cycles)

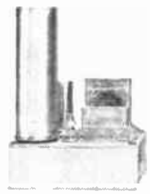

FREQUENCY STANDARD
TYPE 2001-2

Size 3¾" x 4½" x 6" H., Wght. 26 oz.

Frequencies: 200 to 3000 cycles
Accuracy: ±.001% at 20° to 30°C
Output: 5V. at 250,000 ohms
Input: Heater voltage, 6.3 - 12 - 28
B voltage, 100 to 300 V., at 5 to 10 ma.

FREQUENCY STANDARD
TYPE 2111C

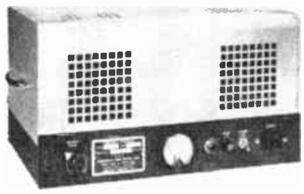

Size, with cover
10" x 17" x 9" H.
Panel model
10" x 19" x 8¾" H.
Weight, 25 lbs.

Frequencies: 50 to 1000 cycles
Accuracy: (±.002% at 15° to 35°C)
Output: 115V, 75W. Input: 115V, 50 to 75 cycles.

ACCESSORY UNITS
for TYPE 2001-2

L—For low frequencies
multi-vibrator type, 40-200 cy.
D—For low frequencies
counter type, 40-200 cy.
H—For high freqs, up to 20 KC.
M—Power Amplifier, 2W output.
P—Power supply.

This organization makes frequency standards within a range of 30 to 30,000 cycles. They are used extensively by aviation, industry, government departments, armed forces—where maximum accuracy and durability are required.

WHEN REQUESTING INFORMATION
PLEASE SPECIFY TYPE NUMBER

American Time Products, Inc.

Watch Master
Timing Systems

Telephone: PLaza 7-1430

580 Fifth Ave., New York 36, N. Y.

Professional Group On Electronic Computers

The electronics computer today stands as one of the most important of all engineering tools and is in widespread use in many military, industrial, and scientific applications. And yet just a decade ago, only a handful of these machines were in existence.

The field of electronic computers is thus one of the youngest and fastest growing branches of the radio engineering art. The rapid expansion of this field led to an urgent need for a means whereby the computer engineer could readily keep abreast of the many developments in this important new field.

In response to this need, the IRE Professional Group on Electronic Computers was formed in October of 1951. Interest in the Group was so great that membership has now grown to more than 8800.

The principal activity of the Group is the Publication of TRANSACTIONS, containing technical papers describing recent developments in the computer field, reviews of current literature, and news. TRANSACTIONS is published quarterly and sent to all Group members who have paid the annual assessment of $4. Thus the Group member is provided with an invaluable source of authoritative information in his particular field of specialization.

Each year the Electronic Computer Group co-sponsors computer conferences on both the East and West Coasts, and organizes several sessions at the IRE National Convention.

In addition to these national meetings, the Group has organized some 19 Chapters all over the country which hold local meetings in conjunction with IRE Sections, thus filling out a program of technical activities which has proved indispensable to the computer engineer.

W. R. G. Baker

Chairman, Professional Groups Committee

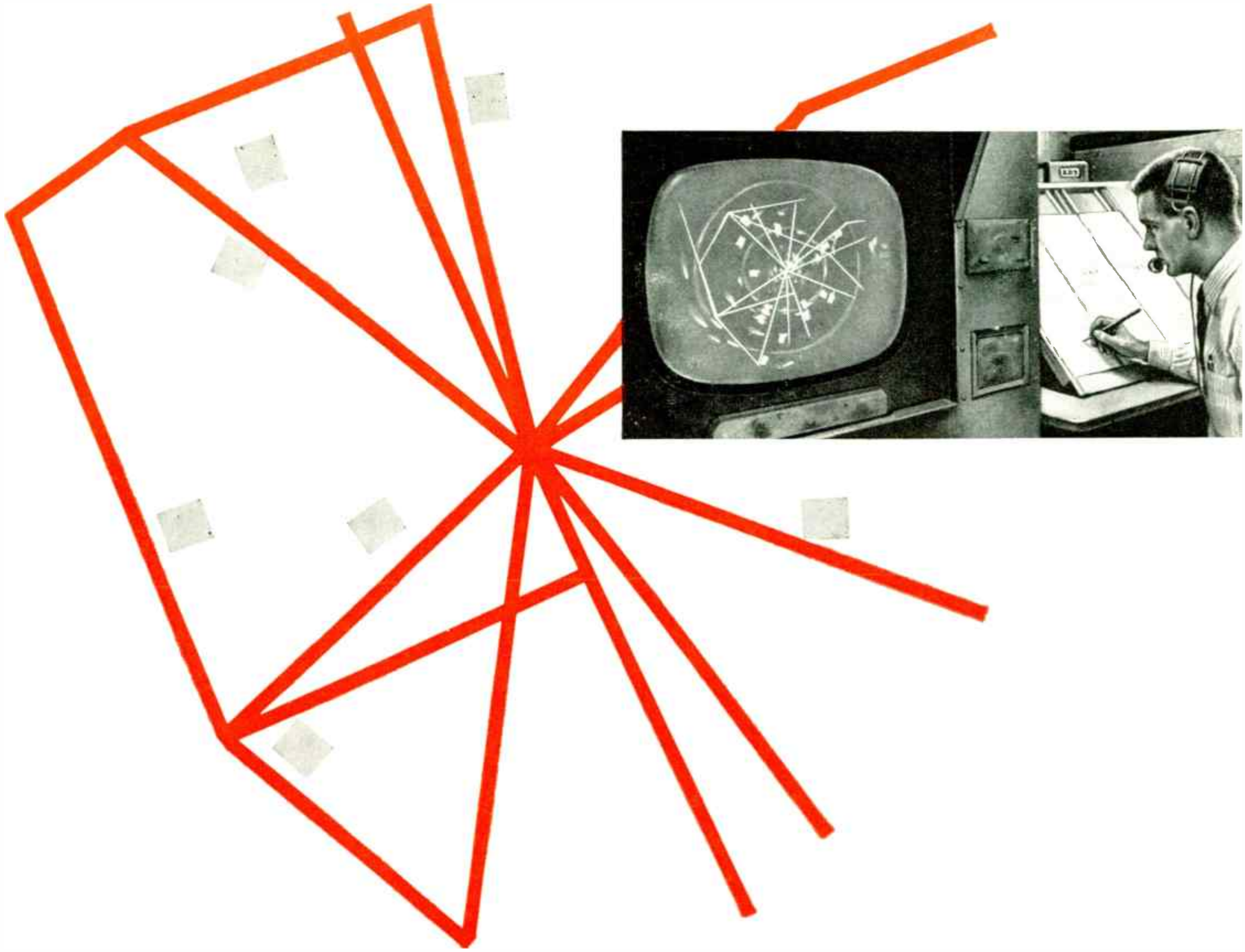

New RCA Scan-Conversion Tube  Makes Possible Brighter and Larger Air-Traffic-Control Displays

Once again RCA Tube Engineers have provided another practical answer to the long-standing problem of large-screen radar display in brightly lighted rooms. The answer . . . RCA-7539 Scan-Conversion Tube.

The 7539 is designed to transform signal information continuously from one time base to another. For example, PPI information generated by a conventional radar system can be processed by this tube for display on a high-resolution, large-screen TV monitor for comfortable viewing in a brightly lighted room.

Depending on system requirements, the persistence of information in the display is adjustable from several seconds to more than a minute. Moreover, writing and reading may take place simultaneously without recourse to rf carrier techniques of signal separation.

The resolution capability of the 7539 is 150 range rings per display radius with a response of 50% or better. To utilize fully the resolution capability of the 7539, the TV monitor system must be designed for resolution in excess of 1000 TV lines.

For complete information about RCA-7539 and its possible applications, contact the RCA Field Office nearest you. Technical bulletin for the 7539 will be available about January 15. For a free copy, write RCA Commercial Engineering, Section B-35-Q, Harrison, N. J.

ANOTHER WAY RCA SERVES YOU THROUGH ELECTRONICS

RCA®

RADIO CORPORATION OF AMERICA ***Electron Tube Division*** ***Harrison, N. J.***

Government Sales: Newark 2, N. J., 415 S. Fifth St., HUmboldt 5-3900; Dayton 2, Ohio, 224 N. Wilkinson St., BAldwin 6-2366; Washington 6, D.C., 1625 "K" St., N.W., District 7-1260
Industrial Tube Products Sales: Newark 2, N. J., 744 Broad Street. HUmboldt 5-3900; Detroit 2, Mich., 714 New Center Building, TRinity 5-5600; Chicago 54, Ill., Suite 1154, Merchandise Mart Plaza, WHitehall 4-2900; Los Angeles 22, Calif., 6355 E. Washington Blvd., RAymond 3-8361

February, 1960
Vol. 48 No. 2

Proceedings of the IRE

Poles and Zeros

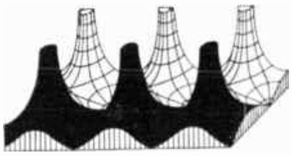

Transition. As a new editor takes over the commas, colons, cedillas, and carets of the IRE publishing activity (and active it is), it is his fervent wish that the transition is sufficiently smooth to avoid any excessive increase in the extremely satisfactory standing-wave ratio established by his predecessors. To follow in the footsteps of Goldsmith, Pierce, Fink, and Ryder, and maintain the excellence of IRE publications to which they have accustomed the reader, is a challenging task. The bylaws assign this task to the Editorial Board, which is charged with the responsibility of advising "the Board of Directors concerning all matters of editorial policy, the publication of the PROCEEDINGS OF THE IRE, including policy determination of its editorial and technical content, and general publication policies for IRE publications." The Editor and the Editorial Board trust that their efforts will be pleasing to the membership.

A specific task that the Editor inherits is that of preparing the text of the Poles and Zeros page established by Editor Fink. From the passive viewpoint of a reader this feature of the PROCEEDINGS has always been interesting and informative and has certainly achieved the intent of its initiator as "a regular page of editorial comment on matters of concern to the IRE membership." From the active viewpoint, forced on one who must author this feature, the striking aspect of Poles and Zeros through its history is an ingenuity of its authors in providing commentary month-by-month on an amazingly diverse series of engrossing topics. A glance at the index over the years reveals subjects ranging from A—"Aids in Preparation and Utilization of IRE Publications" through the alphabet to W—"Wescon." So far no theme has occurred in the X, Y, Z portion of the alphabet. Perhaps this deficiency can be remedied in the coming months. One final point—in a single year Poles and Zeros word-wise requires as much paper and ink, and perhaps writing time, as an average length technical paper; if the topics are of interest (as they have been in the past) the feature is justified, if not, it should, in the words of its founder, be "howled out of existence." To the Editor this means that feedback, positive or negative, is important; suggestions and criticisms are invited.

International Again. Poles and Zeros in December, 1959, told briefly of the Institute and something of its international perspective. To add further emphasis, it is a pleasure to welcome the India Section to the family of IRE and proclaim it number 105. The new Section, which comprises the whole of the country of India, is also the twenty-second outside of the United States. May it grow and prosper (perhaps one day it can entertain the Board of Directors in the shadow of the Taj Mahal).

Peripatetic Presidents. Throughout the history of IRE, and other professional societies as well, one of the natural functions of the society's President seems to have been that of visiting the geographically scattered Sections of the Institute, appearing at conventions, national and regional, and attending special conferences of his own and sister societies. A visit by a President to a Section is rightfully considered a very special occasion, and there is no question of the value of top management learning at first hand the grass root reaction. The wear and tear on the President physically, as well as the tremendous expenditure of time demanded of this nonremunerative office, cannot be ignored.

It has become obvious, as the exponential growth of the Institute continues, that it is unrealistic to expect a President to visit even a fraction of the Institute Sections during this term of office. Try to fit into your own busy life a travel schedule to eighty-three United States and thirteen Canadian Sections. The Board has clearly taken note of the travel problem faced by its President and the Vice-President (residing in North America) and has decreed that annual visits to all Sections by either is neither possible nor practical. It has delegated the responsibility of visiting a nominal number of Sections to the Vice-President (residing in North America) during his period of office. He can devote more time in these fewer visits in the better interest of the Sections and the Institute. The President is thus to be free of the responsibility of Section visits in order to permit him to meet the many other demands on his time that are concomitant with the expanding activities of the Institute. The Board of Directors is confident that this decision will meet with the approval of the Institute membership.

Cumulative Index. Last September Poles and Zeros announced that a new five-year cumulative index would be available soon. It was published last month; to add it to your library see page 14A of this issue of the PROCEEDINGS. No longer can there be complaints about finding material for the years covered by the 1954–1958 index which is striking for its new feature of providing easy access to *all* IRE publications in a simple manner never before available. The index is interesting, too, for the light it sheds on the remarkable growth of the Institute publishing program.

A brief study of earlier indexes, and a comparison with the newest, reveals the astonishing fact that in the five years 1954–1958 more articles were published than in the previous forty-one years of IRE publication. Indeed, the number of articles tripled in both of the last two five-year periods. If this rate continues the present five-year period may produce over 20,000 papers. Editor Ryder's prediction last December that the Professional Groups may have monthly TRANSACTIONS by 1965 would appear to be pessimistic!

Convention Record. The out-of-print sections of the 1959 IRE NATIONAL CONVENTION RECORD and the IRE WESCON CONVENTION RECORD for 1959 have been reprinted and are again available. See pages 22A and 23A for ordering information.

—F. H., Jr.

John N. Dyer

Vice President, 1960

John N. Dyer was born in Haverhill, Mass. on July 14, 1910. He attended Massachusetts Institute of Technology and received the B.S. degree in electrical engineering in 1931.

Upon his return to this country from the Byrd Antarctic Expedition in 1935, Mr. Dyer served as a radio engineer in the General Engineering Department of the Columbia Broadcasting System. In 1937 he became Assistant Chief Television Engineer for that company and was involved in the development of color television. He was associated with CBS for nine years, starting in 1933.

During the war Mr. Dyer was with the Radio Research Laboratory of Harvard University as head of the transmitter group. He was responsible for the line of "carpet" jamming transmitters that are credited with saving large numbers of the Eighth Air Force B-17. He then became director of the American-British Laboratory, Division 15, of the National Defense Research Committee. During 1944 it was his responsibility to assist the services in making maximum use of the countermeasure equipment development at Harvard and other U. S. laboratories.

In 1945 Mr. Dyer joined Airborne Instruments Laboratory, Radar and Air Navigation Section, as Supervising Engineer. He became Director of the Research and Engineering Division in 1950 and Vice President and a member of the Board of Directors of the laboratory in 1951. After he became Vice President, the Research and Engineering Division grew to an organization which has entered into many important military, governmental and industrial programs in different phases of electronics and now numbers more than 1,000 people. Mr. Dyer remained a Director of AIL until the merger of the company with Cutler-Hammer, Inc., in 1958. He is now Vice President and Technical Director of the AIL division, and Assistant Secretary of Cutler-Hammer.

Mr. Dyer joined the IRE in 1930 as a Junior Member. He became an Associate in 1932 and a Senior Member in 1945. In 1949 he received the Fellow Award "for administrative and technical contributions to radio, including polar-expedition communications and important wartime radio countermeasures." Mr. Dyer, a past Chairman of the IRE Policy Advisory Committee and the Fellows Committee, has served on numerous IRE committees. In 1950 he was elected Chairman of the Long Island Subsection. He served as a Director of the IRE in 1955–1956. He is the first to serve in the newly-created office of Vice President Residing in North America under the recently amended IRE Constitution which provides for two IRE Vice Presidents.

Scanning the Issue

PERCOS—Performance Coding System of Methods and Devices Used for Measurement and Control (Keller, p. 148)—Working in close cooperation with the IRE Technical Committee on Industrial Electronics, the author has developed a numeric system for classifying, coding and cataloging the twelve most important functions and performance characteristics of the many components which are found in measurement and control systems. These twelve ratings may then be catalogued by means of edge-coded cards. The result is a system which substantially simplifies the task of a designer in selecting a chain of compatible devices to achieve a system of prescribed accuracy and reliability. It is hoped and believed that this system will find wide application among many industrial and government organizations.

100:1 Bandwidth Balun Transformer (Duncan and Minerva, p. 156)—Within the past year or two important progress has been made in the development of new types of antennas with bandwidths much greater than had previously been thought possible. The future utility of these new antenna designs, however, will depend on the corresponding development of very broad-band components. This paper concerns one such component development. The balun described here is a transmission line section which starts off at one end as a coaxial cable and winds up at the other end as a balanced two-wire transmission line of the type frequently required to feed broad-band antennas. In addition to achieving a physical transition from one type of line to another, the balun also maintains an excellent impedance match over frequency bandwidths as great as 100 to 1.

Measurement of Internal Reflections in Traveling-Wave Tubes Using a Millimicrosecond Pulse Radar (Melroy and Closson, p. 165)—Small irregularities in the helix of a traveling-wave tube cause internal reflections which, in the case of pulse code transmission, may result in echo pulses which could distort the meaning of the code. The accurate location of helix faults has now been made possible by an ingenious technique which employs radar pulses to perform measurements at distances of 2 feet or less and a stroboscopic system for viewing the echoes. This paper will be of interest both as a solution to a very exacting and delicate instrumentation problem and as a method of obtaining valuable new data affecting traveling-wave tube design and performance.

Noise Consideration of the Variable Capacitance Parametric Amplifier (Uenohara, p. 169)—One of the most widely discussed topics in recent months concerns the use of variable capacitance diodes as very-low-noise amplifiers. This paper, in formulating a theoretical model of the noise source in amplifiers of this type, therefore goes to the heart of this timely subject. A simplified theory is developed which introduces a new and useful "quality factor" for representing and calculating the performance potential of diodes. Confirming experiments with a gallium arsenide diode yield a very low 0.9 db noise figure for double-sideband operation and 3.9 db for single sideband. The discussion points up the necessity of differentiating between single- and double-sideband operation when speaking of noise figures, a pitfall into which this column fell in the January, 1959 issue.

Reliability Analysis Techniques (Krohn, p. 179)—This paper presents an excellent nonmathematical picture of the substantial progress that has been in the last few years in developing effective techniques for analyzing the reliability of electronic equipment. The author wrote the paper with the typical nonspecialist particularly in mind. All readers will find this a valuable, introduction to an important subject.

A Stabilized Locked-Oscillator Frequency Divider (Scott, p. 192)—An important class of subharmonic generators is that which makes use of the locking property of oscillators. This paper deals with a particular type within that class which has the combined attributes of other types, namely, it is easily synchronized and at the same time provides a high degree of frequency stability. The circuit is simple, practical and useful, and will be of interest in the design of frequency and interval standards used in almost all phases of electronics. Moreover, the author's graphical analysis technique might well be applied to all types of synchronized oscillators.

IRE Standards on Television: Measurement of Differential Gain and Differential Phase, 1960 (p. 201)—This Standard provides a useful operational and maintenance test for determining whether the phase or amplitude of the chrominance component of a color television signal is being altered by virtue of its being superimposed on a varying base, *i.e.*, the monochrome component. Such tests are important because a variation in phase or amplitude may cause undesirable variations in the colors reproduced by the receiver.

Compandor Loading and Noise Improvement in Frequency Division Multiplex Radio-Relay Systems (Rizzoni, p. 208)—A compandor consists of a device which redistributes the speech volume at the input of a channel for high efficiency of transmission and a device which restores the speech to its original form at the channel output. The effect of a compandor is to improve the intelligibility of speech over noisy circuits and to change, generally for the better, the loading of channels. When used in microwave or scatter communication systems, compandors will permit among other things longer hops, lower antenna gain, lower transmitter power or lower receiver sensitivity. Whether these advantages pay for the expense of the compandors depends on a number of factors, although where high quality is required, compandors always result in the most economical system. This paper provides system designers with the means for calculating the improvement that would result from using compandors, thereby enabling them to arrive at an optimum system design.

Piezoelectric Properties of Polycrystalline Lead Titanate Zirconate Compositions (Berlincourt, *et al*, p. 220)—Valuable data are given on a new piezoelectric ceramic which, despite its forbidding name, seems destined to have very wide application in underwater sound transducers, delay lines and mechanical filters. It has been found that lead titanate zirconate compositions have remarkably higher piezoelectric effects than the presently used barium titanate ceramic, a fact which will interest a wide circle of readers.

Further Consideration of Bulk Lifetime Measurement with a Microwave Electrodeless Technique (Jacobs, *et al.*, p. 229)—A new method of measuring the lifetime of excess carriers in semiconductors has been developed which uses a steady source of light to generate excess holes and electrons. By locating a sample of the material in a waveguide and measuring changes in microwave absorption as the distance between the sample and light source is varied, bulk lifetime can be determined. This technique makes an interesting addition to the list of lifetime measurement methods, one that avoids the complications of electrode attachments and surface recombination effects.

The Application of Linear Servo Theory to the Design of AGC Loops (Victor and Brockman, p. 234)—This paper gives an interesting, well-written description of an application of feedback control theory to the problem of automatic gain control in radio receivers. The key to the authors' contribution is their recognition that an almost linear relationship exists between signal level and receiver attenuation when both are expressed in db relative to unity. By thus linearizing the problem, they have been able to apply linear servo theory to its solution with excellent results.

Scanning the Transactions appears on p. 268.

PERCOS—Performance Coding System of Methods and Devices Used for Measurement and Control*

ERNEST A. KELLER†, SENIOR MEMBER, IRE

The manuscript of Dr. Keller's paper on a proposed Performance Coding System was prepared upon request, and with the active cooperation of the IRE Technical Committee on Industrial Electronics and its Subcommittee 10.3 on Industrial Electronics Instrumentation and Control. Both the proposed system and the definitions suggested therein found approval by potentially large user groups outside of the IRE, such as the Instrument Society of America, and various government and industrial organizations.

By sponsoring the publication of this report in the PROCEEDINGS OF THE IRE, the Industrial Electronics Committee hopes to have contributed to the solution of the ever-increasing problems of equipment classification and specifications. If used consistently both by manufacturers and users of electronic devices, the proposed system could go far toward an unambiguous and clarified language in technical specifications.

Eugene Mittelmann
Chairman
IRE Committee on
Industrial Electronics

Summary—**This paper describes a classifying and coding system of functions and performance characteristics of devices in a way that is useful to the systems designer, who must select a chain of compatible instruments to achieve a measurement or control system of prescribed accuracy and reliability.**

The performance coding system consists of numeric codes for rating a device in terms of twelve parameters of importance to the over-all performance of the system, such as precision, stability of calibration, rate of performance, useful shelf life, mean operating time to failure, average repair time, cost, availability and physical volume.

The numeric codes provide a quantitative description of the performance data to the nearest order of magnitude only. However, this broad classification is consistent with the magnitude of the expected span of performance data of all the devices in a complex system.

An edge coded card system is described for the selection of devices or methods complying with the performance parameters. The individual card specifies the exact technical data of the device, the input and output requirements, and especially the environmental conditions under which the performance parameters are given.

This classification is established for and with the cooperation of IRE Subcommittee 10.3 of the Industrial Electronics Committee.

INTRODUCTION

THE goal of a good classification is to provide a systematic procedure to locate a desired specific piece of information or item out of a large quantity of data or units. The systematic procedure is preferred over the trial method, because the results are generally obtained faster and more easily.

Classification provides as a byproduct a family tree of descriptive terms for the common features of a class or group of units, as well as for the individual details of a specimen.

It is sometimes implied that the quality of a classification can be appraised by the amount of details given for specimens. This is certainly true for many phases of scientific endeavor. In botany, for instance, it is necessary to describe the major and minor differences in logically progressing subdivisions, identifying, finally, one species from another.

* Original manuscript received by the IRE, January 28, 1959; revised manuscript received, August 20, 1959.
† Motorola, Inc., Chicago, Ill.

This type of successive division of classes is very often accomplished by using the decimal coding system. This system has the advantage that neither the quantity of items of the same order nor the number of successive subdivisions is limited. In this respect, the decimal classification system is the most logical and useful coding system.

It should be pointed out, however, that the possibility of subdividing classes into subclasses and sub-subclasses should not be interpreted as a necessity for best service to the user.

The desirable degree of subdivision is determined by the purpose of the classification and by evaluating the ratio of increase in detail data to the gain in new dependable information, derived from this data increase. This ratio of information content per data quantity gains in importance as industry progresses more and more to automatic techniques.

PERCOS, a short name for performance coding system of methods and control, is based on the decimal classification technique, purposely limited to a few classes and to very broad subdivisions in order to be consistent with the information accuracy derived primarily from statistical data.

PURPOSE

The PERCOS system for measurement and control is established primarily for the logical design of systems. It helps in the selection of an economically feasible and, in respect to the requirements, compatible chain of methods or instruments, to obtain results with a given degree of accuracy and reliability under specified environmental conditions.

PERCOS assists in providing the answer to questions of compatibility of requirements. This compatibility depends naturally on the method used to solve a problem, and on the present status of the art. Since there are an infinite amount of factors determining complete compatibility, it is apparent that any practical coding system can only consider the more important aspects, such as accuracy and reliability.

PERCOS selects, out of a number of methods or devices with satisfactory performance in respect to accuracy, those which will also satisfy the requirements of reliability. This reduced number of acceptable solutions can then be screened for the best answers to the problem, considering the economical aspects.

It is immaterial, however, which one of these restricting factors is considered first. PERCOS permits any desired sequence in the selection of compatible parameters.

Organization

The performance coding system is described in two parts. The first part, definitions and coding classes, deals with the actual coding of performance parameters and a series of definitions to clarify the meaning of the coding classes. The definitions follow, as much as possible, the generally inferred meaning of the term.

The second part describes a card file system, organized for random access to any classes described in the first part. It permits, through successive selecting operations, the discovery of a method or device complying with all the prescribed requirements for the solution of a posed problem. This second part is essential for the practical use of PERCOS.

Operational Example

Some of the services offered by PERCOS are best illustrated by a practical example.

In an assumed functional block diagram of a complex communication system, one of the blocks is labelled "multichannel master oscillator." The task consists of finding either the most appropriate design method or a supplier for this instrument. Answers to this problem are found in a three-step approach.

The first step consists of preparing a list of the requirements, complying with the over-all specifications of the entire system. This list is set up according to the twelve classes of PERCOS and contains the PERCOS coding as well as a "rank" scale, indicating the relative importance of the various PERCOS classes for this particular problem. The list may look like Table I.

TABLE I

Item	PERCOS Class	PERCOS Code	Rank
Oscillator	convertor	0	1
Input 60 c ac	electrical	6	2
Output RF	electrical	6	3
Precision minimum	1 part in 10^7	7	5
Stability of calibration	48 hours	6	6
Rate of performance minimum	140–170 mc	8	4
Shelf-life minimum	1 year	4	10
Mean-time-to-failure minimum	10,000 hours	4	7
Repair-time average	4 hours	1	8
Cost limit	$5000.00	3	9
Availability	90 days	2	12
Volume	less than 2 cubic feet	5	11

The second step is the actual selection of the answer cards out of the PERCOS card file. This is accomplished by inserting the search needle into one of the selected code holes around the edges of the file cards. By simply lifting the needle, the cards complying with this code will drop out. These cards are then used to select the next code. The sequence of selection has no effect on the final result.

The third step consists in the evaluation of the selected cards. If too many cards are left, the requirements for reliability or cost may be tightened to reduce quickly the number of cards to a manageable quantity.

In the average case, at least one methods card and several suppliers cards will be left for final consideration. The methods card describes the basic technical solution of the problem, indicating the limits of environmental conditions for which the stated reliability figures are valid, and refers to pertinent literature, without indicating any sources of supply. The suppliers card, on the other hand, describes one available instrument in detail, giving environmental conditions or applicable military specifications as well as pertinent input and output characteristics. The microfilm may give complete schematic diagrams or performance curves under given environmental conditions.

The elimination of all cards in a specific selection process indicates either that the requirements are impossible to meet, or that they reach beyond the present status of the art. For that reason, it is advisable to follow the "rank" order in selecting the classes, to assure that the search limits are imposed by the more important requirements.

Definitions and Coding Classes

Group A—Identification

PERCOS identifies instruments or measuring and control methods with only three codes. These are the instrument itself with ten divisions, and input and output with eleven divisions each. Out of the 1210 possible combinations of all the divisions of these three classes, only about 800 are of use. This rather coarse subdivision serves a very useful purpose in preventing the user of the system from narrowing the possible selection of suitable instruments by searching in too small a domain. The arbitrary choice of only 10 divisions for the instruments has the further advantage of reducing guesswork by the user, by limiting, in an obvious fashion, the possible location of an instrument in the classification.

Class 1—Instruments: All instruments are classified in ten mutually exclusive divisions, each described by a representative term. Each division is identified by a number from 0 to 9. The sequence of the divisions is arbitrary and of no particular significance. The assignment of a specific instrument to a certain class may seem in many cases to be arbitrary. This is due to the necessity of making the divisions mutually exclusive and of providing uniformity of information content.

A debate about whether a particular instrument should be assigned to one division or another is futile, because the logical search process will infallibly find all the instruments which can perform a desired duty. To ease the assignment of instruments to the divisions further, a rather careful study has been made in the selection of the collective names of the divisions and in the specifying definitions used. (See Table II.)

TABLE II

Number	Meaning and Description
0	Converter—Any device which changes one form or kind of energy into another, with efficiency being of primary importance. Examples: oscillator, motors; electrical, hydraulic and pneumatic actuators, motor-generator sets, choppers, inverters, lamps used for illumination or heating, etc.
1	Switch—Any device for connecting and disconnecting a path of information or energy. Examples: samplers, distributors, commutators, electronic gating circuits.
2	Tranducer—Any device which changes one physical quantity into another, with accuracy being of primary interest. Examples: thermocouples, strain gauges, differential transformers, microphones.
3	Amplifier—Any device which changes the level of a physical quantity, part or all of the energy for the output being drawn from a separate supply source. Examples: electronic, magnetic, pneumatic and hydraulic amplifiers with gains greater, equal to, or less than one. Note that passive devices such as transformers, voltage dividers, and resonant circuits are excluded.
4	Passive network—Any device which transfers energy or information between points with or without intentional change, none of the output energy being drawn from a separate supply source. Examples: free space, filters, twin lead, pneumatic or hydraulic signal-tubing, delay line (without recirculation means), cables.
5	Indicator—Any device which changes information signals into quantities recognizable by human senses. Examples: readout devices, oscillographs, data-printers, lamps used to transmit information, mechanical position indicators, voltmeters.
6	Energy Source—Any device capable of providing suitable power to instruments, controls or processes, without supplying information. Examples: ac, dc, RF power supplies, light sources used to excite an optical transducer, pneumatic compressor, temperature-controlled bath.
7	Command element—Any device which initiates specific control actions when provided with predetermined information. Examples: paper tape-, magnetic tape- or punched-card-reading instruments, cam-follower.
8	Comparator—Any device which accepts two inputs and provides an output based upon their relative values. Examples: self-balancing potentiometers, regulators, limit switches, alarm "detectors."
9	Storage element—Any device which retains information for an independently controlled length of time. Examples: self-locking relays, magnetic core logic elements, magnetic drum, magnetic tape, punched-paper tape, punched cards, recirculated delay lines.

Class 2: This describes, in eleven numbers, the general type of input characteristics of an instrument.

Class 3: This describes, for obvious reasons, with the same eleven numbers, the general type of output characteristics.

Table III is applicable for these two classes.

TABLE III

Number	Class 2	Class 3	Description
0	Input	Output	Mechanical
1	Input	Output	Hydraulic
2	Input	Output	Pneumatic
3	Input	Output	Acoustical
4	Input	Output	Thermal
5	Input	Output	Optical (visual)
6	Input	Output	Electrical
7	Input	Output	Magnetic
8	Input	Output	Electromagnetic radiant
9	Input	Output	Chemical
10	Input	Output	Nuclear

Group B—Accuracy and Dynamics

This group contains three classes, namely: precision, stability of calibration, and rate of performance. These three classes determine the level of confidence that can be put in the results of the measurements and give an indication of the speed with which these results may be obtained.

The data of these three classes are in most cases intimately related in a tradeable fashion. It is, for instance, more possible to obtain the highest degree of accuracy if the calibration has only to be maintained for a short time and if rate of performance limits do not impair the careful preparation and checking of the measurement. On the other hand, many instruments are capable of providing results in a rapid sequence, but the accuracy is limited to a nominal value.

The information provided by PERCOS would not be meaningful without an adequate definition of the terms used in the description of the classes. Unfortunately, there seems to be no standard or widely accepted definition for such vital terms as accuracy, precision, resolution, etc. On the contrary, practical evidence (Webster's New Collegiate Dictionary) shows that these terms are either not specifically defined for scientific use, or are labeled as synonyms.

The following definitions are given in an attempt to upgrade the information content of commonly used words by describing the most accepted version and by pointing out the most significant difference between them. It is quite obvious that there are many other ways to express the meanings of the following terms. The definitions chosen are merely one form of them.

Synonyms of the defined principal terms are separated by a comma, antonyms are put in brackets.

Accuracy—Numerically, the extent of agreement of a measured quantity with a predetermined or standard quantity at a specified point within the range of measurement. Note that the extent of agreement is sometimes expressed as a percentage difference between the measured quantity and the standard quantity.

Absolute error—Given by the maximum deviation of a measured quantity from a predetermined or standard quantity, at any given point within the range of measurement.

Accuracy and absolute error define the same borderline which separates the warranted quantity from the unwarranted. Accuracy is intuitively associated with the number of significant digits; hence, "high accuracy" refers to a quantity, described with a "high amount" of digits. Absolute error, on the other hand, emphasizes the deviation. A "large error" refers to a "large" numerical value of the error, as compared to the total numerical value of the quantity to be measured.

Precision (repeatability, relative error)—Defines numerically the degree with which a sequence of measurements of a quantity will coincide with the arithmetic average at any given point within the range of measurement.

Relative error (precision, repeatability)—The maximum deviation from the arithmetic average value, obtained in a series of tests, at any point within the range of measurement.

Precision and relative error have the same relationship as accuracy and absolute error. The observer has the choice of reporting the facts either as precision or as relative error. In many cases, precision and relative error are given, as, for instance, in the probable speed of light, 299,792.6 ± 0.7 km. The precision is given as a seven significant digit number, and the relative error as plus or minus 0.7 km, a numerical quantity.

Sensitivity—Ratio of the output response to a specified change in the measured or controlled variable quantity.

Detectability—The required minimum input signal to cause a useful output signal. Detectability indicates the practical limits of use of an instrument due to noise in the input signal or due to instability of the instrument parameters.

Resolution—Defined as the magnitude of the least significant digit that a measuring system is capable of delivering, or a controlling system to respond. This definition in terms of "significant digits" is probably more useful than the description of resolution as the ratio of a quantity to be measured and the fraction of that quantity that the instrument is able to detect.

Threshold—The minimum detectable energy difference for a given instrument. Threshold is also used in connection with the human senses, describing the minimum stimulus (energy) to cause a definite response of one or more of the human sensitory organs.

Calibrating—The action of making the arithmetic average value of a measured quantity coincide with a predetermined or standard value. Calibration is necessary because of drift. Drift changes the original settings of a device because of aging and environmental conditions. Stability of calibration and drift have the same relationship as precision and relative error.

Stability of calibration—The time during which an instrument provides results with an accuracy half as good as the precision stated for the instrument. The same facts could be described as follows. Drift indicates the probable time at which the average of the measurements of an instrument will show an absolute error of twice the relative error stated for the instrument.

Linearity—The deviation from a constant ratio between dependent and independent variables. Linearity could also be described as the boundary within which all relative errors will fall if an instrument is checked on each significant point within its range.

Hysteresis (backlash: instrument and control usage)—A special form of the relative error (precision), making the magnitude of deviation of a sequence of measurements dependent from the direction of approach. This definition of hysteresis obviously has to be restricted to the use of instruments and controls, for the hysteresis in a magnetic material, for instance, is a physical property and could never be described as some sort of an error. However, the notation pertinent to instrumentation is formed from an analogy to the hysteresis found in nature.

Rate of performance—The number of complete measurement cycles per second, giving results of a prescribed precision.

The following notes do not carry the label of a definition; they are more or less consequences of the previous definitions. They may further clarify the terms.

Calibration is usually carried out to the limit of resolution. Resolution should therefore not be coarser than half the value given for precision. This is consistent with the belief that a digital value derived from a measurement should always be taxed with an error of at least plus or minus one of the least significant digit. This, of course, is a direct consequence of the always finite domain of uncertainty of any practical measurement and of the fact that the resolution of a digital indication is limited to the span of one digit.

The accuracy of a system can, at best, be equal to its precision if the calibration is perfect, but it can never exceed it.

The total absolute error (accuracy) is determined by three component errors: the relative error of the measurement (precision), the error of calibration, and the error of definition of the exact value of the standard. The best approximation to the maximum absolute error of a measurement is given by the sum of the maxima of these three component errors.

The resolution can only be equal to or coarser than the threshold.

The rate of performance and the time constants of a system are naturally related. It is, however, generally not possible to establish a numerical relation between these terms, except in very simple cases where the number, the value, and the dependency of the time constants in an instrument are known to a degree which is consistent with the demands for precision.

For an instrument with a given frequency response characteristic, the rate of performance will decrease in proportion with the increase of demands for precision.

Class 4—Precision: The individual number of the fourth class represents the power of ten by which the range of an instrument has to be divided to obtain the span of the maximum deviation for a large number of measurements at any points within the range. (See Table IV.)

TABLE IV

Number	Description
0	Precise to one part in one or totally random.
1	Precise to ± one part in 10 or better.
2	Precise to ± one part in 10^2 or better.
3	Precise to ± one part in 10^3 or better.
*	* * * * *
9	Precise to ± one part in 10^9 or better.

The tolerance on the value of "one part" is 50 per cent. That means that an instrument with an error of ±1.50 per cent is still within Class 2. But an instrument with an error of ±1.51 per cent belongs to Class 1.

Class 5—Stability of Calibration: The individual number of the fifth class represents the power of ten of seconds of average time, for which the instrument provides results with an accuracy half as good as the precision stated for the instrument, under specified environmental conditions. (See Table V.)

TABLE V

Number	Description
0	Calibration maintained for at least 1 second.
1	Calibration maintained for at least 10 seconds.
2	Calibration maintained for at least 10^2 seconds.
3	Calibration maintained for at least 10^3 seconds or 15 minutes.
4	Calibration maintained for at least 10^4 seconds or 2 hours.
5	Calibration maintained for at least 10^5 seconds or 1 day.
6	Calibration maintained for at least 10^6 seconds or 2 weeks.
7	Calibration maintained for at least 10^7 seconds or 4 months.
8	Calibration maintained for at least 10^8 seconds or 3 years.
9	Calibration maintained for at least 10^9 seconds or 30 years.

Class 6—Rate of Performance: The individual number of the sixth class represents the power of ten of performances per second to achieve measurements or control functions within the precision of class 4. (See Table VI.)

TABLE VI

Number	Description
−3	One performance in 100 to 1000 seconds.
−2	One performance in 10 to 100 seconds.
−1	One performance in 1 to 10 seconds.
0	One performance in 0.1 to 1 second.
1	10 to 100 performances per second.
2	100 to 1000 performances per second.
*	* * * * * *
9	10^9 or more performances per second.

The addition (observing the sign) of the fifth and sixth class gives the power of ten to the possible measurement or control function within one calibration period.

Group C—Reliability

Reliability is defined as the probability that at a given time a device will operate within the prescribed range of precision, calibration, and rate of performance under given environmental conditions.

If an instrument performance deviates beyond the set limits, it is called failing.

One of the few widely accepted quantitative terms describing some aspects of reliability is the "mean time to failure."

Mean time to failure is defined as the arithmetical mean (average) of the operating time between failures under given environmental conditions.

The mean time to failure of an instrument is determined experimentally,

$$T_m = \frac{N \cdot t}{F},$$

where

T_m = mean time to failure (hours),
N = number of identical and independent samples under test,
t = duration of test (hours),
F = number of failures during test.

The same formula is used in many cases to determine the mean time to failure of a system consisting of a multitude of similar elements for which T_m is known. However, certain precautions have to be observed to guard against unwarranted extrapolation.

If, for example, a certain transistor is said to have a T_m of 10,000 hours as a result of a test where 1000 transistors, tested under certain conditions, yielded 100 failures in a 1000-hour test, a closer analysis may reveal that most of these failures occurred during the very early part of the test.

A sample of the same type of transistor, taken from the survivors of a 100-hour aging process, might increase the average T_m to 1,000,000 hours under the same environmental conditions; or 1 failure out of a lot of 1000 transistors during a 1000 hour test.

However, this T_m of 10^6 hours should not be interpreted to mean that the average life of any one of the transistors is in the order of 100 years, because the deterioration of the material may terminate the useful life of a transistor long before that time.

This behavior is found in most life histories of practical components. The mean time of failure applies therefore only to that portion of the component life where the failures per unit time are proportional to the number of identical samples used.

The T_m of an instrument should therefore always be correlated to stated environmental conditions, the number of samples used in the test and the duration of the test.

Sometimes the term "longevity" is used to indicate the longest service life of a component in hours for which the relation of T_m still holds. (See Fig. 1.)

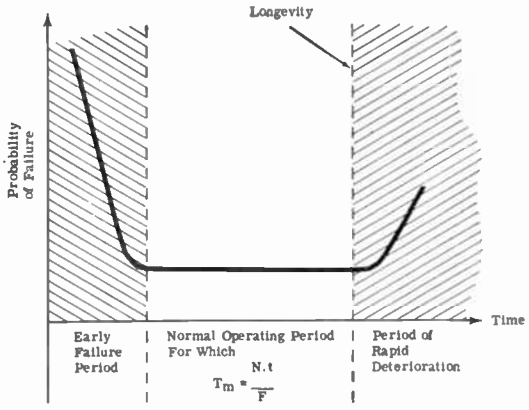

Fig. 1.

The relation between mean time to failure and reliability can be described by

$$R_t = R_0 e^{-t/T_m}$$

where

R_t = probability of satisfactory performance at time t,
R_0 = probability of satisfactory performance at time $t=0$,
T_m = mean time to failure.

Since the probability of satisfactory performance at the time $t=0$ is not necessarily equal to one, it seems to be advisable to introduce another term, similar to the operating mean time to failure.

The "mean shelf life" is defined as the arithmetical mean (average) of time for which a device can be stored under given environmental conditions so that the probability of satisfactory performance at the moment of first use is $1/e$.

Under the same assumptions as given to determine the probability of satisfactory performance after t, operating time can be defined as

$$E_t = E_0 e^{-t/T_0}$$

where

E_t = probability of satisfactory first performance after time t of inoperative storage,
E_0 = probability of satisfactory first performance at the moment of final testing after manufacture (zero storage time),
T_s = mean shelf life.

The probability of satisfactory performance after t_s time of storage and t time of operation can therefore be given as

$$R(t_s + t) = E_0 e^{-(t_s/T_s)(t/T_m)}$$

where E_0 can also be interpreted as the coefficient describing the result of incoming inspection. If, from a large quantity N of identical instruments delivered, the initial inspection detects F failures, E_0 can be defined as

$$E_0 = \frac{N - F}{N}.$$

E_0 therefore describes uniformity of quality at the time of delivery.

A third very useful statistical time record is furnished by the "average repair time," defined as the arithmetical mean (average) of time required to perform the maintenance check program or to locate the cause of failure and to replace the defective part, making the instrument fully operative again.

The utilization factor U of an instrument is determined by

$$U = \frac{T_m - T_r}{T_m} \cdot 100,$$

where

U = per cent of time for which an instrument provides useful service,
T_m = mean time to failure,
T_r = average repair time.

Class 7—Mean Shelf Life T_s: The individual number of the seventh class represents the power of ten of hours as average time for which an instrument can be stored under given environmental conditions, so that the probability of satisfactory performance at the moment of first use is $1/e$. (See Table VII.)

TABLE VII

Number	Description
0	No shelf life.
1	Shelf life of 10 hours or 1 failure out of 10 after 1 hour.
2	Shelf life of 10^2 hours or 1 failure out of 100 after 1 hour.
3	Shelf life of 10^3 hours or 1 failure out of 100 after 10 hours.
4	Shelf life of 10^4 hours or 1 failure out of 100 after 100 hours.
5	Shelf life of 10^5 hours or 1 failure out of 1000 after 100 hours.
6	Shelf life of 10^6 hours or 1 failure out of 1000 after 1000 hours.
7	Shelf life of 10^7 hours or 1 failure out of 10,000 after 1000 hours.
8	Shelf life of 10^8 hours or 1 failure out of 10,000 after 10,000 hours.
9	Shelf life of 10^9 hours or 1 failure out of 100,000 after 10,000 hours.

It is to be understood that the interpretation of the shelf life in Table VII is only one out of many possible interpretations. In other words, number 3 equal to a shelf life of 1000 hours can also mean 2 failures out of 20 samples after 100 hours of storage, etc.

Class 8—Mean Time to Failure T_m: The individual number of eighth class represents the power of ten of hours as average time for which an instrument performs satisfactorily under given environmental conditions. The probability of satisfactory performance is at that time equal to $1/e$. (See Table VIII.)

TABLE VIII

Number	Description
0	Operating time 1 hour.
1	Operating time 10 hours or 100 failures out of 10^3 every hour.
2	Operating time 10^2 hours or 10 failures out of 10^3 every hour.
3	Operating time 10^3 hours or 1 failure out of 10^3 every hour.
4	Operating time 10^4 hours or 1 failure out of 10^3 every 10 hours.
5	Operating time 10^5 hours or 1 failure out of 10^3 every 10^2 hours.
6	Operating time 10^6 hours or 1 failure out of 10^3 every 10^3 hours.
7	Operating time 10^7 hours or 1 failure out of 10^4 every 10^3 hours.
8	Operating time 10^8 hours or 1 failure out of 10^5 every 10^3 hours.
9	Operating time 10^9 hours or 1 failure out of 10^5 every 10^4 hours.

The interpretation in Table VIII of the mean time to failure, "1 failure out of X samples every y hours," is only one example out of many possible interpretations. Any interpretation of the formula

$$T_m = \frac{N \cdot t}{F}$$

is valid provided t is within the normal "operating period" as defined.

Class 9—Mean Repair Time T_r: The individual number of the ninth class represents the power of ten of hours as average time required to repair an instrument after failure, or to perform routine maintenance. (See Table IX.)

TABLE IX

Number	Description
−2	Instantaneous and automatic replacement.
−1	Repair time less than 6 minutes.
0	Repair time less than 1 hour.
1	Repair time less than 10 hours.
2	Repair time less than 100 hours.
3	Repair time less than 1000 hours or 6 weeks.
4	Repair time less than 10,000 hours or 14 months.
5	Instrument cannot be repaired.

Group D—Relative Merits

The last group of relative merits contains 3 classes, representing cost, availability and volume. These three characteristics have been chosen in preference to weight, operability, ease of maintenance, and others of the same nature, because it is felt that the selected three characteristics are more often determining factors in choosing particular instruments.

Class 10—Cost: The individual number of the tenth class represents the power of ten of dollars list price of an instrument. (See Table X.) Higher digits than 5 are probably not useful.

TABLE X

Digit	Description
0	Instrument costs from 1 dollar to 9.99.
1	Instrument costs from 10 dollars or more to 99.99.
2	Instrument costs from 100 dollars or more to 999.99.
3	Instrument costs from 1000 dollars or more to 9999.99.
4	Instrument costs from 10,000 dollars or more to 99,999.99.
5	Instrument costs 100,000 dollars or more.

Class 11—Availability: The individual number of the eleventh class represents the power of ten of days elapsed between the placing of the order for the instrument and the probable delivery. (See Table XI).

TABLE XI

Digit	Description
0	Spare parts at hand.
1	Delivery within 10 days or earlier.
2	Delivery within 100 days or earlier.
3	Delivery within 3 years or earlier.
4	Delivery undetermined.

Class 12—Volume: The individual number of the twelfth class represents the power of ten of cubic centimeters of volume of an instrument. (See Table XII).

TABLE XII

Digit	Description		
−2	Volume 10^{-2} cm³ = 10 mm³	∼ 6.1	10^{-4} cubic inches or less.
−1	Volume 10^{-1} cm³ = 100 mm³	∼ 6.1	10^{-3} cubic inches or less.
0	Volume 1 cm³ =	∼ 6.1	10^{-2} cubic inches or less.
1	Volume 10 cm³ =	∼ 6.1	10^{-1} cubic inches or less.
2	Volume 10^2 cm³ =	∼ 6.1	cubic inches or less.
3	Volume 10^3 cm³ = 1 dm³	∼ 61	cubic inches or less.
4	Volume 10^4 cm³ = 10 dm³	∼610	cubic inches or less.
5	Volume 10^5 cm³ = 100 dm³	∼ 3.5	cubic feet or less.
6	Volume 10^6 cm³ = 1 m³	∼ 34	cubic feet or less.
7	Volume 10^7 cm³ = 10 m³	∼ 13	cubic yards or less.

The Card File System

Group A—Requirements

The only logical means to implement the performance coding system is a card file, whose design parameters are to a large extent prescribed by the requirements of PERCOS.

1) *Information Content:* Each card of the file must contain enough information about one method or device, so that in the majority of cases no further references to books or magazines are required to make a satisfactory decision.

This requirement demands a card of sufficient size to allow a direct readable description of the PERCOS parameters and the environmental conditions or other restrictions affecting the PERCOS data. A separate area on the card has to be reserved for applying a microfilm containing more detailed information.

It should be emphasized at this point that the card gives not only the code number for each class of PERCOS, but the actual value carried out to the least meaningful decimal digit. It is therefore not necessary to subdivide the code number into fractions in order to obtain more precise information. Such a subdivision would only complicate the search operation and would probably make the coding of a specific device obsolete faster.

2) *Search Method:* The amount of written information required makes the use of a common punched card rather difficult due to the possibility of impairing the text by punching out numbers or letters.

It seems to be more advantageous to utilize the edge-coded key sort system, which leaves the center of the card intact. The key sort system has the added advantage that manual search is very easily accomplished. The manual search is probably not only indicated from the economical viewpoint, but also from the user's standpoint in respect to the availability of information independent of sorting machine programs.

The restriction in the number of available holes is not important in the case of PERCOS because the 12 classes require only about 120 holes. Some search systems use miniature holes of ten to twenty thousandths of an inch in diameter. While it is obvious that printed text would not be mutilated even by a large quantity of holes, it is evident that the search operation would be far more time-consuming because of the increased demands for proper alignment between the master and the file card to obtain proper registration. The potential availability of a very large number of holes per card is not an advantage for PERCOS.

The magnetic card search method is principally applicable to PERCOS, since the magnetic coating is only required on one side of the card and does not interfere with the printing on the other side. The magnetic card-reader is capable of very high speeds, offering about the same handling ease as the direct photoelectric reader of the edge-coded card. Both systems are practical, if for some reason the mechanical search is found desirable.

Group B—The Card Organization

The organization of the PERCOS card can best be illustrated by Fig. 2. A card 6.5×7.5 inches is edge perforated with 122 holes (5 holes per linear inch), leaving an area of 37 square inches for text and microfilm. The text area is divided into four parts.

1) The title, giving information about the method or device, the source, and the date of coding.
2) The performance coding, with 12 assigned and 2 spare classes.
3) The notes, giving the conditions under which the performance coding is valid, and any other pertinent information such as input and output impedance, signal level, noise, type of connector used, etc.
4) The microfilm, giving more detailed information, such as schematics, waveform patterns, maintenance instructions, mathematical deductions, cross reference, etc.

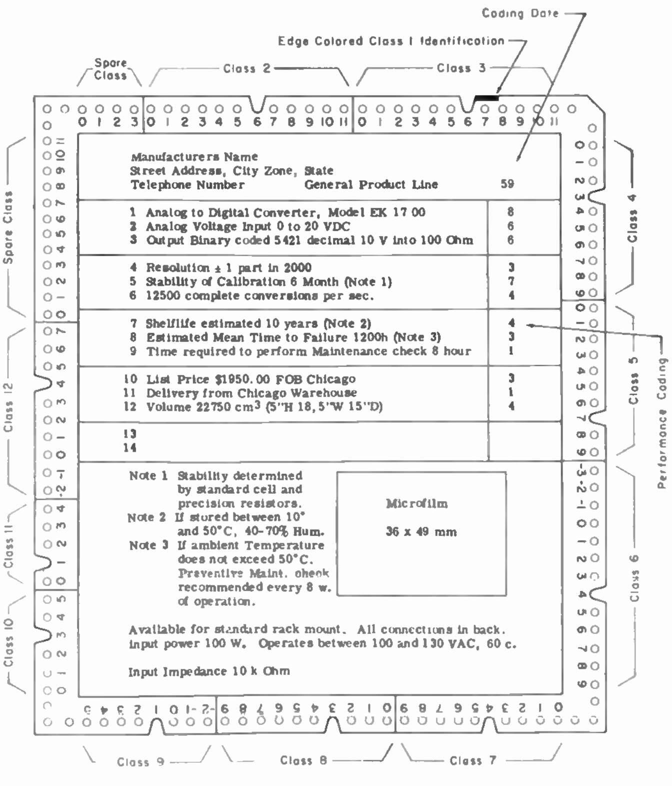

Fig. 2.

It should be noted that the card actually contains two superimposed coding systems. The principal coding system is done by opening the punched holes to the edge of the card. The second system uses the edge printing technique on the two longer edges of the card. The top edge printing serves to identify the number of Class 1. This is done by edge printing all cards of a particular number of Class 1 with a black mark 0.65 inches in length. This length guarantees positive identification even in a case where two adjacent holes are punched out.

Since it is most likely that the cards will be stored according to the numbers of Class 1, it is very easy to spot a misplaced card by merely observing the top of the filing cards in one drawer. The lower edge is used to code the year in which the card is prepared. This gives at one glance a check of the possible obsolescence of the information contained on the card. The spare spaces in the text area and the spare holes are reserved for future additions to PERCOS.

Conclusion

The principles for a useful performance coding system have been outlined. Ahead is the major task of putting this system into practical use. The way to do that is clear. With help from interested industries and governmental agencies, an independent, nonprofit research organization has to be formed. This organization will collect the raw data, correlate the findings of testing laboratories, and perform the coding and printing of the cards, which will then be offered publicly on a subscription basis.

Acknowledgment

The author is deeply indebted to his friends in the IRE Committees 10 and 10.3 for their support and active participation during the conception period of the performance coding system. The author is especially grateful to Dr. E. Mittelmann, chairman of Committee 10, for his many contributions, among which was the suggestion to incorporate the microfilm on the file cards.

100:1 Bandwidth Balun Transformer*

J. W. DUNCAN†, SENIOR MEMBER, IRE, AND V. P. MINERVA†, MEMBER, IRE

***Summary*—The theory and design of a Tchebycheff tapered balun transformer which will function over frequency bandwidths as great as 100:1 is presented. The balun is an impedance matching transition from coaxial line to a balanced, two-conductor line. The transition is accomplished by cutting open the outer wall of the coax so that a cross-sectional view shows a sector of the outer conductor removed. As one progresses along the balun from the coaxial end, the open sector varies from zero to almost 2π, yielding the transition to a two-conductor line.**

The balun impedance is tapered so that the input reflection coefficient follows a Tchebycheff response in the pass band. To synthesize the impedance taper, the impedance of a slotted coaxial line was obtained by means of a variational solution which yielded upper and lower bounds to the exact impedance. Slotted line impedance was determined experimentally by painting the line cross section on resistance card using silver paint and measuring the dc resistance of the section.

The measured VSWR of a test balun did not exceed 1.25:1 over a 50:1 bandwidth. Dissipative loss was less than 0.1 db over most of the range. Measurements show that the unbalanced current at the output terminals is negligible.

INTRODUCTION

In utilizing some of the recently developed broad-band antennas such as the logarithmically periodic antenna, it is sometimes advantageous to excite the antenna from balanced, two-conductor terminals.[1] In order to match the balanced antenna impedance to the unbalanced impedance of a coaxial line, a balun transformer is required. Moreover, the balun transformer must be capable of operating over a very large frequency range if it is to be compatible with the antenna performance. This paper presents the theory and design of a Tchebycheff tapered balun transformer which will function over bandwidths as great as 100:1.

The balun transformer is illustrated in Fig. 1. The balun is an impedance matching transition from coaxial line to a balanced two-conductor open line. The transition is accomplished by cutting open the outer wall of the coax so that a cross-section view shows a sector of the outer conductor removed. The angle subtended by the open sector is denoted by 2α. As one progresses along the balun from the coaxial end, the angle 2α varies from zero to almost 2π, yielding the transition from coax to an open two-conductor line. The cross section of the conductors is then varied as required. One is not limited to conductors having a circular cross section; a transition from coaxial cable to a balanced strip line is one of the possible configurations.

The broad-band impedance matching properties of

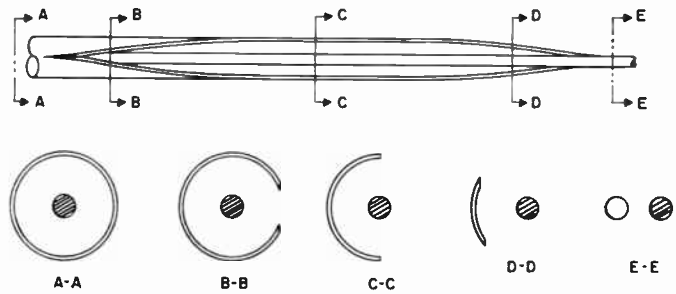

Fig. 1—Tapered balun transformer.

the balun are obtained by utilizing a continuous transmission line taper described by Klopfenstein.[2] The characteristic impedance of the balun transformer is tapered along its length so that the input reflection coefficient follows a Tchebycheff response in the pass band. The length of the balun is determined by the lowest operating frequency and the maximum reflection coefficient which is to occur in the pass band. The balun has no upper frequency limit other than the frequency where higher order coaxial modes are supported or where radiation from the open wire line becomes appreciable.

Before discussing the "balun" property of the device, a brief review of balance conditions on an open transmission line is in order. A balanced two-conductor transmission line has equal currents of opposite phase in the line conductors at any cross section. System unbalance is evidenced by the addition of codirectional currents of arbitrary phase to the balanced transmission line currents. The order of unbalance is measured by the ratio of the codirectional current to the balanced current. Now in a coaxial line, the total current on the inside surface of the outer conductor is equal and opposite to the total current on the center conductor. The ideal balun functions by isolating the outside surface of the coax from the transmission line junction so that *all* of the current on the inside surface of the coax outer conductor is delivered in the proper phase to one of the two balanced conductors. Unbalance of the transmission line currents results if current returns to the generator on the outside surface of the coaxial line.

Consider the Tchebycheff tapered balun transformer which is formed by increasing the slot aperture in the outer wall of the coax until an open two-conductor line is obtained. Over the length of the transition the electromagnetic field changes from a totally confined field in the coax to the "open" field of a two-wire transmission line. It is evident that the total current on the out-

* Original manuscript received by the IRE, April 30, 1959; revised manuscript received, October 5, 1959.

† Collins Radio Co., Cedar Rapids, Iowa.

[1] R. H. DuHamel and F. R. Ore, "Log periodic feeds for lens and reflectors," 1959 IRE NATIONAL CONVENTION RECORD, pt. 1, pp. 128–137.

[2] R. W. Klopfenstein, "A transmission line taper of improved design," PROC. IRE, vol. 44, pp. 31–35; January, 1956.

side surface of the coax at the balun input must result from the summation of wave reflections which originate over the entire length of the open transition. But the slot transition is purposely tapered so that the net reflection at the balun input is arbitrarily small. Consequently, negligible current appears on the outside of the coaxial line at the balun input and electrical balance at the output terminals is very good. In other words, the physical geometry of the transition which produces negligible wave reflections and leads to a broad-band impedance transformer also results in the operation of the device as a balun.

Assuming that the characteristic impedance of the balun at any cross section is equal to the characteristic impedance of a uniform, slotted coaxial line of that particular cross section, it is possible to synthesize the required impedance taper by providing the appropriate cross section at each position along the balun transformer. In order to carry out this procedure, one must know the characteristic impedance of a uniform, slotted coaxial line as the angle 2α varies from zero to 2π. This information was obtained by theoretical analysis and verified experimentally. The characteristic impedance of the slotted line was determined from a variational solution of the two-dimensional boundary value problem. The variational expressions yield upper and lower bounds to the exact characteristic impedance. The upper bound is obtained from a variational expression involving the charge distribution on the outer conductor of the slotted coaxial line, while the lower bound is obtained from a variational expression involving the potential distribution in the slot aperture. Characteristic impedance was determined experimentally by painting the slotted line cross section on resistance card, using silver paint and measuring the dc resistance of the cross section. These data are presented as curves which show characteristic impedance of the slotted coaxial line as a function of the angular opening. The curves allow one to design a balun for matching a large range of impedances with an arbitrarily small standing wave ratio. We proceed to derive variational expressions for the characteristic impedance of the slotted line. The method of analysis is similar to that used by Collin to solve the problem of a symmetrically slotted coaxial line.[3]

Upper Bound to the Characteristic Impedance

Consider the cross-sectional view of the uniform, slotted coaxial line shown in Fig. 2. We choose the cylindrical coordinate system r, θ, z, where r, θ are in the transverse plane and z is the direction of wave propagation along the line. The radius of the inner conductor is $r=a$, while the outer conductor occurs at $r=b$. The slot opening in the outer conductor is defined by the angle 2α. We assume that there is a homogeneous, isotropic medium about the conductors with permeability μ and permittivity ϵ.

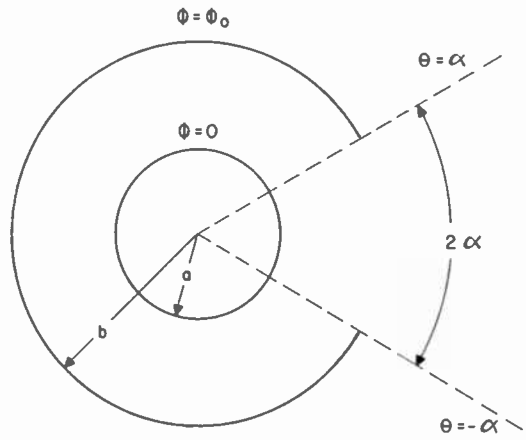

Fig. 2—Cross section of uniform slotted coaxial line.

It may be verified that the solution of Maxwell's equations for the TEM mode of propagation on the line reduces to solving Laplace's equation for the static potential distribution $\phi(r, \theta)$ in the transverse plane. The electric field $\overline{E}(r, \theta)$ is defined by the relation

$$\overline{E}(r, \theta) = -\operatorname{grad} \phi(r, \theta). \tag{1}$$

It follows from Maxwell's equations that the transverse field components are given by

$$E_r = -\frac{\partial \phi}{\partial r} = \frac{1}{\epsilon v} H_\theta$$

and

$$E_\theta = -\frac{1}{r}\frac{\partial \phi}{\partial \theta} = -\frac{1}{\epsilon v} H_r \tag{2}$$

where $v = 1/\sqrt{\mu\epsilon}$ is the velocity of light in the surrounding medium. Thus, all field components may be derived from the scalar potential function $\phi(r, \theta)$ which is the solution of Laplace's equation

$$\frac{1}{r}\frac{\partial}{\partial r}\left(r\frac{\partial \phi}{\partial r}\right) + \frac{1}{r^2}\frac{\partial^2 \phi}{\partial \theta^2} = 0, \tag{3}$$

subject to the boundary conditions of the problem.

We define the potential on the inner conductor $r=a$ as $\phi=0$, while the outer conductor $r=b$, $\alpha \leq \theta \leq 2\pi - \alpha$ is maintained at the constant potential ϕ_0. The potential $\phi(r, \theta)$ at any point in the plane may be expressed in terms of the Green's function $G(r, \theta | r', \theta')$ for the problem. The Green's function is the solution of the inhomogeneous equation

$$\nabla^2 G(r, \theta | r', \theta') = -\frac{1}{\epsilon}\frac{\delta(r - r')\delta(\theta - \theta')}{r} \tag{4}$$

where the polar coordinate form of the delta function

$$\frac{\delta(r - r')\delta(\theta - \theta')}{r}$$

[3] R. E. Collin, "The characteristic impedance of a slotted coaxial line," IRE Trans. on Microwave Theory and Techniques, vol. MTT-4, pp. 4–8; January, 1956.

represents a unit line source at $r=r'$, $\theta=\theta'$. The Green's function satisfies Laplace's equation throughout the r, θ plane except at the source point r', θ' where $G(r, \theta | r', \theta')$ and all its derivatives are singular. Denoting R as the scalar separation between observation point r, θ and source point r', θ', the singularity of G is such that

$$G(r, \theta | r', \theta') \to -\frac{1}{2\pi\epsilon} \ln R \quad \text{as} \quad R \to 0.^{4}$$

The Green's function is subject to the boundary condition $G=0$ on the inner cylinder $r=a$. $G(r, \theta | r', \theta')$ may be viewed as the potential at the point r, θ because of a unit line charge located at r', θ'.

Because of the symmetry of the problem, it is convenient to write the Green's function in the form which derives from unit line sources located as shown in Fig. 3. The positive unit charges are located at $r=b$, $\theta=\pm\theta'$. The images of these line charges in the grounded cylinder $r=a$ occur at $r=a^2/b$, $\theta=\pm\theta'$. The harmonic expansion of the potential caused by this system of sources with the condition that $G=0$ at $r=a$, yields the appropriate Green's function which is

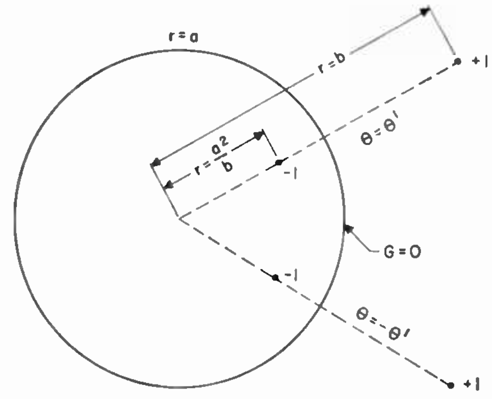

Fig. 3—Unit line charges and images.

$$G(r, \theta | b, \theta') = \frac{1}{\epsilon\pi} \begin{cases} \ln\left(\dfrac{r}{a}\right) + \displaystyle\sum_{n=1}^{\infty} \dfrac{2 \sinh\left(n \ln \dfrac{r}{a}\right) \cos(n\theta) \cos(n\theta')}{n\left[\sinh\left(n \ln \dfrac{b}{a}\right) + \cosh\left(n \ln \dfrac{b}{a}\right)\right]} & \text{where} \quad a \leq r \leq b \\ \ln\left(\dfrac{b}{a}\right) + \displaystyle\sum_{n=1}^{\infty} \dfrac{2 \sinh\left(n \ln \dfrac{b}{a}\right) e^{-n \ln (r/b)} \cos(n\theta) \cos(n\theta')}{n\left[\sinh\left(n \ln \dfrac{b}{a}\right) + \cosh\left(n \ln \dfrac{b}{a}\right)\right]} & \text{where} \quad r \geq b. \end{cases} \tag{5}$$

It now follows that the potential $\phi(r, \theta)$ caused by an arbitrary (but necessarily symmetrical) charge distribution $\sigma(\theta')$ at $r=b$ is given by

$$\phi(r, \theta) = \int_{\alpha}^{\pi} G(r, \theta | b, \theta') \sigma(\theta') b d\theta'. \tag{6}$$

The charge distribution $\sigma(\theta')$ is still unknown, however, imposing the boundary condition that $\phi(r, \theta) = \phi_0$ when $r=b$, $\alpha \leq \theta \leq \pi$ leads to the following integral equation for $\sigma(\theta')$:

$$\phi_0 = b \int_{\alpha}^{\pi} G(b, \theta | b, \theta') \sigma(\theta') d\theta'. \tag{7}$$

To obtain a variational expression for Z_0, we multiply (7) by $\sigma(\theta)$ and integrate with respect to θ over $\alpha \leq \theta \leq \pi$; thus

$$\phi_0 = \frac{b \displaystyle\int_{\alpha}^{\pi} \int_{\alpha}^{\pi} G(b, \theta | b, \theta') \sigma(\theta) \sigma(\theta') d\theta d\theta'}{\displaystyle\int_{\alpha}^{\pi} \sigma(\theta) d\theta}. \tag{8}$$

The total charge Q on the outer conductor resulting from the charge distribution $\sigma(\theta')$ is given by

$$Q = \int_{\alpha}^{2\pi-\alpha} \sigma(\theta') b d\theta' = 2b \int_{\alpha}^{\pi} \sigma(\theta') d\theta'. \tag{9}$$

The characteristic impedance of a uniform, lossless transmission line is given by $1/vC$, where C is the capacitance of the line per unit length and v is the wave velocity. It is sufficient, therefore, to determine C in order to evaluate Z_0. Since C is equal to the ratio of charge on the outer conductor to the potential difference ϕ_0 between the conductors, we obtain

$$Z_0 = \frac{\dfrac{1}{v} \phi_0}{Q}. \tag{10}$$

[4] P. M. Morse and H. Feshbach, "Methods of Theoretical Physics," McGraw-Hill Book Co., Inc., New York, N. Y., pt. 1, pp. 808–810; 1953.

Substituting (8) and (9) into (10) yields the variational form

$$Z_0 = \frac{\frac{1}{2v}\int_\alpha^\pi \int_\alpha^\pi G(b,\theta \mid b,\theta')\sigma(\theta)\sigma(\theta')d\theta d\theta'}{\left[\int_\alpha^\pi \sigma(\theta)d\theta\right]^2}. \tag{11}$$

It may be shown that Z_0 as given by (11) is stationary with respect to arbitrary first order variations in the form of $\sigma(\theta)$ about the correct distribution. (See the Appendix.) The stationary value is an absolute minimum for the "best" approximation to the actual distribution so that (11) yields an upper bound to Z_0. We approximate the true charge distribution by an N term function containing N arbitrary parameters $c_1, c_2, \cdots, c_N$. This function is substituted into (11) for $\sigma(\theta)$ and the expression for Z_0 is minimized with respect to the parameter constants c_ν. To do this, Z_0 is differentiated with respect to the N parameters and the results equated to zero which leads to N homogeneous linear equations in the N unknowns c_ν. Solving for the c_ν and substituting back into (11) yields the stationary value of Z_0.

A suitable expansion for $\sigma(\theta)$ is the cosine series

$$\sigma(\theta) = \sum_{\nu=0}^{N} c_\nu \cos \frac{\nu\pi}{\pi-\alpha}(\theta-\alpha).$$

As one uses a larger number of terms to represent $\sigma(\theta)$, the variational solution converges to the exact value of Z_0; however, the labor of computations increases enormously with N. It will be seen that sufficiently accurate results are obtained by using the simple two term series

$$\sigma(\theta) = c_0 + c_1 \cos k(\theta-\alpha), \tag{12}$$

where

$$k = \frac{\pi}{\pi-\alpha}.$$

Without loss of generality we may define $c_0 = 1$. Proceeding as outlined above, one obtains

$$Z_0 = \frac{1}{2\pi}\sqrt{\frac{\mu}{\epsilon}}\ln\left(\frac{b}{a}\right) + \frac{\sqrt{\frac{\mu}{\epsilon}}}{\pi(\pi-\alpha)^2}\sum_{n=1}^{\infty}\frac{\sin^2(n\alpha)\left[1+\frac{c_1 n^2}{n^2-k^2}\right]^2}{n^3\left[1+\coth\left(n\ln\frac{b}{a}\right)\right]} \text{ ohms}, \tag{13}$$

where

$$-c_1 = \frac{\displaystyle\sum_{n=1}^{\infty}\frac{\sin^2(n\alpha)}{n(n^2-k^2)\left[1+\coth\left(n\ln\frac{b}{a}\right)\right]}}{\displaystyle\sum_{n=1}^{\infty}\frac{n\sin^2(n\alpha)}{(n^2-k^2)^2\left[1+\coth\left(n\ln\frac{b}{a}\right)\right]}}.$$

Selecting $\sqrt{\mu/\epsilon}$, (b/a), and α, one may compute c_1 and evaluate (13) which is an upper bound to the exact characteristic impedance. Before presenting the numerical results obtained with (13) we shall derive a lower bound to Z_0.

Lower Bound to the Characteristic Impedance

The fundamental principle that a system in equilibrium is characterized by a minimum of potential energy consistent with the constraints imposed on the system applies to an electrostatic field.[5] A lower bound to the characteristic impedance may be derived from the integral which yields the total potential energy W of the electrostatic field. For the two dimensional problem under consideration, the total field energy per unit length is given by

$$W = \frac{1}{2}\epsilon\int_0^{2\pi}\int_a^{\infty}\left[\left(\frac{\partial\phi}{\partial r}\right)^2 + \frac{1}{r^2}\left(\frac{\partial\phi}{\partial\theta}\right)^2\right] r dr d\theta \tag{14}$$

which may be recognized as the Dirichlet integral in polar coordinates.

By definition, $W = (1/2)C\phi_0^2$, where C is the capacitance per unit length. Recalling the relation between characteristic impedance and C, we may express $1/Z_0$ in terms of the integral for the total field energy.

$$\frac{1}{Z_0} = vC = \frac{2v}{\phi_0^2}W. \tag{15}$$

It follows from (15) that if W is minimized with respect to the constants of a parameter-laden function, we obtain a *lower bound* to Z_0. The function used to minimize W is an N term approximation to the potential distribution $\phi(b, \theta)$ in the slot aperture.

We pause to discuss briefly the variational expression $1/Z_0$. A *necessary* condition for the integral (14) to be stationary is that its first variation vanish. This condition implies that $\phi(r, \theta)$ must satisfy Laplace's equation.[6] In other words, if a function $\phi(r, \theta)$ *exists* which minimizes (14), it must necessarily satisfy $\nabla^2\phi = 0$ and the boundary conditions of the problem. The reader is referred to Kellogg[7] for proofs that unique solutions of

[5] J. A. Stratton, "Electromagnetic Theory," McGraw-Hill Book Co., Inc., New York, N. Y., pp. 114–116; 1941.
[6] F. B. Hildebrand, "Methods of Applied Mathematics," Prentice-Hall, Inc., Englewood Cliffs, N. J., pp. 138–139; 1952.
[7] O. D. Kellogg, "Foundations of Potential Theory," Dover Publications, Inc., New York, N. Y., pp. 311–315; 1953.

the Dirichlet problem exist under proper conditions on the region, boundary values, and the functions ϕ eligible for the minimization of the integral.

Based on the Green's function analysis we write the following expansion for the potential function $\phi(r, \theta)$ which satisfies the boundary conditions $\phi=0$ at $r=a$ and ϕ continuous at $r=b$.

$$\phi(r,\theta) = \begin{cases} a_0 \ln\left(\frac{r}{a}\right) + \sum_{n=1}^{\infty} a_n \sinh\left(n \ln \frac{r}{a}\right) \cos(n\theta) \\ \qquad \text{where } a \le r \le b \\ a_0 \ln\left(\frac{b}{a}\right) + \sum_{n=1}^{\infty} a_n \sinh\left(n \ln \frac{b}{a}\right) \\ \qquad \cdot e^{-n \ln(r/b)} \cos(n\theta). \\ \qquad \text{where } r \ge b \end{cases} \quad (16)$$

It follows that the potential at $r=b$ is given by

$$\phi(b,\theta) = a_0 \ln\left(\frac{b}{a}\right) + \sum_{n=1}^{\infty} a_n \sinh\left(n \ln \frac{b}{a}\right) \cos(n\theta). \quad (17)$$

Multiplying (17) by $\cos(m\theta)d\theta$ and integrating with respect to θ over $-\pi \le \theta \le \pi$ yields

$$a_0 = \frac{1}{\pi \ln\left(\frac{b}{a}\right)} \int_0^{\pi} \phi(b,\theta) d\theta,$$

$$a_n = \frac{2}{\pi \sinh\left(n \ln \frac{b}{a}\right)} \int_0^{\pi} \phi(b,\theta) \cos(n\theta) d\theta, \quad (18)$$

since $\phi(b, \theta)$ is an even function of θ. If the true potential distribution over the slot aperture were known, the constants a_0, a_n would be determined uniquely by (18), and (16) would yield the exact solution $\phi(r, \theta)$. Instead, we approximate $\phi(b, \theta)$ over the slot by using an appropriate function and then minimize the integral for W with respect to the arbitrary constants.

Substituting the series (16) into (14) and then performing the integration leads to

$$\frac{1}{Z_0} = 2\pi\epsilon v \frac{a_0^2}{\phi_0^2} \ln\left(\frac{b}{a}\right) + \frac{\pi\epsilon v}{\phi_0^2} \sum_{n=1}^{\infty} n a_n^2 \sinh\left(n \ln \frac{b}{a}\right) \cdot \left[\cosh\left(n \ln \frac{b}{a}\right) + \sinh\left(n \ln \frac{b}{a}\right)\right]. \quad (19)$$

Substituting (18) into (19), we obtain the variational expression

$$\frac{1}{Z_0} = \frac{2\epsilon v}{\pi\phi_0^2 \ln\left(\frac{b}{a}\right)} \left[\int_0^{\pi} \phi(b,\theta) d\theta\right]^2 + \frac{4\epsilon v}{\pi\phi_0^2} \sum_{n=1}^{\infty} n \left[1 + \coth\left(n \ln \frac{b}{a}\right)\right] \cdot \left[\int_0^{\pi} \phi(b,\theta) \cos(n\theta) d\theta\right]^2 \quad (20)$$

which is stationary with respect to arbitrary first-order variations in the form of $\phi(b, \theta)$ over the slot aperture.

A suitable representation for the potential $\phi(b, \theta)$ is

$$\phi(b,\theta) = \phi_0 \begin{cases} 1 & \text{where } \alpha \le \theta \le 2\pi - \alpha \\ 1 + \sum_{\nu=1,3,5,\ldots}^{N} c_\nu \cos \frac{\nu\pi}{2\alpha}\theta & \text{where } -\alpha \le \theta \le \alpha \end{cases}$$

Proceeding as outlined for the upper bound, one may substitute this series into (20) and minimize the expression with respect to the c_ν. However, a prohibitive number of terms is needed to describe properly $\phi(b, \theta)$ over the slot for α approaching π. We know that for large α, the potential over the slot remains very small until one approaches the outer conductor at $\theta = \pm\alpha$; consequently one would expect an even-powered polynomial in (θ/α) to provide a good approximation to the true distribution. Excellent results were obtained by using the following simple function containing the single arbitrary constant c_1.

$$\phi(b,\theta) = \phi_0 \begin{cases} 1 & \text{where } \alpha \le \theta \le 2\pi - \alpha \\ 1 - c_1 + c_1\left(\frac{\theta}{\alpha}\right)^4 & \text{where } -\alpha \le \theta \le \alpha. \end{cases} \quad (21)$$

Note that when $\theta=0$, $\phi(b, \theta) = \phi_0(1-c_1)$. Substituting (21) into (20) and minimizing (20) with respect to c_1, yields

$$Z_0 = \frac{\frac{1}{2\pi}\sqrt{\frac{\mu}{\epsilon}} \ln\left(\frac{b}{a}\right)}{1 - \frac{4}{5}\left(\frac{\alpha}{\pi}\right)c_1} \text{ ohms} \quad (22)$$

where

$$\frac{1}{c_1} = \frac{4}{5}\left(\frac{\alpha}{\pi}\right) + \frac{40}{\pi} \ln\left(\frac{b}{a}\right) \sum_{n=1}^{\infty} \cdot \frac{\left[1 + \coth\left(n \ln \frac{b}{a}\right)\right]}{(n\alpha)} \left[\frac{A_n \cos(n\alpha) - B_n \sin(n\alpha)}{(n\alpha)^4}\right]^2,$$

$$A_n = (n\alpha)^3 - 6(n\alpha),$$
$$B_n = 3(n\alpha)^2 - 6.$$

Eq. (22) provides a lower bound to the exact characteristic impedance of the slotted line. The numerator of

(22) may be recognized as the characteristic impedance of a closed coaxial cable with conductor radii b and a. The denominator of (22) is always less than unity for non-zero α. Since (22) is a lower bound to the exact impedance, we see that the slotted coax impedance is always greater than the impedance of closed coaxial line.

Selecting free space values for μ and ϵ so that $\sqrt{\mu_0/\epsilon_0}=120\pi$, (13) and (22) were evaluated for $\log_e (b/a)=0.833$, 1.00, and 1.25 which corresponds to closed coaxial lines of 50-, 60-, and 75-ohm impedance, respectively. Numerical computations were carried out on an IBM 650 computer. These data are presented in the dashed curves of Figs. 4–6 which show the *upper* and *lower bound* to Z_0 as a function of the angle 2α for a particular $\log_e (b/a)$. It is evident that the functional approximations to $\sigma(\theta)$ and $\phi(b, \theta)$ were sufficiently accurate since the difference between the bounds is very small over most of the range 2α. The greatest difference occurs as α approaches π. Since the exact characteristic impedance of the slotted line must lie between the upper and lower bounds, the curves allow one to determine quite accurately the angle 2α required to give a certain impedance Z_0.

The impedance of the slotted line was also determined by using the well-known method where the line cross section is painted on a two dimensional resistive surface and the dc resistance of the cross section is measured.[8] Measurements were performed for $\log_e (b/a)=0.833$, 1.00, and 1.25. These experimental data appear as the plotted points in Figs. 4–6. The solid curve is the *arithmetic mean* of the upper and lower bound to Z_0 for each $\log_e (b/a)$. The experimental data agree quite closely with theory except for the $\log_e (b/a)=1$ data which diverge slightly for large α. Apparently the cross section was not drawn with sufficient accuracy in this case.

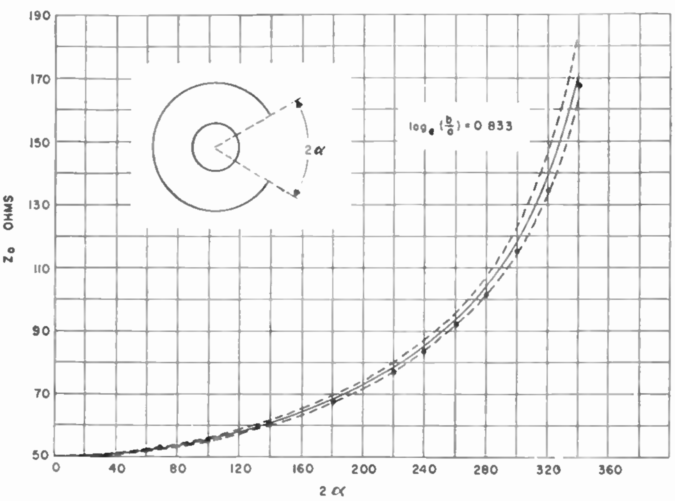

Fig. 4—Characteristic impedance of uniform, slotted coaxial line.

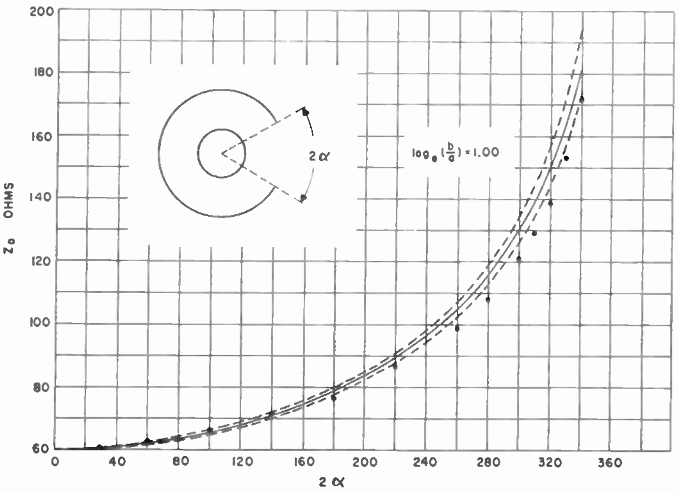

Fig. 5—Characteristic impedance of uniform, slotted coaxial line.

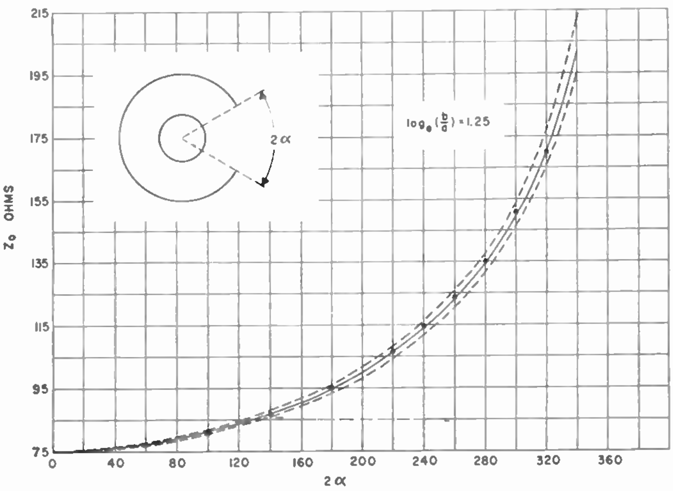

Fig. 6—Characteristic impedance of uniform, slotted coaxial line.

Balun Design and Performance

Having established the characteristic impedance of the uniform, slotted coaxial line, a specific balun design was undertaken. A transition from 50-ohm coaxial line to 150-ohm two-conductor line was selected for the balun. As mentioned previously, the characteristic impedance of the balun transformer is tapered along its length so that the input reflection coefficient follows a Tchebycheff response in the pass band. The maximum allowable reflection coefficient in the pass band was chosen as 0.055. This corresponds to a maximum standing wave ratio of 1.11 to 1. It follows that the length of the balun is $l=0.478\ \lambda$, where λ is the largest operating wavelength.[9] The lowest frequency was selected as 50 mc which fixed the length l as approximately 2.86 meters.

[8] J. D. Kraus, "Electromagnetics," McGraw-Hill Book Co., Inc., New York, N. Y., pp. 426–427; 1953.
[9] Klopfenstein, *op. cit.*, p. 32.

Let the total length l of the balun be defined from $z=-l/2$ to $z=l/2$. Fig. 7 shows the impedance contour required for Tchebycheff response under the prescribed design criteria. The angle 2α which yields the proper impedance at each position along the balun may be extracted from Fig. 4. The outer conductor of the coaxial line had an inside diameter of 1.527 inches. The balun was fabricated by milling through the coax outer conductor to the depth which yielded the angle 2α. The milling cut was performed in discrete 6-inch increments along the balun until the outer conductor was reduced to a thin concave strip having a width equal to the center conductor diameter. This occurred at the position $z/l=0.373$ where $2\alpha=312°$ and $Z_0=131$ ohms. The strip outer conductor was transformed to a circular cylinder identical to the center conductor over a 6-inch length from $z/l=0.373$ to $z/l=0.426$. The spacing between cylindrical conductors at $z/l=0.426$ was such that the impedance was the required 136 ohms as shown in Fig. 7. From $z/l=0.426$ to $z/l=0.5$ the spacing of the cylindrical conductors was gradually increased so that the impedance followed the contour of Fig. 7.

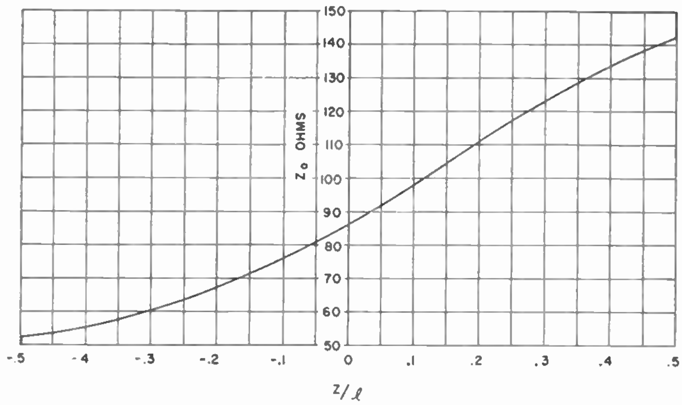

Fig. 7—50- to 150-ohm Tchebycheff impedance taper.

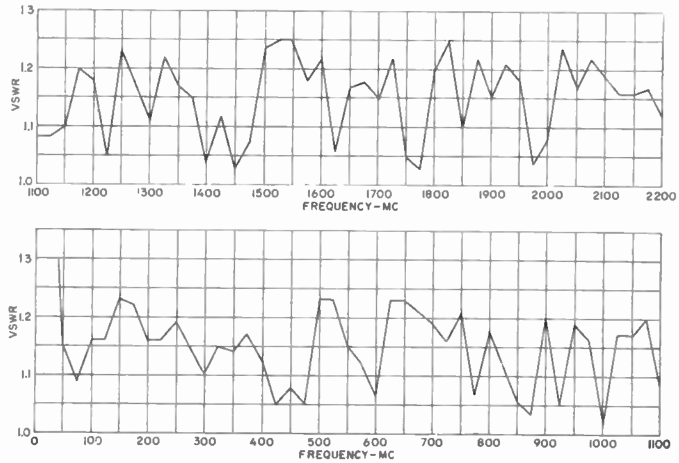

Fig. 8—Experimental performance of tapered balun transformer.

Since the balun may be viewed as a two-port waveguide junction, it was convenient to measure its performance by means of Deschamps' method.[10] The two-conductor output of the balun was terminated in a large, reflecting metal sheet mounted perpendicular to the line. The dissipative loss and scattering matrix coefficients of the balun are readily obtained by locating the reflecting sheet at four equally spaced positions and measuring the corresponding reflection coefficient at the coaxial input.[11] Since the scattering coefficient S_{11} corresponds to the input reflection coefficient for a reflectionless termination of the output line, one thereby obtains the input VSWR for a matched termination of the two-conductor line. This procedure also avoids the considerable difficulties encountered in providing a matched termination for an open wire line. Over the 40- to 500-mc frequency range, measurements were performed by using a General Radio admittance bridge.

The voltage standing wave ratio as a function of frequency is presented in Fig. 8. It may be seen that the VSWR never exceeded 1.25:1 over the 43- to 2200-mc spectrum which represents a 50:1 bandwidth. The rapid increase in VSWR below the 50-mc cutoff frequency is quite apparent. The balun dissipative loss was not measurable below 500 mc. At 1000 mc, the loss was approximately 0.1 db and increased to 0.3 db at 2000 mc. The spacing between cylindrical conductors at 2000 mc was 0.21 λ. It is evident that the tapered balun can be designed to operate over frequency bandwidths as large as 100:1.

It should be noted that the characteristic impedance at any cross section of the balun is slightly different than the Z_0 assumed from theory since the slotted line analysis applied to a coax with infinitely thin outer conductor. The effect of finite wall thickness on impedance is greatest for large apertures 2α. Consequently, the synthesis of the required Tchebycheff impedance contour was not accomplished precisely. It appears that the measured VSWR exceeded the design maximum of 1.11 because of reflections from teflon spacers which were used for mechanical support of the line and because the synthesis of the impedance contour was not exact.

Concerning the electrical balance of the balun, it would be fine to prescribe the exact complex ratio of unbalanced to balanced current which results at the two-conductor output of the balun, but, unfortunately, serious questions arise as to the validity or meaning of such a measurement on the open, two-conductor system. We know that the TEM field of the coaxial line is gradually transformed to the TEM field of an open, two-wire transmission line as one traverses the length of the tapered balun transformer. Obviously, not all of the incident power is converted to the transmission line mode. A fraction of the incident power is lost as stray radiation from the slot aperture which forms the tapered transition. That is, the efficiency of excitation of the transmission line mode is necessarily less than 100 per cent.

[10] G. A. Deschamps, "Determination of reflection coefficients and insertion loss of a waveguide junction," *J. Appl. Phys.*, vol. 24, pp. 1046–1050; August, 1953.

[11] F. L. Wentworth and D. R. Barthel, "A simplified calibration of two-port transmission line devices," IRE TRANS. ON MICROWAVE THEORY AND TECHNIQUES, vol. MTT-4, pp. 173–175; July, 1956.

In addition to the usual TEM transmission line mode, the so-called parallel wave or mode will also be excited.[12] The parallel wave is a transverse magnetic surface wave akin to Sommerfeld's single-wire wave. The parallel wave is evidenced by the superposition of an unbalanced current component (parallel excitation or codirectional currents) with the push-pull currents of the TEM mode. In fact, the common engineering description of this wave phenomenon is to note that the transmission line currents are not balanced, which implies the existence of the parallel wave component of current. The amplitude of the parallel wave field decreases much more slowly with radial distance than does the TEM mode. Because of this fact, the surface wave is quite sensitive to its surroundings and we say that the wave is very loosely bound to the transmission line. At any bends, changes in line cross section, or discontinuities such as line spacers, a significant portion of the mode power will be converted to a radiation field. This is a well-known property of surface wave fields; in fact, some types of surface wave antennas specifically depend upon radiation from obstacles as the mechanism for operation. Wherever radiation occurs, the magnitude of the parallel wave (unbalanced) current will be attenuated. Obviously, then, the measured unbalance on the open two-conductor line will depend upon the line position where the measurement is performed. One questions, therefore, the utility or meaning of an "exact" balance measurement on such an open system.

In order to excite any surface wave mode efficiently, the launching source must produce a field which is quite similar to the mode distribution. If the physical parameters of the problem are such that the surface wave field is of large transversal extent, then the launching source must necessarily have a large physical aperture. It so happens that the parallel wave does have a very large transverse distribution so that the tapered balun transformer, which accomplishes a very gradual transition between two TEM field distributions, is a very poor source of the parallel wave mode. Thus, the initial magnitude of the unbalanced current is quite small compared to the balanced current. Furthermore, it is possible to attenuate the unbalanced current in a short distance from the balun terminals by placing several radiating discontinuities such as spacers on the line. Since only the TEM mode exists at a sufficient distance from the balun output, a reflecting plate may be placed there and a network measurement of dissipative attenuation (Deschamps' method) is valid. In view of the foregoing circumstances it would seem more realistic to evaluate electrical balance by the measurement of balun radiation loss since the "net" result of the unbalanced current is, precisely, radiation which may be included in the total dissipative attenuation of the balun. If the total balun attenuation is small, we can be sure that the unbalanced current is insignificant compared to the balanced current. As a result of the extremely low dissipative attenuation which was measured with the test balun, we conclude that the magnitude of the unbalanced current is negligible and that the tapered balun transformer is inherently a balanced device.

[12] A. Sommerfeld, "Electrodynamics," Academic Press, Inc., New York, N. Y., pp. 198–211; 1952.

As a final demonstration of the electrical balance resulting from the tapered balun, a scaled model of the previous design was constructed for operation in the kilomegacycle frequency region. The balun was fabricated from $\frac{1}{4}$-inch-diameter brass tubing and the total length was approximately 12 inches to permit operation down to 500 mc. The impedance taper of the microwave model was identical to the taper of the low-frequency balun. The balun was used to excite dipole radiators at various frequencies from 500 to 5000 mc. *No asymmetry caused by unbalanced excitation currents was evident in the dipole radiation patterns.*

Conclusion

The performance of the Tchebycheff tapered balun transformer is unique; it provides near perfect impedance matching over frequency bandwidths as great as 100:1. The balun geometry is not limited to a transition from coax to two-wire transmission line; other output configurations such as a balanced strip line are possible. The basic design allows one to match a large range of impedances with an arbitrarily small standing wave ratio. The balun length is determined by the lowest frequency of operation and the maximum reflection coefficient which is to occur in the pass band. It is evident from the very small dissipative attenuation that negligible radiation results from the balun and that the balun is inherently balanced. From the satisfactory performance of the test model baluns, we know that, by simple scaling according to wavelength and with careful regard to construction, tapered baluns may be operated in the kilomegacycle frequency region. It should also be noted that the balun is well suited to high power applications.

Appendix

The formation of a variational principle for the eigenvalue equation

$$\mathfrak{L}(\psi) = \lambda\mathfrak{M}(\psi) \tag{23}$$

is discussed by Feshbach and Morse.[13] Here $\mathfrak{L}$ and $\mathfrak{M}$ are differential or integral operators, ψ is the function upon which $\mathfrak{L}$ and $\mathfrak{M}$ operate, and λ is the quantity (eigenvalue) whose value is desired. Morse and Feshbach show that if $\mathfrak{L}$ and $\mathfrak{M}$ are self-adjoint operators, a variational principle for λ is the form

$$\delta[\lambda] = \delta\left[\frac{\int \psi\mathfrak{L}(\psi)dv}{\int \psi\mathfrak{M}(\psi)dv}\right] = 0, \tag{24}$$

[13] Morse and Feshbach, *op. cit.*, pt. 2, pp. 1108–1109.

which means that the eigenvalue λ is stationary with respect to arbitrary first order variations in the functional form of ψ.

Let the integral operators $\mathfrak{L}$ and $\mathfrak{M}$, and the function ψ be defined as follows:

$$\mathfrak{L} = \frac{b}{v}\int_\alpha^\pi G(b,\theta \mid b,\theta')d\theta',$$

$$\mathfrak{M} = 2b\int_\alpha^\pi d\theta$$

$$\psi = \sigma(\theta').$$

Then

$$\mathfrak{L}(\psi) = \frac{b}{v}\int_\alpha^\pi G(b,\theta \mid b,\theta')\sigma(\theta')d\theta' = \frac{1}{v}\phi_0,$$

$$\mathfrak{M}(\psi) = 2b\int_\alpha^\pi \sigma(\theta')d\theta' = Q, \tag{25}$$

and (23) takes the form

$$\frac{1}{v}\phi_0 = \lambda Q; \tag{26}$$

i.e., the eigenvalue λ is the characteristic impedance Z_0. Substituting (25) and ψ into (24), we obtain the variational principle

$$\delta[Z_0] = \delta\left[\frac{\frac{1}{2v}\int_\alpha^\pi\int_\alpha^\pi G(b,\theta \mid b,\theta')\sigma(\theta)\sigma(\theta')d\theta d\theta'}{\left\{\int_\alpha^\pi \sigma(\theta')d\theta'\right\}^2}\right] = 0, \tag{27}$$

which shows that Z_0 as given by (11) is stationary with respect to arbitrary first order variations in the functional form of $\sigma(\theta)$.

Acknowledgment

The authors are pleased to acknowledge the assistance of Dr. R. H. DuHamel who originally conceived the tapered balun transformer. They also wish to thank R. P. Rhodes who programmed the numerical computations and R. G. Gisel who assisted with the experimental measurements.

Corrections

W. K. Weihe, author of "Classification and Analysis of Image-Forming Systems," which appeared on pages 1593–1604 of the September, 1959, issue of PROCEEDINGS has requested that the following corrections be made to his paper.

In the second paragraph of Section I, on page 1593, the description following the colon on the third line is incomplete. It should read: " . . . the radiation which is being emitted by each individual element and the radiation which is being reflected by the same element and which has its origin inside or outside the scene."

On page 1599, second column, the dimensions in the fourth line after (7) should read $\mathrm{cm}^{-1}\ \mathrm{deg}^{-1}$.

On page 1602, $4\Gamma_0$ in (23) should be replaced by $\Gamma/4L_0$.

In the equation in the middle of the first column on page 1603, r^2 should be replaced by Γ^2.

R. Parthasarathy, R. P. Basler, and R. N. DeWitt, authors of the correspondence entitled "A New Method for Studying the Auroral Ionosphere Using Earth Satellites," which appeared on page 1660 of the September, 1959, issue of PROCEEDINGS, have requested that the following corrections be made to their letter.

In the first paragraph of the second column, the time difference mentioned on the tenth line should be 33 ± 1 seconds and the corresponding height given in the next sentence should be 104 km $\pm$ 3 km.

Measurement of Internal Reflections in Traveling-Wave Tubes Using a Millimicrosecond Pulse Radar*

D. O. MELROY† AND H. T. CLOSSON‡

Summary—**This paper describes a test method which enables one to locate reflections on traveling-wave tube helices and to measure the return loss of each reflection. This information is needed for traveling-wave tubes used in pulse code transmission since "echo" pulses arising from reflections can distort the meaning of the code.**

This test method employs millimicrosecond pulses in a radar circuit with a stroboscopic viewing system. The sensitivity of the system permits easy observation of reflections having return losses as high as 40 db. Using this method we have been able to identify two previously unsuspected sources of helix reflections.

INTRODUCTION

ONE of the requirements for the best operation of traveling-wave tube amplifiers is that the signal be transmitted through the tube with a minimum number of reflections. If the tube is used for pulse amplification, any reflection will increase the apparent pulse width, or, if the pulse is short enough, cause an echo to follow the main pulse.[1] In CW operation, a reflection may cause the operating output match to show a rippled pattern when plotted against frequency. The amplitude of these ripples is a measure of the reflected power, and their frequency spacing is an indication of the distance to the internal reflection point.

In general, these internal reflections are produced by some deviation from a uniform helix structure. A single discontinuity may give a strong reflection at all frequencies. A periodic aberration in the helix structure may cause a small reflection from each of many points which become additive at particular frequencies.[2]

The short pulse measurements reported here locate reflections accurately along a traveling-wave tube helix. Once the location of the reflection is known one can often determine the cause by using a low-power microscope. In some cases it is possible to remove the disturbance and make the helix entirely satisfactory. If this is not possible, it is still important to know the location, since the degree of the signal degradation caused by the reflection depends upon its position along the helix.

If part of the output signal is reflected back into the tube by an imperfect output match, it will travel back along the helix. If part of this reflected signal is again reflected by some disturbance on the helix, it will travel forward with the electron beam and be amplified. For a reflection near the output end, the amplification is small. If, however, the reflection occurs near the edge of the "loss" section of the helix, it will experience almost the full gain of the tube. This may build up an "echo" signal to a level at which it can be confused with the main signal. For this reason the position of the reflection strongly influences the decision as to whether the helix is useable.

The use of millimicrosecond pulses and radar techniques for studies of reflections in waveguides has been reported.[3] A stroboscopic method of pulse observation has been developed at the Bell Telephone Laboratories by Goodall.[4] By use of a stroboscopic gating system one obtains a slowed-down facsimile of the periodically recurring millimicrosecond pulse which may be displayed on any good low frequency oscilloscope. To display these pulses directly would require an oscilloscope having a bandwidth of at least 500 mc. We have adapted the techniques of Beck and Goodall to the measurement of traveling-wave tube reflections, and have developed a stroboscopic system using balanced RF modulators.

OPERATION OF THE TEST SYSTEM

The components and operation of the system appear in Fig. 1. Basically the system consists of a signal source giving millimicrosecond pulses of RF energy which are amplified by a traveling-wave tube. The amplified pulses are coupled into the structure being examined. Any reflected pulses are separated from the incident pulses by a directional coupler. The reflected pulses are amplified by a traveling-wave tube and then detected with a crystal detector. The detected pulses are displayed on an oscilloscope where the separation of the pulses displayed represents the distance between the reflection points along the structure being tested.

The actual display of the reflected pulse is done by use of the stroboscopic gating system previously mentioned. This gating system converts the reflected pulse

* Original manuscript received by the IRE, June 25, 1959; revised manuscript received, October 8, 1959.

† Bell Telephone Labs., Inc., Murray Hill, N. J.

‡ S-F-D Labs., Inc., Varian Associates, Union, N. J. Formerly at Bell Telephone Labs., Inc., Murray Hill, N. J.

[1] A. F. Dietrich, unpublished work.

[2] J. P. Laico, H. L. McDowell, and C. R. Moster, "A medium power traveling-wave tube for 6000-mc radio relay," *Bell Sys. Tech. J.*, vol. 35, pp. 1285–1346; November, 1956.

[3] A. C. Beck, "Waveguide investigation with millimicrosecond pulses," *Bell Sys. Tech. J.*, vol. 35, pp. 35–65; January, 1956.

[4] W. M. Goodall, unpublished work.

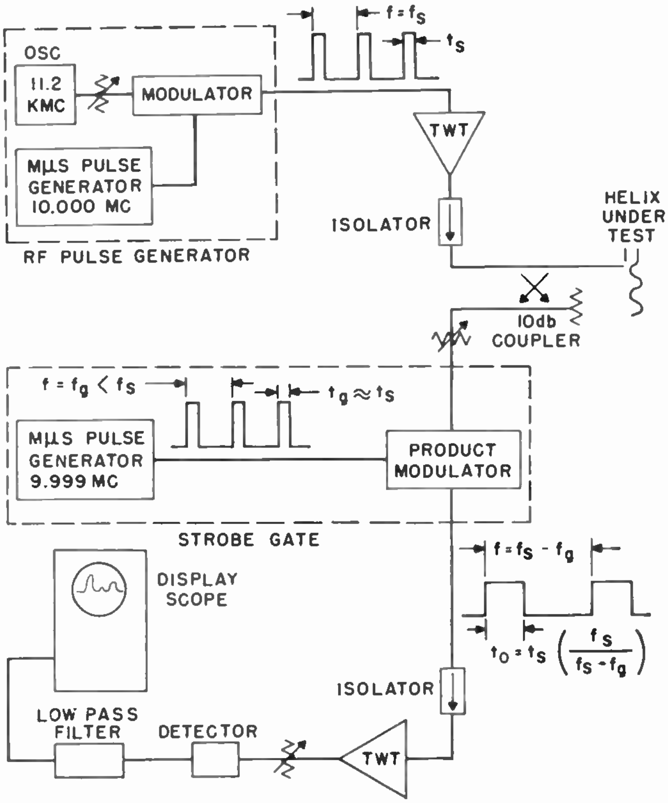

Fig. 1—Millimicrosecond pulse test system.

to low-frequency modulation of the RF pulse train. The modulated RF is amplified by the second traveling-wave tube and detected by a conventional crystal detector. The detected signal can then be displayed on an ordinary low-frequency oscilloscope. The "strobe gate" is essentially a high-speed switch which is normally off and is periodically turned on for a short while by the strobing signal at a repetition rate of f_g. Ideally, the strobe pulse should be much narrower than the signal pulse in order to provide maximum resolution. In practice, however, the strobe and signal pulses are of the same width. The resulting display pulse has about 1.4 times the basic pulse width.

The signal pulses recurrent at frequency f_s and the strobe pulses at frequency f_g may be represented by the Fourier series of harmonic terms. It can be shown that the output of the strobe gate, which is a product modulator, will contain the sum and difference frequencies of the two harmonic series. If a low-pass filter is adjusted to pass only the difference frequencies, then at its output the signal pulses will be reproduced slowed down in time by the factor $K=f_s/(f_s-f_g)$. Values of f_s and f_g may be chosen so that the strobed facsimile of the input pulse may be displayed directly on a low-frequency oscilloscope. The oscilloscope's time base may be calibrated in terms of the input signal by multiplying the scope's sweep speed by the factor K. One may apply this terminology to the more familiar optical stroboscope where f_g is adjusted to equal f_s and K becomes infinite, resulting in "stopped" motion.

The equipment may be calibrated and adjusted quite easily by connecting at the test position a variable attenuator followed by a length of waveguide shorted at the end, as shown in Fig. 2(a). With this arrangement, there are two reflections; the first from the edge of the attenuator vane, and the second from the short at the end of the waveguide. If the distance from the edge of the attenuator vane to the short is 2 feet, the pulse separation will be very close to 5 mμsec, as indicated in Fig. 2(b). These reflections may be used to calibrate the time base of the oscilloscope and checked against the basic 100-mμsec separation of the main pulses. The reflection from the attenuator vane is about 30 db below the incident pulse, so with 15 db in the attenuator, the two pulses will have the same amplitude. With such a display one can easily make adjustments for minimum pulse width by observing the base line separation of the two pulses. The normal base line pulse width is 2 to 3 mμsec, depending on the care used in adjusting the equipment. With care it is possible to measure reflections 45 to 50 db below the main pulse.

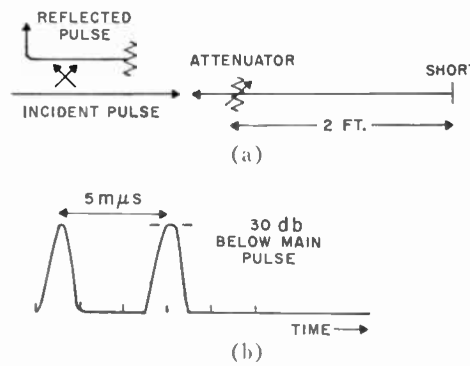

Fig. 2—(a) Waveguide setup for calibration. (b) Oscilloscope display.

Results

The millimicrosecond radar has been used to study the helices for the M1917 traveling-wave tube. This tube is designed for use as a millimicrosecond pulse amplifier in the 10.7- to 11.7-kmc band. Most of the present work has been done with helices prior to assembly into tubes. Results are also presented for several operating tubes.

The helix testing is done by matching into one end of the helix and observing the reflected pulses returning from along the helix. The oscilloscope sweep is triggered by the reflection from the matching section of the helix. Since the other end of the helix is not terminated, it provides a fairly strong reflection which may be used to calibrate the oscilloscope sweep in terms of helix length. The oscilloscope is conveniently adjusted to give a sweep of one or two scale divisions per inch of helix. This makes it easy to identify the position of a

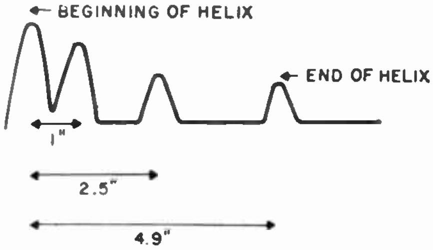

Fig. 3—Reflection pattern from a helix which had pieces of metal placed on the helix at 1.0 and 2.5 inches.

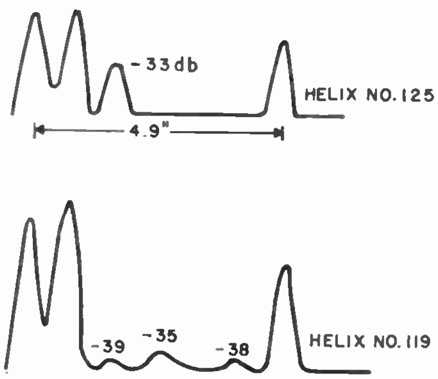

Fig. 4—Typical M1917 helix reflections.

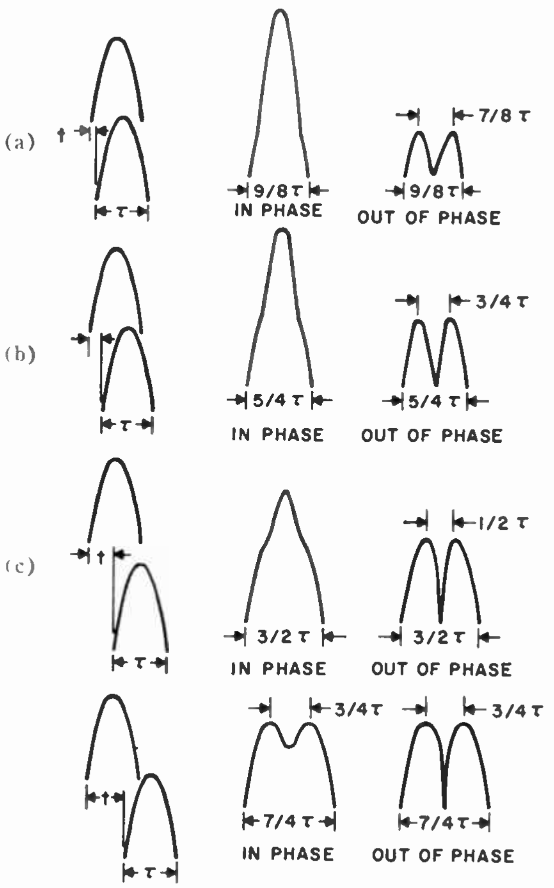

Fig. 5—Interference of overlapping pulses—τ=base pulse width, t=time between reflected pulses. (a) $t=\tau/8$, (b) $t=\tau/4$, (c) $t=\tau/2$.

reflection along the helix. Fig. 3 shows the reflection pattern obtained from a helix on which small bits of wire had been placed at 1.0 and 2.5 inches from the end.

Fig. 4 shows the reflection patterns for two typical M1917 helices. These patterns show a double pulse at the beginning of each helix, the reflection from the helix matching section, and the reflection from the shorting plunger behind the helix. Since these two points are close together the two reflected pulses overlap and one observes an interference pattern in the output trace. A change in plunger position of 0.33 inch gives a phase shift of 180° for the reflected RF pulse. This interference between two pulses can result in a display showing a double pulse with a much greater time separation than would be indicated by the actual separation of the reflection points, as shown in Fig. 5. Because of the double pulse at the beginning of the helix, small reflections close to this end of the helix are not observed. Reflections from this area are seen from the other end of the helix, unless they are very small.

With the first helices examined, a number of reflection points were seen on almost every helix. These were found, in most cases, to be due to one of two defects. Small splinters of wire which formed in the winding of the helix were one source of reflections. The second source was small particles of metal imbedded in the ceramic rods which support the helix. Most of the splinters seen on the wire are very small and easily removed by oxidizing and then reducing the helix assembly. Fig. 6 shows a very large splinter and the reflection obtained from it. The size of the splinter may be estimated by comparing it with the helix wire, which is 0.005 inch in diameter. Splinters of this size may be picked off the helix by hand under a microscope. The metal imbedded in the rods is often covered by the glaze which bonds the helix wire to the ceramic rods, and therefore little can be done to remove it from the finished helix. Examination of the ceramic rods (Alsimag 475) prior to use showed that the particles were already present and distributed throughout the ceramic material. The impurities are bits of iron, stainless steel and nickel introduced during the preparation of the ceramic.

By selecting rods which are free from visible inclusions along the edge which contacts the helix, we have been able to eliminate the worst reflections. However, most helices still show small internal reflections, probably due to particles which lie just below the rod surface.

Several helices have shown a small but broad reflection, as though from a series of points spaced along the helix. Inspection of the helix winding[5] showed periodic

[5] H. T. Closson, W. E. Danielson, and R. J. Nielson, "Automatic measurement of small deviations in periodic structures," *Rev. Sci. Instr.*, vol. 29, pp. 855–859; October, 1958.

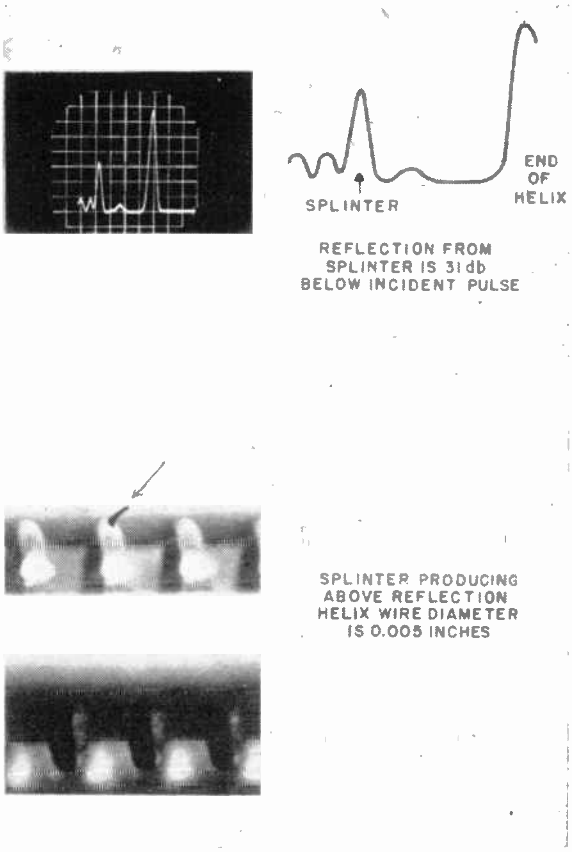

Fig. 6—Reflection from splinter on helix.

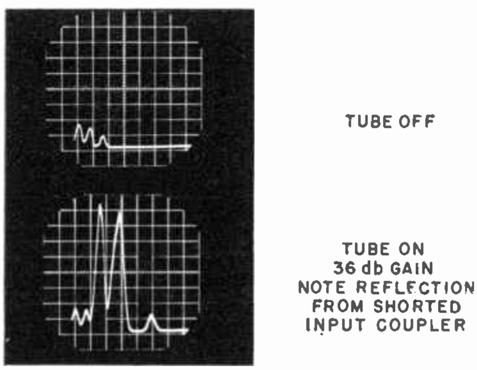

Fig. 7—Growth of helix reflections in operating tube.

aberrations in the region of the reflection and, in one case, a gradual change in pitch.

By using an operating tube one greatly increases the sensitivity of the measuring system, since any reflected pulse will now be amplified by the tube being examined. The output end of the tube being tested is connected to the test system. The incident pulse then travels along the helix against the electron beam, while any reflected pulse travels with the electron beam and is amplified. Fig. 7 shows the result for a typical M1917 tube. The upper trace shows the reflections from the cold tube; the lower trace shows the same tube with full gain. Note that the low total loss of the helix allows one to observe the reflection from the input coupler, which is deliberately mismatched.

In these tests, the full pulse is traveling back along the helix, but in an actual tube this backward power should be only that introduced by the mismatch either at the output coupler or at some other point after the tube. One would expect any such reflection to be 20 db or more below the main signal. This loss would be added to the loss at the internal reflection point to obtain the value of the signal, which would be amplified again. Thus, one should be able to compute the approximate level of any echo pulse. Tests with actual tubes have shown this method to be accurate within 6 db.

The reflected pulse can also be used to measure the rate at which the intrinsic and applied losses increase along the helix. This is done by using a reflecting rod inside the helix and by measuring the amplitude of the reflected pulses as a function of position along the helix. The reflected pulse decreases in amplitude at a rate equal to twice the rate of increase of helix loss. A measurement of this type is shown in Fig. 8, corrected by this factor of two.

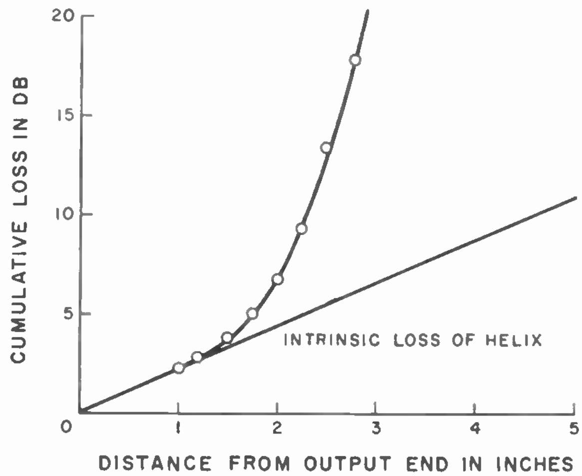

Fig. 8.

Conclusion

These results show that millimicrosecond pulse techniques have provided us with a powerful tool for studying the internal match of traveling-wave tubes. Initial measurements on cold helices have disclosed two major sources of internal reflections. Echoes as small as 40 db below the incident pulse can be measured on the cold helices and even smaller reflections identified in operating tubes. The same equipment can also be used to evaluate various applied loss patterns and to measure the reflection from the edges of this loss. By selecting only helices that have reflections below a selected value we are able to make tubes whose hot match can be predicted and held to some set standards. Perhaps most important of all is that we can now tell, without building a tube, if a change in material, technique, or processing actually results in an improved helix.

Noise Consideration of the Variable Capacitance Parametric Amplifier*

M. UENOHARA†

Summary—**This paper describes a model of the variable capacitance diode in which the spreading resistance is considered as the source of amplifier noise. Gain and noise figure calculations are made for this model and experimental results obtained at 5.84 kmc while pumping at 11.7 kmc are presented for gallium arsenide, silicon and germanium diodes. The qauntity $1/\omega C_0 R_s$ is defined as a "quality factor" where R_s is the spreading resistance and C_0 is the static capacitance at zero bias point. Computations of minimum noise figure, optimum load admittance, optimum pumping factor, are all given in terms of the parameter $\omega C_0 R_s$.**

The essential differences between single- and double-sideband reception are discussed. Over a range of sufficiently large values of the parameter $\omega C_0 R_s$, there is a reasonable correlation of the theory developed with the measurements performed on most of the diodes. In the range of relatively small values of $\omega C_0 R_s$, the model proves inadequate to describe some diodes properly and suggests the need for introducing extra noise sources. These noise sources are also discussed. Of the experimental data obtained thus far, the best result has been with a gallium arsenide diode which yields a 0.9 db double-sideband noise figure and, equivalently, 3.9 db for single-sideband operation with 16 db gain and 25 mc of single-sideband frequency bandwidth.

Introduction

The variable capacitance parametric amplifier is of interest primarily because it shows promise of very low noise amplification.[1–3] A reduction in receiver noise would permit either an equivalent reduction in transmitter power or an increase in range, or both.

In a parametric amplifier, the process of energy transfer from the signal frequency to the idler (image) frequency (and vice versa) complicates the noise problem. The mode of analysis of noise performance in a variable capacitance parametric amplifier is very much the same as for crystal mixers.[4–8] It should be emphasized, however, that the process of energy transfer is caused by a variable capacitance rather than a nonlinear resistance, as is the case for crystal mixers, and that regenerative amplification can be achieved only when the circuit is properly adjusted for both the signal and idler frequencies. When the amplifier is properly adjusted, the variable capacitance exhibits the property of a negative conductance. This negative conductance is the result of a secondary mixing process, namely that between the pump and the idler. The idler frequency band, therefore, cannot be rejected to improve the noise figure as is common practice in mixers.

The noise output in the signal frequency band, f_s, is due to: 1) input noise at f_s which is amplified, 2) input noise at the idler frequency, f_{p-s}, which is converted to f_s while being amplified, 3) noise which originates in the diode and its circuit at f_s and is amplified, and 4) noise from the diode and its circuit at f_{p-s}, which is converted to f_s while being amplified. The noise sources which might be important under 3) and 4) above are as follows:

a) Thermal noise originating in the series resistance (spreading resistance) of the variable capacitance.
b) Noise generated in the junction of the diode. This is mainly shot noise "due to carriers that cross the junction in the forward direction, meander about as minority carriers for a while, and then, escaping any other fate, return in the reverse direction across the junction."[9] Uhlir has shown that this type of noise does not contribute significantly to the noise at the signal and idler frequencies in the microwave region.
c) Thermal noise from the waveguide circuitry.

In addition to the four types of noise mentioned above, there exists still another type. It is caused by pump noise giving rise to a fluctuation of the depletion layer and to a corresponding fluctuation in gain. This noise is probably negligible since for proper adjustment of the amplifier gain it is essentially constant for small variations of pump power.

If the amplifier circuit is designed so that the circuit impedance is very low for all frequencies except for the signal, idler, and pump frequencies, no voltage appears at the circuit terminals except for these three frequencies. However, when the series resistance is not negligible, all currents generated by the variable capacitance flowing through the series resistance will set up corresponding voltages at the terminals. Several mixing proc-

* Original manuscript received by the IRE, March 4, 1959; revised manuscript received, July 29, 1959. A brief presentation of this work was given at the Sixteenth Annual Conf. on Electron Tube Research, Université Laval, Quebec, Can., June, 1958.

† Bell Telephone Labs., Inc., Murray Hill, N. J.

[1] G. F. Herrmann, M. Uenohara, and A. Uhlir, Jr., "Noise figure measurements on two types of variable reactance amplifier using semiconductor diodes," Proc. IRE, vol. 46, pp. 1301–1303; June, 1958.

[2] H. Heffner and K. Kotzebue, "Experimental characteristics of a microwave parametric amplifier using a semiconductor diode," Proc. IRE, vol. 46, p. 1301; June, 1958.

[3] B. Salzberg and E. W. Sard, "A low-noise wide-band reactance amplifier," Proc. IRE, vol. 46, p. 1303; June, 1958.

[4] H. C. Torrey and C. A. Whitmer, "Crystal Rectifiers," M.I.T. Rad. Lab. Ser., McGraw-Hill Book Co., Inc., New York, N. Y., vol. 15; 1948.

[5] P. D. Strum, "Some aspects of mixer crystal performance," Proc. IRE, vol. 41, pp. 875–889; July, 1953.

[6] P. D. Strum, "A note on noise temperature," IRE Trans. on Microwave Theory and Techniques, vol. MTT-4, pp. 145–151; July, 1956.

[7] G. C. Messenger and C. T. McCoy, "Theory and operation of crystal diodes as mixers," Proc. IRE, vol. 45, pp. 1269–1283; September, 1957.

[8] C. T. McCoy, "Present and future capabilities of microwave crystal receivers," Proc. IRE, vol. 46, pp. 61–66; January, 1958.

[9] A. Uhlir, "High frequency shot noise in p-n junctions," Proc. IRE, vol. 44, pp. 557–558; April, 1956.

esses are involved before these currents can give rise to voltages at the idler or signal frequencies, and noise arising from such secondary processes is ordinarily of far less importance than noise arising in the series resistance.

Noise originating in the signal and idler bands is uncorrelated and therefore additive in the output of the amplifier. It is clear that, as compared with normal amplifiers, we are paying a penalty by introducing signal in only one sideband, whereas noise inevitably also comes in through frequency conversion from the idler frequency band. If, however, we generate special signals having proper symmetry about half the pump frequency, signal power as well as noise power will enter in both bands, and the frequency converted signal will add in phase with the nonconverted signal. This type of operation which we shall call "double-sideband reception," offers a considerable advantage in noise performance over "single-sideband reception." The same improvement also occurs when the amplifier is used to receive broad-band noise as, for example, in certain radio astronomy applications. The signal-to-noise ratio for double-sideband reception is better than that of single-sideband reception by a factor of about 2 for $f_s \approx f_{p-s}$. Further, when the background noise temperature goes down below room temperature, the signal-to-noise ratio of the variable capacitance amplifier for normal operation becomes better than for a conventional amplifier having the same noise figure. This is so because a significant amount of noise arises as input noise at the idler frequency. Since the term noise figure is standardized in such a way that excess receiver noise is referred to the available noise from a resistor at room temperature (290°K), we shall employ the term "operating noise figure" to characterize the sensitivity of a receiver for arbitrary source temperatures.[8] The operating noise figure τ_s is defined by

$$\tau_s = (F - 2) + 2\tau_a$$

for single-sideband parametric operation, and

$$\tau_s = (F - 1) + \tau_a$$

for both conventional amplifiers and double-sideband parametric operation. In the above equations F is the noise figure of the amplifier and τ_a is the antenna temperature divided by 290°K. In Fig. 1 the curves indicate the operating noise figures of a single-sideband parametric amplifier and of a conventional amplifier as a function of the apparent temperature of the sky. For example, when the noise figures of the single-sideband parametric amplifier and the conventional amplifier are both 4 db, and the antenna sees a sky temperature of 20°K, then the operating noise figure of the parametric amplifier is −2 db, while that of the conventional amplifier is 2 db. When the noise figure of the parametric amplifier is high, most of the noise originates within the circuit or within the series resistance of the diode; in

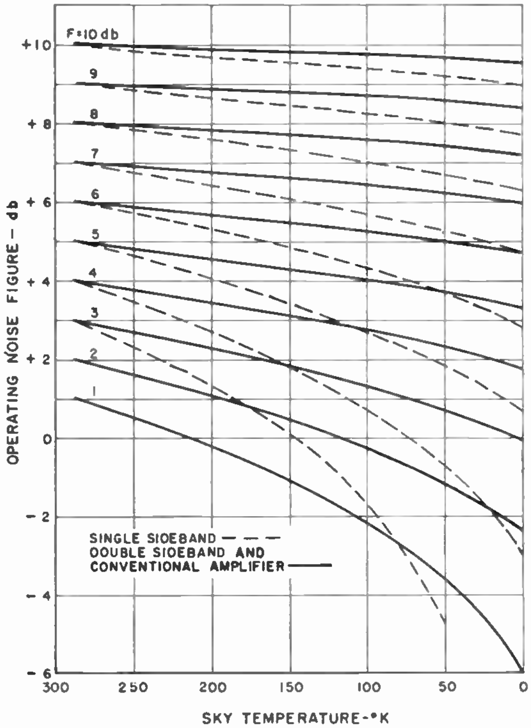

Fig. 1—The operating noise figures of a single-sideband parametric amplifier and of a conventional amplifier or a double-sideband parametric amplifier as a function of the apparent temperature of the sky.

this case the operating noise figure of a conventional and parametric amplifier are approximately equal. However, when the noise figure is small, the output noise is due mainly to input noise so that the distinction between parametric and conventional amplifiers is enhanced. This is shown in the lower portion of Fig. 1.

Available Power Gain of the Variable Capacitance Parametric Amplifier With Series Resistance

The noise figure will be discussed in terms of a circuit having a single external coupling line and using a circulator to separate the incoming and outgoing signals. The experimental arrangement is shown in Fig. 2. Because of the circulator the signal generator is always matched and the amplifier is isolated from the generator while transmitting its output to the load. The equivalent circuit is shown in Fig. 3.

The current flowing into the variable capacitance includes in general the infinite number of frequency components provided by the nonlinearity of the diode. We now assume that the circuit impedance is high only for the signal f_1 and the idler f_2. We assume further that the capacitance is not strongly pumped so that the use of only a first-order nonlinearity term is a good approximation. We observe then that, to within the approximations, $C = C_0 + C_3 \sin(\omega_3 t + \theta_3)$, where ω_3 is the angular frequency of the pump and staisfies the relation $\omega_3 = \omega_1 + \omega_2$. The signal current i_1 and the idler current i_2 are the only important components of the current spectrum. These may be expressed[10,11] in terms of the voltages appearing across the terminals of the variable capacitance, but excluding the series resistance, as

$$\begin{bmatrix} i_1 \\ -i_2^* \end{bmatrix} = \begin{bmatrix} y_{11} & y_{12} \\ y_{21} & y_{22} \end{bmatrix} \begin{bmatrix} e_1 \\ e_2^* \end{bmatrix} = \begin{bmatrix} j\omega_1 C_0 & j\omega_1 \dfrac{C_3}{2} \\ j\omega_2 \dfrac{C_3}{2} & j\omega_2 C_0 \end{bmatrix} \begin{bmatrix} e_1 \\ e_2^* \end{bmatrix}, \qquad (1)$$

where e_1 is the terminal voltage at the signal frequency and e_2^* is the complex conjugate of the corresponding voltage at the idler frequency. Since the depletion-layer capacitance of a junction diode is due to majority rather than minority carriers, and since the motion of these carriers is extremely small, the value of capacitance is practically constant from dc to microwave frequencies and beyond. Strictly speaking, if the series resistance of the diode is appreciable, none of the voltage components at other frequencies can be effectively short-circuited, and we therefore expect a change both in gain and noise output which depend on higher-order modulation products. These effects are considered of little consequence, however, and (1) represents a good approximation.

The currents in (1) are composed of two terms; one is the displacement current flowing through the constant capacitance C_0, and the other is the current generated by the variable capacitance due to the mixing effect. Eq. (1) permits the construction of the equivalent circuit shown in Fig. 4. Energy at the two frequencies is interchanged only through the variable capacitance; evidently no such exchange would take place in a linear passive network. Another form for the equivalent circuit is shown in Fig. 5. Here, the diode is common to both circuits, but currents at the signal and idler frequencies are caused to flow in separate external circuits by the presence of filters. If the circuit impedance is high enough at other frequencies, the representation must include extra circuits connected to the diode through appropriate filters. Since the amplifier has a single external coupling, and the input and output are separated by the circulator, the amplifier can see only one conductance connected in parallel with the signal generator. Let us then redefine G_g as the load conductance as well as the generator conductance for the signal, and G_L as the load for the idler. If the signal is received in double-sideband fashion, an extra current generator should be connected in parallel to G_L. In the equivalent representation, the two circuits appear separately, but in an actual waveguide configuration, the two different

[10] A. E. Bakanowski, "The Nonlinear Capacitor as a Mixer," 2nd Interim Rept., Task 8, Crystal Rectifiers, Signal Corps Projects 2-7-3234; December, 1954.

[11] H. E. Rowe, "Some general properties of nonlinear elements. II. Small signal theory," PROC. IRE, vol. 46, pp. 850–860; May, 1958.

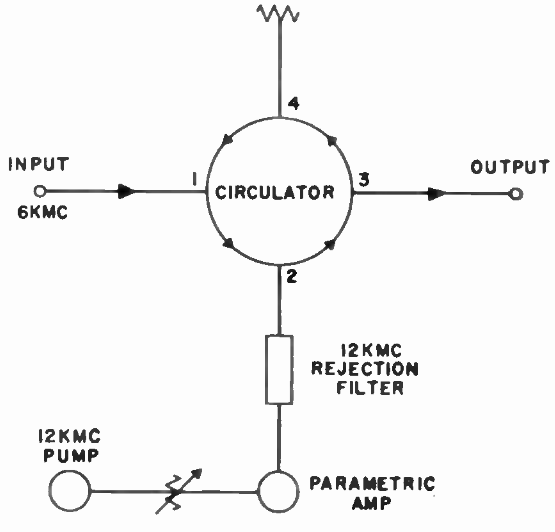

Fig. 2—Experimental arrangement of a circulator parametric amplifier.

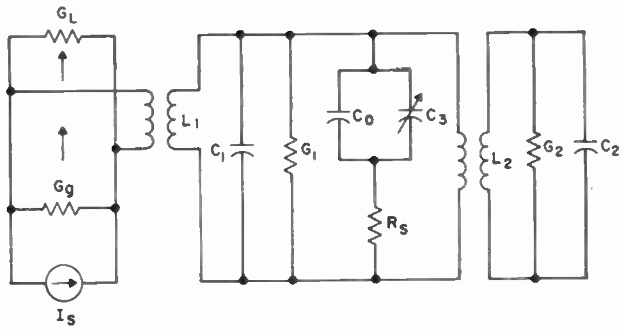

Fig. 3—Equivalent circuit of Fig. 2.

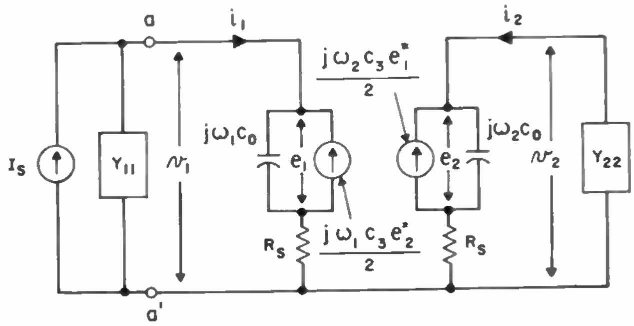

Fig. 4—Equivalent circuit of Fig. 3 based on (1).

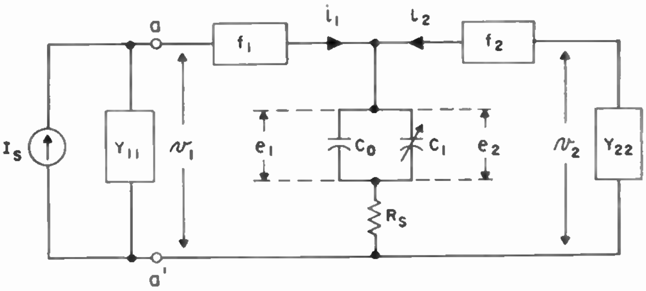

Fig. 5—Revised form of equivalent circuit. Currents at signal and image frequencies are caused to flow in separate external circuits by the presence of filters.

frequencies may be present simultaneously within a single resonant structure. When f_1 is near f_2, G_g and G_L are almost equal.

From the equivalent circuit, the following relations are found:

$$v_1 = e_1 + i_1 R_s. \tag{2}$$

$$v_2^* = e_2^* + i_2^* R_s. \tag{3}$$

$$i_1 = \frac{I_s}{(1 + R_s Y_{11})} - \frac{e_1 Y_{11}}{(1 + R_s Y_{11})} \cdot \tag{4}$$

$$i_2^* = \frac{-e_2^* Y_{22}^*}{(1 + R_s Y_{22}^*)} \cdot \tag{5}$$

where

$$Y_{11} = G_g + G_1 + j\left(\omega_1 C_1 - \frac{1}{\omega_1 L_1}\right) \tag{6}$$

$$Y_{22} = G_L + G_2 + j\left(\omega_2 C_2 - \frac{1}{\omega_2 L_2}\right). \tag{7}$$

From above equations the output voltage v_1 is found to be

$$v_1 = \frac{I_s}{Y_{11} + \dfrac{j\omega_1 C_0 - \dfrac{\omega_1\omega_2 C_3^2}{4Y_2}}{1 + R_3\left(j\omega_1 C_0 - \dfrac{\omega_1\omega_2 C_3^2}{4Y_2}\right)}} = \frac{I_s}{Y_{11} + Y} \tag{8}$$

where Y is the input admittance of the diode seen by the signal at terminal $a - a'$ and Y_2 is the admittance seen looking back from variable capacitance to the idler,

$$Y_2 = -y_{22} + \frac{Y_{22}^*}{(1 + R_s Y_{22}^*)} \cdot$$

Power output at the signal frequency is

$$P_{\text{out}} = v_1 v_1^* G_g. \tag{9}$$

The available power gain, under a high gain approximation is

$$G_{\text{av}} = \frac{P_{\text{out}}}{P_{\text{av}}} = 4G_g^2 \left| \frac{1}{Y_{11} + Y} \right|^2. \tag{10}$$

However, when the logarithmic gain is small or negative, the approximation fails and we determine the available power gain exactly from its equality to the square of the voltage reflection coefficient,[12]

$$G_{\text{av}} = \left| \frac{Y_{11} - Y}{Y_{11} + Y} \right|^2. \tag{10'}$$

If Y is negative, the logarithmic gain is positive, and as the denominator of (10) decreases gain increases. When the denominator passes through zero the gain becomes infinite and the system breaks into oscillation. We now assume that the idler frequency circuit is adjusted to make Y_2 real; then $Y_{11} + Y$ is simplified as follows:

$$\begin{aligned} Y_{11} + Y = {} & G_g + G_1 + j\left(\omega_1 C_1 - \frac{1}{\omega_1 L_1}\right) \\ & + \frac{\left(1 - \dfrac{\omega_1\omega_2 C_3^2 R_s}{4G_2'}\right)\left(-\dfrac{\omega_1\omega_2 C_3^2}{4G_2'}\right) + \omega_1^2 C_0^2 R_s}{\left(1 - \dfrac{\omega_1\omega_2 C_3^2 R_s}{4G_2'}\right)^2 + \omega_1^2 C_0^2 R_s^2} \\ & + j\frac{\omega_1 C_0}{\left(1 - \dfrac{\omega_1\omega_2 C_3^2 R_s}{4G_2'}\right) + \omega_1^2 C_0^2 R_s^2}, \end{aligned} \tag{11}$$

where Y_2 has been replaced by G_2'. If the siganl frequency circuit is adjusted so that its susceptance component is cancelled by that of the diode, the over-all admittance becomes a real conductance and the equation is simplified further.

The diode conductance is a function both of

$$\frac{-\omega_1\omega_2 C_3^2}{4G_2'},$$

which is a negative conductance introduced by the variable capacitance, and of $\omega_1 C_0 R_s$. The normalized conductance of the diode is shown in Fig. 6 as a function of the normalized pumping factor, GR_s, given by

$$GR_s = \left(\frac{\omega_1\omega_2 C_0^2 R_s}{4G_2'}\right)\gamma^2,$$

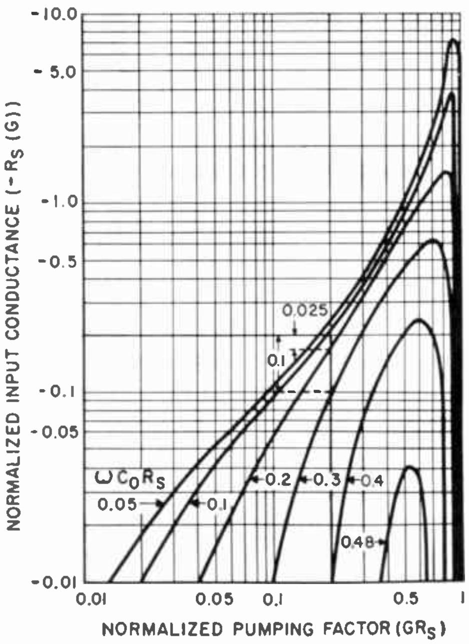

Fig. 6—Normalized conductance of diode as a function of the normalized pumping factor, GR_s. Minimum input conductance is zero when $\omega_1 C_0 R_s$ is 0.5.

[12] C. F. Quate, R. Kompfner, and D. A. Chisholm, "The reflex klystron as a negative resistance type amplifier," IRE Trans. on Electron Devices, vol. ED-5, pp. 173–179; July, 1958.

where γ is the ratio of the variable capacitance C_3 to the static capacitance, C_0, and is proportional to pump power. Curves are shown for 10 values of $\omega_1 C_0 R_s$ ranging from 0.05 to 0.50. As the curves indicate, the negative conductance increases when $\omega_1 C_0 R_s$ is decreased. When $\omega_1 C_0 R_s$ is 0.5, no negative conductance can be observed and this determines the highest frequency at which the diode can be used as an amplifier.[13] Further, it will be shown later that this product $\omega_1 C_0 R_s$ is also important in determining the minimum obtainable noise figure for a given diode, and we shall therefore refer to the inverse of it as "quality factor" of the diode. Since $1/(2\pi C_0 R_s)$ is defined as the diode cut-off frequency at zero bias, the quality factor is equal to the ratio between zero bias cut-off frequency and the signal frequency.

To improve the quality of a diode, both the series resistance R_s and the static capacitance C_0 must be decreased. Both R_s and C_0 depend on the semiconductor material used as well as on the geometry of the diode. In addition C_0 is also a function of the applied bias. While it is desirable to reduce R_s to the lowest possible value, such a reduction cannot be applied to C_0 without, at the same time, limiting the possible capacitance swing. Experimentally, a zero bias has generally been employed for the better diodes, but some negative bias is needed for poorer diodes to obtain optimum gain. The terms "poorer" and "better" refer to diode quality in terms of the quality factor defined above. At lower frequencies, the quality factor of a diode improves, and it is even possible to use small positive bias to cut down the pump power requirements. For example, if the quantity $\omega_1 C_0 R_s$, is 0.5 at 5 kmc, it is necessary to have negative bias to have a gain; but at 500 mc, $\omega_1 C_0 R_s = 0.05$ for the same diode, and ample gain is achieved without external bias. Amplifier gain may be determined using Fig. 6 if the pumping factor and the shunt conductance $(G_g + G_1)$ are known.

The negative conductance is double valued with respect to pumping power in the presence of the series resistance. The question now arises as to how two separate stable regions can exist when only a first-order nonlinearity in the capacitance has been assumed. The answer is related to the tuning conditions implied in making the admittance across the diode real. Looking from the circuit towards the variable capacitance, the negative conductance increases with the pumping factor. However, the over-all loss is greatly changed by changing the susceptance component of the circuit due to reactive current flowing through the series resistance of the diode. The two transition points are found to correspond to two different tuning conditions which occur because the input susceptance of the diode is a function of pump power even though constant load conductance and frequency are maintained. A similar phenomenon has been observed experimentally when a poor crystal is used; *i.e.*, as the pump power increases, the gain at first increases, then oscillation sets in, and finally stable gain is again observed as shown in Fig. 7. It is believed that the higher order terms of nonlinearity are primarily responsible for the observed effect. For better crystals, oscillation cannot be stopped before reaching the avalanche breakdown point by an increase in the pump power alone.

The normalized input capacitance is shown in Fig. 8 as a function of the pumping factor and as (11) indicates, the input susceptance increases as pump power increases. To cancel the imaginary part of the admittance with increasing pump, the inductive susceptance of the circuit must likewise be increased.

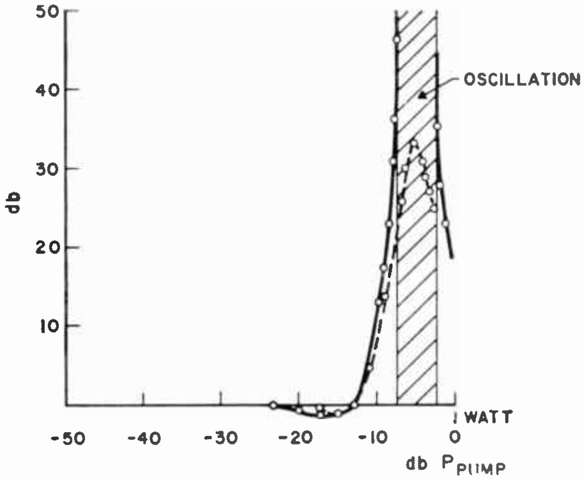

Fig. 7—Gain of a parametric amplifier as a function of pump power. As pump power increases, gain at first increases, then oscillation sets in, and finally stable gain is again observed. When circuit conductance is high no oscillation can be observed, but gain goes down beyond upper limit of optimum pump power.

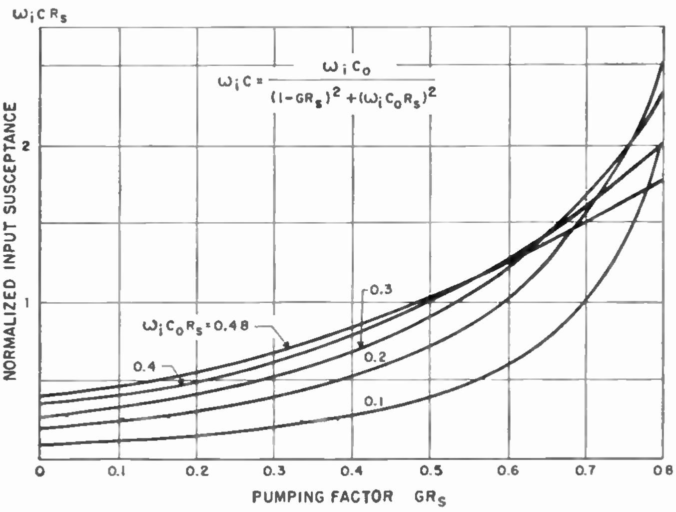

Fig. 8—Normalized input capacitance of variable capacitance diode with parasitic elements as a function of pumping factor.

[13] This statement implies that we are concerned only with a first-order nonlinearity process and that the pump is a purely sinusoidal excitation.

Experimental observations show that the plunger motion of the amplifier cavity is in the appropriate direction to that predicted by the theory; nevertheless, there are separate positions of the plunger required to maximize the idler and signal frequencies individually in the region of lower gain. In the range of higher gains we observe a synchronous tuning at both frequencies. This latter result occurs because the incidental dissipation effects decrease in proportion to the negative resistance as the pump increases, and the idler and signal progressively approach a simultaneous optimization in a fashion consistent with the Manley-Rowe relations.

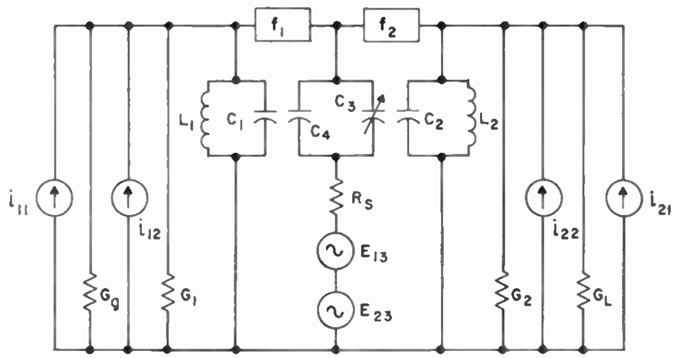

Fig. 9—Equivalent circuit used for noise output calculation.

Noise Figure Calculation

As was discussed in the Introduction, the main noise sources of the amplifier are (Fig. 9):

1) Thermal noise delivered from the series resistance at the diode at frequency bands f_1 and f_2. These noises are introduced by the voltage generators $\epsilon_{13}=\sqrt{4KTB_1R_s}$ and $\epsilon_{23}=\sqrt{4KTB_2R_s}$ connected in series with the series resistance.
2) Thermal noise received from the antenna at frequency bands f_1 and f_2. These noises are introduced by the current generators $i_{11}=\sqrt{4KTB_1G_g}$ and $i_{21}=\sqrt{4KTB_2G_L}$ connected in parallel to G_g and G_L, respectively.
3) Thermal noise generated in amplifier circuit (due to waveguide losses, etc.) at f_1 and f_2. These are represented by the current generators $i_{12}=\sqrt{4KTB_1G_1}$ and $i_{22}=\sqrt{4KTB_2G_2}$ connected in parallel to G_1 and G_2.

The equivalent circuit used for the noise output calculation is shown in Fig. 9.

Assuming that both frequency bandwidths, B_1 and B_2, are the same, the total noise output at signal frequency f_1 is obtained as:

$$P_n = 4KTBG_g\Bigg[(G_g+G_1)\left|\frac{1+R_s\left(j\omega_1C_0-\dfrac{\omega_1\omega_2C_3{}^2}{4G_2'}\right)}{(1+R_sY_{11})\left\{\left(j\omega_1C_0+\dfrac{Y_{11}}{1+R_sY_{11}}\right)-\dfrac{\omega_1\omega_2C_3{}^2}{4G_2'}\right\}}\right|^2$$
$$+(G_L+G_2)\left|\frac{\dfrac{j\omega_1C_3}{2G_2'}\left(\dfrac{1}{1+R_sY_{22}{}^*}\right)}{(1+R_sY_{11})\left\{\left(j\omega_1C_0+\dfrac{Y_{11}}{1+R_sY_{11}}\right)-\dfrac{\omega_1\omega_2C_3{}^2}{4G_2'}\right\}}\right|^2$$
$$+\frac{1}{R_s}\left|\frac{R_s\left(j\omega_1C_0-\dfrac{\omega_1\omega_2C_3{}^2}{4G_2'}\right)}{(1+R_sY_{11})\left\{\left(j\omega_1C_0+\dfrac{Y_{11}}{1+R_sY_{11}}\right)-\dfrac{\omega_1\omega_2C_3{}^2}{4G_2'}\right\}}\right|^2$$
$$+\frac{1}{R_s}\left|\frac{\dfrac{j\omega_1C_3}{2G_2'}\left(\dfrac{1}{1+R_sY_{22}{}^*}\right)Y_{22}{}^*R_s}{(1+R_sY_{11})\left\{\left(j\omega_1C_0+\dfrac{Y_{11}}{1+R_sY_{11}}\right)-\dfrac{\omega_1\omega_2C_3{}^2}{4G_2'}\right\}}\right|^2\Bigg]. \quad (12)$$

where Y_{11} and Y_{22} were defined in (6) and (7).

The noise figure for conventional operation which we shall call single-sideband reception to distinguish it from double-sideband reception (as used above) is defined as

$$F=\frac{P_{n\ \mathrm{out}}}{KTB\,G_{11}}=1+\frac{G_1}{G_g}+\frac{1}{R_sG_g}\left|\frac{R_s\left(j\omega_1C_0-\dfrac{\omega_1\omega_2C_3{}^2}{4G_2'}\right)}{1+R_s\left(j\omega_1C_0-\dfrac{\omega_1\omega_2C_3{}^2}{4G_2'}\right)}\right|^2$$
$$+\frac{G_{21}}{G_{11}}\left[\frac{G_L}{G_g}+\frac{G_2}{G_g}+\frac{1}{R_sG_g}\left|Y_{22}{}^*R_s\right|^2\right], \quad (13)$$

where G_{11} is the available power gain from signal input to signal output, and G_{21} is that from idler input to signal output, and

$$G_{11} = 4G_g^2 \left| \frac{1 + R_s\left(j\omega_1 C_0 - \dfrac{\omega_1\omega_2 C_3^2}{4G_2'}\right)}{(1 + R_s Y_{11})\left[\left(j\omega_1 C_0 + \dfrac{Y_{11}}{1 + R_s Y_{11}}\right) - \dfrac{\omega_1\omega_2 C_3^2}{4G_2'}\right]} \right|^2$$

$$G_{21} = 4G_g^2 \left| \frac{\dfrac{j\omega_1 C_3}{2G_2'}\left(\dfrac{1}{1 + R_s Y_{22}^*}\right)}{(1 + R_s Y_{11})\left[\left(j\omega_1 C_0 + \dfrac{Y_{11}}{1 + R_s Y_{11}}\right) - \dfrac{\omega_1\omega_2 C_3^2}{4G_2'}\right]} \right|^2. \tag{14}$$

When ω_1 and ω_2 are equal, the fourth term in (13) does not appear in the noise figure representation.

For double-sideband reception as defined in the Introduction, the coherent signal comes in at both the signal and idler frequency bands and the frequency converted signal can therefore be made to add in phase with the nonconverted signal. The noise figure for double-sideband reception becomes

$$F = \frac{P_{n\ \mathrm{out}}}{KTB(G_{11} + G_{21})} = \frac{(G_{11}G_g + G_{21}G_L) + (G_{11}G_1 + G_{21}G_2)}{G_g(G_{11} + G_{21})} \tag{15}$$

$$+ \frac{\dfrac{1}{R_s}\left| \dfrac{R_s\left(j\omega_1 C_0 - \dfrac{\omega_1\omega_2 C_3^2}{4G_2'}\right)}{(1 + R_s Y_{11})\left\{\left(j\omega_1 C_0 + \dfrac{Y_{11}}{1 + R_s Y_{11}}\right) - \dfrac{\omega_1\omega_2 C_3^2}{4G_2'}\right\}} \right|^2 + \left| \dfrac{Y_{22}^* R_s \dfrac{j\omega_1 C_3}{2G_2'} \dfrac{1}{1 + R_s Y_{22}^*}}{(1 + R_s Y_{11})\left\{\left(j\omega_1 C_0 + \dfrac{Y_{11}}{1 + R_s Y_{11}}\right) - \dfrac{\omega_1\omega_2 C_3^2}{4G_2'}\right\}} \right|^2}{G_g(G_{11} + G_{21})}.$$

When $G_g = G_L$ and $G_1 = G_2$, and using the further approximation that $Y \approx Y_{22}^* \approx Y_{11}$, (15) reduces to

$$F \approx 1 + \frac{G_1}{G_g} + \frac{1}{R_s G_g} \left| \frac{R_s\left(j\omega_1 C_0 - \dfrac{\omega_1\omega_2 C_3^2}{4G_2'}\right)}{1 + R_s\left(j\omega_1 C_0 - \dfrac{\omega_1\omega_2 C_3^2}{4G_2'}\right)} \right|. \tag{16}$$

Referring to (8), (13), and (16), and the above assumptions, the noise figure for single-sideband reception is about twice that for double-sideband reception. When f_1 and f_2 are widely separated, so that the difference between G_{21} and G_{11} is appreciable, $G_{21}/G_{11} \approx \omega_1/\omega_2$, and the noise figure for single-sideband reception becomes roughly $(1+\omega_1/\omega_2)$ times that for double-sideband reception. This is to say, if f_1 is smaller than f_2, the difference between the noise figure for single-sideband reception and the double-sideband reception is less than 3 db, while it is larger than 3 db if f_1 exceeds f_2. The noise figure for single-sideband reception approaches that for double-sideband reception if ω_1/ω_2 is very small. This we call noise refrigeration due to frequency separation. However, if the quality of the diode at ω_2 is very low, full advantage of refrigeration cannot be taken because the noise temperature of the diode at ω_2 is much higher than at ω_1.

The effects of several of the parameters in (16) on the noise figure are shown in Fig. 10. The term G_1/G_g has been neglected, assuming the circuit loss is very small. The abscissa indicates the normalized pumping factor GR_s and the ordinate shows the excess noise figure, $(F-1)$. The excess noise figure is calculated for different diode quality factors, the dotted line indicating the locus of the calculated minimum noise figure for optimized noise figure adjustment of each diode. These calculations are made under the assumption that the gain is very high, $|G| \approx (G_g+G_1)$. When $\omega_1 C_0 R_s$ is large the excess noise figure is much higher than the ratio between R_s and the load resistance, and it approaches R_L/R_s as $\omega_1 C_0 R_s$ approaches 0.5. However, it approaches the inverse R_s/R_L as $\omega_1 C_0 R_s$ decreases. As seen from Fig. 10, the noise figure varies widely as pump power or load conductance is changed and there is an optimum load conductance for a given diode which provides a minimum noise figure. The optimum load conductance is a function of $\omega_1 C_0 R_s$ and of R_s. When the series resistance is higher the optimum load conductance is also higher. The excess noise figure is, of course, a function of the series resistance, but only through the quality factor, $1/\omega_1 C_0 R_s$. The minimum excess noise figure, $F-1$, the optimum normalized load resistance, and the normalized pumping factor are shown as functions of the inverse quality factor of the diode in Fig. 11.

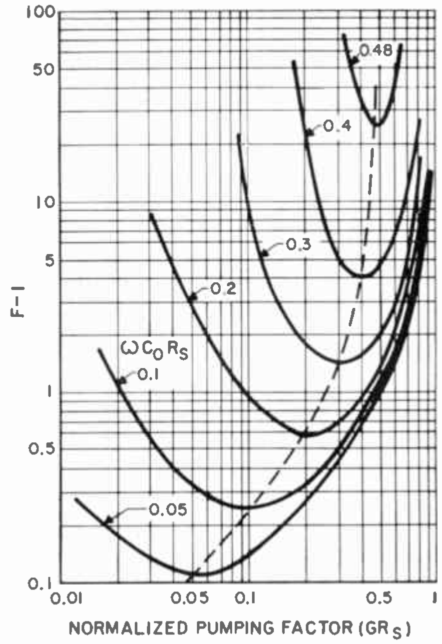

Fig. 10—Excess noise figures, $(F-1)$, of parametric amplifiers with various quality factor as a function of normalized pumping factor. Excess noise from circuit loss is assumed very small.

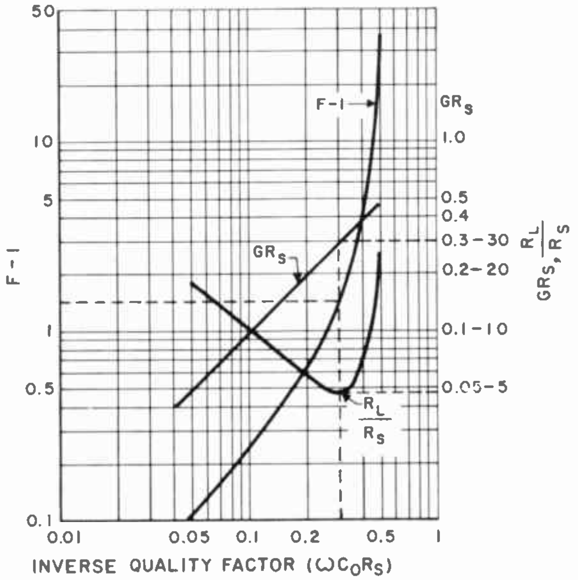

Fig. 11—The minimum excess noise figure, optimum normalized load resistance, and normalized pumping factor as functions of the inverse quality factor of diode.

Up to this point, C_0 has been defined as the static capacitance of the diode at zero bias. However, in actual practice, the pump voltage is swept over a wide range and the assumption of a linear characteristic of the diode is no longer valid. Negative bias is also used for most of the diodes to minimize noise output. Therefore, the average capacitance of the diode at the bias point, which is dependent on the amplitude of pump and the characteristic of the capacitance, must be used to calculate the noise figure. However, as will be discussed later, the average capacitance of the diode at arbitrary bias is usually larger than the static capacitance at zero bias if the coupling is adjusted to the optimum; the minimum obtainable noise figure is well defined by the quality factor given above.

Noise Figure Measurement

It was explained that two different noise figures can be defined for the parametric amplifier. One is the noise figure for single-sideband reception, and the other is that for double-sideband reception; the one with which we associate the measured results is determined by whether the noise generator covers both the signal and idler frequency bands, or only covers the signal frequency band. If the noise generator is broad-band, the measured noise figure is that for double-sideband reception and conversely, appropriately located, a narrow-band noise source provides a single-sideband measure. The noise figure of degenerate operation is put in the category of that for double-sideband reception. In the experiment an argon discharge lamp was used as the noise generator, and no particular band-pass filter was used to eliminate the idler frequency band. Hence, the noise figures measured in this experiment all correspond to double-sideband reception. Since the noise contribution from the idler frequency band has not been eliminated except by refrigerating the idler load thermally or electrically, as discussed previously, it must be emphasized that the ordinary noise figure for operation as a single-sideband amplifier is about 3 db less than the measured value. Throughout the remainder of this section, when "noise figure" is used, it is employed in a double-sideband sense.

One of the most serious measurement errors that is apt to arise is associated with gain variation in the course of measuring noise figure, and it must therefore be carefully avoided. The gain of the amplifier is changed by some stray signal and pump power reflected back from the load and the generator circuits. The amount reflected back will change as changes are made in the circuit impedance. Such changes would include, for example, turning the noise generator on and off and adjustment of the attenuator. The gain of the amplifier was stabilized very well by a circulator and isolators, and by operation in a region where gain is insensitive to pump power. In an absolute measurement of noise figure, it was measured by reference to the noise from a matched load cooled to liquid nitrogen temperature.

Twenty-eight samples—10 silicon *p-n* junction diodes, 6 germanium *p-n* diffused diodes, 6 germanium gold-bonded diodes, and 6 gallium arsenide point contact diodes—were tested as variable capacitance elements at 5.84 kmc while pumping at 11.7 kmc. The parameters, $\omega_1 C_0 R_s$, ranged from 0.06 to 1.13.

In the experiments, the pump voltage used ranged from 0.2 volt to 2 volts depending on the bias voltage. These voltages cannot be considered as small signals and the capacitance characteristic deviates considerably from the linear characteristic. Noise contributions through higher-order nonlinear terms can be eliminated by the careful arrangement of the circuit. However, noise output is higher than that calculated from linear theory because the average capacitance of the diode at the operating point is larger than the static capacitance at the same point. The noise figures of a gallium arsenide diode measured at various bias voltages are plotted in Fig. 12. The input circuit loss was subtracted from the raw noise data to give the "measured" noise figure quoted. The gain of the amplifier was maintained constant at 16 db by adjusting the pump power and the single-sideband frequency bandwidth was about 25 mc. The coupling between the waveguide and the cavity was adjusted for minimum noise output at each bias condition. The pump power, iris size, and the rectified current are also plotted in the same figure. The rectified current is negligibly small, from -0.3 volt of bias voltage to -1.4 volts, with no noise contribution expected in this range other than the thermal noise arising from the series resistance of the diode. The noise figures, calculated theoretically, based on the average capacitance agree very well with the measured values for reverse bias voltages indicated above. For larger reverse bias voltages, the rectified current increases very rapidly as a result of the diode being driven into breakdown. A consequence of this is that the measured noise figures exceed the calculated values, the difference being attributed largely to contributions from shot noise as well as noise of the microplasm type.

To enable calculation of the noise figure theoretically, the pump voltages across the junction were graphically determined from experimental results. The pump voltage for maintaining constant gain was found to be almost linearly proportional to the bias voltage. The average capacitance was determined at each bias from knowledge of both the pump voltage and the capacitance characteristic and $\omega_1 C_0 R_s$ of the diode was calculated. This process is very time-consuming and is impractical to predict the obtainable noise figure. However, the experimental fact was found that the minimum noise figures measured for most diodes were in good agreement with that predicted from the quality factors at zero bias. This resulted because the average capacitance of the diode at the optimum bias voltage was approximately the static capacitance of the diode at zero bias when the circuit coupling was adjusted to the optimum. The experimental results and the theoretical calculations are compared in Fig. 13. The circles indicate the minimum noise figures measured for the individual silicon diodes, the triangles are for the gallium arsenide diodes, and the squares are for the germanium diodes. The solid line indicates the noise figure predicted theoretically. Over a range of sufficiently large values of the parameter $\omega_1 C_0 R_s$, there is a reasonable correlation of the theory developed with the measurements performed on most of the diodes. In the range of relatively small values of $\omega_1 C_0 R_s$, the model proves inadequate to de-

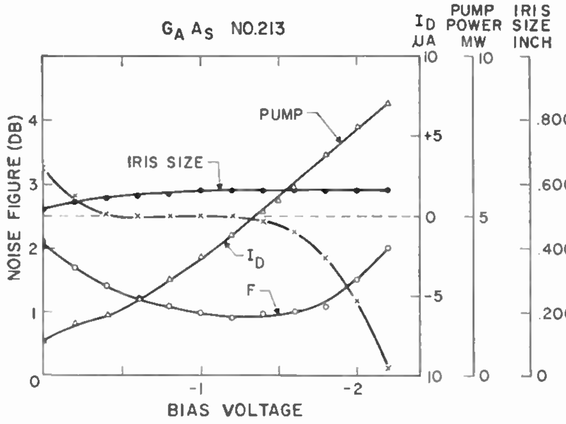

Fig. 12—Measured results of noise figure of a gallium arsenide diode at various bias voltages. Gain was maintained constant at 16 db. Since broad-band noise source is used as noise generator, these values all correspond to double-sideband reception. To determine noise figure for single-sideband reception, about 3 db must be added to these values.

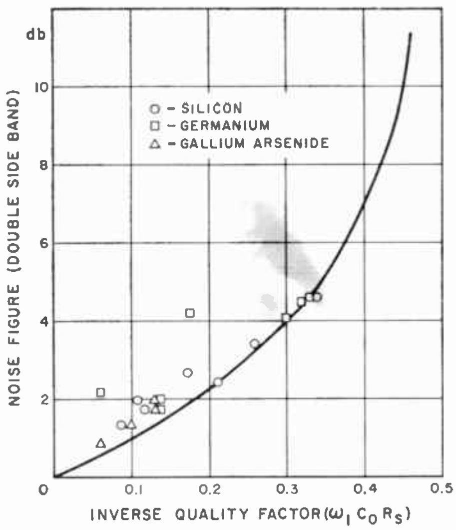

Fig. 13—Measured results of noise figure for various gallium arsenide, silicon and germanium diodes. Solid line indicates noise figure predicted theoretically. Circles indicate the minimum noise figures measured for individual silicon diodes, triangles are for gallium arsenide diode, and squares are for germanium diodes.

scribe some diodes properly and suggests the need for introducing extra noise sources. Of course, circuit losses were neglected in the theoretical curve and they flatten the curve in the range of very small values of $\omega_1 C_0 R_s$. However, the deviation from simple theory is much more than that due to circuit losses[14] and the effects of shot noise, microplasm type noise, higher-order sideband noise, and pump noise should be considered. These noises can be eliminated by knowing the detailed characteristics of the diode and by the circuit adjustment. However, if the amount of impurity doping is too high or the doping is not uniform, the dynamic range[15] of the

[14] The noise contribution from the circuit is about 10°K.

[15] The dynamic range of the diode is defined as the range where pump voltage can be swept without driving into either breakdown or large forward conduction.

diode decreases and it is very difficult to eliminate them without sacrificing other factors, such as coupling, which also increase noise output. This kind of difficulty was enhanced with the germanium diodes, while much less difficulty was experienced with the gallium arsenide diodes.

The quality factor of some germanium diodes was less than 2, and negative bias had to be applied to obtain gain. In this case, the coupling between the cavity and the circuit must be considerably reduced so that the small pump voltage is sufficient to produce an adequate negative conductance, and the operating quality factor can be improved beyond the limit. However, the coupling is much smaller than the optimum value and the noise figure is much higher than the minimum obtainable based on the operating quality factor. The same problem can occur when the dynamic range of the diode is small. The effect on noise figure of coupling between the resonant cavity and the output circuit was measured and is plotted in Fig. 14. The cavity was usually operated in a over-coupled state and coupling was changed by changing the size of a symmetrical waveguide iris. There exists an optimum coupling for minimum noise figure as theory predicts. Noise figure deterioration was larger than theory predicts when coupling was greater than the optimum value. This is because larger pump power is necessary to maintain the gain constant, and the average capacitance C_0 increases and the operating quality factor decreases. Thus noise figure increases much faster than the theory predicts. Some qualitative agreement with theoretical calculations can be found, but a quantitative correlation has not yet been achieved.

Pertinent diode data and experimental results are listed in Table I.

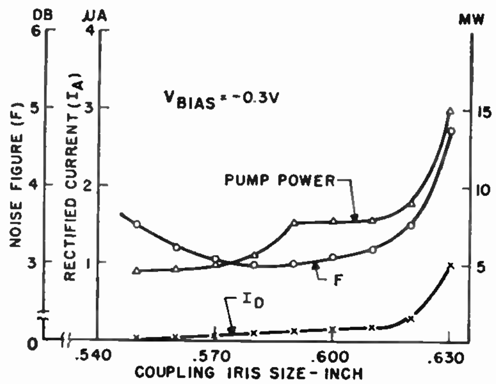

Fig. 14—Data on coupling effect on noise figure. Coupling is changed by changing inductive iris size.

TABLE I

Sample no.	Type	C_0 $\mu\mu$f	$R_s \Omega$	$\omega_1 C_0 R_s$	F_{db}* at zero bias	F_{min}* db	Bias volt	P_{pump} watt	R_0 Ω(1.5v)
451-7	Si p-n junction	2.44	0.99	0.089	2.0	1.4	−0.5	0.15	34 − ∞
422c-2	Si p-n junction	1.88	1.7	0.118	2.5	1.8	−0.6	0.09	33 − ∞
422-10	Si p-n junction	0.7	8.06	0.211	2.87	2.2	−0.4	0.018	40 − ∞
42c-1	Si p-n junction	0.38	18.5	0.258	3.7	3.2	−0.4	0.013	55 − ∞
210	GaAs point contact	0.427	6.4	0.10	3.0	1.4	−1.3	0.0045	42 − ∞
212	GaAs point contact	0.477	7.4	0.130	3.8	1.8	−1.3	0.006	38 − ∞
213	GaAs point contact	0.475	3.44	0.060	2.1	0.9	−1.2	0.004	34 − ∞
295	Ge gold bonded	1.92	4.5	0.33	×	4.5	−3.4	0.450	10.5 − ∞
299	Ge gold bonded	2.20	3.7	0.30	×	4.0	−3.4	0.680	10.5 − 1 M
05-1	Ge gold bonded	2.09	4.1	0.32	×	4.4	−0.8	0.023	16 − 0.5 M
818-5.73-1	Ge p-n diffused	2.036	1.78	0.173	5.7	4.2	−0.5	0.180	17 − ∞
918-11	Ge p-n diffused	0.985	1.62	0.06	4.3	2.1	−0.4	0.020	17 − ∞
919-57-6	Ge p-n diffused	0.87	4.2	0.135	6.0	1.8	−1.4	0.022	19 − ∞

* These are the measured noise figures. They correspond to double-sideband reception. For single-sideband reception 3 db must be added to these values.

Conclusion

It has been demonstrated that a simplified theory, which includes a resistance in series with the variable capacitance, is good enough to predict much of the noise behavior of the parametric amplifier, and can be used in designing a low-noise parametric amplifier. From the facts that 1) no positive gain was obtained for the diodes which have a quality factor smaller than 2, and 2) the minimum obtainable noise figure was fairly well predicted from the quality factor, this factor, $1/\omega_1 C_0 R_s$, is seen to be an appropriate one for representing the performance potential of diodes for use in parametric amplifiers.

The best noise figure measured is 0.9 db excluding the effect of external circuit losses and it applies only to double-sideband reception. If this amplifier is used as an ordinary receiver, however, the obtainable noise figure is worse by about 3 db. The need for communication systems which carry coherent signal information in both the signal and image frequency bands therefore appears to be a real one.

Acknowledgment

The author wishes to express his appreciation to W. E. Danielson, H. Seidel, and E. D. Reed for their stimulating discussions and for their helpful criticism in the preparation of the manuscript.

Acknowledgment is also made to F. J. D'Alessio for helping to carry out the experiments.

Reliability Analysis Techniques*

CHARLES A. KROHN†, MEMBER, IRE

Summary—**Reliability analysis has progressed to the point where a quantification of reliability is possible. Reliability models for electronic equipment and techniques for interpretation of field and laboratory data have been developed. Of more significance, analytical methods leading to higher reliability are available. Reliability estimates enable early pinpointing of low reliability. Catastrophic failures can be controlled and performance change failures reduced through analytical techniques. Redundant techniques allow further reliability improvement even though failures occur. Analytical techniques are a useful aspect of reliability improvement, but they comprise only a part of reliability improvement methods.**

Introduction

THE attainment of increased reliability in electronic equipment during the past several years has received considerable attention throughout the electronics industry. As the field of reliability engineering develops, a system of useful analytical techniques pertinent to reliability is also evolving. Various techniques are presented and related to the whole of such techniques. Generally, the techniques are supported by data indications and reasonable theory.

Treating Reliability Quantitatively

Reliability is an aspect of electronic equipment that can be quantitatively treated; this is desirable from several different viewpoints. In learning how to quantify reliability, equipment designers have a better understanding of their designs and are thus in a position to improve reliability. Operational analysts planning the use of electronic equipment know how useful it will be. Customers procuring equipment can designate their needs and maintenance personnel are in an improved position to plan their programs.

Electronic equipment broadly divides into two logical groups with respect to reliability quantification. These groups are associated with equipment usage. Equipment is either intended for continual use over a long period of time or for a single use for a short time. Long-time use includes communications, computing, instrumentation, navigation, and similar equipment; short-time use equipment principally includes military items such as missile and torpedo electronics, sono-buoys, and projectile proximity fuses. Different approaches to reliability quantification for each of the two groups of equipment are shown.

Continual-Use Equipment

Electronic equipment intended for either long periods of continuous use or for periodic use over long periods of times comes under the continual-use category. In either case, the equipment will be repaired upon failure and returned to operation.

Data for reliability quantification can be obtained by observations of the time-to-failure while actually using the equipment or while testing the equipment under

* Original manuscript received by the IRE, March 23, 1959; revised manuscript received, May 21, 1959.

† Western Military Electronics Center, Motorola, Inc., Phoenix, Ariz.

controlled conditions. A measure of reliability is the failure rate, which is obtained from data by dividing the total equipment operating hours during a given short time interval into the failures during the interval. If failure rate is plotted as a function of time for a typical piece of electronic equipment, the generalized curve will be as indicated in Fig. 1.

An actual failure rate curve best approaches the generalized curve of Fig. 1 as the quantity of equipment under observation increases. Such equipment must be of the same model, with common usage conditions and a common criteria of failure. Failure data, in a laboratory environment from an electronic package, is shown in Fig. 2 and follows the generalized curve shown in Fig. 1.[1] The solid curve is the failure rate of 8 early units; the dashed curve, of 14 later units with subsequent improvements.

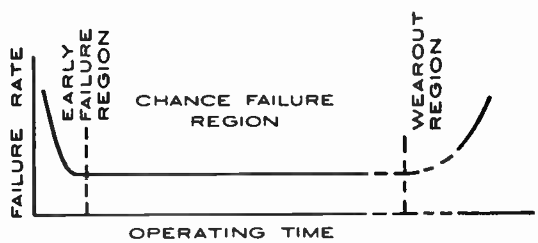

Fig. 1—Failure rate of electronic equipment.

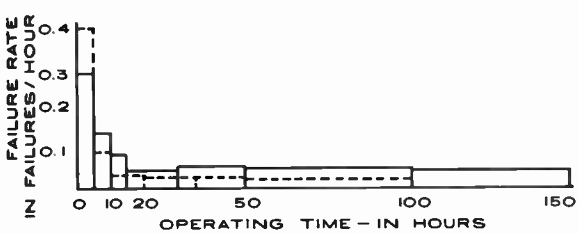

Fig. 2—Measured failure rate of an electronic package; solid line represents early units, dashed line represents later units.

As shown in Figs. 1 and 2, there is an initial higher failure rate called the debugging or burn-in period. This period of high, but decreasing failure rate results from the elimination of marginal parts and materials. Indications show that this period may vary between nearly zero and 200 hours. It is important that this period be determined and removed prior to using equipment in order that the initial use of equipment will be at its lowest failure rate.

Following the higher early failure period, there is an extended period of relatively constant failure rate. In well designed and maintained electronic equipment this period will extend for many thousands of operating hours. This period of relatively constant failure rate describes the useful life of electronic equipment

Failures occur randomly during this period, and chance of failure is independent of age. When a piece of equipment is exhibiting this constant failure rate, replacement of an older model with a newer one will not improve reliability. A constant failure rate results from the accumulation of a large number of failure causes distributed throughout the equipment. These causes include the random occurrence of stresses that exceed inherent strength, some unavoidable human error, and a mixture of unknown or uncontrolled nonrandom variations.

By reducing these causes, the constant failure rate can be lowered. This is illustrated in the two failure rate curves of Fig. 2. Investigation of the reasons for failures in the early units and corrective action resulted in a failure rate improvement.

Finally, the equipment will enter a wearout region, thus indicating an increasing failure rate. The wearout period results from the start of wide-scale deterioration of materials and parts not typically replaced in periodic maintenance. In well designed modern equipment it is doubtful whether wearout will be evidenced as the equipment will experience technological obsolescence and be replaced prior to wearout.

The useful life of a piece of electronic equipment is the period of relatively constant failure rate. During the period of constant failure rate the distribution of failures vs time-to-failure is exponential. Fig. 3 shows time-to-failure data under flight conditions of a military airborne UHF transceiver.[2] The exponential distribution is described solely by its mean M (first absolute moment). Thus M, the mean time-to-failure, is the parameter of interest. The mean time-to-failure of Fig. 3 is 51 hours.

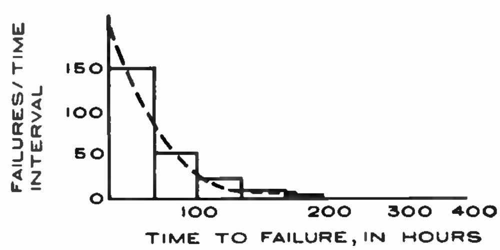

Fig. 3—Time-to-failure distribution for a 55 tube UHF transceiver. Solid line represents data, dashed line is exponential curve for $M=51$ hours.

The failure rate of Figs. 1 and 2, in more exact terms, is the instantaneous probability rate of failure at any time, conditional upon nonfailure at that time.[3] This failure rate is constant with respect to time for equipment whose times-to-failure are exponentially distributed, and is[4]

[1] Western Military Electronics Ctr., Morotola, Inc., Phoenix, Ariz., unpublished internal report.

[2] "Investigation of Electronic Equipment Reliability as Affected by Electron Tubes," Aeronautical Radio, Inc., Washington, D. C., Interbase Rept. No. 1, Contract NObsr-64508, p. 11; March 15, 1955.

[3] D. J. Davis, "An analysis of some failure data," *J. Amer. Statistical Association*, vol. 47, p. 114; June, 1952. A general discussion of reliability models, as well as the referenced point, is contained in this article.

[4] *Ibid.*, p. 117.

$$F = 1/M \quad (1)$$

where (previously used terms will not be defined)

F = failure rate.

Eq. (1) applies to equipment which can be repaired upon failure and returned to operation, as well as to devices having an exponential time-to-failure distribution that cannot be repaired and returned to operation.[5]

Reliability is defined as the probability of a device not failing for a certain period of time under defined usage conditions. Reliability, as a probability, is between 0 and 1. Reliability of electronic equipment whose failure rate is constant and whose times-to-failure follow the exponential distribution is[6]

$$R = \exp[-t/M] \quad (2)$$

where

R = reliability, probability of successful operation;
t = time of successful operation.

Eq. (2) is shown in Fig. 4, and applies at all times when the equipment is in a nonfailed state. Thus reliability for a given time interval does not depend on the previous operating time on the equipment.

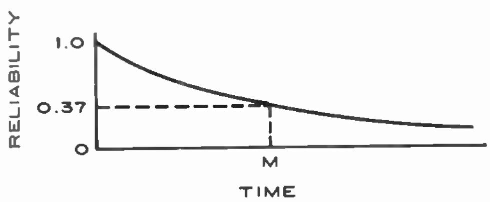

Fig. 4—Reliability of electronic equipment.

It is important to realize that the reliability of a piece of equipment for a period of time equal to its mean time-to-failure is only 0.37. Therefore, we err in thinking that equipment is highly reliable for its mean time-to-failure. As indicated in (2) and Fig. 4, a high reliability, such as 0.99, should be expected for only one per cent of the mean time-to-failure and a 0.90 reliability for 10 per cent of the mean time-to-failure.

If the mean time-to-failure, or its reciprocal, failure rate, is known, probability of operation for any time interval is computed from (2). The communications equipment referred to in Fig. 3 for a 3-hour flight has a reliability of 0.943. A useful approximation for rapid calculation, based on the general exponential expansion of (2), is

$$R \approx 1 - (t/M), \quad (3)$$

and it is reasonably accurate for reliabilities greater than 0.8. Other useful operational reliability information are the percentage and number of pieces of nonfailed equipment expected on the average where a group of similar pieces of equipment are used simultaneously. The per cent of survivors is simply

$$P_s = R100, \quad (4)$$

and the number of survivors is

$$N_s = N_t R, \quad (5)$$

where

P_s = percentage of survivors expected,
N_s = number of survivors expected,
N_t = total similar equipments.

Techniques for analyzing reliability data obtained from either actual equipment use or test have been developed.[7] In measuring reliability as expressed by (2), mean time-to-failure is the parameter of interest. Mean time-to-failure is estimated from

$$\hat{M} = \frac{T}{f}, \quad (6)$$

where

$\hat{M}$ = estimate of the mean time-to-failure;
T = total operating time;
f = number of failures during T.

This is simply the total number of operating hours divided by the number of failures. Eq. (6) applies where failed items are either repaired and returned to operation or not repaired and returned to operation. Further, test termination time or the number of pieces of equipment on test are not mathematically significant.

Estimated mean time-to-failure, $\hat{M}$, is subject to deviation from the true mean time-to-failure because of possible sampling variations. The accuracy of the estimate depends on the number of failures observed.

Confidence limits on $\hat{M}$ can be calculated; these limits embrace the confidence interval. Confidence intervals are the percentage of the intervals that would include the true mean time-to-failure if the tests were to be repeated many times. A useful interpretation of this is that the confidence interval has a probability of the magnitude of the confidence interval of containing the true (but unknown) mean time-to-failure.

Limits of the confidence interval for the estimated mean time-to-failure of the confidence interval are computed from

[5] E. Pieruschka, "Mathematical Foundation of Reliability Theory," U. S. Army Redstone Arsenal, Ala., pp. 15, 23; January, 1958. A discussion of reliability models, as well as derivation of the referenced point, is contained in this article.

[6] C. R. Knight and E. R. Jervis, "A Discussion of Some Basic Theoretical Concepts, and a Review of Progress Since World War II," Aeronautical Radio, Inc., Washington, D. C., ARINC Mono. No. 1, p. 6; May 1, 1955. A general discussion of reliability models, as well as derivation of the referenced point, is contained in this report.

[7] B. Epstein and M. Sobel, "Life testing," *J. Amer. Statistical Assoc.*, vol. 48, pp. 485–502; September, 1953. Derivations of (6) and (7) are contained in this article.

$$\text{lower limit} = \frac{2f\hat{M}}{\chi^2_{(2f,\,\alpha/2)}} \tag{7a}$$

and

$$\text{upper limit} = \frac{2f\hat{M}}{\chi^2_{(2f,\,1-\alpha/2)}} \tag{7b}$$

where $\chi^2_{(2f,\,\alpha/2)}$ and $\chi^2_{(2f,\,1-\alpha/2)}$ = tabulated chi-square values at $2f$ degrees of freedom for $(1-\alpha)$, the desired confidence interval.

Note that $(1-\alpha)$ is the confidence interval. Thus for a 0.90 (or 90 per cent) confidence interval α is 0.10, and the confidence limits are for $(\alpha/2)=0.05$ and $(1-\alpha/2)=0.95$. Tabulated chi-square values are found in most statistics books.

These techniques are useful in analyzing reliability data such as obtained from laboratory reliability measurements or field data. Applying these techniques to the data used to plot the failure rate, shown in Fig. 2 as the later improved models, results in an estimated mean time-to-failure of 40.5 hours (850 hours/21 failures) with 0.90 confidence limits of 31.4 and 55.2 hours. Only that data after the debugging period of 10 hours is used in this computation.

Sampling plans for testing reliability where times-to-failure are exponentially distributed have been developed.[8,9] These are tests where defined equipment operating hours are accumulated and the number of failures are observed. Depending on the quantity of failures observed, a decision is made as to whether or not the specified-reliability exists.

Such sampling plans are not designed to measure reliability but rather, within defined risks, to indicate that a specified reliability exists. Hence they are particularly applicable to production lots where satisfactory reliability of prototypes has previously been demonstrated and the problem is one of allowing only equipment with acceptable reliability to pass the test.

Development of sampling plans is an involved subject and one which is beyond the intended scope of this paper. Sampling plans for reliability are mentioned because they form a logical aspect of reliability analysis. To further illustrate the concept, a reliability sampling plan is shown in Figs. 5 and 6.[10]

Fig. 5 shows a test plan. A group of similar pieces of equipment are tested under defined usage conditions with a certain failure criteria. Failed pieces of equipment are repaired and returned to operation. Total failures are plotted vs total operating time and, as in-

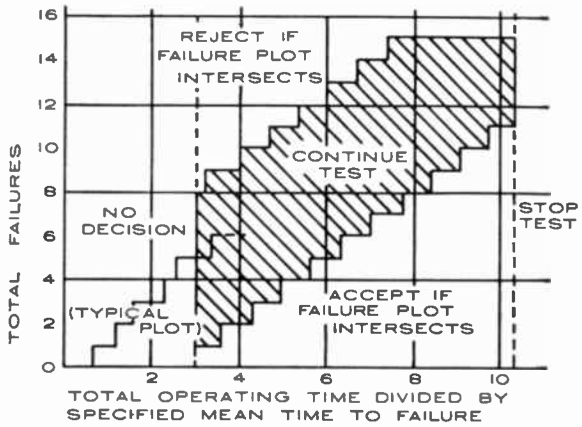

Fig. 5—Reliability sampling plan.

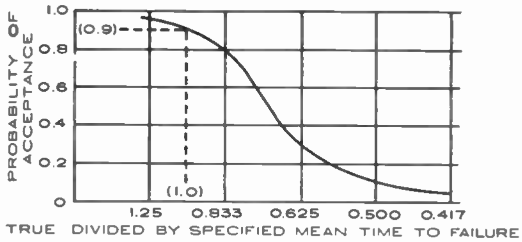

Fig. 6—Operating characteristic curve for the sampling plan shown in Fig. 5.

dicated in Fig. 5, the group is either accepted or rejected at any time, or the test is continued. Fig. 6 is the operating characteristic of this plan and it gives the probability of accepting this group of equipment for various true mean times-to-failure. A great many such plans are possible. Plans with less risk require more testing time.

The pertinency of the techniques for analyzing reliability data discussed to this point depends on assumption of exponential distribution of times-to-failure. Further, common definition of failure, common usage conditions, and similar equipment are necessary when data is to be grouped. The exponential distribution assumption can be tested by application of the standard "goodness of fit" test found in statistics books to the time-to-failure distribution (see Fig. 3).[11] This test is not applicable when there is truncated data; that is, when some tests do not terminate in failure. Techniques have been developed for this situation, and for testing whether or not various data can be grouped.[12]

All discussion to this point has been with respect to the reliability of typical electronic equipment for continued use. The pertinency of the failure rate pattern, as illustrated by Fig. 1, to component parts (resistors, capacitors, vacuum tubes, etc.) in general is, at this time, questionable. Most component-part failure data is acquired under accelerated electrical and environ-

[8] B. Epstein, "Truncated life tests in the exponential case," *Ann. Math. Statistics*, vol. 25, pp. 555–564; September, 1954.

[9] B. Epstein and M. Sobel, "Sequential life tests in the exponential case," *Ann. Math. Statistics*, vol. 26, pp. 82–93; March, 1955.

[10] "Reliability of Military Electronic Equipment," Rept. by the Advisory Group on Reliability of Electronic Equipment, Office of the Asst. Sec'y of Defense, Washington, D. C., pp. 89–90; June 4, 1957.

[11] A. Hald, "Statistical Theory with Engineering Applications," John Wiley and Sons, Inc., New York, N. Y., p. 742; 1952. This test is also shown in many other statistics books.

[12] "Electronic Reliability in Military Applications," Aeronautical Radio, Inc., Washington, D. C., Gen. Rept. No. 2, Contract Nobsr-64508, pp. 243, 246; July 1, 1957.

mental stresses. This allows failures within a reasonable true time, but does not actually represent typical usage conditions. Such component-part failure data, as well as true-time failure data, as the writer has seen have not illustrated a definite leaning toward the failure pattern of Fig. 1.

Although the failure rate pattern of component parts has not been as clearly indicated as has that for equipment, it is reasonable to suspect that certain component parts will exhibit wearout. Wearout results from the start of wide-scale deterioration of materials, and it is highly suspected that component parts subject to exhaustion of some built-in supply of material will exhibit wearout. Such component parts would include contact surfaces of relays, bearings, and brushes and the cathode emissive material of tubes, particularly high power pulse tubes such as magnetrons. If operating time records indicate a wearout phenomena in a component part, the part should be replaced prior to wearout. Such periodic replacement will reduce the equipment failure rate and improve reliability.

Single-Use Equipment

In recent years the short time, single use types of electronic equipment have come to make up a substantial portion of the total electronics effort, with missile electronics being the dominating influence. When actually used, the objective of single-use equipment is satisfactory operation during the short period of usually severe and varying environments. The equipment is often not recoverable for repair when used. The question arises as to what constitutes a meaningful reliability quantification of such single-use equipment.

Data for reliability quantification comes from either direct use observation or from observation under test conditions that may or may not simulate final use conditions. In continual-use equipment these data in the form of times-between-failure can be obtained without excessive difficulty. However, the nature of single-use equipment indicates a different approach to reliability quantification.

Direct use observation of single-use equipment yields data which, when interpreted, primarily indicate the equipment has or has not performed satisfactorily. Typically the use period is short and the environments are severe and varying.

Observation of single-use equipment under controlled test conditions, as a source of reliability quantification data, has limitations. Environmental conditions during such testing can be kept moderate. Under such conditions the equipment under observation will not be harmed and, when failures occur, it can be repaired and returned to operation. Testing can continue for long periods of time, and much time-between-failure data can be obtained. However, there must be a known correlation between the time-between-failure data under moderate test conditions and the performance capabilities during use for the test observations to be meaningful. Such correlation may or may not exist. Thus, time-between-failure data gathered on single-use electronic equipment under moderate test conditions will be questionably useful reliability quantification until the correlation just mentioned both exists and is known.

Instead of using moderate conditions during the test, environments can be made severe in an attempt to simulate actual use. Assuming that this can be accomplished, useful reliability quantification data will be obtained. Various considerations make this approach difficult. Exact use environments are often unknown, and simulation of these environments is difficult, particularly simultaneous simulation of different environments. Subjecting equipment to the severe environment will often have a deteriorating effect, and continuing observations cannot be made on the same piece of equipment. Data obtained can be of a time-to-failure nature, or the test time can be in the order of the short use time with the measure being, simply, satisfactory or unsatisfactory performance. If the former approach is used and the time-to-failure distribution is exponential, the reliability quantification techniques previously presented for continual-use equipment are pertinent, while the latter approach requires a different quantification technique. The latter approach is considered most pertinent, as it is analogous to actual use.

These various considerations lead to the opinion that a meaningful reliability quantification of single-use equipment is simply to judge whether or not satisfactory performance is achieved during use, or tests simulating use. The previous definition of reliability—the probability that a device will perform adequately for an interval of time under certain usage conditions—still applies, but the time interval is now short and essentially constant.

Reliability of single-use equipment is estimated from data by

$$\hat{R} = \frac{N_t - N_f}{N_t}, \tag{8}$$

where

$\hat{R}$ = estimated reliability;
N_t = total number of trials;
N_f = number of trials resulting in failure.

Confidence limits on this estimate are necessary in order to appraise realistically the above illustrations. Estimated reliability here is a simple proportion, and confidence limits are those for the binomial distribution.

Computing confidence limits for proportions is involved, and has been tabulated by the Bureau of Standards.[13] Approximations of confidence limits can be made by using a normal distribution where estimated reliability is between 0.10 and 0.90 and total trials are

[13] Natl. Bur. of Standards, "Table of the Binomial Probability Distribution," U. S. Govt. Printing Office, Washington, D. C., Appl. Math. Ser. 6; 1950.

in the order of 50 or more. Estimates of proportions and their confidence limits are well covered in statistics texts. Various sampling plans for attribute inspections such as the Department of Defense sampling plan, Military Standard 105A, "Sampling Procedures and Tables for Inspection by Attributes," have been formulated. Thus this reliability quantification of single use electronic equipment involves the application of well known, classical methods of statistical analysis.

This reliability quantification technique for single-use equipment is apparent, and the significant point is one of recognizing that an approach different from that employed for continued-use equipment is pertinent. The approach presented for single-use equipment is readily applicable to analysis of existing data accumulated during use or tests simulating use. However, there is difficulty in demonstrating reliability in this manner when it is made a contractual requirement. Since continuing observations on the same piece of equipment cannot be made, large quantities of usually costly equipment are required to satisfactorily demonstrate reliability.

Techniques for Higher Reliability

Areas of reliability analysis that are particularly appealing are those that lead directly to increased reliability. Failure of equipment can be either catastrophic or the change of some performance parameter to an unacceptable level. Analytical techniques, leading to minimization of failures of both types, are available. Techniques for further reliability improvement with the occurrence of failures can be analytically treated. Quantitative reliability estimates lead to optimum system design. Such techniques for higher reliability are discussed below.

Reliability of electronic equipment, when used, is the product of usage reliability and inherent-equipment reliability. Usage reliability reflects such factors as the operator and maintenance personnel ability, maintenance practices, and use environment. Similar equipment under different usage conditions will often realize different reliabilities. Inherent reliability is a complex factor related to component part quality, electrical and mechanical design maturity, and workmanship in assembling the equipment. Further discussion is with respect to inherent reliability, which is under the control of the equipment designer and producer.

Controlling Performance Change Failures

The majority of failures of electronic equipment where a performance parameter has changed to an unacceptable level can be eliminated in design.

Control of performance change failures can be approached by attempting to design circuits which will perform properly when all component part values are simultaneously at their limits. Such an approach may appear feasible where only the typical initial manufacturing tolerance is considered by using circuits requiring a larger quantity of component parts, or precision parts, or both. However, there are many additional causes of part value change other than initial tolerance, and when all part value change causes are considered, the above approach is often impossible. In addition, the larger quantity of component parts to effect the above remedy will have a greater chance of catastrophic failure and thus may offset any total reliability gain.

Component part values of a large quantity of similar parts will be distributed over a range of values, with usually only a few values near the extreme limits. The distribution of the circuit performance variable can be predicted from the distributions of the component part values. Performance variable distribution ranges of the circuit will be smaller than the range obtained by simultaneously using component-part tolerance-limit values in the circuit equation. Control and minimization of performance out of acceptable limits is possible through this realistic prediction of the performance variables distribution.

Exact values of a large quantity of the same component part are distributed over a range of values. Measuring and tabulating values of the same parts from a stable production process over a period of time would reveal the initial distribution of the values. The basic distribution often found is the familiar normal or Gaussian, as shown in Fig. 7. This distribution is completely described by its mean value and standard deviation, sigma.[14] Manufacturing tolerances of perfected production processes are usually 3 sigma or better.

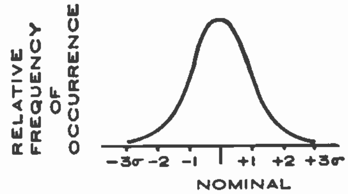

Fig. 7—The familiar normal or Gaussian distribution.

Distributions of performance variables can be estimated from the distributions of component part values.[15] When the analytical expression relating the performance variable to the component part values is

$$y = f(x_1, x_2, \cdots x_n), \tag{9}$$

the standard deviation (see Fig. 7, normal distribution) of the performance variable is obtained from

[14] W. R. Bennett, "Methods of solving noise problems," Proc. IRE, vol. 44, pp. 609–614; May, 1956. A discussion of distributions is contained in this article.

[15] J. B. Heyne, "On an analytical design technique," 1958 IRE National Convention Record, pt. 6, pp. 121–122. Derivation is shown as Appendix A.

$$(\sigma_y)^2 = \left(\frac{\partial y}{\partial x_1}\right)^2 (\sigma_{x_1})^2 + \left(\frac{\partial y}{\partial x_2}\right)^2 (\sigma_{x_2})^2 + \cdots \left(\frac{\partial y}{\partial x_n}\right)^2 (\sigma_{x_n})^2 \quad (10)$$

where

y = performance variable value,
x_n = component part values,
σ = standard deviation of the appropriate distribution.

Nominal component part values are used for numerical determination of the partial derivatives of (10). The nominal value of the performance variable is obtained from using the component parts' nominal value in (9).

This technique is based on the assumptions that component parts are randomly selected for assembly, that component-part value ranges are not large relative to the nominal value, that the various component-part values are independent, and that distributions of component-part values are normal. Techniques are available to treat analytically violation of the assumptions.[16] However, due to the complexity of full treatment and the approximate status of component-part value distributions, the additional effort is not typically warranted.

A moderate portion of component parts in electronics are selected by value from a larger group and have non-normal distributions. The distribution of selected parts often is described essentially by the rectangular distribution shown in Fig. 8. In such instances, the technique of (10) is still useful where there are 3 or more component-part values. The standard deviation of component-part values with rectangular distributions is obtained from

$$\sigma = B/\sqrt{3}, \quad (11)$$

where B is as indicated in Fig. 8.

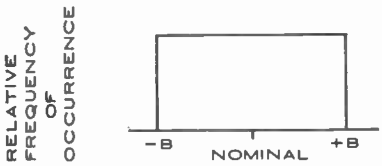

Fig. 8—The rectangular distribution.

The performance value distribution will be nearly normal because of the tendency of combinations of non-normal distributions to approach a normal distribution. As a general rule, where there are only two non-normal component-part values, one should design for both simultaneously at their distribution limits.

Measures of component-part value distributions to be used in the application of this technique are not generally available. Such distributions can be approximated by consultation with component-part manufacturers, examination of test data, and study of component part specifications. Such tabulations of variations are admittedly approximate, but they are still useful in making first approximations as to what the performance value extremes will be realistically.

Tabulations of component-part variations prepared for limited use (short-life guided-missile electronics) are shown in Tables I and II.[17] As indicated in the tabulated variations, there are many additional causes of variations other than the typical manufacturing tolerance of new parts under ambient conditions. Component-part value variations are caused by:

a) Manufacturing tolerance.
b) Applied voltage.
c) Soldering.
d) Operational aging.
e) Nonoperational aging.
f) Ambient temperature.
g) Power dissipation.
h) Operational instability.
i) Short time instability.
j) Humidity.

Further, variations for any cause will be of different types and will be any combination of:

a) Distributions.
b) Mean value change.
c) Reversiblity or irreversibility.

Distributions are assumed to be normal, and $\pm$ values shown in Tables I and II are 3 sigma limits. The mean value change refers to the existence of a shift in the mean value, as indicated in Tables I and II by $a+$ or $a-$. Reversibility or irreversibility is a function of the variation cause, where time is irreversible, temperature typically reversible, and voltage either. Fig. 9 illustrates these points using component-part value variation data from Tables I and II.

The form of the variations of component-part values illustrates that variation causes result in a high and a low set of changes. In using such variations all possible simultaneous causes are separately combined for both high and low value changes. Nominal value changes are algebraically added, while the distributions are statistically added by taking the square root of the sum of the squares. Thus the value changes of each component part reduces to a set of high and low values, both having a

[16] R. H. Hinrichs, "A Second Statistical Method for Analyzing the Performance Variation of Electronic Circuits," Convair, San Diego, Calif., Rept. ZX-7-010, Contract No. AF04(645)-4; February 15, 1956.

[17] "Reliability and Components Handbook," Western Military Electronics Ctr., Motorola, Inc., Phoenix, Ariz., sec. 3.2.1, 3.2.2; initially issued December 19, 1955.

TABLE I

VARIATIONS TO BE EXPECTED IN RESISTORS AND CAPACITORS

	Resistors (Per Cent)			Capacitors (Per Cent)	
	Deposited Carbon	Composition* (1 megohm or less)	Precision Wirewound	Paper	Glass
Typical manufacturing tolerance	±1	±5	±0.25	±5	±5
Change at +125°C	−3.5	+11	+0.25	+5	+1.3
Change at +85°C	−2.1	±4	+0.15	+3	+0.8
Change at −54°C	+2.8	+12	−0.20	−6	−1.0
Aging change	−0.4±1	− 5±2	±0.20	±2	±1
Change with heavy loading (near maximum rating)	−1.8	+ 7	+0.1	—	—
Change due to voltage coefficient (100 volts dc applied)	—	−1.5	—	—	—
Soldering change	—	− 2	—	—	—

* Composition resistors may suffer a +10 per cent additional change if exposed to 95 per cent relative humidity, 55°C, for 100 hours.

TABLE II

VARIATIONS TO BE EXPECTED IN TUBES*

	Transconductance (Per Cent)		Plate Current (Per Cent)		Amplification Factor (Per Cent)	
	Low	High	Low	High	Low	High
Manufacturing tolerance	−8±10	+8±10	−10±14	+10±14	+8±7	+8±7
10 per cent decrease in filament voltage	−5±3	—	− 5±3	—	Negligible	
10 per cent increase in filament voltage	—	+ 5±3	—	+ 5±3	Negiligible	
Aging change	−6±5	—	−10±5	—	—	+2±3
Random change when first energizing	±10	±10	±10	±10	Negligible	

* These data are pertinent to tubes procured to the MIL-E-1 specification and used near their design center values. The low and high conditions, which apply specifically to manufacturing tolerances, result from the MIL-E-1 specification having upper and lower acceptance limits on the tube parameter average (called LAL and UAL in MIL-E-1) and, in addition, an acceptance limit on the dispersion (called ALD in MIL-E-1). If the manufacturing tolerance is adjusted out, it can be omitted from the combined tolerance.

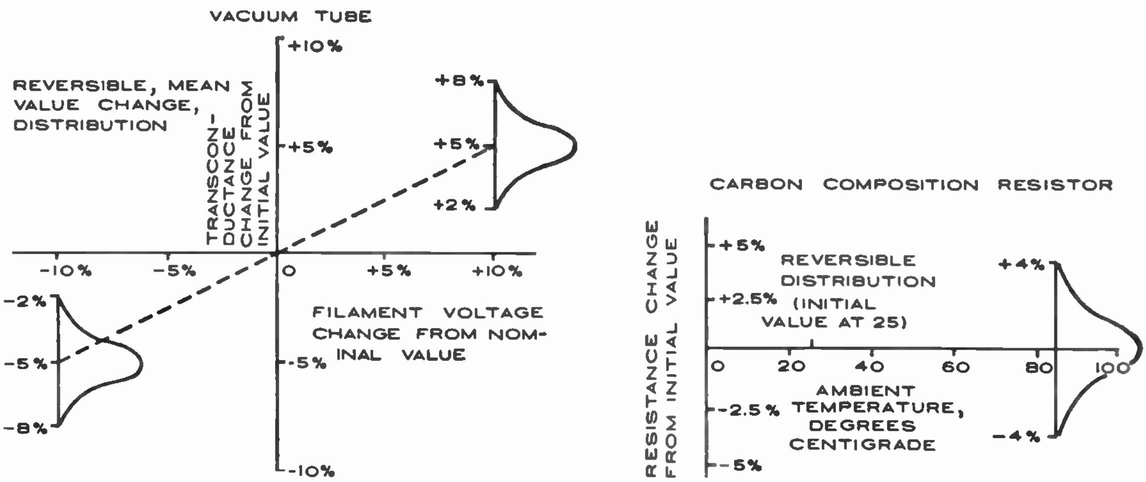

Fig. 9—Examples of component part value variations.

TABLE III
EXPECTED CHANGES

	Resistor, Composition (Per Cent)		Tube, Transconductance Change (Per Cent)	
	Low	High	Low	High
Manufacturing tolerance	±5	±5	− 8±10	+ 8±10
Change at +85°C	±4	—	—	—
Change at −54°C	—	+12	—	—
Aging change	−5±2	—	− 6±5	—
Soldering change	−2*	−2*	—	—
Filament voltage change of ±10 per cent	—	—	− 5±3	+ 5±3
Random change when first energized	—	—	±10	±10
Totals	−7±6.7	+10±5	−19±15	+13±15

* A fixed change that will affect both the low and high conditions.

mean value and a distribution. Table III illustrates the application of this method to the composition resistor and vacuum tube transconductance of Fig. 9 for various causes of changes.

Performance value distributions are next obtained using the two sets of component-part value distributions and the appropriate transfer function. Eqs. (9) and (10) are applied to the appropriate transfer function for both the low and high conditions. The resulting lower distribution limit for the low condition and the high distribution limit for the high condition are realistic extreme performance limits that can be expected for the possible simultaneous combination of variation causes.

The resistance and transconductance of Table III are for a load resistor of 1000 ohms nominal and a tube of 5000 micromhos nominal for a 7-stage IF strip where all stages are similar. The IF strip over-all gain transfer function is

$$A = \prod_{n=1}^{7} G_{m_n} R_{1_n}, \tag{12}$$

where

A = IF strip gain,
G_{m_n} = transconductance of each tube,
R_{1_n} = resistance of each load resistor.

Fig. 10 shows the resulting gain distributions and indicates that the worst probable limits to anticipate under operating conditions are 74.2 and 114 db.

Application of this technique is possible to any circuit or network where the transfer function is known. The technique can be expanded in scope and used to relate circuit performance to equipment performance. Where the transfer function is not known or is too inaccurate, the experimental statistical method of multiple regression will yield an empirical transfer function.

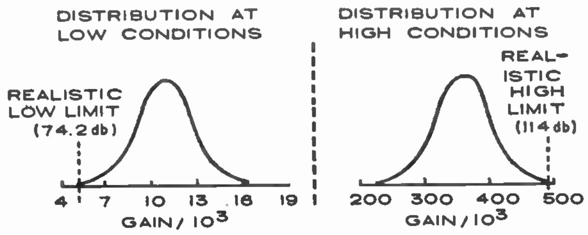

Fig. 10—Distribution of IF strip gain at low and high conditions.

Reducing Catastrophic Failures

Catastrophic failures at the component-part level are such failures as shorted capacitors or open resistors. In most circuits catastrophic failure of a component part will cause catastrophic failure of the circuit. Techniques leading to minimization of such failures have been formulated. Catastrophic failures can be reduced but not entirely eliminated.

Catastrophic failures of component parts are related to electrical and environmental stress levels. Thus, by reducing these stress levels, the incidence of catastrophic failures are reduced. Further stress level reduction will often reduce part parameter variations and thereby assist in minimizing performance change failures.

Stress-level catastrophic failure-rate relationships have been formulated on the basis of the best knowledge available by the Radio Corporation of America.[18] Such relationships are presented in this RCA work as family-of-curves, as shown, in a generalized manner, in Fig. 11. These component-part failure-rate characteristics are available through the Office of Technical Services, Washington, D. C.[18]

[18] "Reliability Stress Analysis for Electronic Equipment," Radio Corp. of America, Camden, N. J., Tech. Rept. No. TR1100; November 28, 1956. Available as Publication No. PB131678, Office of Tech. Services, Dept. of Commerce, Washington, D. C.

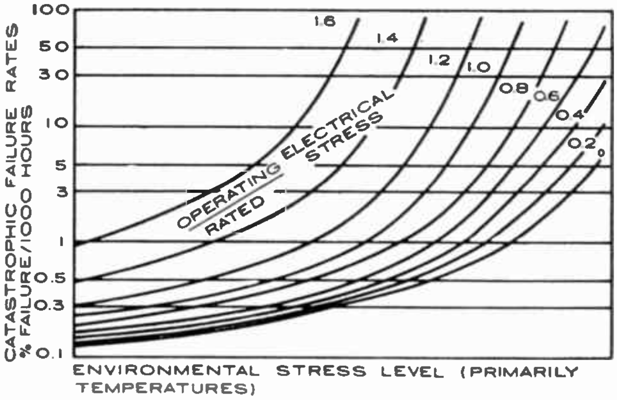

Fig. 11—Format of estimated component part catastrophic failure rate-stress level relationships (RCA TR1100)

Failure rates referred to in these relationships are assumed to be constant, as indicated in Fig. 1, for electronic equipment. In the previous discussion of the treatment of continual-use electronic-equipment reliability quantitatively, the point was made that the pertinency of the constant failure rate conditions to component parts was at this time questionable. Also, the failure-rate quantities assigned are averages and are subject to considerable variation.

These limitations do not detract from the excellency of the curves. They are a very useful guide in controlling and reducing catastrophic failures of component parts by showing designers where electrical and environmental operating level reduction (derating) will be most effective.

Redundancy

The approaches of reducing electrical and environmental stresses on component parts, and designing circuits, tolerant to realistic variations in component part values, that have been discussed increase reliability by minimizing failures. Reliability can be further improved by incorporating additional elements, that serve only to increase reliability of equipment. Reliability is defined as the probability that a piece of equipment will perform satisfactorily for a certain time under specified usage conditions. This definition says nothing about failure, and if a piece of equipment can be made to perform satisfactorily for longer time periods even if failures occur, its reliability has been increased. Redundancy is based on this point.

In typical electronic equipment (nonredundant),

$$R = \prod_{i=1}^{n} R_i \tag{13}$$

where

R = total reliability,
R_i = reliability of the individual elements,

relates equipment reliability to those elements comprising the equipment. Elements can vary from individual component parts to groups of component parts combined into single circuits or groups of circuits. In this discussion of redundancy, elements will be circuits or groups of circuits. The smallest breakdown of elements into individual component parts is a basic portion of practical reliability estimating which is discussed in the subsequent section.

Eq. (13) is based on the assumptions that chance of failure of any element is not related to the chance of any other element failing and that failure of any element causes equipment failure. These assumptions are sufficiently correct in typical equipment to make the concept applicable. The relationship of (13) is based on the application of the general rule of mathematical statistics of multiplication for the probability of joint, independent events to the probability of successful operation of all elements.

When elements are made redundant, reliability of the combination is

$$R = 1 - (1 - R_i)^n \tag{14}$$

where

n = number of redundant elements.

Eq. (14) is for the idealized case of perfect failure detection and switching among elements. The relationship of (14) is based on the application of the general rule of mathematical statistics of multiplication to probability of failure of all elements. Including the reliability of the failure detection and switching mechanism changes total reliability to

$$R = R_s[1 - (1 - R_i)^n], \tag{15}$$

where

R_s = reliability of the failure detection and switching device.

Eq. (15) indicates that R_s has a minimum value below which there is no reliability gain over a single element.

Fig. 12 illustrates those concepts where element-reliability time functions are assumed to be exponential, as shown in Fig. 4. Note that where redundancy is used, the reliability time functions are quite different from the exponential. Hence, a method of comparing various redundant and nonredundant approaches is to compare their reliability time functions.

Investigating further into redundancy reveals that making the complete piece of equipment redundant may not be the optimum technique. Assuming perfect failure detection and switching, optimum results are achieved by making every smallest possible element redundant, as illustrated by Fig. 13. The various reliabilities of the combinations of Fig. 13 are obtained by the appropriate application of the fundamental relationships of (13) and (14). Similarly, reliabilities of the

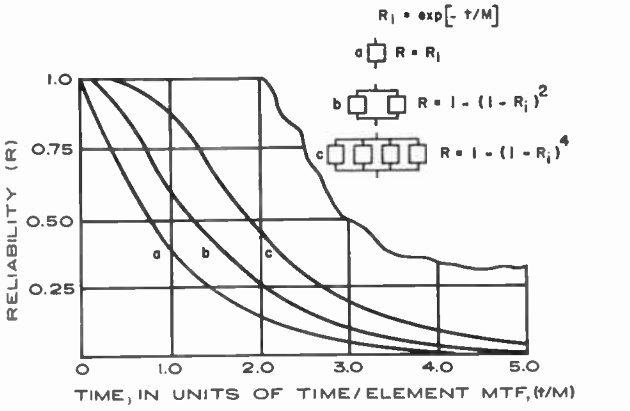

Fig. 12—Idealized reliability improvement with redundancy.

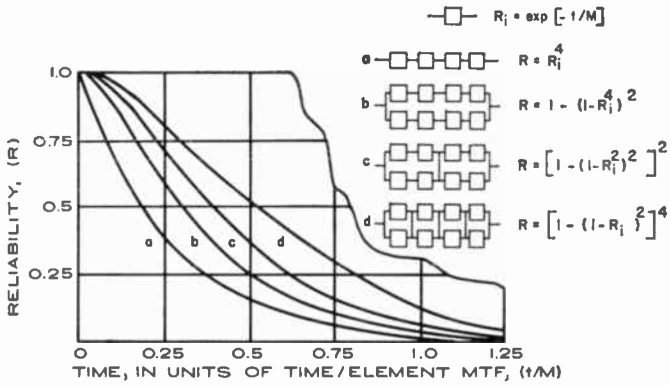

Fig. 13—Idealized reliability improvement for various redundancy levels.

great many possible combination methods are obtained by such application of (13) and (14).

Quantitative appraisal of the reliability of redundant approaches can be carried to further detail than indicated thus far. Total reliability of a redundant combination with switching was expressed by (15). Actually, there are various contingencies, such as erroneous signal from failure detectors or erroneous switching, that lead to a more detailed analysis.[19] Such a contingency also is the criterion of failure for switching circuits.[20] Successful opening of switches in parallel involves the opening of all switches, hence (13) is pertinent for the reliability of opening. Successful closing, however, involves a single switch closing, and hence (14) is pertinent for the reliability of closing. Switches physically in series can be similarly considered and will result in the opposite situation.

The type of redundancy referred to thus far involves switching the signal flow. If electrical power supplying a redundant element is switched instead of, or in addition to, signal, and if there is little chance of an element failing with no power supplied, a different analytical appraisal is pertinent. This situation is often thought of as standby. Reliability of elements on standby, where each element has an exponential time-to-failure distribution, is[21]

$$R = \sum_{i=0}^{n-1} \frac{1}{i!}\left(\frac{t}{M}\right)^i \exp[-t/M]. \qquad (16)$$

Eq. (16) must be individually derived for various time-to-failure distributions (see Fig. 3). However, comparing (16) to (14) for the exponential distribution, and using the same mean time to failure, M, reveals that standby reliability is somewhat higher.

The above discussion of redundancy presents various fundamentals and notes of application that relate the topic to the field of reliability analysis. The concept of redundancy has potentials of significantly increasing equipment reliability. However, this reliability increase will be at the cost of additional size, weight, and money. Considerable study by system and reliability analysts is currently being directed to the feasibility of the concept, and at least one program (AN/SPG-56 Radar for the Talos Missile System) involving equipment is being implemented using extensive redundancy principles.[22]

Reliability Estimating

Estimating reliability is particularly useful in the planning and early design eras of electronic equipment and systems. Estimates indicate whether proposed equipment will have the necessary reliability, allow the comparison of reliabilities of various approaches, and indicate the design emphasis necessary to achieve reliability goals. If reliability of electronic equipment progresses from the present status in military electronics as a qualitative objective or quantitative goal to a quantitative requirement, accurate techniques for estimating reliability will become a necessity.

An ideal equipment reliability estimate relates equipment performance parameters to the characteristics of the individual component parts.[23] The equipment performance is analytically related to part characteristics; the part characteristics are expressed as functions of time and environment. Part characteristics for such a

[19] B. J. Flehinger, "Reliability improvement through redundancy at various system levels," 1958 IRE National Convention Record, pt. 6, pp. 137–151.

[20] J. P. Lipp, "Topology of switching elements vs reliability," IRE Trans. on Reliability and Quality Control, PGRQC-10, pp. 21–33; June, 1957.

[21] To the knowledge of the writer, derivation of (16) is unpublished. As pointed out by J. H. S. Chin, Sperry Gyroscope Co., Great Neck, N. Y., in personal correspondence, (16) is the solution of

$$R = 1 - \int_0^t p(t_1)dt_1 \int_0^{t-t_1} p(t_2)dt_2 \cdots \int_0^{t-\sum_{i=1}^{n-1} t_i} p(t_n)dt_n,$$

where

n = number of elements, i,
t_i = time at which ith element fails,
$p(t_i)$ = failure probability density function of the ith element (see Fig. 3).

[22] R. W. Crosby, "Group Redundancy," presented at the Military Electronics Reliability and Maintainability Symp., Griffiss AFB, Rome, N. Y.; November, 1958.

[23] J. R. Rosenblatt, "On prediction of system performance from information on component performance," *Proc. Western Joint Computer Conf.*, pp. 85–94; February, 1957.

reliability estimate must include the pertinent part parameters expressed as statistical distributions in time and environment and the probability of catastrophic failure as a function of time and environment. With this information, it is possible to obtain the probability of satisfactory equipment performance and the confidence limits of this probability at given combinations of time and stresses.

The ideal equipment reliability estimating technique thus involves utilizing the approaches previously discussed on catastrophic and performance change failures and reliability of combinations. However, while these approaches, when simplified to first order approximations, are useful in reducing failures and increasing reliability, they are not currently practical for widespread use in reasonably-accurate reliability estimating. Highly accurate transfer functions and component-part characteristics are, in most cases, not available. Practical reliability estimating uses a simplified approach that can be reasonably accurate when properly used.

Reliability estimates are made by relating, in a simplified manner, equipment reliability to component-part reliability. Equipment reliability is assumed to be

$$R = \prod_{i=1}^{n} R_i \tag{13}$$

where

R = equipment reliability,
R_i = component part reliability.

This approach is based on the assumptions that chances of failure of the various component parts are independent of each other and the failure of any part will result in equipment failure.

Individual components are assumed to have reliabilities as described by (2). Failure of equipment or component parts is assumed as either catastrophic or as the change of some parameter to an unacceptable level. Hence, (13) becomes

$$\begin{aligned} R &= \prod_{i=1}^{n} \exp\left[-tF_i\right] \\ &= \exp\left[-t\sum_{i=1}^{n} F_i\right] \end{aligned} \tag{17}$$

where

F_i = component part failure rates.

Equipment failure rate F is estimated from

$$F = \sum_{i=1}^{n} F_n. \tag{18}$$

Although, as previously discussed, the assumptions upon which this model is based are not completely satisfied, the method is a useful tool in reliability analysis. In applying this technique reduced equipment performance, different modes of operation and redundancy should be considered.[24] In complex electronic equipment there are often circuits whose failure results in reduced, but still useful, equipment performance. Complex equipment may have various modes of operation where each mode does not utilize all circuits. In these situations, failure rate can be estimated separately for each mode of operation by making the assumption that failure of noncommon circuits in one mode does not cause equipment failure in other modes. Where redundancy exists, the technique above (18) is applied to nonredundant elements; then the appropriate redundant relationships are applied to the nonredundant element reliability time functions.

Component-part failure rates suitable for use in (18) to estimate equipment reliability have been reported by various sources.[25] The reported data show wide divergencies for the same type of component part. As previously cited, inherent equipment reliability is a result of many complex factors such as component-part reliability, electrical and mechanical design approaches and maturity, and manufacturing techniques. Therefore, the wide variations in reported failure rates should be expected because of the wide variations found throughout the electronics industry in the factors just cited that affect reliability.

Examination of many sources of reported component-part failure rates suggests that the failure rates in Table IV are pertinent for the current state of the art on

TABLE IV
COMPONENT PART FAILURE FIGURES FOR RELIABILITY ESTIMATING

Component Part	Failure Rate*	Component Part	Failure Rate*
Capacitors			
Paper	0.67	Relay	5.0
Ceramic	0.67	Resistors	
Mica, glass	0.5	Composition	0.5
Others	2.5	Film	1.0
Choke, coil	1.67	Wirewound	0.5
Connector	1.25	Socket	0.5
Crystal	5.0	Switch	5.0
Delay line	5.0	Synchro	5.0
Diode (semiconductor)	2.5	Thermostat	10.0
Heater	10.0	Transformer	2.5
Magnetic amplifier	1.25	Transistor	5.0
Motor	25.0	Tubes	
Potentiometers		Receiving	20.0
Wirewound	10.0	Other	100.0
Composition	1.67		

* Failures per 10^6 hours.

[24] H. E. Blanton, "Reliability prediction technique for use in design of complex systems," 1957 IRE NATIONAL CONVENTION RECORD, pt. 10, pp. 68–79.
[25] D. E. Johnston and D. T. McRuer, "A Summary of Component Failure Rate and Weighting Function Data and Their Use in Systems Preliminary Design," Wright Air Dev. Ctr., Dayton, Ohio, Tech. Rept. No. 57-668, ASTIA Doc. No. AD-142120.

mature equipment where there has been a high degree of reliability consciousness and gross design errors have been removed. Further, these failure rates are for a typical laboratory environment. In reliability estimates for other more severe environments, these failure rates should be increased. The writer suggests a multiplication of these failure rates by two for typical manned aircraft and by 10 for typical missile flight environments.

The component-part failure rates of Table IV are principally tools of equipment reliability estimating. The failure rates represent an average. Therefore any specific equipment might have little trouble with one component part, but more with another, resulting in a cancelling effect.

In the previous discussion of treating reliability quantitatively, equipment was divided into continual-use equipment and single, short-time-use equipment. This approach toward reliability estimating is directed primarily toward the continual-use equipment, but can be applied to single-use equipment by following the same approach and computing the reliability for the appropriate short time.

This reliability estimating technique can be moderately accurate where an equipment producer develops his own component-part failure-rate data. One such approach has resulted in data that has been ultimately substantiated as being capable of estimating equipment reliability within approximately 15 per cent.[26]

TABLE V

ENGINEERING RELIABILITY ELEMENTS

Use Reliable Component Parts	
Determine best component-part type by: 1) Past experience 2) Evaluative tests. Determine best vendors by: 1) Past experience 2) Screening tests and tests to failure 3) Vendor facility survey.	Control vendors with adequate procurement specification and perform: 1) Qualification tests 2) Lot acceptance tests 3) Requalification tests.
Design for Reliability	
Electrical—reliable circuits by: 1) *Derate component parts 2) *Minimize component-part variation effects through statistical techniques and feedback 3) Simplicity 4) Proven circuits 5) *Redundancy 6) *Reliability estimates aid systems design. Packaging—minimize environmental effects by: 1) Absorb vibratory energy 2) Adequate heat flow 3) Humidity protection 4) Shock protection.	Packaging—maintain a balance among: 1) Reliability—adequate safety margins 2) Maintainability—accessibility for repair 3) Producibility—ease of assembly 4) Operability—ease of operation 5) Size and weight—meet requirements.
Perform Adequate Testing	
Locate weaknesses for corrective action by: 1) Circuit breadboard bench tests 2) System breadboard bench tests 3) Mechanical mock-up environmental tests 4) Engineering model bench tests 5) Engineering model environmental tests.	Measure reliability by (corrective action if inadequate): 1) Controlled Use 2) Defined failure 3) *Statistical analysis.

* Analytically treated in this paper.

Relationship of Analytical Techniques to Effective Reliability Improvement

The approaches discussed to this point on reliability analysis only touch on a portion of a complete engineering effort for high reliability. Many factors affect reliability, and it is difficult to isolate them from the total of all the factors in designing and producing electronic equipment. It is a fundamental fact that the reliability of equipment is established in design, and after the design is committed only gross errors can be fixed within reasonable economic realms.

Elements of a complete reliability program are presented in Table V. Examination of these elements indicates that this is merely a common sense approach to good engineering. The underlying theme of these elements is that of first doing everything reasonable to minimize and eliminate weaknesses and then performing adequate testing in search of existing weaknesses. The objective is to prove the product by design adequacy studies and sufficient testing prior to releasing it from engineering.

The elements of Table V can be applied in varying extents to different engineering programs. On programs where reliability is stressed, the elements should be completely applied. Where reliability is not stressed, the extent of application will be less.

The elements of the reliability effort of Table V which are analytically treated in this paper are coded with an asterisk. Only a few asterisks appear. Analytical techniques only form a part of engineering for reliability and must not be over emphasized at the expense of other equally important elements.

The engineering reliability efforts must be supported by efforts in manufacturing (quality control) to maintain and improve inherent reliability and by efforts in the use of the equipment to improve any gross weaknesses by field changes.

[26] R. L. Vander Hamm, "Component part failure rate analysis for prediction of equipment mean life," 1958 IRE National Convention Record, pt. 6, pp. 72–76. See p. 75.

Conclusion

Analytical techniques leading to improved equipment reliability have evolved in the last few years. The techniques are not precise, but they are effective in reducing failures and increasing reliability. The development of quantitative reliability models is leading to the formal treatment of reliability as a contractual requirement. These analytical techniques are effective but are just a part of total reliability efforts. A total reliability approach is that of essentially sound engineering supplemented by these recently developed analytical techniques.

Considerable research and study of reliability analysis techniques is currently occurring from both a sound theoretical approach and from attempts at practical application. Many electronic equipment producers are experimenting with formal and informal reliability programs. As results are achieved and experience gained, expansion and modification of the material presented herein can be expected.

Acknowledgment

The author is indebted to the other staff members of the Motorola Reliability and Components Group who assisted in gathering the information contained in this paper. To a large extent this is a collection and synthesis of the isolated works of many people. Acknowledgment is extended to these people, and their work, which is referenced throughout the paper.

A Stabilized Locked-Oscillator Frequency Divider*

PHILIP R. SCOTT, JR.†, MEMBER, IRE

***Summary*—This paper presents an analysis of a simple oscillator designed for stabilized frequency divider application. The oscillator combines some of the characteristics of sinusoidal and relaxation oscillators to provide a high degree of frequency stability while allowing sufficient tendency for synchronization. The analytical results are obtained in a graphical form which is easy to handle and which could be used as a design procedure for stabilized frequency dividers. Synchronization of the oscillator is described for the case of an input signal consisting of narrow pulses. It is shown that the circuit can maintain a given frequency division ratio regardless of variations in the amplitude of such a synchronization signal.**

The results of the graphical analysis are confirmed by experimental observations. Performance data are presented indicating that the circuit is capable of frequency division ratios of 30 to 40 without requiring close control of the power supply voltage.

Introduction

The generation of subharmonics, or frequency division, can be performed by several types of circuits.[1–4] An important class of frequency dividers makes use of the locking property of oscillators. This phenomenon has been discussed by a number of writers,[5–10] and for many years has been used as a basis for frequency divider design.[11–18]

Oscillators which generate waveforms rich in harmonics are easier to synchronize than those which generate sinusoidal waveforms.[7,19] For this reason, relaxa-

* Original manuscript received by the IRE, January 30, 1959; revised manuscript received, July 13, 1959. Most of this material was contained in a thesis which the author submitted to the Moore School of Engineering, University of Pennsylvania, Philadelphia, Pa., in partial fulfillment of the requirements for the M.S.E.E. degree.

† Instrumentation Lab., Mass. Inst. Tech., Cambridge, Mass.

[1] H. Sterky, "Frequency multiplication and division," Proc. IRE, vol. 25, pp. 1153–1173; September, 1937.

[2] R. L. Miller, "Fractional-frequency generators utilizing regenerative modulation," Proc. IRE, vol. 27, pp. 446–457; July, 1939.

[3] W. H. Bliss, "Electronic digital counters," *Elec. Engrg.*, vol. 68, pp. 309–314; April, 1949.

[4] K. C. Hu and Y. H. Ku, "Circuit for a magnetic subharmonic pulser," *Trans. AIEE*, pt. I, pp. 137–141; May, 1957.

[5] E. V. Appleton, "The automatic synchronization of triode oscillators," *Proc. Cambridge Phil. Soc.*, vol. 21, pp. 231–248; 1922–1923.

[6] B. van der Pol, "Forced oscillations in a circuit with nonlinear resistance," *Phil. Mag.*, vol. 3, pp. 65–80; January, 1927.

[7] B. van der Pol, "The nonlinear theory of electric oscillations," Proc. IRE, vol. 22, pp. 1051–1086; September, 1934.

[8] D. G. Tucker, "Forced oscillations in oscillator circuits, and the synchronization of oscillators," *J. IEE*, vol. 92, pt. 3, pp. 226–234; September, 1945.

[9] R. Adler, "A study of locking phenomena in oscillators," Proc. IRE, vol. 34, pp. 351–357; June, 1946.

[10] M. L. Cartwright, "Forced oscillations in nearly sinusoidal systems," *J. IEE*, vol. 95, pt. 3, pp. 88–96; March, 1948.

[11] I. Koga, "A new frequency transformer or frequency changer," Proc. IRE, vol. 15, pp. 669–678; August, 1927.

[12] B. van der Pol and J. van der Mark, "Frequency demultiplication," *Nature*, vol. 120, pp. 363–364; September 10, 1927.

[13] W. A. Marrison, "A high precision standard of frequency," Proc. IRE, vol. 17, pp. 1103–1122; July, 1929.

[14] R. M. Page and W. E. Curtis, "The van der Pol four-electrode tube relaxation oscillation circuit," Proc. IRE, vol. 18, pp. 1921–1929; November, 1930.

[15] J. Groszkowski, "Frequency division," Proc. IRE, vol. 18, pp. 1960–1970; November, 1930.

[16] V. J. Andrew, "The adjustment of the multivibrator for frequency division," Proc. IRE, vol. 19, pp. 1911–1917; November, 1931.

[17] V. J. Andrew, "A simplified frequency dividing circuit," Proc. IRE, vol. 21, pp. 982–983; July, 1933.

[18] G. Builder and N. F. Roberts, "The synchronization of a simple relaxation oscillator," *A WA Tech. Rev.*, vol. 4, no. 4, pp. 165–180; 1939.

[19] J. Groszkowski, "The interdependence of frequency variation and harmonic content, and the problem of constant-frequency oscillators," Proc. IRE, vol. 21, pp. 958–981; July, 1933.

tion oscillators are often used as frequency dividers. Relaxation oscillators are sensitive to operating conditions, however, and variation of the synchronizing signal amplitude or of the power supply voltages can cause synchronization to the wrong submultiple of the input frequency. These parameters must be closely controlled to avoid marginal operation. The problem becomes more difficult at high ratios of frequency division.

The locking requirements suggest the use of an oscillator which combines the desirable characteristics of relaxation and sinusoidal oscillators. Such a circuit would have good frequency stability and yet would be easy to synchronize. Builder[20] stabilized a gas tube relaxation oscillator by adding a tuned feedback loop. This reduced the harmonic content of the generated waveform enough to improve stability, while at the same time allowing sufficient tendency for synchronization. Later Sulzer[21] obtained a similar result by increasing the harmonic content of the waveform generated by a sinusoidal oscillator.

This paper presents a study of a simple stabilized frequency divider similar to that described by Sulzer. A graphical solution of the nonlinear differential equation of the circuit is obtained by the piecewise-linear method.[22] The analysis is easy to carry out, and could be used as a basis for the systematic design of stabilized frequency dividers. The mechanism of synchronization is described for the case of an input signal consisting of sharp pulses, and it is shown that the oscillator can be made independent of variations in the amplitude of this type of synchronizing signal.

Circuit Operation

The oscillator of Fig. 1(a) can be adjusted to operate as a stabilized frequency divider. If the resistor R is made very small, the circuit operates as a sinusoidal oscillator. If R is made very large, the effect of the tuned circuit becomes negligible, and the circuit operates as a free running multivibrator. Somewhere between these extremes lies a range of resistor values for which the circuit takes on characteristics of both types of oscillators.

Fig. 1(b) is an approximate equivalent circuit of Fig. 1(a), obtained by neglecting the plate reaction of the triodes as well as the bias resistor R_b and the blocking capacitors C_1. Coil losses are represented by the resistor r_c. The amplifier open circuit output voltage e_o is a nonlinear function $\phi(e_i)$ of its input voltage e_i as illustrated in Fig. 2. To simplify the analysis, the piecewise-linear approximation of Fig. 2(b) will be used.

Referring to Fig. 1(b), and representing the effect of

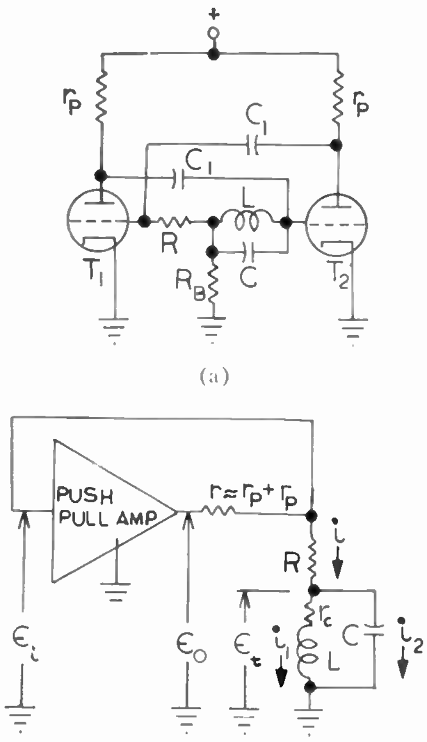

(a)

(b)

Fig. 1—Stabilized frequency divider. (a) Practical circuit. (b) Approximate equivalent circuit.

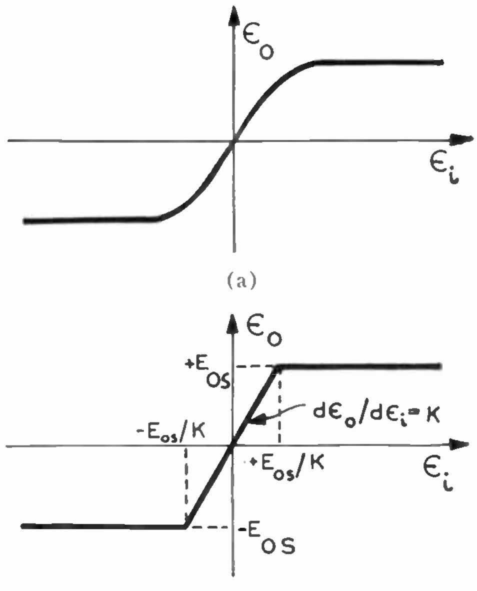

(a)

(b)

Fig. 2—Amplifier function $e_o = \phi e_i$. (a) Actual function. (b) Approximated function.

the tuned circuit by its voltage e_t, the loop equation for the circuit is

$$\phi(iR + e_t) - [i(R + r) + e_t] = 0. \tag{1}$$

This can be illustrated on a graph as shown in Fig. 3. The functions $\phi(iR+e_t)$ and $[i(R+r)+e_t]$ are plotted against the amplifier output current i, and a composite curve is obtained by subtracting the second of these

[20] G. Builder, "A stabilized frequency divider," Proc. IRE, vol. 29, pp. 177–181; April, 1941.

[21] P. G. Sulzer, "Modified locked-oscillator frequency dividers," Proc. IRE, vol. 39, pp. 1535–1537; December, 1951.

[22] A. A. Andronow and C. E. Chaikin, "Theory of Oscillations," English Language ed., Princeton University Press, Princeton, N. J.; pp. 112–118, 163–177; 1949.

curves from the first. The points where the composite curve crosses the current axis are equilibrium points which satisfy (1).

Fig. 3(a) shows the construction for zero voltage e_t. The function $\phi(iR+e_t)$ contains a segment with slope KR, where K is the unsaturated amplifier gain and is greater than plus one. By choosing a resistor R large enough this slope can be made greater than the slope $(R+r)$ of the function $[i(R+r)+e_t]$. As a result, the system has three equilibrium positions labeled a, b, and c. Solutions a and c are stable while b is unstable, and thus the device operates as a bistable or trigger circuit.

As the voltage e_t is moved away from zero, a point is reached where the device becomes monostable. Fig. 3(b) shows the construction for a positive voltage e_t. The effect is to translate the composite curve of Fig. 3(a) upward and to the left. The amount of translation is proportional to the magnitude of e_t. In Fig. 3(b) the shift has been carried so far that solution c is the only one remaining of the original three. A similar result holds for a negative voltage, shown in Fig. 3(c), with the translation occurring downward and to the right.

The transitions between bistable and monostable operation of the amplifier occur when one of the bends d or e in the composite curve is tangent to the current axis. The values of e_t for which these points are tangent are given by

$$e_t = \pm E_j = \pm E_{os}[KR - (R + r)]/Kr. \tag{2}$$

The operation of the circuit for all values of voltage e_t is summarized in Table I.

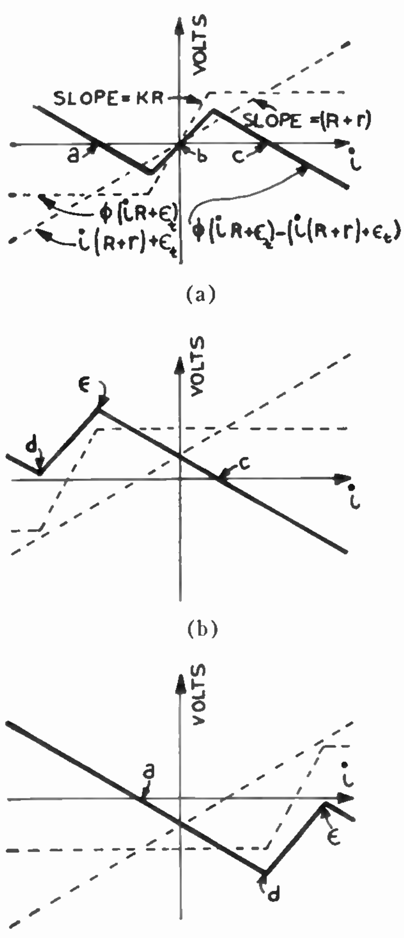

Fig. 3—Graphical determination of amplifier operation as a function of tuned circuit voltage e_t. (a) $e_t=0$. (b) e_t is positive. (c) e_t is negative.

TABLE I

CIRCUIT OPERATION AS A FUNCTION OF e_t FOR $KR>(R+r)$

e_t	Amplifier Operation
$e_t < -E_J$	Monostable: $e_o = -E_{os}$
$-E_J < e_t < +E_J$	Bistable: e_o = either $-E_{os}$ or $+E_{os}$
$+E_J < e_t$	Monostable: $e_o = +E_{os}$

The voltage e_t across the tuned circuit is given by

$$e_t = Li_1' + r_c i_1 \tag{3}$$

where

$$i_1' = di_1/dt.$$

The current i_2 in the capacitive branch is given by

$$i_2 = Ce_t' = CLi_1'' + Cr_c i_1'. \tag{4}$$

The current entering the tuned circuit is the amplifier output current i, the sum of the currents in the inductive and capacitive branches

$$i = i_1 + i_2 = LCi_1'' + Cr_c i_1' + i_1 = \frac{e_0 - e_t}{R + r}$$

or

$$i_1'' + \left[\frac{r_c}{L} + \frac{1}{C(R+r)}\right] i_1' + \left[\frac{R + r + r_c}{(R+r)LC}\right] i_1 = \frac{e_0}{LC(R+r)}. \tag{5}$$

The amplifier open-circuit output voltage e_o assumes one of two possible values $\pm E_{os}$. In practical circuits the coefficient of i_1' in (5) is made much less than the coefficient of i_1, and the equation has an oscillatory solution given by

$$i_1 = I(\exp(-ht)) \cos(\omega_1 t + \alpha) \pm \frac{E_{os}}{R + r + r_c}$$

where

$$h = \frac{1}{2}\left[\frac{r_c}{L} + \frac{1}{C(R+r)}\right],$$

$$\omega_1 = \sqrt{\frac{R + r + r_c}{(R+r)LC} - h^2} \tag{6}$$

and I and α are arbitrary constants depending on the initial conditions.

Differentiating (6) gives

$$i_1' = -I(\exp(-ht))(h\cos(\omega_1 t+\alpha) + \omega_1\sin(\omega_1 t+\alpha)). \quad (7)$$

It is possible to obtain a complete representation of the oscillator operation by using a phase plane plot[23] of i_1' against i_1. In this analysis, however, it is convenient to first make the following transformation:[24]

$$u = \omega_1 i_1; \qquad v = hi_1 + i_1', \quad (8)$$

from which

$$u = P(\exp(-ht))\cos(\omega_1 t+\alpha) \pm \omega_1 E_{os}/(R+r+r_c),$$
$$v = -P(\exp(-ht))\sin(\omega_1 t+\alpha) \pm hE_{os}/(R+r+r_c) \quad (9)$$

where P is an arbitrary constant depending upon the initial conditions.

These equations describe families of clockwise logarithmic spirals in the u, v plane. The transformation to logarithmic spirals is useful because such curves can be constructed easily. Also, this representation provides a simple indication of time, since the angular velocity of the radius vector about its center is a constant ω_1. Thus, the time required to complete any portion of motion in the system can be calculated by measuring the angle of rotation of the radius vector of the spiral segment. This is convenient in studying the effect of synchronizing pulses.

Fig. 4 illustrates the graphical procedure for describing the generation of oscillations. The first step is to locate on the u, v plane the two possible points around which motion can center. These are labeled point A and point B in Fig. 4. Point A has the coordinates $u=+\omega_1 E_{os}/(R+r+r_c)$; $v=+hE_{os}/(R+r+r_c)$. Motion centers about this point when the amplifier output voltage is $+E_{os}$. Point B has the coordinates $u=-\omega_1 E_{os}/(R+r+r_c)$; $v=-hE_{os}/(R+r+r_c)$. Motion centers about this point when the amplifier output voltage is $-E_{os}$.

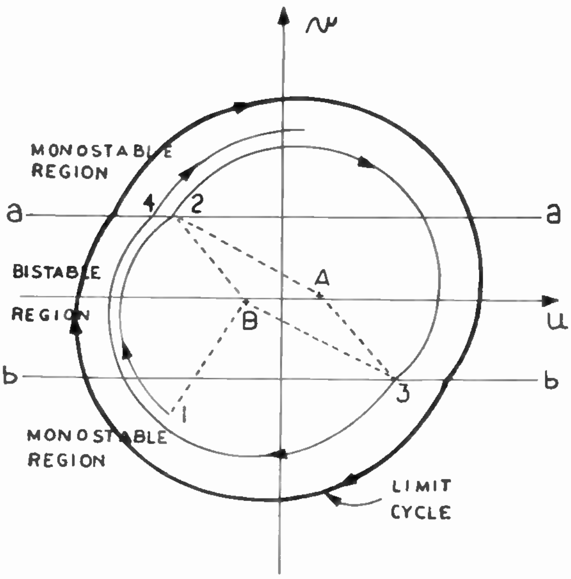

Fig. 4—Graphical representation of the generation of oscillations.

[23] B. van der Pol, "On relaxation oscillations," *Phil. Mag.*, vol. 2, pp. 978–992; November, 1926.
[24] Andronow and Chaikin, *op. cit.*, pp. 18–20.

Next, the voltages $\pm E_J$ are mapped on the u, v plane. Using (3) and (8), the voltage $+E_J$ is mapped as a straight line aa given by

$$v_{aa} = \frac{+E_J}{L} + \left(h - \frac{r_c}{L}\right)\frac{u}{\omega_1}. \quad (10)$$

Line bb maps the voltage $-E_J$.

$$v_{bb} = \frac{-E_J}{L} + \left(h - \frac{r_c}{L}\right)\frac{u}{\omega_1}. \quad (11)$$

According to Table I the portion of the u, v plane above line aa is a region of monostable operation for which the amplifier open circuit output voltage e_o has the value $+E_{os}$ and motion centers about point A. The portion below line bb is also a monostable region for which e_o is $-E_{os}$ and motion centers about point B. Between aa and bb is the bistable region for which e_o can be either $+E_{os}$ or $-E_{os}$, and motion can center about either point A or point B.

The construction begins by selecting some initial point such as 1 in Fig. 4. Since point 1 is below the line bb, it falls on the arc of a logarithmic spiral centered about point B. The radius of the spiral is given by:

$$\text{Radius} = P(\exp(-ht)) = P[\exp(-h\theta/\omega_1)],$$

where

$$\theta = \omega_1 t = \text{angle of rotation in radians},$$
$$P = \text{initial radius}. \quad (12)$$

The spiral is drawn clockwise about point B and passed through the bistable region to point 2 where it intersects the line aa. At this point, the center of motion must switch to point A. Using (12) with the new initial radius, a logarithmic spiral is drawn around point A which intersects line bb at point 3. Here the center of motion switches back to point B. Fig. 4 shows the growth of oscillations from small initial amplitude. This growth approaches the stable operating amplitude or limit cycle.

The limit cycle describes the steady-state operation of the oscillator. From this construction the operating frequency can be calculated, and the waveforms of the voltages at various points in the circuit can be plotted as functions of time. Fig. 5(a) shows the method of calculating frequency. The rotations of the logarithmic spiral segments are θ_1 about point A and θ_2 about point B. These angles, expressed in radians, can be substituted into the following to determine the frequency

$$f_{aa} = \omega_1/(\theta_1+\theta_2), \quad (13)$$

where f_{aa} is the free running or unsynchronized frequency of the oscillator.

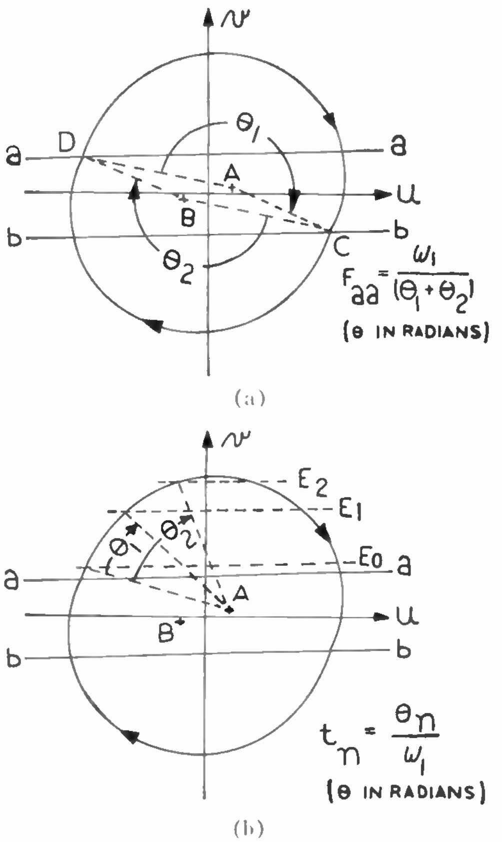

Fig. 5—(a) Calculation of unsynchronized oscillator frequency f_{aa}. (b) Calculation of points for a plot of the waveform of tuned circuit voltage e_t.

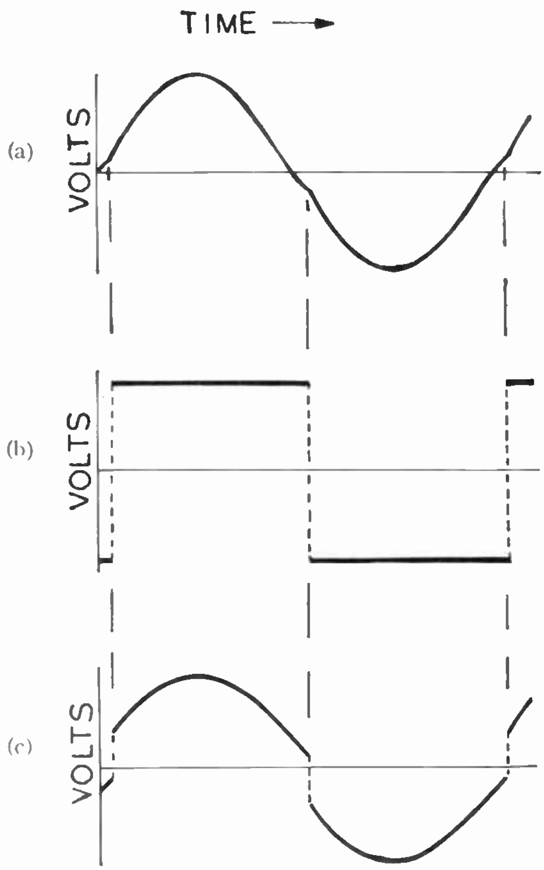

Fig. 6—Typical stabilized oscillator waveforms. (a) Tuned circuit voltage e_t. (b) Amplifier open circuit output voltage e_0 (this cannot be observed on an operating circuit because of loading). (c) Amplifier input voltage e_i.

Fig. (5b) shows the method of calculating points for a plot of the voltage e_t as a function of time. Appropriate values of e_t are mapped onto the u, v plane as straight lines which intersect the limit cycle. Starting from some convenient point, the angles of revolution θ of the spiral segments to each of these intersections is measured in radians. From these measurements, the time corresponding to a value of e_t is given by

$$t_n = \theta_n/\omega_1. \tag{14}$$

The values of e_t are then plotted against the corresponding values of time to obtain the waveform. Fig. 6(a) shows the waveform for a typical oscillator. It is a decaying sine wave which is regenerated every half cycle.

The amplifier open-circuit output voltage e_o is a square wave as shown in Fig. 6(b). Its value is $+E_{os}$ during the time motion is centered about point A, and $-E_{os}$ during the time motion is centered about point B. The waveform of amplifier input voltage e_i is obtained by substituting values of voltage e_t and e_o into the following:

$$e_i = e_t + (e_0 - e_t)R/(R + r). \tag{15}$$

As Fig. 6(c) shows, this is sinusoidal with a superimposed discontinuity caused by the switching of the amplifier.

In order to permit this type of oscillation, the resistor R must be large enough to satisfy the condition $KR > (R+r)$. There is also an upper limit. As R is increased, the points A and B move closer together in the u, v plane, and the lines aa and bb move farther apart. Eventually no limit cycle can be constructed, and the desired type of oscillation becomes impossible. At this point the effect of the blocking capacitors C_1 can no longer be ignored, and the circuit generates relaxation oscillations at a much lower frequency.

It is possible to select starting points for the graphical construction that will not lead to the limit cycle. Consider the shaded area surrounding point A in Fig. 7(a). This area is bounded by the spiral segment centered at point A and tangent to line bb. If the system is represented by a point within this area, and, if motion is centered about point A, the initial spiral segment will not cross line bb. Under these conditions, it is not possible to construct a limit cycle. A similar area exists about point B.

When these areas are small as shown in Fig. 7(a), they do not affect the operation of the circuit. The oscillator will generate relaxation oscillations which provide sufficient impulse to start the desired type of oscillations.

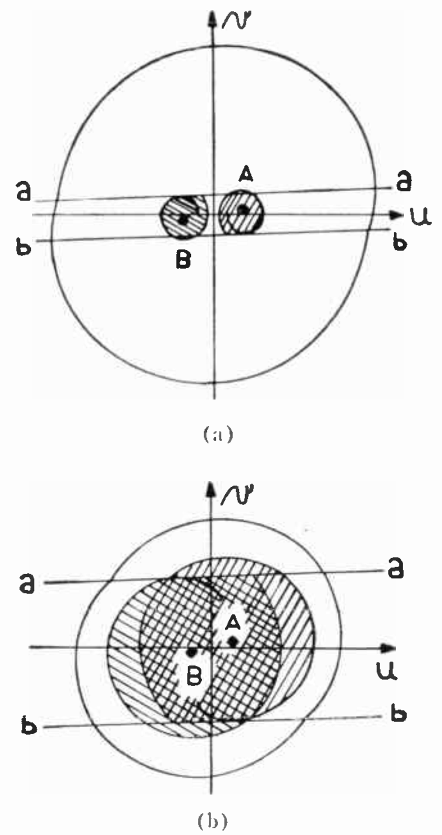

Fig. 7—Initial conditions which do not lead to the limit cycle. (a) Circuit with a small resistor R. (b) Circuit with a larger R.

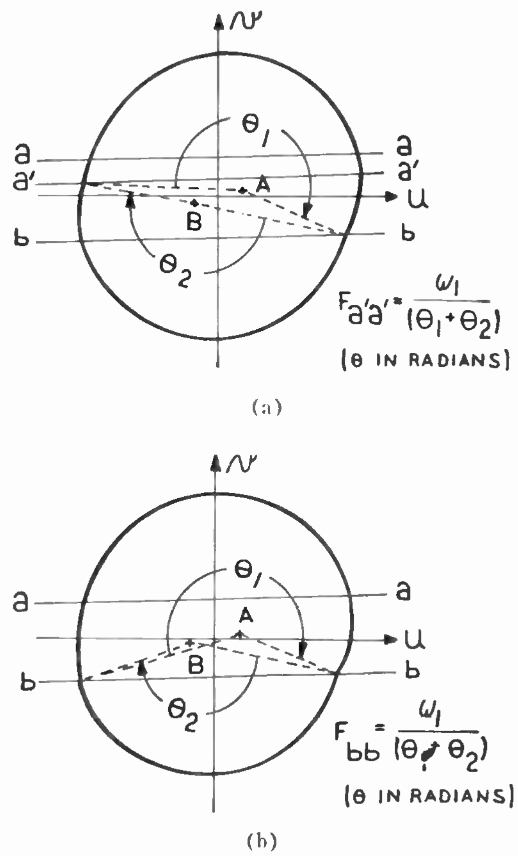

Fig. 8—Graphical representation of the effect of narrow, positive synchronizing pulses. (a) Oscillator synchronized to intermediate frequency $f_{a'a'}$. (b) Oscillator synchronized to maximum frequency f_{bb}.

If the resistor R is made larger, however, the areas overlap and fill most of the area required by the limit cycle, as shown in Fig. 7(b). In this case it sometimes may be necessary to apply an external shock to the circuit to prevent it from continuing to generate relaxation oscillations instead of the desired type.

Synchronization

The oscillator can be synchronized by a signal of proper frequency applied to the input of the amplifier. A signal consisting of narrow positive pulses can affect the circuit only when motion is within the bistable region and centered about point B. The pulses raise the oscillator frequency by causing the center of motion to switch from point B to point A before motion reaches the line aa. When steady state is reached, the circuit operates as though its limit cycle were constructed as shown in Fig. 8(a), by using some line $a'a'$ instead of the line aa. The maximum frequency to which the oscillator can be synchronized by narrow positive pulses is given by the construction of Fig. 8(b) where line $a'a'$ falls on line bb.

The width of the region of bistable operation can be adjusted by varying the resistor R. As R is made smaller, lines aa and bb move closer together and the width decreases. When the following equation is satisfied the oscillator will synchronize only to desired subharmonic regardless of the amplitude of the input pulses:

$$\frac{f}{n+1} < f_{aa} < \frac{f}{n} < f_{bb} < \frac{f}{n-1} \tag{16}$$

where f is the frequency of the input signal, f_{aa} is the oscillator natural frequency, f_{bb} is the maximum possible synchronized frequency, and n is the desired frequency division ratio.

It is not necessary to construct the spiral curves to determine the frequencies f_{aa} and f_{bb}. Referring to Fig. 5(a), the points A and B and the lines aa and bb are located in the u, v plane. Then the points C and D are selected so that the lines CA, DA, DB, and CB satisfy the following:

$$\begin{aligned}(CA/DA) &= \exp(-h\theta_1/\omega_1),\\ (DB/CB) &= \exp(-h\theta_2/\omega_1).\end{aligned} \tag{17}$$

With the aid of a slide rule and a scale, these points can be located in a few tries. Then the angles θ_1 and θ_2 are inserted into (13) to give the frequency f_{aa}. A similar procedure is used to obtain f_{bb}.

Experimental Observations

Fig. 9 shows an experimental circuit designed to operate in the vicinity of 500 cps. The plates of the pentodes are joined to the circuit by electronic coupling and take no part in the generation of oscillations. This provided a method of making accurate frequency measurements without danger of error due to loading from the frequency meter. Synchronizing signal was applied through the 47 $\mu\mu$f capacitor which differentiated the square wave input to approximate a series of narrow pulses. The resistor R was made variable so its effect could be studied.

Fig. 10 presents oscillograms of the amplifier input voltage e_i and the voltage across the tuned circuit e_t with an R of 100 k. The waveforms agree with the graphical constructions of Fig. 6. The e_t waveform shows the irregularities caused by the regeneration of the decaying sine wave. These occur simultaneously with the discontinuities in the e_i waveform.

The operation of the circuit for several values of R is shown in Fig. 11. These waveforms were obtained by connecting the oscilloscope between one of the control grids and ground. When R was zero the waveform was an approximate half sine wave. As R was raised to about 50 k a small discontinuity appeared, indicating the beginning of the bistable region of operation. The discontinuity increased as R was increased. It was found that for values of R between 50 k and 120 k, the circuit generated only the desired type of oscillations. For values between 120 k and 300 k, either the desired type of oscillations or relaxation oscillations could be generated and the oscillator could be switched from one mode to the other by temporarily shorting the resistor R or the tuned circuit. Above 300 k, the circuit generated only relaxation oscillations.

Figs. 12 and 13 show the operation of the oscillator as a synchronized frequency divider. The synchronizing pulses are superimposed on the grid voltage waveforms. Operation at division ratios of 10, 20, and 40 is illus-

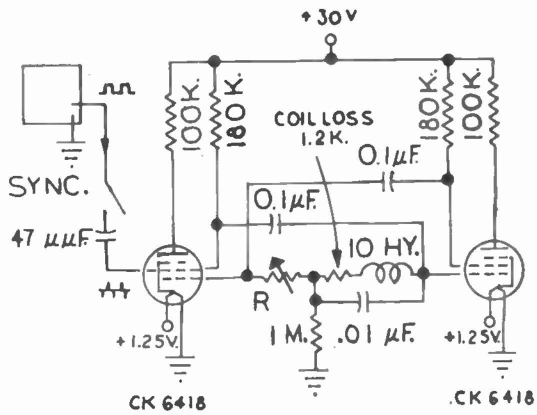

Fig. 9—Experimental circuit.

(a)

(b)

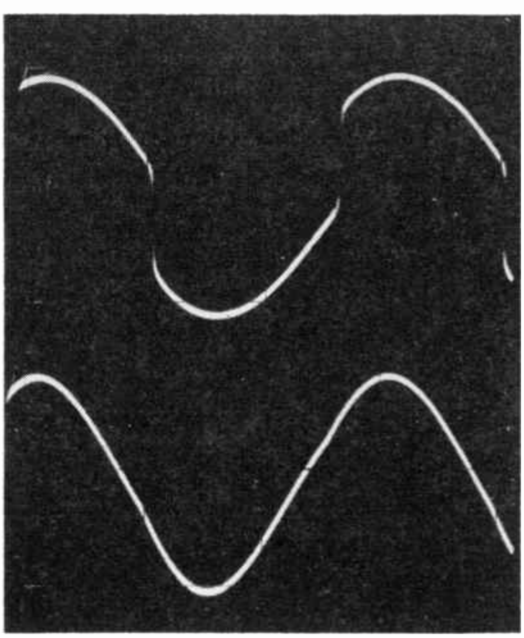

Fig. 10—Oscillator waveforms for $R=100$ k. (a) Amplifier input voltage e_i. (b) Tuned circuit voltage e_t.

(a)

(b)

(c)

(d)

(e)

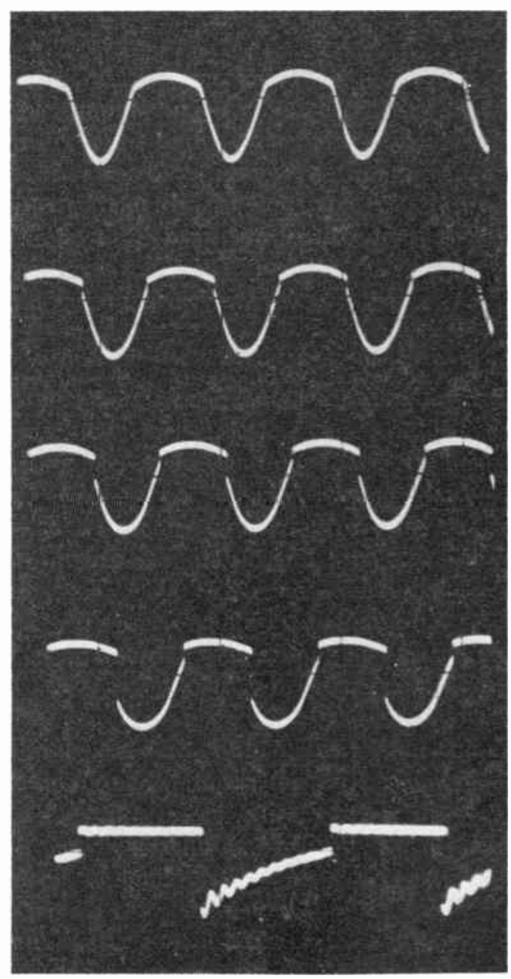

Fig. 11—Control grid waveforms for various values of R. (a) $R=0$. (b) $R=50$ k. (c) $R=100$ k. (d) $R=200$ k. (e) $R=200$ k (operating as a relaxation oscillator at 23 cps).

(a)

(b)

(c)

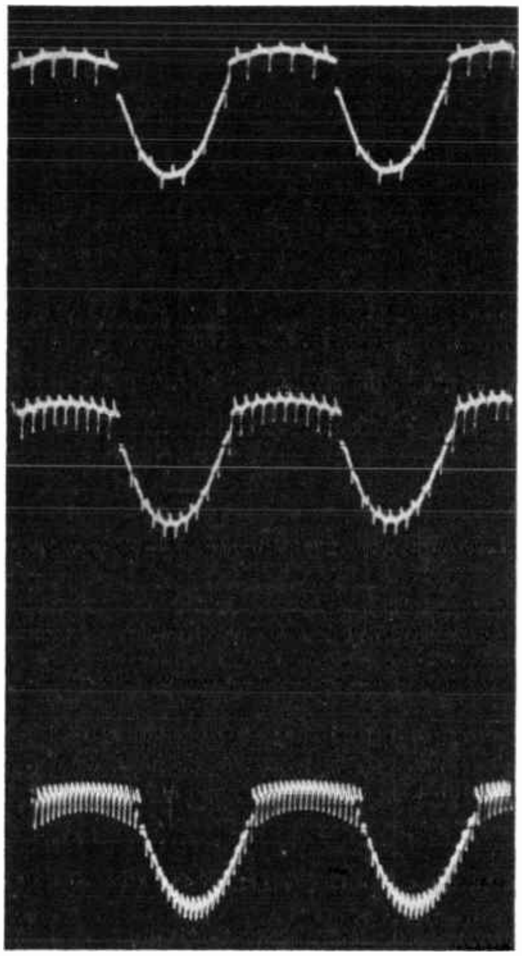

Fig. 12—Operation of the circuit as a frequency divider. (a) 10-to-1 division ratio. (b) 20-to-1 division ratio. (c) 40-to-1 division ratio.

(a)

(b)

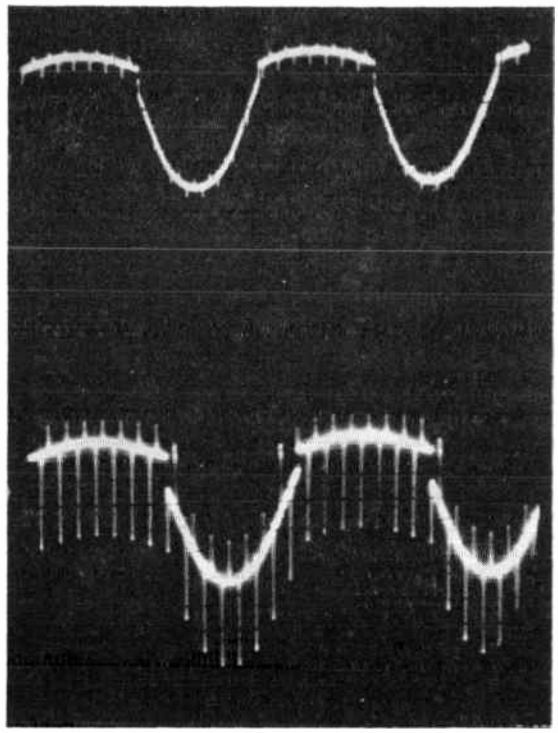

Fig. 13—Operation of the circuit as a 15-to-1 frequency divider over a five-to-one range of synchronizing signal amplitude.

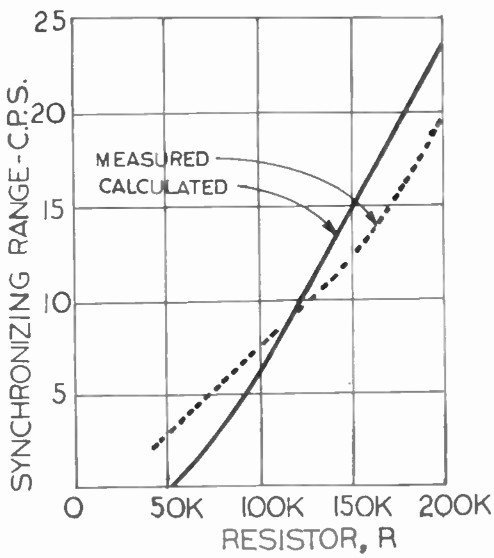

Fig. 14—Frequency range over which synchronization can be maintained.

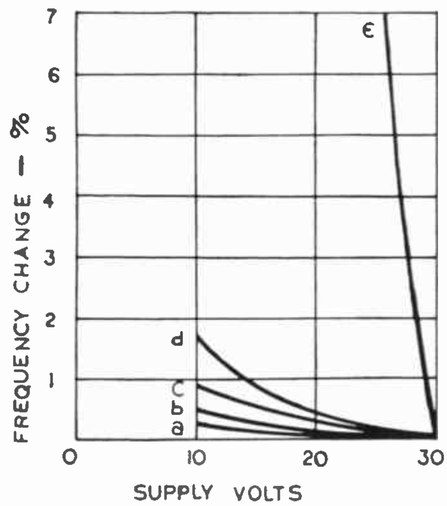

Fig. 15—Per cent change in unsynchronized oscillator frequency caused by varying the supply voltage. (a) $R=0$. (b) $R=50$ k. (c) $R=100$ k. (d) $R=200$ k. (e) $R=200$ k (operating as a relaxation oscillator).

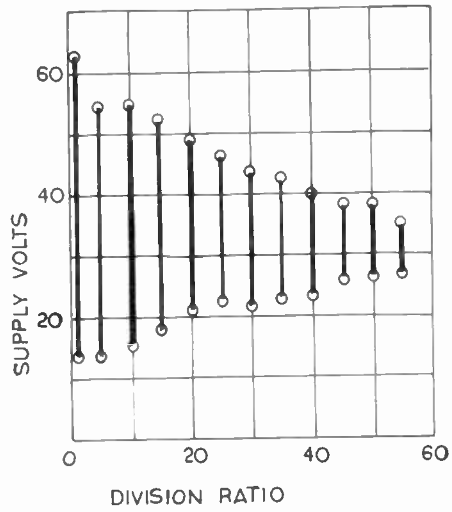

Fig. 16—Range of supply voltage over which synchronization could be maintained for various frequency division ratios.

trated in Fig. 12. Experimental confirmation of the remarks made in connection with (16) is given in Fig. 13. Here the oscillator maintained a division ratio of 15 in spite of a five-to-one variation of synchronizing pulse amplitude. Fig. 13(b) is of interest as it shows that two of the pulses are sufficiently positive to draw grid current during the portion of the cycle when the tube is cut off.

In Fig. 14 the range of frequency over which the oscillator could be synchronized is plotted as a function of R and compared with the results of graphical calculations. It is noted that the measured frequency range did not reduce to zero as R was lowered to 50 k. This is because the synchronizing pulses from the 47 $\mu\mu$f capacitor have a finite width. The circuit parameters used in making the calculations were $L=10$ hy, $C=0.01$ μf, $r=360$ k, $r_c=1.2$ k, and $K=8$. The value of gain K was determined from static measurements of the unloaded push-pull amplifier.

Fig. 15 gives an indication of the frequency stability of the oscillator for various values of resistor R. As expected, the oscillator became more sensitive to supply voltage variation as R was increased, and became extremely sensitive when it operated as a relaxation oscillator. In Fig. 16 the supply voltage range over which synchronization could be maintained is given for several values of division ratio. It appears that the stabilized frequency divider can provide division ratios as high as 30 or 40 without requiring close control of the supply voltage.

Acknowledgment

The author is indebted to Anthony F. Pensabene, Philco Corporation, whose experimental work led to the oscillator circuit described.

Correction

A. Schleimann-Jensen, author of two correspondence items entitled "Experiment Indicating Generation of Submillimeter Waves by an Avalanching Semiconductor" and "Further Notes on Indicated Generation of Submillimeter Waves by an Avalanching Semiconductor," which appeared on pages 1376 and 1378, respectively, of the August, 1959, issue of Proceedings, has requested that the following corrections be made to these letters.

In the first letter, in the section entitled "Small Gap Discharges," located in the second column of page 1376, the word "cathode" on line 19 of the first paragraph should be changed to "anode."

In the second letter, in the section entitled "Generation of Low-Frequency Oscillations," located in the second column of page 1379, the first sentence of the second paragraph should have the words "in the first communication" added to it as a concluding phrase.

IRE Standards on Television: Measurement of Differential Gain and Differential Phase, 1960*

60 IRE 23. S1

COMMITTEE PERSONNEL

Subcommittee on Video Signal Transmission Methods of Measurement

J. M. BARSTOW, *Chairman* 1955–1959
J. L. JONES, *Chairman* 1954–1955

J. M. Barstow 1954–1955
K. B. Benson 1954–1957
R. I. Brown 1955–1957
R. D. Chipp 1954–1958
M. H. Diehl 1955–1958
S. Doba, Jr. 1954–1955
A. B. Ettlinger 1957–1959
M. E. Gloystein 1954–1957
F. J. Herr 1958–1959
H. P. Kelly 1955–1957
H. Mate 1956–1959
L. R. Moffett 1954–1955
R. M. Morris 1954–1959
K. E. Mullenger 1954–1955
R. S. O'Brien 1954–1957
J. R. Popkin-Clurman 1956–1959
E. B. Pores 1955–1959
E. H. Schreiber 1954–1959
L. Staschover 1955–1959
D. Taylor 1958–1959
B. F. Tyson 1954–1955
J. W. Wentworth 1956–1959
W. B. Whalley 1957–1959
J. F. Wiggins 1958–1959

Committee on Video Techniques

G. L. FREDENDALL, *Chairman* 1959–
S. DOBA, JR., *Chairman* 1957–1959
J. M. BARSTOW, *Vice-Chairman* 1959–
G. L. FREDENDALL, *Vice-Chairman* 1957–1959

I. C. Abrahams 1957–1959
S. W. Athey 1957–1959
A. J. Baracket 1957–1958
J. M. Barstow 1957–1959
J. H. Battison 1957–1958
E. E. Benham 1957–1958
K. B. Benson 1957–1959
E. M. Coan 1957–1958
L. B. Davis 1957–1958
S. Deutsch 1958–1959
S. Doba, Jr. 1959–
V. J. Duke 1957–1959
J. R. Hefele 1957–1959
J. L. Jones 1957–1959
R. T. Petruzzelli 1957–1958
W. J. Poch 1957–1959

Ad Hoc Subcommittee for the Review of the Proposed Standard on the Measurement of Differential Gain and Differential Phase, 1959

W. T. WINTRINGHAM, *Chairman*

W. F. Bailey
J. M. Barstow
C. H. Page
S. Doba, Jr.
J. G. Kreer, Jr.

Standards Committee 1959–1960

R. F. SHEA, *Chairman*
J. G. KREER, JR., *Vice-Chairman*
C. H. PAGE, *Vice-Chairman*
L. G. CUMMING, *Vice-Chairman*

J. Avins
W. F. Bailey
M. W. Baldwin, Jr.
J. T. Bangert
W. R. Bennett
J. G. Brainerd
D. R. Brown
P. S. Carter
A. G. Clavier
S. Doba, Jr.
P. Elias
G. A. Espersen
R. J. Farber
D. G. Fink
G. L. Fredendall
E. A. Gerber
A. B. Glenn
V. M. Graham
R. A. Hackbusch
R. T. Haviland
A. G. Jensen
R. W. Johnston
I. Kerney
A. E. Kerwien
G. S. Ley
Wayne Mason
D. E. Maxwell
P. Mertz
H. I. Metz
H. R. Mimno
E. Mittelmann
L. H. Montgomery, Jr.
G. A. Morton
R. C. Moyer
J. H. Mulligan, Jr.
A. A. Oliner
M. L. Phillips
R. L. Pritchard
P. A. Redhead
R. Serrell
W. A. Shipman
H. R. Terhune
E. Weber
R. B. Wilcox
W. T. Wintringham

Measurements Coordinator

J. G. Kreer, Jr.

* Approved by the IRE Standards Committee, June 11, 1959. Reprints of this Standard, 60 IRE 23. S1, may be purchased while available from the Institute of Radio Engineers, 1 East 79 Street, New York, N. Y., at $0.60 per copy. A 20 per cent discount will be allowed for 100 or more copies mailed to one address.

1. INTRODUCTION

1.1 Definitions

THIS Standard describes a method for measuring differential gain and differential phase in equipment transmitting either monochrome or color television signals. The characteristics to be measured are defined as follows.

Differential Gain.[1] In a video transmission system, the difference between (a) the ratio of the output amplitudes of a small, high-frequency sinewave signal at two stated levels of a low-frequency signal on which it is superimposed, and (b) unity.

Note 1: Differential gain may be expressed in per cent by multiplying the above difference by 100.

Note 2: Differential gain may be expressed in db by multiplying the common logarithm of the ratio described in (a) above by 20.

Note 3: In this definition, level means a specified position on an amplitude scale applied to a signal waveform.

Note 4: The low- and high-frequency signals must be specified. For purposes of this standard these signals will be as they are afterwards described in this paper.

Differential Phase.[2] In a video transmission system, the difference in output phase of a small, high-frequency sinewave signal at two stated levels of a low-frequency signal on which it is superimposed.

Note 1: Notes 3 and 4 applied to Differential Gain above, apply also to Differential Phase.

1.2 Scope of Application

The primary application of this Standard is intended to be in the field of routine operational and maintenance tests, where rapid interpretation and communication of test results is necessary or desirable. The basic techniques described here are also applicable to laboratory measurements, proof-of-performance tests, and detailed maintenance procedures.

2. ANALYSIS OF THE MEASUREMENT PROBLEM

2.1 Characteristics of Television Signals

Certain significant characteristics of both monochrome and color television signals are illustrated by Fig. 1. Color television signals differ from monochrome signals, shown in Fig. 1(a), primarily by the addition of two other signal components, which are shown separately in Fig. 1(b). These are:

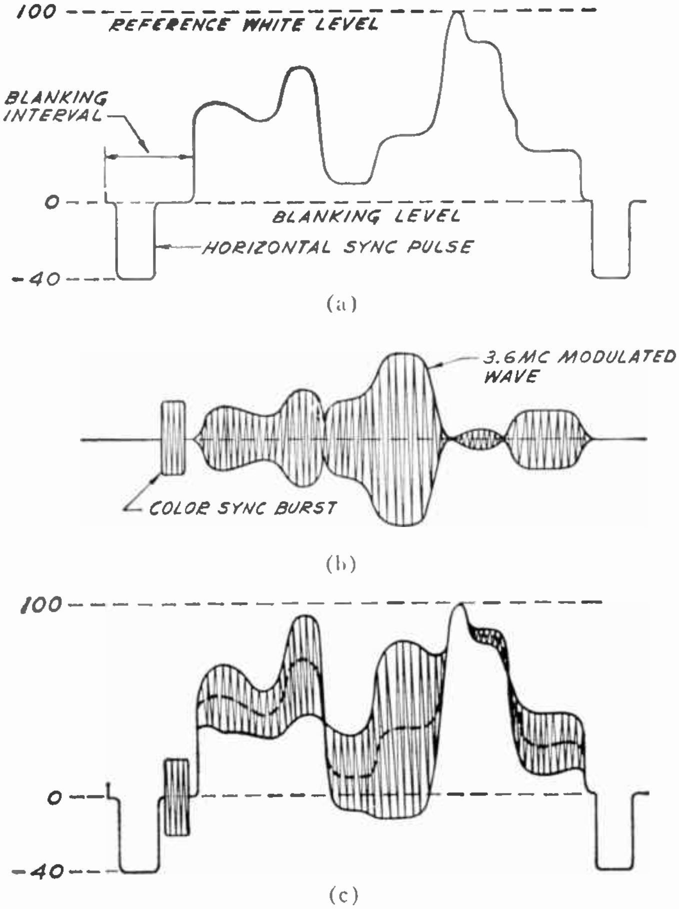

Fig. 1—Waveforms of typical television signals. (a) Luminance or monochrome signal. (b) Chrominance and color sync signals. (c) Composite-color signal.

2.1.1—A burst of about 9 cycles at a subcarrier frequency of approximately 3.6 mc transmitted during the blanking interval following each horizontal sync pulse except during the equalizing pulse and vertical sync pulse intervals. This serves as a phase reference for subcarrier regenerators in color monitors, receivers and test equipment.

2.1.2—A chrominance signal, consisting of the sidebands of the phase-and-amplitude-modulated subcarrier, transmitted during active scanning time. To a first degree of approximation, the phase of the chrominance signal controls dominant wavelength in the reproduced picture, while the amplitude controls purity.

The composite color signal, consisting of the sum of the various components, appears as shown in Fig. 1(c). Note that the effective axis of the chrominance signal may vary through the luminance range since this axis coincides with the level of the monochrome signal component.

2.2 Effects of Differential Gain and Differential Phase

A necessary condition for distortion-free transmission of a color signal is that neither the amplitude nor the phase of the chrominance signal be altered as a function of the level of the associated luminance signal, and that the luminance signal be unaffected by its own level.

[1] This is a revision of the definition of differential gain in "IRE Standards on Television: Definitions of Television Signal Measurement Terms, 1955 (55 IRE 23. S1)," Proc. IRE, vol. 43, pp. 619–622; May, 1955.

[2] This is a revision of the definition of differential phase in "IRE Standards on Television: Definitions of Television Signal Measurement Terms, 1955 (55 IRE 23. S1)," Proc. IRE, vol. 43, pp. 619–622; May, 1955.

Differential gain other than zero in a video transmission system may cause undesirable variations in the purity of reproduced colors as a function of luminance level. Similarly, differential phase other than zero in a video transmission system may cause undesirable variations in dominant wavelength as a function of luminance level.

2.2.1 Differential gain other than zero in a monochrome transmission system produces compression or expansion. The effects of differential phase in a monochrome system are minor and may usually be disregarded.

2.3 Significant Variations in Operating Conditions

The average picture level (APL)[3] of a television signal depends upon the average luminance of the televised scene. For faithful reproduction, the system as a whole must transmit low video signal frequencies extending to zero or dc. It is not necessary to transmit the so-called dc component through all parts of the system, however, since this component can be restored at any desired point by dc restorers or clampers. There are, therefore, two significantly different sets of operating conditions in television systems, depending on whether the dc component is present or absent. These conditions are illustrated in Fig. 2.

2.3.1 When the dc component is present, as shown in Fig. 2(a), the amplitude range required for the monochrome component of a television signal is fixed at 140 IRE scale units.[4]

2.3.2 When the dc component is absent, as shown in Fig. 2(b), the signal for a given luminance varies with the apl. For practical purposes, it is sufficient to consider signal conditions corresponding to variations in the average picture level from 10 per cent to 90 per cent. Under these conditions, the total amplitude range required for the monochrome component of a television signal in ac-coupled equipment is equivalent to 105+96 =201 IRE scale units.

3. REQUIREMENTS FOR STANDARD MEASUREMENTS

3.1 Apparatus Required

The apparatus required to measure differential gain and phase in accordance with the method described in this Standard is shown in block diagram form in Fig. 3. It consists of a test signal generator, an output signal analyzer, and means for displaying or indicating the test results.

[3] APL, or average picture level, is defined as the average signal level, with respect to blanking level, during active picture scanning time (integrated over a frame period, excluding blanking intervals), expressed as a percentage of the difference between the blanking and reference white levels. (*Cf.* Fig. 2).

[4] For a description of the IRE scale for measuring television signal levels see "IRE Standards on Television: Measurements of Luminance Signal Levels, 1958 (58 IRE 23. S1)," Proc. IRE, vol. 46, pp. 482–486; February, 1958.

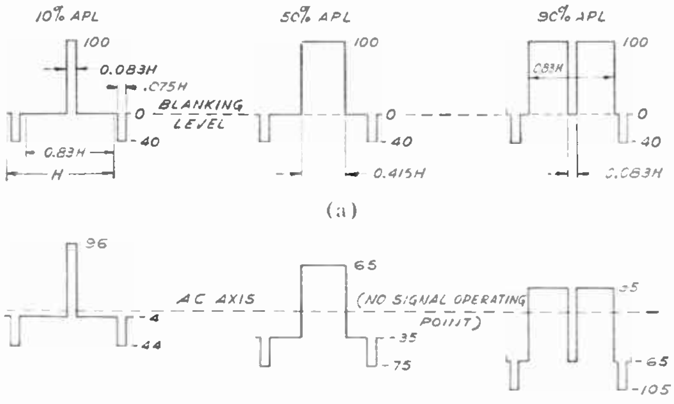

Fig. 2—Variation of signal excursions with APL. (a) DC component present. (b) DC component absent (includes effects of standard sync and blanking signals.)

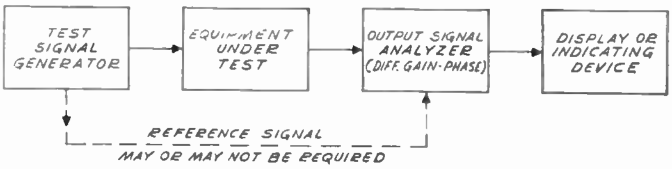

Fig. 3—Apparatus for the measurement of differential gain and differential phase.

3.2 Requirements for the Test Signal

3.2.1 Amplitude Range. The low-frequency component of the test signal should be capable of exploring the amplitude range corresponding to the blanking-to-reference-white range of a normal composite picture signal for each of the following average picture level conditions: 10 per cent, 50 per cent, and 90 per cent.

3.2.2 Continuity. If the low-frequency signal explores the amplitude range in discrete steps, the separation between steps should not exceed 12.5 IRE scale units, where 100 IRE scale units equals the blanking-to-reference-white range.

3.2.3 Frequencies. A high-frequency sinewave of 20 IRE scale units peak-to-peak amplitude and of a frequency approximately equal to the color subcarrier frequency (3.579545 mc) should be added to the low-frequency signal (on the order of 15 kc). (See Section 5.1.)

3.2.4 Additional General Requirements. The test signal should contain such elements of a composite signal (sync pulses, color sync bursts, etc.) as may be required for proper operation of clampers or other control devices included in the specific equipment or circuit under test. The test signal should not alter the normal operating characteristics of the specific equipment or circuit under test.

3.3 Requirements for the Test Signal Analyzer

The test signal analyzer should provide means for measuring the amplitude and phase of the fundamental component of the high-frequency signal as functions of the level of the low-frequency signal.

3.4 Presentation of Test Results

3.4.1. Voltage. The voltage corresponding to 100 IRE scale units (blanking-to-reference-white) should be stated.

3.4.2 Average Picture Level Conditions. Results should be presented for 10 per cent, 50 per cent, and 90 per cent APL conditions separately or for that single condition yielding the largest value of differential gain (or phase). (See Section 5.3.)

3.4.3 Differential Gain Data. Differential-gain data may be expressed as:

a) A function of one of the stated low-frequency levels with the other stated level arbitrarily fixed, or
b) The extreme values of differential gain with respect to that portion of the differential gain function judged to be most nearly constant (plus implies expansion, minus implies compression), or
c) The maximum range of the differential gain (difference of extreme values).

3.4.4 Differential Phase Data. Differential phase data may be expressed as:

a) A function of one of the stated low-frequency levels with the other stated level at blanking level, or
b) The extreme values of differential phase with respect to the value at blanking level (plus implies leading phase; minus implies lagging phase), or
c) The maximum range of the differential phase (difference of extreme values).

3.4.5 Supplementary Information. The general portion of the amplitude range associated with a numerical specification should be designated black, center and white.

3.4.6 Typical Examples of Test Results. The same data for a television transmission circuit may be presented as follows:

(Differential Gain and Phase.) (Low-frequency signal 1.0 volt, blanking to reference white)

A. See Figs. 7–10, for presentations as for a) in both sections 3.4.3 and 3.4.4. Also, refer to Sections 4.3 and 4.4 below.

B. Using methods found in b) of sections 3.4.3 and 3.4.4:

APL	Differential Gain		Amplitude Region	Differential Phase in Degrees
	Per Cent	db		
10 per cent	+2	+0.2	black	0
	0	0.0	center	+0.5
	−7	−0.6	white	−3
50 per cent	+2	+0.2	black	0
	0	0.0	center	+1
	−2	−0.2	white	−2
90 per cent	+5	+0.4	black	0
	0	0.0	center	+1
	−2	−0.2	white	−1

C. Using methods found in c) of sections 3.4.3 and 3.4.4:

Differential Gain Per Cent	*Differential Gain db*	*Differential Phase in Degrees*
+9	0.8	3.5

4. METHODS OF MEASUREMENT[5]

4.1 Low-Frequency Component of the Test Signal

4.1.1 Basic Waveforms. The low-frequency component of the test signal may have any waveform consistent with the requirements of Section 3.2, but simple waveforms such as the sinewave, staircase, and sawtooth, in which the fundamental is on the order of 15 kc, are usually most convenient in practice. Since it is desirable to use a test signal containing horizontal sync pulses, it is convenient, though not essential, to use a low-frequency waveform that is fully contained within a line period. Examples of suitable staircase, sawtooth, and sinewave signals are shown in Figs. 4 and 5.

4.1.2 Provision for Varying the Average Picture Level. Any simple waveform with an inherent duty cycle of 50 per cent during actual presentation time may be used directly as the low-frequency component of the test signal for differential gain measurements under 50 per cent apl conditions. Its peak-to-peak amplitude, exclusive of sync pulses, should be set at 100 IRE scale units. The required variation in the average picture level of the complete signal can be obtained by presenting this 50 per cent APL test information for only one-fifth of the total active scanning time in each field period. The remaining four-fifths of the active scanning time should be used for the transmission of a constant low-frequency level, which should be set at blanking to provide 10 per cent APL conditions, and at reference-white to provide 90 per cent APL conditions. Practical examples of such time-shared signals are shown in Fig. 4.

4.1.3 Special Factors Pertaining to Circuits in Which All Stages are DC Coupled. When *all* stages including the output of the test signal generator are effectively DC coupled, there is no need to vary the APL of the test signal, because the amplitude range occupied by the signal is the same for all APL conditions in each stage.

4.1.4 Special Factors Pertaining to Circuits in Which All Stages are AC Coupled. When *all* stages are ac coupled, and are able to pass a signal of somewhat greater than normal amplitude without overload effects, standard measurements can be made with a test signal whose low-frequency component has a duty cycle of 50 per cent, provided the amplitude of the low-frequency signal is increased to cover the full range occupied by normal picture signals under 10 per cent to 90 per cent APL conditions. Assuming the presence of sync pulses with peak amplitudes of 40 IRE scale units, the low-frequency signal should have a peak-to-peak amplitude of 178 IRE

[5] The methods discussed in Section 4 are for illustration only. They are not intended to preclude other methods now in use, or which may be devised in the future, provided that such methods meet the requirements of Section 3.

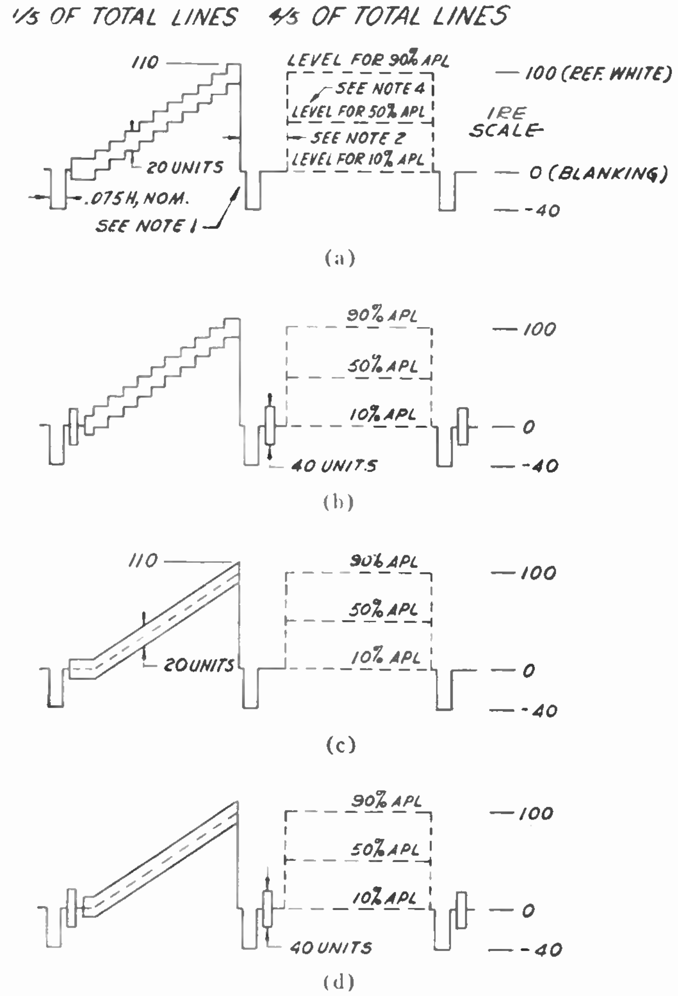

NOTES:

1) Front Porch is optional.
2) Horizontal blanking 17 per cent if 7 per cent vertical blanking is used: 25 per cent if vertical blanking is not used.
3) High frequency component may be transmitted on any portion of the signal provided circuit under test is not adversely affected.
4) 50 per cent APL conditions can also be provided by presenting the test waveform on every line.

Fig. 4—Examples of test signals.

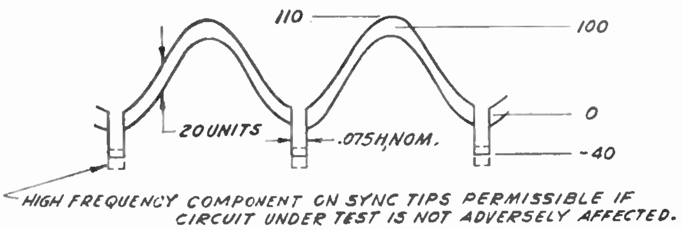

Fig. 5—Examples of a test signal employing a sinusoidal waveform.

scale units when a sawtooth type of signal is used, and horizontal plus vertical blanking is taken into account. When the sinewave type of low-frequency signal is used without additional blanking, the corresponding amplitude is 184 IRE scale units as illustrated in Fig. 6. When these expanded signals are used, the data should be processed so that the results reported for each APL

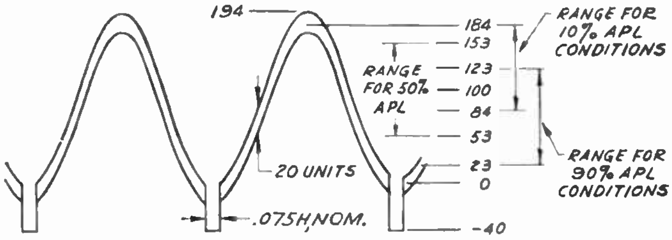

Fig. 6—Example of a test signal of expanded amplitude satisfactory for measurements in circuits in which all stages are AC coupled.

condition correspond to the following ranges relative to the blanking level of the signal.

APL	Significant Ranges	
	Sawtooth waves with sync pulse and blanking	Sine wave and sync pulse, no blanking included
10 per cent	61–161	84–184
50 per cent	30–130	53–153
90 per cent	0–100	23–123

4.2 High-Frequency Component of the Test Signal

4.2.1 Frequency. As stated in Section 3.2.3, the frequency of the high-frequency component of the test signal should be approximately equal to the color subcarrier frequency (3.579545 mc). Unless the equipment under test employs special circuits which require precise control of the subcarrier frequency, deviations of the order of ± 1 per cent from the subcarrier frequency should not appreciably affect the results of tests made in accordance with this standard.

4.2.2 Amplitude During Actual Test Interval. To satisfy the requirements of this standard, the high-frequency component of the test signal should have a peak-to-peak amplitude of 20 IRE scale units during the actual test interval. If a low-frequency signal of greater than normal amplitude is employed for the special case described in Section 4.1.4, it is important that the high-frequency component not be expanded in proportion to the low-frequency signal but remain at the normal of 20 IRE scale units peak-to-peak amplitude, as illustrated in Fig. 6.

4.2.3 Amplitude During Other Intervals. The high-frequency component may be transmitted at any reasonable amplitude (including zero) during other intervals of the test signal, provided the equipment under test is not adversely affected. In the event that the equipment under test requires standard color sync bursts for proper operation, these must be added to the test signal. Fig. 4 illustrates several possible test signals with and without separate color sync bursts.

4.3 Measurement of Differential Gain

4.3.1 A Method Suitable for Test Signals with Staircase or Sawtooth Waveforms. Fig. 7(a) is a simplified block diagram illustrating the measurement of differential gain by means of test signals similar to those in Fig. 4. In this method, the output signal from the equipment

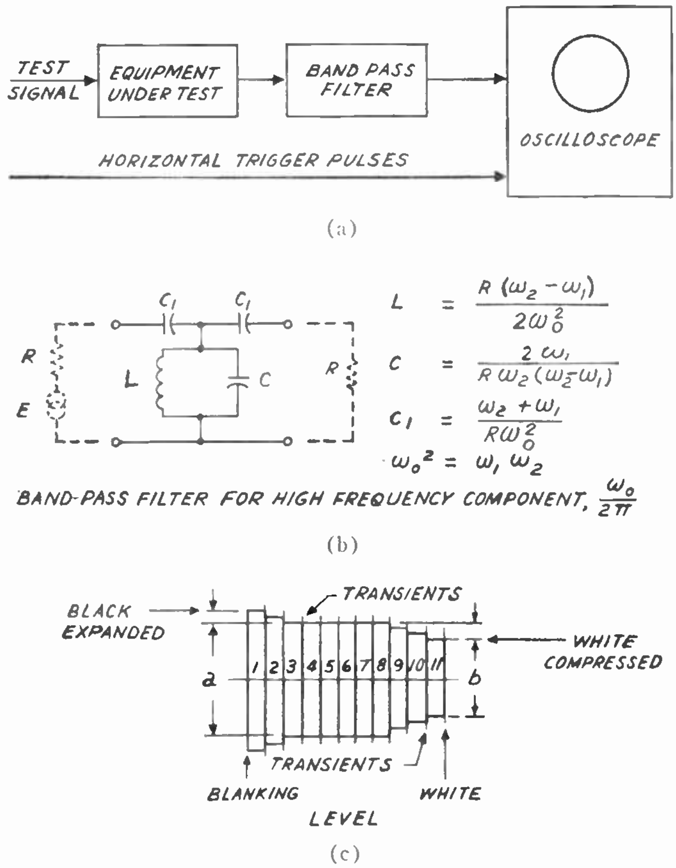

Differential gain in per cent at level $11 = 100(b/a - 1)$
Differential gain in db at level $11 = 20 \log b/a$

Fig. 7—Diagrams illustrating the measurement of differential gain when using the test signal of Fig. 4(a).

under test is passed through a band-pass filter (order of 1 mc bandwidth centered at the high frequency), which rejects the low-frequency components. A filter suitable for this purpose is shown in Fig. 7(b), in which R is the nominal impedance of the circuits between which the filter is intended to operate, $\omega_0/2\pi$ is the center of the pass band, and $\omega_1/2\pi$ and $\omega_2/2\pi$ are the frequencies at the nominal limits of the pass band. The high-frequency component is then directly displayed on an oscilloscope. Fig. 7(c) illustrates such a display for the test signals of Fig. 4(a). Differential gain appears as a variation in the envelope of the high-frequency signal. Transients occur at the riser positions of the stairsteps and should be disregarded.

4.3.2. A Method Suitable for Test Signals with Sinusoidal Waveforms. Fig. 8(a) is a simplified block diagram of equipment[6] which may be used to measure differential gain by means of a test signal like that shown in Fig. 5. In this method, the high-frequency component of the output signal received from the equipment under test is separated from the complete signal, and is applied to an envelope detector,[7] the output of which is displayed

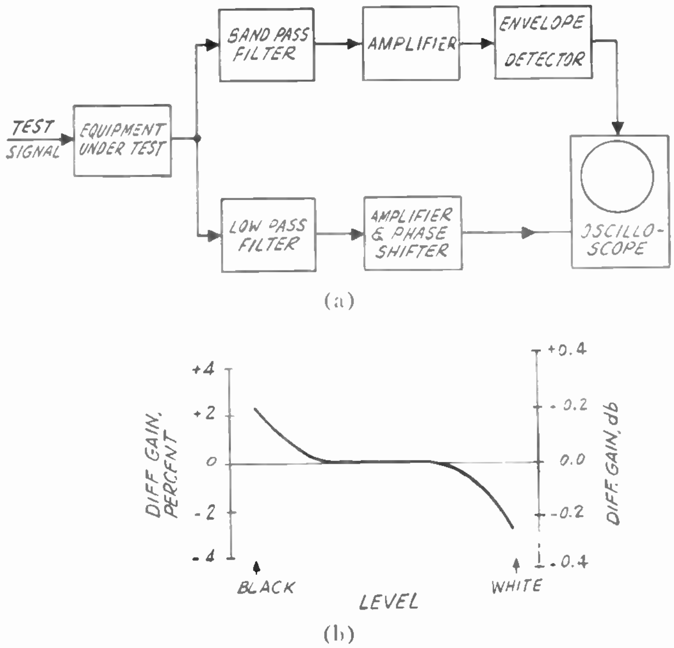

Fig. 8—Simplified block diagram and waveform illustrating the measurement of differential gain using a test signal of the type shown in Figs. 5 or 6.

on an oscilloscope. As shown in Fig. 8(b) the vertical deflection of the oscilloscope trace is proportional to the differential gain. Horizontal deflection for the oscilloscope may be provided by the use of a low-pass filter to recover the low-frequency sinewave from the test signal. A phase shifter in the horizontal deflection circuit compensates for the delay difference between the horizontal and vertical circuits.

4.4 Measurement of Differential Phase

4.4.1 A Method for Test Signals with Staircase or Sawtooth Waveforms. Fig. 9(a) is a simplified block diagram of equipment which may be used to measure differential phase with test signals similar to those in Fig. 4. The high-frequency component of the test signal, separated from the complete signal by a suitable band-pass filter [see Fig. 7(b)] (order of 1 mc bandwidth, centered at the high frequency), may be compared with a reference signal of the same frequency in a phase detector.[8] The reference signal may be regenerated from the color sync burst or derived from the high-frequency component of the test signal. A phase shifter may be used to obtain a zero indication on the part of the oscilloscope trace corresponding to blanking level.

As shown in Fig. 9(b) the vertical deflection of the oscilloscope trace is very nearly proportional to differential phase. Differential phase can also be measured by introducing a known phase shift (by means of a calibrated phase shifter) to bring any particular portion of the trace to the signal zero reference.

4.4.2 A Suitable Method for Test Signals with Sinus-

[6] H. P. Kelly, "Differential phase and gain measurements in color television systems," IRE Trans. on Broadcast and Television Receivers, vol. BTR-1, pp. 14–17; July, 1955.
[7] *Ibid.*, see Fig. 11.

[8] *Ibid.*, see Fig. 9.

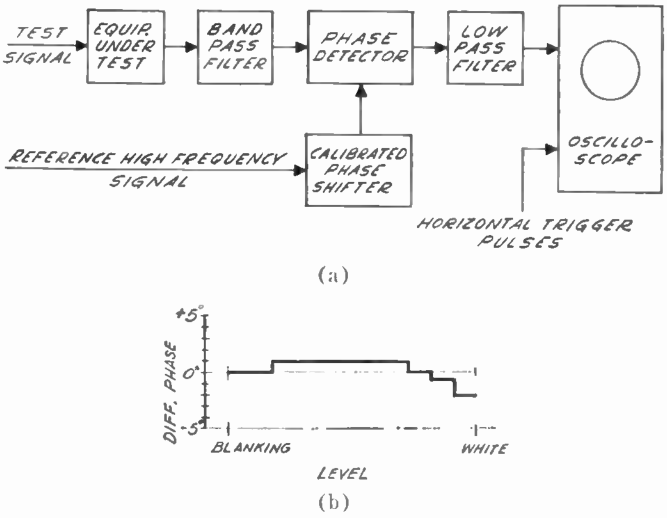

Fig. 9—Simplified block diagram and waveform illustrating the measurement of differential phase using the test signals of Fig. 4(a).

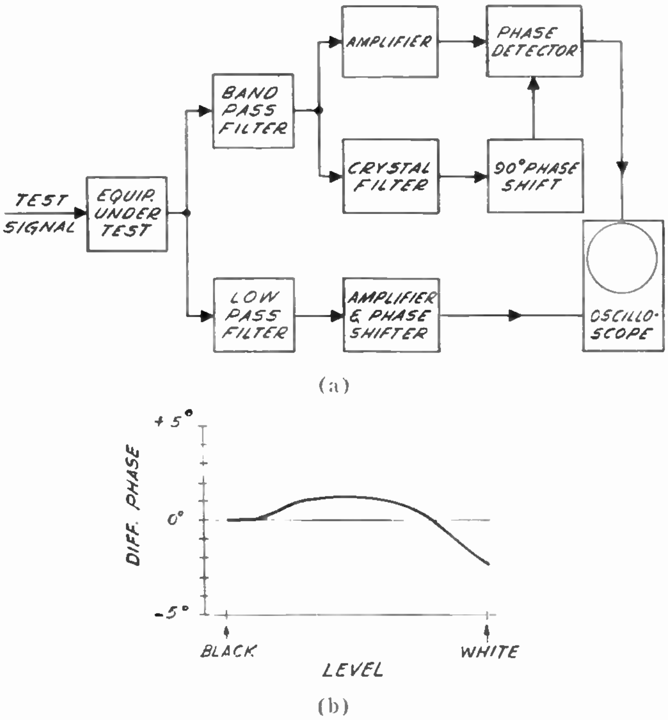

Fig. 10—Simplified block diagram and waveform illustrating the measurement of differential phase using a test signal of the type shown in Figs. 5 or 6.

oidal Waveforms. Fig. 10(a) is a simplified block diagram of equipment[6] which may be used to measure differential phase with a test signal such as that shown in Fig. 5. This apparatus is similar to that shown in Fig. 8(a) except that the high-frequency component of the output signal is compared with a reference high-frequency signal in such a way that the trace on the oscilloscope represents the differential phase characteristic. This is accomplished by using a 90° phase shifter and a phase detector.[6] Over a reasonable operating range, the output of the detector is very nearly proportional to the differential phase, and the oscilloscope can be calibrated to be direct reading as shown in Fig. 10(b).

5. LIMITATIONS AND COMMENTS

5.1 High-Frequency Signal

The primary objective of this standard is the measurement of differential gain or phase in the chrominance frequency region. It should be noted that measurements of differential gain or phase with a specified high-frequency signal such as the color subcarrier do not necessarily indicate the performance of the system at other frequencies. This is particularly true in the case of circuits which employ spectrum separation, pre-emphasis or de-emphasis techniques. However, it should be noted that when the frequency separation between the high- and low-frequency components is reduced, the difficulty of making a measurement may be increased and measurements are practically impossible when the low and high frequencies are barely separable by filters.

5.1.1 Frequency. A frequency other than 3.579545 mc may be used for special purposes. When such a frequency is used, it should be stated when presenting the results of measurements.

5.1.2 Amplitude. A high-frequency component amplitude of other than 20 IRE scale units peak-to-peak may be used for special purposes, but should be specified when presenting test results. For example, greater resolution in measuring differential gain or phase characteristics in low-noise transmission circuits may be achieved by decreasing the high-frequency component amplitude.

5.2 Relation to FCC Rules[9]

To provide data with reasonable correlation to FCC transmission requirements, it is recommended that the low-frequency exploratory signal, exclusive of sync pulses, be adjusted to 80 IRE scale units, peak-to-peak, and that the superimposed high-frequency signal have a peak-to-peak amplitude of 40 IRE scale units. This test signal then simulates conditions which are somewhat more severe than FCC requirements. Measurements should be made at 10 per cent, 50 per cent and 90 per cent APL.

5.3 Significance of 50 per cent APL Conditions

It is recognized that the amplitude ranges occupied by normal picture signals under 10 per cent and 90 per cent APL conditions overlap each other, and that tests at 50 per cent APL do not provide information beyond that contained in the results of tests made at 10 per cent and 90 per cent APL. Tests at 50 per cent APL are significant, however, because this condition comes closest to

[9] See Section 3.682, paragraph 20-VII of Part 3, in the "FCC Rules Covering Radio Broadcast Services." The FCC standards for color television broadcasts specify tolerances which apply to 1) the phase shifts and 2) the amplitudes of subcarriers for saturated primaries and their complements at 75 per cent of full amplitude, with respect to a) the sync burst phase and b) standard values. No requirements are specifically given for differential gain and phase *as such.*

simulating average transmission conditions. Where time or facilities permit tests under only one APL condition, the results are most significant if 50 per cent APL is selected.

5.4 Noncomposite Signals

The standard tests do not fully cover the case of noncomposite signals, since the maximum excursion of the subcarrier signal in the black direction (for the 90 per cent APL condition) is increased by about 4 IRE scale units when the sync pulses are absent. If there is any reason to suspect difficulty with noncomposite signals, a further test may be made either by removing the sync pulses from the test signal or by slightly increasing the amplitude of the low-frequency signal.

5.5 Sync Compression or Expansion

The standard tests do not directly provide for the measurement of sync compression or expansion, although this characteristic may be readily measured by direct observation of the test signal on an oscilloscope using the IRE scale.

5.6 Color Sync Burst Distortion

Distortion of the amplitude or phase of the color sync burst relative to the chrominance signal may be introduced by such factors as poorly adjusted clampers or burst regenerators. Therefore, such equipment should be adjusted properly before measurements of differential gain and phase are made.

Compandor Loading and Noise Improvement in Frequency Division Multiplex Radio-Relay Systems*

EITEL M. RIZZONI†, SENIOR MEMBER, IRE

Summary—**Graphical and numerical means are developed to compute the additional effective loading caused by the use of syllabic compandors on the input of a multichannel radio-relay system, and to evaluate the noise improvement yielded by the compandor in a telephone channel.**

Introduction

In modern commercial and military multichannel radio-relaying, an increasingly large number of telephone channels are carried on wide-band equipment, employing either conventional microwave propagation, or scatter propagation, at VHF, UHF, and SHF frequencies. High circuit quality and reliability are normally required. Some applications require reliable transmission of a small number of voice channels on narrow-band equipment, often over long hops, using the technique of scatter propagation.

Theoretical considerations, experimentally proved by many working compandored circuits, show that the use of syllabic compandors permits the attainment of the desired performance economically.

The system designer is thus confronted with the problems of 1) evaluating the additional effective load which compandors introduce on the common equipment, and 2) estimating the improvement in circuit quality resulting from their action. These problems are dealt with in Parts I and II, respectively.

* Original manuscript received by the IRE, March 26, 1959; revised manuscript received, August 25, 1959.

† RCA International Division, Clark, N. J.

A basic explanation of the compandor principle of operation and circuitry, as well as of multichannel loading theory, is not included in this paper. (This is available in the literature.[1,2])

Part I

Introduction

A syllabic compandor is made of two separate devices: a compressor inserted at the channel input and an expandor inserted at the channel output, as shown schematically in Fig. 1. The compressor processes the speech input for high efficiency of transmission, and the expandor restores the speech output to its original value and introduces substantial loss during silent pauses when noise output would otherwise be present.

The insertion of a compressor in a channel may modify the channel loading on the radio system. The insertion of the expandor at the channel output may modify both speech and noise levels, hence the signal-to-noise ratio, and does not affect the loading of the system.

To evaluate the effect of channel dynamic compression on the multichannel rms load and multichannel peak factor, most of the classical work published by

[1] B. D. Holbrook and J. T. Dixon, "Load rating theory for multichannel amplifiers," *Bell Sys. Tech. J.*, vol. 18, pp. 624–644; October, 1939.

[2] C. W. Carter, A. C. Dickieson, and D. Mitchell, "Application of compandors to telephone circuits," *Trans. AIEE* (*Commun. and Electronics*), vol. 65, pp. 1079–1086; 1946.

Holbrook and Dixon in 1939[1] has been repeated, starting from a compandored distribution of speech volume. Numerical data and curves are shown together with corresponding data and curves for uncompandored speech. This permits a direct appraisal of the contribution of compressors on the multiplex loading and of their effect on the multichannel peak factor.

In the following analysis, single-sideband carrier-suppressed 4-kc channels are considered. The effects of signalling tones are not included.

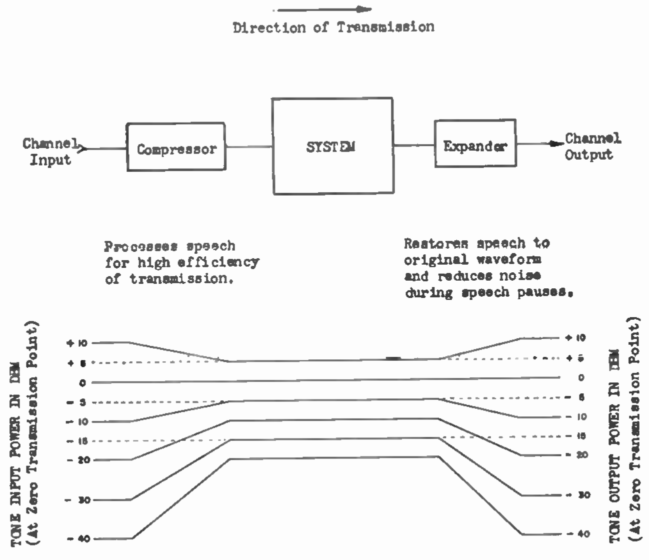

Fig. 1—A compandor is made of two devices: the compressor and the expandor.

Single-Channel Loading

In a syllabic compandor, the average power of the applied signal over a short time interval is used to control the transmission gain. The insertion of a compressor in a telephone channel has the effect of raising speech volume which is below the compandor crossover level and of lowering speech volume which is above the crossover level. The compandor crossover level is defined as that level at which the use of the compandor introduces no gain or loss on the input signal.

The speech volume at the compressor output is a function of the speech volume at the compressor input and of the setting of the compandor crossover level (other parameters such as the compandor time constants, the compression ratio, etc. are assumed to be standardized constants). Therefore, both input volume distribution and compandor crossover level must be known for determination of the volume distribution at the compressor output.

Uncompandored Channel

Holbrook and Dixon[1] found that the probability distribution of the average-talker volume follows approximately the Gaussian law. That is, the probability that the speech volume will be equal to or greater than a value V, is given by:

$$P(V) = \frac{1}{\sigma\sqrt{2\pi}} \int_{-\infty}^{V} \exp - \frac{(V - V_0)^2}{2\sigma^2} (dV), \qquad (1)$$

where

V_0 = mean value of the distribution in volume units (VU)

σ = standard deviation of the distribution in decibels.

The average-talker cumulative distribution of (1) is plotted in Fig. 2, curve A. In Appendix I an explanation is given of the units used in Fig. 2. For distribution A of Fig. 2, the parameters are:

$$V_0 = -10 \text{ VU}$$

$$\sigma = 5.8 \text{ db.}$$

The volume, V_{0p}, corresponding to the average speech power of the log-normal distribution is given by:[3]

$$V_{0p} = V_0 + (0.115)\sigma^2(\text{VU}). \qquad (2)$$

For distribution A of Fig. 2:

$$V_{0p} = -10 + (0.115)5.8^2 \cong -6.1 \text{ (VU)}. \qquad (3)$$

In Appendix I it is shown that the relationship between volume, V, and average speech power, P, is

$$V(\text{VU}) \cong P(\text{dbm}) + 3.8 \text{ (db)}. \qquad (4)$$

Therefore, a volume of -6.1 VU corresponds approximately to an average speech power of -9.9 dbm0 (denotes dbm referred to a point of zero transmission level), which is thus found to be the average loading on the baseband by an uncompandored active channel carrying continuous speech of an average talker.

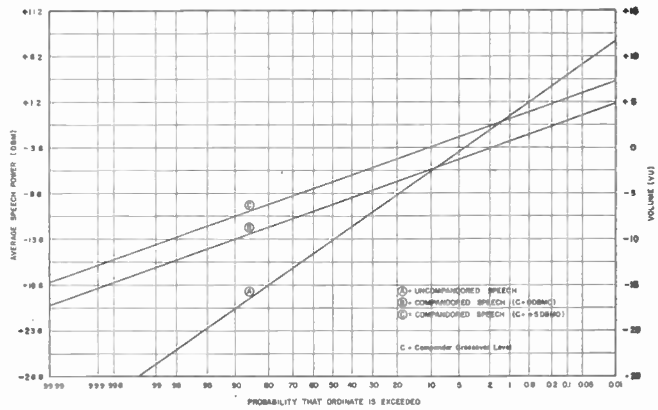

Fig. 2—Average-talker volume distribution and corresponding average speech power. (All levels referred to zero transmission point.)

Compandored Channel

Let us consider a compandored channel. Fig. 3 shows typical compandor characteristics and their crossover levels. The figure also shows that the output powers from the compressor (expander) for sinewave input and

[3] W. R. Bennett, "Cross modulation requirements on multichannel amplifiers below overload," *Bell Sys. Tech. J.*, vol. 19, pp. 587–610; October, 1940.

speech or noise input of same rms power differ by three decibels. The explanation of this behavior is given in Appendix II.

At the output of the compressor, the talker volume distribution will be altered according to the compressor characteristic. Thus, channel input volume lower than the crossover level will be raised, and input volume higher than the crossover level will be lowered. The result is a compression of the speech dynamics to one-half, and the halving of the standard deviation of the volume distribution.

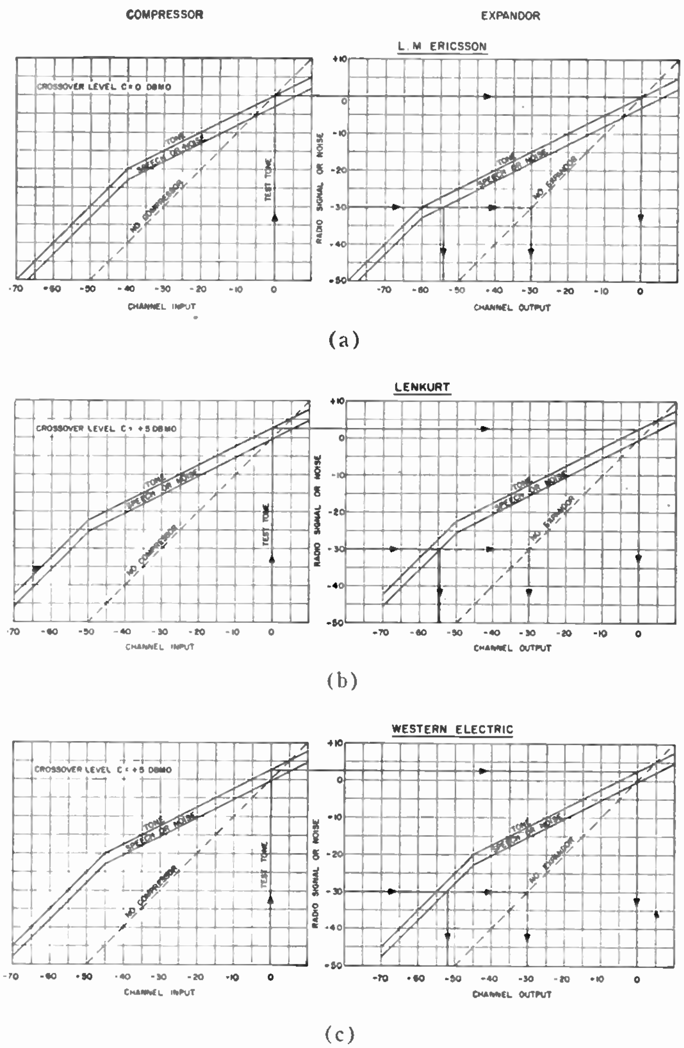

Fig. 3—Typical characteristics of compandors. (All powers are in dbm at a point of zero transmission level.)

The average-talker distribution A of Fig. 2, compressed through a compandor with zero dbm0 crossover level, results in distribution B of Fig. 2. Distribution A, through a compandor with $+5$ dbm0 crossover level, results in distribution C of Fig. 2. The significance of dynamic compression is that the resulting decreased fluctuation of speech volume permits a more constant, hence efficient, loading of the baseband. In fact, weak signals are substantially amplified and unnecessarily strong signals are attenuated.

The compressed distributions are again log-normal and their mean value and standard deviation can be read on Fig. 2, or directly calculated by recalling that in the practical range of speech the compression ratio is two to one. The volume corresponding to the average speech power of the compressed distributions is calculated with (2); and the average speech power with (4). The results are summarized in Table I, where L (db) is the increase in loading on the baseband, because of the compressor action in one active channel. In Appendix III it is shown that the variation in average load, L, is a linear function of the compandor crossover level, C. From Table I:

$$L = 0.5C + 1.1. \tag{5}$$

Eq. (5) shows that when the crossover level is adjusted to -2.2 dbm0, the compressor will introduce no change in average load on the baseband. Physically, it means that the average speech power at the compressor input is equal to the average speech power at the compressor output. Mathematically, this can be easily checked by applying (2) before and after compression.

Multichannel Loading

A. Case of All Volumes Controlled to Single-Channel Average Speech Power. In a practical multichannel system, each active channel will carry speech at varying volume within the values of the volume distributions shown in Fig. 2. However, if the number of channels is sufficiently large, the multichannel rms power resulting from the combination of all individual active channels will be approximately equal to the single-channel average speech power multiplied by the number of active channels.

The fraction of time for which overloading may be tolerated is generally taken as one per cent. Therefore, it is necessary to find the multichannel speech power

TABLE I

Channel	Distribution of Fig. 2	V_0 (VU)	σ (db)	V_{0p} (VU)	Average Speech (dbm) Power	Average Load Increase L (db)
Uncompandored Speech	A	−10	5.8	−6.1	−9.9	Reference
Compandored with crossover level $C=0$ dbm0	B	− 6	2.9	−5	−8.8	+1.1
Compandored with crossover level $C=+5$ dbm0	C	−3.5	2.9	−2.5	−6.3	+3.6

exceeded for one per cent of the time in a system of N compandored channels, when the volume in each compandored channel is held to the same constant value. The number, n, of active channels exceeded for one per cent of the time in a system of N channels is shown in Fig. 4 (from Holbrook and Dixon[1]). The average power for n active channels will be n times that of one channel, which is given by Table I, or:

n—channel average power $=(-8.8+10\log_{10}n)$ dbm, for compandors with $C=0$ dbm0 (6)

n—channel average power $=(-6.3+10\log_{10}n)$ dbm, for compandors with $C=+5$ dbm0. (7)

The multichannel speech power and the equivalent volume [defined by (4) when P is now the total power because of the contributions of all active channels] exceeded for one per cent of time computed from (6) or (7) and from Fig. 4 are plotted in Fig. 5 vs the number, N, of compandored channels. The case of uncompandored channels is also shown for direct comparison.

It is seen that for the particular case of all volumes controlled to average speech power, the multichannel load increase caused by the insertion of compressors in all N channels is equal to the single-channel load increase, L.

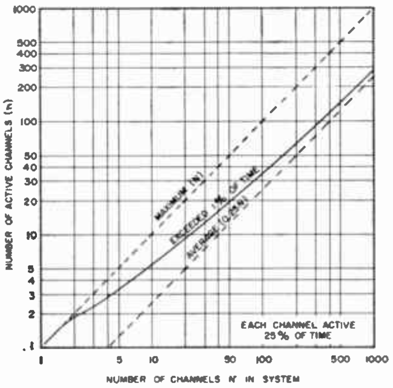

Fig. 4—Number of active channels vs number of channels in system.

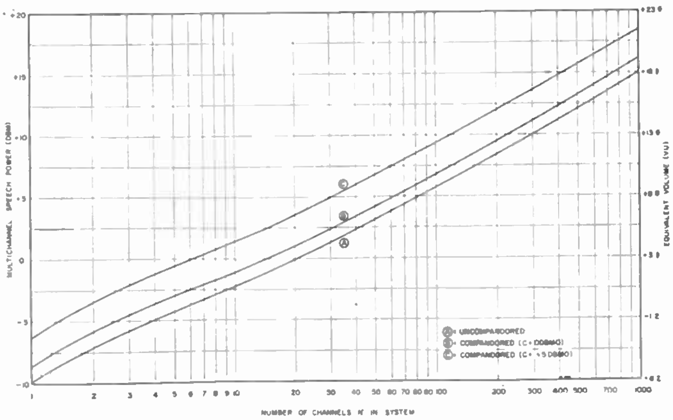

Fig. 5—Multichannel speech power and equivalent volume exceeded one per cent of time. (Volumes controlled to single-channel average speech power. All levels referred to zero transmission point.)

When only a partial number of channels, Nc, are compandored in an N-channel system, the increase in multichannel load will be smaller than L. Let Lm be the increase in multichannel load in decibels for systems partially compandored. If busy channels are assumed at random, it can be shown that:

$$Lm = 10\log_{10}\left\{\left(\text{antilog}_{10}\frac{L}{10}-1\right)\frac{Nc}{N}+1\right\}. \quad (8)$$

By virtue of (5), (8) becomes:

$$Lm = 10\log_{10} \cdot\left\{\left(\text{antilog}_{10}\left[\frac{(0.5C)+1.1}{10}\right]-1\right)\frac{Nc}{N}+1\right\}. \quad (9)$$

Fig. 6 shows relationship (9) in nomogram form for direct application.

B. Case of Uncontrolled Volumes. When the number of active channels is not sufficiently large, the simple method of summation used in the preceding section to compute the multichannel power exceeded for one per cent of the time is not valid. In the more general case, each channel will carry speech at any volume according to the probability shown in Fig. 2, and the multichannel power will be the sum of the power contributions from all active channels.

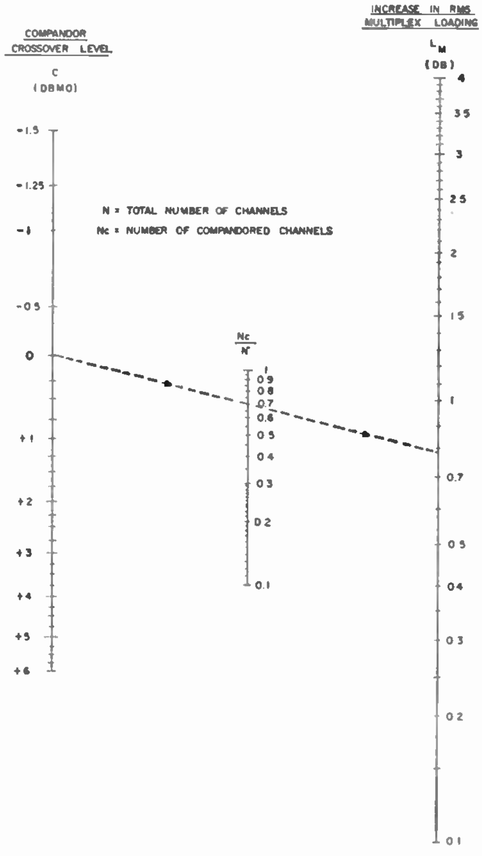

Fig. 6—Loading effect of compandors on radio baseband. (Case of controlled volumes.)

The multichannel speech power exceeded for one per cent of the time in a system of N compandored channels, when the volume in each of n active channels varies at random with distribution as in Fig. 2, corresponds to the one per cent probability of the following cumulative distribution:[1]

$$P_N(V) = \sum_{n=1}^{N} p(n) \cdot p_n(V). \tag{10}$$

The term $p(n)$ is the probability that n channels be simultaneously active in an N-channel system, and is given by:

$$p(n) = \frac{N!}{n!(N-n)!} \tau^n (1-\tau)^{N-n},$$

with $\tau = 0.25$ being the activity factor of a busy channel. Tables of binominal probability[4,5] give $p(n)$ directly.

The term $p_n(V)$ represents the probability that, with n active channels, the volume V is exceeded. The function $p_n(V)$ is the cumulative distribution of the sum of n independent probability variables whose logarithms (volumes) have the same Gaussian distribution as in Fig. 2.

To the knowledge of the writer, the problem of expressing the function $p_n(V)$ analytically has not yet been solved for the general case of $n > 2$. An approximate numerical method of calculating $p_n(V)$ was used by Holbrook and Dixon.[1] Here, a more direct approximate graphical method is employed.[6] This graphical method offers good accuracy for the higher levels of volume [lower values of probability $p_n(V)$] and hence is readily applicable for the range of values affecting the present calculation.

Examples of the cumulative distribution curves $p_n(V)$ of equivalent volume for n active compandored channels are given in Fig. 7, together with the corresponding distributions for uncompandored channels.[1] Similarly, Fig. 8 gives examples of the cumulative distribution curves $P_N(V)$ of equivalent volume for systems of N compandored channels, together with the corresponding distribution for uncompandored channels.[1]

The equivalent volume and the corresponding speech power exceeded one per cent of the time, read from curves as in Fig. 8, are plotted in Fig. 9 vs the number, N, of channels for compandored and uncompandored systems.

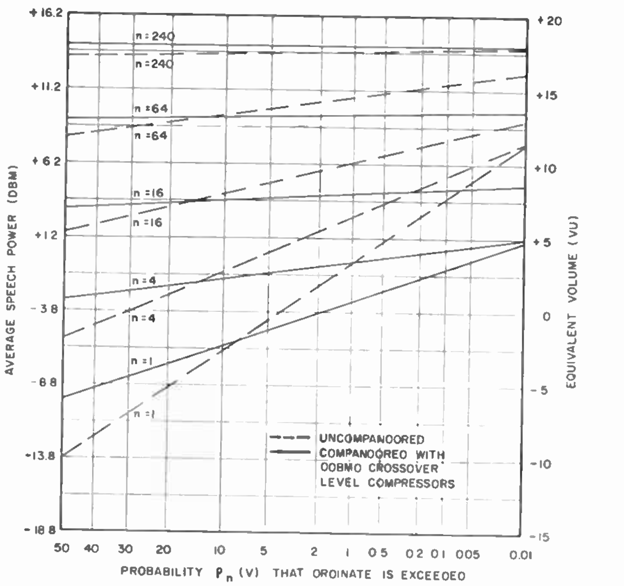

Fig. 7—Equivalent volume distribution for n active channels.

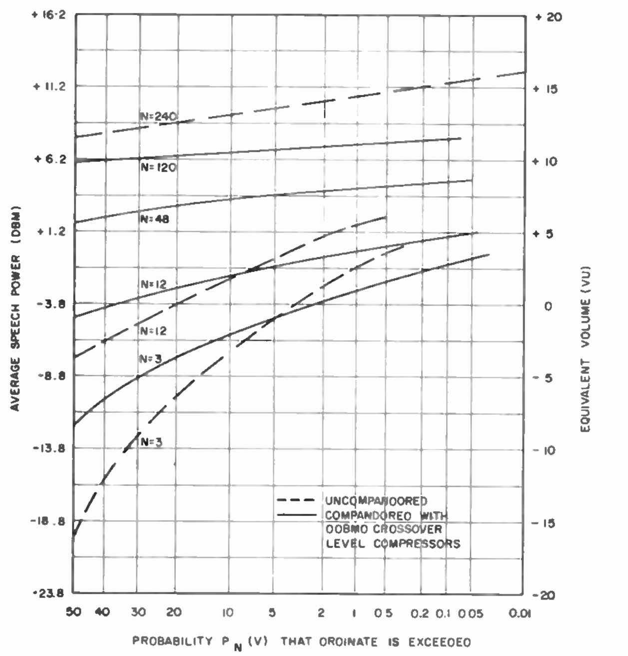

Fig. 8—Equivalent volume distribution for systems of N channels.

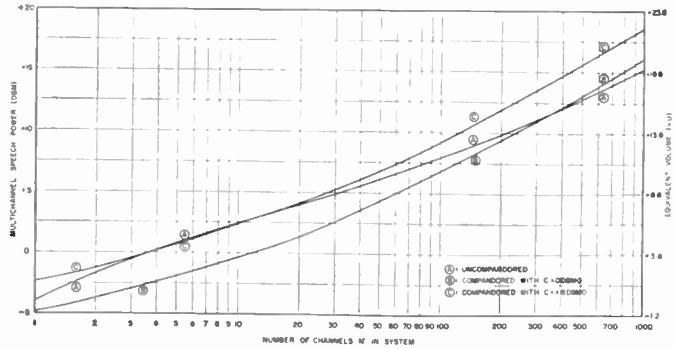

Fig. 9—Multichannel speech power and equivalent volume exceeded one per cent of time. (Uncontrolled volumes. All levels referred to zero transmission point.)

[4] "Tables of Binominal Probability Distribution," Dept. of Commerce, Natl. Bur. of Standards, Washington, D. C., Appl. Math. Series.

[5] "Tables of Cumulative Sums of Binominal Probabilities," U. S. Army Ordnance Dept., Washington, D. C.

[6] J. Dutka and S. J. Mehlman, "The Distribution of Noise Power in an N-Hop FM Radio Relay System," presented at the Second Natl. Symp. on Global Communications, St. Petersburg, Fla.; December, 1958.

The computation of (10) has been carried out up to $N=120$ channels. For $N>120$, the extrapolation has been performed in the following manner. Fig. 7 clearly shows that the volume fluctuations are largely reduced when a number of channels are combined together. For a very large number of channels, the equivalent volume tends to stay constant; that is, the speech power exceeded for one per cent of the time is approximately equal to the average speech power of the composite signal. The latter is given by (6) or (7), which can thus be used to compute the multichannel load also for a very large number of channels with uncontrolled volumes. This computation has been done for $N=1000$ ($n=300$; see Fig. 4), and the points $N=120$ and $N=1000$ in Fig. 9 have been joined by a smooth curve.

When only a number $N_c(<N)$ of channels are compandored in an N-channel system, the difference δ between compandored and uncompandored curves in Fig. 9 must be corrected to a value δ' which, assuming busy channels at random, is shown on the nomogram of Fig. 10.

Multichannel Peak Factor

Superimposed on the speech volume, constantly changing at a relatively slow rate, there are instantaneous voltage variations occurring at a relatively fast rate because of rapid transients which constitute the very nature of speech. The probability distribution of the ratio of instantaneous voltage to rms voltage for different numbers of channels was derived by Holbrook and Dixon from actual tests[1] and was found to be independent of volume. The multichannel peak factor was defined[7] as the upper limit of the ratio of instantaneous voltage to rms voltage. Speech at the compressor input can be regarded as a succession of volumes slowly varying, each having superimposed instantaneous voltages. It is desired to estimate the effect of compression on the instantaneous voltages in a channel and in a multichannel system.

The syllabic compressor has an attack time-constant of about 3 milliseconds, and its variolosser follows faithfully all voltage variations having rise-time longer than 3 milliseconds. Thus, such slow voltage variations are compressed. By contrast, the compressor variolosser is too sluggish to follow rapid variation lasting less than 3 milliseconds. Thus, such rapid voltage variations are not compressed. Therefore, the action of a compressor on the instantaneous voltages is to compress all peaks having rise time greater than 3 milliseconds.

It is known that only rarely do vowel sounds build up to full amplitude within one or two milliseconds.[8] More frequently, speech sounds reach full amplitude in about fifty milliseconds, while for the great majority of syllables the build-up is even more gradual.

[7] Holbrook and Dixon, *op. cit.*, Figs. 3 and 4.
[8] R. O. Drew and E. W. Kellog, "Starting characteristics of speech sounds," *J. Soc. Mot. Pic. Telev. Engrs.*, vol. 34, pp. 43–58; January, 1940.

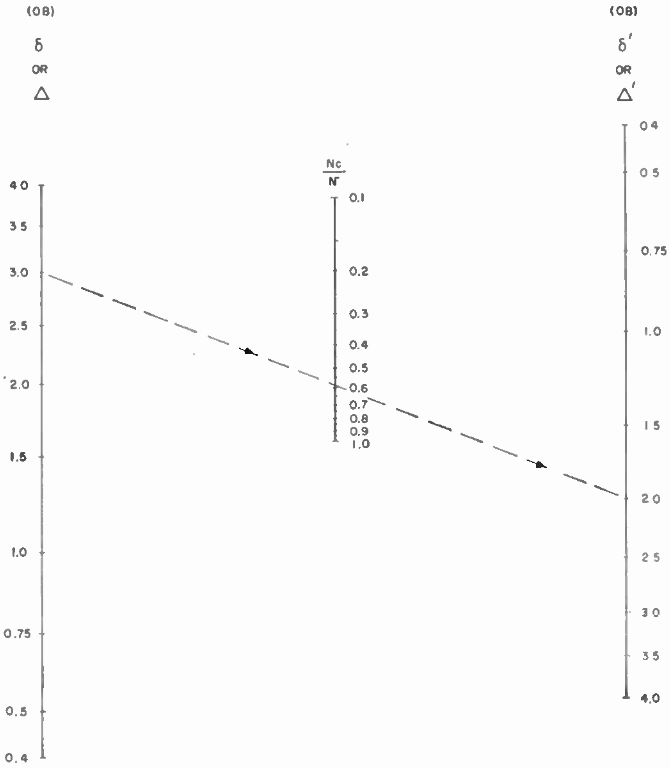

Fig. 10—Nomogram for partially-compandored systems.

Thus, the insertion of a compressor in a channel will have the effect of compressing the great majority of instantaneous voltage variations. It follows that a given peak amplitude will be reached with a smaller percentage of occurrence.

In a multichannel system where speech in all channels is uncorrelated, peaks will have random magnitude, phase, and duration. At any given instant, there will be some peak compression in a number of channels and there may be no peak compression in some other channels. Thus, the effect of a number of compressors is again to compress the bulk of instantaneous voltages in the composite multiplex signal. However, as the number of channels is increased, the probability of occurrence of short uncompressed peaks in the composite signal will increase; and for an infinite number of channels, dynamic syllabic compression will not modify the multichannel peak factor.

Comparative oscillographic measurements of single and multichannel peak factor with compandored and uncompandored active channels have been carried out, employing compressors with zero dbm0 crossover level.[9] The measured peak factor for n active channels, expressed as

$$20 \log_{10} \frac{V \text{ inst max}}{V \text{ rms}},$$

[9] Telefonaktiebolaget, L. M. Ericsson, Stockholm, Rept. No. 865-1084 (unpublished); see also, L. M. Ericsson Leaflet No. 1260e.

and modified by the solid line of Fig. 4, is plotted in Fig. 11 vs the number N of channels in system.[10]

Notice that curve B of Fig. 11 is valid also for systems compandored with +5 dbm0 crossover-level compressors. In fact, the crossover level affects solely the amount of volume compression; but the distribution of instantaneous voltages to rms voltage, hence the peak factor, was found to be independent of volume;[1] therefore, the peak factor is also independent of crossover level.

If only a partial number of channels $N_c(<N)$ are compandored in an N-channel system, the corresponding multichannel peak factor will be somewhere in between curves A and B of Fig. 11. Let Δ represent the difference between these two curves. The decrease in peak factor from the uncompandored case, assuming busy channels at random, will be given by Δ' shown on the nomogram of Fig. 10.

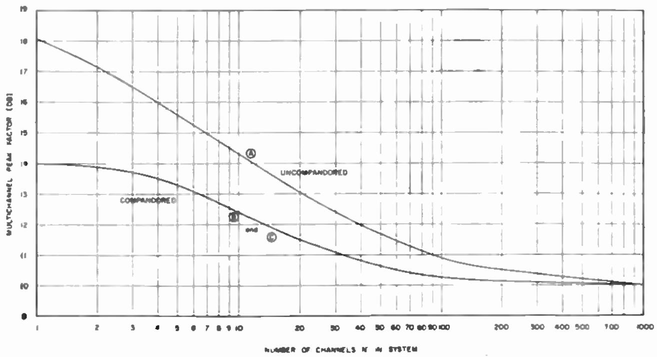

Fig. 11—Multichannel peak factor.

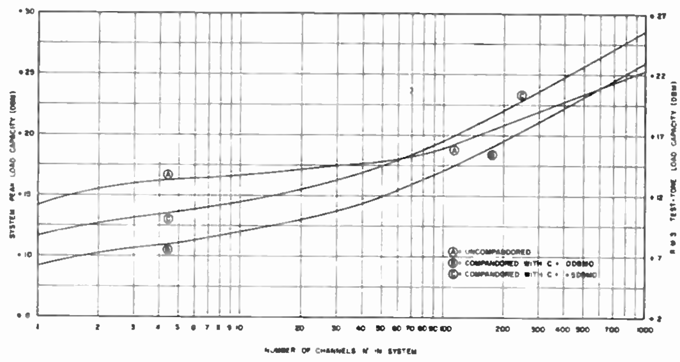

Fig. 12—Multichannel instantaneous peak load capacity. (All levels referred to zero transmission point.)

System Peak Load Capacity

The multichannel rms speech power not exceeded for more than one per cent of the time is shown in Fig. 9. To determine the instantaneous peak-load capacity of the sytem, the multichannel peak factor of Fig. 11 must be added to the rms speech power. The system peak-load capacity, so obtained, is plotted in Fig. 12 vs the number N of channels in system. The rms test-tone load capacity, also shown in Fig. 12, is three decibels lower than the peak-load capacity.

Conclusion

For system design purposes, Figs. 9 and 12 show the important parameters. Fig. 9 shows the multichannel speech power exceeded one per cent of the time vs the number of channels in a system when channel volumes are uncontrolled (practical case). Intermodulation noise at the output of a system is a function of the multichannel input power and of the amplitude and phase characteristics of the system. Intermodulation can be estimated when these parameters are known. Generally, the equipment is tested in order to determine the relationship between output intermodulation noise and input power level. A random noise source of proper bandwidth and of level deduced from Fig. 9 is used to simulate a number of telephone conversations, and the intermodulation noise is measured in an idle channel.[11] Fig. 12 shows the peak-load capacity required of the equipment vs the number of channels in a system to maintain overloading below one per cent of the time. Fig. 12 can be safely used for modern multiplex equipment which presents a certain amount of peak limiting.

From Figs. 9 and 12 it is seen that compandors decrease the rms load and the peak load in systems with small and medium number of channels. Physically, this is due to the fact that, before input to the sytem, speech is processed for a more constant loading of the equipment, thus increasing the over-all efficiency of transmission. The figures also show that compandors increase the rms and peak loading in systems with very many channels. The reason is that the composite uncompandored speech for very many channels presents little volume fluctuation, and the reduction of such fluctuation, resulting from the introduction of compandors, is overridden by the increase in mean

[10] $V_{inst\ max}$ is the maximum value observed on an oscilloscope for a physical signal; hence, it represents the upper limit of the observations. For the uncompandored case, it should be noted that the maximum voltages measured by Telefonaktiebolaget L. M. Ericsson are somewhat lower than the upper limit of Holbrook-Dixon observations (see Holbrook and Dixon, *op. cit.*, broken line of Fig. 3). Instead, they check closely with Holbrook and Dixon overload expectation of 0.1 per cent (curve $\epsilon = 0.001$ of their Fig. 3).

The peak factor is a decreasing function of the number, n, of active channels. In the case of controlled volumes, for a given number, N, of channels in system, n is the number of active channels exceeded one per cent of the time, as shown in Fig. 4. In the case of uncontrolled volumes, for a given N, there is no way of determining the exact number, n, of active channels. It can only be said that n will likely be somewhere between the maximum possible value $n = N$, and the average value $n = 0.25N$. Holbrook and Dixon have chosen conservatively the value $n = 0.25N$ (dotted line of their Fig. 4). Here, the slightly less conservative value of n equal to the number of channels exceeded one per cent of the time is used (solid curve of their Fig. 4). This choice is arbitrary. However, its justification is found in the statement by Holbrook and Dixon (*op. cit.*, p. 642) that their approximation—$n = 0.25N$—tends to give load capacities slightly higher than required for a very small number of channels but that the difference diminishes rapidly as the number of channels is increased.

[11] R. W. White and J. S. Whyte, "Equipment for measurement of interchannel crosstalk and noise on broadband multichannel telephone system," *P. O. Elec. Engrs. J.*, vol. 48, pt. 3, pp. 127–132.

power caused by the compressors. Moreover, the multichannel peak factor for very many channels is not modified significantly by the compandor action.

Also from Figs. 9 and 12, it appears that compandors with zero dbm0 crossover levels are more advantageous than compandors with +5 dbm0 crossover level. This is true insofar as loading of line and radio equipment is concerned. However, in Part II it will be seen that the improvement in signal-to-noise ratio may be greater when the higher crossover-level compandors are used.

Part II

Introduction

The improvement in signal-to-noise ratio (SNR) yielded by a compandor in a telephone channel is given by the instantaneous magnitude of the expandor loss.

The gain of the expandor varioloss circuit is controlled by the average power of its input signal over a short interval of time. Input signal during speech is made of two components, the desired signal (compressed at the transmitting point) and the channel noise introduced along the system up to the receiving point. Channel noise alone is present at the expandor input during pauses or in the absence of speech. Therefore, the expandor loss is controlled by speech power (assumed to be higher than noise) during syllables, and by noise power during pauses or in the absence of speech.

To deduce the compandor noise improvement, it is convenient to proceed as follows:

Step 1: Estimate the compandor noise improvement when speech is absent from the channel under consideration (normally the top channel in the baseband, where noise is greatest).

Step 2: Estimate the compandor noise improvement when speech is present in the channel under consideration.

Step 3: Perform electrical and aural tests to measure and appraise the improvement under conditions 1 and 2 above and compare the test results with the estimates.

Noise Improvement in an Idle Channel

When speech is absent in the channel under consideration, it is convenient to regard the compandor as a static device, or in other words to assume steady-state conditions. Expandor characteristics as well as channel noise level must be known. Expandor characteristics of commercial compandors are shown in Fig. 3. Channel noise is a statistical variable with probability distribution depending upon the distribution of fading, traffic over the system, external interferences, etc. Assuming that the channel noise probability distribution is known, the level of noise corresponding to a certain probability can be chosen. Entering the expandor characteristic with this level of noise will permit one to obtain the improvement yielded by the expandor.

By repeating this process for various levels of noise, corresponding to different probabilities of occurrence, the probability distribution of the compandor noise improvement can be found.

From a practical viewpoint, however, one value of noise improvement is of interest, namely that corresponding to the value of reliability for which the system is designed.

Let us assume that the value of channel noise is given for the chosen reliability (for instance, corresponding to one per cent of the time). It is desired to find out the compandor noise improvement in an idle channel. The procedure is more easily followed by working out a numerical example. Fig. 13 shows a system block diagram with relative levels at several points, as well as the top channel thermal and intermodulation noise at the expandor input. Compandors with zero dbm0 are employed, with characteristics as in Fig. 3(a).

Multichannel loading is in accordance with Fig. 9. System *A* is the reference. In System *B* the intermodulation noise is lower than in System *A*, because of the decrease in multichannel loading introduced by the compressors, as shown in Fig. 9. The channel noise undergoes a loss through the expandor according to the expandor characteristics of Fig. 3(a). This loss determines the noise improvement. In System *C* (Fig. 13), the effect on the noise improvement of compandoring only a partial number of channels is considered.

The example shows theoretical noise improvement in an idle compandored channel of the order of 25 db. This value may not be obtained in practice, as the expandor characteristic may deviate from its theoretical slope.

Noise Improvement in an Active Channel

When speech is present in a channel, the instantaneous expandor loss depends upon the short-term average power of the compressed speech. As a numerical example, let us assume a speech level of −10 dbm (talker average power) at the channel input. Table II shows speech levels read off Fig. 3, characteristics (a) and (b).

It is seen that the order of magnitude of noise improvement, during speech, is of only a few decibels. For compandors with +5 dbm0 crossover level, the noise improvement is always 2.5 db higher than for compandors with zero dbm0 crossover level.

It should be noticed that the stronger the speech, the smaller the noise improvement. For high enough values of speech, there is actual impairment of SNR. However, the level of noise during syllables is unimportant as long as it stays below the speech level, as noise is then masked by speech. During pauses or between syllables, owing to the short time-constant of the expandor variolosser, the compandor improvement approaches the value of noise improvement in an idle channel. Speech following a silent interval thus becomes more intelligible as adaptation to higher sensitivity during a quiet interval is a property of the human ear.

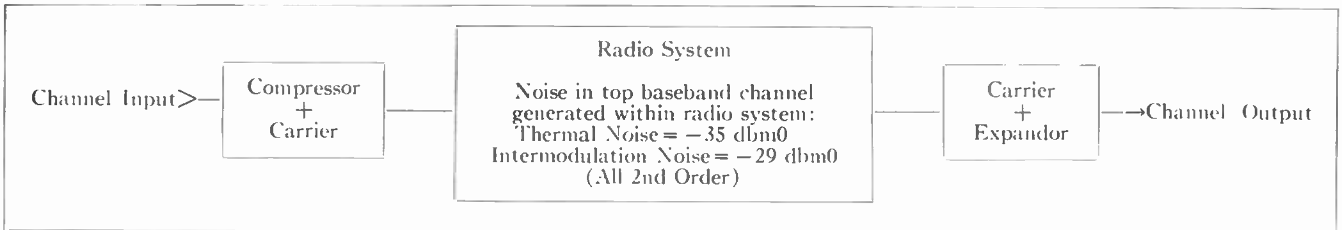

	Channel Input (dbm0)	After Compressor (dbm0)	Before Expandor (dbm0)	Channel Output (dbm0)	Test Tone Noise (db)	Theoretical Noise Improvement (db)
A) *System without compandors*						
Test Tone Level	0	0	0	0		
Thermal Noise	—	—	−35			
Intermodulation Noise 1)	—	—	−29			
Total Noise	—	—	−28	−28	28	Reference
B) *System with all channels compandored* ($N=72$)						
Test Tone Level	0	0	0	0		
Thermal Noise	—	—	−35			
Intermodulation Noise 2)	—	—	−32			
Total Noise	—	—	−30.2	−54.4	54.4	26.4
C) *System with only 47 channels compandored* ($N_c=47$)						
C.1 Compandored channel						
Test Tone Level	0	0	0	0		
Thermal Noise	—	—	−35			
Intermodulation Noise 3)	—	—	−31			
Total Noise	—	—	−29.5	−53	53	25
C.2 Uncompandored channel						
Test Tone Level	0	0	0	0		
Thermal Noise	—	—	−35			
Intermodulation Noise	—	—	−31			
Total Noise	—	—	−29.5	−29.5	29.5	1.5

1) For multichannel speech power as in Fig. 9, curve *A* for $N=72$.
2) For multichannel speech power as in Fig. 9, curve *B* for $N=72$. Notice that as intermodulation noise is all of 2nd order, its absolute value changes at twice the rate of change of loading in decibels.
3) For multichannel speech power as in Fig. 9, curve *B* for $N=72$, and nomogram of Fig. 10 for $N_c=47$.

Fig. 13—Example of static insertion of compandors with zero dbm0 crossover level in a 72-channel radio-relay system.

TABLE II

	For $C=0$ dbm0	For $C=+5$ dbm0
Compressor input	−10 dbm	−10 dbm
Compressor output	− 8 dbm	− 5.5 dbm
Expandor input	− 8 dbm	− 5.5 dbm
Expandor output	−10 dbm	−10 dbm
Noise improvement	2 db	4.5 db

Tests

Extensive aural tests under different conditions have been reported.[2,12,13] The results of these tests are plotted in Fig. 14 and show that the ear's appraisal of the noise improvement in the presence of speech is only a few decibels lower than the calculated and measured noise improvement in the absence of speech. For design purpose, subjective noise improvement can reasonably be assumed as five decibels lower than the theoretical noise improvement in the absence of speech.

Crossover Level Setting

The compandor crossover level determines the amount of speech compression and of speech and noise expansion, and affects the following parameters:

1) The signal to thermal noise ratio. From inspection of the expandor characteristics of Fig. 3, it is seen that the signal to thermal noise ratio is a linearly increasing function of the crossover level within the range of one to two expansion ratio.

2) The signal to intermodulation noise ratio. This ratio depends upon the multiplex power at the input of the system, which in turn is a function of the crossover level as shown in Fig. 9 (for uncontrolled volumes), and in Fig. 5 (for controlled volumes). From inspection of

[12] M. C. Harp, M. H. Kebby, and E. J. Rudisuhle, "Application of compandors to FM radio relay systems with frequency division multiplex," IRE TRANS. ON MICROWAVE THEORY AND TECHNIQUES, vol. MTT-2, pp. 36–40; April, 1954.
[13] Caruthers and Boxall, "A Miniature Compandor for General Use in Wire and Radio Communication System," Lenkurt Electric Co., San Carlos, Calif., Rept. No. 0-509.

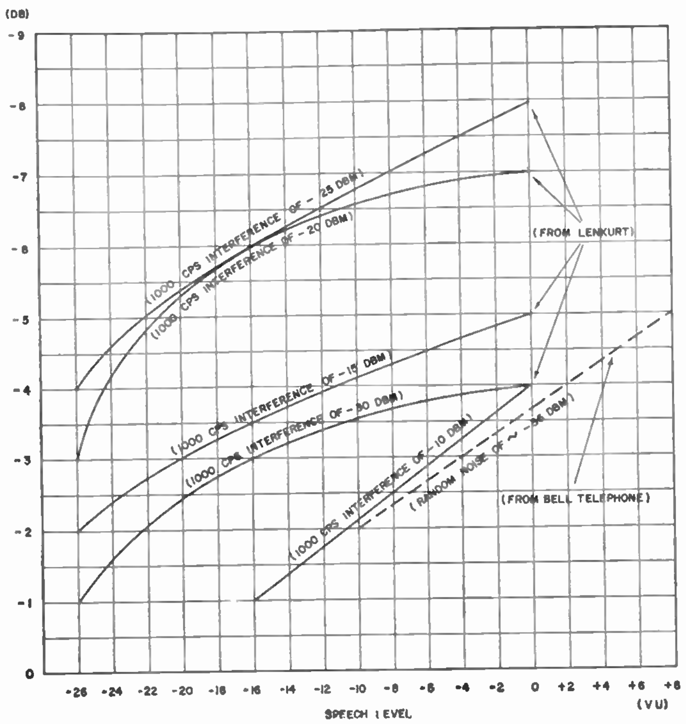

Fig. 14—Difference between subjective compandor improvement in the presence of speech, and theoretical noise improvement in the absence of speech.

the figures, it is seen that the signal to intermodulation ratio is a decreasing function of the crossover level, inasmuch as higher volume of crossover level results in a higher value of speech power at the input of the radio system, hence in higher crosstalk.

Thus, increasing the crossover level improves the signal to thermal noise ratio but simultaneously impairs the signal to intermodulation ratio. Theoretically, a compromise would be desirable to balance these opposite effects and optimize the system performance. In practice, because of continuously changing conditions of speech and noise, a balance can be attained only for short intervals. However, this balance is not critical at all, as compandors with either zero dbm0 or +5 dbm0 crossover level are about equally effective from a subjective viewpoint. Recently, the CCITT has recommended the standardization of crossover level to zero dbm0.[14]

Economical and Technical Considerations

The best design compromise of a particular multichannel system requires the simultaneous considerations of many factors depending upon the basic requirements of that system. (See for instance, Beverage, *et al.*[15]) As these factors vary with system parameters and as they may be of different relative importance, it is not possible to state that the use of compandors will always entail the most economical solution. The system engineer, therefore, should attempt to optimize the design of the system for the desired performance with and without compandors and then compare the economics of the two cases. Where high quality is required, however, it will be found that the use of compandors always results in the most economical system.

It is interesting to notice that some mutiplex manufacturers (*e.g.*, the one described by Carpani[16]) include compandors in the basic design of the multiplex, thus attaining a more economical design while preserving quality.

For a qualitative appreciation of the economy resulting from the use of compandors, the following list contains some of the most important parameters affected by compandors in a radio-relay system. For equal overall transmission performance (with and without compandors) their insertion permits:

- longer hops
- lower antenna gain
- lower transmitted power
- lower receiver sensitivity
- lower frequency deviation, hence smaller bandwidth or higher number of channels
- higher equipment amplitude and phase distortion, or higher number of channels
- poorer antenna match and sidelobe attenuation
- higher external RF interference
- longer transmission lines.

Intelligibility tests[17] show that no significant reduction in speech quality is noticed, even with 10 compandored circuits connected in series. Intelligibility in noisy circuits, in fact, is greatly enhanced by the insertion of compandors.

Compandors are also very useful under threshold conditions, in conjunction with radio squelch circuit.[18] On scatter circuits, where operating conditions are near FM threshold for a considerable percentage of the time, it is found to be very effective to use a compression ratio larger than the expansion ratio. Typical values are 10-to-1 for compression ratio and 1-to-2 for expansion ratio. The level of low-volume speech is thus raised enough above noise so that under marginal conditions intelligibility is preserved.

It should be appreciated that inherent level instability is introduced by the nature of the expansion process. The expandor, in fact, with its 1-to-2 expansion ratio doubles all input-level variations, thus halving the level stability. Therefore, more severe level stability requirements may be specified for a compandored system.

[14] "Red Book," Internatl. Tel. and Tel. Consultative Comm., vol. 1, pp. 239–304; June, 1957.

[15] See, for instance, H. H. Beverage, E. A. Laport, and L. C. Simpson, "System parameters using tropospheric scatter propagation," *RCA Rev.*, vol. 16, pp. 432–457; September, 1955.

[16] D. Carpani, "Telettra," *Tech. Info. Bull.*, pp. 10–17; July, 1957.

[17] G. Haessler, "Sprachubertragung mit Dynamikkompression," *FTZ*, vol. 12, pp. 659–664.

[18] T. A. Combellick, "Channelizing frequency modulated scatter communication system," *Signal*, vol. 12, pp. 51–52; August, 1958.

Tone-level regulation in the multiplex equipment is standard practice in high quality circuits, and is sometimes applied directly to the radio equipment.[19]

Conclusion

The compandor improvement can be resolved into separate contributions: quieting of the circuit by the expandor in absence of speech or between syllables, and an increased SNR by the compressor for weak speech. The introduction of noise into the channel between compressor and expandor is the condition necessary to this behavior.

For system design purposes, knowledge of improvement in SNR introduced by the compandors is necessary in order to arrive at a performance figure for the system. An analysis as shown in Fig. 13 may be carried out, where the value of intermodulation noise refers to the chosen loading and the value of thermal noise corresponds to a given multihop propagation fade (for instance, exceeded for one per cent of the time). The subjective improvement in circuit quality for speech can be estimated by subtracting five decibels from the calculated performance figure.

Appendix I

Holbrook and Dixon plot the average-talker volume distribution in "db above reference," the unit of speech and program volume used at the time the measurements were taken (1939).[1] The parameters of the average-talker volume distribution are:

$$V_0 = -16 \text{ db}$$
$$\sigma = 5.8 \text{ db.}$$

The volume V_{0p} corresponding to the average speech power of the distribution is given by:[2]

$$V_{0p} = V_0 + (0.115)\sigma^2\text{db} = -16 + (0.115)5.8^2$$
$$= -12.1 \text{ db.} \tag{12}$$

Holbrook and Dixon[1] also show the measured relationship between "db above reference" and long-term average speech power, P, in dbm:

$$0 \text{ db} \cong +2.2 \text{ dbm.} \tag{13}$$

The average speech power of the distribution, in dbm, is obtained as follows:

$$P \cong V_{0p} - 2.2 = -12.1 + 2.2 = -9.9 \text{ dbm.} \tag{14}$$

After the Holbrook-Dixon work was published, a newer type of volume meter-reading volume in volume units (VU) was standardized. The relationship between "db above reference" and volume units for speech in a telephone channel was found to be approximately:[20]

$$0 \text{ db} = +6 \text{ VU.} \tag{15}$$

Therefore, the parameters of the average-talker volume distribution measured by Holbrook and Dixon, but expressed in volume units, are:

$$V_0 = -10 \text{ VU}$$
$$\sigma = 5.8 \text{ db}$$
$$V_{0p} = -6.1 \text{ VU}$$

from (12) and (15)

$$0 \text{ VU} \cong -3.8 \text{ dbm} \tag{16}$$

from (13) and (15)

$$P \cong -9.9 \text{ dbm.} \tag{17}$$

Volume measurements shown by Holbrook and Dixon[1] were carried out, reading the highest peaks occurring within intervals of about ten seconds. The average speech power was measured over a much longer interval of time. However, in first approximation, it seems reasonable to assume the average speech power to be the same in every ten-second interval, when the volume is held constant. This assumption permits us to set a scale of speech power in dbm for the average-talker distribution, according to (16). The setting of a scale of speech power on the volume-distribution graph is necessary for two reasons:

1) to set the scale of compandor crossover level in dbm0 (dbm referred to a point of zero transmission level),
2) to translate measurements of volume (VU) into average speech power (dbm)—the latter being used to compute the multiplex loading.

In 1953, Subrizi reported on a number of measurements of talker volume.[20] Because of talkers' changing habits, improvements in telephone sets, and other factors, the average-talker volume distribution could be expressed approximately by the following parameters:

$$V_0 = -15 \text{ VU}$$
$$\sigma = 5 \text{ db}$$
$$V_{0p} = -12 \text{ VU.}$$

Also, the relationship between volume units and speech power in dbm was modified as follows:

$$0 \text{ VU} \cong -1.4 \text{ dbm.} \tag{18}$$

Therefore, the average speech power of the cumulative distribution resulted as:

$$P \cong -13.4 \text{ dbm.} \tag{19}$$

American, British, and French experimenters have, from time to time, measured talker volume over different circuits. Widespread results have been obtained

[19] "Design of a Nation-Wide Multichannel VHF System for the Empresa Nacional de Telecommunicaciones, Colombia, S. A.," RCA Internatl. Div., Clark, N. J. (Unpublished).

[20] V. Subrizi, "A speech volume survey on telephone message circuits," *Bell Labs. Rec.*, vol. 31, pp. 292–295; August, 1953.

for the parameters of the average talker distribution.[21] An approximate indication of the measured range is given below:

V_0 from -16 to -6 VU

σ from 4.0 to 7.8 db

P from -16 to -8 dbm.

It should be appreciated that these differences depend upon different habits of different talkers, the type of speech, the type of material being spoken, different telephone sets and plants, etc. Different administrations and laboratories may use different values for V_0, σ, P, and for the conversion between VU and dbm.

In 1958, the CCIR suggested a formula for standardizing the rms white noise loading of radio systems to simulate the telephone load, for systems with 12 channels or more.[22] The CCIR rms white noise loading is plotted in Fig. 15, together with Holbrook-Dixon rms speech power exceeded for one per cent of the time. It is seen that the two curves differ by at most ± 1 db.

From the above considerations and because the Holbrook-Dixon monograph is the most extensive existing study of load-rating theory for uncompandored speech, Holbrook-Dixon results are used in this paper as the reference values. Since this paper aims only at a comparison between compandored and uncompandored systems, the absolute values used are not of primary concern. Nevertheless, adjusting the values used herein to a different reference is easily done by simply shifting the scales of volume and speech power on the graphs to the desired reference.

Appendix II

The standard volume meter is an rms type of instrument with a time-constant of about 300 milliseconds. For complex speech, it averages whole syllables or words. The dynamic compressor has a considerably shorter time-constant of only a few milliseconds; hence, its action is sufficiently fast to follow the envelope of syllables. Thus, a fast level variation lasting an interval of time shorter than the VU meter time-constant, but longer than the compressor time-constant, will not be detected by the VU meter, while it will act upon the compressor variolosser, thereby changing its transmission gain.

Therefore, it is to be expected that the average power at the compressor output will be a function of the input waveform. By comparing the compressor output powers in a telephone channel for inputs of a 1000-cps sinewave of known power and of speech volume having the same

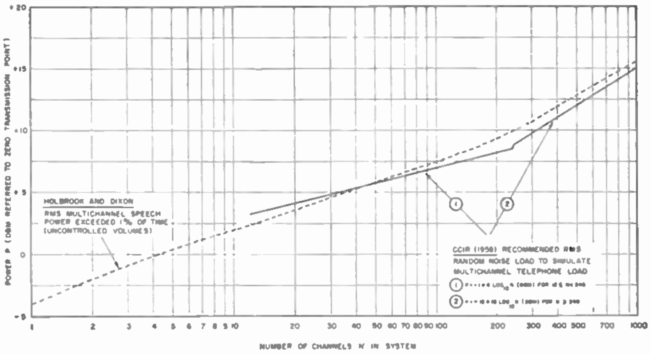

Fig. 15—Loading comparison between Holbrook and Dixon (1939) and CCIR recommendation.

rms power, we can evaluate the effect of speech waveform on the transmission gain. Measurements made with zero dbm0 crossover level compandors,[9] show that the compressor output level for speech input is approximately three decibels lower than for sine-wave input of the same power. This relationship was found to be independent of the input signal level. The same relationship can be assumed to hold in first approximation between sinewave and random noise, inasmuch as speech and random noise have similar waveform characteristics. Identical results for speech are reported by a different source.[17]

Thus it is seen that the relationship between compressed speech or noise output and compressed tone output depends upon the compressor time constants, but is independent of the volume input level. Hence, it is independent also of the crossover level, since the latter changes only the amount of volume compression. It follows that the results obtained with zero dbm0 crossover level compandors can be directly applied to the characteristics with +5 dbm0 crossover level shown in Fig. 3.

Appendix III

Given a compandor with fixed compression ratio (*i.e.*, 2-to-1), apply the volume distribution [Fig. 2(a)] to the compressor input. The volume distribution at the compressor output is altered according to the compressor characteristic. Now vary the compandor crossover level and show that the resulting variation of loading, L, is a linear function of the crossover level C.

To prove the above, refer to Fig. 16. Recall that V_{0p} corresponds to the average loading of an active channel, and that

$$V_{0p} = V_0 + (0.115)\sigma^2. \tag{20}$$

The variation in average loading of a channel can be written as:

$$L = \Delta V_{0p} = \Delta V_0 + \Delta[(0.115)\sigma^2]. \tag{21}$$

[21] M. Toutan and M. Thue, "Determination experimentale de al puissance transmisse par un circuit telephonique," *Cables and Transm.* (*Paris*), vol. 10, no. 2, pp. 145–151; April, 1956.

[22] Documents, CCIR Study Groups, Period 1956–1959, Doc. No. IX/78-E, p. 3; August 20, 1958.

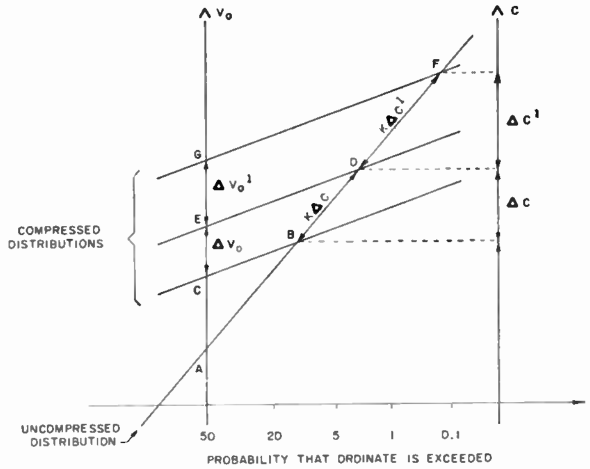

Fig. 16—Additional average loading is proportional to compandor crossover level.

But for all compressed distribution, σ is a constant (2.9 db) since the compression ratio is constant and all compressed distributions are parallel straight lines. It follows that

$$\Delta[(0.115)\sigma^2] = 0; \tag{22}$$

therefore,

$$L = \Delta V_0. \tag{23}$$

Then, it will be sufficient to show that the variations of V_0, ΔV_0, are linearly related to the variations of compandor crossover level C, ΔC. Owing to the similarity of triangles ABC, ADE, AFG, the following proportion among the sides of the parallelograms can be written down at once:

$$\frac{CE}{BD} = \frac{EG}{DF} = \frac{\Delta V_0}{K\Delta C} = \frac{\Delta V_0{}^1}{K\Delta C^1}, \tag{24}$$

where K is a constant of proportionality.

Eqs. (23) and (24) show the proportionality between average loading and crossover level.

Acknowledgment

The author is indebted to L. C. Simpson for many hours of inspiring discussions and for his advice. The contribution of Telefonaktiebolaget L. M. Ericsson in making available the results of their experiments is gratefully acknowledged.

Piezoelectric Properties of Polycrystalline Lead Titanate Zirconate Compositions*

D. A. BERLINCOURT†, MEMBER, IRE, C. CMOLIK†, AND H. JAFFE†, SENIOR MEMBER, IRE

Summary—**Detailed data are given for the piezoelectric, elastic, and dielectric properties of lead titanate zirconate ceramic compositions near the rhombohedral-tetragonal phase boundary. These compositions have markedly higher electromechanical coupling factors, remanent ferroelectric charge, and coercive field, than ceramic barium titanate. Another interesting feature is a pronounced change in the free permittivity $\epsilon_{33}{}^T$ by the poling process; this change is in opposite directions for rhombohedral and tetragonal compositions. The dielectric and elastic anisotropy ratios of poled lead titanate zirconate are much greater than those of barium titanate, indicating a greater degree of alignment of domains during poling.**

I. Introduction

Lead titanate and lead zirconate form a complete solid solution system. A phase boundary which is virtually temperature independent exists near the composition $PbZr_{.55}Ti_{.45}O_3$;[1,2] solid solutions richer in zirconium are rhombohedral, and those richer in titanium have tetragonal symmetry. In 1954, B. Jaffe[3] and co-workers reported that solid solutions near the phase boundary could be permanently poled. They obtained highest piezoelectric coupling at the phase boundary, with best values approximately equal to typical values for good barium titanate.

By close control of chemical composition and processing, the present authors were able to obtain the substantially higher values of piezoelectric coupling reported in this paper. The combination of high piezo-

* Original manuscript received by the IRE, April 24, 1959; revised manuscript received, September 4, 1959. This work was supported by Sandia Corp., Albuquerque, N. Mex., under Purchase Orders WC-727 and 51-4232.

† Clevite Corp., Electronic Res. Div., Cleveland, Ohio.

[1] G. Shirane and K. Suzuki, "Crystal structure of $Pb(Zr, Ti)O_3$," *J. Phys. Soc. Japan*, vol. 7, p. 333; May-June, 1952.

[2] E. Sawaguchi, "Ferroelectricity versus antiferroelectricity in solid solutions of $PbZrO_3$ and $PbTiO_3$," *J. Phys. Soc. Japan*, vol. 8, pp. 615–629; September-October, 1953.

[3] B. Jaffe, R. S. Roth, and S. Marzullo, "Piezoelectric properties of lead zircoanate-lead titanate solid-solution ceramic ware," *J. Appl. Phys.*, vol. 25, pp. 809–810; June, 1954.

electric effects with high Curie point (about 350°C) makes these ceramics important for applications involving high power level or a wide range of ambient temperatures. Variation of the ratio of zirconium to titanium in these compositions allows one to cover a considerable range of permittivity. Partial replacement of lead, titanium, or zirconium by other elements[4,5] provides even wider variation of permittivity and substantial modification of other physical properties. Transducer characteristics of commercial lead titanate zirconate ceramics as function of temperature have been presented elsewhere.[6]

The present study presents complete sets of low-signal elastoelectric parameters at 25°C for poled lead titanate zirconate ceramics ranging from $PbZr_{.48}Ti_{.52}O_3$ to $PbZr_{.6}Ti_{.4}O_3$, and not chemically modified. These data are supplemented by information on total piezoelectric charge released by high compressive stress parallel to the polar axis, and by some observations on pyroelectricity.

piezoelectric (electromechanical) coupling factors[10] are defined as follows:

$$k_{31} = d_{31}/\sqrt{\epsilon_{33}^T s_{11}^E}, \tag{1}$$

$$k_p = k_{31}\sqrt{\frac{2}{1-\sigma^E}}\,. \tag{2}$$ [11]

$$k_{33} = d_{33}/\sqrt{\epsilon_{33}^T s_{33}^E}, \tag{3}$$

and

$$k_{15} = d_{15}/\sqrt{\epsilon_{11}^T s_{55}^E}, \tag{4}$$

where $\sigma^E = -s_{12}^E/s_{11}^E$ is Poisson's ratio under constant-field conditions.

One poled disk of each composition served as the basis for all measurements, but each disk was representative of about 15 disks of the same composition prepared concurrently. The disks were fully plated, about 1.2 mm thick and 17 mm in diameter and poled parallel to the thickness. Measurement of f_r and f_a then yielded coupling factor k_p and elastic compliance s_{11}^E by:

$$\frac{k_p^2}{1-k_p^2} = \frac{(1-\sigma^E)J_1[\eta_1(1+\Delta f/f_r)] - \eta_1(1+\Delta f/f_r)J_0[\eta_1(1+\Delta f/f_r)]}{(1+\sigma^E)J_1[\eta_1(1+\Delta f/f_r)]}, \tag{5}$$

$$\frac{1}{s_{11}^E} = \frac{\pi^2 d^2 f_r^2(1-\sigma^E)\rho}{\eta_1}, \tag{6}$$

II. Procedures

A. Measurement of Piezoelectric, Dielectric, and Elastic Constants

Piezoelectric, elastic, and dielectric constants were measured using methods recommended in an IRE Standard on Piezoelectric Ceramics which is in preparation,[7] and presented in part in an earlier paper.[8] Preference is given to measurements of the resonance frequency, f_r, and antiresonance frequency, f_a, of the fundamental mode of disks. For the materials here discussed, f_r may be identified with the frequency of minimum impedance, and f_a with the frequency of maximum impedance. The symbols for piezoelectric constants, permittivities, and elastic constants here used follow the 1949 Standards on Piezoelectric Crystals.[9] In addition, four

where

$\Delta f = f_a - f_r$,
J_0 = Bessel function of first kind and zero order,
J_1 = Bessel function of first kind and first order, and
η_1 = lowest positive root of $(1+\sigma^E)J_1(\eta) = \eta J_0(\eta)$.

For $\sigma^E = 0.31$, $\eta_1 \cong 2.05$. The change of η with σ^E is negligible for the range of σ^E found in these ceramics.

ρ = density (kg/m³), and
d = disk diameter (meter).

The hydrostatic strain constant $d_h = d_{33} + 2d_{31}$ of these disks was obtained from the measured response to a calibrated hydrostatic pressure (about 3 psi RMS).

At this point three bars were cut from each disk. The bars had the following approximate dimensions:

Bar	l	w	t
A	15 mm	2 mm	1.2 mm
B	14	5.5	1.2
C	5	1.8	1.2

f_a and f_r of A bars, fully plated on the faces 15 mm by 2 mm, were then measured to obtain k_{31} and s_{11}^E by

$$\frac{k_{31}^2}{1-k_{31}^2} = \frac{\pi}{2}\frac{f_a}{f_r}\tan\frac{\pi}{2}\frac{\Delta f}{f_r}, \tag{7}$$

[4] B. Jaffe, R. S. Roth, and S. Marzullo, "Properties of piezoelectric ceramics in the solid-solution series lead titanate-lead zirconate-lead oxide: tin oxide and lead titanate-lead hafnate," *J. Res. Natl. Bur. Standards*, vol. 55, pp. 239–254; November, 1955.

[5] F. Kulcsar, "Electromechanical properties of lead titanate zirconate ceramics with lead partially replaced by calcium or strontium," *J. Amer. Ceram. Soc.*, vol. 42, pp. 49–51; January, 1959; and "Electromechanical properties of lead titanate zirconate ceramics modified with certain three- or five-valent additions," *J. Amer. Ceram. Soc.*, vol. 42, pp. 343–349; July, 1959.

[6] D. Berlincourt, B. Jaffe, H. Jaffe, and H. H. A. Krueger, "Transducer properties of lead titanate zirconate ceramics," 1959 IRE National Convention Record, pt. 6, pp. 227–232, and IRE Trans. on Ultrasonics Engineering, PGUE-8, February, 1960.

[7] IRE Committee on Piezoelectric Crystals, Proc. IRE, to be published.

[8] W. P. Mason and H. Jaffe, "Methods for measuring piezoelectric, elastic, and dielectric coefficients of crystals and ceramics," Proc. IRE, vol. 42, pp. 921–930; June, 1954.

[9] "IRE Standards on Piezoelectric Crystals, 1949," Proc. IRE, vol. 37, pp. 1378–1395; December, 1949.

[10] "IRE Standards on Piezoelectric Crystals: Determination of the Elastic, Piezoelectric, and Dielectric Constants—The Electromechanical Coupling Factor, 1958," Proc. IRE, vol. 46, pp. 765–778; April, 1958.

[11] k_p is identical with the "radial electromechanical coupling coefficient k_r," of Mason and Jaffe, *op. cit.*

and

$$\frac{1}{s_{11}^E} = 4\rho f_r^2 l^2. \tag{8}$$

The length-to-width ratio of the A bars is sufficient to reduce Rayleigh corrections to less than 1 per cent. The coupling factor k_{31} calculated by (2) from k_p of the original disk was in all cases within 1 per cent of that measured on the corresponding A bar.

The permittivities ϵ_{33}^T and ϵ_{33}^S were obtained on type B bars fully plated on the faces 14 mm by 5.5 mm. The capacitance was measured over a frequency range from 50 kc to 20 mc. The data were plotted on semilog graph paper, and values well above the fundamental thickness resonance near 1.5 mc and the first few overtones were extrapolated back to 50 kc to give ϵ_{33}^S, while the measured value at 50 kc gave ϵ_{33}^T. In this manner the variation of ϵ with frequency was eliminated.

New electrodes were applied to A bars on the faces 14 by 1.2 mm, and the capacitance of each bar was measured in the frequency range 50 kc to 15 mc to give ϵ_{11}^T and ϵ_{11}^S. The data were plotted on semilog graph paper, and the measurements well above 1 mc were extrapolated to 1 mc (near the fundamental thickness shear antiresonance frequency) to give ϵ_{11}^S; measurements below 1 mc were also extrapolated to 1 mc[12] to give ϵ_{11}^T. The coupling factor k_{15} was then obtained using the relationship

$$k_{15}^2 = 1 - \frac{\epsilon_{11}^S}{\epsilon_{11}^T}. \tag{9}$$

Bars C were depoled by heating to 600°C. The faces 1.2 by 1.8 mm were electroded and the bars were repoled. The fundamental resonance and antiresonance frequencies were measured using a special crystal holder which effectively placed all stray capacitances across the signal generator rather than across the test specimen. This precaution was taken in the present case because of the very low capacitance of the test specimens. Relationships used are listed below.

$$k_{33}^2 = \frac{\pi}{2}\frac{f_r}{f_a}\tan\left(\frac{\pi}{2}\frac{\Delta f}{f_a}\right), \tag{10}$$

$$\frac{1}{s_{33}^D} = 4\rho l^2 f_a^2, \tag{11}$$

and

$$s_{33}^E = s_{33}^D/(1 - k_{33}^2). \tag{12}$$

In order to obtain a coherent set of data, not involving another poling process, another value for k_{33} was calculated from d_h and d_{31} measured on the original disk, ϵ_{33}^T measured on B bars, and s_{33}^E from (12). Values of k_{33}, so calculated, differed by less than 5 per cent from values measured on C bars after repoling.

The elastic stiffness c_{33}^D was obtained from overtones of the thickness mode antiresonance frequency of type-B bars electroded on the faces 14 by 5.5 mm. In each case the fifth, seventh, ninth, and eleventh harmonics were divided by the appropriate order and averaged. The relationship is

$$c_{33}^D = 4\rho f_a^2 l^2. \tag{13}$$

The elastic compliance s_{44}^D was obtained from overtones of the thickness shear modes of C bars electroded on the faces 5 by 1.8 mm. The fifth, seventh, ninth, and eleventh harmonics were measured. The relationship used is

$$\frac{1}{s_{44}^D} = 4\rho f_a^2 l^2. \tag{14}$$

Poisson's ratio, $-s_{12}^E/s_{11}^E$, was determined on square plates 5.5 mm on a side cut from B bars. The resonance frequencies of the two contour-extensional modes were measured, and from the ratio of these frequencies $-s_{12}^E/s_{11}^E$ was obtained using Table III of the 1958 IRE Standards on Piezoelectric Crystals.[10]

The described measurements furnish a complete set of independent constants. Additional constants contained in Table I follow from the defining relations of 1949 IRE Standards on Piezoelectric Crystals.[9]

B. Measurement of Total Electric Moment

The total ferroelectric moment was determined by measurement of charges released as test specimens were depoled by application of high compressive stress parallel to the polar axis. Cylindrical axially-poled test specimens were used, and the released charges were collected on a shunt capacitance three orders of magnitude greater than the capacitance of the test specimen. The compressive stress was applied by an hydraulic press, and the test specimens were proportioned so that hydrostatic stresses were negligible. This required a diameter/thickness ratio not greater than three.

C. Pyroelectric Measurements

Pyroelectric measurements were made at constant stress, and therefore included both the primary and secondary effects defined by Cady.[13] Above about 130°C anomalous dielectric charges are also included; this is discussed further in the next section. A sensitive galvanometer was connected across the test specimen, which was heated slowly. Discharge current and temperature were recorded as functions of time.

[12] The extrapolation was made to 1 mc because the fundamental resonance was near this frequency, and the degree of extrapolation was thus minimized. For $\epsilon_{33}^{S,T}$ the extrapolation was to 50 kc because the resonance of the fundamental lateral mode was near this frequency. For application in (15), this is convenient, since nearly all other constants were measured near 50 kc also.

[13] W. G. Cady, "Piezoelectricity," McGraw-Hill Book Co., Inc., New York, N.Y., p. 40; 1946.

TABLE I

DIELECTRIC, ELASTIC, AND PIEZOELECTRIC CONSTANTS OF LEAD TITANATE ZIRCONATE COMPOSITIONS

Comp Zr/Ti atom ratio	k_{31}	k_p	k_{15}	k_{33}	K_{11}^T	K_{11}^S	K_{33}^T	K_{33}^S Meas.	K_{33}^S Calc.	s_{11}^E	s_{11}^D	s_{33}^E	s_{33}^D	s_{44}^E	s_{44}^D	s_{66}	s_{12}^E	s_{12}^D	s_{13}^E	s_{13}^D	Density
48/52	0.170	0.289	0.408	0.435	663	551	666	540	537	10.8	10.5	10.9	8.83	28.3	23.6	28.3	−3.35	−3.66	−3.21	−2.40	7.59
50/50	0.230	0.397	0.504	0.546	855	631	846	585	585	12.4	11.7	13.3	9.35	32.8	24.5	32.9	−4.06	−4.72	−4.22	−2.60	7.55
52/48	0.313	0.529	0.694	0.670	1180	612	730	399	389	13.8	12.4	17.1	9.35	48.2	25.0	38.4	−4.07	−5.38	−5.80	−2.56	7.55
54/46	0.280	0.470	0.701	0.626	990	504	450	253	268	11.6	10.7	14.8	9.0	45.0	22.9	29.9	−3.33	−4.24	−4.97	−2.68	7.62
56/44	0.267	0.450	0.657	0.619	840	477	423	246	258	11.0	10.2	14.0	8.65	39.8	22.6	28.4	−3.22	−4.01	−4.63	−2.57	7.59
58/42	0.254	0.428	0.646	0.607	751	437	397	243	246	10.5	9.85	12.8	8.10	37.7	21.9	27.1	−3.07	−3.75	−4.12	−2.33	7.64
60/40	0.238	0.400	0.625	0.585	672	410	376	240	245	10.4	9.75	12.05	7.92	36.9	22.5	26.7	−2.96	−3.55	−3.72	−2.17	7.60
$BaTiO_3$ Ceramic[17]	0.208	0.354	0.467	0.493	1620	1260	1900	1420		8.55	8.18	8.93	6.76	23.3	18.3	22.3	−2.61	−2.98	−2.85	−1.95	5.7

Comp Zr/Ti atom ratio	g_{31}	g_{33}	g_{15}	$g_{33}-g_{31}$	d_{31}	d_{33}	d_{15}	$d_{33}-d_{31}$	$s_{33}^D+s_{11}^D-2s_{13}^D$	Q_M	Q_E	P	c_{33}^D	$\frac{-s_{12}^E}{s_{11}^E}$	$\frac{-s_{12}^D}{s_{11}^D}$	$\frac{-s_{13}^E}{\sqrt{s_{33}^E s_{11}^E}}$	$\frac{-s_{13}^D}{\sqrt{s_{33}^D s_{11}^D}}$
48/52	−7.3	18.7	28.4	26.0	43.0	110	166	153	24.1	1170	380	17	14.0	0.310	0.349	0.296	0.250
50/50	−9.35	23.1	33.2	32.4	70.0	173	251	243	26.2	950	370	27	13.5	0.328	0.404	0.329	0.249
52/48	−14.5	34.5	47.2	49.0	93.5	223	494	316	26.9	860	360	36	13.4	0.295	0.434	0.376	0.238
54/46	−15.1	38.1	50.3	53.2	60.2	152	440	212	25.1	680	300	42.5	14.8	0.288	0.396	0.380	0.273
56/44	−14.5	37.8	48.0	52.3	54.3	142	357	196	24.0	490	190	48	15.3	0.293	0.394	0.373	0.274
58/42	−13.9	36.7	48.8	50.6	48.9	129	325	178	22.6	500	200	43	15.8	0.292	0.381	0.355	0.261
60/40	−13.3	35.2	49.3	48.5	44.2	117	293	161	22.0	600	210	33	15.6	0.285	0.365	0.332	0.247
$BaTiO_3$ Ceramic	−4.7	11.4	18.8	16.1	−79	191	270	270	18.8	430	200	8–10	18.9	0.305	0.365	0.326	0.262

Units of s are in 10^{-12} m^2/newton, g in 10^{-3} voltmeters/newton, d in 10^{-12} coulombs/newton, P in 10^{-2} coulombs/m^2, c in 10^{10} newton/m^2, and density in 10^3 kg/m^3. Dielectric constants K are relative to air: $\epsilon = 8.85 \cdot 10^{-12}$ K farad/m.

III. Results and Discussion

A. Dielectric, Elastic, and Piezoelectric Constants

Piezoelectric, elastic, and dielectric properties of a series of lead titanate zirconate compositions are shown in Figs. 1 through 6; these data are listed in Table I. Highest values of piezoelectric coupling and mechanical compliance were obtained with the 52/48[14] limiting tetragonal composition. In other compositional series the peak piezoelectric response was obtained at 52/48 in some cases and 53/47 in others, always at the limiting tetragonal composition. The zirconium compounds used in this study contained 1 to 2 atom per cent hafnium. This fact was, however, disregarded in computing molar ratios from actual weight ratios.

The character of the curves showing the compositional dependence of the dielectric constant is particularly interesting (see Fig. 4). The isotropic dielectric constant before poling was maximum at the 52/48 or limiting tetragonal composition. After poling, the maximum values of ϵ_{33}^T, ϵ_{33}^S, and ϵ_{11}^S all occurred at the 50/50 composition. The peak value of ϵ_{11}^T was still at 52/48. With the exception of ϵ_{11}^T the poling process moved the curves of permittivity vs mol per cent $PbZrO_3$ to the left. One may infer that the poled state favors the rhombohedral phase. This may be ascribed to the greater number of possible positions for the polar axes in a rhombohedral crystal (eight) than in a tetragonal crystal (six), which permits a closer average approach of the polar axes of crystallites to the applied field direction. A phase change by application of an electric field at constant temperature has also been found in barium titanate ceramic[15] near the orthorhombic-tetragonal polymorphic transition. In this case the or-

[14] Henceforth the composition will be given as a simple numerical ratio with atom per cent Zr^{4+} as numerator and atom per cent Ti^{4+} as denominator.

[15] H. G. Baerwald and D. Berlincourt, "Electromechanical response and dielectric loss of prepolarized barium titanate under maintained electric bias," *J. Acoust. Soc. Amer.*, vol. 25, pp. 703–710; July, 1953.

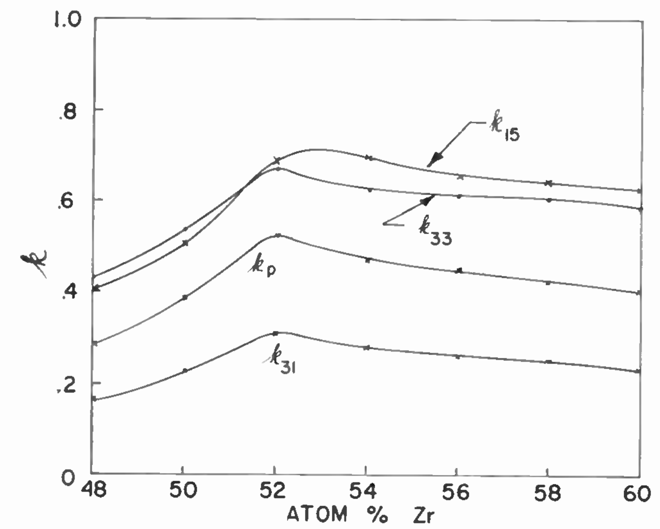

Fig. 1—Variation of piezoelectric coupling with atom per cent Zr^{4+} in $Pb(Zr, Ti)O_3$.

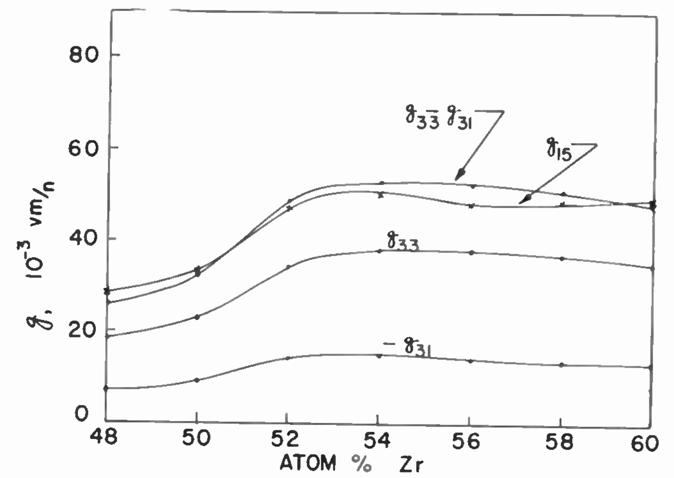

Fig. 2—Variation of piezoelectric strain constants g_{33}, g_{31}, and g_{15} with atom per cent Zr^{4+} in $Pb(Zr, Ti)O_3$.

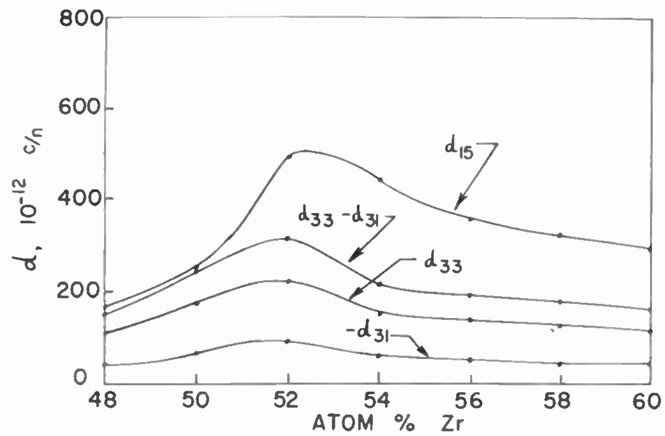

Fig. 3—Variation of piezoelectric strain constants d_{33}, d_{31}, and d_{15} with atom per cent Zr^{4+} in $Pb(Zr, Ti)O_3$.

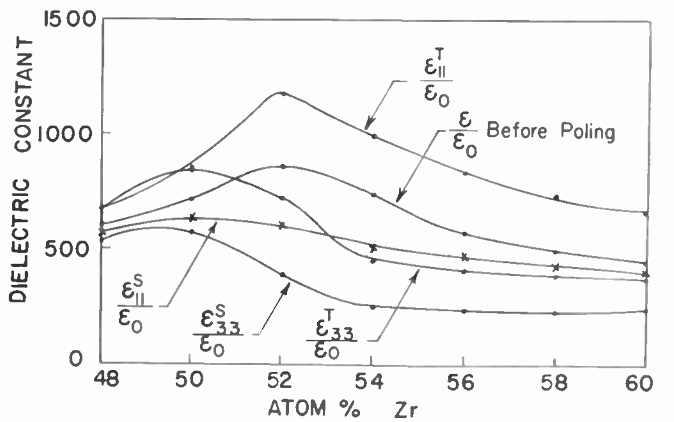

Fig. 4—Variation of dielectric constants with atom per cent Zr^{4+} in $Pb(Zr, Ti)O_3$.

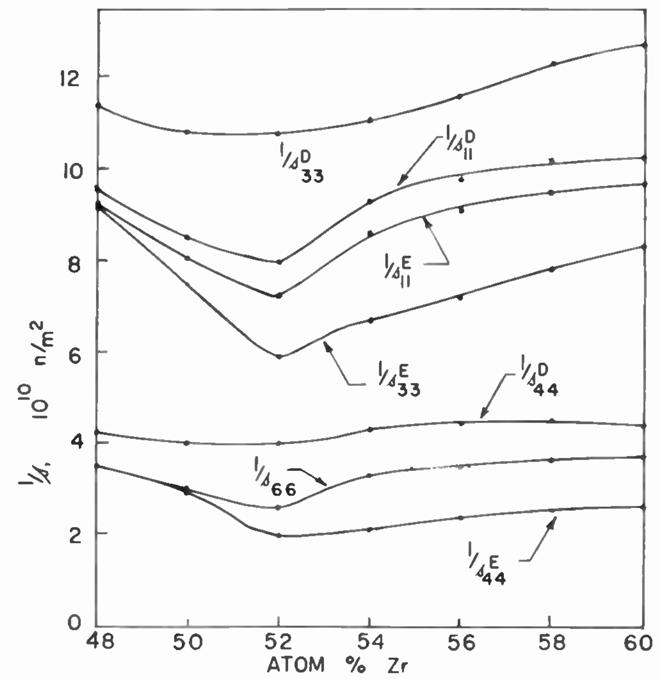

Fig. 5—Variation of elastic compliances with atom per cent Zr^{4+} in $Pb(Zr, Ti)O_3$.

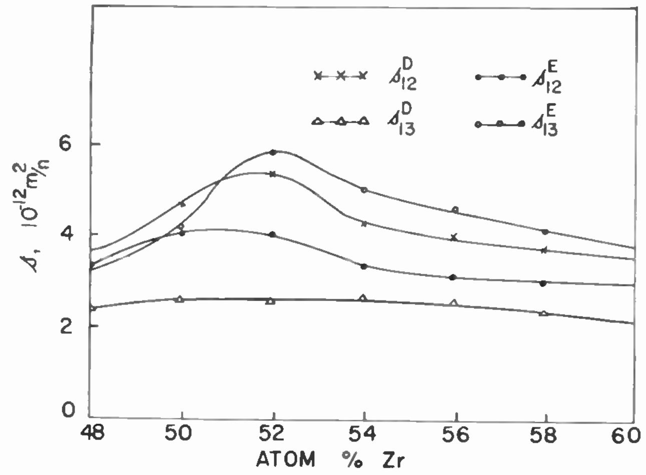

Fig. 6—Variation of elastic compliances with atom per cent Zr^{4+} in $Pb(Zr, Ti)O_3$.

thorhombic phase is favored. With barium titanate ceramics this effect is not maintained upon removal of the electric field, but a remanent effect in lead titanate zirconate may be explained by the much larger energy involved in the poling process.

The dielectric anisotropy of poled lead titanate zirconate is clearly demonstrated in Fig. 7, where the ratios $\epsilon_{11}{}^T/\epsilon_{33}{}^T$ and $\epsilon_{11}{}^S/\epsilon_{33}{}^S$ are plotted. Peak values occur at 54/46, the limiting rhombohedral composition, and there is relatively little dielectric anisotropy in the tetragonal 48/52 and 50/50 compositions. Table II lists the dielectric anisotropy ratios for typical tetragonal and rhombohedral lead titanate zirconate compositions and for single crystal[16] and ceramic[17] barium titanate.

The elastic constants of the lead titanate zirconate compositions are shown in Fig. 5, and the elastic anisotropy ratios are plotted as functions of composition in Fig. 8. Again the greatest anisotropy was obtained with the 54/46 limiting rhombohedral composition, and the tetragonal compositions show relatively little anisotropy. Table II lists elastic anisotropy ratios for typical tetragonal and rhombohedral lead titanate zirconate, and for single crystal and ceramic barium titanate. Barium titanate ceramic is in this respect quite similar to the $PbZr_{.50}Ti_{.50}O_3$ composition, but the two lead titanate zirconate compositions listed in Table II are markedly different.

With ceramic barium titanate 90° domain reorientation is only about 12 per cent complete in poled specimens, but 180° reorientation is virtually perfect.[18] The elastic and dielectric anisotropies of the ceramics are markedly less than in a single-domain crystal, just as would be expected with very little 90° reorientation. With the limiting tetragonal lead titanate zirconate composition, on the other hand, 90° domain reorientation is about 44 per cent complete,[18] and elastic and dielectric anisotropies are relatively high. Elastic and dielectric data have not yet been obtained on single domain lead titanate zirconate crystals, so a comparison cannot be made. The poled rhombohedral ceramics have the greater anisotropy in spite of the smaller distortion of the crystal from cubic symmetry. It has generally been found that 180° domain reorientation is virtually complete, and this is not affected by crystal distortion. Switching by other than 180° accounts for the elastic and dielectric anisotropy, and the smaller distortion and greater number of degrees of freedom in the rhombohedral material allow more complete reorientation of this type than in the tetragonal ceramic.

The piezoelectric constants d_{33}, d_{31}, and d_{15} have peak values at the limiting tetragonal composition, but the peak values of g_{33}, g_{31}, and g_{15} occur at the limiting rhombohedral composition (Figs. 2 and 3). It is interesting to note that in all cases $g_{15} \sim g_{33} - g_{31}$, as pre-

[16] D. Berlincourt and H. Jaffe, "Elastic and piezoelectric coefficients of single-crystal barium titanate," *Phys. Rev.*, vol. 111, pp. 143–148; July 1, 1958.

[17] R. Bechmann, "Elastic, piezoelectric, and dielectric constants of polarized barium titanate ceramics and some applications of the piezoelectric equations," *J. Acoust. Soc. Amer.*, vol. 28, pp. 347–350; May, 1956.

[18] D. Berlincourt and H. H. A. Krueger, "Domain processes in lead titanate zirconate and barium titanate ceramics," to be published in *J. Appl. Phys.*

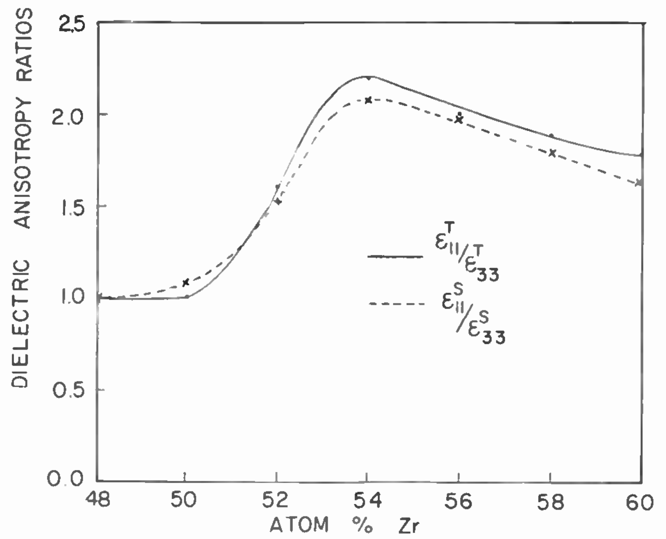

Fig. 7—Variation of dielectric anisotrophy ratios with atom per cent Zr^{4+} in $Pb(Zr, Ti)O_3$.

TABLE II
ANISOTROPY RATIOS

Composition	$\epsilon_{11}^T / \epsilon_{33}^T$	$\epsilon_{11}^S / \epsilon_{33}^S$	s_{33}^E / s_{11}^E	s_{33}^D / s_{11}^D	s_{44}^E / s_{66}	s_{44}^D / s_{66}	s_{13}^E / s_{12}^E	s_{13}^D / s_{12}^D
$PbZr_{.50}Ti_{.50}O_3$	1.01	1.08	1.07	0.80	1.00	0.75	0.96	0.55
$PbZr_{.56}Ti_{.44}O_3$	1.99	1.94	1.27	0.85	1.40	0.80	1.44	0.64
$BaTiO_3$ (ceramic)[17]	0.86	0.90	1.04	0.83	1.04	0.82	1.09	0.66
$BaTiO_3$ (crystal)[56]	17.4	18.1	1.95	1.49	2.08	1.40	2.32	1.03

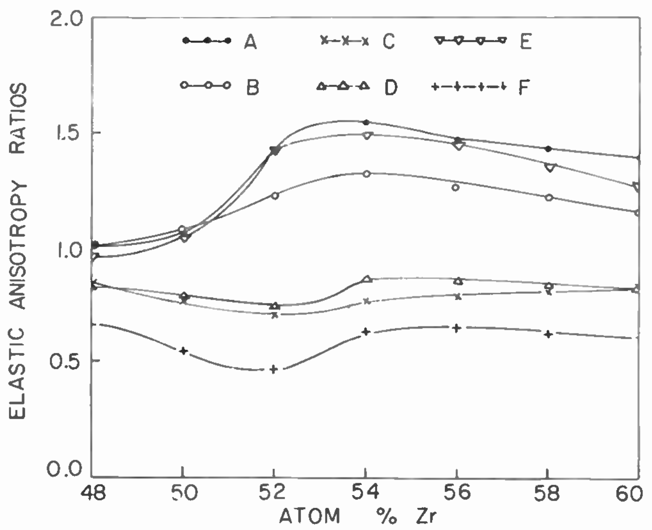

Fig. 8—Variation of elastic anisotropy ratios with atom per cent Zr^{4+} in $Pb(Zr, Ti)O_3$; $A = s_{44}^E/s_{66}$, $B = s_{33}^E/s_{11}^E$, $C = s_{44}^D/s_{66}$, $D = s_{33}^D/s_{11}^D$, $E = s_{13}^E/s_{12}^E$, $F = s_{13}^D/s_{12}^D$.

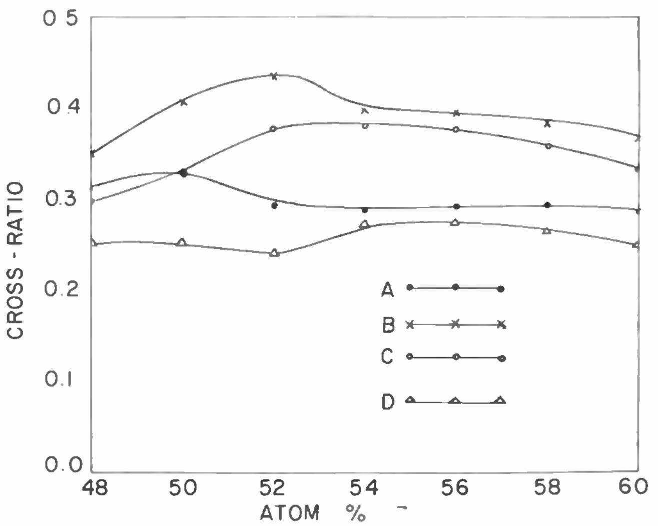

Fig. 9—Variation of elastic cross-ratios with atom per cent Zr^{4+} in $Pb(Zr, Ti)O_3$; $A = -s_{12}^E/s_{11}^E$, $B = -s_{12}^D/s_{11}^D$, $C = -s_{13}^E/\sqrt{s_{11}^E s_{33}^E}$, $D = -s_{13}^D/\sqrt{s_{11}^D s_{33}^D}$.

dicted by Jaffe[19] and Mason.[20] Baerwald[21] later derived an expression which showed that g_{15} should differ from the sum $g_{33}-g_{31}$ by a term proportional to P_0^2. He pointed out that one would expect this term to be positive. This has always been the case with barium titanate and tetragonal lead titanate zirconate, but with most rhombohedral lead titanate zirconate the term is negative (see Fig. 2).

As a check on the measured value of ϵ_{33}^S, a value was calculated using the free permittivity ϵ_{33}^T, the piezoelectric constants d_{33} and d_{31}, and the elastic compliances s_{13}^E, s_{33}^E, s_{11}^E, and s_{12}^E, using the following expression:[16]

$$\epsilon_{33}^T - \epsilon_{33}^S = \frac{2d_{31}^2 s_{33}^E + d_{33}^2(s_{11}^E + s_{12}^E) - 4d_{31}d_{33}s_{13}^E}{(s_{11}^E + s_{12}^E)s_{33}^E - 2(s_{13}^E)^2}. \quad (15)$$

The calculated value is included in Table I along with the measured value.

The electrical quality factor Q_E listed in Table I and plotted in Fig. 10 is the reciprocal of the dissipation factor obtained from bridge measurements at 1 kc and about 1 volt/mm. The mechanical quality factor Q_M was determined from resistance R at resonance of the thin disks by the relation

$$1/Q_M = 2\pi f_r RC(f_a^2 - f_r^2)/f_a^2, \quad (16)$$

where C is the low frequency (1 kc) capacitance.

It will be noted that both electrical and mechanical Q factors are higher on the tetragonal side of the phase boundary. The closest approach between electrical and mechanical Q factors occurs near the phase boundary, where the coupling between electrical and mechanical effects is highest. The mechanical Q is not the same for different modes, and may be expected to be lower for a shear than for the planar extensional mode used here.

B. Total Ferroelectric Moment

The total ferroelectric moments of the lead titanate zirconate compositions are listed in Table I. They were obtained by a measurement of short-circuit charge resulting from high compressive stress along the polar axis. The values listed were measured during stress application to 58,000 psi, a stress sufficient to cause substantially complete depolarization. With barium titanate ceramic it is also possible to determine the total ferroelectric moment by means of charge-field hysteresis loops or by measurement of total charges released on heating through the Curie point. In practice it is not possible to obtain meaningful data with lead titanate zirconate from hysteresis loops because of the extremely high coercive fields at room temperature. At temperatures high enough so that the coercivity is sufficiently low, the volume resistivity is not high enough to prevent leakage, so hysteresis loops are of poor quality. As will be discussed shortly, measurement of total charges released on heating through the Curie point does not give a meaningful result for the total polarization in these ceramics, due to anomalous dielectric charges which flow above about 150°C. These anomalous charges total about one order of magnitude greater than the true ferroelectric charges.

Typical curves showing released charge as a function of compressive axial stress are shown in Fig. 11. It will be noted that total charges released were much higher for the lead titanate zirconate compositions than for barium titanate. Fig. 12 shows released charges at various levels of stress as a function of composition. It will be noted that the highest ferroelectric moment was obtained with the rhombohedral 56/44 composition. This is again probably due to more complete domain alignment in the rhombohedral compositions. As mentioned before, the crystal distortion is higher in the tetragonal compositions, and would as such favor higher polarization in an equally aligned tetragonal composition.

C. Pyroelectric Measurements

Temperature variations severely affect the magnitude of the polarization both through a change in domain alignment and a change in the spontaneous polarization of individual domains. These changes are particularly severe in temperature ranges in which crystal symmetry is altered. Barium titanate ceramics, for instance, suffer a severe loss of charge as the temperature is increased through the orthorhombic-tetragonal transition near 15°C.[22] As the temperature rises through the Curie point, substantially all ferroelectric charges are irreversibly released. With lead titanate zirconate there are no phase transitions from −200°C to the Curie point. There are, however, anomalous dielectric charges, which begin to flow above about 100 to 150°C. In Fig. 13 ferroelectric currents are shown as positive. Near 150°C the current began to decrease and at about 230°C the current actually reversed. The anomalous charges flowing in the temperature range 25° to 400°C amounted to about 1000 μcoul/cm², over twenty times the ferroelectric polarization. Charge flow above the Curie point has also been observed with poled barium titanate ceramic (Fig. 14). Here anomalous charge flow began at about 270°C, and total anomalous charges were over an order of magnitude greater than the ferroelectric polarization.

With lead titanate zirconate charge flow up to 130°C is quantitatively reversed on cooling, and this flow of

[19] H. Jaffe, "Volume electrostriction in barium titanate ceramics," *Phys. Rev.*, vol. 73, p. 1261; May 15, 1948.

[20] W. P. Mason, "Electrostrictive effect in barium titanate ceramics," *Phys. Rev.*, vol. 74, pp. 1134–1147; November 1, 1948.

[21] H. G. Baerwald, "Thermodynamic theory of ferroelectric ceramics," *Phys. Rev.*, vol. 105, pp. 480–486; January 15, 1957.

[22] D. Berlincourt, "Recent developments in ferroelectric transducer materials," IRE Trans. on Ultrasonics Engineering, vol. 4, pp. 53–65; August, 1956.

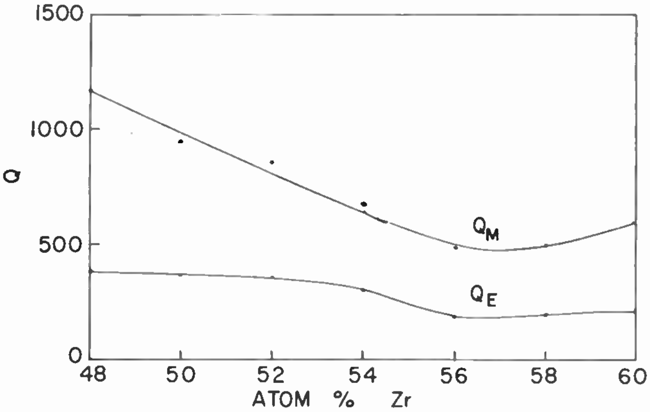

Fig. 10—Variation of mechanical and electrical Q factors with atom per cent Zr^{4+} in Pb(Zr, Ti)O_3.

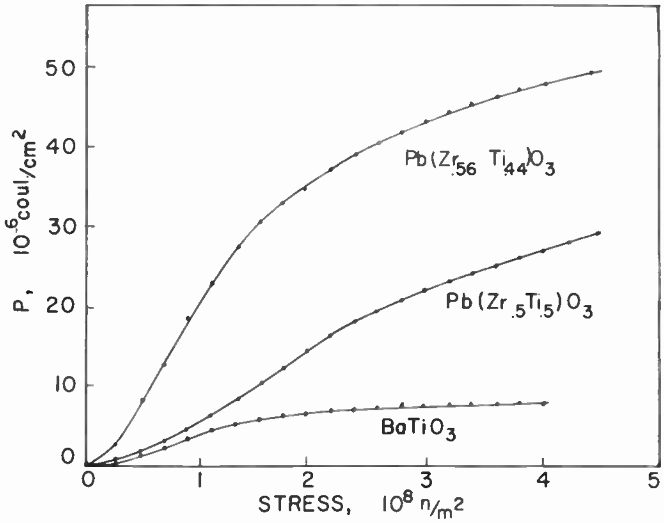

Fig. 11—Short-circuit charge vs stress parallel to polar axis, $PbZr_{.53}Ti_{.47}O_3$, $PbZr_{.56}Ti_{.44}O_3$, and $BaTiO_3$.

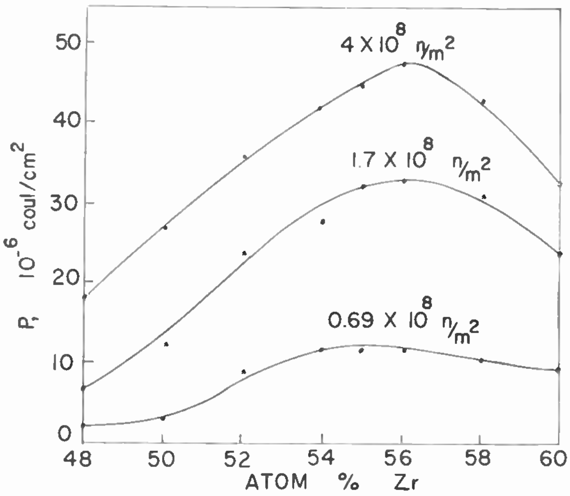

Fig. 12—Variation of short-circuit charge with atom per cent Zr^{4+} in Pb(Zr, Ti)O_3.

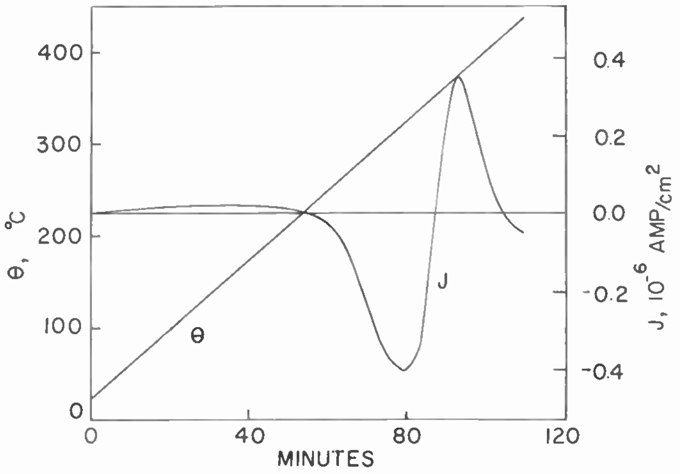

Fig. 13—Variation of discharge current and temperature with time for slowly heated $PbZr_{.53}Ti_{.47}O_3$ disk.

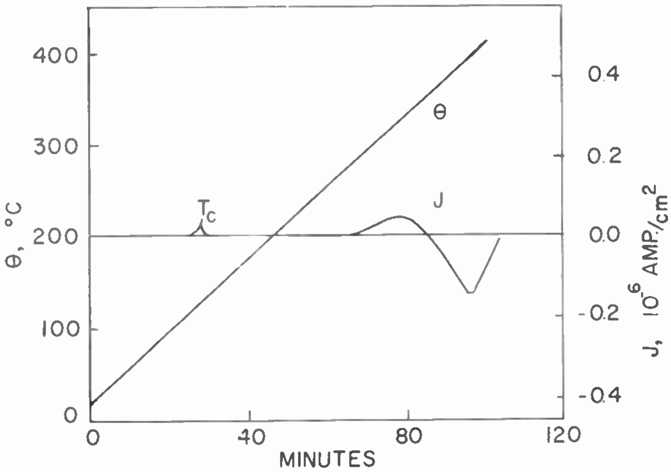

Fig. 14—Variation of discharge current and temperature with time for slowly heated $BaTiO_3$ disk.

charges of alternate polarity on heating and cooling can be repeated indefinitely. This is not the case at higher temperatures. Thus there is an experimental distinction between pyroelectric and anomalous dielectric charge flow.

Modified lead titanate zirconate compositions recently developed begin to release substantial anomalous charges only above about 350°C, and in this case the total ferroelectric charge may be determined from integrated current flow. These modified lead titanate zirconate ceramics have volume resistivity about two and one-half orders of magnitude higher than the unmodified material above 100°C, and with both the modified and unmodified compositions anomalous charge flow occurs only at temperatures above which the volume resistivity drops below about 10^9 ohm cm. These modified compositions have markedly reduced coercivity as well, and the ferroelectric polarization may, therefore, be determined from charge-field hysteresis loops. With these compositions there has been very close agreement between the three methods used in measuring the total ferroelectric moment.

IV. Acknowledgment

The authors wish to thank F. Brunarski for the preparation of numerous test specimens and some of the measurements reported, and B. Jaffe for the pyroelectric measurements. We also gratefully acknowledge the continued interest of Dr. G. W. Anderson and Dr. F. Nielson of Sandia Corp., Albuquerque, N.Mex.

Further Consideration of Bulk Lifetime Measurement with a Microwave Electrodeless Technique*

H. JACOBS†, A. P. RAMSA‡, AND F. A. BRAND†, MEMBER, IRE

Summary—A new method for measurement of the lifetime of excess carriers in semiconductors is described. Using a steady light source and measuring changes in microwave power absorption as a function of position of the sample in a waveguide, bulk lifetime can be determined. Measurements described here were made at 9600 mc. The new technique offers the following advantages: First, the method does not require electrode attachments, thus making the preparation of the samples less difficult and the actual experiment less subject to error due to non-ohmic contacts. Second, the effects of surface recombination are made less important, thus giving a greater assurace of the evalaution of bulk lifetime.

Introduction

When equilibrium conditions in a semiconductor are disturbed due to the presence of light, heat, or injected current carriers, and the source of disturbance is removed, a finite amount of time is required for equilibrium to be established again. For instance, in the case of a pulse of light incident upon germanium, excess holes and electrons are created. After the light is removed, it is generally found that recombination occurs in an exponential manner until equilibrium is restored. The time for the carrier density to be reduced to e^{-1} of its maximum value is defined as the lifetime.

Quite recently, a pulsed-light electrodeless technique for lifetime measurements was disclosed.[1] As shown in Figs. 1 and 2, a germanium sample was inserted in a waveguide in such a manner that light and microwave radiation would fall on the sample simultaneously. As light was removed from the surface the decay in conductivity could be measured by the decay in microwave absorption of the sample. Following this, correlation was established between the standard photoconductive decay methods and the electrodeless microwave method. In what follows, we shall call the latter method of measurement the pulsed light microwave electrodeless technique. It has certain advantages: first, no contacts are required at the ends of the sample, and second, a considerable range of lifetimes can be studied. With this technique, however, we are still concerned with a problem common to the photoconductive decay techniques; that is, the role of the surface.

In lifetime determinations the role of the surface is often ambiguous. In the work of Stevenson and Keyes,[2] and in reports by Shockley,[3] it is shown that for a rec-

* Original manuscript received by the IRE, June 11, 1959; revised manuscript received, August 25, 1959.

† U. S. Army Signal Res. and Dev. Lab., Ft. Monmouth, N. J.
‡ Monmouth College, West Long Branch, N. J.

[1] A. P. Ramsa, H. Jacobs, and F. A. Brand, "Microwave techniques in measurement of lifetime in germanium," 1959 IRE National Convention Record, pt. 3, pp. 159–168.

[2] D. T. Stevenson and R. J. Keyes, "Measurement of carrier lifetimes in germanium and silicon," *J. Appl. Phys.*, vol. 26, pp. 190–195; February, 1955.

[3] W. Shockley, "Electrons and Holes in Semiconductors," D. Van Nostrand Co., Inc., N. Y. p. 323; 1950.

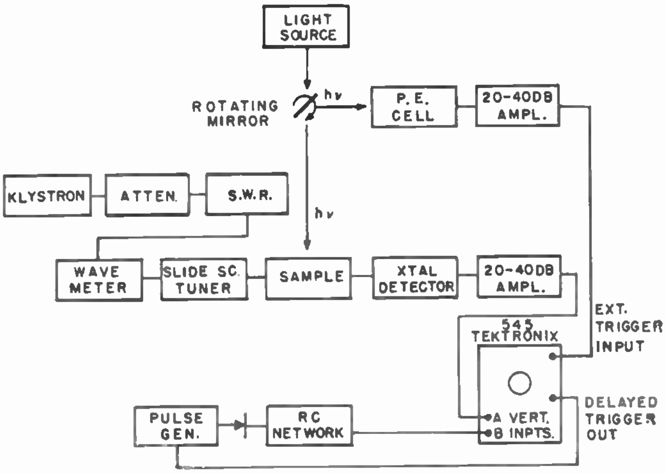

Fig. 1—Schematic arrangement for the measurement of lieftime by pulsed-light microwave electrodeless technique. This arrangement allows for a comparison with the time constant of an RC network to facilitate measurement of lifetime.

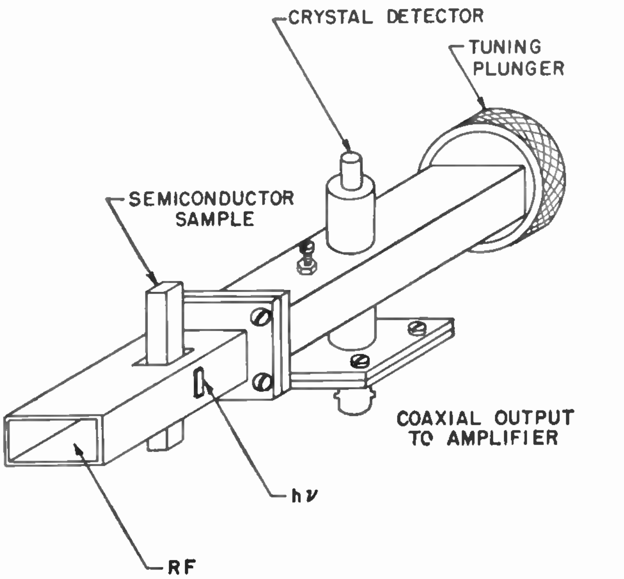

Fig. 2—Arrangement of a sample in a holder for the measurement of lifetime by pulsed-light microwave electrodeless technique. The light from a projector lamp and rotating mirror injects excess carriers in the germanium sample, thus resulting in a decrease in power as measured with a crystal detector. The recovery time after cessation of the light pulse is then used as a measure of lifetime.

tangular cross-section rod with uniform distribution of excess carriers,

$$1/\tau_{pl} = 1/\tau_p + \nu_s, \tag{1}$$

where τ_{pl} is the measured lifetime, τ_p is the bulk lifetime, and ν_s is a term due to surface recombination. In addition,

$$\nu_s = \left(\frac{\pi^2 D_p}{4}\right)\left(\frac{1}{B^2}+\frac{1}{C^2}\right), \qquad S \to \infty \tag{2}$$

where $2B$ and $2C$ are the cross sectional dimensions of the sample, D_p is the diffusion constant and S is the surface recombination velocity. For the case of $S \to 0$,

$$\nu_s = S(1/B + 1/C). \tag{3}$$

In the case of the experiments involving pulsed light and photoconductive decay, the assumption of uniform injected carrier distribution is not valid. The excess carrier concentration distribution may fall off exponentially with distance due to the absorption of light. Hence, empirical methods must be used to determine ν_s; *i.e.*, changing the nature of the surface, or increasing the size of the sample. Even this, however, does not provide data which can always be applied to (2) and (3) because it can be shown experimentally that most of the light is usually absorbed very near the surface facing the light and no matter how large the sample is, an appreciable amount of the carriers can diffuse out to the surface region and recombine there instead of in the bulk.

It appears that the photoconductive decay methods of measuring lifetime, as described above, may be approximately correct if the surface has a low recombination velocity. One way of showing this is by considering the ratio of surface recombination current to bulk current. If this ratio is small, it can be assumed that most of the carriers are in the volume, and the techniques described above are valid. Calculations can be carried out as follows:

$$I_s = qp_sS, \tag{4}$$

and

$$I_p = qp_sD_p/L_p. \tag{5}$$

Combining these, the ratio is

$$\frac{I_s}{I_p} = \frac{L_pS}{D_p} \tag{6}$$

where I_s is surface recombination current, I_p is bulk hole current directed in and away from the surface, p_s is excess hole density on the surface due to light, D_p is the diffusion constant for holes, and L_p is the diffusion length.

For a lifetime of 200 μsec and $S = 100$, the ratio I_s/I_p is in the order of 0.2, and this indicates that lifetime measurements describe bulk properties, particularly if the volume to surface ratio of the crystal is so high that varying the sample size does not change the resulting values as determined by the experiments.

There is still, however, a possible error if the surface recombination velocity is higher than the assumed value. For this reason, when measuring lifetime, it is best to try to eliminate surface recombination as much as possible.

To circumvent surface recombination, Blakemore[4] used a series of very thick silicon filters so that the light that penetrated the filters would go to an appreciable depth in the silicon sample tested. This technique requires a high degree of amplification and is subject to small amounts of light leakage. In the method to be described, the more realistic assumption is made that with visible light all of the carriers are indeed generated

[4] J. S. Blakemore, "Lifetime in *p*-type silicon," *Phys. Rev.*, vol. 110, pp. 1301–1308; June 15, 1958.

in the region just next to the surface itself and as time progresses diffusion allows carriers to enter the bulk.

With this assumption, we shall describe a method of approximating the bulk lifetime in a manner which is relatively independent of the surface recombination velocity relating to the surface facing the light. In addition, we shall show that an electrodeless method of lifetime measurement can be combined in the proposed procedure.

Experimental Method

Assume that the sample is arranged as shown in Figs. 3 and 4. The light source is steady, and in electrical terms can be called a dc light source. The light beam itself is assumed to be comprised of parallel rays. The monitored microwave generator supplied a square wave modulation of the microwave energy transmitted through the sample. Measurements were made during the course of the experiment of the change in absorption of microwave energy as a function of the distance "d" which the surface of the semiconductor extends out of the waveguide. It is assumed that under the dc light conditions, the excess carriers decreased exponentially with distance from the surface facing the light.

It is assumed further that the excess minority carrier density is given by

$$p = p_s e^{-kx} \tag{7}$$

where p is the excess density, p_s is the surface excess density, and $k = 1/L_p$ is the reciprocal of the diffusion length. The total number of excess carriers in the waveguide (region of interaction with the microwave) is

$$p' = \int_d^\infty p dx = p_s \int_d^\infty e^{-kx} dx$$

$$= -\frac{p_s}{k} e^{-kx}\Big]_d^\infty \tag{8}$$

and

$$p' = Ke^{-kd}, \tag{9}$$

where $K = p_s L_p$ and p' is the total number of excess carriers. The plane d is the distance from the end of the semiconductor to the plane of the waveguide. Hence if the light source is kept at a constant level, variations of the distance the sample extends from the waveguide should produce a change in the total number p'.

It is assumed the p' is linearly related to the change in power absorbed, A, for small increments. In considering the ln of both sides of (9) and plotting ln A vs d, we should expect a straight line. The slope here should be $-k$ or $-1/L_p$.

In determining L_p experimentally, and using the relation

$$L_p = \sqrt{D_p \tau_p}, \tag{10}$$

we can determine the lifetime τ. This technique has several advantages and several possible pitfalls. On the

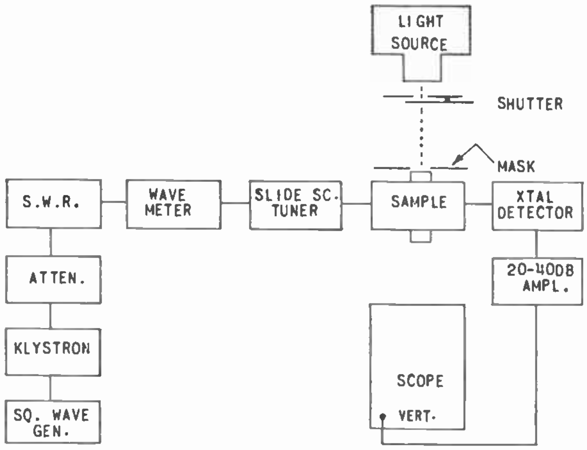

Fig. 3—Schematic arrangement for the measurement of lifetime by dc light microwave electrodeless technique. Klystron source supplies a square wave 1000 cycles per second. Changing the position of this sample causes little or no change in attenuation with the light off. However, with the light on, the change in power absorbed increases as the surface facing the light approaches the waveguide surface. All measurements were made at 9600 mc per second.

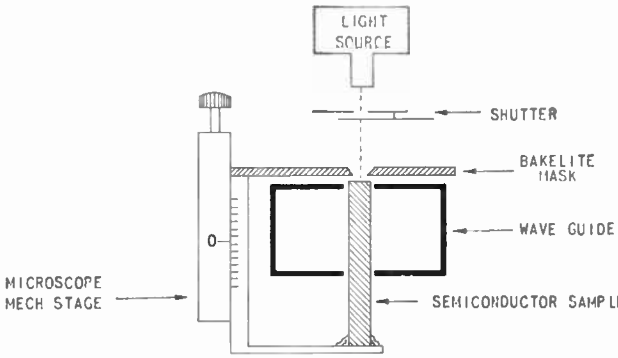

Fig. 4—Arrangement of a germanium sample in a holder for the measurement of lifetime by dc light microwave electrodeless technique. The distance d is the measured distance from the end of the sample to the upper surface of the waveguide. In the experiment, the change of absorption due to the presence of light is measured as a function of this distance.

advantageous side we can list the following factors. First, we have here a new electrodeless technique for the measurement of lifetime. We shall refer to this as the dc light microwave electrodeless method of lifetime measurement. Second, and most important, if the surface facing the light should have a high surface recombination velocity and, hence, have a dominant role in the lifetime characteristics, the dc light source will cancel out the effect of recombination on this surface. With this technique, since it is steady state in nature, it is only assumed that the decay is exponential with distance into the bulk. The absolute value of the excess carrier density at the surface is not critical because in the equations used we assumed only that the surface density was constant. The dc light microwave electrodeless method of lifetime measurement will thus measure lifetime resulting from recombination primarily in the bulk and in some cases, and to a lesser extent, recombination on the surfaces other than the surface facing the light.

In making comparisons of the two methods, we should expect that using the dc light source should give values approximately equal to the values of lifetime obtained by pulsed light methods when the surface recombination velocity is low. However, when surface recombination velocities are high, we should expect the dc light source method to give lifetime values higher than the pulse light method since the latter is more subject to surface domination. In addition, we might consider the new technique as a check on samples previously measured by more conventional means such as the photoconductive decay method or the newer pulsed-light electrodeless method. This would provide greater assurance that the measurements were bulk dominated rather than affected by the surface.

The disadvantage of the proposed method is that the distance at which the microwave electric field is practically zero and attains a maximum is not as clearly defined as would be desirable. Hence measurements were necessarily made on long lifetime samples, so that even if this region is not a sharp line, the lack of definition would not be a critical factor. Experiments were carried out with samples of various lifetime to assure the fact that the region of uncertainty of d was small compared to the diffusion length.

Experimental Data

Experiments were arranged as indicated in Figs. 3 and 4. Samples of germanium which were 3.5 mm wide by 3.5 mm thick and 3 cm long were tried. In Table I we have indicated the data obtained. In arriving at the data in Table I, the column referring to the pulsed light source contains data measured directly by experiment. The data in the column referring to the dc light source was computed as follows. Experiments were conducted, with results indicated in Figs. 5 and 6, where the logarithm of the changes in absorption is plotted against the distance from the end of the sample to the upper waveguide walls. From these plots the slopes were computed giving $1/L$. Having determined L by experiment, τ was computed using the relationship $L^2=D\tau$. The question arises as to what value of D to choose. Since the samples used were measured at a resistivity of 42.8 ohm cm at room temperature, the germanium crystal was assumed to be intrinsic. Hence the ambipolar diffusion constant of $D=60.3$ was used, assuming $D_n=96$ and $D_p=44$. Using the value of $D=60.3$, τ was calculated. It can be observed that where the surface processing was such as to give low surface recombination velocities both methods gave good agreement. However, when the surface recombination velocity was increased by exposure to ammonia vapor, the dc light source method gave slightly longer values of lifetime than the pulsed light source technique, as was predicted.

In the course of these experiments, an assumption is made that the power absorbed is linearly related to the number of carriers in the semiconductor portion located in the waveguide. This is further explained in the Appendix. The skin depth for a sample of the resistivity stated and at 9600 mc per second has been calculated to be approximately one centimeter. This corresponds to the equilibrium condition of no excess minority carriers. Since the sample dimensions were about one third of this distance, the assumption was made that the sample was "viewed" homogeneously by the microwave field. In addition, the excess carrier density added to the specimen by incident light must be small, and hence the change in power absorbed was as small as practicable from a measurements viewpoint.

TABLE I*

Experimental Data

Sample 90 AE 42.8 ohm cm Germanium Run Number	Surface Treatment	Lifetime in Seconds using Electrodeless Technique with Continuous Light Source	Lifetime in Seconds using Electrodeless Technique with Pulsed Light Source
A	CP4 etched and distilled water washed. Exposure to air 24 hours	1.45×10^{-3}	$1.2\ \times10^{-3}$
B	Repeat A	1.45×10^{-3}	$1.2\ \times10^{-3}$
E	Repeat A	1.65×10^{-3} to $2.7\ \times10^{-3}$	$2.0\ \times10^{-3}$
K	Repeat A	1.80×10^{-3}	$1.3\ \times10^{-3}$
M	Following procedure A, the sample was exposed to ammonia vapor and then exposed to air for several hours	1.57×10^{-3}	0.88×10^{-3}
N	Second test after M	1.49×10^{-3}	0.88×10^{-3}
O	After N, sample was allowed to stand in air for 48 hours	1.85×10^{-3}	0.97×10^{-3}
S	Sample in O exposed to air another 48 hours	2.30×10^{-3}	0.97×10^{-3}
T	Sample CP4 etched again and exposed to air for 48 hours	1.40×10^{-3} to 2.24×10^{-3}	1.75×10^{-3}

* Note the same sample is used in all cases. In the first four runs listed in the table, with low lifetime surfaces, there is good agreement in the dc light microwave electrodeless technique and in the pulsed light microwave electrodeless technique. As the surface is contaminated by the ammonia, the dc light technique gives longer values of lifetime as predicted since this method more accurately measures bulk lifetime. In the last step (T) the sample was again surface cleaned and the agreement in the two techniques reappears. It should be noted that the ambipolar diffusion constant was used. Calculations indicate that for material of this specific resistivity, $D=60.3$. In using a different resistivity specimen, it is necessary to recalculate the diffusion constant based upon the resistivity and type of semiconductor in order to interpret the slope correctly in terms of lifetime.

Conclusion

A variation of the microwave electrodeless method of measurement of lifetime using dc light has been de-

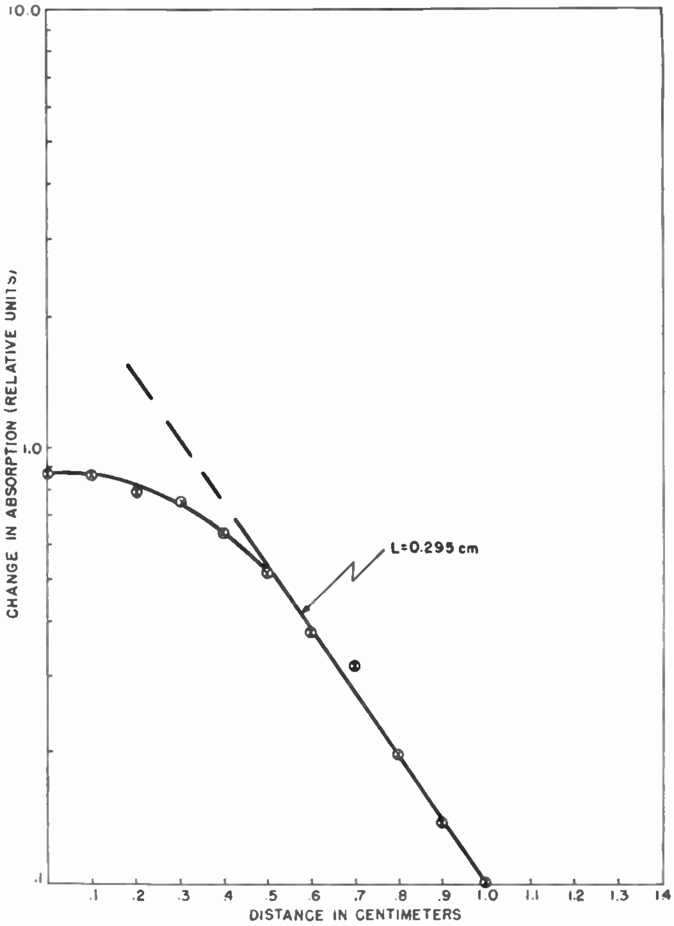

Fig. 5—Experimental data giving the change in the absorption of microwave power as a function of *d*. In considering the region where ln *A* changes linearly with *d*, the following parameters can be obtained: $L=0.295$ cm, $\tau=1.45$ msec.

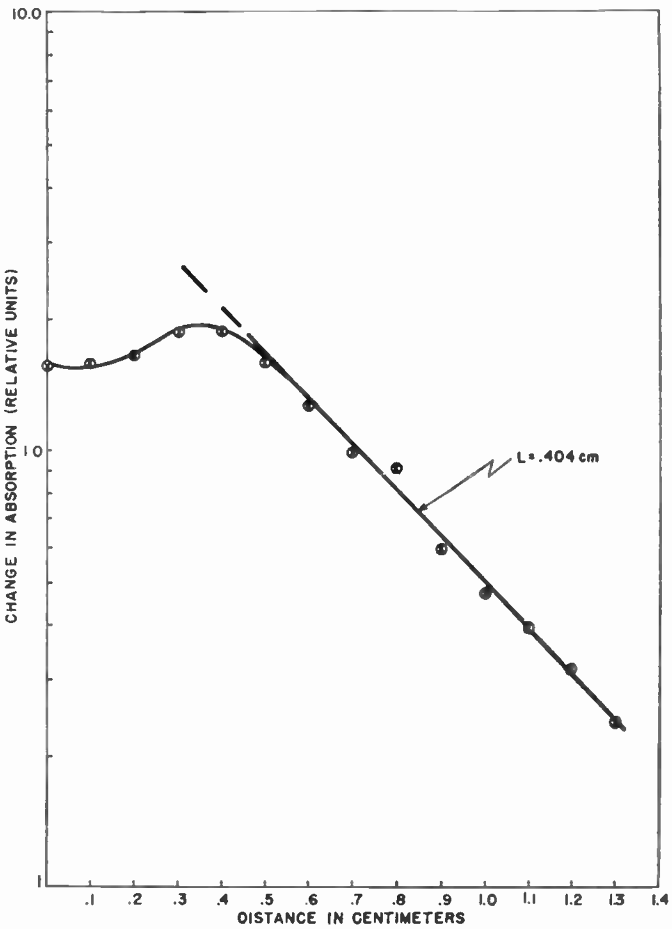

Fig. 6—Experimental data giving the change in the absorption of microwave power as a function of *d*. In considering the region where ln *A* changes linearly with *d*, the following parameters can be obtained: $L=0.404$ cm, $\tau=2.50$ seconds.

scribed. This technique is advantageous in that no contacts are required at the ends of the semiconductor sample. In addition, it is less sensitive to surface recombination velocities than previously described techniques such as the more conventional photoconductive decay method or the pulsed light microwave electrodeless method. Finally, in carrying out these experiments, an independent check was made on the values of lifetime determined by earlier methods.

Appendix

Linear Relationship in Power Absorbed and Conductivity

In measuring lifetime during the course of the experiment, the technique involved moving the sample in various measured positions and determining the power transmitted with the light on, and off. The difference in power transmitted was attributed to injected carriers.

In mathematical language this gives

$$P = P_0 e^{-a_0 x} \qquad (1)$$

with the light off, and

$$P' = P_0 e^{-a_0(1+c)x} \qquad (2)$$

with the light on.

Assume now that a_0 is constant, as is x and P_0. The change in power transmitted due to the incident light is $P-P'$. That is,

$$P - P' = P_0 e^{-a_0 x}\left[1 - e^{-a_0 c x}\right]. \qquad (3)$$

If $a_0 cx$ is small, the exponential can be expanded and, retaining only the second term,

$$P - P' = P_0 e^{-a_0 x}\left[a_0 c x\right]. \qquad (4)$$

Thus, if the change in absorption is small, the term $P-P'$ will be linearly related to c. Furthermore, the attenuation constant is linearly related to conductivity and, hence, the total number of carriers in a given volume providing $\sigma < \omega\epsilon$.

Combining these relationships, the change in power transmitted is linearly related to the change in the total number of carriers in the volume of the waveguide.

Acknowledgment

The authors wish to thank Dr. G. Goubau of the U. S. Army Signal Research and Development Laboratory, Fort Monmouth, N. J. for his advice, and Dr. W. Caldwell of Bendix Aviation Corporation, Long Branch, N. J. for furnishing samples of highly perfect germanium crystals.

The Application of Linear Servo Theory to the Design of AGC Loops*

W. K. VICTOR† AND M. H. BROCKMAN†

Summary—**An analytical technique for designing automatic gain control (AGC) circuits is presented. This technique is directly applicable to high-gain high-performance radio receiving equipment. Use of this technique permits the designer to specify the performance of the AGC system completely with respect to step changes in signal level, ramp changes in signal level, frequency response, receiver gain error as a function of receiver noise, etc., before the receiver is constructed and tested. When used in conjunction with the statistical filter theory the technique has been used to synthesize optimal AGC systems when the characteristics of the signal and noise are appropriately defined.**

The mathematical derivation of the closed-loop equations is presented. The resulting expressions are simple and easy to understand by anyone acquainted with linear servo theory. Furthermore, the underlying assumptions used in theory have been tested experimentally, and the close agreement between theory and experiment attests the usefulness of the design technique.

Automatic gain control (AGC) is a closed-loop regulating system which automatically adjusts the gain of a receiver to maintain a constant signal amplitude at the receiver output. The AGC loop is normally capable of operating over a very wide range of signal input levels. When the signal is narrow-band and its amplitude is detected synchronously, the loop is capable of performing efficiently in the presence of wide-band noise. The purpose of this paper is to derive the basic equations of the AGC loop which minimize the mean square error in the estimate of receiver gain when the signal level, noise level, and transient performance are specified.

Fig. 1 is a block diagram showing the principal elements of the AGC loop with the waveform equations at various points in the loop. The desired output of the receiver is unity. The amplitude of the signal $a(t)$ is expressed as a fraction with respect to unity. The gain of the receiver is expressed as (attenuation)$^{-1}$, or $1/a^*(t)$. When $a(t)=1$, $a^*(t)=1$; the gain is unity, and the receiver output is also unity. When $a(t)=0.1$, for example, $a^*(t)=0.1$, the gain is $1/a^*(t)=10$, and the receiver output is unity. The attenuation of the receiver is introduced as a useful concept because it is the attenuation of the receiver that is required to follow the changes in signal level. The variation in attenuation of the receiver is some function of the control voltage b; thus, the receiver may be considered as a voltage-controlled attenuator. This idea is expressed in block diagram form in Fig. 2.

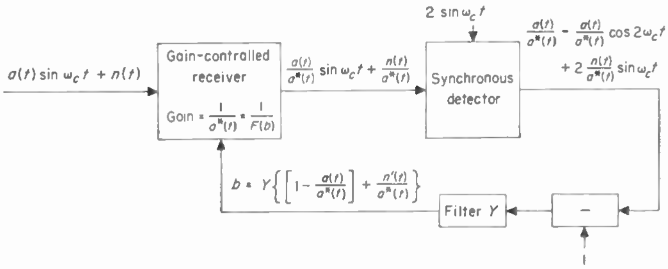

Receiver attenuation $a^*(t)$ =

$$F(b) = \text{Function } Y\left\{\left[1-\frac{a(t)}{a^*(t)}\right]+\frac{n'(t)}{a^*(t)}\right\};$$

where

$a(t)$ = amplitude of RF carrier expressed as a fractional part of unity,
ω_c = radian frequency of the carrier,
$n(t)$ = interference of flat spectral density over a range of frequencies about ω_c,
$n'(t) = n(t)[2\sin\omega_c t]$ = interference of same spectral density as $n(t)$,

$$YX(t) = \int_0^\infty y(\tau)X(t-\tau)d\tau,$$

$$y(\tau) = \text{weighting function of filter} = \frac{1}{2\pi j}\int_{-j\infty}^{+j\infty} Y(s)\epsilon^{s\tau}ds.$$

Fig. 1—Conventional AGC circuit with coherent detection.

Fig. 2 illustrates a recognition of the fact that the output of the AGC loop is the receiver attenuation $a^*(t)$ and that this output signal is required to match the input signal $a(t)$ with a minimum error. The synchronous detector is easily eliminated because it does nothing more than frequency-translate the signal and the noise $n(t)$ from the carrier frequency ω_c to zero frequency, or dc. In proceeding from Fig. 1 to Fig. 2 it should be noted that the two circuits are mathematically equivalent; the solution for the output attenuation $a^*(t)$ is

$$\text{Func } Y\left\{\left[1-\frac{a(t)}{a^*(t)}\right]+\frac{n'(t)}{a^*(t)}\right\}$$

in each case. The diagram is rearranged to provide a better understanding of what actually takes place when the loop is functioning.

The next step in the analysis is to choose a function for the variation of receiver attenuation with control voltage. If b is the control voltage (see Fig. 3), $F(b)$ is chosen to be $10K_A{}^{b/20}$; K_A is a constant associated with the attenuator (or amplifier) and has the dimension db/volt. Although $F(b)$ is highly nonlinear, it should be noted that log $F(b)$ is a linear function.

* Original manuscript received by the IRE, April 6, 1959; revised manuscript received, September 1, 1959. This paper presents the results of one phase of research carried out at the Jet Propulsion Laboratory, California Institute of Technology, under Contract No. DA-04-495-Ord 18, sponsored by the Department of the Army Ordnance Corps.

† Jet Propulsion Lab., California Inst. of Technology, Pasadena, Calif.

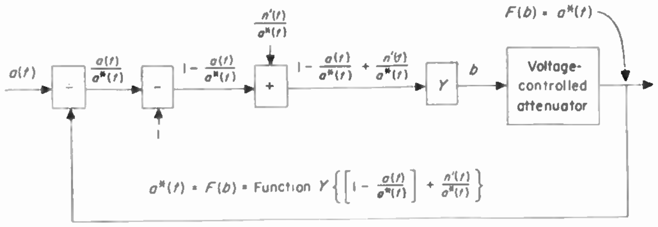

Fig. 2—Modified conventional AGC circuit.

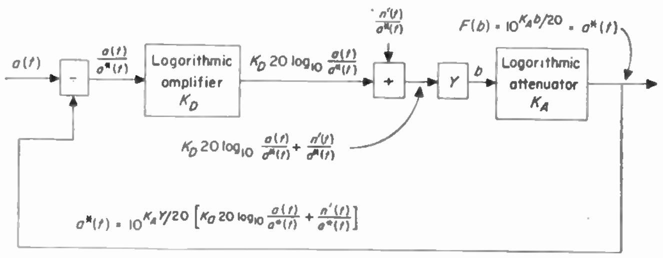

Fig. 3—Nonlinear equivalent AGC circuit.

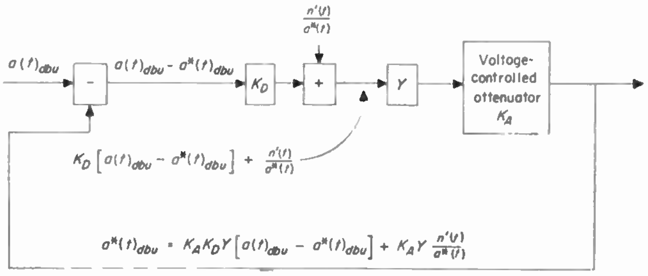

where

$$a(t)_{\text{dbu}} = 20 \log_{10} \frac{a(t)}{1} = \text{amplitude of signal expressed in db}$$

with respect to unity

$$a^*(t)_{\text{dbu}} = 20 \log_{10} \frac{a^*(t)}{1} = \text{attenuation of receiver in db}$$

with respect to unity

Fig. 4—Linear AGC system.

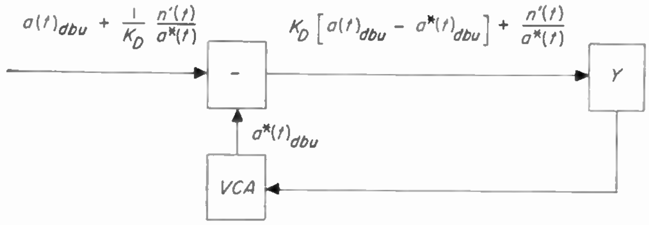

Fig. 5—Simplified linear AGC system.

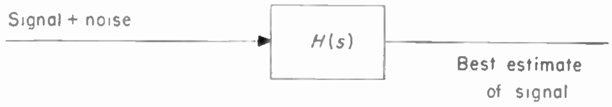

Fig. 6—Standard servo problem.

Having made the decision (see Fig. 3) that the attenuator characteristic should be linear in decibels, the function $1-a(t)/a^*(t)$ is studied and found to be approximately equal to 20 $\log_{10} a(t)/a^*(t)$ over the range of 3 db, or 30 per cent variation in $a^*(t)$. Therefore, the differencing function in Fig. 2 can be replaced by the logarithmic amplifier in Fig. 3 without altering the nature of the loop, providing the loop error does not exceed 3 db. (This limitation is similar to the requirement in automatic phase-control systems that the phase error not exceed 30°.) Within this restriction, then, Fig. 3 is a true representation of the AGC loop, and K_D is the constant associated with the logarithmic amplifier in volts/db. The equation of the loop as indicated in Fig. 3 is

$$a^*(t) = 10^{K_A Y/20}\left[K_D 20 \log_{10} \frac{a(t)}{a^*(t)} + \frac{n'(t)}{a^*(t)}\right].$$

This equation can be solved for $a^*(t)$ by taking the logarithm of both sides and, for convenience, expressing the answer in decibels relative to unity. When this is done

$$a^*(t)_{\text{dbu}} = K_D K_A Y[a(t)_{\text{dbu}} - a^*(t)_{\text{dbu}}] + K_A Y \frac{n'(t)}{a^*(t)}.$$

It is now apparent that when the signal level and the receiver attenuation are expressed as a logarithm, the AGC loop becomes a linear system. This system is shown in Fig. 4 and may be simplified still further to the system shown in Fig. 5. The problem has been reduced to the standard servo problem indicated in Fig. 6 and can be solved for the $H(s)$ which gives the minimum rms error in receiver gain.

This problem has been solved using the Weiner methods outlined in a previous paper.[1] The input signal was

[1] E. Rechtin, "The Design of Optimum Linear Systems," Jet Propulsion Lab., California Inst. Tech., Pasadena, Calif., External Publication No. 204; April, 1953.

assumed to be in the form of small step changes in amplitude. The transient error was defined as the infinite time integral of the squared error:

$$\text{transient error} = \int_0^\infty [a(t)_{\text{dbu}} - a^*(t)_{\text{dbu}}]^2 dt$$

and was assumed to be independent of the amplitude noise. The additive noise is assumed to be essentially flat over the spectrum, producing a gain-jitter, σ_N^2, which is

$$\text{gain error due to noise} = \frac{1}{2\pi j}\int_{-j\infty}^{+j\infty} |H(s)|^2 \Phi_N(s)ds.$$

The closed-loop transfer function which minimizes the gain-jitter while holding the transient error to a specified maximum value is of the form

$$H(s) = \frac{1}{1 + \dfrac{1}{K_B}s}$$

where K_B is a parameter in sec^{-1} which depends upon the amplitude step and the noise spectral density. The solution of the loop equation for filter Y yields $Y(s) = K_B/s$, a pure integrator. If the loop gain is high, $1/s$ may be approximated by $1/(1+\tau s)$, a low-pass filter. Solving for $H(s)$ yields

$$H(s) = \frac{GY(s)}{1 + GY(s)} = \frac{1}{\left(\dfrac{1}{G} + 1\right) + \dfrac{\tau}{G}s} \approx \frac{1}{1 + \dfrac{\tau}{G}s}$$

where G is the dimensionless product of K_D and K_A and is greater than 10.

To demonstrate the usefulness of the theory and the validity of the assumptions made in linearizing the loop, three experiments were performed on the AGC loop of a particular synchronous receiver.

1) The frequency response of the loop was measured using sine-wave variations in the input signal level.
2) The transient response of the loop was measured using exponential changes in the input signal level.
3) The rms error in receiver gain was measured as a function of the input-noise spectral density.

The AGC loop forming a part of this system is similar to the diagrams shown in Figs. 1 through 6. The filter Y is a low-pass filter having essentially a single time constant of 0.4 second. The loop gain has been measured at several different values of input signal level and varied from 66 for a -40-dbm signal level to 38 at -80 dbm. However, over a signal-level range of 3 to 6 db, the gain is essentially constant.

Frequency Response

Using the measured values of gain, the frequency response of the AGC loop was calculated for signal levels of -40, -60, and -80 dbm, and the curves have been plotted in Figs. 7, 8, and 9. The frequency response of the loop was then measured using a sine-wave modulating voltage which attenuated the carrier approximately 2.5 db. The measured points are plotted in Figs. 7, 8, and 9 for comparison with the calculated curves. The experimental data may be observed to agree generally within 1.5 db of the calculated curve.

Transient Response

The transient response of the AGC loop to an exponential change in input signal level of magnitude Δa under the restrictions outlined above can be determined by using transform relation

$$A^*(s) = H(s)A(s)$$

where $A(s)$ = Laplace transform of the input signal and $A^*(s)$ = Laplace transform of the resultant output signal or

$$A^*(s) = \frac{1}{\left(1 + \dfrac{1}{G}\right) + \dfrac{\tau}{G}s} \times \frac{\Delta a}{s(1 + \tau_{\text{in}}s)}$$

where τ_{in} = rise time of the input signal.

The solution of this equation expressed as a function of time is

$$a^*(t)_{\text{dbu}} = \frac{\Delta a_{\text{db}}}{1 + \dfrac{1}{G}}\left[1 - \frac{\dfrac{1}{\tau_{\text{in}}}e^{-(G/\tau)t} - \dfrac{G}{\tau}e^{-(t/\tau_{\text{in}})}}{\left(\dfrac{1}{\tau_{\text{in}}} - \dfrac{G}{\tau}\right)}\right]$$

where $a^*(t)_{\text{dbu}}$ represents the resultant change in receiver attenuation. The amplitude of the input signal Δa is expressed in decibels. Using the measured values of loop gain, the transient response of the AGC loop was calculated for a 3-db exponential change in signal level at input signal levels of -40 and -80 dbm. The calculated AGC output is plotted in Figs. 10 and 11 as resultant change in receiver attenuation.

The transient response of the AGC loop was then measured by introducing known changes in the input signal level and recording the resultant AGC output (see Figs. 10 and 11). The change in input signal level was accomplished using a current-controlled microwave ferrite attenuator which was varied by a step change in control current. The rise time of the input signal change was 4 to 5 times faster than the rise time of the resultant AGC voltage change. The measured AGC voltage change was expressed as db attenuation change using the measured value of K_A. The experimental results are plotted in Figs. 10 and 11 for comparison with the calculated curves. The experimental data agree with the calculated results to within 0.5 db.

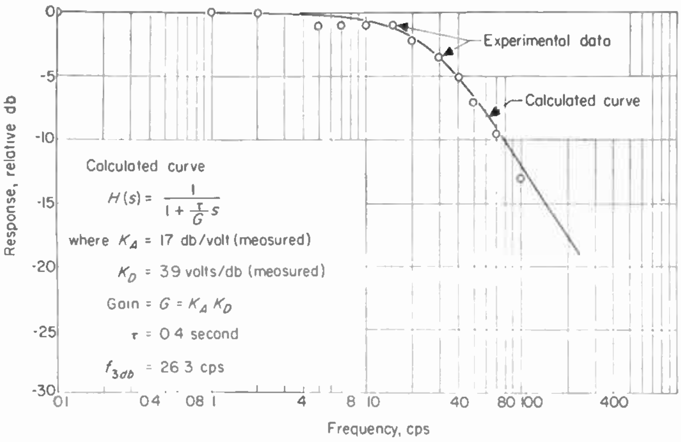

Fig. 7—Frequency response of AGC loop; input signal level = −40 dbm.

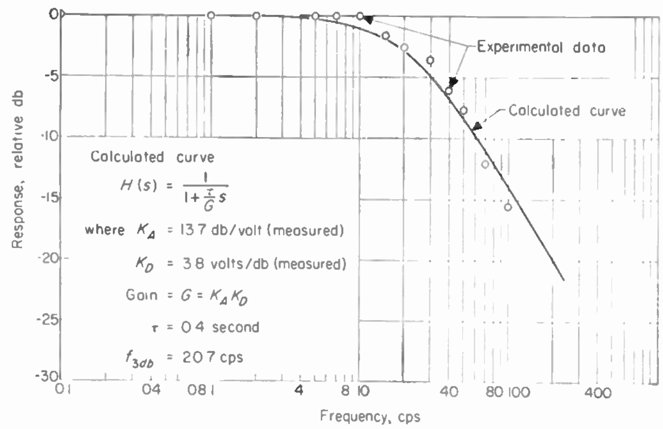

Fig. 8—Frequency response of AGC loop; input signal level = −60 dbm.

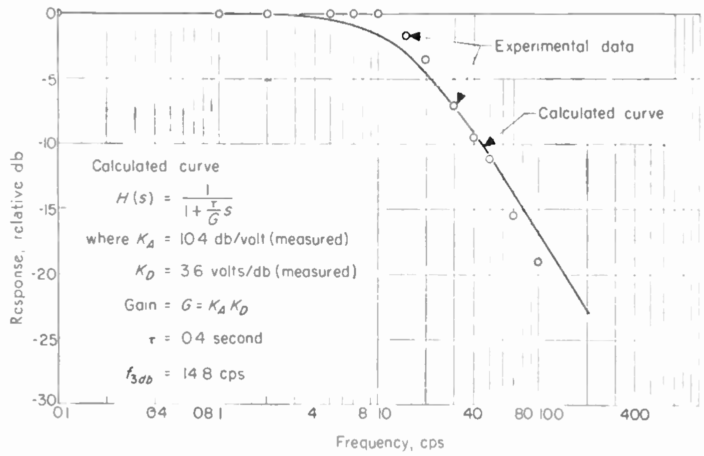

Fig. 9—Frequency response of AGC loop; input signal level = −80 dbm.

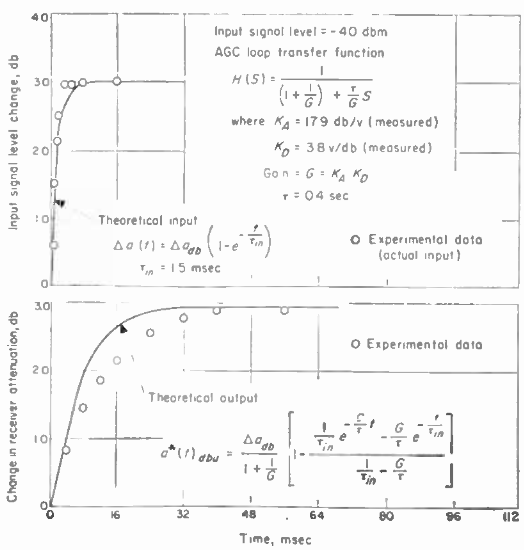

Fig. 10—Transient response of AGC loop.

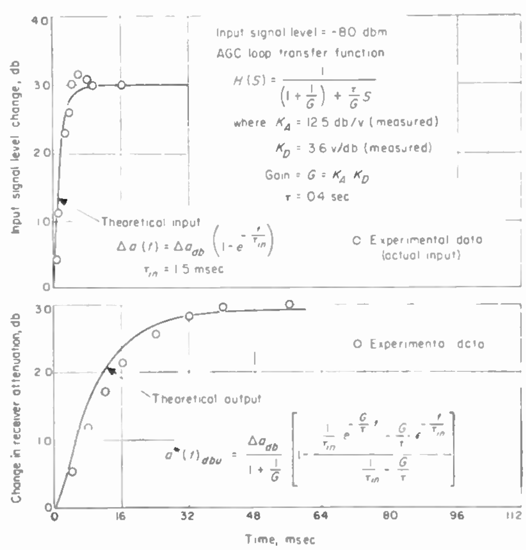

Fig. 11—Transient response of AGC loop.

RMS Error in Receiver Gain

The operation of the AGC loop was analyzed with random noise jamming, and the root-mean-square (rms) error in receiver gain was calculated. An experiment was then performed using a synchronous receiver to determine if the AGC system performed according to the theory. The analytical method is presented first.

The mean square error for the linear system with an error spectral density of $\Phi_\epsilon(\omega)$ is given by

$$\sigma^2 = \frac{1}{2\pi}\int_{-\infty}^{\infty} \Phi_\epsilon(\omega)d\omega. \tag{1}$$

If the system is considered to be distortionless with respect to the signal, the mean square error can be written as

$$\sigma^2 \text{ distortionless} = \frac{1}{2\pi}\int_{-\infty}^{\infty} \Phi_N(\omega)\,|H(j\omega)|^2 d\omega \tag{2}$$

where $\Phi_N(\omega)$ is the noise spectral density at the input in units determined by those of the signal, and $H(j\omega)$ is the system transfer function (dimensionless).

The jamming noise was assumed to have an rms amplitude of N volts and a flat spectral density of

$$\Phi_N(\omega) = \Phi_N(0) = \left[\frac{\Delta a(FS)}{\Delta a'(0)}\right]^2 \left(\frac{N}{S}\right)^2 \frac{1}{2B_N}\ \frac{\text{db}^2}{\text{cps}} \tag{3}$$

where

$\Delta a(FS)$ = full-scale value of the gain error curve = 12 volts,

$\Delta a'(0)$ = slope of the error curve in volts/db at zero gain displacement for the signal level under investigation,

S = rms amplitude of the signal in volts, and

$2B_N$ = the effective bandwidth of the input noise.

$$\sigma^2 \text{ distortionless} = \Phi_N(0)\,\frac{1}{2\pi}\int_{-\infty}^{\infty} |H(j\omega)|^2 d\omega \ \text{db}^2$$

$$= \left[\frac{\Delta a(FS)}{\Delta a'(0)}\right]^2 \left(\frac{N}{S}\right)^2 \frac{1}{2B_N}\,\frac{1}{2\pi}\int_{-\infty}^{\infty} |H(j\omega)|^2 d\omega \ \text{db}^2 \tag{4}$$

$$= \left[\frac{\Delta a(FS)}{\Delta a'(0)}\right]^2 \left(\frac{N}{S}\right)^2 \frac{B_L}{B_N}\ \text{db}^2 \tag{5}$$

where

$$2B_L = \frac{1}{2\pi}\int_{-\infty}^{\infty} |H(i\omega)|^2 d\omega, \tag{6}$$

and the approximate AGC loop transfer function is given by

$$H(j\omega) = \frac{1}{1 + j\omega\dfrac{\tau}{G}} \tag{7}$$

where

$\tau = 0.4$ second,

G = gain of the AGC loop, dimensionless $= K_D K_A$;

where

K_D = AGC detector constant expressed in volts/db, and

K_A = constant associated with the gain of the receiver expressed in db/volt.

The rms error in receiver gain is obtained by taking the square root of (5).

$$\sigma \text{ distortionless} = \frac{\Delta a(FS)}{\Delta a'(0)} \times \frac{N}{S} \times \sqrt{\frac{2B_L}{2B_N}}\ \text{db rms}. \tag{8}$$

Eq. (8) appears in graphical form in Fig. 12 for the receiver under test. Superimposed on the graph are the measured values for comparison purposes. Agreement between measured and calculated values is within 1 db.

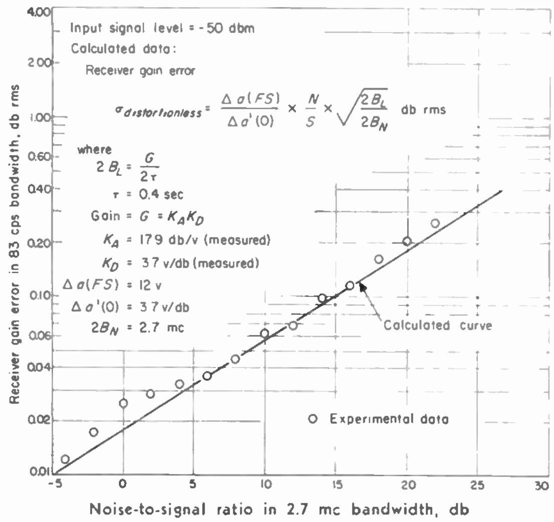

Fig. 12—Receiver gain error vs input noise-to-signal ratio.

Conclusion

AGC systems utilizing synchronous detection may be analyzed with considerable accuracy using the simple theoretical approach outlined here. The assumptions made in linearizing the AGC loop are valid for noise-free and noise-perturbed signals alike, and the analytical technique is a useful design tool.

The ability to achieve this goal is based on the recognition that an almost linear relationship exists between signal level and receiver attenuation when they are both expressed in decibels relative to unity. With the establishment of this fact, more advanced noise theory may be directed toward the synthesis of optimum AGC systems.

Correspondence

WWV Standard Frequency Transmissions*

Since October 9, 1957, the National Bureau of Standards radio stations WWV and WWVH have been maintained as constant as possible with respect to atomic frequency standards maintained and operated by the Boulder Laboratories, National Bureau of Standards. On October 9, 1957, the USA Frequency Standard was 1.4 parts in 10^9 high with respect to the frequency derived from the UT 2 second (provisional value) as determined by the U. S. Naval Observatory. The atomic frequency standards remain constant and are known to be constant to 1 part in 10^9 or better. The broadcast frequency can be further corrected with respect to the USA Frequency Standard, as indicated in the table; values are given as parts in 10^{10}. This correction is *not* with respect to the current value of frequency based on UT 2. A minus sign indicates that the broadcast frequency was low.

The WWV and WWVH time signals are synchronized; however, they may gradually depart from UT 2 (mean solar time corrected for polar variation and annual fluctuation in the rotation of the earth). Corrections are determined and published by the U. S. Naval Observatory.

WWV and WWVH time signals are maintained in close agreement with UT 2 by making step adjustments in time of precisely plus or minus twenty milliseconds on Wednesdays at 1900 UT when necessary; retarding time adjustments were made at WWV and WWVH on November 4 and 18, 1959.

NATIONAL BUREAU OF STANDARDS
Boulder, Colo.

WWV FREQUENCY†
WITH RESPECT TO U. S. FREQUENCY STANDARD

1959 1600 UT	Parts in 10^{10}‡
November 1	−32
2	−32
3	−32
4	−32
5	−32
6	−33
7	−33
8	−33
9	−33
10	−33
11	−33
12	−32
13	−33
14	−33
15	−33
16	−32
17	−32
18	−32
19	−31
20	−31
21	−31
22	−31
23	−31
24	−31
25	−31
26	−31
27	−31
28	−31
29	−30
30	−30

* Received by the IRE, December 28, 1959.

† WWVH frequency is synchronized with that of WWV.

‡ 30-day moving average seconds pulses at 15 mc. Method of averaging is such that an adjustment of frequency of the control oscillator appears on the day it is made. No change or adjustment in the control oscillator was made during November, 1959.

Note: Beginning January 1, 1960, the value of the USFS has been arbitrarily increased by 74 parts in 10^{10} to bring it into agreement with a cesium resonator frequency of 9,192,631,770 cps. See "National standards of time and frequency in the United States," PROC. IRE, vol. 48, p. 105; January, 1960.

Parametric Oscillations with Point Contact Diodes at Frequencies Higher than Pumping Frequency*

This letter is written to describe negative resistance effects obtained experimentally with point contact diodes operating as parametric oscillators at frequencies higher than the pumping frequency.[1] The signal and idler frequency in the operation reported herein are located symmetrically with respect to "m" times the pumping frequency. These results are shown to be consistent with the Manley-Rowe relations.

The types of point contact diodes which were used in these experiments have the same physical dimensions as the microwave rectifiers described in a previous paper.[2] A gallium arsenide diode with the capacity-bias curve of Fig. 1 produced oscillation at 11.63 kmc when pumped at 11.03 kmc. The dc bias point for this operation is indicated by an X on Fig. 1. The corresponding symmetrical lower sideband, located at 10.430 kmc, was also observed. The circuits used were such as to suppress the 600-mc difference frequency. Approximately 10 mw of pump power was used.

In a second experiment this diode achieved low-level oscillation at 530 mc when pumped at 480 mc. The symmetrical signal at 430 mc was observed. The pump power was about 20 mw into a matched load. (Actual power absorbed by the diode was not determined.)

A gallium phosphide diode with capacitance-bias voltage curve as shown in Fig. 2 produced oscillation at 530 mc when pumped at 470, 460, and 450 mc, respectively. (Circuit tuning was adjusted in each case.) The

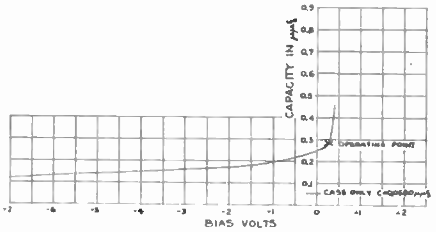

Fig. 1—Gallium arsenide point contact diode. Capacitance at 100 kc vs bias voltage.

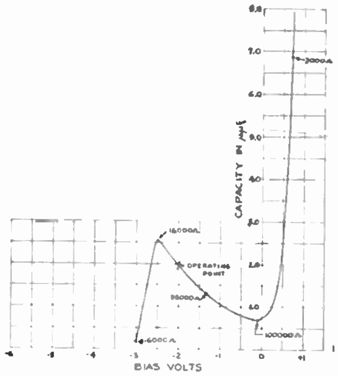

Fig. 2—Gallium phosphide point contact diode. Capacitance at 100 kc vs bias voltage.

best bias for this operation with a pump power of approximately 30 mw is indicated by an X on Fig. 2. (Actual power absorbed by the diode was not determined.)

It is shown below that this type of operation can be obtained if the diode possesses nonlinearities in its reactance beyond the usual linear term, *i.e.*, C_1/C_0. Thus for a nonlinear capacity device with a large second-order harmonic term in the equation describing the capacity vs voltage characteristic, we can expect the capacity to vary at a $2f$ rate while pumping at f. Note that $2f_{\text{pump}}$ is not necessarily generated, but the capacitance variation at $2f$ produces the same effect. Similarly a capacitance variation containing a large 4th, 6th, etc., harmonic content will allow other types of operation; *i.e.*, $m=2, 4$, etc.

The relations governing this type of operation can be obtained from the Manley-Rowe relations.[3]

$$\sum_{m=0}^{m=\infty}\sum_{n=-\infty}^{n=\infty}\frac{mW_{mn}}{mf_1+nf_0}=0$$

$$\sum_{m=-\infty}^{m=\infty}\sum_{n=0}^{n=\infty}\frac{nW_{mn}}{mf_1+nf_0}=0. \qquad (1)$$

For the case where negative resistance is obtained at frequencies symmetrically located about mf_1, these relations become

* Received by the IRE, November 16, 1959.

[1] This type of operation was discussed by K. K. N. Chang and S. Bloom, "A parametric amplifier using lower frequency pumping," PROC. IRE, vol. 46, pp. 1380–1387; July, 1958.

[2] W. M. Sharpless, "High frequency gallium arsenide point contact rectifiers," *Bell Sys. Tech. J.*, vol. 38, pp. 259–269; January, 1959.

[3] J. M. Manley and H. E. Rowe, "Some general properties of nonlinear elements—part 1, general energy relations," PROC. IRE, vol. 44, pp. 904–913; July, 1956.

$$\frac{W_{1,0}}{f_1} + \sum_{m=0}^{m=\infty} \frac{mW_{m,\pm 1}}{mf_1 \pm f_0} = 0$$

$$\sum_{m=-\infty}^{m=\infty} \frac{W_{m,1}}{mf_1 + f_0} = 0. \qquad (2)$$

For the experimental results above, the two frequencies were located symmetrically about the pump frequency, *i.e.*, $m=1$,

$$\frac{W_{1,0}}{f_1} + \frac{W_{1,-1}}{f_1 - f_0} + \frac{W_{1,1}}{f_1 + f_0} = 0$$

$$\frac{W_{-1,1}}{-f_1 + f_0} + \frac{W_{1,1}}{f_1 + f_0} = 0 \qquad (3)$$

where $W_{1,0}$ is the pump power entering at f_1. Similar results can be written for $mf_1 \pm f_0$ frequencies. Since

$$\frac{W_{1,-1}}{f_1 - f_0} = \frac{W_{1,1}}{f_1 + f_0}$$

and $W_{1,0}$ is power entering the device, power must leave the device at $f_1 \pm f_0$. (We have assumed that no power flows at frequencies other than $f_1 \pm f_0$ and f_0 is suppressed by circuit design.) The ratio of input power to output power is given by

$$G_{p+} = -\frac{f_1 + f_0}{f_1 - f_0} \text{ (up converter)}$$

$$G_{p-} = -\frac{f_1 - f_0}{f_1 + f_0} \text{ (down converter)}.$$

These relations indicate that power may also be delivered at both input and output ports in the absence of input (signal) power, thus acting as a generator.

The general power relations for an amplifier of this type pumped at f_1 and operating at $mf_1 \pm f_0$ are

$$G_{p+} = -\frac{mf_1 + f_0}{mf_1 - f_0}$$

$$G_{p-} = -\frac{mf_1 - f_0}{mf_1 + f_0}.$$

A small signal analysis similar to Rowe's[4] confirms that for operation described by (3), a large C_2/C_0 is required. For operation at $mf_1 \pm f_0$ a large C_{2m}/C_0 would be required of the nonlinear device.

It is evident from the curves of Figs. 1 and 2 that these two diodes possess nonlinearities in their $C-V$ curves that will satisfy the C_{2m}/C_0 requirement for the experimental results reported.

The diodes were furnished to the author by W. M. Sharpless of these Laboratories. His assistance and encouragement is gratefully acknowledged.

L. U. KIBLER
Bell Telephone Labs., Inc.
Holmdel, N. J.

[4] H. E. Rowe, "Some general properties of nonlinear elements, part II—small signal analysis," PROC. IRE, vol. 46, pp. 850–860; May, 1958.

On the Frequency Dependence of the Magnitude of Common-Emitter Current Gain of Graded-Base Transistors*

It has been experimentally observed and generally accepted that the magnitude of the common-emitter short-circuit current gain of graded-base transistors falls at a rate of 6 db per octave with increasing frequency. Considerable departure from this behavior has also been observed, however, for certain transistors. So far, little attention has been paid to the detailed theoretical examination of this important property, possibly owing to the mathematical difficulties involved in simplifying the current-gain expression for the transistor. To avoid such difficulties, the common-base current gain a is often[1,2] empirically approximated by

$$a = a_0 \frac{e^{-jKf/f_a}}{(1 + jf/f_a)} \qquad (1)$$

where a_0 is the low-frequency value of the current gain, f_a its 3-db cutoff frequency, and K a constant. This expression is found sufficiently accurate for most practical design problems, with appropriate choice of K. Using this empirical relationship, it has been shown that the common-emitter current-gain modulus $|b| = |a/(a-1)|$ exhibits a 6-db per octave fall over a *limited* frequency range,[3] but common experience suggests that such behavior may exist over a much wider range of frequencies. Questions arise as to whether the 6-db per octave fall of $|b|$ is an exact law or an approximation, whether this property is governed directly by any physical mechanism, and what the reason is for the observed departure from the 6-db per octave law in certain cases. In this letter, the theoretical current gain of a transistor with exponential base impurity grading is examined in order to throw more light on this matter, and adequate answers to the above questions are given.

Assuming an exponentially graded-base region resistivity, negligible recombination of minority carriers, low injection level and an ideal one-dimensional geometry, the intrinsic short-circuit current gain a (common base) may be expressed in the well-known form:[4]

$$a = a_0 \frac{e^{\epsilon}}{\dfrac{\epsilon}{\theta} \cdot \sinh \theta + \cosh \theta} \qquad (2)$$

where

$2\epsilon = \Delta V \cdot q/kT = m$

$\Delta V =$ "built in" potential difference across the base width W

$\theta = (\epsilon^2 + j\omega W^2/D_p)^{1/2}$

$D_p =$ diffusion constant for holes in the base of a p-n-p transistor structure.

If all extrinsic effects were absent (zero depletion capacitances and $r_{bb'}$), a would also be the terminal short-circuit current gain α of the transistor. This ideal case is examined first, the important effects of the emitter depletion capacitance C_{te} being considered after certain properties of the intrinsic transistor have been established.

At very low frequencies, *e.g.*, when the phase angle of a is less than about 5°, expression (2) may be simplified to[5]

$$a = a_0/(1 + j\omega/\omega_r) \qquad (3)$$

where

$$\omega_r = \frac{2D_p}{W^2} \frac{m^2}{2(m - 1 + e^{-m})}$$

$$\simeq \frac{D_p}{W^2} \cdot \left(\frac{m^2}{m-1}\right) \text{ when } m \geq 4. \qquad (3a)$$

The time constant $(1/\omega_r)$ appearing in (3) may be shown to be identical to the base transport time τ_b, which is defined as

$$\tau_b = C_b/g_{ee}(=1/\omega_r) \qquad (4)$$

where

$C_b =$ the "base-charging" capacitance, obtained by integrating the excess equilibrium (dc) hole concentration in the base region and differentiating the "integrated charge" with respect to the emitter-base voltage, and where

$g_{ee} = (q/kT) \cdot I_e$, the differential emitter junction conductance.

The reciprocal of the low-frequency common-emitter current gain b may be written, from (3), as

$$\frac{1}{b} = \frac{1-a}{a} = \frac{1}{a_0} - 1 + j\omega/\omega_r a_0. \qquad (5)$$

Eq. (5) indicates that for an ideal transistor, with $a_0 = 1$, the 6-db per octave fall of b at low frequencies is a natural law and represents the charging of the base region with minority carriers as a *succession of steady states; i.e.*, the instantaneous base charge distribution is negligibly different to that in the steady state for the emitter-base voltage concerned, and the total base charge accurately represented by the charge on the lumped base-charging capacitance C_b. For practical transistors, if the real part of (5) is small compared to its imaginary part, within the assumed low-frequency limit, this law will still apply. Now, accepting the experimentally-observed fact that for all except certain exceptional transistors, $|b|$ falls at 6 db per octave at much higher frequencies than defined before (3), it is to be expected that $\omega_r/2\pi$ will be the frequency at which $|b|$ falls to unity (commonly denoted by f_1 or f_T); it will be shown that this property has theoretical justification.

* Received by the IRE, July 15, 1959.

[1] D. E. Thomas and J. L. Moll, "Junction transistor short-circuit current gain and phase determination," PROC. IRE, vol. 46, pp. 1177–1184; June, 1958.

[2] R. L. Pritchard, "Electric network representation of transistors—a survey," IRE TRANS. ON CIRCUIT THEORY, vol. CT-3, pp. 5–12; March, 1956.

[3] F. J. Hyde, "The Current Gains of Diffusion and Drift Types of Junction Transistors," presented at the IEE International Convention on Transistors and Associated Semiconductor Devices, May 23, 1959. To be published in *Proc. IEE*, vol. 106, pt. B, suppl. no. 17.

[4] H. Kroemer, "On the diffusion and drift transistor theory," *Arch. elek. Übertr.*, vol. 8, pp. 223–228; May, 1954.

[5] M. B. Das and A. R. Boothroyd, "Measurement of Equivalent Circuit Parameters of Transistors at VHF," presented at the IEE International Convention on Transistors and Associated Semiconductor Devices, May 27, 1959. To be published in *Proc. IEE*, vol. 106, pt. B, suppl. no. 15.

Subject to the assumption that the field factor $m \geq 4$, the general current-gain expression (2) may be simplified to

$$a \simeq 2a_0 e^{-\epsilon(x-1)} \frac{x + jy}{1 + x + jy} \cdot e^{-j\epsilon y} \qquad (6)$$

where

$$x = \sqrt{\tfrac{1}{2}\{(1 + \delta^2)^{1/2} + 1\}};$$

$$y = \sqrt{\tfrac{1}{2}\{(1 + \delta^2)^{1/2} - 1\}}$$

$$\delta = \omega/\omega_n$$

and

$$\omega_n = m^2 D_p / 4W^2.$$

It is noted that the normalizing frequency $\omega_n/2\pi$ is approximately $m/8$ times the 3-db cutoff frequency f_a. Assuming $\delta^2 \ll 1$, (6) may, by expanding in power series and neglecting all except the first order term in δ^2, be simplified to give

$$\left|\frac{1}{b}\right| = \left|\frac{1}{a} - 1\right|$$

$$\simeq \sqrt{\left(\frac{1}{a_0} - 1\right)^2 + A\delta^2} \qquad (7)$$

where

$$A = 1/4(\epsilon - 1/2a_0)^2 + \left(\frac{1}{a_0} - 1\right)\left(\frac{\epsilon}{2} - \frac{3}{8}\right)\frac{1}{a_0} + \frac{\epsilon^2}{4}\left(\frac{1}{a_0} - 1\right).$$

Eq. (7) may be further simplified, by putting $a_0 \simeq 1$ and using (3a), to give

$$\left|\frac{1}{b}\right| \simeq \delta(\epsilon - \tfrac{1}{2})/2 = \frac{\omega W^2}{D_p}\left(\frac{m - 1}{m^2}\right)$$

$$= \frac{\omega}{\omega_T}. \qquad (8)$$

A disregard of terms in δ^4 and higher powers in the above series expansions is found to cause negligible error even for δ^2 as high as 0.5 or $\delta = 0.7$. Thus, from (8), it might be expected that the 6-db per octave behavior should hold for frequencies up to about 0.7 $f_a(\simeq 1.2 f_1)$ for $m = 8$, or 0.5 $f_a(\simeq 0.85 f_1)$ for $m = 6$. It is difficult to extend this analytical approach further, to include much higher frequencies; it is also difficult to extend it without restriction of the value of m. However, the exact value of $|b|$ may be examined by plotting $|1/b|$ against $\omega W^2/2D_p$, computed directly from (2) as shown in Fig. 1. Theoretical curves of $|1/b|$ are given for several values of m, and for a uniform base transistor ($m = 0$), assuming $a_0 = 1$; the frequencies f_a and f_1 are indicated. It is seen that the 6-db per octave fall of $|b|$ is a good approximation over a surprisingly wide range of frequency, much wider than expected from the above approximate analysis. At very high frequencies, the fall of $|b|$ is at a much higher rate than 6 db per octave. In view of the very wide frequency range over which the behavior expressed in (8) is found to be approximately valid, it might perhaps be expected that the simple representation of base-region charging by the lumped base input capacitance C_b, derived from the steady-state base charge, should also be valid over a similar frequency range. This is not so, however, for the base input capacitance (in common emitter with zero collector load) is found to be considerably frequency dependent over this range.

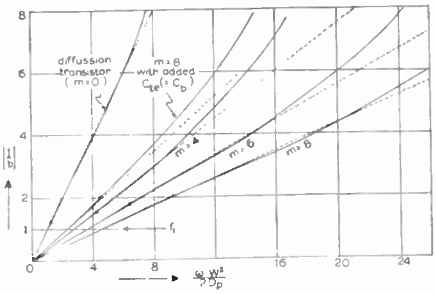

Fig. 1—High-frequency behavior of common-emitter current gain b. Solid lines: theoretical behavior of $|1/b|$. Dotted lines: 6-db per octave approximation. x indicates 3-db cutoff frequency.

The presence of the emitter junction depletion capacitance has not yet been discussed but it usually modifies the ideal behavior of the transistor considerably. The modified current gain a' may be expressed as:

$$a' = a \cdot \frac{1 + j\omega \dfrac{C_{de}}{g_{ee}}}{1 + j\dfrac{\omega}{g_{ee}}(C_{te} + C_{de})} \qquad (9)$$

where C_{de} is the emitter diffusion capacitance. This capacitance and the emitter conductance g_{ee} are, in general, frequency dependent; however, the associated frequency $g_{ee}/2\pi C_{de}$ is about $m/2$ times the 3-db cutoff frequency f_a of the transistor and it increases at higher frequencies. Eq. (9) may, for the present purpose, be simplified to

$$a' \simeq a \cdot \frac{1}{1 + j\omega/\omega_{te}} \qquad (10)$$

where

$$\omega_{te} = g_{ee}/C_{te}.$$

Combining (6) and (10), and simplifying in the same manner as in the derivation of (7) and (8), the following expression for $|1/b'|$ is obtained:

$$|1/b'| = \left|\frac{1}{a'} - 1\right|$$

$$\simeq \omega\left(\frac{1}{\omega_{te}} + \frac{1}{\omega_T}\right)\sqrt{1 + \frac{\omega^2}{(\omega_{te} + \omega_T)^2}}. \qquad (11)$$

Thus, when $\omega_T \gg \omega$, or vice versa, the fall of $|b'|$ is at 6-db per octave although the frequency at which $|b'|$ falls to unity is determined by both ω_T and ω_{te}. But, when ω_T and ω_{te}, *i.e.*, C_b and C_{te}, are of the same order of magnitude, the rate of fall of $|b'|$ is greater than 6-db per octave. The influence of C_{te} is illustrated in the figure where the behavior of $|b'|$ is plotted for $C_{te} = C_b$ in the case of $m = 8$. The departure from the 6-db per octave law is obvious.

It may be concluded that the 6-db per octave fall of the common-emitter short-circuit current-gain magnitude can be a good approximation to its actual behavior over the useful frequency range of the transistor, but that care must be taken not to generalize this behavior when the emitter junction capacitance is present.

M. B. Das
A. R. Boothroyd
Imperial College of Science and Technology
Elec. Engrg. Dept.
London, S.W.7, Eng.

A Simple Technique for Measuring the Signal-to-Noise Ratio at the Output of a Pulsed Sinusoid Matched Filter*

The usual method for measuring signal-to-noise ratios in teletype receiving systems is to make the separate measurements of signal and noise following a band-pass filter of the system. For a matched filtering system this signal-to-noise ratio may then be converted by use of bandwidth ratios to its corresponding value at the output of the matched filter where error rates may be readily calculated for comparison with experimental values.

This method of measuring signal-to-noise ratios, however, is wholly dependent on knowing the noise bandwidth of the band-pass filter and the figure of merit of the matched filter. If these are not known precisely, the accuracy of the resultant measurements will suffer. The following technique for measuring signal-to-noise ratios at the output of the matched filter does not require a band-pass filter preceding the matched filter. If, however, the signal-to-noise ratio at the input of the matched filter is known this measurement technique could be used to determine an equivalent noise figure or figure of merit for the matched filter.

If the input signal to the matched filter is defined as

$$g(t) = E \cos \omega t, \qquad 0 < t < T;$$

the impulse response of the matched filter is

$$h(t) = Kg(T - t) = A \cos \omega t, \quad 0 < t < T;$$

where $A = KE$ is an arbitrary gain constant of the filter and T is the duration of the pulse or baud. The output signal of the matched filter is given by the convolution integral as

$$f(\tau) = \int_0^{\tau} h(t)g(\tau - t)dt$$

$$= \frac{AE\tau}{2}\cos \omega\tau, \qquad \begin{matrix} 0 < \tau < T \\ \omega \gg \dfrac{AE}{4} \end{matrix}. \qquad (1)$$

* Received by the IRE, May 19, 1959.

The maximum output of the matched filter is obtained at the end of the baud and is

$$f(T) = \int_0^T h(t)g(T-t)dt$$
$$= \frac{1}{K}\int_0^T h^2(t)dt = \frac{AET}{2} \qquad (2)$$

where T is a multiple of $2\pi/\omega$ or the time variation of (1) is sampled at a peak of the sinusoidal variation.

The output of this filter may also be determined for a white noise spectrum of N_0 watts per cycle at the filter input. The noise power spectrum at the filter output is

$$\Phi(f) = N_0 |H(f)|^2, \qquad (3)$$

and the total power at the filter output at the end of the baud is

$$\sigma^2(T) = \int_{-\infty}^{\infty} N_0 |H(f)|^2 df. \qquad (4)$$

This same power is given in terms of a time integration by the Parseval Theorem as

$$\sigma^2(T) = N_0 \int_0^T h^2(t)dt, \qquad (5)$$

and the time variation of output power for the specified matched filter is

$$\sigma^2(\tau) = N_0 \int_0^\tau h^2(t)dt$$
$$= \frac{N_0 A^2 \tau}{2} \qquad 0 < \tau < T. \qquad (6)$$

Thus both the signal voltage and the noise power increase linearly throughout the baud interval, and therefore the signal-to-noise power ratio also increases linearly and reaches a maximum at time T, the end of the baud. Using (2) and (5) this optimum signal power to noise power ratio is

$$\left(\frac{S}{N}\right)_{\text{opt.}} = \frac{f^2(T)}{\sigma^2(T)} = \frac{\frac{1}{K^2}\int_0^T h^2(t)dt}{N_0} = \frac{E^2T}{2N_0}. \qquad (7)$$

In order to measure the maximum value of the signal-to-noise ratio with a true rms voltmeter, it is necessary to calculate the relation between the maximum value of signal and the rms signal over the whole baud and the maximum value of noise compared to the rms value over the baud. If V_s and V_n represent the reading of a true rms voltmeter for signal and noise, respectively, then using (1) and (6)

$$V_S = \frac{AE}{2}\sqrt{\frac{1}{T}\int_0^T \tau^2 \cos^2 \omega\tau d\tau}$$
$$= \frac{AET}{2\sqrt{6}} \qquad (8)$$

and

$$V_N = \left(\frac{N_0A^2}{2}\right)^{1/2}\sqrt{\frac{1}{T}\int_0^T \sqrt{\tau^2 d\tau}}$$
$$= \sqrt{\frac{N_0A^2T}{4}}. \qquad (9)$$

The signal power to noise power ratio corresponding to these meter readings is

$$\left(\frac{S}{N}\right)_{\text{meter}} = \frac{V_S^2}{V_N^2} = \frac{\frac{A^2E^2T^2}{24}}{\frac{N_0A^2T}{4}} = \frac{E^2T}{6N_0}. \qquad (10)$$

Comparison of this ratio with (7) shows that the optimum signal-to-noise ratio at the filter output can be obtained from the rms voltage measurements by the following relation,

$$\left(\frac{S}{N}\right)_{\text{opt.}} = 3\frac{V_S^2}{V_N^2}. \qquad (11)$$

Thus the signal-to-noise ratio determined by a true rms voltmeter at the output of the pulsed sinusoid matched filter is 4.8 db less than the optimum value at the end of the baud.

H. E. White
U. S. Army Sig. Res. and Dev. Lab.
Ft. Monmouth, N. J.

The Reliability Function*

Most attempts to measure reliability of complex systems quantitatively thus far have utilized the general Poisson formula. This may be used to describe the failure of systems in the following way:

$$P_n = \frac{\left(\frac{t}{t_m}\right)^n e^{-t/t_m}}{n!} \qquad (1)$$

where

t = Some time interval in which minimum failures are desired.
P_n = Probability of n failures in time, t.
t_m = Mean time between failures.
t/t_m = Ratio of critical interval, t, to mean time between failures, t_m.

However, only the case of zero failures is of interest, not how many failures occur within a larger interval of time. For $n=0$ only, the formula reduces to

$$P_n = e^{-t/t_m}. \qquad (2)$$

This formula is virtually the unanimous proposal of the literature as the best description of systems failures. A failure distribution may be illustrated as in Fig. 1. This is a typical Poisson plot of the form a large number of these intervals to failure take. The largest number of failures tend to cluster around the value of central tendency, t_m, or mean time to failure. The probability distribution of t around t_m can be solved to give the probability of a failure after time t. If the probability of no failures in time t is plotted vs t/t_m, Fig. 2 results. Now if Fig. 2 is superimposed on Fig. 1, the effects of varying t_m and t on probability of successful operation during time t can be compared.

Investigation of Fig. 3 discloses an important relationship. For the probabilities of successful operation to time t of complex systems to approach 1.00, the mean time to failure must be very large with respect to the desired operation interval, t. Or, if one is concerned with raising the probability of successful operation in time t with regards to a proposed system, either the critical time interval, t, must be lowered significantly or the mean time to failure must be drastically increased. This region of scant return in increased probability of successful operation for rather large increases in mean time to failure can readily be seen from the nomograph.

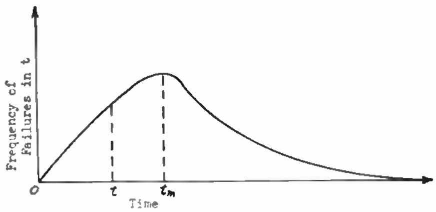

Fig. 1—Failure time distribution.

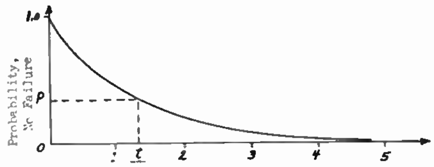

Fig. 2—Probability of no failure vs t/t_m.

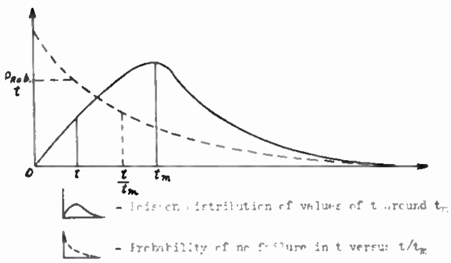

Fig. 3—Effect of changes in t and t_m on probability.

The nomograph (Fig. 4) is scaled to solve (2). Simply draw a straight line through any two known variables and read the third directly. As the column heading shows, the scale on the right serves a dual purpose. The left side of the line is scaled to read the quotient of t/t_m. The right side of the same line is scaled to represent the corresponding probability of successful operation during a time interval, t. The nomograph should provide a rapid solution to the formula for anyone who is often concerned with reliability problems.

Consider, for example, the following problem. A complex electronics system has been found to operate, on the average, 55 hours between failure of some component at random. If it is desirable to find the probability with which the system should operate at least 10 minutes successfully, we need only connect 55 hours on the t_m scale and 10 minutes on the t scale and read probability $=0.9970$.

The nomograph was drawn to 4 times page ($8\frac{1}{2}\times 11$) size and reduced to increase

* Received by the IRE, September 29, 1958.

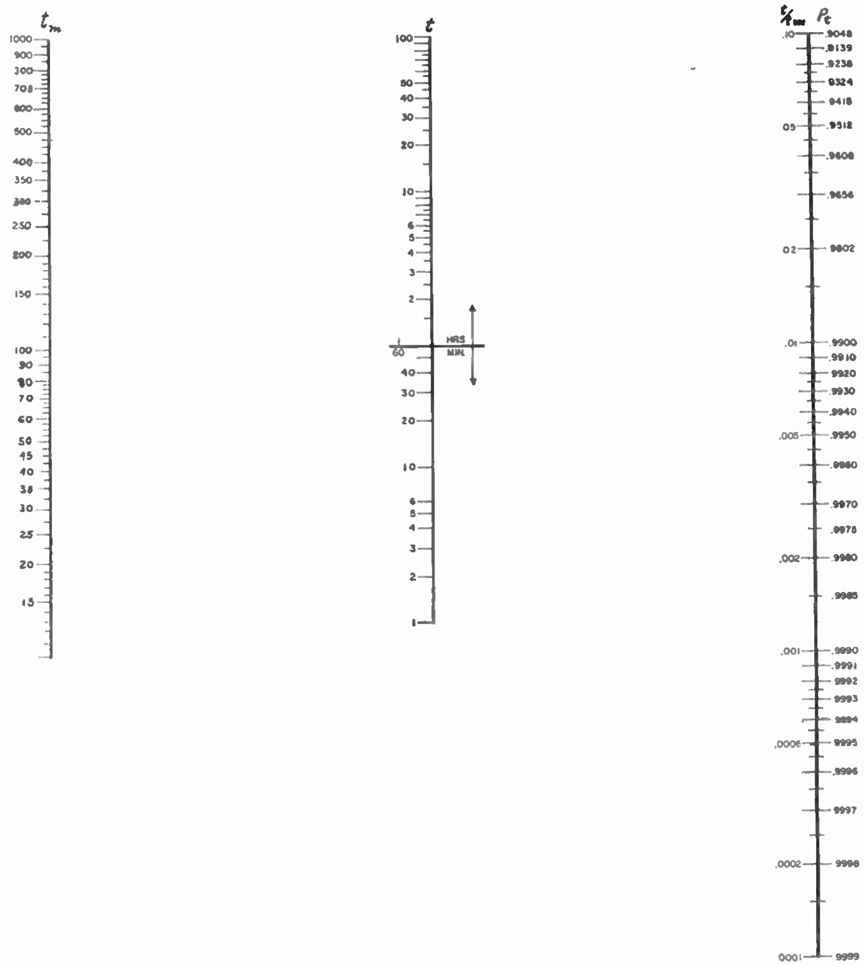

Fig. 4—Reliability nomograph $P_t = e^{-t/t_m}$.

its accuracy. It solves the formula accurately to the fourth decimal place and a fifth place may be interpolated by anyone familiar with logarithmic interpolation, as on a slide rule.

J. L. Colley
The Western Elec. Co.
Winston-Salem, N. C.
Formerly at
Dept. of Industrial Admin.
Yale University
New Haven, Conn.

A High-Speed Binary Counter Based on Frequency Script Techniques*

The work reported here[1] constitutes a continuation and extension of previous experimental investigations on bistable oscillators.[2] Specifically, the high speed capabilities of the circuit shown in Fig. 1 were to be investigated.

The block diagram of Fig. 1 depicts a frequency domain flip-flop, as well as an additional gating circuit for scale of two operations. Instead of the biased diodes commonly employed for pulse/no-pulse scripts,[3] band-pass filters may serve as a means to distinguish between binary states for a frequency script.

Summarizing previous results,[2] the bistable oscillator may be characterized as follows:

1) Assume sustained oscillation at f_1. Then, an RF pulse applied to the input with length T, power level P_i, and carrier frequency f_2 initiates oscillation at f_2 and terminates oscillation at f_1. Analogously, due to symmetry, this is also true for switching from f_2 to f_1.

2) The input power level necessary for switching of the bistable oscillator, P_i, is significantly lower than its stable output power level, P_0.

3) The instruction time, T, of the bistable oscillator defines the minimum pulse length for a given pulse amplitude, required to switch the device from one stable state to the other. It approximately equals the delay plus transient time within the loop of the bistable oscillator. Instruction times $T = 7$ mμsec could be demonstrated for the 200 mc mode-spacing S-band system previously described.[2]

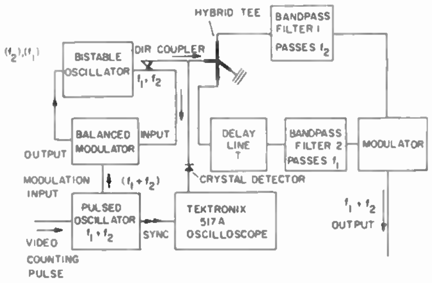

Fig. 1—Block diagram of a frequency script scale of two binary counter.

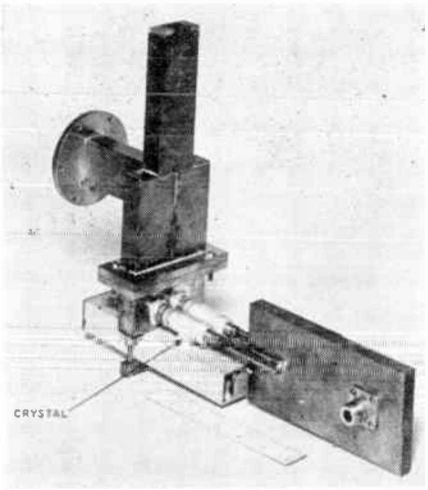

Fig. 2—Balanced modulator assembly.

In Fig. 1, the balanced modulator serves as a device to produce the alternate frequency, or, as a binary negation gate. It is readily seen that this requires a modulation input of frequency f_1+f_2, or f_1-f_2 (assuming $f_1>f_2$), which usually will be applied in pulse-form. Theoretical considerations reveal that the choice of f_1+f_2 is more advantageous.[4] Accordingly, the broadband balanced modulator shown in Fig. 2 has been developed for high level operation of two RF signals in the respective frequency ranges of 3 and 6 kmc, and has been successfully operated with a conversion loss of around 8 db. The various elements of the modulator are so arranged as to obtain balanced operation, resulting in 20-db suppression of both the input as well as the modulating-signal.

The functioning of the scale of two circuit of Fig. 1 is most readily explained on hand of the time diagram, Fig. 3. At a specific time, t_0, a counting pulse switches the bistable oscillator from f_1 to f_2, and f_2 is transmitted through bandpass filter 1 into the modulator. The second input of the modulator still receives f_1 through the delay

* Received by the IRE, April 24, 1959; revised manuscript received, June 1, 1959.

[1] Contract N 123(62738)6578A, sponsored by the Naval Ordnance Res. Lab., Corona, Calif., 1956.

[2] V. Met, "On multimode oscillators with constant time delay," Proc. IRE, vol. 45, pp. 1119–1128; August, 1957.

[3] To the best of the author's knowledge, the term script has been introduced by L. Fein, in connection with microwave logic research, performed under Contract NONR 2127(00), in 1956.

[4] Modulation with f_1-f_2 leads to two new frequencies, one of which is the desired one, while the other one, closely adjacent, is highly undesirable since it represents a degenerate mode-frequency. For a modulation frequency f_1+f_2 this undesired component lies far outside the useful band.

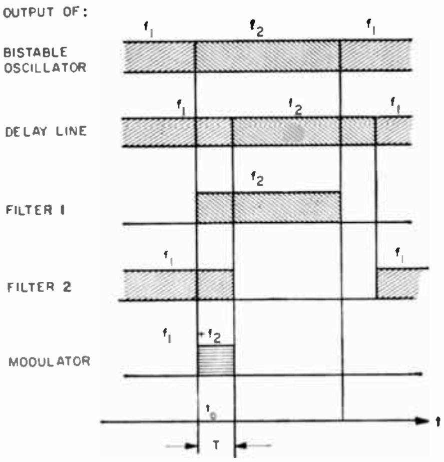

Fig. 3—Time diagram for the scale of two operation.

line and bandpass filter 2. Thus, an output of f_1+f_2 appears at the modulator, which lasts until the delay line has emptied its content of f_1. Accordingly, the length of the resulting pulses is equal to T, or, more generally, the delay of the line used, and their repetition rate is half the rate of the incoming pulses.

We have stated that a combination of a bistable oscillator and a balanced modulator represents a flip-flop for frequency script. With no external modulation signal f_1+f_2 applied to the balanced modulator, the circuit is bistable with an output frequency of either f_1 or f_2. Monostable operation may be obtained by making one mode of the bistable oscillator conditionally stable. Also, we may achieve astable operation of the device if the modulating signal f_1+f_2 is applied in CW fashion. Then, the bistable oscillator will switch alternatingly from state to state, and the period of the switching waveform, t_s, may serve as a criterion for the ultimate switching speed of the counter, although the process of regeneration involves a certain loss of speed. It seems appropriate to refer to the modulation signal as bias-signal, and to its frequency f_1+f_2 as bias-frequency, to carry through the analogy to the multivibrator. For display purposes, a frequency sensitive detector may be used to convert frequency script into amplitude script.

Let us consider the influence of the length of the bias frequency pulse on the circuit performance. If the pulse duration is shorter than the instruction time, T, of the bistable oscillator, no switching will occur. Increasing the pulse length to a certain characteristic value, which theoretically should be equal to T, will then produce switching from f_1 to f_2 for one pulse, and back to f_1 from f_2 at the consecutive pulse, to give a specific example. If the length of the bias frequency pulse is increased more and more, the final state in which the system is left at the end of the pulse will depend on the number of free running switching periods t_s contained in this time-interval. This is illustrated by Fig. 4.

For the experimental investigations the S-band TWT bistable oscillator available from previous experiments[2] was combined with the balanced modulator shown in Fig. 2.

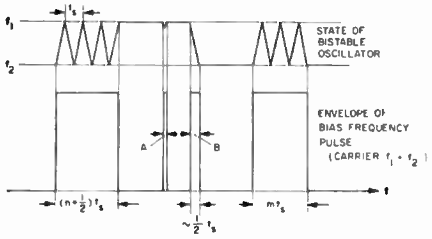

Fig. 4—Theoretical switching waveforms. Insufficient pulse length A, minimum switching length, B.

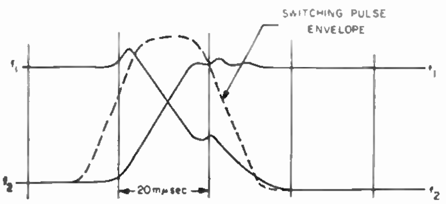

Fig. 5—Observed switching waveform using selective detector.

The mode frequencies $f_1=2995$ mc and $f_2=2800$ mc led to a modulation frequency $f_1+f_2=5790$ mc. The external modulation or bias-frequency pulses were obtained by grid modulating a TWT amplifier fed from a standard signal generator, with pulses of 10 mμsec rise time and variable length. Unfortunately, the circuit parameters were such that the maximum output available from the balanced modulator was merely 5 db above the instruction threshold, $P_{i\ min}$, of the bistable oscillator, due to an increase in conversion loss of 12 db at the correspondingly high input levels. From previous experience[2] we realize that this instruction level is insufficient to achieve an instruction time $T=7$ mμsec. The waveforms observed are sketched in Fig. 5.

It is believed that the performance of the circuit used for the experiments could be improved, to render a switching time of 10 mμsec, or less (approaching 7 mμsec), if, a) the rise time of the bias-frequency pulses were shorter, and b) the balanced modulator and bistable oscillator were better matched.[5]

The principle described here seems to be well applicable for operation with 1 mμsec pulses (a generally accepted goal at present), considering the following possibilities of circuit improvement. The mode-spacing could be increased to 1000 mc at X-band, if a 1 mμsec transit-time, medium bandwidth (20 per cent) TWT were available. The need for such an element has long been felt, and has also been expressed by others.[6] Minimum transit-time may be purchased at the expense of bandwidth, either by using a medium-bandwidth slow-wave circuit, or by extending the principle of the extended interaction gap klystron.[7] It is realized that

[5] The use of a 1 watt TWT prohibited optimum efficiency of the crystal modulator, which functions most satisfactorily in the mw range.

[6] B. L. Havens, "High-frequency carrier techniques for computer logic," presented at the PGEC Meeting, Palo Alto, Calif.; May 19, 1959.

[7] T. Wessel-Berg, "A General Theory of Klystrons with Arbitrary Extended Interaction Fields," Microwave Lab., Stanford University, Stanford, Calif., Rept. No. 376; March, 1957. Wessel-Berg describes cavity oscillations as undesired effects which should be of the multimode oscillator type. Also, H. Golde, "Extended Interaction Klystrons with Traveling-Wave Cavities," Microwave Lab., Stanford University, Stanford, Calif., Rept. No. 582; April, 1959.

with a binary frequency script one essentially wastes half the bandwidth available, but one also has the advantage that a combination of bandpass filters may replace the usual diode gates found in amplitude script devices.

Recent advances in microwave computer techniques[8] have demonstrated the merits of certain solid state circuits to perform logical operations with a minimum of cost and complexity. Still, it seems probable that, for a class of applications, a circuit involving a short-delay TWT might be preferable either for reasons of fast regeneration due to large bandwidth or due to the choice of script which lends itself most readily.

V. Met
Gen. Elec. Microwave Lab.
Palo Alto, Calif.

[8] Presented by several authors at the Symp. on Microwave Techniques for Computing Systems, Office of Naval Res., Washington, D. C.; March 12, 1959.

Reduction of Frequency-Temperature Shift of Piezoelectric Crystals by Application of Temperature-Dependent Pressure*

New military communication systems are in urgent need of frequency-control devices with a higher degree of stability, especially with respect to varying temperature. This requirement is coupled with the necessity for miniaturization and low power consumption. Crystal ovens, therefore, which consume a great deal of power, are not practical and must be replaced by other techniques.

One possible new technique will be described in this note. It is based on the sensitivity of the frequency of thickness-shear quartz crystal resonators to external pressure. Fig. 1 shows the influence of a compressional stress of 100 grams on the frequency of a 3rd overtone AT quartz crystal resonator as a function of the orientation of such stress with respect to the crystallographic axes.[1] It is noted that the observed frequency change can be either positive or negative depending upon the orientation of the stress. Additionally, it has been found that the frequency change for one particular stress orientation is always proportional to the amount of stress. If the stress is made temperature-dependent and applied to selected spots at the circumference of the crystal plate, the frequency-temperature behavior of the plate can be modified.

The solid curve in Fig. 2 represents a typical frequency-temperature relationship for an AT cut quartz crystal resonator. The frequency drift due to temperature change remains within $1\cdot 10^{-6}$ for a temperature range from 0° to 43°C. Application of temperature-dependent pressure could change the frequency of the resonator as indicated

* Received by the IRE, July 10, 1959.

[1] E. A. Gerber, "Precision frequency control for guided missiles," *Proc. First IRE Natl. Convention on Military Electronics*, pp. 91–98; June 17–19, 1957.

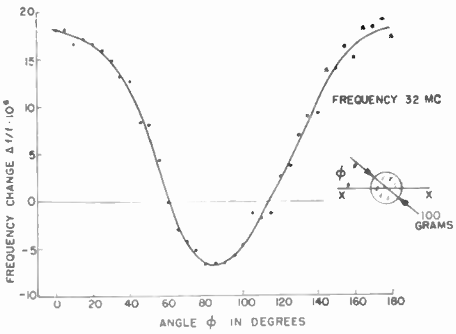

Fig. 1—Influence of the direction of a compressional stress on the frequency of a 32-mc AT crystal resonator.

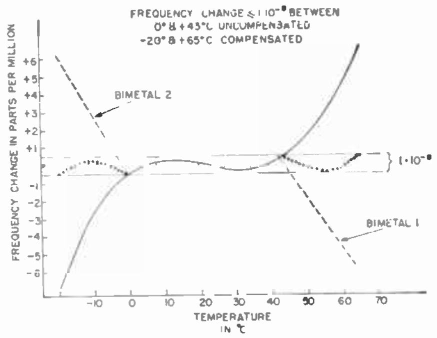

Fig. 2—Modification of the frequency-temperature curve of an AT crystal resonator by the application of temperature dependent pressure.

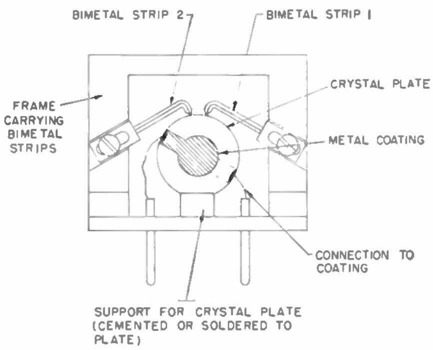

Fig. 3—Design of a crystal unit with two compensating bimetal strips.

by the two dashed lines. The two dotted curves then show how the original frequency-temperature curve of the resonator has been modified by the application of pressure. The temperature range for a frequency tolerance of $1\cdot10^{-6}$ is extended to twice its original value. As indicated in Fig. 2 and shown in detail in Fig. 3, bimetal strips are used to create the temperature-dependent pressure. Strip 1 starts to touch the circumference of the crystal at a temperature of 43°C and its pressure, which increases with temperature, causes the frequency shift represented by the dashed line. To compensate for the frequency excursion at lower temperatures, a second bimetal strip is used which increases its pressure with decreasing temperature. The proper points of contact with respect to the crystallographic axes of the crystal plate can be selected with the help of the curve in Fig. 1. Additionally, a wide choice regarding the dimensions of the bi-

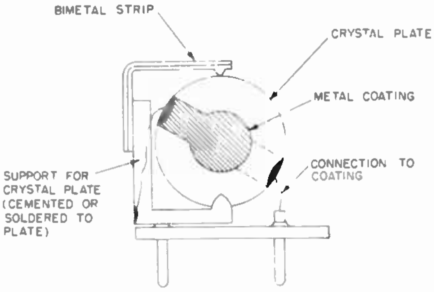

Fig. 4—Design of a crystal unit with one compensating bimetal strip.

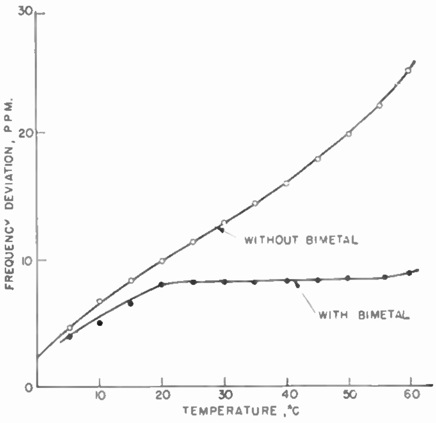

Fig. 5—Frequency-temperature curve of a 32-mc 3rd overtone crystal unit, with and without compensating bimetal strip; orientation angle of stress ϕ (see Fig. 1) $\approx 70°$.

metals permits one to adapt this method to almost any given condition. The relation between the dimensions and properties of a bimetal, the mechanical force F appplied by the strip to the crystal, and the temperature difference $\Delta\Theta$ has been derived from Bernoulli's theory of the cantilever beam

$$\frac{F}{\Delta\Theta} = \frac{3bt^2(\alpha_1 - \alpha_2)}{4a} \cdot \frac{1}{2}(E_1 + E_2);$$

where

a = length of the bimetal strip,
b = width of the bimetal strip,
t = thickness of each of the two metal layers constituting the bimetal strip,
α_1, E_1 = expansion coefficient and Young's modulus of metal 1, respectively,
α_2, E_2 = expansion coefficient and Young's modulus of metal 2, respectively.

It is obvious that many modifications of the above principle are possible. The simplified design of Fig. 4 can be used if a compensation at high or low temperatures only is desired. The use of more than two strips is indicated for compensation over a wide temperature range.

Preliminary measurements on two crystal units designed according to Fig. 4 are depicted in Figs. 5 and 6. Only the upper temperature range is compensated. The great improvement is obvious. Fig. 6 shows, in addition to frequency measurements, values of the resonance resistance of the crystal as a function of temperature. It is noted that the resistance does not increase with higher temperature, *i.e.*, with increasing pressure.

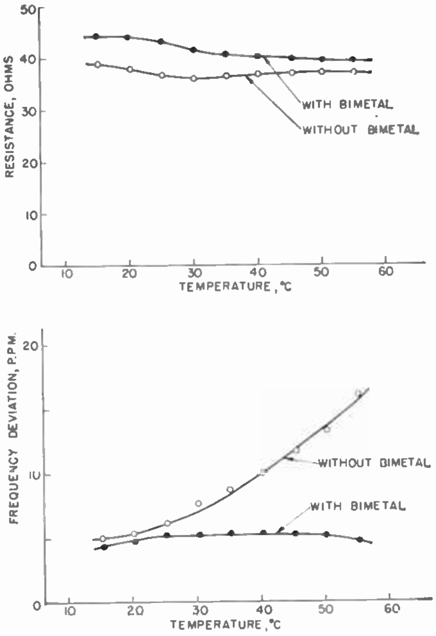

Fig. 6—Frequency and resistance as a function of temperature for a 54-mc 3rd overtone crystal unit, with and without compensating bimetal strip; orientation angle of stress ϕ (see Fig. 1) $\approx 80°$.

Aging will be greatly reduced by using the new device instead of ovens, since the crystal will operate at a much lower average temperature.

E. A. GERBER
U. S. Army Signal Res. and Dev. Lab.
Fort Monmouth, N. J.

On the Synthesis of Multiloop Systems*

It is usual to fix pole locations in multiloop systems by cut-and-try adjustment of gains. In special cases, it is possible to select gains without resorting to trial-and-error techniques. The method to be described provides for prediction of root loci for certain multiloop systems of order one.[1] In essence, the technique involves factoring the common transmission from the total loop transmission, $L(s)$, and recognizing a function of the adjustable parameters which, when the function is held constant, will fix the roots of the remainder of $L(s)$. Thus, with known pole and zero locations, the root locus for the system may be predicted.

For certain practical systems, such as the rate feedback system of Fig. 1, the required function of variable gains is readily recognized.

For Fig. 1:

$$T(s) = \frac{K_1G_p(s)}{1 + K_1G_p(s) + K_2sG_p(s)} = \frac{K_1G_p(s)}{1 + K_2G_p(s)\left[s + \dfrac{K_1}{K_2}\right]}. \quad (1)$$

* Received by the IRE, June 23, 1959.
[1] J. G. Truxal, "Automatic Feedback Control System Synthesis," McGraw-Hill Book Co., Inc., New York, N. Y., pp. 99–101; 1955.

In this case, with K_1/K_2 held constant, the locus for increasing K_1 and K_2 is predictable by considering the poles and zeros of $G_p(s)$ and an additional zero at $s=-(K_1/K_2)$.

When a single-index system with the configuration of Fig. 2 is considered,

$$T(s) = \frac{H_1(s)G_p(s)}{1+G_p(s)[H_2(s)+H_1(s)H_3(s)]}. \quad (2)$$

It is evident that $[H_2(s)+H_1(s)H_3(s)]$ can be selected to produce compensating poles and zeros. For example, if $H_1(s)=K_1$, $H_2(s)=K_2s^2$, and $H_3(s)=s+a$,

$$L(s) = K_2G_p(s)\left[s^2+\frac{K_1}{K_2}s+\frac{K_1}{K_2}a\right].$$

Again, the additional zeros are fixed for a constant ratio of $K_1:K_2$ and the locus can be readily predicted. In a similar manner, for $H_1(s)=K_1(s+a)$, $H_2(s)=K_2/(s+b)$, and $H_3(s)=K_3/(s+c)$,

$$L(s)=K_1K_3G_p(s)$$

$$\cdot\left[\frac{s^2+\left(a+b+\frac{K_2}{K_1K_3}\right)s+\left(ab+c\frac{K_2}{K_1K_3}\right)}{(s+b)(s+c)}\right].$$

In this latter case, the compensating poles and zeros are fixed by the value of K_2/K_1K_3, and the root locus for K_2/K_1K_3 equal to a constant may be generated.

It is instructive to consider the rate feedback system of Fig. 1 for a particular $G_p(s)$. If the controlled process, $G_p(s)$, can be approximated by a pair of complex poles, the root locus may be drawn immediately. When

$$G_p(s) = \frac{1}{s^2+2\zeta\omega_ns+\omega_n^2},$$

(1) becomes

$$T(s) = \frac{K_1}{s^2+(2\zeta\omega_n+K_2)s+(\omega_n^2+K_1)}$$

and the poles of $T(s)$ are described by

$$s = -\left(\frac{2\zeta\omega_n+K_2}{2}\right)$$

$$\pm j\sqrt{(\omega_n^2+K_1)-\frac{(2\zeta\omega_n+K_2)^2}{2}}.$$

It is noted at this point, that the magnitude of the real part of the migrating pole equals $\zeta\omega_n+(K_2/2)$; thus, a series of vertical lines may be drawn intersecting the real axis at

$$\sigma = -\left(\zeta\omega_n+\frac{K_2}{2}\right).$$

Further, it can be shown[2] that the locus of the poles of $T(s)$, for K_1/K_2 held constant, is a circle centered at $\sigma=-(K_1/K_2)$. Given the poles of $G_p(s)$, the loci for various values of K_1 and K_2 are known. Conversely, given the poles of $G_p(s)$ and the desired location of the

[2] The distance, d, between $\sigma=-(K_1/K_2)$ and

$$s = -\left(\zeta\omega_n+\frac{K_2}{2}\right)$$

$$\pm j\sqrt{\omega_n^2+K_1-\left(\zeta\omega_n+\frac{K_2}{2}\right)^2}$$

is a constant for a fixed ratio of K_1 and K_2.

$$d^2=\left(\frac{K_1}{K_2}\right)^2-2\zeta\omega_n\left(\frac{K_1}{K_2}\right)+\omega_n^2.$$

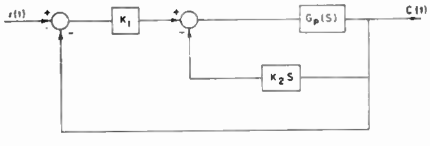

Fig. 1—Rate feedback system.

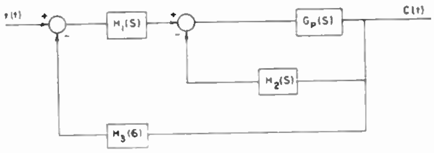

Fig. 2—Single index system.

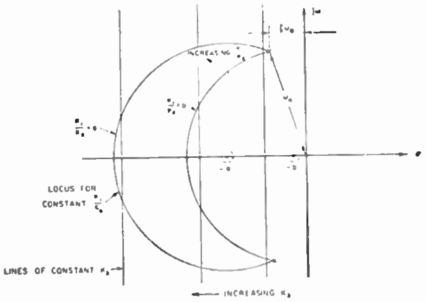

Fig. 3—Loci for rate feedback system with

$$G_p(s) = \frac{1}{s^2+s\xi\omega_n+\omega_n^2}$$

poles of $T(s)$, the required values of K_1 and K_2 may be determined. Fig. 3 illustrates these loci.

It is felt that the described technique promises substantial improvement over the usual trial-and-error method of analyzing multiloop systems. Certainly, the technique provides for the rapid prediction of root-loci for a large class of practical systems; it remains, however, to determine the limits to which this method can be usefully extended.

John D. Glomb
Microwave Res. Inst.
Polytechnic Inst. of Brooklyn
Brooklyn, N. Y.

Noise Temperature in a Radar System*

Amplifying parametric circuits have been operated as the preamplifiers in an L-band high-power radar system. One of the circuits was an inverting up converter, two others were amplifiers. Substantial improvements in receiver sensitivity were secured in each case. The best results were obtained with the inverting up converter. The excess temperature of the entire antenna-duplexer-transmission line system was 190°K. The excess temperature caused by the up converter and the succeeding components of the receiver was 140°K.

* Received by the IRE, June 22, 1959.

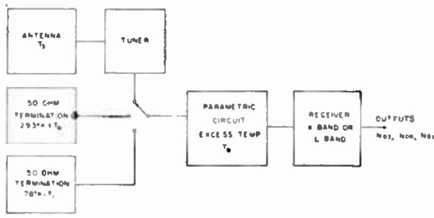

Fig. 1—Noise temperature measurement arrangement.

The measurement system is shown in Fig. 1.

The input to the parametric circuit was switched alternately to each of the three sources; two of them at a known temperature, the antenna at an unknown temperature. The antenna temperature can be computed from relative values for the noise output of the receiver. It is given by

$$\frac{T_3}{T_R}=\frac{N_{03}}{N_{0R}}+\frac{T_e}{T_R}\left[\frac{N_{03}}{N_{0R}}-1\right].$$

T_e can be computed from

$$\frac{T_e}{T_R}=\frac{\left(\frac{N_{01}}{N_{0R}}\right)-\left(\frac{T_1}{T_R}\right)}{1-\left(\frac{N_{01}}{N_{0R}}\right)}.$$

Two amplifiers were also utilized in similar arrangements. They were operated singly and in cascade. L-band Y circulators were used for isolating the amplifiers from the antenna and from each other. An excess noise temperature of 300°K was observed for one amplifier in one set of measurements. The circulator forward loss could account for about 20°K of this excess. The L-band receiver following the amplifiers had a 10-db noise figure. The gain of the parametric amplifier was somewhere in the range of 15 to 20 db, and the 10 db receiver could therefore account for excess noise of 80°K to 30°K.

The tuner shown in Fig. 1 was used to match the antenna to the up converter or amplifier-input line to a VSWR of no more than 1.05. The two terminations were also matched to a VSWR of 1.05 at the specified operating temperatures.

The radar antenna was a cosecant squared fan beam. The output noise level varied very little with azimuth in the test location. The parametric circuits easily withstood the transmitter leakage. The TR box had to be completely removed before permanent damage to the parametric diodes occurred. Burnout then occurred in about one minute of operation.

For operating reasons, careful studies of the distribution of excess noise over the various components in the antenna and duplexer system could not be carried out. The transmitter leakage levels were also not evaluated. The minimum discernible signal of the radar receiver was improved at least 6 db by the use of the up converter. During the noise-temperature tests no unexpected difficulties were encountered.

H. H. Grimm
Electronics Lab.
General Electric Co.
Syracuse, N. Y.

Surface Resistance of Corrugated Conductors*

It was reported by Gent[1] that the attenuation of a waveguide consisting of spaced discs with central circular hole transmitting on circular modes is considerably less than that of a plain circular waveguide of internal diameter equal to that of the circular hole.

This result is very doubtful because of the fact that, in some cases, much of the energy lost in corrugated conductors may have originated from those cross-products of the spatial harmonics which are neglected in Gent's paper. The author believes that the attenuation of any waveguide whose wall is corrugated cannot be less than that of the plain circular waveguide. To show this, we shall prove that the macroscopic or average surface resistance of any periodically corrugated wall cannot be smaller than that of the plain surface.

Fig. 1 shows a typical example of periodically corrugated conductors. The period p of the wall structure is assumed to be much smaller than the wavelength in question so that we can treat the field near the wall surface quasi-statically. Furthermore, when the depth of penetration is very small, in comparison with all the structural dimensions, the wall behaves as a perfect conductor, as far as the outer field is concerned. Then the energy lost in the wall can be calculated from this first approximation by the usual method.

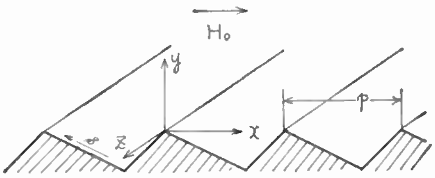

Fig. 1.

For the sake of convenience, we take a right-handed system of Cartesian coordinates as shown in Fig. 1. It is evident that the average surface resistance parallel to the x-axis is larger than that of the plain wall, because of the longer path length of the surface current.

Next, we consider the average surface resistance parallel to the z-axis. At first sight, it may seem that this can be smaller than that of the plain wall because the path width of the surface current is wider in this case. It will be shown in the following discussion, however, that this advantage is over-canceled by the fact that the distribution of the surface current now becomes nonuniform.

Let us assume that $H_x=H_0$ and $H_y=0$ at $y=\infty$. To calculate the average surface resistance, we can assume without any loss of generality that $H_0=2\pi/p$ numerically. By s we denote the length along the cross-sectional curve measured towards the direction inverse to the magnetic field. Then the value of the magnetic potential U is a monotonically increasing function of s so that the magnetic field on the surface is given by $|H|=dU/ds$. Therefore, if R_s is the surface resistance of the plain wall, the energy lost in the corrugated wall is given by

$$P = R_s \int |H|^2 ds = R_s \int |H| \, dU. \quad (1)$$

If V is the conjugate harmonic function of U, the components of the magnetic field must also be the harmonic function of two variables U and V, and may be written as

$$\begin{aligned} H_x &= H_0 + (A_1 \cos U - B_1 \sin U)e^{-V} \\ &\quad + (A_2 \cos 2U - B_2 \sin 2U)e^{-2V} + \cdots \\ H_y &= (A_1 \sin U + B_1 \cos U)e^{-V} \\ &\quad + (A_2 \sin 2U + B_2 \cos 2U)e^{-2V} + \cdots \quad (2) \end{aligned}$$

where the A's and B's are constants whose values are to be determined from the actual form of the corrugation.

For the plain conductor, the A's and B's are all zero and the energy lost per structural period is given by

$$P_0 = R_s \int_0^{2\pi} H_0 dU = R_s H_0^2 p. \quad (3)$$

This checks with the result obtained by the usual method.

For the energy lost per structural period of a corrugated wall, we get from (1), (2), and (3)

$$\begin{aligned} P &= R_s \int_0^{2\pi} \sqrt{H_x^2 + H_y^2} \, dU \geq R_s \int_0^{2\pi} H_x dU \\ &= R_s \int_0^{2\pi} H_0 dU = P_0. \quad (4) \end{aligned}$$

The result given by this equation can be expressed as the following theorems.

1) Under the condition of the same total current per structural period, the energy lost in a corrugated wall cannot be smaller than that lost in the plain surface of the same material.
2) The integral of the x-component of the magnetic field with respect to the magnetic potential is an invariant under corrugation.

If the power lost in the wall is divided by the current flowing per structural period, we get the average surface resistance. Thus we have the Theorem 3.

3) The average surface resistance of any corrugated conductor cannot be smaller than that of the plain conductor.

To illustrate an elementary application of the foregoing discussion, consider a rectangular corrugated surface with infinite corrugation depth as shown in Fig. 2. In this case, there are only x-components of the magnetic field on the horizontal parts of surface and only y-components on the vertical parts. We can then conclude from Theorem 2 that, in spite of the reduction in horizontal length by the ratio w/p, the energy lost in one of the horizontal parts is still equal to that lost in the length p of the plain surface. Thus the total energy lost in this corrugated surface must be larger than that for the plain conductor by the amount which is lost in the vertical parts.

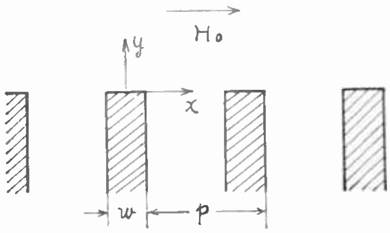

Fig. 2.

So far we have considered the case in which the quasi-static treatment is valid. There has been no complete solution of the problem when a dynamic treatment is needed. Since, in dynamic cases, the magnetic field can go into the gap regions with less attenuation than in the quasi-static case, the author believes that the energy lost in a corrugated conductor, in this case, must be still larger than that lost in the plain conductor. To confirm this conclusion analytically, we must perform Gent's analysis without neglecting the cross-products of the spatial harmonics.

Toshio Hosono
Faculty of Engineering
Nihon University
Kanda-Surugadai
Tokyo, Japan

* Received by the IRE, June 19, 1959.

[1] A. W. Gent, "The Attenuation and Propagation Factor of Spaced-Disc Circular Waveguides," presented at IEE Convention on Long-Distance Transmission by Waveguide, January 29–30, 1959.

The Electromagnetic Energy Stored in a Dispersive Medium*

In sinusoidal time variation, the following expression is commonly used as the mean electric energy stored per unit volume of a dielectric medium:

$$U = \tfrac{1}{4}\epsilon |E|^2, \quad (1)$$

where ϵ is the dielectric constant or permittivity of the medium, and $|E|$ is the absolute value of the electric field. This expression is valid only in the case where ϵ is independent of frequency. There are, however, many materials whose permittivities are not independent of frequency in some region of the spectrum; *e.g.*, an ionized gas near its plasma frequency, some gaseous dielectrics in the microwave region, and most solid dielectrics in the infrared. In such cases we must extend the above expression for the energy storage. For this purpose we first remind ourselves of the formula in which, in circuit theory, the energy stored in a lossless passive linear two-terminal network is given by

$$U = \frac{|V|^2}{4} \cdot \frac{\partial Y(\omega)}{j\partial\omega} \quad (2)$$

where $Y(\omega)$ is the admittance of the network and $|V|$ is the absolute value of the voltage between the terminals as shown in Fig. 1.

Consider a condenser which is insulated by a medium with frequency dependent permittivity as shown in Fig. 2. The expression

* Received by the IRE, June 8, 1959.

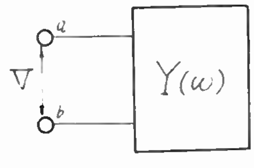

Fig. 1—Two-terminal network with frequency dependent admittance $Y(\omega)$.

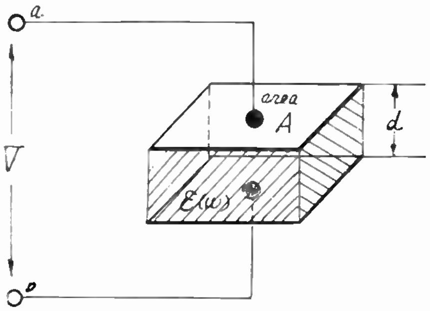

Fig. 2—Condenser-insulated dielectric medium having frequency dependent permittivity $\epsilon(\omega)$.

for the electric energy stored in this condenser is derived as follows. First the admittance of the condenser is calculated as

$$Y(\omega) = j\omega C(\omega), \quad C(\omega) = \epsilon_s(\omega)C_0 \quad (3)$$

where ϵ_s is the specific permittivity of the insulator and C_0 is the capacitance in empty space. The permittivity $\epsilon(\omega)$ is written as $\epsilon_0\epsilon_s(\omega)$, where ϵ_0 is the permittivity of empty space. Substituting (3) into (2), we obtain

$$U = \frac{|V|^2}{4} \cdot \frac{\partial[\epsilon_s(\omega)\omega C_0]}{\partial\omega}. \quad (4)$$

Since the capacitance in empty space is known to be

$$C_0 = \frac{\epsilon_0 A}{d} = \frac{\epsilon_0 A d}{d^2},$$

(4) can be transformed into the equation

$$U = \frac{1}{4}\left(\frac{V}{d}\right)^2 \Omega \frac{\partial[\omega\epsilon(\omega)]}{\partial\omega} \quad (5)$$

where Ω is Ad, the volume of the condenser. Thus the mean energy stored per unit volume is given by

$$u = \frac{U}{\Omega} = \frac{1}{4}\frac{\partial[\omega\epsilon(\omega)]}{\partial\omega}|E|^2, \quad (6)$$

where $|E| = V/d$ is the intensity of the electric field in the medium. Eq. (6) shows the energy stored per unit volume in a dispersive medium.

If we get the explicit expression for the permittivity, we can easily calculate the mean energy storage per unit volume of the medium by making use of (6). The result can be shown to coincide with the one obtained by the microscopic theory which was considered by L. Brillouin in his famous paper.[1] The use of (6), however, permits us to get the same result without complicated considerations.

Now let us show the appropriateness of (6). We consider a dielectric medium which contains N molecular resonators per unit volume, each having the resonance frequency ω_0, mass m, and charge e. Then the mean energy storage per unit volume, being calculated microscopically, is given by

$$u = \frac{1}{2}\epsilon_0\overline{|E|^2} + N(\tfrac{1}{2}m\overline{\dot{S}^2} + \tfrac{1}{2}m\omega_0^2\overline{S^2}), \quad (7)$$

where S is the displacement of the electron from its equilibrium position, $\dot{S}$ the derivative of S with respect to time t, and the bars over the letters indicate the time average. These terms represent the energy of the electric field, the kinetic energy and potential energy of the resonator, respectively.

Now for a lossless system the displacement S, which is found by solving the equation of motion for the electron under the action of the external electric field $E = |E| \cos \omega t$, is represented as

$$S = \frac{e}{m}\frac{|E| \cos \omega t}{\omega_0^2 - \omega^2}. \quad (8)$$

Taking (8) into account, (7) will be transformed into

$$u = \frac{1}{4}|E|^2\left[\epsilon(\omega) + \frac{Ne^2}{m}\frac{2\omega^2}{(\omega_0^2 - \omega^2)^2}\right], \quad (9)$$

where the permittivity is given by

$$\epsilon(\omega) = \epsilon_0 + \frac{Ne^2}{m}\frac{1}{\omega_0^2 - \omega^2}. \quad (10)$$

However, this can be found by substituting (10) into (6).

If the expression for permittivity $\epsilon(\omega)$ can be determined in some way, (6) yields a simple method to obtain the mean energy storage. Furthermore, in the case of a magnetic substance whose permeability is dependent on frequency, we can get a result similar to that obtained for a dielectric substance.

Thus electromagnetic energy stored per unit volume of a medium whose permittivity and permeability are both dependent on frequency is given by

$$U = \frac{1}{4}\frac{\partial[\omega\epsilon(\omega)]}{\partial\omega}|E|^2 + \frac{1}{4}\frac{\partial[\omega\mu(\omega)]}{\partial\omega}|H|^2. \quad (11)$$

T. Hosono
T. Ohira
Faculty of Engineering
Nihon University
Tokyo, Japan

[1] L. Brillouin, "Sur la propagation de la lumière dans un milieu dispersif," *Compt. Rend. Acad. Sci.*, vol. 172, p. 1167; December 5, 1921.

Immittance Properties of Nonreciprocal Networks*

In a previous communication[1] dual representations of the general two-terminal-pair network were given in terms of a topological nonreciprocal element called the unitor. Apart from reciprocal end-loading, each representation consisted of a single normally-orientated unitor having both series (Z_b) and shunt (Z_a) loading, as shown in Fig. 1(a). This basic unitor circuit may be taken as the typical representation of the general non-reciprocal network; as such its driving-point and transfer immittance properties are of importance.

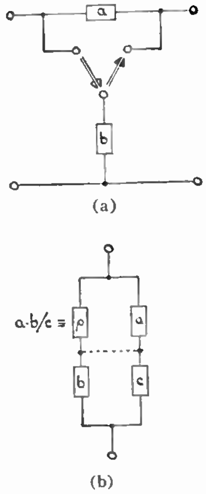

Fig. 1—(a) The unitor model of the typical nonreciprocal network; (b) the equivalent circuit of the driving-point impedance of the network in (a) when terminated in Z_c.

The open-circuit impedance matrix of the circuit of Fig. 1(a) is

$$[Z] = \begin{bmatrix} Z_b & Z_b \\ -Z_a + Z_b & Z_b \end{bmatrix} \quad (1)$$

the determinant of which is $\Delta Z = Z_a \cdot Z_b$. With loading Z_c at one end, the driving-point impedance at the other end is

$$Z_d = z_{11} - \frac{z_{12} \cdot z_{21}}{z_{22} + Z_c} = \frac{\Delta Z + z_{11}Z_c}{z_{22} + Z_c} \quad (2)$$

$$= \frac{(Z_a + Z_c)Z_b}{Z_b + Z_c} = \frac{(\rho + Z_b)Z_c}{Z_b + Z_c}, \quad (3)$$

where $\rho = Z_a \cdot Z_b / Z_c$, which reduces to $Z_d = Z_c$ at $Z_a \cdot Z_b = Z_c^2$. Because of the equality of the principal diagonal elements in (1), and of the symmetry in $z12$, $z21$ of (2), the value of Z_d given by (3) is invariant under transposition of the network with respect to its terminations; moreover, because of the symmetry of the internal loading, it is invariant also to transposition of the unitor about terminal 2.

An explanation of this result is readily given in terms of the properties of the unitor. In the forward direction the unitor sets up a current v_1/Z_b, a proportion $Z_c/(Z_a+Z_c)$ of which flows through Z_a and the input source, increasing the current which would flow in the absence of the unitor by the factor $(Z_b+Z_c/Z_b$, as though Z_a and Z_c were shunted by an additional fictitious impedance $\rho = Z_a \cdot Z_b/Z_c$, and by Z_b, respectively, as shown in Fig. 1(b). In the backward direction, (*i.e.*, with source and load transposed), the action of the unitor is to preserve a balanced bridge condition between Z_a, Z_b, Z_c and a fourth, fictitious, element ρ whose value is given, as before, by the bridge balance condition as $\rho = Z_a \cdot Z_b / Z_c$. Evaluation of

Received by the IRE, July 6, 1959.
[1] A. W. Keen, "A topological nonreciprocal network element," Proc. IRE, vol. 47, pp. 1148–1150; June, 1959. The following corrections have been submitted by the author. In the third paragraph, line 10 should read 123 instead of 132; in Fig. 4, the bracketed portion in the caption should continue ". . . this becomes a circulator"; and in footnote 9, the third word in the title should read "topology." This paper has now been published in IRE Trans. on Circuit Theory, vol. CT-6, pp. 188–196; June, 1959.

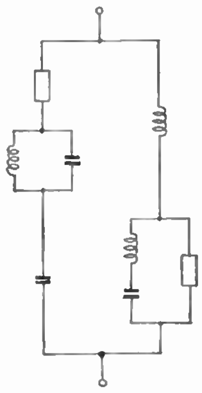

(a)

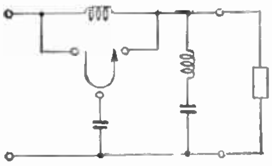

(b)

Fig. 2—(a) The form of the Bott-Duffin cycle; (b) a unitor equivalent of (a) in which an alternative graphical representation of the unitor is shown.

the terminal impedance of the equivalent circuit of Z_d in Fig. 1(b) confirms the result already given at (3).

It will be noted that in case $Z_a \cdot Z_b = R_0^2$, where R_0 is a real constant, ρ and Z_c comprise an inverse pair. An immediate application of this result is to driving-point immittance synthesis. It is known that the Bott-Duffin method of realizing a positive-real immittance function produces a cycle which is of balanced bridge form [Fig. 2(a)] and has the advantage of avoiding the need for a pair of perfectly-coupled coils or an ideal transformer (as required by the classical Brune method) per cycle, at the cost of requiring an excessive number of immittance elements. By correlation of Figs. 1(b) and 2(a), one may obtain unitor forms of the Bott-Duffin cycle; one of these is given in Fig. 2(b), in which the fictitious impedance ρ needed to account for the unitor action replaces the remainder impedance, thereby reducing the realization to canonical form. This development will be discussed in detail in a separate paper.

A constant-resistance form of Fig. 1(a) may be had by making Z_a and Z_b an inverse pair with respect to a resistive termination R_0; under this condition the determinant of the impedance matrix in (1) is a constant, for $\Delta Z = Z_a \cdot Z_b = R_0^2$. Alternatively, setting $Z_a = Z_b = R_0$, with Z_c arbitrary, results in a driving-point impedance $Z_d = R_0$, independently of the load Z_c because ρ is maintained at the inverse value of Z_c with respect to R_0 by the unitor action. The network may then be reorientated in either of two ways to bring $Z_a(=R_0)$ or $Z_b(=R_0)$ into the load position, as shown in Fig. 3(a) and 3(b) respectively. In each case, transposition of the unitor itself about terminal 2 leaves the constant-resistance property unchanged. Using the same networks immittance, transformation by a real constant may be achieved with Z_a (or, dually, Z_b) and Z_c similar in kind but of different magnitude;

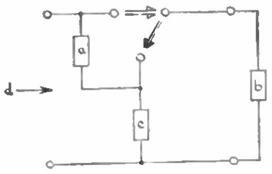

(a)

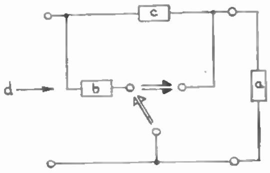

(b)

Fig. 3—Circuits obtained by re-orientation of Fig. 1(a): with $a = b = R_0$ these are constant-resistance forms; with a and c in (a) of similar kind and of large, but different, magnitudes, a Z_b transformer is obtained; dually, with b and c in (b) similar in kind and of small, but different, magnitudes, a Z_a transformer is obtained.

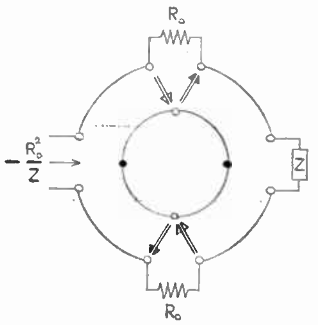

(a)

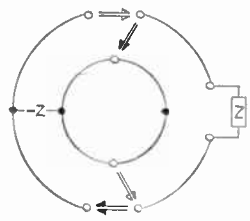

(b)

Fig. 4—(a) Unit negative impedance inversion; (b) unit negative impedance conversion.

i.e., such that their ratio is a real constant. If $Z_a(Z_b)$ and Z_c are increased (decreased) together, keeping their ratio constant, the driving-point impedance Z_d will tend to a scalar multiple of Z_b (Z_a) which is a simple function of the desired immittance transformation ratio.

Either positive or negative inversion of an immittance may be obtained with a pair of unitors in a feedback loop. Negative impedance inversion with respect to a constant R_0 is shown at Fig. 4(a), where the shunt-loaded (R_0) unitors, the impedance under inversion, and the access terminal-pair comprise a shunt-shunt feedback loop. In the dual, negative-admittance inversion circuit, the unitors are series loaded with conductances G_0 and are connected, together with the admittance under inversion and the access terminal-pair, in a series-series feedback configuration. For positive inversion in either case it is necessary to invert the loop gain by inserting an ideal unit-ratio

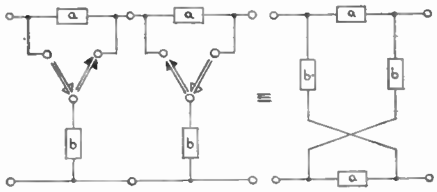

(a)

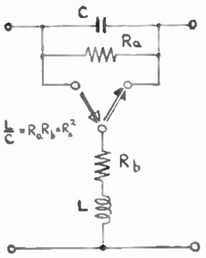

(b)

Fig. 5—(a) A unitor network equivalent of the symmetrical lattice; (b) a simple nonreciprocal image-parameter equalizer.

inverting transformer, thereby producing the unitor forms of three-terminal impedance and admittance gyrator, the latter of which was given in Fig. 4 of the previous communication. Unit negative immittance conversion may be had with a pair of unitors in a positive feedback loop, with one unitor orientated for unit current gain and the other for unit voltage gain. The shunt-series feedback form shown in Fig. 4(b) provides unit negative impedance conversion (UNIC); the dual series-shunt configuration provides unit negative admittance conversion (UNAC).

The short- and open-circuit values of Z_d are simply $z_{s1} = z_{s2} = Z_a$ and $z_{01} = z_{02} = Z_b$, giving for the image (and iterative) impedances of the Fig. 1(a) network:

$$Z_{I1} = Z_{I2} = Z_I = \sqrt{z_s z_0} = \sqrt{Z_a Z_b}$$

as for the correspondingly annotated lattice (Fig. 5(a); and for the image transfer constant

$$\theta_I = \tanh^{-1} \sqrt{\frac{z_s}{z_0}} = \tanh^{-1} \sqrt{\frac{Z_a}{Z_b}},$$

which is exactly one half of that of the same lattice. An image parameter equivalent of the symmetrical may therefore be obtained by cascading a pair of similar unitor circuits; for exact equivalence, however, one member of the pair must be reversed with respect to the other in order to secure symmetry, as shown in Fig. 5(a). This equivalence may be confirmed by Bartlett's bisection theorem or by matrix methods. The forward-acting unitor of the pair has a voltage gain $(R_0 - Z_a)/R_0$ and provides zeros of the transfer function; the backward-acting unitor has a voltage-gain $R_0/(R_0 + Z_a)$ and produces the poles of this function: the overall gain is the product of the separate factors, *viz.* $(R_0 - Z_a)/(R_0 + Z_a)$, as for the lattice.

The importance of the equivalence revealed in Fig. 5(a) follows from the invariance of the image parameters of the unitor cascade under reversal of either one of the two unitor half-sections. The reciprocity restriction may, in this way, be removed, thereby extending the class of networks which may be produced by the classical image-parameter method to include active-network networks in which the unitors may be approximated by thermionic amplifier tubes or transistors on the basis of the unitor equivalents of these elements which were given in Fig. 3 of the previous communication. A very simple example of a non-reciprocal equalizer is given in Fig. 5(b): if R_a is sufficiently large to absorb r_a/μ a close approximation may be obtained by replacing the unitor by a thermionic amplifier tube, preferably of high ra and high μ. Thus, by means of electronic realizations of the equivalent unitor cascade pair, the lattice form may be used as a basis for the synthesis and design of active, as well as of passive networks.

A. W. Keen
Technical College
Coventry, England

A System of Nonuniform Transmission Lines*

In view of the recent interest in tapered lines[1] the N-port generalization of a single transmission line is indicated below. Because of the generality of the approach adopted, the discussion gains in simplicity and clarity.

The customary transmission line equations are

$$\frac{dV}{dz} = -ZI \tag{1}$$

$$\frac{dI}{dz} = -YV \tag{2}$$

or, in vector notation

$$\frac{d}{dz}\boldsymbol{\phi} = A\boldsymbol{\phi} \tag{3}$$

where

$$\boldsymbol{\phi} = \begin{pmatrix} V \\ I \end{pmatrix} \quad \text{and} \quad A = \begin{pmatrix} 0 & -Z \\ -Y & 0 \end{pmatrix}. \tag{4}$$

We will now consider the generalization of (3) wherein $\boldsymbol{\phi}$ is a column with N entries and A is a square matrix with N^2 entries. For the moment let us consider the exponential taper

$$A = e^{-L_0 z}A_0 e^{L_0 z} \tag{5}$$

where each of the N^2 entries of the square matrices A_0 and L_0 are constants (independent of z). (Of course if A_0 and L_0 commute, *i.e.*, $A_0L = LA_0$, then $A = A_0$). Define $\hat{\boldsymbol{\phi}}$ by

$$\boldsymbol{\phi} = e^{-L_0 z}\hat{\boldsymbol{\phi}}. \tag{6}$$

When (6) and (5) are substituted into (3) one obtains

$$\frac{d}{dz}\hat{\boldsymbol{\phi}} = (A_0 + L_0)\hat{\boldsymbol{\phi}} \tag{7}$$

and hence

$$\hat{\boldsymbol{\phi}}(z) = e^{(A_0+L_0)z}\hat{\boldsymbol{\phi}}(0). \tag{8}$$

By combining (6) and (8) one obtains

$$\boldsymbol{\phi}(z) = e^{-L_0 z}e^{(A_0+L_0)z}\boldsymbol{\phi}(0) \tag{9}$$

as the solution to (3) when the matrix A has the exponential taper specified by (5). In particular, when L_0 and A_0 are partitioned in a consistent manner with

$$L_0 = \begin{pmatrix} L_1 & 0 \\ 0 & L_2 \end{pmatrix}$$

and

$$A_0 = \begin{pmatrix} 0 & A_1 \\ A_2 & 0 \end{pmatrix}$$

then A is given by

$$A = \begin{pmatrix} 0 & e^{-L_1 z}A_1 e^{L_2 z} \\ e^{-L_2 z}A_2 e^{L_1 z} & 0 \end{pmatrix}. \tag{10}$$

In order to consider more general tapers let $K(z)$ denote the solution to the matrix equation

$$\frac{d}{dz}K = L(z)K, \qquad K(0) = I, \tag{11}$$

where I is the identity matrix. One can then verify that

$$\boldsymbol{\phi}(z) = K^{-1}(z)e^{(A_0+L_0)z}\boldsymbol{\phi}(0) \tag{12}$$

is the solution to

$$\frac{d}{dz}\boldsymbol{\phi}(z) = K^{-1}(z)(A_0 + L_0 - L(z))K(z)\,\boldsymbol{\phi}(z) \tag{13}$$

where A_0 and L_0 are arbitrary constant matrices. Thus, the solution to the nonuniform line specified in (13) is given explicitly in (12). The matrix coefficient in (12) is precisely the transfer matrix for a line of length z. Finally, one should note that the exponential taper in (5) is the special case of (11) and (13) wherein $L(z) = L_0$ so that $K = e^{L_0 z}$.

H. Kurss
W. K. Kahn
Microwave Res. Inst.
Polytechnic Inst. of Brooklyn
Brooklyn, N. Y.

* Received by the IRE, July 10, 1959. This work was performed in connection with the U. S. Army Signal Res. and Dev. Lab., Contract No. DA-36-039 sc-78001.

[1] I. Jacobs, "A generalization of the exponential transmission line," Proc. IRE, vol. 47, pp. 97–98; January, 1959.

TM Waves in Submillimetric Region*

Karbowiak concludes in a recent paper[1] that, with all transverse magnetic (TM) waves in metal waveguides, the attenuation becomes proportional to (frequency)$^{-5/2}$ at sufficiently high frequencies. It is the purpose of this letter to show that the TEM and TM_{01} waves in planar waveguides and the TM_{01} wave in circular waveguides do not have this characteristic.

For planar waveguide, Karbowiak uses the equation

$$jZ_s k_0 = h \tan ah, \tag{1}$$

where

$k_0 = 2\pi/\lambda$,
a = distance between waveguide surfaces,
$h = h_r + jh_i$
Z_s (for copper waveguide) $= 6.8 \times 10^{-6} k_0^{1/2} \angle 45°$.

The propagation constant is related to h by the equation

$$\gamma = \alpha + j\beta = \sqrt{h^2 - k_0^2} \tag{2}$$

He obtains two sets of approximate solutions for h. One set is for $a|Z_s|k_0 \ll 1$ (at low frequencies) and is in the vicinity of $h_0 = n\pi/a$ (n = order of the mode); the other is for $a|Z_s|k_0 \gg 1$ (at extremely high frequencies) and is in the vicinity of $h_0' = (n - \frac{1}{2})\pi/a$.

Eq. (1) applies to the case where only one of the two planar surfaces is an imperfect conductor. To include the practical case where both surfaces are imperfect, we will deal with the following.

$$jZ_s k_0 = h \tan(ah/2), \ n \text{ even}. \tag{3}$$

$$jZ_s k_0 = -h \cot(ah/2), \ n \text{ odd}. \tag{4}$$

The solution of (3) will be applied to (1) by means of an obvious modification. For $Z_s = |Z_s|\angle 45°$, (3) and (4) can be put into the following forms.

$$\sinh ah_i = \mp\left(\frac{ah_r + ah_i}{ah_r - ah_i}\right)\sin ah_r, \tag{5}$$

$$ak_0|Z_s| = \frac{\sqrt{2}\sinh ah_i}{\cosh ah_i \pm \cos ah_r} \cdot \left[\frac{(ah_r)^2 + (ah_i)^2}{ah_r + ah_i}\right], \tag{6}$$

where the upper sign applies for n even and the lower, for n odd.

Fig. 1 shows the solution of (3) and Fig. 2 shows the solution of (4). These curves were traced by solving (5) for 0.1 intervals of ah_r/π by means of successive approximations. It should be noted that the arrows in the curves point in the direction of increasing frequency (increasing $ak_0|Z_s|$).

Fig. 1 describes the solution of (1) if the abscissa and ordinate values are divided by two. Then the curve labeled TM_{02} in the figure corresponds to the TM_{01} wave. For this case (only one plane imperfect) the TM_{01} wave by (2) converts at high frequencies to one having a negative attenuation-frequency slope as stated in the reference paper. All higher order modes do so also. However, Fig. 1 shows that the TEM wave does not behave in this manner and that the value of $h_0' = \pi/(2a)$, which Karbowiak associates with both the TEM and TM_{01} waves, belongs only to the latter.

Fig. 2 shows that the attenuation of the TM_{01} wave increases without limit with the frequency for the practical case of both planes being imperfect.

The general behavior of the TM_0 waves in circular waveguide is similar to that of the odd order waves in planar waveguide. This

* Received by the IRE, June 1, 1959.

[1] A. E. Karbowiak, "Guided wave propagation in submillimetric region," Proc. IRE, vol. 46, pp. 1706–1711; October, 1958.

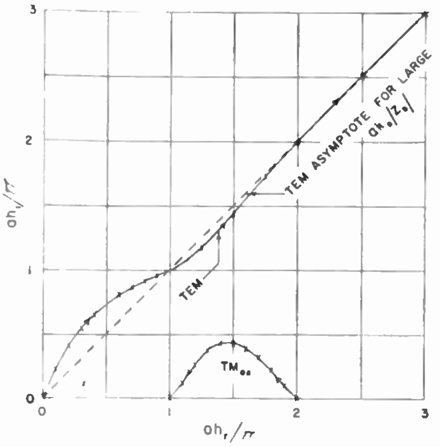

Fig. 1—Solution of $jk_0|Z_s|\angle 45° = h \tan (ah/2)$; even order modes in planar waveguide; arrows point in the direction of increasing frequency.

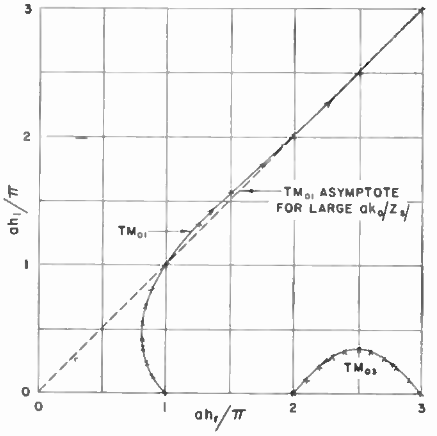

Fig. 2—Solution of $jk_0|Z_s|\angle 45° = -h \cot (ah/2)$; odd order modes in planar waveguide; arrows point in the direction of increasing frequency.

may be seen from the similarity of (4) and the corresponding equation for circular waveguides, which is

$$jZ_s k_0 = -h(J_0(hs)/J_1(hs)), \quad (7)$$

where s is the guide radius.

The circular TM_{01} wave behaves as the TM_{01} wave of Fig. 2 except that it takes off (low frequencies) at $sh_r = 2.405$ rather than at $ah_r/2 = \pi/2$. The circular TM_{02} wave behaves very nearly as the TM_{03} wave of Fig. 2 except that it takes off at $sh_r = 5.520$ rather than at $ah_r/2 = 3\pi/2$, and terminates at $sh_r = 3.832$ rather than at $ah_r/2 = \pi$.

C. A. Martin
RCA Labs. Div.
Rocky Point, N. Y.

Author's Comment[2]

Mr. Martin has made a valuable contribution. Whereas I have analyzed a waveguide with one imperfect wall and have derived the property of negative slope of the attenuation-frequency curve, Mr. Martin's analysis is more general and reveals new features. Thus in a waveguide where all walls are imperfectly conducting (although the negative slope of the attenuation curve is still a feature of most modes) the TEM and TM_{01} modes are notable exceptions. Dr. Oliner has recently drawn my attention to the possibly exceptional behavior of these two modes in a waveguide with two imperfect walls (as distinct from one imperfect wall). It certainly is a very interesting and significant observation.

A. E. Karbowiak
Standard Telecommunication Labs., Ltd.
Enfield, Middlesex, England

² Received by the IRE, July 6, 1959.

Efficient Harmonic Generation*

A harmonic generator using a rectifier multiplier followed by an amplifier is more efficient than its equivalent class-C multiplier. A proposed rectifier-transistor harmonic generator is capable of high efficiency that is nearly independent of harmonic number.

Electronic systems often need efficient means for generating harmonic power. This note is a review of practical harmonic generator performance with emphasis on a circuit that seems to have been neglected.

Harmonic generators may be active or passive devices, depending on whether or not the device is supplied with power in addition to that at the fundamental frequency. For either type, we shall be concerned mainly with the ratio of harmonic output power to fundamental input power, defined as the conversion gain $G_c(n)$, where n is the harmonic number. The fundamental input power is all such power supplied to the device. The harmonic output power is that which is available at the input of any transformer used to match the device to its load, and thus includes any transformer loss.

The conventional frequency multiplier is the class-C multiplier of Fig. 1 whose resonant output circuit is tuned to a harmonic of the driving frequency f. For simplicity, we assume that the output current pulse is a clipped sinusoid of phase duration 2α at the fundamental frequency. If the amplitude of the fundamental driving voltage is E_1, then the maximum nth harmonic output power is obtained when $\alpha = \pi/n$ and is

$$P_n = \frac{2}{\pi^2}(g_m E_1)^2 R_L \left[\frac{\sin(\pi/n)}{n^2-1}\right]^2, \quad (1)$$

where g_m is the transconductance and R_L is the effective load resistance. Even if the amplifier itself requires no driving power, the input power must supply the transformer loss represented by the shunt resistance R_G. The input power is then

$$P_1 = E_1^2/2R_G \quad (2)$$

and the conversion gain is

$$G_c(\text{class-}C) = \frac{4}{\pi^2}(g_m^2 R_G R_L)\left[\frac{\sin(\pi/n)}{n^2-1}\right]^2. \quad (3)$$

* Received by the IRE, June 18, 1959.

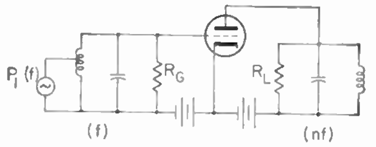

Fig. 1—Class-C frequency multiplier.

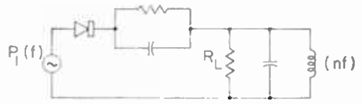

Fig. 2—Rectifier-frequency multiplier.

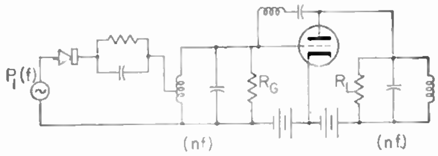

Fig. 3—Rectifier-amplifier frequency multiplier.

A passive harmonic generator is the rectifier multiplier of Fig. 2. This type of multiplier is specified by a conversion efficiency

$$\epsilon_d = G_0 + G_c \quad (4)$$

where G_0 is the fraction of the input power converted to dc. Page[1] has shown that for $\epsilon_d = 1$ the maximum conversion gain is

$$\max.\ G_c(\text{rect.}) = 1/n^2. \quad (5)$$

This maximum is approached, even ideally, only as both input and output powers approach zero. In practice, a G_c of about $\frac{1}{2}n^2$ seems obtainable, and ϵ_d may be almost unity.

Now suppose that the amplifier of Fig. 1 is used to amplify linearly the output of the rectifier multiplier of Fig. 2, as described by Shaull.[2] In Fig. 3, the harmonic output power is

$$P_n = \frac{1}{2}(g_m E_n)^2 R_L \quad (6)$$

where E_n is the amplitude of the harmonic driving voltage. Assuming a practical rectifier conversion gain,

$$\frac{E_n^2}{2R_G} = \frac{P_1}{2n^2} \quad (7)$$

so that

$$G_c(\text{rect.-amp.}) = \frac{1}{2}(g_m^2 R_G R_L)\left[\frac{1}{n}\right]^2. \quad (8)$$

This conversion gain exceeds that of the class-C multiplier for all $n \geq 2$. In addition, if the rectifier develops sufficient harmonic power, the amplifier may be operated class-C, with an improvement in plate efficiency as well. Shaull[2] found rectifier-amplifiers to be noisier than class-C multipliers. A recent experiment at the National Bureau of Standards does not confirm this inferiority; Shaull's noise may have been due to non-optimum circuit impedances or to cascading

¹ C. H. Page, "Harmonic generation with ideal rectifiers," Proc. IRE, vol. 46, pp. 1738–1740; October, 1958.

² J. M. Shaull, "Frequency multipliers and converters for measurement and control," *Tele-Tech. & Electronic Ind.*, vol. 14, pp. 86–89, 7 ff.; April, 1955.

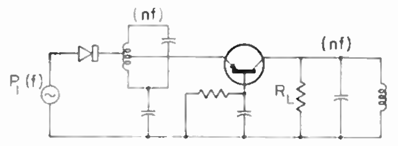

Fig. 4—Rectifier-transistor frequency amplifier.

two rectifier stages before amplification rather than the single stage shown in Fig. 3.

Finally, the rectifier-multiplier becomes much more attractive if some use can be made of the input power that is unavoidably converted to dc. A method for doing so uses the rectifier-transistor multiplier of Fig. 4, where both harmonic and dc power supply the transistor amplifier. With a rectifier conversion efficiency $\epsilon_d = 1$ and an optimum ratio of G_c(rect.) to G_0, the maximum transistor output power is

$$P_n = GG_c(\text{rect.})P_1 = \epsilon_c G_0 P_1 \quad (9)$$

where G is the transistor power gain, and ϵ_c is the transistor collector efficiency. But $G_0 = 1 - G_c(\text{rect.})$, so that

$$G_c(\text{rect.}) = \frac{\epsilon_c}{\epsilon_c + G} \quad (10)$$

and

$$G_c(\text{rect.-trans.}) = \frac{\epsilon_c G}{\epsilon_c + G} \quad (11)$$

with (10) as a condition. (For large n, it may be impossible to satisfy (10); previous assumptions require that $G \geq (2n^2 - 1)\epsilon_c$, but this inequality will almost always hold for any n of practical interest. Note that (10) usually requires a rectifier conversion gain considerably less than the possible maximum. Thus, if the transistor has appreciable power gain, it pays to convert most of the input power to dc.) Typical values in (11), at least where the transistor is operated at moderate frequency in class-C, are $\epsilon_c = 0.9$ and $G = 100$, yielding G_c (rect.-trans.) $= 0.9$. The rectifier-transistor multiplier is therefore a "passive" device whose conversion gain is essentially high and independent of harmonic number.

The circuits of Figs. 3 and 4 should be useful in transmitter exciters, radio receivers, and stable clocks. The method of Fig. 4, *i.e.*, using a vacuum tube whose dc plate supply and ac excitation are both generated by a rectifier multiplier, may also be useful at high power.

G. Franklin Montgomery
Natl. Bureau of Standards
Washington, D. C.

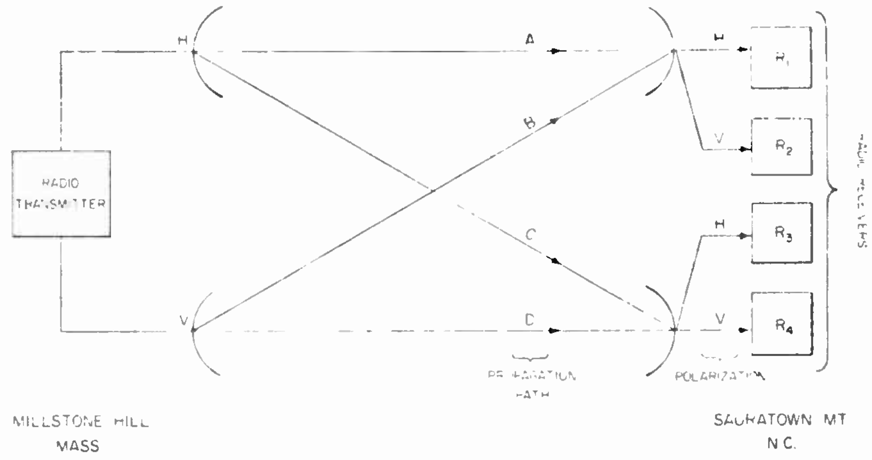

Fig. 1—Block diagram of diversity system.

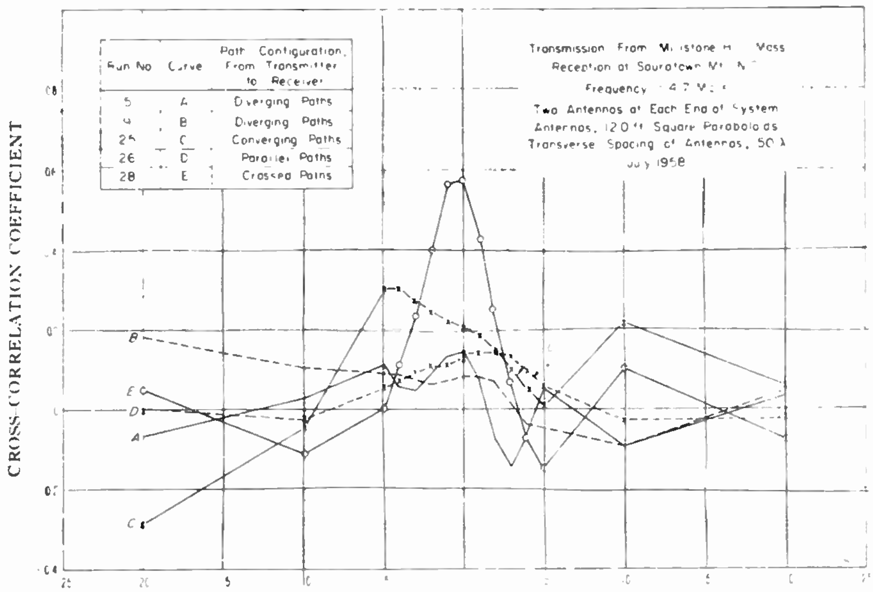

Fig. 2—Cross correlation of tropospheric carrier envelopes vs time displacement of the envelopes relative to each other.

A Note Regarding the Mechanism of UHF Propagation Beyond the Horizon*

Since appreciable controversy still exists regarding the mechanism of beyond-the-horizon propagation of UHF radio waves, it is believed that the following observations may be of interest to workers in this field. Recently E. F. Florman and R. W. Plush recorded simultaneously in pairs the carrier envelope amplitudes obtained from four diversity receivers in the Millstone, Mass. to Sauratown, North Carolina 638-mile path, at a frequency of 417 mc. Antennas at both terminals were square parabolic sections of 120-by-120 feet. Measurements made with only one polarization at the transmitter indicated that the conversion of energy on the path from horizontal to vertical polarization or vertical to horizontal was very small; and as a result, if different polarizations are employed at the transmitters, we can consider that four independent paths are available at the receivers, as shown in Fig. 1.

It is well known that when sufficient spacing exists between receiving antennas, the carrier intensity level received from the diverging paths A and C or B and D will not be correlated. This was, in fact, observed as is shown in Fig. 2. The same results were also found for the converging or parallel paths. When, however, the crossed paths B and C were compared, an appreciable correlation was observed as is seen in Fig. 2.

If the mechanism by which energy is transferred is primarily dependent on atmospheric turbulence either over the complete path or in the foreground of the antennas, it would appear that paths B and C should be as independent as the diverging, converging, or parallel paths. On the other hand, if the energy is transferred via a common "scatter volume," it would appear possible, but not necessary, that correlation could exist between paths B and C.

It should be emphasized that the results given here are for one specific path, and cross correlation over 30-minute intervals. In some other transhorizon propagation cases the atmospheric turbulence in the antenna foreground could possibly become important.

A. D. Watt
E. F. Florman
R. W. Plush
Natl. Bureau of Standards
Boulder, Colo.

* Received by the IRE, June 15, 1959.

Unusual Propagation at 2500 KC*

As is generally known, frequencies of the order of three megacycles constitute "borderline territory" between the high-frequency spectrum, with its ionospheric propagation, and the medium frequency range.

Studies made of the signal strength of station WWV, Beltsville, Md. from this location on 2500 kc indicate a 40- to 50-db variation between daytime and evening levels, caused undoubtedly by D-layer absorption. The typical daytime signal observed here is steady, with a slow fading characteristic, and rather weak, with levels generally between 20 and 50 μv.[1] Nighttime levels may reach 10,000 μv, although they usually average about 2000.

This weak daytime condition poses an intriguing question: Can the presence of a swift-moving body in the upper ionosphere, such as an earth satellite, have any effect upon 2.5-mc propagation, as it does at 20 mc? Theory answers with an unequivocal no, pointing out that the high absorption rates at this frequency would cancel out any reflection which might be linked, directly or indirectly, with the satellite.

Indeed, experimentation showed that for the conditions described above any satellite-linked effects are so small as to be immeasurable.

However, on occasion a different daytime condition has been found to exist. This is a rapid fading effect, with a variation rate of about 100 per minute and peak levels of 50–100 μv.[1] No clear explanation of this is available, although the rapid flutter strongly suggests some type of skywave effect, possibly sporadic-E backscatter, on at least one component of the wave, necessarily accompanied by a lessening of the absorption rate. At any rate, satellite-linked propagation disturbances can and do occur under this type of condition. A detailed description of one case follows.

Such rapid flutter was observed on May 31, 1959, with a peak level of about 75 μv (higher towards the end of the observation period, about 150 μv), and an average level of 25–30 μv. The observation period lasted from 12:50 p.m. to 1:11 p.m., EDST. At 12:52, the flutter suddenly stopped and a clear, steady beat note emerged, with a signal level of 50–70 μv, ending at 12:54, at which time the flutter resumed. At exactly this interval, the Vanguard I carrier rocket was passing in an easterly direction, just east (71° W.) of the propagation path, at 34° N. lat., and at an altitude of 700 miles. The fading effect continued with a rising peak level until 12:57, when it again gave way to a steady slow-fading signal, with levels of 70–140 μv. At 12:59, the flutter resumed, and lasted with peak levels of about 150 μv until after the end of the observation period. At the time of the second interruption, Explorer IV was several hundred miles west of the propagation path, moving southeast at an altitude of 750 miles. No frequency variation was noticed, although the calculated maximum possible Doppler shift is far below the measurement capabilities of the receiver; this aspect, then, cannot be given much importance.

No attempt at speculation will be made here as to the cause of the effect, except to note that four other such disturbances have been noted. In all cases the flutter residual signal was noted, a correlation was established with a satellite pass, and the level of the "reflected" signal roughly equalled the peak of the residual flutter. This is not to say, however, that such disturbances *always* occur under the flutter condition.

It has been said that many discoveries in science resulted from apparent inconsistencies with prevailing theory. Here is one such inconsistency.

RAPHAEL SOIFER
33 Fifth Avenue
New York 3, N. Y.

* Received by the IRE, June 25, 1959.

[1] All strength readings were taken with a standard S meter calibrated in microvolts at antenna terminals; although this may not be a perfect absolute standard, it does provide a relatively unchanging scale with which to compare measurements. The receiving equipment consisted of a Hallicrafters model SX-96 dual-conversion receiver and a dipole antenna resonant at 7050 kc; it was therefore relatively omnidirectional at this frequency.

Generalized Energy Relations of Nonlinear Reactive Elements*

Manley and Rowe[1] have been referred to very frequently by the authors working with parametric amplifiers. While their theory is based upon the interaction between two applied frequencies, it is possible to generalize it to any number of applied frequencies. The derivation of the equations follows a pattern similar to Manley and Rowe's with the exception that a Fourier summation of n variables is used. The resultant energy relations are

$$\left.\begin{aligned}
&\sum_{m_1=0}^{\infty}\sum_{m_2\cdots m_n=-\infty}^{\infty}\cdots\sum \frac{m_1 W_{m_1,m_2,\cdots,m_n}}{m_1f_1+m_2f_2+\cdots+m_nf_n}=0,\\
&\sum_{m_2=0}^{\infty}\sum_{m_1,m_3\cdots m_n=-\infty}^{\infty}\cdots\sum \frac{m_2 W_{m_1,m_2,\cdots,m_n}}{m_1f_1+m_2f_2+\cdots+m_nf_n}=0,\\
&\cdots\cdots\cdots\cdots\cdots\cdots\\
&\sum_{m_n=0}^{\infty}\sum_{m_1,m_2,\cdots m_{n-1}=-\infty}^{\infty}\cdots\sum \frac{m_n W_{m_1,m_2,\cdots,m_n}}{m_1f_1+m_2f_2+\cdots+m_nf_n}=0,
\end{aligned}\right\}\quad(1)$$

where $W_{m_1,m_2,\cdots,m_n}$ are the average power flowing into the nonlinear reactance at frequencies $\pm[m_1f_1+m_2f_2+\cdots+m_nf_n]$, $m_1, m_2 \cdots m_n$ are integers, and $f_1, f_2\cdots f_n$ are the applied frequencies.

* Received by the IRE, July 20, 1959. This work was supported by Project MICHIGAN under Department of the Army contract (DA36-039SC-78801), administered by the U. S. Army Signal Corps.

[1] J. R. Manley and H. E. Rowe, "Some general properties of nonlinear elements—part I. General energy relations," PROC. IRE, vol. 44, pp. 904–913; July, 1956.

An example of the application of (1) is a two-pump parametric amplifier. In this case, we have two pumping frequencies, f_1 and f_2 and a signal frequency f_3. Eq. (1) reduces to

$$\left.\begin{aligned}
&\sum_0^{\infty}\sum_{-\infty}^{\infty}\sum_{-\infty}^{\infty}\frac{m_1W_{m_1,m_2,m_3}}{m_1f_1+m_2f_2+m_3f_3}=0,\\
&\sum_{-\infty}^{\infty}\sum_0^{\infty}\sum_{-\infty}^{\infty}\frac{m_2W_{m_1,m_2,m_3}}{m_1f_1+m_2f_2+m_3f_3}=0,\\
\text{and}\quad&\\
&\sum_{-\infty}^{\infty}\sum_{-\infty}^{\infty}\sum_0^{\infty}\frac{m_3W_{m_1,m_2,m_3}}{m_1f_1+m_2f_2+m_3f_3}=0.
\end{aligned}\right\}\quad(2)$$

Further simplification of (2) is accomplished by introducing the property of high-Q resonant circuits, each tuned to f_1, f_2, f_3 and f_4 $(=f_1+f_2-f_3)$ respectively. Then (2) reduces to

$$\left.\begin{aligned}
&\frac{W_{1,0,0}}{f_1}+\frac{W_{1,1,-1}}{f_1+f_2-f_3}=0,\\
&\frac{W_{0,1,0}}{f_2}+\frac{W_{1,1,-1}}{f_1+f_2-f_3}=0,\\
\text{and}\quad&\\
&\frac{W_{0,0,1}}{f_3}-\frac{W_{1,1,-1}}{f_1+f_2-f_3}=0.
\end{aligned}\right\}\quad(3)$$

Eq. (3) is sometimes rewritten in a more familiar form as

$$\frac{W_1}{f_1}=\frac{W_2}{f_2}=-\frac{W_3}{f_3}=-\frac{W_4}{f_1+f_2-f_3},\quad(4)$$

where $W_1=W_{1,0,0}$, $W_2=W_{0,1,0}$, $W_3=W_{0,0,1}$ and $W_4=W_{1,1,-1}$.

CHAI YEH
Willow Run Labs.
University of Michigan
Ann Arbor, Mich.

P-N-P Variable Capacitance Diodes*

The purpose of this letter is to describe the properties of a p-n-p semiconductor diode when it is used as a low-loss, voltage variable capacitor. To arrive directly at the fundamental characteristics of such a structure, we shall neglect the possibility of transistor action and consider the diode to consist of two single-ended diodes placed back to back with a common base. Under this assumption, the diode and its electrical circuit models are given in Fig. 1.

In the circuit model of Fig. 1(b), R_C is the contact resistance, R_P is the bulk resistance of the p-type material, and R_N is the bulk resistance of the n-type material. C_1 and C_2 are the transition capacitances of the two junctions, and R_1 and R_2 are the usual nonlinear junction resistances associated with minority carrier injection effects. For the direction of bias indicated in Fig. 1(a), junction (2) is back biased, so R_2 is very large and, except at very low frequencies,

* Received by the IRE, July 15, 1959. This work was supported in part by the Office of Naval Research.

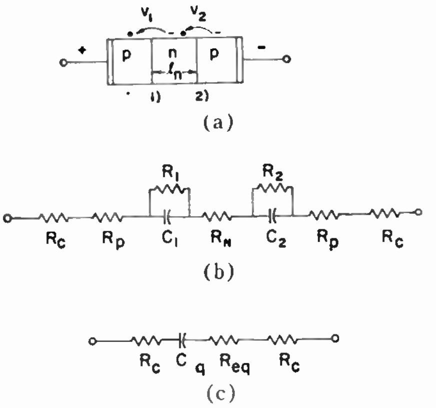

Fig. 1—P-n-p diode and circuit models. (a) diode; (b) circuit model; (c) approximate circuit model.

its effect in shunting C_2 may be neglected. Furthermore, the dc operating current level will be essentially that of a reverse biased junction. If the diode is made of silicon and operated at a voltage less than the avalanche breakdown voltage, this operating current level will be extremely small. As a result, the junction resistance R_1 will be large, and the minority carrier charge stored in the base will be very small. It follows from this reasoning that for biases less than breakdown voltage, 1) the shunting effect of R_1 on C_1 may be neglected except at low frequencies, and 2) conductivity modulation effects may be neglected in calculating R_N, the resistance of the base layer.

If we now define

$$C_{eq} = (C_1C_2)/(C_1 + C_2)$$
$$R_{eq} = R_N + 2R_P \tag{1}$$

the circuit model for this diode simplifies to that given in Fig. 1(c) (except at low frequencies). The Q of this circuit is then defined by

$$Q = 1/2\pi C_{eq}(R_{eq} + 2R_C)f \tag{2}$$

where the symbols are as defined before and f is the frequency in cps.

Eq. (2) indicates the steps that must be taken to make a high Q p-n-p diode capacitor. Before discussing device design, however, it is interesting to consider several unique properties which the structure has.

First, it follows from the physical symmetry of the device that reversing the polarity of bias on the diode merely interchanges the roles of the junctions and does not change the terminal characteristics. Hence, the capacitance vs voltage characteristic of the device is symmetrical, as shown in Fig. 2. This characteristic is of possible utility in parametric amplifiers since the diode can be operated at zero bias, and pumped at a frequency f_0 to get significant capacitance variations at $2f_0$ (see Fig. 2). It is therefore conceivable that parametric oscillations at a frequency up to $2f_0$ can be obtained readily from a pump at f_0.[1]

A second property of interest is the capacitance modulation which occurs when a light beam is focused on the p-n junctions. This capacitance modulation comes about because the light source produces hole-electron pairs in and near the junctions, thus

[1] The authors are indebted to Prof. H. Heffner for pointing out these facts.

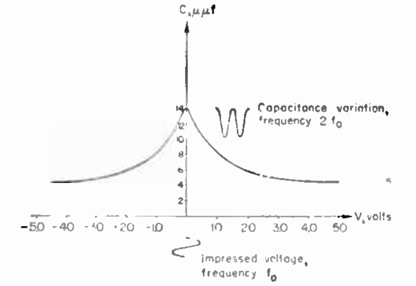

Fig. 2—Capacitance vs voltage for a p-n-p diode.

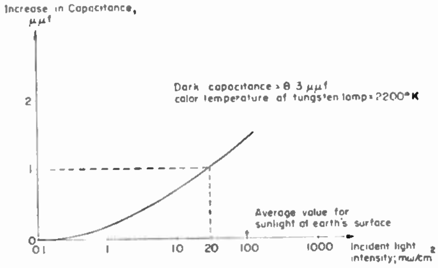

Fig. 3—Change of zero-bias capacitance vs incident light intensity.

causing a change in the voltages existing across the junctions and hence a change in the junction capacitances. A typical zero-bias capacitance vs light intensity plot is given in Fig. 3. In connection with this figure, it should be mentioned that the diode headers were not designed for maximum light interception at the junction; hence, the light energy actually falling on the junctions was much less than the incident light flux.

This capacitance modulation property of the diode provides a simple means of varying the tank circuit capacitance in an oscillator and thereby producing an oscillator output frequency which is related to the incident light intensity. This effect has been used in an FM transmitter operating at 128 mc to produce a frequency shift of 3.24 mc for an incident light intensity of 20 mw/cm². Using the curve of Fig. 3 and the tank circuit relation

$$\Delta f = \frac{f\Delta C}{2C}$$

we calculate a frequency change of 3.85 mc for this light intensity. The difference in measured and calculated frequency shifts may readily be accounted for by observing that the tank voltage also modulates the diode capacitance, causing its average value to be somewhat less than the small signal value indicated in Fig. 3.

Returning now to the problem of making a high Q diode capacitor, (2) indicates that R_C should be eliminated or reduced to a practical minimum. Since this resistance is to be compared with R_{eq}, which can be 0.001 ohm or lower for a p-n-p device of typical dimensions, it cannot always be neglected as unimportant. However, for the purposes of estimating the ultimate performance of a p-n-p diode, we shall neglect R_C and concentrate entirely on the $C_{eq}R_{eq}$ product.

To have a concrete example before us, we shall consider the device design problem assuming that the diode is to be used in a parametric amplifier. For this case, a suitable figure of merit for the diode as far as gain and noise figure of the parametric amplifier are concerned is the $f\alpha Q$ product, where $\alpha = \Delta C/C$. To maximize the $f\alpha Q$ product, it is necessary to maximize the fQ product of the diode at zero bias. Specification of fQ at a large reverse bias is unrealistic for this application, though Q increases with increasing bias voltage, since C_{eq} decreases with increasing bias voltage.

Neglecting R_C and rewriting (2), we have

$$fQ = 1/(2\pi C_{eq}R_{eq}). \tag{3}$$

It follows from this that the fQ product is independent of the area of the device, since C_{eq} depends directly on area, while R_{eq} depends inversely on area. That is, the fQ product is a material property of the diode.

The fQ product may be expressed in terms of device geometry and parameters by substituting the appropriate expressions for C_{eq} and R_{eq} into (3). If we assume that both p-n junctions are linearly graded, the equivalent capacitance per unit area may be expressed as

$$C_{eq} = \epsilon(2aq)^{1/3}/2(3\epsilon\phi)^{1/3} \tag{4}$$

where q is the electronic charge, ϵ is the dielectric constant, a is the gradient of impurity density at either p-n junction, and ϕ is the built in potential across either p-n junction.

Unfortunately, the expression for R_{eq} cannot be written so readily, since there are two types of resistance contributing to the total loss. First, there is the bulk resistance of the p- and n-type regions. Since the p-type regions will be much more heavily doped than the n-type region, we may neglect the bulk contributions of R_p to the total resistance and write the bulk resistance per unit area as

$$R_{\text{Bulk}} = R_{N\ \text{Bulk}} = l_N(q\mu_N N_D) \tag{5}$$

where l_N is the length of the n-type region (see Fig. 1), q is the electronic charge, μ_N is the mobility of electrons in the base, and N_D is the base doping density.

There is also a resistance contribution arising from the fact that near the junctions there is a nonuniform doping density associated with the impurity density gradient. While the extent of this region in neutral material is small, the resistivity of the region is high, and its contribution to the series resistance of the device is appreciable. In fact, the ultimate fQ product of diffused p-n-p diodes will be determined by this resistance, since the bulk resistances can be made relatively small by carefully controlled fabrication techniques. An analytical expression for this resistance may be obtained when the entire diffusion profile is known, but it is usually simpler to make a graphical estimate of its value.

An upper bound on the fQ product may be obtained by using the bulk resistance formula given in (5). Using (4) and (5) in (3), one obtains

$$fQ < (q\mu N_D)(3\epsilon\phi)^{1/3}/\pi(\pi l_N\epsilon)(2aq)^{1/3}$$

where symbols are as defined earlier. Using $\mu = 300$ cm²/volt-second, $N_D = 10^{18}$/cm³, $N_A = 10^{20}$/cm³ (bulk doping density for the p-regions), $l_N = 15$ microns $= 15 \times 10^{-4}$ cm, and $a = 10^{22}$/cm⁴, one obtains a zero bias bound on fQ of 100 kmc. When the resistance associated with the nonuniform doping density near the p-n junctions is added, the fQ product decreases to about 30 kmc. With due care, this latter figure can be approached; this still represents a respectable fQ product. To compare this figure with single p-n junction diodes of either the alloy or mesa type, one should multiply by a factor of 2 or 3, since it is customary to quote fQ figures with several volts of reverse bias applied to the diode. Using this factor, the p-n-p diode is about the same as the p-n diode in terms of fQ product.

Because of fabrication difficulties, the p-n-p diodes constructed to date have larger junction areas than those of p-n diodes, and, as a consequence, the impedance level at any given frequency is higher in the latter configuration. In a typical p-n diode of either the mesa or gold bonded construction, the capacitance of the diode at a small back bias is about one micromicrofarad. At a frequency of 1 kmc, this has an impedance of 160 ohms. For an area of 0.01 cm² and the doping parameters quoted earlier, the p-n-p diode has a zero bias capacitance of 250 $\mu\mu$f and an impedance of 0.64 ohm at 1 kmc. As a consequence of this fact, special techniques would have to be used to produce the extremely small areas required to get the proper impedance level in the p-n-p diode for a parametric amplifier application (about 50 ohms at S band). For lower frequency work, however, compromises can be made which reduce the capacitance drastically without too much loss in fQ product. For example, using a base layer doping of $N_D = 10^{16}$/cm³, one can readily obtain an fQ product of 6 kmc at zero bias. The zero bias capacitance for a diffused p-n-p diode with $N_D = 10^{16}$ is about 8 $\mu\mu$f for an area of 0.001 cm².

P-N-P diodes have been constructed from several different base materials ranging from $N_D = 10^{16}$ to $N_D = 10^{18}$. The fabrication technique is essentially as follows: a silicon slice is first lapped to a thickness of 45 microns, put in a grooved quartz boat, and placed in a diffusion furnace. Boron from either a BCl_3 or B_2O_3 source is then deposited on the surface of the slice and diffused in from each side at a temperature of 1200°C to a depth of about 15 microns. (It should be noted that a p-n-p diode is the natural product of such a diffusion operation unless masking techniques are employed.) The slice is then removed and given a light HF etch to remove possible surface oxides. Gallium-gold contacts are evaporated onto each side of the slice and alloyed in. The slice is then diced into small pieces, usually 0.01 to 0.001 cm² in area. These chips are then mounted in microwave diode headers to complete the unit. Typical zero-bias fQ products for diodes made in this way are given in Table I.

TABLE I

Base Resistivity Ω-cm	Base doping density atoms/cc	Upper bound on fQ calculated from (6) kmc	Calculated fQ (kmc) including nonuniform doping effects	fQ measured kmc
.6	10^{16}	12.2	6.1	6
.1	10^{17}	47	18	10
.02	10^{18}	102	34	16

The agreement between the last two columns is seen to be reasonably good; it may be improved by including the effects of contact resistance. A contact resistance of 10^{-4} ohm-cm² will bring the measured and calculated values of fQ into coincidence for the $N_D = 10^{18}$ case. This same contact resistance will decrease the calculated fQ product for the $N_D = 10^{17}$ to 16 kmc, so that the measured and calculated values of fQ are reasonably close.

Finally, it should be pointed out that p-n-p diodes in materials which do not display very low junction current when reverse biased will have quite different properties from those described here. In particular, if there is appreciable injection from the forward-biased diode, the Q of the capacitor will be severely deteriorated in certain frequency ranges.

J. F. GIBBONS
Stanford Electronics Labs.
Stanford University
Stanford, Calif.
G. L. PEARSON
Bell Telephone Labs.
Murray Hill, N. J.

Some Possible Causes of Noise in Adler Tubes*

Adler,[1,2] has recently described a new type of low-noise amplifier in which the signal is carried on an electron beam in the form of orbiting motion of the electrons in a magnetic field. A particular feature of this amplifier is that the conditions for coupling the signal onto the beam from the input circuit are identical to those for coupling a signal off it. Any noise on the beam, therefore, will be absorbed by the input circuit, and the amplifier should have a noise figure of zero db to a first approximation. Actual measurements show that the noise is not quite so low as this. The best noise figure reported so far,[2] is 1.3 db, of which about 0.4 db was accounted for by circuit losses. The purpose of this letter is to suggest reasons which might account for some of the remainder.

Consider, first, the nature of the noise signal which is absorbed from the beam. Noise arises because of random motion of the electrons at right angles to the beam axis caused by thermal velocities. Since we are concerned here with only two degrees of freedom, the average energy per electron will be kT_e, where T_e is the effective temperature of the beam for these two degrees of freedom. In the plane at right angles to the beam axis, each electron will pursue a circular orbit of random magnitude and phase. At any instant in time, the electron will feed an amount of current proportional to its component of velocity in that direction into the coupling plates. The sum of the instantaneous currents caused by all the electrons between the plates is the instantaneous noise current. The summation must take sign into account, so that the sum is on the average zero and the noise is merely the rms deviation from zero. The rms value of the noise current is given by

$$i_n = \frac{l}{d}\sqrt{\frac{G_0 \times k \times T_e \times B}{2}},$$

where

l = transit length of plates,
d = spacing of plates,
G_0 = dc beam conductance,
k = Boltzmann's constant,
T_e = electron temperature,
B = bandwidth.

When the correct matching impedance is connected between the plates, the noise current is reduced by a factor two, so that the noise power is given by

$$P_n = \tfrac{1}{4} i_n^2 \times R,$$

where

$$R = 8\left(\frac{d}{l}\right)^2 \times \frac{1}{G_0}$$

so that

$$P_n = k \times T_e \times B.$$

This noise signal should not be confused with the total thermal power on the beam, which, in general, is many orders of magnitude greater, and is given by

$$P_{th} = \frac{k \times T_e \times I_0}{e}.$$

P_{th} is simply the sum of all the lateral thermal energies of the electrons. For example, taking T_e as 1000°K and B as 50 msec,

$$P_n = 6.9 \times 10^{-13} \text{ watts}$$

whereas

$$P_{th} = 3.0 \times 10^{-6} \text{ watts}.$$

It is clear, therefore, that when the noise signal is removed from the beam, the thermal power of the electrons remains virtually unaltered. All that has happened is an almost imperceptible readjustment of the amplitude and phase of the orbit of each electron which results in the wiping out of the statistical fluctuation with time of the sum of their currents. To be more exact, the smoothing applies only to a limited band of frequencies. This is the same as saying that the summation must be carried out over a time interval of $1/B$ or longer.

The removal of noise from the beam represents, therefore, a delicate state of balance rather than any real physical removal of the source of the noise. The positive and negative thermal velocities of the electrons in the direction of the plates have been equalized for the beam as a whole, but the velocities themselves are still as great as ever. Anything which happens to upset this state of balance will thus reintroduce noise. Some of the ways this might happen are suggested below.

1) *Partition noise*

Any electron which is removed from the beam will upset the balance. Thus, interception current anywhere after the input

* Received by the IRE, June 15, 1959.

[1] R. Adler, "Parametric amplification of the fast electron wave," PROC. IRE, vol. 46, pp. 1300–1301; June, 1958.

[2] R. Adler, G. Hrbek, and G. Wade, "A low noise electron-beam parametric amplifier," PROC. IRE, vol. 46, pp. 1756–1757; October, 1958.

plates will cause noise. Whether the interception occurs before or after the pump is immaterial because, although the signal level is higher after the pump, the thermal orbits are also. Thus, the removal of an electron after the pump injects a larger noise signal into the beam. The likelihood of interception occurring is greater after the pump because the expansion of the thermal orbits will cause spreading of the beam. The seriousness of this effect must therefore depend on the gain of the tube as well as on the geometry of the beam and the output plates. A further point is that the actual magnitude of this noise signal is greater than would be expected on the basis of simple partition noise because only the most energetic electrons are intercepted.

An example will serve as an illustration of the magnitude of partition noise. Suppose an interception of 1 per cent is observed. The average energy of the intercepted electrons might typically be two and one-half times kT_e. The noise power fed into the output plates will thus be 0.025 kT_eBG, where G is the power gain in the tube. This has to be compared with the amplified generator noise KT_0BG. Taking $T_0=290°$K and $T_e=1000°$K, the noise figure is therefore 1.086 or 0.36 db.

2) *Noise caused by nonuniform electric field between the plates*

If there is a nonuniform electric field between the plates, the contribution of each electron to the noise current will depend not only on its velocity but also on the relative field strength at that point. The cancellation of noise is therefore of a different form from that which would have occurred with a uniform field between the plates. The noise current induced in the output plates will only be zero if the relative field experienced by each electron is the same at the output as it was at the input plates. This would be achieved, for example, by making the input and output plates identical, provided that the electrons maintained their positions in the beam. However, if space charge forces are appreciable, this will not be the case, so that the only practicable solution is to maintain as uniform a field as possible between both input and output plates.

By way of example, suppose that the input plates are divided into two equal regions in one of which the field is 10 per cent stronger than in the other, and that the output plates are similar but have the positions reversed. After the beam has been through the input plates, there will be no noise on the beam as a whole, but there will be equal and opposite noise currents in each half of the beam, of magnitude $i_n/\sqrt{2}$. At the output plates, one of these currents will be increased by 10 per cent and the other will be decreased by the same amount. The resultant current will, therefore, be $(0.2/\sqrt{2})i_n$. The noise fed into the output plates will be 0.02 KT_eBG, corresponding to a noise figure of 1.069 or 0.29 db.

3) *Noise caused by spread of axial velocities in the beam*

So far the assumption has been made that the electrons all move forward with equal velocity. If this is not the case, then we have to consider to what extent a relative axial displacement of different parts of the beam will upset the balance of the noise. To simplify the situation let us consider that the beam is divided into two equal parts moving at slightly different velocities. Each half of the beam will carry a noise current, but after passing through the input plates, they will be equal and opposite, and of magnitude $i_n/\sqrt{2}$. Noise cancellation will be upset if, and only if, the relative axial displacement of the two halves results in a relative phase difference between them. This will depend upon what frequency we are considering. At the cyclotron frequency, there would be no phase difference. At other frequencies, it is given by

$$\phi = 2\pi(f_c - f_n) \times \tau \times (v_1 - v_2).$$

ϕ = phase difference between the two parts of the beam,

where

τ = transit time between input and output plates at velocity v_1,

f_c = cyclotron frequency,

f_n = frequency of noise component,

and v_1 and v_2 are the velocities of the two parts of the beam.

Thus, we should expect no deterioration of the noise at the center of the band, but it would get progressively worse as we move outwards from the center. The magnitude of this effect can be judged from the following example:

$$f_c = 500 \text{ msec},$$

$$f_n = 525 \text{ msec},$$

$$\tau = 5 \times 10^{-8} \text{ seconds } (i.e., 25 \text{ cycles}),$$

$$\left(\frac{v_1 - v_2}{v_1}\right) = 0.015,$$

then

$$\phi = 6.8°,$$

$$\text{noise current} = \frac{2i_n}{\sqrt{2}} \times \sin\frac{6.8°}{2} = 0.084 i_n,$$

$$\text{noise power} = 0.007 T_e BG.$$

and

$$\text{noise figure} = 1.024 = 0.1 \text{ db}.$$

4) *Noise caused by collisions between electrons and ions*

If there are any ions present in the beam, either positive or negative, this may give rise to noise by disturbing the thermal orbits of the electrons. It is not yet clear whether this effect would be important in any practical cases. A safe precaution would be to use a beam potential at which the rate of ion formation is small.

By way of summary, the most important form of noise suggested is partition noise caused by interception of the beam caused, in turn, by amplification of the thermal orbits of the electrons. This is fundamental to this type of tube and must limit the gain at which any particular tube can be operated. An important contributory cause of the noise may be nonuniformity of the field between the plates. Space charge depression of potential in the beam should have no effect at the center of the band, but might be a contributory cause at the edges of the band in particular cases. More detailed calculations on these effects are in progress.

C. P. LEA-WILSON
Services Electronics Res. Lab.
Harlow, Essex, England

Authors' Comment[3]

Lea-Wilson, in the first part of his letter, has given an excellent account of the physical situation which exists when fast-wave noise is cancelled. His explanation will answer many questions; his description of the noise absorption process as "an almost imperceptible readjustment of the amplitude and phase of the orbit of each electron . . ." should clarify this matter once and for all.

The following comments, based on experiments with a number of tubes and on a theoretical examination of their behavior, might be in order. As was recently reported,[4] when the electron gun potentials are adjusted empirically for optimum noise figure and the input coupler is terminated by a matched load at room temperature, we find that the noise temperature measured at the output coupler remains significantly above room temperature even with the pump turned off. Hence a significant amount of noise originating in the beam appears at the output even with no pumping present. This excess noise, in combination with the circuit losses, is large enough to account for the noise figure measured with the pump turned on. This would indicate that partition noise, which would increase strongly with pumping, cannot be a large factor. It seems to become a large factor when the gun is purposely misadjusted; in that case the noise figure deteriorates rapidly as pump power is increased. With optimum gun adjustment, on the other hand, only a slight increase in noise figure occurs for very high gain (30 db or over).

In view of these experimental findings, the most interesting sources of residual noise are those not affected by pumping. Lea-Wilson's sources 2)–4) are in this class. Source 2), the contribution due to nonuniform electric field between the plates, is probably negligible in our experimental tubes in view of their geometry.

Contributions to the excess noise from certain other sources not considered by Lea-Wilson have also been examined and reported.[4] For example, noise carried by the other transverse waves of the beam (the slow wave and the intermediate or synchronous wave) can produce measurable effects. Noise in the intermediate wave appears to be especially significant in some tubes.[5] This noise does not involve transverse electron motion but results from spatial fluctuations of the center of gravity of the beam about its axis due to the finite thickness of the beam. These fluctuations, moving along at the velocity of the stream, may induce a

[3] Received by the IRE, July 13, 1959.

[4] R. Adler, G. Hrbek, and G. Wade, "The noise behavior of quadrupole parametric amplifiers," presented at the Conference on Electron Tube Research, Mexico City, Mexico; June 26, 1959.

[5] This possibility was first suggested to us some months ago by R. Kompfner of Bell Telephone Laboratories.

voltage in the input coupler which is then re-impressed upon the steam in the form of fast wave noise. For the dimensions of our experimental tubes, an easily calculated maximum possible value for this contribution is 0.6 db. The actual value must be much lower than this.

We have recently reported[4] a substantial improvement in experimental tubes; using a gun in which the small first-anode aperture originally employed is replaced by a small virtual cathode, we have obtained over-all noise figures of slightly better than 1 db at both 425 and 780 mc. Circuit losses still account for close to 0.5 db, leaving a little less than 0.5 db or an excess noise temperature of 35° K to be accounted for. Thus, with this new gun there is little noise left to explain. These experiments, as well as the theoretical examination mentioned above, will be published in detail in the near future.

R. Adler
G. Hrbek
Research Department
Zenith Radio Corp.
Chicago, Ill.
G. Wade
Electronics Laboratory
Stanford University
Stanford, Calif.

A New Concept in Computing*

Wigington[1] points out that the design of logic networks consisting of majority decision elements may be carried out by using permanent-source inputs to reduce the majority elements to OR's and AND's. This practice permits the use of familiar design techniques, since the majority elements are made to behave as familiar elements. By failing to utilize the logical properties of the majority elements, however, this technique sometimes produces extravagant designs.

An alternative design method depends on operating on conventional Boolean expressions (in terms of AND, OR, NOT, etc.) to convert them to equivalent expressions in "majority form." An expression is said to be in majority form if it is expressed exclusively in terms of Boolean literals (with and without negation), grouping symbols (parentheses, etc.), and the majority decision operator. The discussion that follows gives a method for conversion to majority form and presents examples that show that the corresponding networks are somewhat simpler than those developed by Wigington's method.

The conversion method, as given here, is restricted to networks having 1) no more than three inputs, 2) no more than three inputs per element, and 3) no storage function.

The first step is to put the given function, $f(A_1, A_2, A_3)$, in the following form:

$$f(A_1, A_2, A_3) = X[f_1(Y, Z) + f_2(Y, Z)] + X'f_3(Y, Z)f_4(Y, Z), \quad (1)$$

where X, Y, and Z are Boolean literals A_1, A_2, and A_3 (not necessarily respectively) or negations thereof, and f_1, f_2, f_3, and f_4 are functions chosen to satisfy (1). With the understanding that f_1, f_2, f_3, and f_4 are functions of Y and Z only, (1) may be simplified to read:

$$f(A_1, A_2, A_3) = X(f_1 + f_2) + X'f_3f_4. \quad (2)$$

The second step—which requires that the given function be in form (2)—is to apply the conversion theorem:

$$X(f_1 + f_2) + X'f_3f_4 \equiv \mathrm{Maj}\,[X, (Xf_1 + X'f_3), (Xf_2 + X'f_4)]. \quad (3)$$

If, after this second step, any term of the right-hand member of (3) is not in majority form (that is, if any term contains AND, or OR, etc.), that term is converted by a second application of the two-step procedure described above. The two-step procedure is applied repeatedly until conversion to majority form is complete.

The conversion procedure described above is illustrated by derivations of majority-element networks for 1) a parity checker, and 2) a binary adder stage.

Since, by convention, an even-parity code is an erroneous one, a three-bit parity-error detector is given by:

$$\text{Error} = A_1A_2A_3' + A_1A_2'A_3 + A_1'A_2A_3 + A_1'A_2'A_3'. \quad (4)$$

Arbitrarily selecting A_1 as X (any other choice would serve as well), we factor (4) to give:

$$\text{Error} = A_1(A_2A_3' + A_2'A_3) + A_1'(A_2A_3 + A_2'A_3'). \quad (5)$$

Conversion of (5) to form (2) is completed by expressing $A_2A_3 + A_2'A_3'$ as a product (which is done by double negation and repeated application of De Morgan's laws) to give:

$$\text{Error} = A_1(A_2A_3' + A_2'A_3) + A_1'(A_2 + A_3')(A_2' + A_3). \quad (6)$$

Eq. (6), has the desired form; comparison with (2) shows $A_1 = X$, $A_2A_3' = f_1$, $A_2'A_3 = f_2$, $A_2 + A_3' = f_3$, $A_2' + A_3 = f_4$. Application of (3) yields:

$$\text{Error} = \mathrm{Maj}\,[A_1, (A_1A_2A_3' + A_1'A_2 + A_1'A_3'), (A_1A_2'A_3 + A_1'A_2' + A_1'A_3)]. \quad (7)$$

Application of (3) to each of the latter two terms within the brackets of (7) yields:

$$\text{Error} = \mathrm{Maj}\,[A_1, \mathrm{Maj}\,(A_1', A_2, A_3'), \mathrm{Maj}\,(A_1', A_2', A_3)]. \quad (8)$$

Fig. 1 expresses (8) in diagrammatic form. The added "D" represents a delay that might be required to synchronize the inputs to the final element.

Derivation of a binary adder stage proceeds in a similar fashion. If A_1, A_2, and A_3 are the addend, augend, and low-order carry inputs to a binary adder stage, the carry (K) and sum (S) outputs are given by:

$$K = \mathrm{Maj}\,(A_1, A_2, A_3) \quad (9)$$

$$S = A_1A_2A_3 + A_1A_2'A_3' + A_1'A_2A_3' + A_1'A_2'A_3. \quad (10)$$

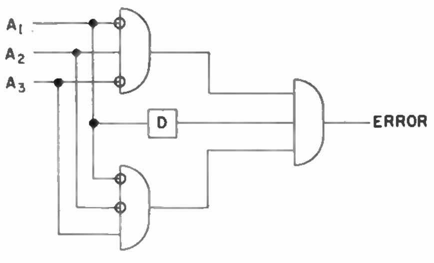

Fig. 1—Parity-error detector.

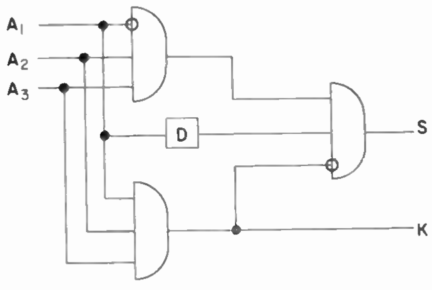

Fig. 2—Adder stage.

Conversion of (10) to majority form is as follows:

$$\begin{aligned} S &= A_1(A_2A_3 + A_2'A_3') + A_1'(A_2A_3' + A_2'A_3) \\ &= A_1(A_2A_3 + A_2'A_3') + A_1'(A_2 + A_3)(A_2' + A_3') \\ &= \mathrm{Maj}\,[A_1, (A_1A_2A_3 + A_1'A_2 + A_1'A_3), (A_1, A_2'A_3' + A_1'A_2' + A_1'A_3')] \\ &= \mathrm{Maj}\,[A_1, \mathrm{Maj}\,(A_1', A_2, A_3), \mathrm{Maj}\,(A_1', A_2', A_3')] \\ &= \mathrm{Maj}\,[A_1, \mathrm{Maj}\,(A_1', A_2, A_3), K']. \end{aligned} \quad (11)$$

Fig. 2 expresses (9) and (11) in diagrammatic form. It uses three three-input majority decision elements and (perhaps) a delay element. Wigington's adder stage requires six majority decision elements, of which two are five-input devices.

Richard Lindaman
Remington Rand Univac
St. Paul, Minn.

* Received by the IRE, June 24, 1959.

[1] R. L. Wigington, "A new concept in computing," Proc. IRE, vol. 47, pp. 516–523; April, 1959.

A S/N Improvement Factor on PAM-FM Whose Received Pulse is Cosine-Squared*[1]

The S/N improvement factor, which is the ratio of the channel signal output S/N to the carrier S/N, is an important factor in measuring the properties of the communication system. In PAM-FM, the ratio S/N of the carrier is improved by the frequency discriminator, then the noise is limited through the pulse low-pass filter, and further improvement of S/N is achieved by sampling. Formerly, Landon[2] obtained S/N,

* Received by the IRE, July 13, 1959.

[1] The original work in Japanese appeared in the *Natl. Tech. Rept.*, vol. 4, pp. 61–63; March, 1958.

[2] V. D. Landon, "Theoretical analysis of various systems of multiplex transmission," *RCA Rev.*, vol. 9, p. 322; June, 1948.

without integration, by determining the effective noise bandwidth of the pulse filter and sampling the noise. Hölzler-Holzwarth[3] calculated S/N by taking the frequency characteristics of the pulse low-pass filter as the square of the cosine, without considering sampling at receiving. Moreover, Ezaki[4] added what was lacking in the above treatment—he took the characteristics of the pulse low-pass filter into consideration, and obtained the integrated demodulation type S/N, approaching very near to practice. However, Ezaki's result is too complicated for general use. Although in practice many low-pass filters make the receiving pulses cosine squared, and the integrated demodulation circuit is employed, no consideration is given to them anymore and no useful formula for the S/N improvement factor of them is known; this point is clarified in this paper.

First, let the waveform and the frequency spectrum of the cosine-squared impulse and the rectangular pulse of the width $2T_0$ be respectively:

$$\begin{cases} f(t) = \cos^2 (\pi t/2T) & (1) \\ g(\omega) = T \dfrac{\sin \omega T}{\omega T(1 - \omega^2 T^2/\pi^2)} & (2) \end{cases}$$

$$\begin{cases} F(t) = \begin{cases} 1 & -T_0 < t < T_0 \\ 0 & |T_0| < t \end{cases} & (3) \\ G(\omega) = 2T_0(\sin \omega T_0)/(\omega T_0). & (4) \end{cases}$$

Then, if the above narrow rectangular pulse is passed through the filter with the following frequency characteristic,

$$\frac{\omega T_0}{\sin \omega T_0} \frac{\sin \omega T}{\omega T(1 - \omega^2 T^2/\pi^2)}, \tag{5}$$

the cosine-squared pulse whose height is $2T_0/T$ appears in the output. Generally, since the width of the input pulse is narrower than that of the output pulse, the first term can be assumed approximately unity within the variation range of the second term. The filter is divided into two parts, which are installed on the sending and the receiving sides. At present, for the convenience of calculation, let both sides have the same characteristics. As the receiving side bandwidth is taken to be narrower, the above assumption will make S/N the minimum, which, however, does not have much affect in practice. Therefore let

$$\sqrt{\frac{\sin \omega T}{\omega T(1 - \omega^2 T^2/\pi^2)}} \tag{6}$$

be the characteristics of the sending side, and the height of the output waveform is calculated from the equation

$$f_1(t)\big|_{t=0} = \frac{2T_0}{\pi T} \int_0^\infty \sqrt{\frac{\sin \omega T}{\omega T(1 - \omega^2 T^2/\pi^2)}}\, T d\omega; \tag{7}$$

the result is approximately $(4.52/\pi)(2T_0/T)$, which is multiplied by approximately 0.69 after it leaves the receiver filter.

Next, let C be the peak amplitude of the carrier, e, $\sqrt{2}$ times the effective noise voltage in a one cycle per second band, and f_x, the frequency difference of the carrier wave and the noise; then, assuming the coefficient is unity, the noise output voltage of the frequency discriminator[2] is expressed by $\sqrt{2} f_x e/C$ which, after passing through the receiver filter, becomes

$$\sqrt{2} \frac{e}{C} f_x \sqrt{\frac{\sin \omega T}{\omega T(1 - \omega^2 T^2/\pi^2)}}. \tag{8}$$

This is sampled and integrated. In integrating, a step function can be assumed which keeps the voltage constant until the next pulse comes. According to Kleene,[5] let $\alpha = 0$, $\beta = 1$, and f_p be the repeating frequency, then the relative gain is

$$\sin \pi T_p(bf_p - f_x)/[\pi T_p(bf_p - f_x)]. \tag{9}$$

However, the audio components fall within the range of $|bf_p - f_x| \leqq f_m$, where f_m is the maximum audio frequency. Hence the noise energy E_n in the audio bandwidth can be obtained from the following integration under the above conditions. By transforming $x = \omega T$;

$$E_n = 2 \frac{e^2}{C^2} \left(\frac{1}{2\pi T}\right)^2 \int_0^\infty x^2 \frac{\sin x}{x(1 - x^2/\pi^2)} \frac{\sin^2 [(T_p/T)(bx_p - x)/2]}{[(T_p/T)(bx_p - x)/2]^2} dx$$
$$|bx_p - x| \leqq x_m = 2\pi f_m t. \tag{10}$$

Since the third term of the integrand varies much faster than the first and second term, it can be independently integrated with expansion form $\sin^2 u/u^2 \simeq 1 - u^2/4$, then;

$$\frac{1}{\pi} \int_{bx_p - x_m}^{bx_p - x_m} \frac{\sin^2 [(T_p/T)(bx_p - x)/2]}{[(T_p/T)(bx_p - x)/2]^2} dx \simeq \frac{2f_m}{f_p} \left[1 - \frac{1}{12} \left(\pi \frac{f_m}{f_p}\right)^2\right]. \tag{11}$$

The total noise energy is

$$E_n = 2 \frac{e^2}{C^2} \left(\frac{1}{2\pi T}\right)^3 \frac{2f_m}{f_p} \left[1 - \frac{1}{12}\left(\pi \frac{f_m}{f_p}\right)^2\right] \pi^2 \int_0^\infty \frac{x \sin x}{\pi^2 - x^2} dx, \tag{12}$$

replacing $T = \mu/nf_p$ and integrating the last term, this becomes

$$E_n = \frac{1}{4\mu^3} \left[1 - \frac{\pi^2}{12} \left(\frac{f_m}{f_p}\right)^2\right] n^3 f_m f_p^2 \frac{e^2}{C^2}. \tag{13}$$

On the other hand, the signal voltage is multiplied by ν after leaving the frequency discriminator and passing through the receiver filter, and assuming that the voltage itself is kept constant by integration, it is expressed by νf_d. Then S/N (voltage) is obtained from

$$\frac{2\mu\sqrt{\mu\nu}}{\sqrt{1 - \dfrac{\pi^2}{12}\left(\dfrac{f_m}{f_p}\right)^2}} \frac{f_d}{n\sqrt{n}\sqrt{f_m f_p}} \frac{C}{e}. \tag{14}$$

Assuming that the effective noise bandwidth of the intermediate frequency is approximately the intermediate frequency bandwidth B, the S/N improvement factor can be obtained by dividing (14) by the carrier S/N, $C/(e\sqrt{B})$. Similarly, the cosine-squared pulse nonintegration type and Landon's equivalent bandwidth nonintegration type can be obtained.[1] Their S/N improvement factors are respectively as follows:

1) the cosine-squared pulse integration type

$$\left[\frac{2\mu\sqrt{\mu\nu}}{\sqrt{1 - \dfrac{\pi^2}{12}\left(\dfrac{f_m}{f_p}\right)^2}}\right] \frac{f_d\sqrt{B}}{n\sqrt{n}\sqrt{f_m f_p}} \tag{15}$$

2) the cosine-squared pulse nonintegration type

$$\left[2\mu\sqrt{\mu\nu} \frac{\pi/(2\mu)}{\sin (\pi\xi/2\mu)}\right] \frac{f_d\sqrt{B}}{n\sqrt{n}\sqrt{f_m f_p}}, \tag{16}$$

3) the equivalent bandwidth nonintegration type (Landon type)

$$\left[\frac{\pi\xi}{\sqrt{2\zeta}} \frac{\nu}{\sqrt{1 - \dfrac{\sin 2\pi\xi\zeta}{2\pi\xi\zeta}}}\right] \frac{f_d\sqrt{B}}{n\sqrt{n}\sqrt{f_m f_p}}, \tag{17}$$

where

$T = \mu/(nf_p)$ half amplitude bandwidth of the cosine-squared pulse. $0 < \mu < 1$
ν = signal pulse ratio of output to input in the receiver pulse low-pass filter $0 < \nu < 1$
$\tau = \xi/(nf_p)$ width of receiver sampling pulse $0 < \xi < 1$
$F_e = \zeta n f_p$ effective noise bandwidth of the receiver pulse low-pass filter $0 < \zeta$
n = number of division
f_d = maximum frequency deviation
f_p = repeating frequency
f_m = maximum signal frequency
B = bandwidth of the intermediate-frequency amplifier.

To investigate each first term, let $f_m = 3400$ cps, $f_p = 8000$ cps, $\mu = 3/4$, $\nu = 0.69$, $\xi = 1/5$, $\zeta = 0.7$, then

1) 0.966
2) 0.913
3) 1.04,

which, however, are not justifiable to compare those three methods. These values vary around the above values according to conditions. Since they are very close to unity, the S/N improvement factor of PAM-FM is approximately calculated from

$$I = \frac{f_d\sqrt{B}}{n\sqrt{n}\sqrt{f_m f_p}}. \tag{18}$$

For example, let $f_d = 1$ mc, $B = 3$ mc, $n = 12$, $f_m = 3400$ cps, $f_p = 8000$ cps, then,

$$I \simeq 0.924 \cdot 10^2 \simeq 39.3 \text{ db}.$$

Or, if $f_d = 3$ mc, $B = 10$ mc, $n = 24$, then

$$I \simeq 1.69 \cdot 10^2 \simeq 44.6 \text{ db}.$$

The values are rather reasonable and they clarify the meaning of the S/N improvement factor fairly well.

AKINORI WATANABE
Central Laboratories
Matsushita Electric Industrial Co., Ltd.
Kadoma, Kitakawachi, Osaka
Japan

[3] E. Hölzler and H. Holzwarth, "Theorie und Technik der Pulsmodulation," Springer-Verlag, Berlin, Germany, pp. 394–398; 1957.
[4] T. Ezaki, "A S/N Improvement Factor on PAM-FM with Storage Demodulation," presented at the IEE Conference of Japan, no. 224; October, 1955. (Abstract in Japanese.)

[5] S. C. Kleene, "Analysis of lengthening of modulated repetitive pulses," PROC. IRE, vol. 35, pp. 1049–1053; October, 1947.

The Efficiency of 100 Per Cent Inspection*

The increasing demand for high reliability components in the electronic industry places stringent limits on the efficiency of 100 per cent testing. With the quality levels continually decreasing, the efficiency of inspection must constantly be increased. Although many components must be 100 per cent tested before being submitted to the Quality Control Department, such testing is never a guarantee of 100 per cent acceptable quality.

The following formula will determine the efficiency required to pass any desired quality level.

$$E = \frac{P(1 - P')}{P(1 - 2P') + P'}$$

where

E = the probability of making a correct decision on any unit.

P = fraction defective before test (percentage of defective units entering the test station).

P' = AQL (Acceptable Quality Level).

By substituting an AQL of 1 per cent for P' and several values of P from 5 per cent to 50 per cent, Table I can be calculated.

TABLE I

P	*Total E*	C_4	C_5	C_6
0.05	0.839	0.957	0.966	0.971
0.10	0.917	0.979	0.983	0.986
0.20	0.962	0.990	0.992	0.994
0.30	0.977	0.994	0.995	0.996
0.40	0.985	0.996	0.997	0.997
0.50	0.990	0.997	0.998	0.998

The *Total E* column is the efficiency for the entire inspection station. Suppose there are four, five, or six tests to be conducted at the station, the efficiency of each individual test is given by

$$\sqrt[c]{E}$$

where

C = the number of tests that are to be performed

Table I indicates that E must increase when the per cent defective that enters the station increases. The efficiency of the individual tests must also be increased as the number of tests increases. These two factors are of prime importance when considering the merits of any testing facility. The efficiency value must be designed and built into the station.

The efficiency of 200 per cent inspection can be calculated by the formula

$$E_1 = 1 - \sqrt{1 - E_T}.$$

E_T is the total E value in Table I.

E_1 is the efficiency of the first 100 per cent inspection and E_2 is the efficiency of the second 100 per cent inspection. In this formula E_1 and E_2 are considered to be equal as in the case of most automatic test equipment.

Table II can be calculated for a 200 per cent inspection based on a 1 per cent AQL.

TABLE II

P	*Total E*	C_4	C_5	C_6
0.05	0.599	0.880	0.903	0.918
0.10	0.712	0.919	0.934	0.945
0.20	0.808	0.947	0.958	0.965
0.30	0.848	0.960	0.968	0.973
0.40	0.878	0.968	0.974	0.979
0.50	0.900	0.974	0.979	0.983

The efficiency of the inspection station can be materially reduced by submitting the units twice. Consideration must be given to the cost of reinspection vs the cost of obtaining high efficiency in the test facilities. The high reliability demanded by the Space Age can be achieved only through reliability of design. However, because the "state of the art" cannot, in all cases, achieve this goal, the interim alternative is to test the required reliability into the product.

CHARLES R. TOYE
Quality Control Supervisor
Texas Instruments, Inc.
Dallas, Tex

* Received by the IRE, July 28, 1959.

Ferromagnetic Amplifiers*

In the course of experiments on ferromagnetic amplifiers we have observed an effect which has not, to our belief, been previously reported. When a magnetized yttrium iron garnet sphere is placed in a microwave field havings its H component parrallel with the magnetization and its frequency approximately twice that corresponding to the magnetization, an absorption of microwave power occurs when the amplitude of the field exceeds a threshold value. Fig. 1 shows the appearance of the absorption as the steady field is varied. Fig. 2 shows how the peak absorption varies with microwave power. A preliminary experiment has shown the threshold value of the microwave field to be about 0.5 oersted and has shown it to vary little, with either orientation, or shape, of the YIG sample.

We suggest that the cause of the absorption is parametric excitation of pairs of spin wave modes of the material. Attempts to detect radiation with a well matched receiver have failed, as have attempts to influence the absorption by feeding in power at right angles to the pump field and at frequencies appropriate to the steady field. We therefore conclude that the mode numbers involved must be so high that there is negligible coupling of the excited modes to the surroundings.

If our explanation proves, in future experiments, to be correct, it may also account for our failure to obtain amplification from CW pumped amplifiers. The high-order spin wave modes, being more easily excited, may begin to absorb power from the pump and limit its field before appreciable gain from low-order couplable modes have appeared. The reported successes (which we confirm) of amplifiers using pulsed pump sources can be explained as due to there being insufficient time for the spin wave excitation to build up to limit the pump field. Indeed, we have observed a time of several milliseconds to reach peak absorption at pump powers a few per cent above the threshold value.

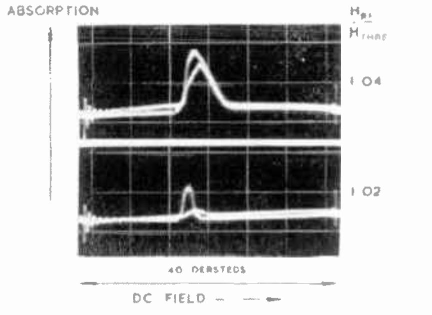

Fig. 1.

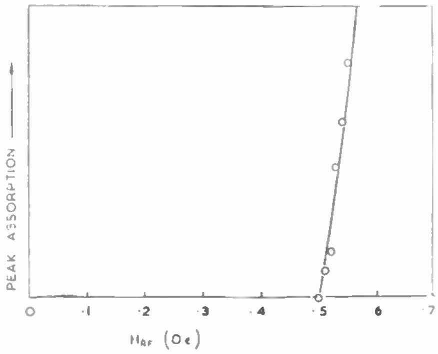

Fig. 2.

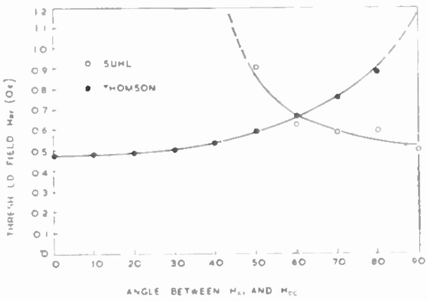

Fig. 3.

The mechanism of spin wave excitation appears to differ from that discussed by Suhl[1] in two respects. First, it occurs at fields corresponding quite closely to half the pump frequency while Suhl's mechanism works at fields about 70 per cent of the pump resonant field. Secondly, it causes an absorption over a much narrower range of field. In Fig. 3 the thresholds for the two mechanisms are plotted against the angle between the dc and RF fields. The lowest thresholds appear to be equal but, though neither phenomenon shows exactly a

$$\frac{\cos\theta}{\sin\theta}$$

variation, our phenomenon deviates from such a law less than does Suhl's.

A. F. H. THOMSON
Services Electronics Res. Lab. Ext.
Harlow, Essex, Eng.

[1] H. Suhl, "Subsidiary peaks in ferromagnetic resonance at high signal levels", *Phys. Rev.*, vol. 101, pp. 1437–1438; February, 1956.

* Received by the IRE, July 20, 1959.

A Tunable X-Band Ruby Maser*

A tunable solid-state ruby maser has not only been successfully operated at X-band, but also shown to maintain constant characteristics of 20-db gain and 10-mc bandwidth over a continuous tuning range of 205 mc (from 9405 to 9610 mc). Subsequent tests have indicated that the continuously-tunable range will be extended to at least 400 mc. Although voltage-gain bandwidth products of 100 mc were easily achieved, products of up to 230 mc were also reached, even without fully optimizing all the parameters.

A 0.5 per cent chromium-doped ruby crystal almost filled the rectangular cavity, thus assuring a fairly large filling factor. Pump frequencies ranged from 22.85 kmc to 23.85 kmc. DC magnetic fields were of the order of 3900 to 4300 oersteds, oriented at about 54° with respect to the ruby C-axis, thus utilizing the "push-pull" double-pumping principle. Helium bath temperatures ranged from 1.35°K to 1.5°K.

The tuning mechanism of this cavity consists of only two external controls controls mounted on the maser superstructure, as shown in Fig. 1. The frequency tuning control consists of a worm and gear which turns a threaded rod mounted along the outside of the waveguide run. On this rod rides a noncontacting shorting plunger, shown in the cutaway sketch of the cavity in Fig. 2. This plunger simultaneously tunes the signal and pump resonant frequencies as required. A large gear reduction through the worm and worm gear results in an extremely small plunger travel for each revolution of the driving shaft, allowing for very fine frequency tuning. Occasional slight compensating changes in magnetic field strength and pump frequency will maintain a constant voltage-gain bandwidth product.

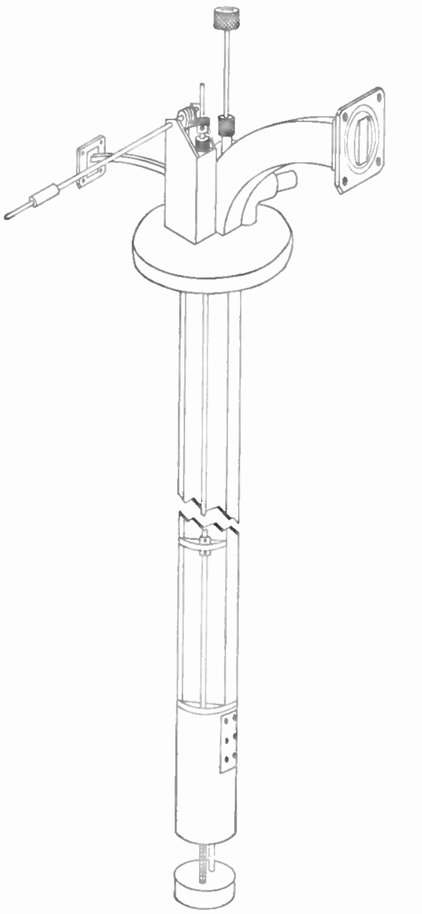

Fig. 1.

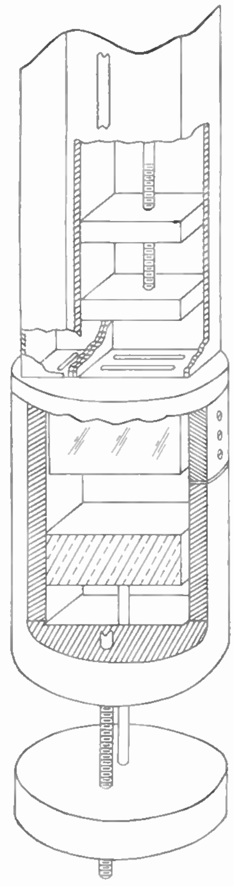

Fig. 2.

The second control is shown on the superstructure as a vertical rod topped by a knurled knob. It consists of a dielectric slug tuner made of two quarter-wave-thick teflon blocks. These are inserted down the center of the X-band guide to control the signal-frequency coupling into the cavity. The blocks are shown in the cutaway portion of the X-band guide in Fig. 2. A given position of this slug tuner has been found to give satisfactory performance over at least a 4 per cent bandwidth.

Fig. 2 also shows the coupling irises from the K- and X-band guides into the cavity.

It should be noted that the magnetic field orientation remains fixed at 54° and that no external pump tuning mechanism is required because the large piece of ruby crystal with its high dielectric constant causes many more modes to appear in the pump circuit resulting in many pump resonances.

The crystal was saturated at CW signal powers of about 0.02 μw. CW pump powers were of the order of 30 to 60 mw.

The authors feel that these simplified tuning principles can be used at any band.

P. D. Gianino
F. J. Dominick
Ewen Knight Corp.
Needham Heights, Mass.

* Received by the IRE, July 27, 1959.

Frequency Response of the Two-to-One Autotransformer*

It may be of interest to some readers of the Ruthroff paper[1] to know that the equation which he derives for the insertion function of the two-to-one "transmission-line" autotransformer also applies to transformers constructed with the more usual winding scheme of one wire layer over another (provided that these layers are of equal width). These concentric layers may be considered as forming a helical delay line (of length l) at sufficiently high frequencies (see Fig. 1).

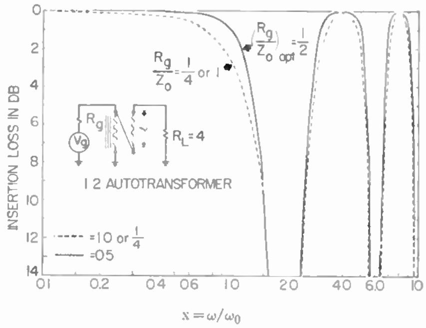

Fig. 1.

It is also interesting (and, in some cases, distressing) to observe that there exists a large number of multiple responses beyond the nominal (first) cutoff frequency with this type of transformer. The insertion loss returns to zero (in loss-free theory) at the center of each spurious response band as may be seen from an examination of Fig. 1. The solid curve is for the optimum characteristic impedance,

$$Z_0 = 2R_g,$$

while the dashed curve is relevant to a characteristic impedance, either

$$Z_0 = R_g,$$

or

$$Z_0 = 4R_g.$$

The frequency scale x in Fig. 1 is normalized in terms of the $\lambda/4$ frequency ω_0.

The insertion-loss zeros occur at every frequency where the associated delay line has an electrical length which is an integral multiple of 2π radians. The phase characteristics of this transformer have also been computed and are available to interested readers.

Experimental evidence demonstrates that this transformer does exhibit spurious responses as indicated by theory.[2]

T. R. O'Meara
Hughes Res. Labs.
Culver City, Calif.

* Received by the IRE, September 22, 1959.

[1] C. L. Ruthroff, "Some broad-band transformers," Proc. IRE, vol. 47, pp. 1337–1342; August, 1959.

[2] See, for example, P. Gillette, K. Oshima, and R. M. Rowe, "Measurement of parameters controlling pulse front response of transformers," IRE Trans. on Component Parts, vol. CP-3, pp. 20–25; March, 1956.

On the Use of Physical Rather Than Four-Pole Parameters in a Standard Transistor Specification*

A plea has been made by Armstrong[1] for the standardization of transistor notation and terminology. While endorsing the purposes of standardization, particularly the attempt to simplify the teaching of transistor circuitry, this writer would like to suggest a possible danger of standardization on common-emitter parameters as proposed by Armstrong. This can be illustrated by the following comparison between the common-emitter and common-base configurations for linear circuit applications.

The common-emitter configuration is widely used in the design of cascaded amplifier stages; indeed, in such amplifiers using direct-coupling or RC-coupling between stages, this choice of configuration is necessary to achieve stage gain. However, if interstage coupling transformers are used, a choice between common-emitter and common-base stages is possible, though again, it would appear that the common-emitter configuration is the more commonly used. Nevertheless, good arguments exist for choosing the common-base configuration for cascaded amplifier stages with interstage transformers; these follow from the advantages to be gained by having the stage gain dependent on the common-base current gain α rather than on the relatively more variable and less stable common-emitter current gain β. Not only is β more dependent than α on transistor bias and environmental changes, but as a function of frequency, β varies much more rapidly in magnitude and phase than does α. The result is that over a wide range of frequencies, the common-base configuration permits the greater definition of amplifier performance by circuit elements external to the transistor. Similar advantages are found for the common-base configuration used in oscillator circuits.[2]

The choice of one configuration for specifying the transistor could be dangerous if it led to a perpetuation of the present situation —a naive restriction on the part of many transistor circuit designers to one configuration for most applications. Rather, the solution might be an undertaking on the part of transistor manufacturers to provide simply the physical parameters of the device in the form, for example, of the common-base physical equivalent circuit in which the carrier base transit characteristic (α as a function of frequency) and all the necessary loss elements (resistances of junctions, base region, etc.) and storage elements (junction and equivalent base storage capacitances) are given quantitatively with tolerances. It would then be left to the circuit designer to calculate (using his own notation) the over-all four-pole terminal and transfer parameters relevant to his choice of configuration and frequency. Also, the following arguments exist for a standardization on physical rather than over-all parameters.

A specification of over-all parameters is of limited use because one must ultimately express these in physical terms if their variations with frequency are to be known. A similar observation applies when the circuit dependence upon temperature, bias, and other environmental effects is to be known. It might be argued, therefore, that the teaching of transistor circuitry should be based on the student's need of a grasp of transistor mechanics in physical terms. The student also requires, of course, a facility for evaluating and using over-all parameters, but it would seem that these should be taught only as a shorthand technique for handling the true physical parameters. In this regard, it would seem unwise to teach transistor circuitry using parameters similar to those used for vacuum-tubes, such as mutual conductance. The relationship between transistors and vacuum-tubes can certainly be made analytically via over-all parameters. But if circuit design is to proceed in physical terms (surely not in the analytical abstract), the transistor seems most easily considered as a current amplifier.

A further argument for a standardization on the physical transistor parameters rather than an arbitrarily chosen four-pole parameters follows from the fact that charge-control parameters are most appropriate for the design of transistor switching circuits.[3] Such charge-control parameters are also physical, representing the dynamic behavior of the physical equivalent circuit parameters used for linear circuit design. Providing high-level injection effects are avoided, these two sets of physical transistor parameters can be related, so that an assessment can be made of transient performance from a knowledge of the physical linear equivalent circuit.

D. F. Page
Def. Res. Telecommun. Estab.
Ottawa, Ont., Can.

* Received by the IRE, July 29, 1959.

[1] H. L. Armstrong, "On the need for revision in transistor terminology and notation," Proc. IRE, vol. 46, pp. 1949–1950; December, 1958.

[2] D. F. Page, forthcoming paper.

[3] R. Beaufoy and J. J. Sparkes, "The junction transistor as a charge-controlled device," *ATE J.*, vol. 13, pp. 310–327; October, 1957.

Effect of Initial Stress in Vibrating Quartz Plates*

Introduction

It has been observed recently that a compressional stress applied to the edge of a vibrating circular quartz plate of the *AT* type excited in the third overtone mode causes a change in frequency.[1] This frequency change may be positive, negative, or zero, depending on the azimuth ψ of the applied force in the plane of the *AT* plate. When the compressional stress, measured from the *X* axis, is applied at about 60°, the frequency change is zero. The effect of compressional stress in an *AT* plate is illustrated in Fig. 1 where the abscissa represents the angle ψ of applied force plotted against the pressure coefficient

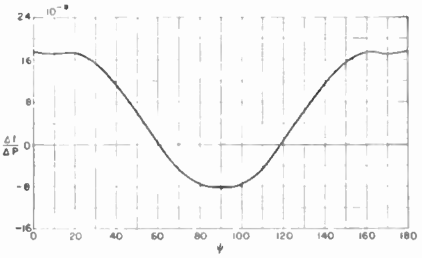

Fig. 1—Effect of compressional stress on a quartz *AT* plate as a function of the azimuth ψ.

$$\frac{1}{f_0}\frac{\Delta f}{\Delta P}.$$

Systematic experimental and theoretical studies of initial stress have been made on a variety of differently oriented circular and square quartz plates. This effect is of great interest with respect to the mechanism of thickness vibrations of plates. The zero effect of pressure is of practical interest for mounting *AT* quartz plates exposed to shock and vibration.

In the present paper, the essential experimental facts are summarized, while the theoretical explanation of this effect will be given at at a later date.

Equipment and Measurement Facilities

Circular and square plates of various orientations were excited by electrodes plated on the surfaces perpendicular to the thickness direction. The electrodes were gold strips parallel to the Z' axis, overlapping in the center of the plate. Electrically-conducting bonding cement was placed on the rim of the crystal, beginning at each electrode and continuing almost around to the other electrode.

A conventional crystal holder was modified by bending the crystal support wires inward and by filing notches in the ends to support the crystal at two diametric points on its periphery.

The holder provided the electrical connections from the crystal to the oscillator and thereby served as the means by which pressure was applied to the plate. The holder was mounted in a metal frame constructed inside a crystal oven to provide a constant temperature. All measurements were made at 25°C.

The metal frame was equipped with a lever arrangement by which the lowering of a weight would cause a force to be applied to the holder arms and hence to the crystal. The weight was controlled from outside the oven.

The coaxial leads from the holder were connected to a crystal impedance meter, the output of which was amplified and beaten to a lower frequency when necessary; *i.e.*, for the purpose of measuring overtone crystal modes. A frequency counter was used to determine the difference in frequency. The measurement equipment is shown schematically in Fig. 2. The plate diameters in all cases were approximately 0.55 inch and the frequencies of the fundamental mode were about 10 mc. The force applied was 100 grams.

* Received by the IRE, July 24, 1959.

[1] E. A. Gerber, "Precision frequency control for guided missiles," 1957 IRE National Convention Record, pt. 1, pp. 90–98.

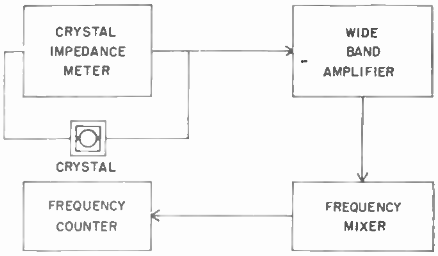

Fig. 2—Block diagram of equipment for measurement of frequency change cause by applied stress.

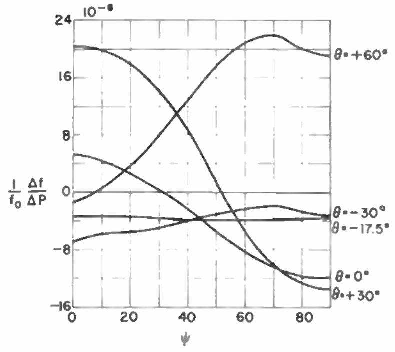

Fig. 3—Effect of compressional stress on various quartz plates of the orientation $(YXl)\theta$ vibrating at the thickness-shear mode as a function of the azimuth ψ.

MEASUREMENTS

The effect of compressional stress on frequency is linear in the range investigated, up to 200 grams. The effect is independent of the order of overtone. For example, the zero pressure angle for a circular AT cut coincides for the fundamental and the overtone modes. The pressure, when applied to circular disks or square plates and oriented so that the edge to which a pressure is applied is perpendicular to the azimuth, shows a similar effect; only a slight difference in the order of 5° was observed between circular and square plates. The pressure effect on square plates depends slightly on the amount of the width to which pressure is applied. Fig. 3 shows the effect of pressure on five circular quartz disks of the orientation $(YXl)\theta$, $\theta=-30°$, $-17.5°$, $0°$, $30°$, $60°$ as function of the azimuth ψ. The ordinate indicates the pressure coefficient of frequency defined as

$$Pf = \frac{1}{f_0}\frac{\Delta f}{\Delta P}.$$

In all cases, the angle of azimuth ψ in the plane of the plate is measured from the X axis. The pressure P is measured in grams. The pressure coefficient of plates $(YXl)\theta$ as function of θ, measured at intervals of 5°, at constant azimuth angles $\psi=0°$, $30°$, $60°$, $90°$, is shown in Fig. 4. Finally, Fig. 5 shows the location of zero pressure coefficient as function of the angles θ and ψ for circular plates having an orientation $(YXl)\theta$.

The effect of pressure in quartz plates is different on the positive and negative side of the orientation angle θ. For the BT cut, $\theta=-49°$, the pressure coefficient is always negative. Quartz plates of the orientation $(XYl)\theta$, $\theta>0°$ have also been investigated. Usually all three thickness modes, the two shear modes, and the extensional mode are excitable.

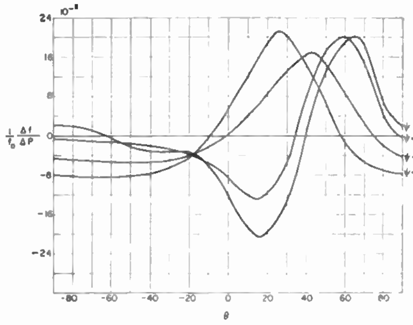

Fig. 4—Effect of compressional stress in vibrating quartz plates $(YXl)\theta$ as a function of orientation θ and the azimuth ψ.

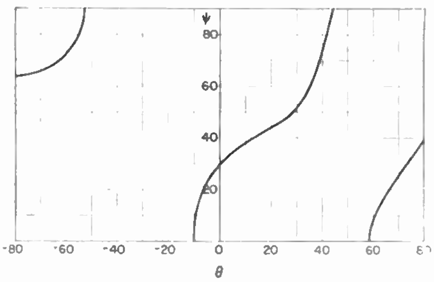

Fig. 5—Locus of pressure coefficient

$$\frac{1}{f_0}\frac{\Delta f}{\Delta P}=0$$

for quartz plates of the orientation $(YXl)\theta$ as a function of θ and ψ.

Of particular interest is the behavior under pressure of the thickness modes of quasi-isotropic plates, *e.g.*, plates made from poled barium titanate or PZT, where thickness-shear or thickness-extensional modes can be excited. Studies on these materials are being carried out.

A. D. BALLATO and R. BECHMANN
U. S. Army Signal Res. and Dev. Lab.
Fort Monmouth, N. J.

Some Bounds on the Error in the Unit Impulse Response of a Network*

Bounds are placed on the error in the unit impulse response of a network caused by a deviation of the transfer function from some desired value. These bounds are modifications of some work published previously by the author.[1] Much of the discussion of this former work is applicable here and will not be repeated.

Throughout, the transfer function of the network in question will be written here as $T(\omega)\exp j\theta(\omega)$ where the amplitude function $T(\omega)$ is never negative and $T(0)>0$. The maximum magnitude of the error in the unit impulse response will be written as $|\delta|$ and will be normalized with respect to $T(0)$. Thus, if $W(t)$ is the actual (or desired) unit impulse response, and $W_1(t)$ is the approximate unit impulse response,

$$|\delta| = \frac{|W(t)-W_1(t)|_{\max}}{T(0)}.$$

The error is normalized with respect to $T(0)$ since this gives a measure of the relative error rather than the absolute error (*i.e.*, if $T(\omega)$ were replaced by $kT(\omega)$, the absolute error would increase whereas the relative error would remain constant). For the same reason, if a definite cutoff frequency ω_c is present, we shall normalize with respect to it and use the following definition:

$$|\delta_1| = \frac{|W(t)-W_1(t)|_{\max}}{\omega_c T(0)}.$$

The proofs of the following theorems are similar to those of the previously mentioned paper[1] and will be omitted.

It is often convenient to assume that the transfer function of a network is zero for all frequencies above a given cutoff frequency ω_c. This is called a band-limiting approximation, and the error introduced is bounded by the following theorem.

Theorem 1

If $T(\omega)/T(0)\le G(\omega)$ for $\omega>\omega_c$, then

$$|\delta_1| \le \frac{1}{\pi\omega_c}\int_{\omega_c}^{\infty} G(\omega)d\omega.$$

A very common expression for $G(\omega)$ is

$$G(\omega)=\epsilon\left(\frac{\omega_c}{\omega}\right)^n \quad \text{where} \quad n>1.$$

Utilizing this expression, we obtain

Corollary 1(a): If $T(\omega)/T(0)<\epsilon(\omega_c/\omega)^n$ for $\omega>\omega_c$, then

$$|\delta_1| \le \frac{\epsilon}{\pi(n-1)}.$$

When an arbitrary transfer function is not realized exactly, but is only approximated, an error appears in the unit impulse response. Two theorems are presented here. The first bounds the error which results when the desired transfer function $T(\omega)\exp j\theta(\omega)$, is approximated by $[T(\omega)+T_\epsilon(\omega)]\exp j\theta(\omega)$. It will be assumed that the integral of the magnitude of the amplitude error function $\int_0^\infty|T_\epsilon(\omega)|d\omega$ exists, then $|\delta|$ can be bounded.

Theorem 2[2]

If the amplitude error function $T_\epsilon(\omega)$ exists then

$$|\delta| \le \frac{1}{\pi}\int_0^\infty \left|\frac{T_\epsilon(\omega)}{T(0)}\right| d\omega.$$

The second theorem bounds the error produced when the desired amplitude function $T(\omega)\exp j\theta\omega$ is approximated by $T(\omega)\exp j[\theta(\omega)+\phi(\omega)]$ where $\phi(\omega)$ is the phase error function. It will be assumed here that the following integrals exist.

$$\int_0^\infty \frac{T(\omega)}{T(0)}|\phi(\omega)|d\omega \quad \text{and} \quad \int_0^\infty \frac{T(\omega)}{T(0)}[\phi(\omega)]^2 d\omega.$$

* Received by the IRE, August 12, 1959.

[1] P. Chirlian, "Bounds on the error in the unit step response of a network," *Quart. Appl. Math.*, vol. 16, pp. 432–435; January, 1959.

[2] The proof of this theorem is similar to one given by A. H. Zemanian, "An approximate method of evaluating integral transforms," *J. Appl. Phys.*, vol. 25, pp. 262–266; February, 1954.

Theorem 3

If the phase error function $\phi(\omega)$ exists,

$$|\delta| \le \frac{1}{\pi}\int_0^\infty \frac{T(\omega)}{T(0)}\{2\sin^2[\phi(\omega)/2] + |\sin\phi(\omega)|\}d\omega$$

and

$$|\delta| \le \frac{1}{\pi}\int_0^\infty \frac{T(\omega)}{T(0)}\left\{\frac{[\phi(\omega)]^2}{2} + |\phi(\omega)|\right\}d\omega.$$

If, in addition, $T(\omega)/T(0) \le M$ where M is a positive constant, then we obtain: *Corollary 3(a): If the phase error function $\phi(\omega)$ exists and $T(\omega)/T(0) \le M$, then*

$$|\delta| \le \frac{M}{\pi}\int_0^\infty \{2\sin^2[\phi(\omega)/2] + |\sin\phi(\omega)|\}d\omega$$

and

$$|\delta| \le \frac{M}{\pi}\int_0^\infty \left\{\frac{[\phi(\omega)]^2}{2} + |\phi(\omega)|\right\}d\omega.$$

P. M. CHIRLIAN
New York University
New York, N. Y.

On the Performance of a Class of Hybrid Tubes*

It was noted previously[1] that the bandwidth (that is, Q_L the loaded Q) of the output cavity is one of the determining factors where efficiency and flat gain characteristics of a broadband multicavity klystron are concerned.

In practice, the beam radii that are chosen in klystrons operating at different frequencies are such that the parameter $\omega r_0/u_0$ goes up with frequency (where, ω is the operating angular frequency, u_0 the dc velocity of the beam, and r_0 the nominal unperturbed beam radius). Under these conditions one finds that for a given value of beam perveance, the loaded Q of the output cavity goes up with frequency, and hence reduces the frequency bandwidth over which efficient operation of the multicavity klystron as a broadband device can be obtained.

A method of improving the bandwidth characteristic of multicavity klystrons by the use of coupled cavities for power extraction has recently been suggested.[2] In the present communication we investigate a "hybrid" tube where the beam bunching section of the tube consists of a multicavity klystron (stagger tuned) and the output or power extraction section is a traveling-wave circuit whose passband is broader than the operating frequency bandwidth of the bunching section. The experiments were performed at X-band.

Calculations have been made of a hybrid tube which consists of: 1) a bunching section, which is a five-cavity (multicavity) klystron structure, and 2) an output section (for power extraction) in a slow wave structure. In the present case it is a disc loaded waveguide operating on the forward space harmonic. Fig. 1 shows a photograph of the tube. One can compute the conventional gain parameter C and the space-charge parameter QC as defined by Pierce[3] of the TW circuit.

$$C^3 = \frac{KI}{4V_0}$$

and

$$4QC^3 = \left[\frac{\omega_q}{\omega}\right]^2[1 + (\omega_q/\omega)^2],$$

where K is the circuit impedance, I and V_0 are the dc beam current and beam voltage, and ω_q is the reduced plasma angular frequency. A fairly good approximate treatment of the problem is possible (since some of the equations do not strictly hold under large signal conditions)as indicated below.

1) Calculate the ac current, i, and the a velocity, v, of the bunched beam at the input to the slow wave circuit. (This can be obtained by the application of the multicavity klystron theory[4]).
2) Write then the usual TWT matching equations[3] to find the circuit voltage at the input to the slow wave circuit.

These equations are

$$\frac{ju_0C}{\eta}v = \sum_{k=1}^{3} V_k/\delta_k$$

$$-2V_0\frac{C^2}{I}i = \sum_{k=1}^{3} V_k/\delta_k^2,$$

and

$$V = \sum_{k=1}^{3} V_k = 0,$$

where the parameters V_1, V_2, and V_3 are the circuit voltages corresponding to the three forward waves (backward wave is neglected here, since the slow wave circuit is assumed to be properly terminated) δ_1, δ_2, and δ_3 are the δ's (as defined by Pierce) associated with the propagation constants of the three forward waves, and V is the total circuit voltage. One finds, for instance, with the above equations (assuming synchronism, that is, velocity parameter $b=0$, and neglecting losses in the slow-wave circuit, that is, loss parameter $d=0$) that the circuit voltage $V_1^{(in)}$ at the input to the slow wave circuit corresponding to the growing wave is given by

$$V_1^{(in)} = \frac{1}{3}\left[e^{j\pi/3}\frac{u_0C}{\eta}v + e^{j2\pi/3}\left(\frac{2V_0C^2}{I}\right)i\right].$$

From the above expression for $V_1^{(in)}$ knowing the gain parameter C, space-charge parameter QC, velocity parameter b and loss parameter d, employing some of the published curves,[4,5] one can calculate the output power of the tube. In the present case the computations yielded:

1) the bandwidth obtainable is approximately 170 mc,
2) power output $\simeq$300 kilowatts (peak),
3) efficiency $\simeq$18 per cent.

If a cavity were used (instead of the TW section) as a power extraction device when obtaining the same bandwidth, the efficiency would have dropped to a value much lower than 18 per cent.

Figs. 2 and 3 show the experimental data obtained with the hybrid tube under different operating conditions. The observed efficiency of the tube is approximately 17 to 18 per cent over a 3 db bandwidth of roughly 200 mc (2.2 per cent). Also, a power output in the vicinity of 375 kilowatts was obtained.

The main factor that appears to determine the efficiency of the present tube (just as in a TWT) is the gain parameter C of the TW circuit. From this it is clear that in the class of hybrid tubes considered here, it is preferable to use a TW circuit which has a large C. It is not out of place to remark here that there are many more types of hybrid tubes which are attractive under different conditions.

The author would like to thank L. T. Lindsay, J. P. Polese, and others of this Laboratory, for their assistance in mechanical design, construction and testing of this tube.

S. V. Yadavalli
Power Tube Dept.
G.E. Microwave Lab.
Palo Alto, Calif.

Fig. 1—Photograph of the "hybrid" tube.

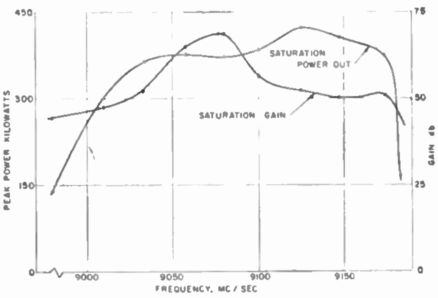

Fig. 2—Performance characteristics of the hybrid tube.

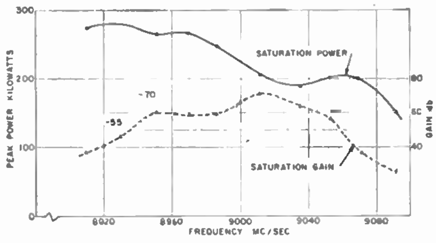

Fig. 3—Performance characteristics of the hybrid tube.

* Received by the IRE, August 11, 1959.

[1] S. V. Yadavalli, "Effect of beam coupling coefficient on broad-band operation of multicavity klystrons," PROC. IRE, vol. 46, pp. 1957–1958; December, 1958.

[2] W. L. Beaver, R. L. Jepson, and R. L. Walter, Wide band klystron amplifiers," 1957 WESCON CONVENTION RECORD, pt. 3, pp. 111–113.

[3] J. R. Pierce, "Traveling Wave Tubes," D. Van Nostrand Co., Inc., Princeton, N. J.; 1950.

[4] C. K. Birdsall and G. R. Brewer, "Traveling wave tube characteristics for finite values of C," IRE TRANS. ON ELECTRON DEVICES, vol. ED-1, pp. 1–11; August, 1954. See for instance, S. V. Yadavalli, "Application of the potential analog in multicavity klystron design and operation," PROC. IRE, vol. 45, pp. 1286–1287; September, 1957.

[5] G. R. Brewer and C. K. Birdsall, "Traveling wave tube propagation constants," IRE TRANS. ON ELECTRON DEVICES, vol. ED-6, pp. 140–144; April, 1957.

Contributors

Don Berlincourt (S'47–A'50–M'56), was, born on January 10, 1924 in Fremont, Ohio. He received the B.S. degree in electrical engineering from Case Institute of Technology, Cleveland, Ohio, in 1949 and the M.S. degree in applied physics from Harvard University, Cambridge, Mass., in 1950.

D. Berlincourt

Since 1950 he has been with The Brush Development Co., which became part of Clevite Corp., Cleveland, Ohio, in 1952. He is now head of the Electrical Properties Section, where his field is solid-state physics, particularly ferroelectricity and piezoelectricity.

Mr. Berlincourt is a member of the Acoustical Society of America.

❖

Frank A. Brand (M'58) was born in Brooklyn, N. Y., on June 26, 1924. He attended Hofstra College, Hempstead, N. Y., from 1946 to 1948 and the Polytechnic Institute of Brooklyn, Brooklyn, N. Y., from which he received the B.S. and M.S. degrees in physics in 1950 and 1958, respectively.

F. A. Brand

In 1950, he joined the U. S. Army Signal Research and Development Laboratory, Fort Monmouth, N. J., as a research physicist and has since been engaged in research and development activities concerned with electron devices and semiconductor physics. He is currently chief of the Physical Electronics Branch, U. S. Army Signal Research and Development Laboratory at Fort Monmouth. Since 1958, Mr. Brand has been a part-time faculty member of the Electronic Engineering Department of Monmouth College, West Long Branch, N. J.

❖

M. H. Brockman (S'43–A'54–M'50–SM'53) was born on September 8, 1918 in Richmond Beach, Wash. He received the B.S.E.E. degree from the University of Washington, Seattle, in 1943 and did graduate work at Harvard University, Cambridge, Mass., Northwestern University, Evanston, Ill., and the Polytechnic Institute of Brooklyn, Brooklyn, N. Y., from which he received the M.E.E. degree in 1953.

From 1943 to 1945, he was a special research associate at the Radio Research Laboratory of Harvard University, and from 1946 to 1955, he was a member of the engineering staff at Airborne Instruments Laboratory, Mineola, N. Y. In 1955, he joined the staff of the Jet Propulsion Laboratory, California Institute of Technology, Pasadena, as a senior research engineer, where, since 1957, he has been a research group supervisor in the electronic research section and is engaged in research in the area of deep-space communication and tracking. He has participated in the Explorer series satellite experiments and the Lunar probe experiments (Pioneer III and IV).

M. H. Brockman

Mr. Brockman is a member of Tau Beta Pi and Zeta Mu Tau and an associate member of the AIEE and Pi Mu Epsilon.

❖

H. Terry Closson was born in Orange, N. J., on May 30, 1926.

He joined the Bell Telephone Laboratories, Murray Hill, N. J., in 1951, where he was concerned with the development of traveling-wave tubes and, more recently, broadband variable reactance amplifiers. He has recently accepted a position with S-F-D Labs. Inc., a subsidiary of Varian Associates in Union, N. J., where he is working on high-power, crossed-field devices and beam-type parametric amplifiers.

H. T. Closson

❖

Clarence Cmolik was born on June 7, 1921 in Cleveland, Ohio. He received the B.S. degree from Western Reserve University, Cleveland, in 1943.

He joined The Brush Development Co. (now part of Clevite Corp.) in 1943 and did research and development on magnetic recording media and ultrasonics until 1952. Since that time he has carried out research and development projects on ceramic titanates. He is presently ceramic engineer with Clevite Electronic Components, Division of Clevite Corp., Cleveland, Ohio.

C. Cmolik

Mr. Cmolik is a member of the American Ceramic Society and the American Chemical Society.

❖

James W. Duncan (A'53–SM'59) was born in Decatur, Ill., on September 15, 1926. He attended Millikin University, Decatur, Ill. from 1946–1948, and in 1950 received the B.S. degree in electrical engineering from the University of Colorado, Boulder. He received the M.S. and Ph.D. degrees in electrical engineering in 1955 and 1958, respectively, from the University of Illinois, Urbana.

J. W. Duncan

From 1944–1946 he served as an electronic technician with the U. S. Navy, and from 1950–1953 he was a development engineer at the Sandia Corporation, Albuquerque, N. M. During the years from 1953 to 1958, he was on the staff of the Electrical Engineering Department of the University of Illinois, Urbana. As a research associate in the Antenna Laboratory, he was engaged in research on surface wave launchers and antennas. Since 1958, he has been with the Collins Radio Company, Cedar Rapids, Iowa where he is head of the Antenna Research Department.

Dr. Duncan is a member of Sigma Xi, Tau Beta Pi, Eta Kappa Nu, Sigma Tau, and Pi Mu Epsilon.

❖

Harold Jacobs was born in Port Chester, N. Y., on November 21, 1917. He received the B.A. degree from Johns Hopkins University, Baltimore, Md., in 1938 and the M.A. and Ph.D. degrees from New York University, New York, N. Y., in 1940 and 1945, respectively.

H. Jacobs

He was employed as a physicist at RCA, Lancaster, Pa., from 1942 to 1945 and at Sylvania Electric Products, Kew Gardens, N. Y., from 1945 to 1949. He joined the U. S. Army Signal Research and Development Laboratory in 1949 where, as chief of the Tube Techniques Section, he performed research pertaining to electron emission, high vacua, gas discharges and semiconductor phenomena. In 1955, he was appointed chief of the Solid-State Devices Branch in the same organization and is presently director of this Solid-State Devices Division. He has also participated in instructional activity, having been associated with Polytechnic Institute of Brooklyn, Brooklyn, N. Y., as an instructor in electrical engineering from 1946 to 1950. At present, he is Chairman of the Electronic Engineering Department of Monmouth College, West Long Branch, N. J.

❖

H. JAFFE

Hans Jaffe (SM'53), was born in Heidelberg, Germany, on February 25, 1909. He received his training at the Universities of Heidelberg, Berlin, and Goettingen, Germany, and received his doctorate in physics in 1934 from the University of Goettingen.

From 1935 to 1939 he was an assistant in piezoelectricity with Professor W. G. Cady at Wesleyan University, Middletown, Conn. Since 1940 he has been with The Brush Development Co., which became part of Clevite Corp., Cleveland, Ohio, in 1952. He is now director of electronic research and his field is solid-state physics with emphasis on ferroelectricity, piezoelectricity, crystal optics, and crystal growth phenomena.

Dr. Jaffe is a member of the American Physical Society and the American Crystallographic Society.

❖

E. A. KELLER

Dr. Ernest A. Keller (A'49–SM'55) was born in Zurich, Switzerland, on March 2, 1913. He received a Physics and Mathematics degree, equivalent to an M.S. degree in 1938 and a Doctor of Technical Sciences degree in 1942, both from the Swiss Federal Institute of Technology, Zurich, Switzerland.

From 1938 to 1951, he was affiliated with Oerlikon Machine Tool Works in Switzerland. During the first six years he was physicist in charge of interior and exterior ballistics for 20-mm guns and the development of electronic test gear for gun powder evaluation and shell developments. In 1941 he designed and built the first digital computer in Switzerland. In 1944 he became manager of Oerlikon's Research and Development Department. Among its most important developments are the Ipsophone in 1946, a completely automatic telephone answering device, and the first magnetic sheet dictating machine in 1947. In 1950 he was appointed technical executive and was sent to the United States for market studies. In 1951 he joined Daystrom Electric Corp., Poughkeepsie, N. Y., in charge of sound recording and reproducing systems development. He worked on basic developments on printed circuits and conducted European market analysis for tape recorder components. He was responsible for the IEC recommendation of in-line recording heads for stereophonic recordings. From 1955 to 1958, he was director of research for Panellit Inc., Skokie, Ill. He was responsible for the development of solid-state and magnetic-core computer elements and the design of single purpose digital systems.

Now with Motorola Inc., Chicago, Ill., he is staff scientist to the director of engineering in the military electronics field, where his major interest is in complex system performance criteria and in the reliability and accuracy considerations for computing and data processing systems and components.

Dr. Keller has had thirty-five European and five U. S. patents granted and two U. S. applications are pending. He is Vice Chairman of Technical Committee 10 IRE and a member of the Administrative Committee of PGIE. He is a member of the Instrument Society of America, Acoustical Society of America, Rocket Society of America, National Security Industrial Association, and the Armed Forces Communications and Electronics Association.

❖

C. A. KROHN

Charles A. Krohn (M'56) was born in New Orleans, La. on August 31, 1930. He received the B.E.E. degree in 1956 and the M.S. degree in industrial management in 1957, both from the Georgia Institute of Technology, Atlanta, Ga. He has also taken additional courses in engineering and statistics.

Prior to college, he was trained and served as an electronic technician in the U. S. Navy. Throughout undergraduate school, he was employed on a part-time basis as an electronic technician in the area of data recording and analysis equipment for sea-clutter studies at the Georgia Institute of Technology Engineering Experiment Station. Following graduation, he remained at this location in the capacity of assistant research engineer, and worked on the development of data recording and analysis equipment for radar polarization studies. He is presently a project electronic engineer at the Motorola Western Military Electronic Center in Phoenix, Ariz., and is in the staff Reliability Group, where he is concerned with the development of reliability programs and reliability analysis techniques. He is also active in reliability education, having instructed reliability engineering techniques in both collegiate and industrial reliability courses.

Mr. Krohn is a member of Phi Eta Sigma, Tau Beta Pi, Eta Kappa Nu, and Phi Kappa Phi.

❖

D. O. MELROY

D. O. Melroy was born in Chatham, N. J. on June 12, 1928. He received the B.S. degree in education in 1950 and the M.S. degree in physics in 1952 from the University of Florida, Gainesville.

He joined Bell Telephone Laboratories, Murray Hill, N. J., in 1952 where he worked on the development of traveling-wave tubes. From 1954 to 1956 he was at White Sands Proving Grounds, N. M., with the U. S. Army, engaged in the evaluation of ground guidance equipment. Upon returning to Bell Laboratories in 1956 he continued work on traveling-wave tubes. He is currently engaged in the development of millimeter traveling-wave tubes.

Mr. Melroy is a member of the American Physical Society and Phi Kappa Phi, and is an associate member of Sigma Xi.

❖

V. P. MINERVA

Vito P. Minerva (S'51–M'58) was born in Cicero, Ill., on December 8, 1931. He received the B.S.E.E. and M.S.E.E. degrees from the University of Illinois, Urbana, in 1954 and 1955, respectively.

From 1954 to 1955 he was a research assistant at the University of Illinois Antenna Research Laboratory, where he was engaged primarily in flush mounted aircraft antenna studies. In 1957, after two years as a guided missile officer in the U. S. Army, he joined the antenna group of Collins Radio Company, Cedar Rapids, Iowa, where most of his work has been in the design and development of high-frequency ground-based antennas. He was primarily responsible for the design and development of the Collins 237A series log periodic antennas, and is presently engaged in the further development of log period antennas.

❖

Alexander P. Ramsa was born in Zakopane, Poland, on August 23, 1916. He attended X Ray Diffraction School at the Polytechnic Institute of Brooklyn, Brooklyn, N. Y., and also attended Monmouth

College, West Long Branch, N. J. for two years.

He served with the Civilian Technical Corps, United Kingdom Air Liaison Mission, and with the U. S. Army Signal Corps from 1941 to 1942. From 1951 to 1955, he worked at the U. S. Army Signal Research and Development Laboratory, Fort Monmouth, N. J., as a specialist in vacuum tube techniques. In 1955 he was employed as a junior engineer in the Solid-State Devices Laboratory at CBS laboratories, New York, N. Y. From 1957 to 1959 he has been associated with the electronic engineering department, Monmouth College, West Long Branch, N. J. He is the co-author of several papers on point contact transistors and also holds a patent on the formation of junctions in semiconductors and has a patent application for small-sized helices and the method of their fabrication.

A. P. Ramsa

❖

Eitel M. Rizzoni (S'50–A'52–M'57–SM'58), was born in Palermo, Italy, on January 15, 1925. He received the bachelor degree (cum laude) in industrial engineering from the University of Palermo in 1947, a postgraduate diploma (cum laude) in electrical communication from the Polytechnic of Turin, Italy, in 1949, and the M.S. degree in electrical communication from the Massachusetts Institute of Technology, Cambridge, in 1952.

E. M. Rizzoni

From 1952 to 1955, he was with RCA Italiana, Rome, Italy, an associated company of the Radio Corporation of America, where, after the installation of a record factory, he was in charge of the recording department. In 1955, he transferred to the systems marketing and engineering group of RCA International Division, Clark, N. J., as a telecommunication system engineer. Since then, he has been engaged in the design and planning of multichannel radiotelephone systems. At present, he is in Bogota, Colombia, for the supervision of the installation and testing of a nation-wide multichannel microwave system.

❖

Philip R. Scott, Jr. (M'58) was born in Worcester, Mass., on April 13, 1930. He received the B.S. degree in electrical engineering from Worcester, Polytechnic Institute, Worcester, Mass., in 1952, and the M.S.E.E. degree from the University of Pennsylvania, Philadelphia, Pa., in 1958.

P. R. Scott, Jr.

From 1952 to 1959, he was employed at Philco Corporation, Philadelphia, Pa., working mainly on the application of pulse circuits to special communication systems. He recently joined the Instrumentation Laboratory of the Massachusetts Institute of Technology, Cambridge, Mass.

❖

Michiyuki Uenohara (S'52–A'54–M'57), was born in Kushikino City, Kagoshima Perfecture, Japan, on September 5, 1925. He received the B.E. degree in electrical engineering from Nihon University in Tokyo in 1949, and the M.S. and Ph.D. degrees in electrical engineering from Ohio State University, Columbus, in 1953 and 1956.

After graduating from Nihon University, he was appointed assistant in the Department of Electrical Engineering, where he taught and conducted research on microwave tubes from 1949 to 1952. In 1952, he received an appointment as a research assistant in the Electron Device Laboratory, Department of Electrical Engineering at Ohio State University. In July, 1954, he was appointed a research associate at Ohio State University and held this position for two years while he completed the requirements for the Ph.D. degree. He then taught at Nihon University for one year, and in 1957, joined Bell Telephone Laboratories, Murray Hill, N. J. He also received the Doctor of Engineering degree from Tohoku University, Sendai, Japan, in 1958.

M. Uenohara

Dr. Uenohara is a member of Sigma Xi, Pi Mu Epsilon, Eta Kappa Nu, American Physical Society, and the Institute of Electrical Communication Engineers in Japan.

❖

W. K. Victor was born in 1922 in New York, N. Y. He attended the University of Texas, Austin, where he received the B.S. degree in mechanical engineering in 1942.

W. K. Victor

Prior to his military service, he was with the Sperry Gyroscope Company, working on airborne computer and fire-control systems. During the war, he served with the Air Corps as a twin-engine pilot instructor. Since September, 1953, he has been associated with the Jet Propulsion Laboratory, Pasadena, Calif., where he is currently chief of the Electronics Research Section. He was previously in charge of flight and ground electronic instrumentation for the Army satellite program and was responsible for the design of the communication system used in the Pioneer lunar probes launched by the U. S. Army.

Mr. Victor is a member of Tau Beta Pi.

Books

Soldering Manual, Ed. by AWS Committee on Brazing and Soldering

Published (1959) by American Welding Society, 33 W. 39 St., N. Y. 18, N. Y. 154 pages+16 index pages+ix pages. Illus. 6×9¼. $5.00.

Prepared by the Committee on Brazing and Soldering of the American Welding Society, this manual covers the main details of joining metals by soldering, the shaping of the edges or surfaces of the joints, precleaning the surfaces, fluxes and methods of fluxing, jigs and fixtures, composition of solders and methods of heating, and subsequent cleaning operations. While to most radio people soldering refers mainly to the joining of wires to terminals, this reference covers for the most part the many other applications and the joining of many different metals, with practical descriptions and illustrations of procedures. In fact, while the information is useful for the joining of electrical connections, the user should supplement the information given here with data on which fluxes and solders are permitted for wiring military (and for that matter, commercial) equipment. There are no distinctions made between approved materials and other materials. With this limitation in mind, the book provides an authoritative source of recommended practices in this art.

RALPH R. BATCHER
Consultant
Douglaston, N. Y.

Microwave Data Tables, by A. E. Booth

Published (1959) by Illiffe and Sons, Ltd., Dorset House, Stamford St., London S.E. 1, Eng. 61 pages. 26 tables. 10¾×7¼. $3.85.

This reference book contains twenty-six tables selected by the author for their usefulness to microwave engineers. These include tables of db vs power and voltage ratio, VSWR vs voltage and reflection coefficient, VSWR vs transmission loss by reflection, frequency to free-space wavelength in centimeters, frequency to guide wavelength in centimeters for nine rectangular waveguide sizes, dimensions and electrical characteristics of twenty-eight British-standard rectangular-waveguide sizes, mode cutoff wavelengths and guide wavelengths in centimeters for two circular-waveguide sizes, and microwave-frequency-band designations. In addition, there are more generally useful tables of reciprocals, squares, and centimeter-to-inch conversions.

The British-standard rectangular-waveguide dimensions are identical to the JAN- or RMA-standard dimensions of this country for all of the commonly used sizes. The guide-wavelength tables cover the JAN waveguide sizes for frequency bands from 2.6 through 18.0 kmc, and also for the 26.5 to 40, and 60 to 90 kmc bands.

The tables involving VSWR adhere to the British practice of expressing VSWR as a number less than unity. This greatly detracts from the usefulness of these tables in this country, where VSWR is customarily defined as a ratio greater than unity. Although corresponding VSWR values may be converted by the table of reciprocals in this book, the added inconvenience would usually make use of the tables inadvisable.

Tables of most of the quantities covered by this book have been published in various references in this country, although generally with coarser increments. For example, tables of db vs power and voltage ratios,[1,2] and of VSWR (>1) vs voltage and power reflection coefficient and transmission loss[2] are appended to two readily available equipment catalogs. Tables of f vs λ_g in centimeters for the principal waveguide sizes have been published by the IRE Professional Group on Microwave Theory and Techniques.[3] The latter reference is even more complete than this book in that it also tabulates λ_g in inches, the ratios λ_g/λ and λ/λ_g, and the quantity $1/\lambda_g$ in reciprocal inches.

In this reviewer's opinion, the book is not sufficiently well adapted to American practice to justify its purchase in this country. It will be found much more useful in countries where VSWR values less than unity are used, and where the references[1-3] are not available. This reviewer hopes that the author will prepare a revised and more complete edition better suited for use in America.

SEYMOUR B. COHN
Stanford Res. Inst.
Menlo Park, Calif.

[1] "Catalog P," General Radio Co., West Concord, Mass., pp. 245-248; April, 1959.

[2] "Microwave Equipment," DeMornay-Bonardi Corp., Pasadena, Calif., pp. D56-D62; 1960.

[3] "Tables of constants for rectangular waveguides," unattached supplement to IRE TRANS. ON MICROWAVE THEORY AND TECHNIQUES, vol. MTT-4; July, 1956. Reprints available from Sperry Gyroscope Co., Great Neck, L. I., N. Y.

Modern Electronic Components, by G. W. A. Dummer

Published (1959) by Philosophical Library, Inc., 15 E. 40 St., N. Y. 16, N. Y. 467 pages+5 index pages +viii pages. Illus. 5¾×8¾. $15.00.

In his present effort, the author has condensed into one volume the characteristics of the more-commonly-used component parts from a previous series of books (a series that was directed to the component-parts engineer and the component-parts application specialist). Nearly 300 pages of completely new material have been added to this condensation.

The above might lead one to imagine that the subject compendium is meant to serve the design engineer—the general practitioner, rather than the component-parts application engineer. This is basically true. However, few of us are experts on all types of parts, and all of us could find the present book of considerable value as a reference outside of our own special field of major interest. In particular, the bibliography of 327 references—properly arranged at the end of each chapter—provides excellent further reading, even for the specialist.

As might be expected, the book has a certain English flavor; "valves" instead of "vacuum tubes," "components" instead of "component parts," "programme" and "colour" instead of "program" and "color," etc. But beneath this British veneer is a wealth of American, and some international material.

Chapter 1 introduces "A Brief History of Component Development in Great Britain." Chapter 2, "Component Specifications and Publications," lists 161 ASESA and 168 British military and commercial specifications. In addition, the author makes an attempt to internationalize the book by listing 20 NATO "Stranag" series military specifications and six International Electrotechnical Commission "IEC Publication" series commercial specifications, covering resistors, capacitors, RF cables, waveguides, and quartz crystals. It is in this chapter that we find the only basis for serious criticism. A more complete list of specifications, including the Military of France and West Germany, and the commercial specifications of other countries (such as EIA in the U.S.A.) would perhaps have given a broader international tenor to the publication. The further addition of a comprehensive cross index to the suggested specification list would have made this a truly great book.

Chapter 3, "Color Codes of Components," and Chapter 4, "Conventional Symbols for Components," compare these two specification sections of the British Services and the Standards Institution with those of the International Electrotechnical Commission.

Chapters 5 through 8 make up over 40 per cent of the book and, being technical rather than of a standards nature, have no particular national flavor, or perhaps more correctly, are completely international. The excellent bibliographies, appended to each chapter, are quite world-wide—approximately half being U. S. references. Characteristics and definitions are discussed in the chapters, which also provide guides for selection and use and discuss manufacturing methods of some 20 basic types of each of these more-commonly-used component parts.

Chapters 9 through 17 are much briefer than the previous chapters. Chapter 9, "Wires, Covered Wires, and Sleeving," also treats "litz" and magnet wire, including ceramic covering. Chapter 10, "Radio Frequency Cables," has received the first truly international treatment. Thirteen NATO RF cable types are related to equivalent International Electrotechnical Commission varieties, as well as British, Canadian, French, U.S.A., Swedish, and Russian varieties.

Chapter 11, "Plugs and Sockets," includes a summary of the properties of twelve commonly-used insulating materials. Chapter 12, "Relays," and Chapter 13, "Switches," include gauged and rotary types. Chapter 14, "Inductors and Magnetic Materials," lists by properties 10 quench-hardened steels and the trade name used in various countries. A comparative table of 65 British and American permanent magnets is provided.

The last 15 chapters cover what might be called horizontal subjects, cutting across most of the previous subjects and taking on a more international flavor.

In the Preface the author summarizes your reviewer's opinion with, "This is the first comprehensive book of its kind written in the world. . . . " The book constitutes a very worthwhile contribution to the engineering literature.

ALFRED R. GRAY
The Martin Co.
Orlando, Fla.

Scanning the Transactions

A fly almost caused a plane crash recently. As the pilot was entering the final phase of his approach, landing instructions from the airport tower were momentarily obliterated at a critical moment by an interfering signal. The cause of the interference? Arcing due to a fly landing on an electric fly-killing device in the airport restaurant. Unwanted electromagnetic radiation is becoming a growing menace. The above case is by no means an isolated example. Last year a radio cab dispatcher's voice caused a missile to explode. Radar on a military plane touched off a shelf-full of flash bulbs. An electroencephalograph located near a hospital elevator was found to be sending people to institutions because of spurious brain waves. An industrial heater in a Louisville factory disrupted airline communications at Cleveland, St. Louis, and Chicago. In one community an astute political candidate played havoc with his rival's radio speeches by retiring to his work shop and running his unsuppressed electric drill whenever his opponent went on the air. So far, comparatively few people are concerned with interference control. But it is a problem that is rapidly growing in magnitude. Not only are new sources of interference being invented daily, but electronic equipment is being made more and more sensitive. We are fast approaching the point of trying to operate a microvolt civilization in a millivolt interference environment. Interference control may well become a major field of electronics in the near future. (R. Daniels, "Trouble with a capital I," IRE STUDENT QUARTERLY, December, 1959.)

Among the several stereo broadcast techniques currently being investigated is one which relies on an interesting psychoacoustic phenomenon known as the Precedence Effect. If a sound reaches a listener from two directions at the same instant, it will appear to him to emanate from a source midway between the two. However, if the sound from one direction is delayed slightly (from 1 to 30 msec) the listener will totally disregard it and will locate the sound source by the direction of the first arriving sound only. This effect offers a novel way of making the 2-channel 2-receiver method of stereo broadcasting compatible. A number of radio stations currently broadcast one channel of a stereophonic program on AM and the other channel on FM. If the broadcaster tried for a full stereophonic effect, the listener with only one receiver would hear an incomplete or poorly balanced program. Consequently, broadcasters have had to dilute the stereophonic effect in order to preserve satisfactory reception for single-channel listeners. Under the Precedence Effect system, the AM and FM transmitters are cross connected through two delay lines. Thus both transmitters carry the full program, but with the left channel delayed slightly in one and the right channel delayed in the other. This delay will go unnoticed by the listener with a single receiver. Meanwhile, thanks to the Precedence Effect, the stereo listener will disregard the directions of the delayed sounds and will hear the left channel as coming from the left loudspeaker only, and similarly for the right channel. (F. K. Becker, "A compatible stereophonic sound system," IRE TRANS. ON BROADCASTING, November, 1959.)

Those interested in test equipment, whether it be in the AF, RF, or microwave range, would no doubt have enjoyed seeing the 30 instruments which were shown at the Soviet exhibit at the New York Coliseum last July. For the benefit of those who didn't, the Washington Chapter of the IRE Professional Group on Instrumentation made arrangements with the Soviet Press Attaché to take pictures of the instruments and to examine their exterior appearance and electrical performance specifications. The 30 photographs, together with translated panel markings and detailed descriptions of performance ratings, have now been published by the Chairman of the Washington Chapter in what amounts to an unusual guided picture tour of the exhibit. The tour is augmented by an enlightening commentary based on technical discussions which Chapter members had with one of the Russian engineers at the scene. The Washington Chapter is to be congratulated for undertaking this novel and informative project. (B. O. Weinschel, "Russian test equipment for audio, radio, and microwave measurements," IRE TRANS. ON INSTRUMENTATION, December, 1959.)

Man on the moon. A paper on lunar exploration in the last issue of PGSET TRANSACTIONS is worthy of note. While it does not stress the electronic aspects of space exploration, it is interesting to electronic engineers in that it represents concrete plans for what will probably be the first trip of man to the moon *and back*. The need for electronic instrumentation and navigation is apparent between the lines and the requirements for light weight, reliability and accuracy are recognized as the details of the trip through space are unfolded. A realization of the magnitude of the trip is obtained from the weight breakdown table where it is seen that for a launching weight of 6,700,000 pounds, only 8000 pounds is returned to earth. (M. W. Rosen and F. C. Schwenk, "A rocket for manned lunar exploration," IRE TRANS. ON SPACE ELECTRONICS AND TELEMETRY, December, 1959.)

External noise is receiving as much attention in the design of communications equipment as the noise generated within electronic systems, thanks to the recent advent of extremely quiet amplifiers. All the noises which arrive at the antenna from outer space and which arise in the antenna itself and in the coupling to the first amplifier must now be given careful consideration. An examination of the problem reveals that a handsome total of at least eight sources of external noise must be considered, namely, sky background radiation, reradiation by the atmosphere, leakage from the warm earth via minor lobes of the antenna pattern, warm-earth radiation that is scattered by particles into the main lobe, noise due to the finite conductivity of metallic antenna surfaces, losses through duplexing components, and leakage from the transmitter during beam-off condition. While present information concerning many of these factors is adequate for making usable design approximations, there still remains a considerable area which is in need of further attention, especially with respect to noise due to the nonhomogeneous character of the atmosphere. (H. W. Grimm, "Fundamental limitations of external noise," IRE TRANS. ON INSTRUMENTATION, December, 1959.)

Designing a Yagi antenna is still a problem in spite of the fact that this type of array has been with us for more than 30 years. During this time, it has found many applications due to its constructional simplicity and its usefulness at practically all frequencies. But despite its popularity, no one has been able to develop a general method for designing Yagi antennas for maximum gain. Gain is dependent on the height, spacing, and diameter of the elements in the array. The problem is to find the optimum set of dimensions of these parameters, which in turn requires discovering how they are related to one another under conditions of maximum gain. Investigators have now come up with a new design approach which makes this possible at last. By introducing the notion of a surface wave traveling along the array, they have found that the maximum gain occurs at a definite value of phase velocity. This value is a function of the height, spacing and diameter of the elements, and thus a criterion has been found for specifying the optimum combination of these parameters. (H. W. Ehrenspeck and H. Poehler, "A new method for obtaining maximum gain from Yagi antennas," IRE TRANS. ON ANTENNAS AND PROPAGATION, October, 1959.)

Abstracts of IRE Transactions

The following issues of TRANSACTIONS have recently been published, and are now available from the Institute of Radio Engineers, Inc., 1 East 79th Street, New York 21, N. Y. at the following prices. The contents of each issue and, where available, abstracts of technical papers are given below.

Sponsoring Group	Publication	Group Members	IRE Members	Non-Members*
Aeronautical and Navigational Electronics	ANE-6, No. 3	$1.10	$1.65	$3.30
Antennas and Propagation	AP-7, No. 4	2.25	3.85	7.65
Broadcasting	PGBC-14	0.60	0.90	1.80
Component Parts	CP-6, No. 4	1.50	2.25	4.50
Instrumentation	I-8, No. 3	1.25	1.85	3.75
Microwave Theory and Techniques	MTT-7, No. 4	1.60	2.40	4.80
Space Electronics and Telemetry	SET-5, No. 4	1.55	2.35	4.65

* Libraries and colleges may purchase copies at IRE Member rates.

Aeronautical and Navigational Electronics

Vol. ANE-6, No. 3, September, 1959

The Editor Reports (p. 158)

Vector Principles of Inertial Navigation—A. M. Schneider (p. 159)

A vector equation, which is derived from first principles, describes the mechanization of inertial navigation systems for use anywhere in space. A specialized form of this equation applies directly to three-dimensional motion at any speed, any altitude, over an elliptical, rotating earth. The usefulness of this equation is illustrated by working out an example of a system design. Behavior of errors in inertial systems is also discussed.

Position Information Using Only Multiple Simultaneous Range-Measurements—H. L. Groginsky (p. 178)

Three-dimensional generalized position-measurement systems are analyzed in this paper. In these systems, target position is obtained by trilateration using only range data collected by a group of ν stations located in an arbitrary geometry.

The method of maximum likelihood is used to obtain a joint estimator for the target coordinates which makes optimal use of the redundant data when the noise is Gaussian. A simple recursion formula for the estimator is obtained for this purpose and is shown to be convergent. This formula makes it possible to add data from a redundant number of stations at will and in proportion to their relative reliability. Further, it is shown that the recursion formula can be written entirely in terms of the changes in the successive iterative target position estimates. This technique offers a new means of obtaining tracking data on a moving target since it permits changes in target position to be computed directly as new data are obtained.

The covariance matrix of the joint three-dimensional estimator is obtained in the case in which the measurement noise is small compared to the distances measured. The mean-square position error, namely, the trace of the covariance matrix, is shown to have a simple form for the general two-dimensional system in which the target and stations are coplanar. The geometry enters the variance expression only through the angles of cut θ_{ij}, which are the angles between the lines joining the target and the stations.

The surveillance regions of various redundant two-dimensional systems obtained by using the joint estimator are compared to that obtained by using only pair-wise estimation. It is found that little improvement is made when the distance of the target to all the stations is much greater than the distance between stations.

C.P.I.—A Crash Position Indicator for Aircraft—D. M. Makow and H. T. Stevinson (p. 187)

A novel, light, simple and inexpensive position indicator for crashed aircraft has been developed and subjected to severe tests. A special pulsed transmitter with trickle-charged batteries and an internal antenna is potted in shock-absorbing foam transparent to radio waves and placed inside a special aerofoil. This device, held on the tail of the aircraft, is released automatically upon detection of any abnormal structural disturbance. Then it tumbles away from the aircraft in time to clear the danger zone, slows down to a safe landing and transmits a distress signal from any position and under wide environmental conditions.

Contributors (p. 201)

Roster of Members (p. 202)

Antennas and Propagation

Vol. AP-7, No. 4, October, 1959

Leaky-Wave Antennas I: Rectangular Waveguides—L. O. Goldstone and A. A. Oliner (p. 307)

A microwave network approach is employed for the description and analysis of leaky-wave antennas. This approach is based on a transverse resonance procedure which yields the complex propagation constants for the leaky waves. A perturbation technique is then applied to the resonance equation to obtain results in simple and practical form. These procedures are illustrated by application to a number of practical leaky rectangular waveguide structures. Very good agreement is obtained between the theoretical results and the measured values.

A Flush-Mounted Leaky-Wave Antenna with Predictable Patterns—R. C. Honey (p. 320)

This paper describes the design and the measured performance of a large, flat antenna consisting of an inductive grid spaced over a conducting surface. The analysis employs the transverse-resonance method to determine the radiating properties of the structure. This analytical technique is shown to predict very accurately the amplitude and phase of the illumination along the aperture of the antenna.

An antenna was built with an 18- by 24-inch aperture and tested over the frequency band from 7-to-13 kmc. The results of these tests confirm the theoretical predictions in every detail. A pencil beam from the antenna scans in the H plane (perpendicular to the antenna) from 20° to 60° from the normal to the aperture as the frequency changes from 7-to-13 kmc. The H-plane beamwidth remains virtually constant over most of this band. The first H-plane sidelobe or shoulder is at least 29 db below the main lobe from 7-to-10 kmc, and at least 23 db below from 10-to-13 kmc. All H-plane sidelobes beyond three or four beamwidths on either side of the main lobe are at least 40 db below the main lobe everywhere in the 7-to-13 kmc band. At the design frequency the measured pattern agrees with the theoretical pattern within a fraction of a db down to 40 db below the peak of the main lobe, even though the gain of the antenna at this frequency is only 33 db.

The Unidirectional Equiangular Spiral Antenna—John D. Dyson (p. 329)

Circularly polarized unidirectional radiation, over a bandwidth which is at the discretion of the designer, is obtainable with a single antenna. The antenna is constructed by wrapping balanced equiangular spiral arms on a conical surface. The nonplanar structure retains the frequency-independent qualities of the planar models, and, in addition, provides a single lobe radiation pattern off the apex of the cone. Practical antennas have been constructed with radiation patterns and input impedance essentially constant over bandwidths greater than 12 to 1 and there is no reason to assume that these cannot be readily extended to more than 20 or 30 to 1.

Closely-Spaced Transverse Slots in Rectangular Waveguide—Richard F. Hyneman (p. 335)

The traveling-wave modes associated with an infinite, periodic structure are considered. An approximate equation for the propagation constants of these modes is derived through the use of Fourier analysis and an approximate application of the reaction concept. In the homogeneous case considered, it is found that two dominant modes may exist: an attenuated fundamental mode representing a perturbation of the dominant mode of a closed rectangular waveguide, and an unattenuated surface wave, which is similar to the wave associated with a corrugated surface waveguide. By means of the appropriate variation of physical parameters, including the slot length and spacing, essentially independent control of the attenuation constant and phase velocity of the fundamental mode is possible over a wide range. Typical curves of the propagation constant in terms of these parameters are given, and the results of experimental measurements are shown to be in close agreement with the theory.

Generalizations of Spherically Symmetric Lenses—Samuel P. Morgan (p. 342)

The purpose of this paper is to generalize the solutions of some spherically symmetric lens and lens-reflector problems recently treated by Kay. The original problem was to find a variable-index structure, with a point source at its surface or at infinity, which would produce a beam of finite angular width, having a prescribed variation of intensity with angle. It is shown that a prescribed exit beam can be obtained from a point source at any given distance from the lens, and that the index of refraction may be specified more or less arbitrarily in the outer part of the lens. A special case is solved in terms of tabulated functions.

Radiation Properties of a Thin Wire Loop Antenna Embedded in a Spherical Medium—Orval R. Cruzan (p. 345)

Formulas for certain radiation properties of a spherical antenna are derived theoretically. The antenna, which consists of a spherical medium, such as ferrite, with a thin wire loop embedded just below the surface in an equatorial plane, is driven by a slice generator. For the spherical medium, the permeability K_m and the dielectric constant K, are assumed to be scalars and, in general, complex. The solutions are facilitated through the expansion of the fields in terms of characteristic orthogonal spherical vector wave functions. The properties for which formulas are derived are current distribution, input impedance, input power, radiated power, power loss in the spherical medium, and the efficiency of the antenna. For radiation resistance, not only the general case formula but also the formula for electrically small antennas is given, and the difference between these formulas, for media assumed lossless, is shown graphically.

The Conductance of Dipoles of Arbitrary Size and Shape—K. Franz and P. A. Mann (p. 353)

The real part of either the impedance or the admittance of dipoles of arbitrary size and shape can be computed rigorously without solving a boundary value problem of a partial differential equation. In analogy to a well-known method of potential theory, fields of standing waves can be generated by integrals over current filaments so that for a given frequency there exist dipole shaped surfaces normal to the electric field surrounded by distant surfaces of vanishing electric field strength. Boundaries of perfect conductors may be supposed to coincide with a dipole shaped surface and a distant closed surface. The transients of such fields of standing waves are intimately related to the steady state of the free radiating dipole, since, before the first waves reflected from the distant enclosure have come back, the dipole cannot know whether or not it is enclosed. Corresponding to the type of current filament, either the resistance, or the conductance, of the radiating dipole can be calculated by direct integrations, while the shape of the dipole is determined by an ordinary differential equation of first order. As an example, we compute a family of dipoles that all have the same conductance $G=(254\ \Omega)^{-1}$ and a length $2h$ between limits $\lambda/2 \leq 2h \leq 1.36 \cdot \lambda/2$.

The Launching of Surface Waves by a Parallel Plate Waveguide—C. M. Angulo and W. S. C. Chang (p. 359)

The excitation of the lowest TM surface wave in grounded dielectric slab by a terminated parallel plate waveguide is discussed. The ground plane is the continuation of the lower plate of the waveguide and the infinite dielectric slab is partially filling the waveguide. The thickness of the slab, the height of the parallel plate waveguide, and the frequency are such that only the lowest slow wave can propagate in the partially filled waveguide and the grounded dielectric slab.

The Fourier transform of the field scattered by the termination of the upper plate of the waveguide is found by means of the Wiener-Hopf technique and the far fields obtained by the method of steepest descents. The percentage of power reflected back into the waveguide, of power transmitted to the surface wave in the slab, and of power radiated into the open space are plotted vs the thickness of the slab for different heights of the waveguide and $\epsilon = 2.49$.

This method of excitation is found to be very efficient. If the dimensions of the waveguide and the slab remain within a considerably wide range, the efficiency obtained for a given frequency is very close to the optimum. Therefore, the adjustments for maximum efficiency are not critical.

Random Errors in Aperture Distributions—R. H. T. Bates (p. 369)

The effects of random manufacturing errors on polar diagrams of antennas are analyzed in terms of the radius of correlation and mean square magnitude of the errors. The basis of the method is the Wiener-Khintchine theorem. Approximate general formulas are given for the reduction in gain and lowest probable sidelobe level. The implications of the theory are discussed.

Successive Variational Approximations of Impedance Parameters in a Coupled Antenna System—M. K. Hu and Y. Y. Hu (p. 373)

In this paper, a new variational formulation for a single impedance parameter of an m-antenna system is presented. This formulation enables one to determine any self impedance Z_{ii}, one at a time, merely by exciting antenna i alone and leaving all the other antennas open circuited. For determining any mutual impedance Z_{ij}, only two independent excitations, one the same as that used for determining Z_{ii} and the other for determining Z_{jj}, are required. Thus, if all the $m(m+1)/2$ impedance are required, only m independent excitation conditions are needed. In contrast to this, the formulation available in the literature is based on $m(m+1)/2$ independent excitation conditions. Because of a reduced number of excitation conditions and the way they are assumed, the physical nature of the problem is made simpler and easier to comprehend. Such comprehension helps considerably in the choice of trial current distributions for a specific application.

Two methods of evaluating the successive higher-order approximations are also given. One is based upon an orthogonalization process, and the other is based upon the successive inversion of matrices. In the evaluation of a certain order approximation, both methods have the advantage of utilizing all the work already done for the lower-order approximations; and at the same time, additional work required is considerably reduced. It is believed that the formulation, as well as the two methods of successive approximations, will also be useful in other problems.

A New Method for Obtaining Maximum Gain from Yagi Antennas—H. W. Ehrenspeck and H. Poehler (p. 379)

In conventional Yagi design, optimum performance requires separate adjustments in a number of parameters—the array length and the height, diameter, and spacing of the directors and reflectors.

By introducing the notion of a surface wave traveling along the array, it is possible to demonstrate experimentally the interrelationship between these parameters. With this, the gain then depends only on the phase velocity of the surface wave (which is a function of the height, diameter, and spacing of the directors) and on the choice of the reflector. Thus, maximum gain for a given array length, for any director spacing less than 0.5 λ, can be obtained by suitable variation of the parameters to yield the desired phase velocity.

A design procedure that provides maximum gain for a given array length is presented.

A Dipole Antenna Coupled Electromagnetically to a Two-Wire Transmission Line—S. R. Seshadri and K. Iizuka (p. 386)

The properties of a dipole antenna coupled electromagnetically to a two-wire transmission line are studied experimentally. It is found that the coupling of the antenna to the transmission line can be maximized by a proper choice of 1) the angular position of the antenna with respect to the transmission line, 2) the length of the antenna, and 3) the separation of the antenna from the transmission line. The effect of the spacing between the wires of the transmission line on the optimum parameters is investigated. It is found that the optimum angular position of the antenna is not noticeably altered if, instead of a single antenna, an array of properly located antennas is used as the load. The advantage of an antenna array built on this coupling principle is discussed.

An Ionospheric Ray-Tracing Technique and Its Application to a Problem in Long-Distance Radio Propagation—D. B. Muldrew (p. 393)

A method is given for the determination of the equation of a ray path in a known ionosphere where there are no horizontal gradients. It can partially take into account the effects of the magnetic field of the earth. The method was applied to an oblique path between Ottawa and Slough (5300 km) to determine certain properties of the one-hop mode. From this it is shown that at times one-hop direct ray propagation is possible over this path.

The Effect of Multipath Distortion on the Choice of Operating Frequencies for High-Frequency Communication Circuits—D. K. Bailey (p. 397)

Harmful multipath distortion on high-frequency facsimile services and telegraphic services operating at high speeds occurs when the received signal is composed of two or more components arriving by different modes over the same great-circle path with comparable intensities, but having travel times which differ by an amount equal to an appreciable fraction of the duration of a signal element. The dependence of multipath distortion on the relationship of the operating frequency to the MUF is discussed and a new term, the multipath reduction factor (MRF), is introduced which permits calculation in terms of the MUF of the lowest frequency which can be used to provide a specified measure of protection against multipath distortion. The MRF has a marked path-length dependence and is calculated as a function of path length for representative values of the other parameters involved by making use of an ionospheric model. It is then shown how the MRF can be used in connection with world-wide MUF prediction material to determine the minimum number of frequencies which must be assigned to a high-frequency communication service of continuous availability operating at high speed. Some comparisons with observations are discussed, and finally conclusions are drawn concerning manner of operation and choice of operating frequencies to reduce or to eliminate harmful multipath distortion.

Analysis of 3-CM Radio Height-Gain Curves Taken Over Rough Terrain—H. T. Tomlinson and A. W. Straiton (p. 405)

This report describes the effect of terrain and meteorological conditions on the height-gain pattern of 3.2-cm radio waves over various short transmission paths. Equivalent reflection coefficients are obtained and potential reflection areas are investigated. A study of the time variations in the height of nulls in the signal strength pattern is made and the relationship between movement of the nulls and the corresponding refractive index distribution is considered.

Electron Densities of the Ionosphere Utilizing High-Altitude Rockets—O. C. Haycock, *et al.* (p. 414)

The problem of determining the electron densities in the E-region of the ionosphere is approached by using 6-mc pulse transmissions from a rocket to several ground receiving stations.

A logical and complete development, using dyadic techniques, is given for obtaining the propagation constant of the dissipative, anisotropic ionosphere. Special cases of the magnetoionic formulas are given, and comparison of the ionosphere with a distributed-constant transmission line is made.

In a nondissipative ionosphere, formulas are developed establishing the relationship between the effective electron density and the relative transmission delay of the 6-mc pulse.

A description of the University of Utah's vertical incidence experiment is given in which a 6-mc pulse from an airborne transmitter is received simultaneously at several ground receiving stations.

The relative 6-mc time-delay data from three Aerobee high-altitude rockets launched from Holloman Air Development Center on July 1, 1953, November 3, 1953, and June 13, 1956, were obtained and, from these, electron density was calculated. Curves showing the profile of electron density as a function of altitude as calculated both during the rocket ascent and descent are presented. The curves indicate a general increase of electron density throughout the *E*-region, rising from nearly zero at 85 km to a maximum of about 2×10^{11} electrons/m^3. The maximum altitude attained by the rockets allowed exploration up to 137 km above sea level.

A Scatter Propagation Experiment Using an Array of Six Paraboloids—Lorne H. Doherty (p. 419)

Using an antenna system whose aperture could be varied in four-foot steps between 4 and 24 feet, aperture-to-medium coupling loss measurements have been made on a 2720-msec, 216-mile path. These measurements reveal an intrinsic variability in the scattering mechanism which is not accounted for in most current theories. Diversity and fading-rate measurements were also made. A simple mathematical model of the diffracted field yields calculated values of the normal component of the wind which agree well with the measured wind. Calculated and measured values of fading rate are also seen to be in good agreement. An estimate is made of the turbulent wind velocity.

Sweep-Frequency Studies in Beyond-the-Horizon Propagation—W. H. Kummer (p. 428)

This paper considers the bandwidth characteristics of the propagating medium in tropospheric beyond-the-horizon propagation.

To study this problem, a frequency-sweep experiment was performed over a 171-mile experimental circuit. A 4.11-kmc transmitter was frequency modulated at a 1000-cps rate over a 20-mc band. The receiver was swept nonsynchronously over the same band at a 30-cps rate. The resultant pulses were displayed on an oscillograph and photographed at the rate of one frame every two seconds.

The experiment used a 28-foot transmitting antenna and 8-, 28- and 60-foot receiving antennas.

Sequences of selected sweep-frequency pictures are shown for various antenna combinations and transmission conditions. The bandwidths from the experiment are compared with a calculation based on the common volume geometry.

Photographs of signals received simultaneously from a twin-feed horizontal diversity system are also shown and discussed.

Communications (p. 434)

Contributors (p. 441)

Broadcasting

PGBC-14, November, 1959

Forward (p. 1)

Optimized Compatible AM Stereo Broadcast System—H. B. Collins, Jr. and D. T. Webb (p. 2)

A two-channel multiplex system for compatible AM broadcasting is described. System objectives including compatibility, service area, and program quality are discussed. Three different methods of creating the equivalent transmitted signal are reported, and conversion of present-day monaural stations to stereo by each method is indicated. The design of receivers for recovering the two stereo tracks is examined showing the signals derived by various means of detection. Emphasis is placed on a design resulting in a reliable, minimum cost receiver. Field test equipment and results are briefly considered and the level of performance that can be obtained from the system is stated.

A Compatible Stereophonic Sound System—F. K. Becker (p. 16)

New Dimensions in Sound—H. E. Sweeney and C. W. Baugh, Jr. (p. 19)

Component Parts

Vol. CP-6, No. 4, December, 1959

Information for Authors (p. 236)

Who's Who in PGCP (237)

High Dielectric Constant Ceramics—Fielding Brown (p. 238)

Currently available high dielectric constant ceramics enjoy certain special advantages for use in capacitor design. However, there are also severe limitations which must be well understood by engineers attempting their application. This paper summarizes the principal electrical characteristics, favorable or otherwise, of these materials and attempts to relate them to well-known basic dielectric properties. In addition, a brief review of present knowledge of ferroelectricity in barium titanate is given, since many of the practical problems encountered in the use of high dielectric constant ceramics are rooted in the inherent ferroelectricity of the material. A few remarks are included concerning avenues of future advance in high-*K* ceramic applications.

Component-Part Screening Procedures Based on Multiparameter Measurements—Ralph E. Thomas (p. 252)

A screening methodology based on measurements of several parameters is proposed. The methodology provides an improved semiquantitative basis for the selection and evaluation of screening criteria. The method is devised 1) to yield a minimum number of parameters required for effective screening with a linear function, 2) to determine the gain in reliability obtained by screening on the basis of two parameters rather than one, three rather than two, etc., 3) to determine the parameters which may be interchanged for measurement or cost reasons without changing the effectiveness of the screening procedure, 4) to determine the probabilities of screening out a superior component and failing to screen out an inferior component, 5) to determine the costs associated with making the screening procedure more stringent, 6) to permit modification of the screening criteria for small changes in component-part design, or lot characteristics, 7) to determine the effect of alternative failure criteria on the screening criteria, and 8) to indicate when practical screening cannot be achieved using a linear function of the parameters selected for measurement. The methodology is based on a combination of standard statistical techniques, and is novel only in maintaining a tractable analysis of the over-all problem of screening individual component parts by variables inspection.

Aircraft Secondary Power Generator With Direct Compensation Frequency Control—L. J. Johnson and S. E. Rauch (p. 259)

The variable speed constant frequency alternator system provides accurate frequency control independent of the shaft speed. The method employed is completely electrical in contrast with the more conventional mechanical speed control systems. The principle of operation depends upon a constant angular velocity magnetic field in the alternator armature, the angular velocity being the vector sum of the mechanical velocity of the shaft and the velocity of an electromagnetic rotating field induced by the excitation of a polyphase field winding. The polyphase field winding is driven by a variable frequency polyphase exciter, its frequency being directly proportional to the speed deviation from synchronous speed of the alternator rotor and shaft. The frequency control system as described in this paper is the open-loop type and, as such, accomplishes absolute frequency control with no errors arising from load or speed transients.

An experimental brushless, constant frequency, three-phase alternator is discussed.

Delay-Line Specifications for Matched-Filter Communications Systems—R. M. Lerner, *et al.* (p. 263)

Specifications for a wide-band multitap delay-line are rationalized by the demands of a matched-filter communication system employing a pair of such delay lines. The delay line is specified in terms of time-domain characteristics.

Some Rating and Application Considerations for Silicon Diodes—H. C. Lin (p. 269)

The dissipation in a silicon rectifier depends on the characteristics of the rectifier (threshold voltage and ohmic resistance) and the circuit constants (inductive, resistive, or capacitive load). Dissipations under these different conditions are calculated.

The maximum permissible dissipation is limited by maximum junction temperature and thermal stability. The stability criterion depends on the thermal resistance, the reverse characteristic and its change with respect to temperature, the reverse voltage, and the circuit configuration. Derating curves are obtained, based on known variations of the reverse characteristics of silicon rectifiers with temperature and voltage.

The maximum permissible transient dissipation depends on the total surge energy. The energy dissipated in the rectifier is high when the load capacitance is high and the external series resistance is low.

A design embodying all the foregoing considerations is illustrated.

Correction to "A Comparison of Thin Tape and Wire Windings for Lumped-Parameter Wide-Band High-Frequency Transformers"—Thomas R. O'Meara (p. 273)

Contributors (p. 274)

Annual Index, 1959 (follows p. 275)

Instrumentation

Vol. I-8, No. 3, December, 1959

Russian Test Equipment for Audio, Radio, and Microwave Measurements—Washington Chapter PGI—Bruno O. Weinschel (p. 67)

During July, 1959, some Russian instruments were exhibited in New York City. Photographs of 30 of such electronic test instruments are shown, including a translation of the panel inscription. The Russign specifications, reproduced in English, appear with each photograph. Comments on items of lesser familiarity are offered.

A Time Gate for Echo-Measuring Radar Installations—J. Bacon and J. Q. Burgess (p. 79)

Emphasis on higher operating speed in echo-measuring radar installations necessitates the tightening of performance specifications on certain component parts of the system. A case in point is the time gate and it provides the principal topic of this paper. A design having a linear dynamic range of 50 db for an error not exceeding ±0.3 db is presented. Out-of-gate rejection is 58 db below maximum signal. Gating is accomplished by using a Zener diode. Signal and gate pulses are separated by using a principle which eliminates balancing. This adds a measure of stability unattainable when using balancing techniques. Without unduly stressing detail, sufficient essentials are presented in order to duplicate the quoted results. Principal weight is placed on the design features which may be modified to fit a number of similar situations.

A Transistor Temperature Analysis and Its Application to Different Amplifiers—Werner Steiger (p. 82)

The equivalent input drift of an amplifier, which is the correction necessary at the input to restore the output to its "pre-drift" condition, is a convenient concept for the temperature analysis of transistor differential amplifiers. In this paper general expressions are derived for the equivalent input drift of a dc amplifier with one transistor. The results are then applied to differential stages. Conclusions for the design of low-drift differential amplifiers are drawn with the possibilities of drift compensation being taken into consideration. Experimental verification indicates that it is possible to reduce the equivalent input drift voltage under certain conditions to the order of 1 millivolt per 100 centigrades.

Logarithmic Amplifier Design—S. J. Solms (p. 91)

The logarithmic amplifier is useful for signal compression, analog computation and IAGC in wide-range pulse receivers; it has numerous possible applications in instrumentation. A lin-log amplitude characteristic may be obtained by cascading a number of stages having a dual-slope amplitude characteristic. This approximation, being analyzed in detail, leads to expressions for dynamic range and approximation error.

Measurement of the bandwidth of a lin-log amplifier is discussed as well as maximization of bandwidth as affected by the choice of the number of stages. The problem of temperature compensation as it affects bandwidth and power consumption is also discussed. The problem of recovery transients imposed by the use of ac coupling and the advantage of bipolar design for the control of recovery characteristics are discussed.

A lin-log transistor bipolar amplifier design having an 80-db dynamic range and a small signal bandwidth of 2.5 mc is presented. Experimental results including temperature effects and pulse response characteristics are given. The dependence of the amplitude response on duty factor imposed by the ac coupled bipolar design is mentioned.

Fundamental Limitations of External Noise—Henry H. Grimm (p. 97)

The development of low-noise microwave amplifiers has prompted the author to re-evaluate noise sources preceding the first low-noise amplifier of a microwave receiver. This paper presents design relations, or analytical methods, which permit approximate evaluation of most noises encountered. Noise sources discussed are those due to the antenna and transmission line components, the atmosphere, the warm earth, and space beyond the ionosphere. The discussion utilizes the concept of excess noise temperature currently popular in the low-noise receiver art. The conclusions reached are that: 1) excess noise due to absorbing media at uniform temperatures is easily evaluated using present information; 2) noise due to the nonhomogeneous atmosphere is beginning to get some attention and the need for more intensive work is indicated; 3) antenna noise leakage data are inadequate at present, but suitable measurements and computations will clearly be required in the near future; and 4) radio sky background temperatures are in the least satisfactory stage of all the pertinent factors at present, and absolute background measurements cannot be made before antenna sidelobe leakage is more carefully evaluated.

Comparison of Deviations from Square Law for RF Crystal Diodes and Barretters—G. U. Sorger and B. O. Weinschel (p. 103)

The properties of barretters and crystal diodes as square law video detectors are examined both theoretically and experimentally. The deviation from square law characteristic as a function of input and output levels is presented. Maximum RF levels and audio output levels at which the over-all deviation exceeds 0.1 db are given for the PRD 610A, PRD 631C, FXR Z220A barretters and for the crystal diode 1N32 at frequencies between 1 and 10 kmc. Minimum usable signals are also discussed, and the maximum range of accurate power ratio measurements is shown to be approximately 53 db for a barretter and 38 db for a video crystal. However, the crystal has the advantage in that the lower edge of its accurate range is 20 db below that of the barretter.

Correspondence (p. 112)
Contributors (p. 112)
Annual Index 1959 (follows p. 113)

Microwave Theory and Techniques

Vol. MTT-7, No. 4, October, 1959

Frontispiece (p. 400)
Guest Editorial (p. 401)

Mechanical Design and Manufacture of Microwave Structures—A. F. Harvey (p. 402)

The paper gives an account of the various aspects of the design and manufacture of microwave structures. The presentation of design information such as dimensions and tolerances is first discussed. Machining and other fabrication processes are then examined. Several methods of metal casting and associated techniques are described and the electrodeposition of waveguide components studied. Such final stages as inspection procedure, protective finishing and packaging are considered. The survey concludes with a bibliography.

The Dependence of Reflection on Incidence Angle—Raymond Redheffer (p. 423)

A lossy dielectric sheet has complex dielectric constant $\epsilon=\epsilon(x)$ and complex permeability $\mu=\mu(x)$, where x is the distance to one interface. This sheet is backed by a conducting surface and used as an absorber. If $|\epsilon(x)\mu(x)|\gg\epsilon_0\mu_0$, so that $(\epsilon/\epsilon_0)(\mu/\mu_0)-\sin\theta$ is nearly independent of the incidence angle θ, then the amplitude reflection $R(\theta)$ is wholly determined by $R(0)$. Typical results: When $R(\theta_0)=0$ at one polarization, then at $\theta=\theta_0$ the reflection for the other polarization corresponds to a voltage standing-wave ratio SWR$=\sec^2\theta_0$. At perpendicular polarization max $|R(\theta)|$ on (θ_1, θ_2) is least, for given $|R(0)|$, if $R(0)$ is real and positive; and then $R(\theta)=0$ at $\tan^2\theta/2=R(0)$. But for parallel polarization $R(0)$ must be real and negative to get optimum performance. When the absorber functions at both polarizations the best obtainable result is $|R(\theta)|=\tan^2\theta/2$, no matter what interval (θ_1, θ_2) is specified. The error in the approximation is investigated theoretically and experimentally. A complete set of graphs is included, suitable for design of those absorbers to which the theory applies. The analysis also yields an exact expression for the limiting behavior of the reflection at grazing incidence. This can be used in problems such as computation of the field due to a dipole over a plane earth. Finally, the theory of the Salisbury screen is re-examined as an aid in checking the other developments.

Analytical Asymmetry Parameters for Symmetrical Waveguide Junctions—M. Cohen and W. K. Kahn (p. 430)

This paper presents a systematic approach to the evaluation of (waveguide) junctions from the standpoint of their conformance to certain symmetries. Preferred sets of asymmetry parameters are found which are complete, minimal in number, which go to zero when the junction represented is symmetrical, and which may often be identified with a corresponding structural symmetry defect. The asymmetry parameters are first introduced for general linear junctions, but special attention is given to reciprocal and lossless junctions. The derivation of these preferred sets is based on the theory of group representations hitherto employed in the analysis of ideally symmetric junctions. One of the applications of these preferred parameters yields first-order relations among the defects of a nearly perfect hybrid-T junction which are believed to be new.

Orthogonality Relationships for Waveguides and Cavities with Inhomogeneous Anisotropic Media—Alfred T. Villeneuve (p. 441)

A modified reciprocity theorem forms the basis of development of orthogonality relationships for modes in waveguides and in cavities containing inhomogeneous, anisotropic media. In the lossless case certain of these may be interpreted in terms of power flow and energy storage. The special case of magnetized gyrotropic media is discussed for longitudinal and transverse magnetization.

Mismatch Errors in Cascade-Connected Variable Attenuators—G. E. Schafer and A. Y. Rumfelt (p. 447)

The treatment of mismatch errors is extended to cover variable attenuators cascade-connected in a system which is not free from reflections. The method of analysis is applicable to any number of cascaded attenuators, but only the analysis of two and three variable attenuators in cascade is presented. Graphs are given to aid in estimating the limits of mismatch error.

In an example, which is considered representative of rigid rectangular waveguide systems, the limits of error are: for two attenuators in cascade, 0.19 db in a 3-db measurement, and 0.17 db in a 40-db measurement; and for three attenuators is cascade, 0.25 db in a 40-db measurement and 0.23 db in a 75-db measurement.

A Nonreciprocal, TEM-Mode Structure for Wide-Band Gyrator and Isolator Applications—E. M. T. Jones, *et al.* (p. 453)

The theoretical and experimental operation of a novel form of TEM transmission-line network capable of operation over octave bandwidths is described. This network consists, basically, of a parallel arrangement of two conductors and a ferrite rod within a grounded outer shield. The conductors may be connected in a two-port configuration which provides, in the absence of the ferrite rod, complete isolation from zero frequency to the cut-off frequency of the first higher mode. With an unmagnetized ferrite rod properly inserted, the broad-band isolation is virtually unaffected. When the rod is magnetized by an axial magnetic field, coupling occurs between the two ports by a process analogous to Faraday rotation.

The device may be used as a broad-band gyrator, switch, or modulator, and with the addition of a resistance load, as an isolator. The bandwidth of these components is inherently limited only by the bandwidth capability of the ferrite material itself.

High-Power Microwave Rejection Filter Using Higher-Order Modes—Joseph H. Vogelman (p. 461)

In order to obtain filters capable of handling very high power, the use of radial lines and uniform line discontinuities was investigated. Forty-five-degree tapers and uniform lines were used to design a high-power microwave filter capable of handling 700 kw at 15 pounds pressure in a 0.900 by 0.400 ID waveguide. In addition to the filtering which results from the discontinuities in the TE_{10} mode in the waveguide, high insertion loss elements are effected when the enlarged uniform line section is larger than the TE_{10} mode waveguide wavelength and when the length of the enlarged section is approximately $(2n-1)\lambda_g/4$. Extremely large insertion losses are possible by the cascading of these elements. Tuning, in the standard-size waveguide, has no effect on the insertion loss of the higher-mode enlarged waveguide at its resonant frequency. Empirical design formulas are evolved and the design procedure for band-rejection filters is given, using these high insertion loss elements.

A Method for Accurate Design of a Broad-Band Multibranch Waveguide Coupler—K. G. Patterson (p. 466)

A new approach is made to the problem of tapering the branch impedances for broadband performance. A taper is proposed, which, for a 3-db branch coupler, is shown to give much better results in theory and practice than the currently used binomial taper.

Also, simple expressions are developed which enable the effects of waveguide junction discontinuities to be adequately corrected, thus allowing a greater accuracy in design to be achieved than was hitherto possible.

Correspondence (p. 473)

Contributors (p. 482)

Call for Papers for 1960 PGMTT Symposium (p. 485)

Space Electronics and Telemetry

Vol. SET-5, No. 4, December, 1959

A Rocket Manned for Lunar Exploration—M. W. Rosen and F. C. Schwenk (p. 155)

The exploration of the moon is within view today. If it may be assumed that Project Mercury in the U. S. A. and similar efforts by the U. S. S. R. will establish that man can exist for limited periods of time in space, then a trip to the moon requires mainly the design, construction and proving of a large rocket vehicle. In one concept of a manned lunar vehicle, the entire mission, the trip to the moon and the return, is staged on the earth's surface. A highly competitive technique is to stage the lunar mission by refueling in a low earth orbit. This would permit the use of a smaller launching vehicle but would require development of orbital rendezvous techniques.

This paper presents a parametric study of vehicle size for the direct-flight manned lunar mission. The main parameter is the take-off thrust which is influenced by many factors, principally the propellants in the several stages and the flight trajectory. A close choice exists in the second stage where conventional and high-energy propellants are compared. The size of the final stage and hence the entire vehicle is governed mainly by the method of approach to the earth's surface, whether the approach is made at elliptic, parabolic or hyperbolic velocities. The various design choices are applied to an illustrative vehicle configuration.

Contemporary Plasma Physics—Louis Gold (p. 162)

The manifold aspects of plasma physics are briefly described. The basic science and advanced technology embodied in this interdisciplinary field are delineated following an identification of what constitutes a plasma. With regard to the former, such highlights as the evolution of the method of adiabatic invariants to deal with highly nonlinear properties of plasmas are offered. Hypersonics, high impulse fuel systems, the Sherwood program, nuclear explosives, and microwave tubes represent key areas in modern technology demanding more basic knowledge of plasma interactions.

A New Approach to the Linear Design and Analysis of Phase-Locked Loops—Charles S. Weaver (p. 166)

Using the techniques and philosophy of control systems theory, the phase-locked loop is analyzed as a conventional feedback loop. The root-locus method yields graphs which specify how the transient response changes with signal strength. This method also reveals two thresholds which explain why a small change in signal strength or modulation may cause complete loss of detection. Charts show how the transients vary with various pole-zero patterns for both step and ramp inputs. The feedback equation shows why the phase-locked loop is an FM detector, and simplifies its design analysis to that of a simple audio network. The application of Wiener's criterion is simplified, and a new method of solution for the filter is presented which is applicable to almost any kind of signal. Because the phase-locked loop is nonlinear, there is no known solution for the filter except when the noise is white. The optimum transfer function may easily be reduced to the loop components. When used in an AM detector the phase-locked loop should be designed for minimum phase shift independent of the modulation.

Space-To-Ground Transmissions Beyond the Line-of-Sight Distance—Janis Galejs (p. 179)

Radio-wave transmission from above the maximum-intensity ionospheric layer to ground surface locations beyond the direct line-of-sight distance is examined in this paper. Transmission involving penetration of the F-layer, and subsequent ground-to-F-layer reflections, is found to be more reliable than transmission, depending upon ducting either along the F-layer or between the E- and F-layers.

At a frequency approximately three times the maximum plasma frequency (measured with respect to the transmitter location) transmission must take place in a direction along which the maximum plasma frequency increases. The transmission path is reciprocal. At a frequency approximately 20 per cent higher than the plasma frequency, transmission may take place along a constant or even slightly decreasing plasma frequency contour, but the transmission is severely attenuated.

The Application of Radio Interferometry to Extraterrestrial Metrology—Marcel J. E. Golay (p. 186)

Following an introductory discussion of the interferometric method, the essential building block of an interferometric system, the interferometric link, is discussed, especially with reference to the transmit-receive problem and to the noise problem in a frequency tracking circuit. One form of phase-locked loop is discussed in connection with the latter.

Several possible interferometric applications are listed and a table is presented in which an attempt has been made at estimating the essential parameters of each system.

Standards for Pulse Code Modulation (PCM) Telemetry (p. 194)

The Tracking of Pioneer IV: The Elements of a Deep Space Tracking System (Abstract)—H. L. Richter, Jr., and R. Stevens (p. 196)

An Interplanetary Communication System—G. E. Mueller and J. E. Taber (p. 196)

Exploring of space by means of space probes poses some challenging problems if all useful data acquired at the probe's location is to be made available on earth. There exists a monotonic relationship for every communication system between the received energy required per unit of received information. The quantity of received data can be increased by an increase in the received energy or more subtly by varying this montonic relationship through the choice of a more efficient communication system. Proper screening and processing of data before their transmission can increase the amount of useful information received at the expense of other data not so valuable and can ease ground data handling problems. A telemetry system, entitled "Telebit," which makes use of some of these principles, and is a forerunner to the application of others, is described.

Deltamodulation for Cheap and Simple Telemetering—F. K. Bowers (p. 205)

Deltamodulation is a simple binary pulse transmission method that can be readily adapted to transmit dc signal levels. It is particularly useful where only a few channels are to be sent, and where one per cent accuracy suffices. A signal-channel demonstration system has been built and tested. The high-speed limitation of such a system takes the form of a finite rate-of-rise, well suited to most telemetering. If, on the other hand, sudden large signal changes are expected, then the system may be modified accordingly. The modified system has the interesting property of giving accuracy varying exponentially with the pulse rate (as in PCM), but still without the necessity of framing the pulses.

Contributors (p. 209)

Annual Index 1959 (follows p 210)

Abstracts and References

Compiled by the Radio Research Organization of the Department of Scientific and Industrial Research, London, England, and Published by Arrangement with that Department and the *Electronic and Radio Engineer*, incorporating *Wireless Engineer*, London, England

NOTE: The Institute of Radio Engineers does not have available copies of the publications mentioned in these pages, nor does it have reprints of the articles abstracted. Correspondence regarding these articles and requests for their procurement should be addressed to the individual publications, not to the IRE.

The Index to the Abstracts and References published in the PROC. IRE from February, 1957 through January, 1958 is published by the PROC. IRE, May, 1958, Part II. It is also published by *Electronic and Radio Engineer*, incorporating *Wireless Engineer*, and included in the March, 1957 issue of that journal. Included with the Index is a selected list of journals scanned for abstracting with publishers' addresses.

The number in heavy type at the upper left of each Abstract is its Universal Decimal Classification number. The number in heavy type at the top right is the serial number of the abstract. D.C. numbers marked with a dagger (†) must be regarded as provisional.

U.D.C. NUMBERS

Certain changes and extensions in U.D.C. numbers, as published in PE Notes up to and including PE 666, will be introduced in this and subsequent issues. The main changes are:

Artificial satellites:	551.507.362.2	(PE 657)
Semiconductor devices:	621.382	(PE 666)
Velocity-control tubes, klystrons, etc.:	621.385.6	(PE 634)
Quality of received signal, propagation conditions, etc.:	621.391.8	(PE 651)
Color television:	621.397.132	(PE 650)

The "Extensions and Corrections to the U.D.C.," Ser. 3, No. 6, August, 1959, contains details of PE Notes 598–658. This and other U.D.C. publications, including individual PE Notes, are obtainable from The International Federation for Documentation, Willem Witsenplein 6, The Hague, Netherlands, or from The British Standards Institution, 2 Park Street, London, W.1., England.

ACOUSTICS AND AUDIO FREQUENCIES

534.22-8-14 **1**
Speed of Sound in Distilled Water as a Function of Temperature and Pressure—W. D. Wilson. (*J. Acoust. Soc. Amer.*, vol. 31, pp. 1067–1072; August, 1959.) Detailed report of measurements made using an ultrasonic pulse technique.

534.286-8 **2**
Ultrasonic Interferometry and the Determination of the Absorption Coefficient of Liquids—R. Cerf. (*Compt. Rend. Acad. Sci., Paris*, vol. 248, pp. 3536–3538, June 22, 1959.) A simple method of measurement is described, based on the theory of the Pierce interferometor and assuming that the reciprocal of the equivalent-circuit resistance is a linear function of the total damping of resonator, liquid and reflector.

534.75 **3**
Additivity of Different Types of Masking—R. C. Bilger, (*J. Acoust. Soc. Amer.*, vol. 31, pp. 1107–1109; August, 1959.) At moderately high levels the combination of critical-band masking with either remote masking or the masking of frequencies above the band resulted in a 6-db increase in masking. This supports the hypothesis that the summation takes place within the ear or in the nervous system.

534.75 **4**
Residual Masking at Low Frequencies—C. M. Harris. (*J. Acoust. Soc. Amer.*, vol. 31, pp. 1110–1115; August, 1959.) The temporary shift in the threshold of hearing following the cessation of a masking source is termed "residual" masking; its variation with frequency and with the level of a white-noise masking source is investigated.

534.75 **5**
Masking Patterns of Tones—R. H. Ehmer. (*J. Acoust. Soc. Amer.*, vol. 31, pp. 1115–1120; August, 1959.) Monaural masking patterns for pure tones from 250 c/s to 8 kc are discussed with reference to the auditory masking mechanism.

534.75 **6**
Identification of Elementary Auditory Displays and the Method of Recognition Memory—I. Pollack. (*J. Acoust. Soc. Amer.*, vol. 31, pp. 1126–1128; August, 1959.)

534.75 **7**
Relation between Loudness and Duration of Tonal Pulses: Part 1—Response of Normal Ears to Pure Tones Longer than Click-Pitch Threshold—F. Miskolczy-Fodor. (*J. Acoust. Soc. Amer.*, vol. 31, pp. 1128–1134; August, 1959.)

534.84 **8**
On the New Reverberation Chamber with Nonparallel Walls (Studies on the Measurement of Absorption Coefficient by the Reverberation-Chamber Method: Part 2)—K. Sato and M. Koyasu. (*J. Phys. Soc. Japan*, vol. 14, pp. 670–677; May, 1959.) Details of construction and performance are given. The chamber has a volume of 513 meter³ and a reverberation time of 22 s at 500 c/s. Part 1: 3916 of 1959.

621.395.623.52 **9**
Method of Improving Acoustic Transmission in Folded Horns—R. W. Carlisle. (*J. Acoust. Soc. Amer.*, vol. 31, pp. 1135–1137; August, 1959.) The development of a conoidal insert for the bend of a folded horn is described.

681.84.087.7 **10**
The Transmission of Stereophonic Sound Field Distribution over a Single Channel using Pilot Frequencies below Threshold Level—F. Enkel. (*Elektron. Rundschau*, vol. 12, pp. 347–349; October, 1958.) A compatible l.f. system of stereophonic transmission is outlined. Amplitude-modulated and suitably phased pilot signals derived from the envelope of the output waveforms of two spaced microphones followed by a delay system are transmitted at a level close to the noise level, as part of the AF modulation. A method of obtaining compatible stereophonic magnetic-tape recordings in this way is proposed, and the use of additional pilot signals to give greater detail of the spatial sound distribution is suggested.

ANTENNAS AND TRANSMISSION LINES

621.315.212:[621.395.4+621.397.13 **11**
Multichannel Systems along Coaxial Cables—J. Bauer. (*Tech. Mitt. PTT*, vol. 36, pp. 423–435; November 1, 1958. In German and French.) Expanded version of 2958 of 1958.

621.372 **12**
Relations between the Variations of Amplitude and Phase in the Propagation of Vibratory Phenomena—J. C. Simon and G. Broussaud. (*Compt. rend. Acad. Sci., Paris*, vol. 248, pp. 3693–3695; June 29, 1959.) A three-branch junction, formed by two extremities of the same feeder and a third branch capable of absorbing a certain quantity of energy, is considered; a matrix analysis leads to a general statement of phase relations involved in energy transfer.

621.372.2:621.315.212 **13**
Propagation of an Electromagnetic Impulse in a Medium in which the Dielectric Loss Angle is almost Independent of Frequency—M. Cotte. (*Compt. Rend. Acad. Sci., Paris*, vol. 248, pp. 3142–3144; June 1, 1959.) An analytical treatment gives results which are applicable to the propagation of the principal wave in a coaxial cable.

621.372.22 **14**
The Transient Response of Tapered Transmission Lines—F. J. Young, E. R. Schatz and J. B. Woodford. (*Commun. and Electronics*, no. 43, pp. 223–228; July, 1959.) Determination of the transient response of the tapered line as a function of its terminations and nominal characteristic impedance. See also 15 below.

621.372.22:621.372.51 **15**
The Optimum Transmission-Line Pulse Transformer—F. J. Young, E. R. Schatz and

J. B. Woodford. (*Commun. and Electronics*, no. 43, pp. 220–223; July, 1959.) A theory based on transient response is developed for determining the optimum taper of a transmission line.

621.372.8 16

Synthesis of a Bent Waveguide with Continuous Variation of Curvature—M. G. Andreasen. (*Arch. elekt. Übertragung*, vol. 12, pp. 463–471; October, 1958.) The optimum bending curve is derived for a specified limit of energy conversion to any given undesirable mode. The excitation of higher modes is less in a waveguide with variable curvature than in one with constant curvature (see 3929 of 1959).

621.372.8 17

Reflection of a Pyramidally Tapered Rectangular Waveguide—K. Matsumaru. (IRE Trans. on Microwave Theory and Techniques, vol. MTT-7, pp. 192–196; April, 1959. Abstract, Proc. IRE, vol. 47, p. 1285; July, 1959.)

621.372.8:537.226 18

The Efficiency of Excitation of a Surface Wave on a Dielectric Cylinder—J. W Duncan. (IRE Trans. on Microwave Theory and Techniques, vol. MTT-7, pp. 257–268; April, 1959. Abstract, Proc. IRE, vol. 47, p. 1286; July, 1959.)

621.372.8:621.372.2 19

A Guide to the Practical Application of Tchebycheff Functions to the Design of Microwave Components—R. Levy. (*Proc. IEE*, Pt. C, vol. 106, pp. 193–199; September, 1959.) Practical formulas giving the broadest possible bandwidth in a given physical length are derived for stepped transformers, stepped twists and multielement directional couplers. Microwave band-pass filters with Tchebycheff equal-ripple characteristics are also described.

621.372.8:621.39 20

Waveguide as a Long-Distance Communication Medium—A. E. Karbowiak. (*Electronic Eng.*, vol. 31, pp. 520–525; September, 1959.) A discussion giving comparison of plain metallic waveguides with dielectric-coated ring and helix types.

621.372.823 21

Measurement of Attenuation in Ring Waveguides—Yu. N. Kazantsev and V. V. Meriakri. (*Radiotekh. Elektron.*, vol. 4, pp. 131–133; January, 1959.) A brief description of the apparatus for measurements on ring waveguides which consist of several equal metal rings on a common axis and separated by thin slots. This type of structure gives only small additional losses in the H_{01} wave when compared with a normal circular waveguide of the same diameter. It can be used for waveguide bends and also as a wave filter. Values of attenuation for the H_{01} wave with different ring parameters are tabulated.

621.372.823:621.372.832.43 22

Directional Couplers for Generating H_{01} Waves in Circular Waveguide—A. Jaumann. (*Arch. elekt. Übertragung*, vol. 12, pp. 440–446; October, 1958.) The mode selectivity of a long-slot directional coupler is calculated in terms of slot length and waveguide radius. Measurements on a 35-kmc/s directional coupler give results in agreement with calculations of TE_{01}-mode purity obtainable.

621.372.824 23

On the Problem of the Dispersion Properties of a Coaxial Waveguide both Conductors of which are Loaded with Disks—N. M. Chirkin. (*Radiotekh. Elektron.*, vol. 4, pp. 126–127; January, 1959.) The waveguides investigated have a zero dispersion over a wide band of frequencies, which decreases with increasing retardation.

621.372.831 24

Concerning the Junction of Two Different Plane Waveguides—N. P. Mar'in. (*Radiotekh. Elektron.*, vol. 4, pp. 3–11; January, 1959.) The incidence of an electromagnetic wave at a junction of two plane waveguides which have their walls directed along different coordinate systems is considered. The solution is given of an infinite system of equations in which the unknown quantities are the amplitudes of the forward and reflected waves.

621.372.831.25:621.372.852.22 25

Characteristics of a Ferrite-Loaded Rectangular Waveguide Twist—A. E. Barrington. (IRE Trans. on Microwave Theory and Techniques, vol. MTT-7, pp. 299–300; April, 1959.) Brief report of experiments with a tapered cylindrical Ni-Co ferrite mounted centrally midway between the flanges of a 90° waveguide twist. In the region of 8900 mc a reversal of the magnetic field caused a reduction of 10 db in the transmitted power.

621.372.832.8 26

The Synthesis of Symmetrical Waveguide Circulators—B. A. Auld. (IRE Trans. on Microwave Theory and Techniques, vol. MTT-7, pp. 238–246; April, 1959. Abstract, Proc. IRE, vol. 47, p. 1286; July, 1959.)

621.372.85+621.372.413 27

Perturbation of Waveguides and Cavities by Spheres and Cylinders—W. Hauser and L. Brown. (*J. Appl. Phys.*, vol. 30, pp. 1460–1461; September, 1959.) A brief account of a theoretical investigation of the effect of a plane wall on the fields in a nearby cylinder or sphere.

621.372.85 28

On Network Representations of Certain Obstacles in Waveguide Regions—H. M. Altschuler and L. O. Goldstone. (IRE Trans. on Microwave Theory and Techniques, vol. MTT-7, pp. 213–221; April, 1959. Abstract, Proc. IRE, vol. 47, p. 1286; July, 1959.)

621.372.85:537.226 29

Propagation in a Dielectric-Loaded Parallel Plane Waveguide—M. Cohn. (IRE Trans. on Microwave Theory and Techniques, vol. MTT-7, pp. 202–208; April, 1959. Abstract, Proc. IRE, vol. 47, p. 1286; July, 1959.)

621.372.852.1 30

Absorptive Filters for Microwave Harmonic Power—V. Met. (Proc. IRE, vol. 47, pp. 1762–1769; October, 1959.) The cutoff properties of certain lossy periodic waveguide structures are utilized to obtain insertion loss up to 50 db for second-harmonic power and less than 0.1 db for the fundamental at S-band frequencies.

621.372.852.22 31

Precise Control of Ferrite Phase Shifters—D. D. King, C. M. Barrack and C. M. Johnson. (IRE Trans. on Microwave Theory and Techniques, vol. MTT-7, pp. 229–233; April, 1959. Abstract, Proc. IRE, vol. 47, p. 1286; July, 1959.)

621.372.852.223 32

A Resonance Isolator for Use at 4000 Mc/s—A. D. Cartwright and C. F. Davidson. (*P.O. Elec. Engrg. J.*, vol. 52, Pt. 1, pp. 69–73; April, 1959.) A description of the use of ferrite material to provide nonreciprocal attenuation in a waveguide.

621.372.852.223:538.221:621.318.134 33

The Behaviour of Ni-Zn and Mg-Mn Ferrites in Ferromagnetic-Resonance Nonreciprocal Attenuators in the 9000-Mc/s Range—U. Milano. (*Note Recensioni Notiz.*, vol. 7, pp. 611–633; November/December, 1958; and vol. 8, pp. 3–20; January/February, 1959.) Tests were made on specimens of commercial-type material in isolators in the form of a slab placed lengthwise in rectangular waveguide and supported by polystyrene or immersed in styrofoam.

621.396.67.006.2 34

The Aerial Testing Station at Brück—E. Missler. (*Tech. Mitt. BRF, Berlin*, vol. 2, pp. 79–82; September, 1958.) A description of a testing site near Berlin with details of existing and planned metal-free masts for measurements on antennas of any type and size. The proposed expansion of facilities including the use of helicopters is outlined.

621.396.67.029.62 35

A Common Aerial System for Simultaneous Transmission and Reception of VHF Signals—J. K. Grierson. (*Electronic Engng.*, vol. 31, pp. 546–549; September, 1959.) "A common antenna system that consists of five sections is described. The sections are a transmitter, a transmission coupling network, a receiver, a reception coupling network and an antenna. The transmission and reception coupling networks enable a single antenna to be used for transmission and reception of frequency-spaced signals without the necessity of time sharing. The coupling networks are considered in detail and practical values of components are assigned."

621.396.677.029.6:621.391.822 36

Effective Antenna Temperatures due to Oxygen and Water Vapour in the Atmosphere—D. C. Hogg. (*J. Appl. Phys.*, vol. 30, pp. 1417–1419; September, 1959.) "Calculations of the effective noise temperature at the terminals of a high-gain antenna due to oxygen and water vapor in the atmosphere are given for the frequency range 0.5 to 40 kmc/s. In the 1 to 10 kmc/s band, the effective temperature increases from about 3° to 100°K as the zenith angle is increased from 0° to 90°. Calculated values of the total attenuation through the atmosphere are given."

621.396.677.8 37

Electromagnetic Prisms in Microwave Links—C. Rudilosso. (*Note Recensioni Notiz.*, vol. 7, pp. 634–645; November/December, 1958.) The insertion loss of a pair of reflectors which are arranged so as to replace a single reflector is calculated. An expression for the gain of such a "prism," relative to a single reflector, is derived by analogy with geometrical optics.

621.396.677.83 38

An Unusual Application of an Aerial Reflector—R. Possenti. (*Note Recensioni Notiz.*, vol. 7, pp. 736–741; November/December, 1958.) A note on the solution of difficulties due to load limits of an existing radio-link antenna mast in Milan. Radiation at a height of at least 20 meters was required in three different directions and a single plane reflector was mounted on the mast and illuminated from below by three paraboloidal radiators oriented to give the correct reflected-beam direction while allowing for certain site restrictions.

621.396.677.832 39

The Design of the Corner-Reflector Antenna—H. P. Neff and J. D. Tillman. (*Commun. and Electronics*, no. 43, pp. 293–295; July, 1959.) Simplified design procedures are described.

621.396.677.833.029.65:535.854 40

Reflectors for a Microwave Fabry-Perot

Interferometer—W. Culshaw. (IRE TRANS. ON MICROWAVE THEORY AND TECHNIQUES, vol. MTT-7, pp. 221–228; April, 1959. Abstract, PROC. IRE, vol. 47, p. 1286; July, 1959.)

621.396.679 41
Fields in Electrically Short Ground Systems: An Experimental Study—A. N. Smith and T. E. Devaney. (*J. Res. Nat. Bur. Stand.*, vol. 63D, pp. 175–180; September/October, 1959.) Measurements of magnetic field distribution are described for a simplified radial ground system on poorly conducting soil under an electrically short, top-loaded monopole.

AUTOMATIC COMPUTERS

681.142 42
Pattern Detection and Recognition—S. H. Unger. (PROC. IRE, vol. 47, pp. 1737–1752; October, 1959.) Both processes have been carried out on an IBM 704 computer which was programed to simulate a spatial computer. The programs tested included the recognition process for reading hand-lettered sans-serif alphanumeric characters.

681.142 43
Compact Memories have Flexible Capacities—D. Haagens. (*Electronics*, vol. 32, pp. 50–53; October 2, 1959.) A digital data storage system with capacity up to 8192 bits, and random and/or sequential access is described.

681.142 44
An Electronic Analogue Computer for Solving Systems of Linear Equations—E. Hempel. (*NachrTech.*, vol. 8, pp. 453–455; October, 1958.) Mathematical derivation of the operating principle and stability conditions for a computer consisting of amplifiers.

681.142 45
Electronic Coordinate Transformer—J. Gónzález-Ibeas and V. Aleixandre. (*Electronic Radio Eng.*, vol. 36, pp. 360–365; October, 1959.) Circuit details are given for the construction of an electronic calculating unit which enables the polar coordinates of a vector (modulus and cosine or sine of the argument) to be derived from those of a rectangular system of axes.

681.142:061.3 46
The British Computer Society—A. S. Douglas. (*Nature*, vol. 184, pp. 945–946; September 26, 1959.) Report of a conference held in Cambridge, June 22nd–25th, 1959.

681.142:621.374.3 47
Millimicrosecond Digital Computer Logic—N. F. Moody and R. G. Harrison. (*Electronic Engng.*, vol. 31, pp. 526–529; September, 1959.) "A system of fast pulse logic is described which combines the efficiency of transformer coupled stages with digit delay tolerances approaching that of dc coupled systems. Logical circuits for OR, AND, INVERTOR and RECLOCK are shown, together with a driver which permits a 'fan out' factor of 5. Transistor circuits are used throughout."

681.142:621.374.3 48
Binary Circuits Count Backwards or Forwards—H. J. Weber. (*Electronics*, vol. 32, pp. 82–83; September 25, 1959.) A transistorized module is described that can be used to build logical circuits. A complete reversible counter measures 3.25×3.8×0.75 inches.

CIRCUITS AND CIRCUIT ELEMENTS

621.3.049.7 49
3-D Packaging Reduces Size of Electronic Units—E. C. Hall and R. M. Janssen. (*Electronics*, vol. 32, pp. 62–65; October 9, 1959.) Greater component densities are obtainable using a module technique in which miniature circuit elements are placed side by side, with electrical connection made on a three-dimensional basis by a spot-welding process.

621.318.57:621.318.134 50
The Square-Loop Ferrite Core as a Circuit Element—C. H. Lindsey. (*Proc. IEE*, Pt. C, vol. 106, pp. 117–124; September, 1959.) The shape of the output waveforms when the cores are switched is explained by a quantitative theory which takes into account the residual loss. Reasonable agreement with experimental evidence is shown.

621.318.57:621.372.44:681.142 51
Switching Circuits using Bidirectional Nonlinear Impedances—T. B. Tomlinson. (*J. Brit. IRE*, vol. 19, pp. 571–591; September, 1959.) A general review of circuit logic is developed for a bidirectional nonlinear switching element. The design of *p-n-p* transistor driver stages is considered. A binary octal decoder circuit and a simple binary full-adder circuit are discussed as examples.

621.318.57:621.382.2 52
High-Speed Microwave Switching of Semiconductors: Part 2—R. V. Garver. (IRE TRANS. ON MICROWAVE THEORY AND TECHNIQUES, vol. MTT-7, pp. 272–276; April, 1959. Abstract, PROC. IRE, vol. 47, p. 1286; July, 1959.) Part 1: 1054 of 1958 (Garver *et al.*).

621.318.57:621.382.3 53
Design of Bistable Switching Circuits using Junction Transistors—C. Mira. (*Compt. rend. Acad. Sci., Paris*, vol. 248, pp. 3284–3286; June 8, 1959.) The relations between the different parameters which affect the switching circuit may be obtained by plotting on the same diagram a load line and the theoretical curve of the static characteristic of the circuit.

621.372.413+621.372.85 54
Perturbation of Waveguides and Cavities by Spheres and Cylinders—Hauser and Brown. (See 27).

621.372.413 55
On the Theory of the Cavity Resonator comprising Two Confocal Paraboloids of Revolution—H. Baumgärtel. (*Tech. Mitt. BRF, Berlin*, vol. 2, pp. 67–72; September, 1958.) A solution is found for a system of equations given by Buchholz (2159 of 1952).

621.372.413:537.533.8 56
The Excitation of Cavity Resonators by Secondary-Electron Resonance Multiplications—K. Krebs and H. V. Villiez. (*Z. Phys.*, vol. 154, pp. 27–33; January 19, 1959.) Experimental investigation of the suitability for frequency multiplication of the process analyzed in 101 below.

621.372.5 57
Some Generalizations of Duhamel's Integral for Linear Quadripoles—G. Wunsch. (*NachrTech.*, vol. 8, pp. 470–472; October, 1958.)

621.372.5 58
The Stable and Unstable Image Parameters in Quadripole Theory—G. Ulrich. (*NachrTech.*, vol. 8, pp. 521–525; November, 1958.) The definition of stable and unstable image impedances by Feldtkeller is extended to related parameters, and their position in the complex plane is determined.

621.372.51 59
Matching Quadripoles—U. Kirschner. (*Elektron. Rundschau*, vol. 12, pp. 338–341; October, 1958.) Design formulas are derived for π and T-sections and groups of curves are given from which practical design parameters can be obtained.

621.372.54 60
Optimum Tchebycheff Third-Order Filters—H. S. Heaps and L. J. Mason. (*Electronic Radio Eng.*, vol. 36, pp. 388–391; October, 1959.) A theoretical analysis is given of a design for the detection of rectangular pulsed signals on a background of white noise, and it is shown that resulting signal/noise ratios are smaller than those obtained by the use of optimum Butterworth filters.

621.372.54:621.372.2 61
Cascade Directional Filter—O. Wing. (IRE TRANS. ON MICROWAVE THEORY AND TECHNIQUES, vol. MTT-7, pp. 197–201; April 1959. Abstract, PROC. IRE, vol. 47, pp. 1285–1286; July, 1959.)

621.372.543.2:621.376 62
Transient Response of Band-Pass Filters to Modulated Signals—D. Q. Mayne. (*Proc. IEE*, Pt. C, vol. 106, pp. 144–152; September, 1959.) Laurent's low-pass band-pass transformation is used with suitable approximations to obtain the response to a suddenly applied carrier. The *m*-derived filter is analyzed.

621.372.6 63
The Order of Complexity of Electrical Networks—P. R. Bryant. (*Proc. IEE*, Pt. C, vol. 106, pp. 174–188; September, 1959.) An expression for the order (*i.e.*, the number of natural frequencies) is derived for a RLC network. Complete sets of dynamically independent network variables are obtained from the network equations.

621.372.6:621–52 64
The Stability Criteria for Linear Systems—O. P. D. Cutteridge. (*Proc. IEE*, Pt. C, vol. 106, pp. 125–132; September, 1959.) The various criteria can be obtained and interrelated by means of continued fractions. The Hurwitz determinants are condensed to about half their original order.

621.372.622:538.221:621.318.134 65
The Efficiency of a Ferrite as a Microwave Mixer—L. Lewin. (*Proc. IEE*, Pt. C, vol. 106, pp. 153–157; September, 1959.) It is shown theoretically that a polycrystalline ferrite should behave like a single-crystal sample. Magnetization measurements taken previously are explained by assuming a basic permeability line width of a few gauss and a spread in resonant fields from point to point. The efficiency appears to be 14 db lower than for a conventional crystal mixer.

621.373 66
Selective Properties of an Oscillator System Synchronized by a Harmonic Signal—Yu. I. Samoĭlenko. (*Radiotekh. Elektron.*, vol. 4, pp. 39–42; January, 1959.) A theoretical investigation of the dependence of the amplitude and phase oscillations of an oscillator on the interference of a quasi-harmonic EMF. The effect on the system of harmonic and fluctuation noise is briefly examined.

621.373.4:621.391.822 67
On the Amplitude Fluctuation of Oscillations of a Self-Excited Valve Oscillator—L. I. Gudzenko. (*Radiotekh. Elektron.*, vol. 4, pp. 97–108; January, 1959.) Mathematical analysis of the amplitude fluctuations of an oscillator due to thermal noise and shot effect for the case of weak and strong modes of excitation.

621.373.421.13 68
Short-Time Stability of a Quartz-Crystal Oscillator as Measured with an Ammonia Maser—A. H. Morgan and J. A. Barnes.

(PROC. IRE, vol. 47, p. 1782; October, 1959.) Appreciable improvement in the short-time stability is achieved by immersing the crystal in liquid helium. Control of the pressure of the gas above the liquid improves the long-time stability through adversely affecting the short-time stability.

621.373.421.14 69

The Reactance Characteristics of Concentric-Line Circuits with Interrupted Inner Conductor—C. Boden. (*Elektron. Rundschau*, vol. 12, pp. 335–338; October, 1958.) Oscillator circuits in which the inner conductor is interrupted, *e.g.*, those comprising disk-seal tubes, are investigated to determine the reactance as a function of gap and line section lengths. Normally the higher resonant frequencies of the circuit are not harmonics of the fundamental frequency.

621.373.43:621.374.5 70

Application of Delayed Feedback in Electronic Circuits—Z. Náray. (*Brit. J. Appl. Phys.*, vol. 10, pp. 400–403; September, 1959.) A short general theory is given of a method of generating periodic signals of controlled shape. Two simple applications of a delay line as a feedback loop are given. The signal frequency depends on the delay time and under certain conditions on the triggering frequency, and this provides a method of measuring the delay time of an element in the feedback loop.

621.373.431:621.376.32 71

Use of Relaxation Oscillators in the Generation of Frequency-Modulated Oscillations—A. A. Vasilev. (*Dokl. Akad. Nauk SSSR*, vol. 129, pp. 85–87; November 1, 1959.) An analysis of the operation of a relaxation oscillator as a frequency modulator, with a series of diode circuits for transformation of the triangular waveform into sinusoidal form.

621.373.44 72

Millimicrosecond Pulse Generator Capable of 10 Million Pulses per Second—M. Nakamura. (*Rev. Sci. Instr.*, vol. 30, pp. 778–782; September, 1959.) The generator has a repetition rate of up to 10^7/second, pulse rise time less than 2.5 mμsec and pulse widths from 2.5 to 25 mμsec. The negative output pulse is adjustable over a range of 0 to 12 volts into a 125 Ω load. There are facilities for gating, single pulses, and triggering from an outside source.

621.373.44:519.2 73

Electronic Probability Generator—G. M. White. (*Rev. Sci. Instr.*, vol. 30, pp. 825–829; September, 1959.) Description of a random-pulse generator simulating the tossing of a coin 500 times per second. The probability of a particular side of the "coin" can be varied from 0 to 1.

621.373.52 74

On the Problem of Starting Conditions of the Avalanche Process in Relaxation Oscillators on Point-Contact Triodes—V. N. Yakovlev. (*Radiotekh. Elektron.*, vol. 4, pp. 70–74; January, 1959.) It is shown that the oscillators can be considered as nonlinear voltage or current amplifiers. Conditions governing the formation of the avalanche process are given and formulas are derived for coefficients of voltage and current amplification. Circuits are shown.

621.374.4 75

Frequency Divider with Direct Lock-In—T. S. Fedosova and K. A. Samoilo. (*Radiotekh. Elektron.*, vol. 4, pp. 43–53; January, 1959.) Investigation is carried out by the phase-pulse method. The effect of phase shift in the feedback circuit and of anode reaction on the divider regime is considered. The effect of the shape of the synchronized and pedestal pulses on the divider is also examined. Theoretical data are verified by experimental results.

621.374.4:621.372.44:621.382.2 76

Generation of Harmonics and Subharmonics at Microwave Frequencies with *P-N* Junction Diodes—D. Leenov and A. Uhlir, Jr. (PROC. IRE, vol. 47, pp. 1724–1729; October, 1959.) The performances of a nonlinear resistance and a nonlinear capacitance in a wide-band harmonic generator circuit are analyzed. The nonlinear capacitance is shown to have a considerably higher efficiency. Results of experiments with a graded-junction Si nonlinear-capacitance diode are given.

621.374.4:621.373.3.029.64 77

A New Microwave Harmonic Generator—K. D. Froome. (*Nature*, vol. 184, Suppl. no. 11, p. 808; September 12, 1959.) Microwave power is used to maintain a very short mercury arc between a "pool" cathode and a tungsten wire "anode" (see 1722 of 1957). With an estimated input power of a few watts at 2.5 kmc/s, an output in excess of 1 mw was obtained at 10 kmc/s; a strong signal at 30 kmc/s was detected by a spectrum analyzer placed close to the arc tube.

621.374.4.029.65:621.382.2 78

Improved Diode for the Harmonic Generation of Millimetre and Submillimetre Waves—Ohl, Budenstein and Burrus. (See 344.)

621.375.4 79

The Stability Factor and Static Gain of Transistor Amplifiers—G. Giralt. (*Compt. rend. Acad. Sci., Paris*, vol. 248, pp. 3415–3417; June 15, 1959.) A general method relating the stability factor of disturbances of thermal origin to static gain is described.

621.375.4.078:621.316.86 80

Use of the Silicon Resistor in the dc Stabilization of Transistor Circuits—J. T. Zakrzewski and D. H. Mehrtens. (*Nature*, vol. 184, Suppl. no. 11, pp. 811–812; September 12, 1959.) Stabilization of grounded-emitter small-signal stages over a wide range of temperatures is achieved with a Si resistor of high positive temperature coefficient in the emitter circuit.

621.375.432 81

Local Feedback in Transistor Amplifiers—H. Pfyffer. (*Electronic Engng.*, vol. 31, pp. 550–555; September, 1959.) The effects of negative feedback on common-emitter amplifiers are calculated and compared with the measured results.

621.375.9:538.569.4 82

Proposal for a Tunable Millimetre-Wave Molecular Oscillator and Amplifier—J. R. Singer. (IRE TRANS. ON MICROWAVE THEORY AND TECHNIQUES, vol. MTT-7, pp. 268–272; April, 1959. Abstract, PROC. IRE, vol. 47, p. 1286; July, 1959.)

621.375.9:538.569.4 83

The Molecular Amplifier—H. C. Wolf. (*Z. angew. Phys.*, vol. 10, pp. 480–488; October, 1958.) The principles of molecular amplification and the main characteristics of the various types of maser are reviewed. 39 references.

621.375.9:538.569.4 84

Theory of Maser Oscillation—J. C. Kemp. (*J. Appl. Phys.*, vol. 30, pp. 1451–1452; September, 1959.) The experimentally observed amplitude-modulated nature of the signal from an inverted spin system undergoing maser oscillation or coherent spontaneous emission is explained.

621.375.9:538.569.4 85

Silvered Ruby Maser Cavity—L. G. Cross. (*J. Appl. Phys.*, vol. 30, p. 1459; September, 1959.) Preparation and properties are described.

621.375.9:621.372.44 86

Noise Figure of Reactance Converters and Parametric Amplifiers—A. van der Ziel. (*J. Appl. Phys.*, vol. 30, p. 1449; September, 1959.) A simple derivation of noise figure correcting a formula of Heffner and Wade (77 of 1959).

621.375.9:621.372.44 87

Phase Considerations in Degenerate Parametric Amplifier Circuits—G. A. Klotzbaugh. (PROC. IRE, vol. 47, pp. 1782–1783; October, 1959.) A theoretical examination of the negative resistance in the signalling circuit as a function of the phase angle between the pump and signal voltages. See also 1690 of 1958 (Bloom and Chang).

621.375.9:621.372.44 88

Self-Quenching in Superregenerative Parametric Amplifiers—I. Hefni. (*Electronic Engng.*, vol. 31, p. 559; September, 1959.) A qualitative reasoning of the behavior of cavity-type parametric amplifiers in the UHF range using Ge diodes is given for the condition of self-bias, or external bias with high internal resistance, applied to the diode. Increase in pump power makes frequency response multipeaked as with regenerative tube amplifiers in the coherent state.

621.375.9:621.372.44:621.385.6 89

Use of the Principles of Conservation of Energy and Momentum in Connection with the Operation of Wave-Type Parametric Amplifiers—J. R. Pierce. (*J. Appl. Phys.*, vol. 30, pp. 1341–1346; September, 1959.) Some limitations on operation are explained in simple terms and certain general relations governing behavior, including the Manley-Rowe relation (2988 of 1956) are derived.

621.375.9:621.372.44:621.385.6 90

The Quadrupole Amplifier, a Low-Noise Parametric Device—Adler, Hrbek and Wade. (See 361.)

621.375.9:621.372.832.8 91

Analysis of a Negative-Conductance Amplifier Operated with a Non-ideal Circulator—E. W. Sard. (IRE TRANS. ON MICROWAVE THEORY AND TECHNIQUES, vol. MTT-7, pp. 288–293; April, 1959. Abstract, PROC. IRE, vol. 47, p. 1287; July, 1959.)

621.375.9:621.372.85:621.318.134 92

The Gain of Travelling-Wave Ferromagnetic Amplifiers—P. J. B. Clarricoats. (*Proc. IEE* (*London*), Pt. C, vol. 106, pp. 165–173; September, 1959.) The gain of an amplifier using a circular waveguide and axial ferrite rod of small cross section is determined by a general perturbation method. Methods for overcoming the low efficiency are discussed and other possible waveguide configurations and practical aspects of construction are described.

GENERAL PHYSICS

530.12:538.569.4:621.375.9 93

Two Maser Experiments to Test General Relativity—H. Yilmaz. (*Phys. Rev. Lett.*, vol. 3, pp. 320–321; October 1, 1959.) A comparison of the velocities of light in two directions can be made to an accuracy within 1 in 10^{12} using maser techniques. The two experiments involve such comparisons to test the principle of equivalence and the local isotropy of the space-time continuum, respectively.

535.37 94

A Model of Phosphors on the Basis of Quantum Mechanics: Part 3—Transition Probabilities with Constant Defects and a Dis-

crete Spectrum—H. Stumpf. (*Z. Naturforsch.*, vol. 13a, pp. 171–183; March, 1958.)

Part 1: 2691 of 1958.

Part 2: *ibid.*, vol. 12a, pp. 465–478; June, 1956.

537.226 95

The Quantum Mechanical Theory of the Dielectric Orientation Polarization of Gases: Part 2—The Orientation Polarization of a Dipolar Gas consisting of Symmetric Spin Molecules in an Attenuating Electric Field—W. Maier and H. K. Wimmel. (*Z. Phys.*, vol. 154, pp. 133–149; February 6, 1959.)

Part 1: 2901 of 1959.

537.322.2 96

Influence of the Thomson Effect on the θ-ϕ Relationship for a Constrictive Resistance in Thermal Equilibrium—W. Davies. (*Nature*, vol. 184, suppl. no. 13, p. 975; September 26, 1959.)

537.52 97

Investigation of a High-Frequency Resonant Discharge—A. A. Glazov and D. L. Novikov. (*Zh. Tekh. Fiz.*, vol. 28, pp. 2295–2301; October, 1958.) An experimental study of a discharge in a magnetic field in the frequency range 50–100 mc. A theoretical and experimental analysis is made of the breakdown conditions and characteristics and the properties of the plasma in the discharge.

537.523 98

The Application of Schottky's Diffusion Theory to Discharges with several Types of Ions and Excited Neutral Particles—J. Wilhelm. (*Z. Phys.*, vol. 154, pp. 361–375; March 4, 1959.)

537.525 99

The Low-Pressure Plane Symmetric Discharge—E. R. Harrison and W. B. Thompson. (*Proc. Phys. Soc.* (*London*), vol. 74, pp. 145–152; August 1, 1959.)

537.525 100

Pulse Technique for Probe Measurements in Gas Discharges—J. F. Waymouth. (*J. Appl. Phys.*, vol. 30, pp. 1404–1412; September, 1959.)

537.533.8 101

Frequency Multiplication by Secondary Electrons in the Centimetre-Wavelength Range—K. Krebs. (*Z. Phys.*, vol. 154, pp. 19–26; January 19, 1959.) Fourier analysis of the electron current produced by secondary-electron resonance multiplication [see 737 of 1957 (Krebs and Meerbach)] shows that many harmonics are generated, so that the process appears suitable for frequency multiplication in the cm λ range.

537.56:538.56 102

Theory of Spatially Growing Plasma Waves—M. Sumi. (*J. Phys. Soc. Japan*, vol. 14, pp. 653–657; May, 1959.) See also 2534 of August.

537.56:538.566 103

On the Growth of Longitudinal Waves Propagating in Plasma—G. F. Filimonov. (*Radiotekh. Elektron.*, vol. 4, pp. 75–87; January, 1959.) An analytical treatment based on a single solution of the one-dimensional linear kinetic equation describing the propagation of high-frequency signals produced by a given external force. It is shown that for a low temperature of the electron gas, it is possible to use the ordinary single-velocity approximation. The analysis of the results permits a determination of the direction of propagation of natural waves in a plasma and a solution of the problem of the existence of increasing waves in a rectilinear electron beam.

538.221:538.569.4:537.311.62 104

Anomalous Skin Effect in Ferromagnetics—V. L. Gurevich. (*Zh. Tekh. Fiz.*, vol. 28, pp. 2352–2354; October, 1958.) A brief mathematical analysis of the anomalous skin effect which is present in ferromagnetic materials at resonance at low temperature and at high frequencies when the depth of the skin layer is of the order of the length of a free path of the conduction electrons.

538.3 105

On the Singular Electromagnetic Field in the Born-Infeld Theory—S. Kichenassamy. (*Compt. rend. Acad. Sci., Paris*, vol. 248, pp. 3690–3692; June 29, 1959.) It is shown that for this singular case the Born-Infeld theory gives the same results as Maxwell's theory.

538.566 106

Simple Derivation of Sommerfeld's Formula for the Dipole Function—O. Steiner. (*Arch. elekt. Übertragung*, vol. 12, pp. 457–462; October, 1958.)

538.566 107

Transmission and Reflection by a Parallel Wire Grid—M. T. Decker. (*J. Res. Nat. Bur. Stand.*, vol. 63D, pp. 87–90; July/August, 1959.) Experimental results are given for the transmission and reflection coefficients of a plane grid of parallel wires at frequencies near 9 kmc. The results are compared with theory.

538.566:535.42 108

Diffraction by a Slit—R. Plonsey and Hwei-Piao Hsu. (*J. Appl. Phys.*, vol. 30, p. 1468; September, 1959.) Several methods of calculation of the aperture field are compared.

538.566:535.42 109

Diffraction of Electromagnetic Waves by Smooth Obstacles for Grazing Angles—J. R. Wait and A. M. Conda. (*J. Res. Nat. Bur. Stand.*, vol. 63D, pp. 181–197; September/October, 1959.) "The diffraction of electromagnetic waves by a convex cylindrical surface is considered. Attention is confined primarily to the region near the light-shadow boundary. The complex-integral representation for the field is utilized to obtain a correction to the Kirchhoff theory. Numerical results are presented which illustrate the influence of surface curvature and polarization on the diffraction pattern. Good agreement with the experimental results of Bachynski and Neugebauer (3957 of 1959) is obtained. The effect of finite conductivity is also considered."

538.566:535.43 110

The Scattering of Electromagnetic Waves by a Corrugated Sheet—T. B. A. Senior. (*Canad. J. Phys.*, vol. 37, pp. 787–797; July, 1959.) The "physical optics" method is used to determine the scattering of a plane wave by a perfectly conducting sheet having sinusoidal corrugations.

538.566.029.6:537.562 111

Microwave Conductivity of Slightly Ionized Air—H. Margenau and D. Stillinger. (*J. Appl. Phys.*, vol. 30, pp. 1385–1387; September, 1959.) Values computed from experimental data are compared with others derived from simple formulas.

538.569.4:535.853:621.372.413 112

Cavity Resonators for Dielectric Spectroscopy of Compressed Gases—H. E. Bussey and G. Birnbaum. (*Rev. Sci. Instr.*, vol. 30, pp. 800–804; September, 1959.) Tunable sealed-off resonators for frequencies 1, 2, 9 and 24 kmc at pressures of 1000 lb/in² are described.

538.569.4.029.65:535.853 113

Dispersion Measurements on NaCl, KCl and KBr between 0.3- and 3-mm Wavelength—L. Genzel, H. Happ and R. Weber. (*Z. Phys.*, vol. 154, pp. 13–18; January 19, 1959.) Report of tests made with the spectrometer described in 114 below.

538.569.4.029.65:535.853 114

A Grating Spectrometer for the Far-Infrared Range and Short Microwaves—L. Genzel, H. Happ and R. Weber. (*Z. Phys.*, vol. 154, pp. 1–12; January 19, 1959.) A special diffraction grating is incorporated in the equipment described which covers the wavelength range 0.2–4.5 mm. For measurements below 1.2 mm λ the source is a mercury-vapor lamp; above 1 mm λ a klystron with frequency multiplier is used.

538.63 115

Negative and Oscillatory Longitudinal Magnetoresistance—R. Barrie. (*Canad. J. Phys.*, vol. 37, pp. 893–896; July, 1959.) A report on the result of numerical calculations of the longitudinal magnetoresistance of semiconductors and semimetals for the case in which electron scattering is due to the acoustic modes of the lattice vibrations and the magnetic field is so large that the quantization of the electron orbit is important.

538.632 116

Methods of Improving the Stability in Devices based on the Hall Effect—D. D. Voeĭkov. (*Zh. Tekh. Fiz.*, vol. 28, pp. 2248–2254; October, 1958.) The investigation shows that the main reasons for the temperature instability in these devices are a) the inhomogeneity of the crystal lattices of the sample and b) the rectification and the insufficient equipotentiality of the Hall contacts.

539.12 117

A Comparison of the Charges of the Electron, Proton and Neutron—A. M. Hillas and T. E. Cranshaw. (*Nature*, vol. 184, suppl. no. 12, pp. 892–893; September 19, 1959.) A report of experiments to determine whether matter in which there is an excess of neutrons is electrically neutral. For a comment by H. Bondi and R. A. Lyttleton, see *ibid.*, vol. 184, suppl. no. 13, p. 974; September 26, 1959.

GEOPHYSICAL AND EXTRATERRESTRIAL PHENOMENA

523.164:551.507.362.2 118

Measurement of Cosmic Noise at Low Frequencies above the Ionosphere—J. P. I. Tyas, C. A. Franklin and A. R. Molozzi. (*Nature*, vol. 184, pp. 785–786; September 12, 1959.) A description of the basic design features of a 2–15-mc frequency-sweep radiometer. The equipment is to be launched as an artificial satellite for the measurement of cosmic noise.

523.164.32 119

Solar Investigations in Japan—T. Khatanaka. (*Priroda*, no. 8, pp. 77–81; August, 1959.) A description of interferometric investigations carried out during the IGY by Tokyo Observatory, in the range 67–9500 mc of the intensity distribution over the solar disk. The radio noise on 200 mc seems to originate in the solar atmosphere 50,000 km above the visible solar surface. Recordings of radio noise between 200 and 9400 mc are shown and the relations of solar flares, magnetic storms and radio wave attenuation are considered.

523.164.32 120

Observations of the Fine Structure of Enhanced Solar Radio Radiation with a Narrow-Band Spectrum Analyser—O. Elgaröy. (*Nature*, vol. 184, suppl. no. 12, pp. 887–888; September 19, 1956.) An extension of the work described earlier (1141 of 1958).

523.164.32:32:523.75 121
Association of Radio Outbursts with Solar Flares—L. D. de Feiter, A. D. Fokker and J. Roosen. (*Nature*, vol. 184, suppl. no. 11, pp. 805–806; September 12, 1959.) Data covering the period July, 1957–December, 1958 have been examined for a relation between RF bursts and flares. A greater-than-normal percentage of impulsive flares of importance 1 were accompanied by RF bursts.

523.164.32:523.75 122
Distribution of Flares on the Solar Disk associated with Noise—L. R. McNarry. (*Nature*, vol. 184, suppl. no. 11, p. 806; September 12, 1959.) Results for periods between June, 1957 and July, 1958 indicate that present conditions in the solar corona favor noise emission at VHF from flares occurring in the northwest quadrant of the solar disk.

523.164.32:523.78 123
Eclipse Observations of Microwave Radio Sources on the Solar Disk on 19 April 1958—H. Tanaka and T. Kakinuma. (*Rept. Ionosphere Research, Japan*, vol. 12, pp. 273–284; September, 1958.) Results are given of observations of flux density, polarization and brightness distribution made in Japan on four frequencies in the range 1000 mc–9400 mc.

523.164.32:550.385.4 124
On the Relation of Solar Eruptions to Geomagnetic and Ionospheric Disturbances: Parts 1 and 2—K. Sinno and Y. Hakura. (*Rept. Ionosphere Research, Japan*, vol. 12, pp. 285–300; September, 1958.) A statistical analysis of data indicates that the characteristics of solar RF bursts can be related to S_c type storms, short-wave fades or a combination of both types of disturbances. See 1178 of 1959 (Hakura).

523.164.4 125
Red-Shift Absorption Spectrum of the Cygnus-A Radio Source—R. D. Davies and R. C. Jennison. (*Nature*, vol. 184, suppl. no. 11, pp. 803–804; September 12, 1959.) Results do not confirm the observations of Lilley and McClain (*Astrophys. J.*, vol. 123, pp. 172–175; January, 1956.)

523.165 126
Terrestrial Corpuscular Radiation—A. E. Chudakov and E. V. Gorchakov. (*Priroda*, no. 8, pp. 86–89; August, 1959.) A note on the two Van Allen zones which are attributed to charged particles moving in closed trajectories formed by magnetic traps due to the earth's magnetic field. A graph based on American and Russian rocket data shows the variation of the intensity of those zones with height. A maximum intensity is recorded at a distance between 20 and 30×10^3 km from the center of the earth.

523.165 127
Fermi Acceleration of Electrons in the Outer Van Allen Belt—J. A. Crawford. (*Phys. Rev. Lett.*, vol. 3, pp. 316–318; October 1, 1959.)

523.34 128
The Physical Nature of the Surface of the Moon—G. Fielder. (*J. Brit. Interplanetary Soc.*, vol. 17, pp. 57–58; March/April, 1959.) "Evidence concerning the structure of the lunar rock is reviewed. It is probable that it is vesicular in nature."

523.75:621.391.812.5 129
Apparent Observation of Solar Corpuscular Clouds by Direct Continuous-Wave Reflexion—J. D. Kraus and W. R. Crone. (*Nature*, vol. 184, pp. 965–966; September 26, 1959.) A report of observations in Ohio of Doppler signals centered on 15 mc which were first recorded at 0631 U.T. on 15th April 1959. The observations are discussed in relation to a solar flare of importance 3 which reached a maximum at about 0900 U.T. on April 13, 1959.

523.755 130
Kellogg and Ney's Model of the Solar Corona—D. E. Blackwell and D. W. Dewhirst: E. P. Ney and P. J. Kellogg. (*Nature*, vol. 184, pp. 1120–1123; October 10, 1959.) Critical comment on 2943 of 1959 and authors' reply.

550.38:551.507.362.1 131
Some Results Obtained by Measuring the Magnetic Field at the Earth with a Space Rocket—S. Sh. Dolginov and N. V. Pushkov. (*Dokl. Akad. Nauk SSSR*, vol. 129, pp. 77–80; November 1, 1959.) Results obtained using magnetometers with a range of $\pm 3000\ \gamma$ and a telemetry channel sensitivity of 600 γ/V, where $1\gamma = 1 \times 10^{-5}$ oersted, indicate that at a distance of 2–5 earth radii the magnetic field does not depend only on the earth potential but also on external sources such as charged solar particles. Measured values, recorded by space rocket, are lower than calculated ones. The difference between these values reaches a maximum at 22×10^3 km and a minimum at 23×10^3 km.

550.384 132
The Analytical Representation of the Geomagnetic Field—G. Fanselau and H. Kautzleben. (*Geofis. pura e appl.*, vol. 41, pp. 33–72; September–December, 1958. In German.) The representation of the geomagnetic field for the epoch 1945 by series of spherical functions up to 15th order are discussed. Within the limits of accuracy reached the permanent geomagnetic field may be derived only with respect to sources within the earth.

550.385 133
On the Characteristic Intervals of Pulsations of Diminishing Periods (10–1 sec) in the Electromagnetic Field of the Earth and their Connection with Phenomena in the Upper Atmosphere—V. A. Troitskaya and M. V. Mel'nikova. (*Dokl. Akad. Nauk SSSR*, vol. 128, pp. 917–920; October 11, 1959.) Investigation by high-speed recording of the daily variation of the earth's electromagnetic field has shown that during strong magnetic storms characteristic intervals of pulsation occur. The decreasing period of these pulsations can be directly correlated with the sharp atmospheric disturbances and the development of aurora in lower latitudes. Records obtained during two severe magnetic storms in 1958 are discussed.

550.385:551.510.536 134
Evidence concerning Instabilities of the Distant Geomagnetic Field: Pioneer I—C. P. Sonett, D. L. Judge and J. M. Kelso. (*J. Geophys. Res.*, vol. 64, pp. 941–943; August, 1959.) A report of some preliminary observations suggesting directional instability in the field.

550.385:621.317.42 135
Measurement of the Rapid Fluctuations of the Earth's Magnetic Field—M. Sauzade and E. Stefant. (*Compt. rend. Acad. Sci., Paris*, vol. 248, pp. 3325–3327; June 8, 1959.) A ferroxcube probe in circuit with a photoelectric fluxmeter [3371 of 1958 (Sauzade)] may be used to observe fluctuations at frequencies up to 20 c/s.

550.385.4 136
Geomagnetic Storms and the Earth's Outer Atmosphere—T. Obayashi. (*Rept. Ionosphere Research, Japan*, vol. 12, pp. 301–335; September, 1958.) Hydromagnetic oscillations of the ionized outer atmosphere are considered theoretically and discussed in relation to observations of geomagnetic pulsations (see 3673 of 1959). The geomagnetic storm on February 11, 1958 is analyzed in terms of hydromagnetic disturbances in the outer atmosphere. During such storms a corpuscular "cavity" 2–5 earth radii in size is formed enclosing the earth's magnetic field. A model of the interplanetary space is proposed. 42 references.

550.385.4(98) 137
On the Electric Field of the Polar Magnetic Storm—S. Akasofu. (*Rept. Ionosphere Research, Japan*, vol. 12, pp. 268–272; September, 1958.) It is suggested that proton and electron streams rushing into the ionosphere have a common powerful polarized field between them which might give rise to the currents associated with polar magnetic storms.

551.507.362.1+629.19 138
The Laws of Motion of Artificial Celestial Bodies—Yu. A. Ryabov. (*Priroda*, no. 8, pp. 11–18; August, 1959.) The critical velocities of artificial satellites are discussed and the observed trajectory of the first cosmic rocket launched on January 2, 1959 is examined. A rocket designed to reach the moon must have an initial velocity of approximately 10,780 meters/second.

551.507.362.2 139
An Application of Dynamic Programming to the Determination of Optimal Satellite Trajectories—R. Bellman and S. Dreyfus. (*J. Brit. Interplanetary Soc.*, vol. 17, pp. 78–83; May–August, 1959.)

551.507.362.2 140
Orbits of Artificial Satellites—W. T. Thomson. (*J. Brit. Interplanetary Soc.*, vol. 17, pp. 83–87; May–August, 1959.) Orbits are specified by three nondimensional parameters at rocket burn-out and expressions giving the periods of closed orbits in terms of the parameters are derived.

551.507.362.2 141
The Continued Progress of Satellite 1958-δ2 (Sputnik III)—B. R. May and D. E. Smith. (*Nature*, vol. 184, pp. 765–767; September 12, 1959.) Report of the progress of the satellite since November 1, 1958 and of the methods used for predicting its flight at the Radio Research Station, Slough. Earlier progress has been reviewed by King-Hele (1545 of 1959).

551.507.362.2:539.16 142
Satellite Observations of Electrons Artificially Injected into the Geomagnetic Field—J. A. Van Allen, C. E. McIlwain and G. H. Ludwig. (*J. Geophys. Res.*, vol. 64, pp. 877–891; August, 1959.) The geomagnetically trapped electrons resulting from the high-altitude nuclear detonations of the Argus experiment have been observed on four radiation detectors in satellite 1958ε (Explorer IV). The measurements for several satellite passes through the Argus "shells" are described and the significance of the results is summarized.

551.507.362.2:551.510.53 143
Mass-Spectrometer Measurements of the Ionic Composition of the Atmosphere by the Third Artificial Earth Satellite—V. G. Istomin. (*Dokl. Akad. Nauk SSSR*, vol. 129, pp. 81–84; November 1, 1959.) Discussion of results obtained from an analysis of 15,000 mass-spectrograms taken between the 15th and 25th of May, 1958 at heights of 225–980 km in the latitude interval 27°–65°N. Graphs show the variations of relative ionic intensity as a function of height and latitude. Above 500 km molecular ions are no longer observed.

551.507.362.2:621.391.812.33 144

The Faraday Fading of Radio Waves from an Artificial Satellite—F. H. Hibberd. (*J. Geophys. Res.*, vol. 64, pp. 945–948; August, 1959.) "Faraday fading of signals from an artificial satellite is analysed in terms of the difference between the Doppler shifts of the ordinary and extraordinary components in the ionosphere. A procedure is outlined for determining the vertical distribution of electron density in the upper ionosphere. Explanations are given for the apparently excessive values of electron content yielded by measurements of Faraday fading and for the observation that the rate of Faraday fading is not exactly inversely proportional to the square of the wave frequency."

551.507.362.2:621.396.969.35 145

Radio Detection of Silent Satellites—C. Roberts, P. Kirchner and D. Bray. (*QST*, vol. 43, pp. 34–35; August, 1959.) A brief description of the characteristics of reflected signals from a standard-frequency transmitter within the skip distance received on 10, 15 and 20 mc. See also 3805 of 1958 (Kraus and Dreese).

551.510.52 146

Diurnal and Semidiurnal Variations of Wind, Pressure, and Temperature in the Troposphere at Washington, D. C.—M. F. Harris. (*J. Geophys. Res.*, vol. 64, pp. 983–995; August, 1959.)

551.510.535 147

Turbulence at Meteor Heights—C. O. Hines. (*J. Geophys. Res.*, vol. 64, pp. 939–940; August, 1959.) An outline of a new method of studying motions at meteor heights by assuming that they are perturbations associated with oscillating waves propagated through the atmosphere.

551.510.535 148

Study of the New Model of the Ionosphere: Part 1—O. Burkard. (*Geofis. pura e appl.*, vol. 41, pp. 133–140; September–December, 1958. In German.) The variation with height of the electron density is calculated for three cases, and good agreement is obtained between the model (3705 of 1959) and the results of moon echo observations.

551.510.535 149

Effect of Small Irregularities on the Constitutive Relations for the Ionosphere—K. G. Budden. (*J. Res. Nat. Bur. Stand.*, vol. 63D, pp. 135–149; September/October, 1959.) A theoretical treatment of the modification of refractive index due to small irregularities. The latter may play an important part in the propagation of VLF radio waves.

551.510.535 150

Stratification in the Lower Ionosphere—C. Ellyett and J. M. Watts. (*J. Res. Nat. Bur. Stand.*, vol. 63D, pp. 117–134; September/October, 1959.) A survey of the evidence for stratification at heights below 100 km. Over 100 references.

551.510.535 151

Electron Collision Frequencies in Nitrogen and in the Lower Ionosphere—A. V. Phelps and J. L. Pack. (*Phys. Rev. Lett.*, vol. 3, pp. 340–342; October 1, 1959.) By using an improved version of the electron drift-velocity tube in the laboratory measurements, and an improved analysis of rocket data, the two sets of results are brought into agreement. Reevaluation of the rocket data involves the energy dependence of the electron collision frequency.

551.510.535 152

The Possible Occurrence of Negative Nitrogen Ions in the Atmosphere—F. D. Stacey. (*J. Geophys. Res.*, vol. 64, pp. 979–981; August, 1959.) If negative ions are formed, and laboratory experiments show that they may be, a strong pressure dependence of the electron-ion recombination coefficient is to be expected. At the very low F-region pressures, the rate of disappearance of free electrons could follow an attachment law.

551.510.535 153

Tides in the F_2 Ionospheric Layer—P. Herrinck. (*Nature*, vol. 184, suppl. no. 14, pp. 1055–1056; October 3, 1959.) A brief report of the results of a harmonic analysis of the mean diurnal variation of the layer semithickness y_m during the period 1952–1958 at Léopoldville-Binza, Belgian Congo.

551.510.535 154

A Theory of Spread F based on a Scattering-Screen Model—J. Renau. (*J. Geophys. Res.*, vol. 64, pp. 971–977; August, 1959.) Oblique rays from the sounder are scattered by a scattering screen into the F region whence they are reflected back to the sounder. For frequencies appreciably higher than the F-region penetration frequency, there is a linear relation between the minimum virtual height of the returned signal and the operating frequency. All virtual heights above this minimum value and below the normal vertical incidence value are possible; this fact accounts for spread echoes being enclosed by two sharply defined boundaries. This hypothetical picture agrees with that obtained from actual ionograms but requires that the screen be above E-region heights.

551.510.535 155

Magnetic Control of the Variations of the Critical Frequency of the F_2 Layer of the Ionosphere—R. G. Rastogi. (*Canad. J. Phys.*, vol. 37, pp. 874–879; July, 1959.) The true magnetic latitude reference is shown to give more satisfactory results than the idealized geomagnetic latitude reference when considering diurnal and latitudinal variations of f_0F_2 at low latitudes. See also 2245 of July, 1959.

551.510.535 156

Measurement of Ionospheric Electron Densities using an RF Probe Technique—J. E. Jackson and J. A. Kane. (*J. Geophys. Res.*, vol. 64, pp. 1074–1075; August, 1959.) The probe consists of a 28-foot dipole operating at 7.75 mc and has been flown in a rocket over Fort Churchill. Above 110 km it behaves as a capacitor, the capacitance of which is telemetered to the ground. The local electron density in the ionosphere may be calculated from these values by using a simplified form of the Appleton-Hartree equation. The electron densities obtained using such probes are in good agreement with those obtained by normal methods.

551.510.535:523.164 157

Investigation of Winds and Inhomogeneities in the Ionosphere using a Radio-Astronomy Method—V. V. Vitkevich and Yu. L. Kukurin. (*Radiotekh. Electron.*, vol. 4, pp. 17–20; January, 1959.) Description of measurements made using three parabolic mesh-type reflectors of area 170m² spaced approximately 300 meters apart, and operating at a wavelength of 6 meters. Ionospheric wind velocities of 70–90 meters/second were recorded.

551.510.535:621.391.812.63 158

Ionospheric Investigations using the Sweep-Frequency Pulse Technique at Oblique Incidence—V. Agy and K. Davies. (*J. Res. Nat. Bur. Stand.*, vol. 63D, pp. 151–174; September/October, 1959.) A review of oblique incidence investigations, especially those carried out at the National Bureau of Standards showing diurnal and seasonal variations on two east-west paths of 1150 km and 2370 km. There is a discrepancy of about 3 per cent between the observed and calculated MUF.

551.510.535:621.391.812.63 159

The D Region of the Ionosphere—(See 307.)

551.510.536:539.16 160

The Argus Experiment—N. C. Christofilos. (*J. Geophys. Res.*, vol. 64, pp. 869–875; August, 1959.) "A geophysical experiment on global scale was conducted last fall. Three small A-bombs were detonated beyond the atmosphere at a location in the south Atlantic. The purpose of the experiment was to study the trapping of the relativistic electrons (produced by the β-decay fission fragments) in the geomagnetic field. The released electrons are trapped by this field oscillating along the magnetic lines between two mirror points. In addition to this motion the electrons drift eastward, creating a thin electron shell around the earth. The lifetime and location of the thus-created global electron shell were measured by satellite- and rocket-borne instruments. Auroral luminescence was observed at the conjugate points. The electron shell exhibited remarkable stability during its lifetime. No motion of the shell or change in its thickness was detected."

551.510.536:539.16 161

Optical, Electromagnetic, and Satellite Observations of High-Altitude Nuclear Detonations: Part 1—P. Newman. (*J. Geophys. Res.*, vol. 64, pp. 923–932; August, 1959.) "After each of the high-altitude detonations in the Argus experiment, visual auroras were observed in the detonation area. After the third event an aurora was observed in the conjugate area. After the second and third events, signals attributed to hydromagnetic waves were detected in the conjugate region; these signals had a periodicity of about 1 cycle/second. The maximum change in the magnetic field was about 1 gamma. If propagated along the magnetic line of force the velocity was about 2000 km/second. Sporadic E was observed after the third event in the conjugate area. Comparative records of the 5577 Å and 3914 Å lines were obtained in the detonation area."

551.510.536:539.16 162

Optical, Electromagnetic, and Satellite Observations of High-Altitude Nuclear Detonations: Part 2—A. M. Peterson. (*J. Geophys. Res.*, vol. 64, pp. 933–938; August, 1959.) "The radio effects of the Argus detonations were measured using a) 30-mc radars designed to obtain echoes from the aurora or from the earth's surface mirrored in an enhanced ionospheric layer, b) VLF receivers for monitoring distant transmitters or atmospheric noise sources in search of changes in signal strength, c) riometers for recording cosmic noise absorption or VHF shot-created noise at 30, 60, and 120 mc. Results included 1) auroral echoes in the vicinity of the launch point after all three shots and near the conjugate points after the first and third shot, 2) sudden depressions of 6 to 12 db of the signal from England (19.6 kc) at Madrid and the Azores, 3) no ionospheric absorption at the conjugate location."

551.510.536:539.16 163

Project Jason Measurement of Trapped Electrons from a Nuclear Device by Sounding Rockets—L. Allen, Jr., J. L. Beavers, II, W. A. Whitaker, J. A. Welch, Jr., and R. B. Walton. (*J. Geophys. Res.*, vol. 64, pp. 893–907; August, 1959.) High-altitude sounding rockets have been used to observe electrons injected into the geomagnetic field from the high-altitude nuclear detonations of the Argus experiment. The results of these observations agree with those measured by satellite Explorer IV. The trapping of neutron decay β particles from large-yield high-altitude explosions in the Pacific was also observed.

551.510.536:539.16 164

Theory of Geomagnetically Trapped Electrons from an Artificial Source—J. A. Welch, Jr., and W. A. Whitaker. (*J. Geophys. Res.*, vol. 64, pp. 909–922; August, 1959.) The history of electrons resulting from the high-altitude nuclear detonations of the Argus experiment is treated theoretically, and the results are compared with the Jason rocket data and the Explorer IV satellite data.

551.594.21 165

Modern Theories of Thunderstorm Electrification—J. A. Chalmers. (*Geofis. pura e appl.*, vol. 41, pp. 189–193; September–December, 1958. In English.) Critical comparison of theories [*e.g.*, 444 of 1957 (Wilson)]. Suggestions are made for investigations to determine the correctness of convection theories. 18 references.

551.594.221 166

Very-Low-Frequency Radiation Spectra of Lightning Discharges—W. L. Taylor and A. G. Jean. (*J. Res. Nat. Bur. Stand.*, vol. 63D, pp. 199–204, September/October, 1959.) An analysis is given of the ground-wave portion of 33 "sferics" waveforms recorded from cloud-to-ground discharges between 150 and 600 km from Boulder, Colo. Frequencies of peak energy lie between 5 and 20 kc.

551.594.5 167

Diurnal Variation of Aurora and Geomagnetic Disturbance at New Zealand Antarctic Stations—T. Hatherton and G. G. Midwinter. (*Nature*, vol. 184, suppl. no. 12, pp. 889–890; September 19, 1959.) A relation exists between aurora and geomagnetic disturbance but the main features of diurnal variation of auroral incidence are not related to local geomagnetic variations.

551.594.5 168

Low-Frequency (100-kc/s) Radio Noise from the Aurora—R. L. Dowden. (*Nature*, vol. 184, suppl. no. 11, p. 803; September 12, 1959.) Strong RF noise, recorded on one occasion at frequencies up to 180 kc is reported.

551.594.5:550.385 169

Auroras, Magnetic Bays, and Protons—R. C. Bless, C. W. Gartlein, D. S. Kimball and G. Sprague. (*J. Geophys. Res.*, vol. 64, pp. 949–953; August, 1959.) Observational evidence indicates that aurora and magnetic bays both have the same cause and occur at the same geographic location. Calculations show that these bays can be explained by a wind movement of positive ions generated by incoming solar protons.

551.594.6 170

Observations of "Whistlers" and Very-Low-Frequency Phenomena at Godhavn, Greenland—E. Ungstrup. (*Nature*, vol. 184, suppl. no. 11, pp. 806–807; September 12, 1959.)

LOCATION AND AIDS TO NAVIGATION

621.396.96 171

A Unified Analysis of Range Performance of C.W., Pulse, and Pulse Doppler Radar—J. J. Bussgang, P. Nesbeda and H. Safran. (Proc. IRE, vol. 47, pp. 1753–1762; October, 1959.)

621.396.96:621.391.82 172

Detection of a Signal in Normal Noise and Chaotic Reflections—V. D. Zubakov. (*Radiotekh. Elektron.*, vol. 4, pp. 28–38; January, 1959.) Examination of the mathematical theory of optimum detection of radar signals in the presence of noise and reflection from local objects.

621.396.96:621.391.82 173

Realistic Simulation of Radar Clutter—J. Atkin, H. J. Bikel and M. Weiss. (*Electronics*, vol. 32, pp. 78–81; September 25, 1959.) A Gaussian noise source at 30 mc and a delay line are used.

621.396.969.3 174

Radar Echoing Area Polar Diagram of Birds—J. Edwards and E. W. Houghton. (*Nature*, vol. 184, suppl. no. 14, p. 1059; October 3, 1959.) Measurements have been made with a high-resolution X-band radar, of the echoing area of single birds in various attitudes of flight.

621.396.969.36 175

Electromagnetic Back-Scattering Measurements by a Time-Separation Method—C. C. H. Tang. (IRE Trans. on Microwave Theory and Techniques, vol. MTT-7, pp. 209–213; Abstract, Proc. IRE, vol. 47, p. 1286; July, 1959.)

MATERIALS AND SUBSIDIARY TECHNIQUES

535.215:546.23 176

Saturated Photocurrents in Hexagonal Selenium—M. Polke, G. Storch and F. Stöckmann. (*Z. Phys.*, vol. 154, pp. 51–61; January 19, 1959.) The photoconductivity of thin vapor-deposited Se films was ivnvestigated in the temperature range $-180°$ to $+20°C$.

535.215+535.37:546.48'221 177

Photoconductivity Excitation and Luminescenoe Spectra of CdS Crystals—V. L. Broude, V. V. Eremenko and V. S. Medvedev. (*Zh. Tekh. Fiz.*, vol. 28, pp. 2263–2265; October, 1958.) Investigation at 20°K showed a close relation between the yellow luminescence and photoconductivity in CdS crystals. It also revealed two types of orange luminescence of different origin.

535.215:546.48'221 178

Nonstationary Processes in Photoconductors: Part 2—Slow Build-Up of Photoconduction in CdS Single Crystals for Low Excitation Intensities—K. W. Böer and H. Wantosch. (*Ann. Phys., Lpz.*, vol. 2, pp. 406–412; January 27, 1959.)

Part 1: 1061 of 1956 (Böer and Vogel).

535.215:546.48'221 179

Photosensitive Spin Resonance in CdS—J. Lambe, J. Baker and C. Kikuchi. (*Phys. Rev. Lett.*, vol. 3, pp. 270–271; September 15, 1959.) Direct observation and identification of a trapping center in CdS crystals with traces of iron impurities is reported.

535.215:546.48'221 180

Photoconduction of Activated Cadmium Sulphide Layers with Electron Excitation—F. Lappe. (*Z. Phys.*, vol. 154, pp. 267–285; March 4, 1959.) Report on investigations of reversible changes of conductivity in polycrystalline activated CdS layers under constant and modulated bombardment with electrons of energy 10–80 kev.

535.215:546.48'221 181

Investigation of the Spectral Distribution of Photoconductivity in CdS Single Crystals at 77 and 20°K—V. L. Broude, V. V. Eremenko and M. K. Sheĭnkman. (*Zh. Tekh. Fiz.*, vol. 28, pp. 2142–2151; October, 1958.) An examination of the spectral dependence of the photocurrent and the photocarrier lifetime and also of the relation of these magnitudes to the absorption coefficient of light at different wavelengths.

535.215:546.48'221:537.311.33 182

Investigations of Charge-Carrier Diffusion and other Forms of Energy Transport in CdS—J. Auth and R. Riddler. (*Ann. Phys., Lpz.*, vol. 2, pp. 351–364; January 27, 1959.) The distribution of charge-carrier concentration in partially illuminated CdS crystals is investigated at room temperature and at 80°C using the method described in 792 of 1957 (Auth and Niekisch).

535.215:546.561–31 183

Spectral Distribution of Photoconductivity in Cu_2O Crystals at 20°K—V. V. Eremenko. (*Zh. Tekh. Fiz.*, vol. 28, pp. 2261–2263; October, 1958.) Investigation of the absorption spectrum of Cu_2O at low temperature reveals a number of narrow lines or exciton lines which, by confirming the mechanism of the internal photoeffect, have a maximum disposed at the fringe of the light absorption in the crystal. Results of a comparison of the spectrum with the spectrum distribution of photoconductivity at low temperature are shown graphically.

535.215:546.817'221 184

Modification of PbS Noise Spectra by Radiation—R. L. Williams. (*Canad. J. Phys.*, vol. 37, pp. 841–847; July, 1959). Detailed wavelength studies at CO_2 temperatures have shown that generation-recombination noise can be obtained with light of the 2.4-μ region and 1/f noise with radiation of the 1.0-μ region.

535.215–15 185

Relationship between Signal-to-Noise Ratio and Threshold of Response of Infrared Photoconductors Limited by Generation-Recombination Noise—W. E. Spicer. (*J. Appl. Phys.*, vol. 30, pp. 1381–1384; September, 1959.) The signal/noise ratio varies as exp $\beta Ei/2kT_D$ where Ei is the threshold response of the photoconductor, T_D its temperature, and β is a constant between 1 and $\frac{1}{2}$.

535.37:535.215 186

The Temperature-Dependence of the Fluorescence of Photoconductors—H. A. Klasens. (*J. Phys. Chem. Solids*, vol. 9, pp. 185–197; March, 1959.) Theoretical discussion of the effect of temperature on a two-state model of a fluorescent photoconductor

535.37:546.47'221 187

Associated Donor-Acceptor Luminescent Centres in Zinc Sulphide Phosphors—E. F. Apple and F. E. Williams. (*J. Electrochem. Soc.*, vol. 106, pp. 224–230; March, 1959.) A comprehensive study of ZnS-*x* (Cu or Ag), *y* (Ga or In) shows two emission bands. The shorter wavelength band does not involve the ground state of the coactivator or donor whereas the longer wavelength band does. Both bands involve the ground state of the activator or acceptor.

537.37:546.47'221 188

ZnS Phosphors with P, As, Sb, Coactivators—E. F. Apple. (*J. Electrochem. Soc.*, vol. 106, pp. 271–272; March, 1959.)

535.37:546.47'221 189

Emission Spectrum of Copper-Activated Zinc Sulphide in the Region of Partial Thermal Extinction—H. Payen de la Garanderie and D. Curie. (*Compt. rend. Acad. Sci., Paris*, vol. 248, pp. 3151–3153; June 1, 1959.) Interaction between optical centers and the crystalline lattice accounts satisfactorily for the effects observed.

535.37:546.47'221 190

Changes in Trapping Levels of Zinc Sul-

phide Phosphors Resulting from Positive-Ion Bombardment—W. T. Allen and C. H. Bachman. (*J. Electrochem. Soc.*, vol. 106, pp. 211–217; March, 1959.) Report of experimental procedure and the results obtained from measurements of the amount of visible light emitted by ZnS-Ag phosphors 5.0 msec after excitation by weak ultraviolet radiation. Bombardment by ions caused an increase in the number of traps at the lowest trapping level 0.28 ev deep as well as the creation of new traps at depths slightly greater and slightly less than 0.28 ev. This effect was independent of the ions used for bombardment. New traps also appeared at deeper trapping levels: 0.37ev for Ar^+, 0.38 ev for H_2^+, and 0.39 ev for O_2^+ ion bombardment.

535.37-15:538.569.4 191
Paramagnetic Resonance Detection of the Optical Excitation of an Infrared Stimulable Phosphor—R. S. Title. (*Phys. Rev. Lett.*, vol. 3, pp. 273–274; September 15, 1959.) The results for SrS-Eu,Sm agree with those obtained by other methods and support the simplified band-theory model.

535.376:546.561-31 192
Electroluminescence at Point Contacts in Cuprous Oxide and the Mobility of Cu^+ Ions at Room Temperature—R. Frerichs and I. Liberman. (*Phys. Rev. Lett.*, vol. 3, pp. 214–215; September 1, 1959.) The measured value of the mobility is about 5×10^{-10} cm²/volt-second.

537.226+538.221 193
Arrangement of Boundary Surfaces between Dielectrics or Ferromagnetics—K. Funk. (*Elektron. Rundschau*, vol. 12, pp. 349–350; October, 1958.) An increase in capacitance or reduction of losses in capacitors or ferrite cores with air gap can be achieved by suitably shaping the boundary surfaces.

537.226 194
Relaxation Polarization Dielectrics. An Assessment of the System (Sr, Ba, Ca) TiO_3–Bi_2O_3–TiO_2—R. M. Glaister and J. W. Woolner. (*J. Electronics Control*, vol. 6, pp. 385–396; May, 1959.) Ceramic solid solutions of the system $SrTiO_3$–$Bi_2O_3\cdot nTiO_2$, with n from 0 to 4, have been investigated, and the effects of substituting Ba or Ca for Cr studied. Results of measurements of permittivity and loss tangent are given.

537.227 195
New Ferroelectrics of the Complex Forms $Pb_2Fe^{3+}NbO_6$ and Pb_2YbNbO_6—G. A. Smolenskii, A. I. Agranovskaya, S. N. Popov and V. A. Isupov. (*Zh. Tekh. Fiz.*, vol. 28, pp. 2152–2153; October, 1958.) A brief report of an investigation of the temperature dependence of dielectric conductivity and loss angle.

537.227/.228.1 196
Dielectric Polarization and Piezoelectric Properties of Ferroelectric Solid Solutions Consisting of Metaniobates of Calcium, Strontium and Barium in Lead Metaniobate—V. A. Isupov and V. I. Kosyakov. (*Zh. Tekh. Fiz.*, vol. 28, pp. 2175–2185; October, 1958.) An investigation of the dependence of the Curie temperature of these solutions on the content of lead metaniobate. The spontaneous polarization in these polycrystalline specimens has a value greater than 20 microcoulombs/cm.² Piezoelectric characteristics are shown graphically.

537.227:546.431'824-31 197
Theoretical Treatment of the Movement of 180° Domain in $BaTiO_3$ Single Crystal—R. Abe. (*J. Phys. Soc. Japan*, vol. 14, pp. 633–642; May, 1959.)

537.227:546.824-31 198
Ferroelectric Properties of a Material made of Titanium Oxide—L. Nicolini. (*Nuovo Cim.*, vol. 13, pp. 257–264; July 16, 1959. In English.) A report of tests made to prove the existence of ferroelectric properties in a ceramic-type material prepared from TiO_2 by a technique described in 1048 of 1953.

537.228.1 199
Lead Zirconate Piezoelectric Ceramics—A. E. Crawford. (*Brit. Commun. Electronics*, vol. 6, pp. 516–519; July, 1959.) The effects of additives on the characteristics of lead-zirconate-titanate are briefly discussed. See also 4086 of 1959 (Jaffe).

537.311.31:538.632 200
Hall Effect in Copper and Cu_3Au at Low Temperatures—W. F. Love. (*J. Phys. Chem. Solids*, vol. 9, pp. 281–284; March, 1959.) Measurements on single crystals at temperatures down to 4°K.

537.311.33 201
Semiconducting Compounds with a General Formula ABX_2—V. P. Zhuze, V. M. Sergeeva and E. L. Shtrum. (*Zh. Tekh. Fiz.*, vol. 28, pp. 2093–2108; October, 1958.) Investigation of ternary compounds which crystallize in the chalcopyrite (Cu Fe S_2) pattern and which were first synthesized in 1953 by Hahn. Data are given on new compounds some of which crystallize in tetragonal systems. All these compounds proved to be semiconductors.

537.311.33 202
***P–N* Junctions at Low Temperature**—B. M. Vul. (*Dokl. Akad. Nauk SSSR*, vol. 129, pp. 61–63; November 1, 1959.) The investigation shows that at a sufficiently low absolute temperature T, when the energy of ionization in semiconductors is less than kT, where k is the Boltzmann constant, the electron concentration in the conduction band and the hole concentration in the valence band are very low compared to the impurity concentration.

537.311.33 203
Delineation of Junctions in Semiconductors by Electroscopic Powders—J. A. Amick and B. Goldstein. (*J. Appl. Phys.*, vol. 30, pp. 1471–1472; September, 1959.) Materials are used in the form of dry powders or suspensions of triboelectrically charged powders. Techniques and observed results are described.

537.311.33 204
The Influence of Internal Electric Fields in a Semiconductor on its Field Emission—M. I. Elinson. (*Radiotekh. Elektron.*, vol. 4, pp. 140–142; January, 1959.) A brief mathematical analysis.

537.311.33:535.215 205
Measurement of Minority-Carrier Lifetime by means of the Surface Photovoltaic Effect—P. Gosar. (*Compt. rend. Acad. Sci., Paris*, vol. 248, pp. 3139–3141; June 1, 1959.) A calculation is made of the concentration of minority carriers near the illuminated surface of a semi-infinite semiconductor. Results are in quantitative agreement with measurements of rate of signal decay.

537.311.33:538.632:621.317.3 206
Hall Effect Measurement in Semiconductor Rings—R. G. Pohl. (*Rev. Sci. Instr.*, vol. 30, pp. 783–786; September, 1959.) The ring is placed in an alternating magnetic field normal to the plane of the ring. The current induced in the ring interacts with the field to produce a Hall voltage between the inner and outer edges which can be expressed as a function of parameters of the material. The advantages of this method are described and mobilities determined using this and normal techniques are compared.

537.311.33:546.28 207
Energy Bands in Silicon Crystals—F. Bassani. (*Nuovo Cim.*, vol. 13, pp. 244–245; July 1, 1959. In English.) An extension of the work described in 1178 of 1958 to include energy values at the points where K is equal to $2\pi a^{-1}$ ($\frac{1}{2}$, $\frac{1}{2}$, $\frac{1}{2}$) and to $2\pi a^{-1}$ ($\frac{1}{2}$, 0, 0).

537.311.33:546.28 208
The Solubility of Oxygen in Silicon—H. J. Hrostowski and R. H. Kaiser. (*J. Phys. Chem. Solids*, vol. 9, pp. 214–216; March, 1959.) "The intensity of the fine structure of the 1100 cm^{-1} silicon-oxygen absorption at 4.2°K has been used to determine the temperature-dependence of the concentration of oxygen in solid solution. Above 1000°C the logarithm of this concentration is a linear function of the reciprocal of the absolute temperature, and the heat of the precipitation reaction is 22 ± 2 kcal/mole."

537.311.33:546.28 209
Effect of Oxygen in Silicon on Phosphorus Diffusion—J. L. Hartke. (*J. Appl. Phys.*, vol. 30, pp. 1469–1470; September, 1959.)

537.311.33:546.28 210
The Diffusion of Impurities into Evaporating Silicon—R. L. Batdorf and F. M. Smits. (*Bell. Lab. Record*, vol. 37, pp. 330–333; September, 1959.) A vacuum system for the simultaneous diffusion of P and Ga into evaporating Si is described.

537.311.33:546.28 211
Investigation of Surface Conditions during Impurity Diffusion in Silicon—G. Feuillade. (*Compt. rend. Acad. Sci., Paris*, vol. 248, pp. 3136–3138; June 1, 1959.) A "limiting condition" for diffusion is defined and diffusion processes are classified in three groups according to the nature of the surface reactions.

537.311.33:546.28 212
Hot Electrons and Carrier Multiplication in Silicon at Low Temperature—W. Kaiser and G. H. Wheatley. (*Phys. Rev. Lett.*, vol. 3, pp. 334–336; October 1, 1959.) At temperatures where most carriers are frozen out on impurity levels, new effects of an applied electric field are observed. The electrical resistivity and Hall coefficient in phosphorus-doped silicon were measured at 20°K as a function of the electric field (0.5 to 10³v/cm), particular attention being paid to the breakdown region.

537.311.33:546.28:535.215 213
On the Current/Voltage Characteristic of Diffusion-Type Silicon *n-p* Junctions—V. M. Tuchkevich and V. E. Chelnokov. (*Zh. Tekh. Fiz.*, vol. 28, pp. 2115–2123; October, 1958.) The samples were illuminated by a 500-watt lamp provided with a water filter in order to cut out the infrared part of the spectrum. The V/I characteristic and temperature dependence of the photovoltage and photocurrent of these junctions are shown graphically.

537.311.33:546.28:535.37 214
Recombination Light Emission and Electron Multiplication in Silicon—S. Müller. (*Z. Naturforsch.*, vol. 13a, pp. 240–241; March, 1958.) The effect noted earlier [*e.g.*, 1088 of 1956 (Newman)] is investigated by tests on n-type Si disks with resistivity 10 Ω cm to determine whether carrier multiplication occurs at the luminous regions. The results are in agreement with the assumption of Chynoweth and McKay (3096 of 1956).

537.311.33:546.28:535.37 215
Visible Light Emission from Metal/Silicon Contact—M. Kikuchi. (*J. Phys. Soc. Japan*, vol. 14, p. 682; May, 1959.) A brief report on the appearance of light spots at a back-biased contact, and correlation with its photoresponse.

537.311.33:546.28:539.12.04 216
Electron Bombardment of Silicon—D. E. Hill. (*Phys. Rev.*, vol. 114, pp. 1414–1420; June 15, 1959.) After bombardment with high-energy electrons, the following properties of single-crystal Si were measured: carrier removal rate and temperature dependence of resistivity and Hall coefficient.

537.311.33:546.28:539.12.04 217
Some Effects of Fast Neutron Irradiation on Carrier Lifetimes in Silicon—R. W. Beck, E. Paskell and C. S. Peet. (*J. Appl. Phys.*, vol. 30, pp. 1437–1439; September, 1959.)

537.311.33:546.28:621.314.63 218
Silicon as a Material for Power Rectifiers—F. W. G. Rose, J. Shields and I. Williams. (*Trans. S. Afr. Inst. Elec. Eng.*, vol. 49, pt. 12, pp. 391–410; December, 1958. Discussion, pp. 410–416.) A review with 50 references.

537.311.33:546.289 219
Effect of Various Etches on Recombination Centers at a Germanium Surfaces—G. Wallis and S. Wang. (*J. Electrochem. Soc.*, vol.106, pp. 231–238; March, 1959.) Ge samples were etched with CP-4, H_2O_2, iodine A, electrolytic and silver etch. Iodine A and electrolytic etches produce recombination centers of one type and the remaining etches centers of another type. The effects of baking on the etched samples are discussed.

537.311.33:546.289 220
Investigation of the Industrial Etching of the Surface of Single-Crystal Germanium before Fusing Indium into It—R. E. Smolyanskii, V. M. Gurevich, A. M. Raikhlin and M. I. Lukasevich. (*Zh. Tekh. Fiz.*, vol. 28, pp. 2135–2141; October, 1958.) The thickness of the Ge surface layer distorted by cutting and polishing is found to be 90 μ. Some technical advice is given concerning the etching of Ge to be used in different types of apparatus and having a fused In-Ge *p-n* junction. The best etching solution was found to be one of NaOH in H_2O_2.

537.311.33:546.289 221
Micropyramids on Germanium Formed during Microalloying—R. Zuleeg. (*J. Appl. Phys.*, vol. 30, pp. 1461–1462; September, 1959.)

537.311.33:546.289 222
***g*-Factor of Electrons in Germanium**—L. M. Roth and B. Lax. (*Phys. Rev. Lett.*, vol. 3, pp. 217–219; September 1, 1959.) Theoretical and experimental values are compared.

537.311.33:546.289:534.2–8 223
Attenuation of Sound in a Germanium Crystal at Ultra High Frequencies and Low Temperatures—E. R. Dobbs, B. B. Chick and R. Truell. (*Phys. Rev. Lett.*, vol. 3, pp. 332–334; October 1, 1959.) The ultrasonic attenuations of compressional and shear waves in a high purity Ge crystal were measured at frequencies up to 650 mc and temperatures down to 1.5°K. Results at the highest frequencies (at room temperature) show evidence of dislocation resonance. Attenuation is very small at temperatures below about 20°K.

537.311.33:546.3–1'87'86 224
Temperature Dependence of the Electrical Properties of Bismuth-Antimony Alloys—A. L. Jain. (*Phys. Rev.*, vol. 114, pp. 1518–1528; June 15, 1959.) Resistivity, Hall effect and lattice parameters are discussed.

537.311.33:546.48'221:621.317.321 225
Measurements of Contact Potential on Cadmium Sulphide—W. Schaaffs and H. Woelk. (*Z. angew. Phys.*, vol. 10, pp. 456–458; October, 1958.) Measurements were made on a number of CdS crystals with different impurity content and structure using a rotating-armature method described *ibid.*, vol. 10, pp. 424–428; September, 1958 (Schaaffs). For an acoustic method of measuring contact potential see *ibid.*, vol. 10, pp. 455–456; October, 1958 (Schaaffs).

537.311.33:546.49'241 226
Preparation and Properties of HgTe and Mixed Crystals of HgTe-CdTe—W. D. Lawson, S. Nielsen, E. H. Putley and A. S. Young. (*J. Phys. Chem. Solids*, vol. 9, pp. 325–329; March, 1959.) HgTe is found to be a semiconductor with activation energy ~0.01 ev and mobility ratio ~100. It is opaque to infrared radiation, but mixed crystals of HgTe-CdTe show absorption edges which vary in position with composition. Photoconductivity has been observed in mixed crystals.

537.311.33:546.681'86 227
Oscillatory Magneto-Absorption in Gallium Antimonide JA—1149—S. Zwerdling, B. Lax, K. J. Button and L. M. Roth. (*J. Phys. Chem. Solids*, vol. 9, pp. 320–324; March, 1959.) Measurements at photon energies just above the intrinsic absorption edge show an oscillatory spectrum similar to that for direct transitions in Ge. The energy gap is found to be 0.813±0.001 ev, and the electron effective mass (0.047±0.003) m_0.

537.311.33:546.682'19 228
Anomalous Electrical Properties of *p*-Type Indium Arsenide—J. R. Dixon. *J. Appl. Phys.*, vol. 30, pp. 1412–1416; September, 1959.) Anomalies in the Hall-constant/temperature relation were investigated experimentally. An explanatory mechanism is proposed and predictions based on this model about the removal of the anomalies are confirmed by experiment.

537.311.33:546.682'86 229
A Reliable Method for the Production of High-Purity Indium Antimonide—K. F. Hulme. (*J. Electronics Control*, vol. 6, pp. 397–402; May, 1959.)

537.311.33:546.682'86:539.23 230
Investigation of Thin Films Obtained by Evaporation of Indium Antimonide in a Vacuum—G. A. Kurov and Z. G. Pinsker. (*Zh. Tekh. Fiz.*, vol. 28, pp. 2130–2134; October, 1958.) Films produced after only ten or twelve evaporations in vacuo are of the *n* or *p* type in which the mobility of the charge carrier depends on the size of the crystals.

537.311.33:546.682'86:539.23 231
Electron-Optical Investigations of the Structure of Vapour-Deposited InSb Films—L. Reimer. (*Z. Naturforsch.* vol. 13a, pp. 148–152; February, 1958.) The crystal structure of InSb films 500Å thick was investigated as a function of the temperature of the supporting SiO film, using electron diffraction and microscopy. The best structure was obtained for a support temperature above 400°C during deposition. Hall-effect measurements on films >1 μ thick give results in agreement with these findings.

537.311.33:546.742–31 232
Optical Properties of Nickel Oxide—R. Newman and R. M. Chrenko. (*Phys. Rev.*, vol. 114, pp. 1507–1513; June 15, 1959.)

537.312.62:621.318.57 233
High-Speed Superconductive Switching Element Suitable for Two-Dimensional Fabrication—V. L. Newhouse and J. W. Bremer. (*J. Appl. Phys.*, vol. 30, pp. 1458–1459; September, 1959.) Results are given of experiments on the superconducting-to-normal transition of Sn films due to the magnetic field of current in an adjacent transverse film.

537.533.8 234
Electron Reflection and Secondary Electron Emission from Metallic Surfaces for Low-Energy Primary Electrons: Part 1—I. M. Bronshtein and V. V. Roshchin. (*Zh. Tekh Fiz.*, vol. 28, pp. 2200–2208; October, 1958.) A description of the apparatus and the method for measuring the reflection and the secondary electron emission coefficients of Ni in the range 0.2–30 ev. The reflection coefficient for Ni is found to be 0.13.

537.582 235
Temperature Dependence of the Work Function of Silver, Sodium and Potassium—C. R. Crowell and R. A. Armstrong. (*Phys. Rev.*, vol. 114, pp. 1500–1506; June 15, 1959.)

538.22:538.569.4 236
Sign of the Ground-State Cubic-Crystal Field Splitting Parameter in Fe^{3+}—S. Geschwind. (*Phys. Rev. Lett.*, vol. 3, pp. 207–209; September 1, 1959.) It is shown experimentally that the parameter is positive for Y=Ga garnet and Rb=Al sulphate.

538.221 237
Antiphase Antiferromagnetic Structure of Chromium—L. M. Corliss, J. M. Hastings and R. J. Weiss. (*Phys. Rev. Lett.*, vol. 3, pp. 211–212; September 1, 1959.) A model which fits the observations is suggested.

537.221 238
Direct Measurement of Domain Wall Energy—L. F. Bates and P. F. Davis. (*Proc. Phys. Soc.*, vol. 74, pp. 170–176; August 1, 1959.) The energy of a Bloch wall has been measured in a thin perminvar ring by a modification of a method used by Williams and Goertz (*J. Appl. Phys.*, vol. 23, pp. 316–323; March, 1952.)

538.221 239
The Silver-Based Heusler Alloys—E. O. Hall. (*Phil. Mag.*, vol. 4, pp. 730–744; June, 1959; plates.) The structures of some fifty alloys have been studied with a view to explaining their magnetic properties

538.221 240
Transitions from Ferromagnetism to Antiferromagnetism in Iron-Aluminium Alloys. Theoretical Interpretation—H. Sato and A. Arrott. (*Phys. Rev.*, vol. 114, pp. 1427–1440; June 15, 1959.)

538.221 241
Transitions from Ferromagnetism to Antiferromagnetism in Iron-Aluminium Alloys. Experimental Results—A. Arrott and H. Sato. (*Phys. Rev.*, vol. 114, pp. 1420–1440; June 15, 1959.)

538.221:534.213–8 242
The Behaviour of Plane Ultrasonic Waves in Homogeneously Magnetized Single Crystals—G. Simon. (*Z. Naturforsch.*, vol. 13a, pp. 84–89; February, 1958.) The velocity of ultrasonic wave propagation in ferromagnetic single crystals is affected by the magnetic state of the crystal, and the damping of waves depends on the electrical conductivity of the crystal (see also 1278 of 1959). An expression is derived for calculating these effects.

538.221:534.6–8 243
A Resonance Method for the Measurement of Ultrasonic Absorption in Ferromagnetic Specimens—H. J. Goehlich. (*Z. Naturforsch.*, vol. 13a, pp. 90–98; February, 1958.) A method is described for the measurement at 10^7 cps of sound absorption and velocity, and damping effects due to magnetic processes in small disk specimens. The underlying theory and difficulties of the method are discussed.

538.221:538.632 244
Remarks on the Measurement of the Hall Effect in Ferromagnetics—K. M. Koch, W. Rindner and K. Strnat. (*Z. Naturforsch.*, vol. 13a, pp. 113–116; February, 1958.) The importance of the accurate alignment of ferromagnetic strip specimens with the direction of the field is discussed with reference to measurements and to the separation of the ordinary from the extraordinary component of the Hall effect at low field strengths.

538.221:539.2 245
Canted Spin Arrangements—P. G. de Gennes. (*Phys. Rev. Lett.*, vol. 3, pp. 209–211; September 1, 1959.) A discussion of the "ordered" Fe-Al alloy and Sn-substituted Y-Fe garnet spin systems.

538.221:539.2:537.311.31 246
Spin-Dependence of the Resistivity of Magnetic Metals—R. J. Weiss and A. S. Marotta. (*J. Phys. Chem. Solids*, vol. 9, pp. 302–308; March, 1959.) The theory of Friedel and de Gennes (*J. Phys. Chem. Solids*, nos. 1–2, pp. 71–77; 1958.) is extended in terms of the spin-dependence of the magnetic resistivity, and applied to metals of non-half-integral spin such as Ni and Co.

538.221:621.318.134 247
The Influence of Hydrostatic Pressure on the Curie Point of a Ni-Zn Ferrite—K. Werner. (*Ann. Phys., Lpz.*, vol. 2, pp. 403–405; January 27, 1959.) The application of hydrostatic pressure up to 6000 atm. to a ferrite (15 per cent NiO, 35 per cent ZnO, 50 per cent Fe_2O_3) raises the Curie temperature by about 5°C. See also 2142 of 1954 (Patrick).

538.221:621.318.134 248
The Effect of Dispersion Corrections on the Refinement of the Yttrium-Iron Garnet Structure—S. Geller and M. A. Gilleo. (*J. Phys. Chem. Solids*, vol. 9, pp. 235–237; March, 1959.) Recalculation allowing for dispersion of the $CoK\alpha$ radiation by the metal atoms. See 3180 of 1958.

538.221:621.318.34 249
Size Effects on the Ferrimagnetic Resonance Absorption of Polycrystalline Ferrites and Garnets—H. Yonemitsu. (*J. Phys. Soc. Japan*, vol. 14, pp. 688–689; May, 1959.) Measurements at 9345 mc show that the resonance line width is of the form $a+\alpha D^2$ where D is the diameter of the spherical sample, and a, α are constants for a given sample. α depends strongly on porosity.

538.221:621.318.134:538.569.4 250
Dipolar Magnetodynamic Ferrite Modes—W. H. Steier and P. D. Coleman. (*J. Appl. Phys.*, vol. 30, pp. 1454–1455; September, 1959.) The characteristic equation for axially symmetric modes is given, and an experimental arrangement for their observation is described. Experimental and theoretical values of resonant frequency as a function of biasing magnetic field are compared, for a particular mode.

538.221:621.318.134:621.318.57 251
Uniform Rotational Flux Reversal of Ferrite Toroids—E. M. Gyorgy and F. B. Hagedorn. (*J. Appl. Phys.*, vol. 30, pp. 1368–1375; September, 1959.) A mechanism is proposed for high-speed flux reversal, and analysis gives results in very good agreement with those obtained from uniform rotation in isotropic thin films. Experimental confirmation of a high-speed switching mode in ferrite toroids is given.

538.221:621.318.134:621.372.622 252
The Efficiency of a Ferrite as a Microwave Mixer—Lewin. (See 65.)

538.221:621.318.57 253
A Contribution to the Study of Switching in a Ferromagnetic Core fed by a Perfect Voltage Source—C. Durante. (*Compt. rend. Acad. Sci., Paris*, vol. 248, pp. 3412–3414; June 15, 1959.) Using Maxwell's equations it is possible to predict behavior of a ferromagnetic core under the action of a constant voltage. Expressions are derived for the switching time and the dynamic hysteresis cycle.

538.221:621.318.57 254
Influence of Different Parameters on the Switching Time of Ferromagnetic Cores—J. Lagasse and C. Durante. (*Compt. rend. Acad. Sci., Paris*, vol. 248, pp. 3539–3540; June 22, 1959.) The expression derived in 253 above is discussed and applied to the construction of coils with cores having nearly equal switching times.

538.222 255
The Heat Capacities of Seven Rare-Earth Ethyl Sulphates at Low Temperatures—H. Meyer and P. L. Smith. (*J. Phys. Chem. Solids*, vol. 9, pp. 285–295; March, 1959.)

538.222 256
Thermal and Magnetic Properties of Praseodymium Ethyl Sulphate below 1°K—H. Meyer. (*J. Phys. Chem. Solids*, vol. 9, pp. 296–301; March, 1959.)

538.222:537.311.31 257
Theory of the Resistance Minimum in Dilute Paramagnetic Alloys—A. D. Brailsford and A. W. Overhauser. (*Phys. Rev. Lett.*, vol. 3, pp. 331–332; October 1, 1959.) The resistance minimum is explained theoretically in terms of the scattering of conduction electrons by paramagnetic ions in random solution.

538.222:538.569.4 258
Paramagnetic Resonance Line Shapes—P. Swarup. (*Canad. J. Phys.*, vol. 37, pp. 848–857; July, 1959.) A study of the line shape of the transitions of various concentrations of Cr^{+++} ions in potassium cobalticyanide and potassium aluminium alum single crystals has been made at 9300 mc. The shape changes gradually from Lorentzian to Gaussian with increasing Cr concentration. A Lorentzian shape is reported for the Gd^{+++} ion in lanthanum ethyl sulphate.

538.222:538.569.4 259
Stress and Temperature Dependence of the Paramagnetic Resonance Spectrum of Nickel Fluosilicate—W. M. Walsh, Jr. (*Phys. Rev.*, vol. 114, pp. 1473–1485; June 15, 1959.)

538.222:538.569.4 260
Pressure Dependence of the Paramagnetic Resonance Spectra of Two Dilute Chromium Salts—W. M. Walsh, Jr. (*Phys. Rev.*, vol. 114, pp. 1485–1490; June 15, 1959.) The results obtained are not adequately explained by theory.

538.222:538.569.4 261
Synthetic Ruby as a Secondary Standard for the Measurement of Intensities in Electron Paramagnetic Resonance—L. S. Singer. (*J. Appl. Phys.*, vol. 30, pp. 1463–1464; September, 1959.)

538.222:538.569.4:621.375.9 262
Controlling the Habit of Potassium Cobalticyanide Crystals—A. E. Rennie and S. Nielsen. (*Brit. J. Appl. Phys.*, vol. 10, p. 429; September, 1959.) Growth conditions affecting crystal shape are noted, with reference to the shape suitable for maser applications.

541.133:621.319.45 263
A Method of Measurement for the Objective Assessment of Electrolytes for Electrolytic Capacitors—P. Werner. (*NachrTech.*, vol. 8, pp. 467–469; October, 1958.) A quality factor for electrolytes is proposed based on a measurement of oxidation time with constant oxidation current.

548.5:621.365.42 264
Production of Crystals from Unstable Alloys—A. Fischer. (*Z. Naturforsch.*, vol. 13a, pp. 105–110; February, 1958.) A 40-kva graphite-tube oven is described for working at 2500°C and a pressure of 150 atm. The decomposition of unstable semiconductor and phosphor crystals is thereby avoided.

MEASUREMENTS AND TEST GEAR

621.3.018.41(083.74) 265
Comparison and Evaluation of Caesium Atomic-Beam Frequency Standards—J. Holloway, W. Mainberger, F. H. Reder, G. M. R. Winkler, L. Essen and J. V. L. Parry. (PROC. IRE, vol. 47, pp. 1730–1736; October, 1959.) "Caesium atomic beam frequency standards of different design have been compared, and the principal sources of errors in these devices have been studied. The unresolved discrepancy found between the standards was about 2 parts in 10^{10}. The characteristics of the standard, sources of errors, and the details of the comparison tests are discussed in this paper."

621.317.3.029.63:621.391.822 266
A Noise Source with Saturated Diode for 20-cm Wavelength and its Absolute Calibration by Comparison with a Heated Resistor—H. Prinzler. (*NachrTech.*, vol. 8, pp. 495–500; November, 1958.) Details are given of the noise generator and its control circuit, the reference standard, and the calibration circuit with trombone section which enables errors due to mismatch to be eliminated. See also 1492 of 1958 (Mollwo).

621.317.31.014.6 267
Simple dc Amplifier for Measuring Very Small Currents—G. Elliott and J. A. Radley. (*J. Sci. Instr.*, vol. 36, pp. 410–411; September, 1959.) A single-stage push-pull amplifier is used with a sensitive galvanometer to measure currents of the order of 5×10^{-6} μA. Stability precautions are listed.

621.317.311.081.1 268
Suggested Modifications to a Method for the Determination of the Absolute Ampere—M. Romanowski and R. Bailey. (*Canad. J. Phys.*, vol. 37, pp. 896–898; July, 1959.) The induction method is discussed and it is proposed that in addition to Briggs' modification (*J. Sci. Instr.*, vol. 13, pp. 127–129; April, 1936) the search-coil should be replaced by a homopolar generator, thus eliminating the need to calibrate the large mutual inductance and the problems associated with current reversal.

621.317.335.3 269
The Method of Layer Doubling—E. Biller. (*Z. angew. Phys.*, vol. 10, pp. 458–459; October, 1958.) A method is described for determining complex dielectric constants by means of standing waves in the microwave range using specimens of the same materials with lengths in the ratio 1:2.

621.317.336:029.62 270
The Measurement of Balanced Impedances at VHF—H. N. Edwardes. (*Proc. IRE (Australia)*, vol. 20, pp. 343–349; June, 1959.) A balanced standing-wave detector accurate to within about ±3 per cent is described.

621.317.34 271
Measurement of Nonlinear Distortion of Dipoles and Quadripoles—I. L. Dekker. (*PTT-Bedrijf*, vol. 9, pp. 1–9; April, 1959.) Basic circuits for the measurement of nonlinear distortion are described. Results obtained using

these circuits show the importance of high-quality resistors in transmission equipment.

621.317.39:531.78 272

Sensitive Transducers use One-Tube Crystal Oscillator—L. J. Rogers. (*Electronics*, vol. 32, pp. 48–49; October 2, 1959.) A single tube oscillator for use with electromechanical transducers is described. A sensitivity up to 250 v/pf of transducer capacitance with long-term stability equivalent to 4 parts in 10^3 is obtained.

621.317.4:537.311.33 273

Small Magnetic-Field Mapping Probes of Thin Semiconducting Films—J. W. Buttrey. (*Rev. Sci. Instr.*, vol. 30, pp. 815–817; September, 1959.) "The Hall effect in thin semiconducting films has been employed to produce a magnetic field mapping probe of very small active area. Germanium probes having active areas of approximately 10 square microns were found to have a sensitivity of approximately 100 oersteds. Results obtained on thin InSb films indicate small area probes of this material should be sensitive to fields smaller than five oersteds."

621.317.44.087.4 274

Sensitive Recording Magnetic Fluxmeter—P. Lerond and A. Thulin. (*J. Sci. Instr.*, vol. 36, pp. 388–389; September, 1959.) A ballistic galvanometer with a taut suspension is used. Its restoring torque is balanced out by photo-electric-mechanical feedback governed by the galvanometer spot position.

621.317.723 275

Using Feedback in Electrometer Design—D. Allenden. (*Electronics*, vol. 32, pp. 71–73; October 9, 1959.) The design of a high-sensitivity wide-band electrometer is described, for measuring currents in the range 10^{-11}–10^{-15} A. Feedback-path integration is an optional feature for use when maximum bandwidth is the main requirement.

621.385.3:621.317.723 276

The Development of a New Type of Electrometer Valve—Frommhold. (See 359.)

621.317.729 277

New Method for Mapping Electric Fields—G. M. Gershtein. (*Radiotekh. Elektron.*, vol. 4, pp. 137–139; January, 1959.) The method is based on the Shockley-Ramo theorem of induced currents. The electric-field intensity along the line of motion of a charged probe is represented by a CRO trace of the current induced in the probe. Two models are described, using a) rectilinear probe movement, and b) a fixed probe adjacent to a rotating cyclinder with segmented structure.

621.317.75.001.4:621.373.44 278

Spectrum Generator for Testing of Pulse-Height Analysers—J. E. Draper and W. J. Alston, III. (*Rev. Sci. Instr.*, vol. 30, pp. 805–809; September, 1959.) The generator produces voltage pulses of width 1–4 μsec having three pulse-height frequency distributions: a) delta shaped over the range 0–100 v, or 0–0.1 v; b) uniform over the same range; c) triangular.

OTHER APPLICATIONS OF RADIO AND ELECTRONICS

535.854:621.3.029.6 279

Asymmetric Fringes in Multiple-Beam Systems—J. L. Farrands. (*Optik*, vol. 16, pp. 14–18; January, 1959. In English.) The asymmetrical sawtooth shape of interference fringes can be produced by the addition of a coherent wave of variable phase. Suitable apparatus is described and applications for microwave interferometry are noted.

537.534.9:620.18 280

Improved Method of Etching by Ion Bombardment—T. K. Bierlein and B. Mastel. (*Rev. Sci. Instr.*, vol. 30, pp. 832–833; September, 1959.) The etching process involves 165 mc excitation to increase ionization in the chamber.

621–52:629.113 281

Electronics guides your Car—V. K. Zworykin and L. E. Flory. (*Radio and Electronics*, vol. 30, pp. 99–101, 104; April, 1959.) Report of stages in the development of a vehicle control system from one in which the guidance equipment is part of the road, to one which is completely automatic, with equipment in both vehicle and road surface.

621.318.381.078.3:538.569.4 282

A Synchronized Autodyne Detector and its Application to the Stabilization of Magnetic Fields with Proton Resonance—W. Müller-Warmuth and P. Servez-Gavin. (*Z. Naturforsch.*, vol. 13a, pp. 194–203; March, 1958.) With the circuit described a relative field stability better than 1 part in 10^6 can be obtained.

621.36:537.322 283

Theory of Reversible Electric Heating—R. Dahlberg. (*Z. angew. Phys.*, vol. 10, pp. 467–470; October, 1958.) Theoretical treatment of thermoelectric heating in line with the investigation of cooling (3449 of 1959).

621.362:621.387 284

Thermoelectric Properties of the Plasma Diode—Lewis and Reitz. (See 366.)

621.384.611 285

Stochastic Acceleration in a 5-mev Cyclatron—R. Keller, L. Dick and M. Fidecaro. (*Compt. rend. Acad. Sci., Paris*, vol. 248, pp. 3154–3156; June 1, 1959.) A 5-mev cyclotron has been constructed fed by a generator which, unlike that of a synchrocyclotron, does not follow a frequency program but produces a voltage varying in a random manner. The resulting beam is more intense than that of a synchrocyclotron of corresponding voltage.

621.384.612.11 286

The World's Largest Synchrophasotron—A. A. Kolomenskii and M. S. Rabinovich. (*Priroda*, No. 8, pp. 57–61; August, 1959.) A general description of the accelerator built in 1957. It has a magnetic ring weighing over 36,000 tons, and diameter 70 meters. Protons can be accelerated to an energy of 10^{10} ev.

621.384.8 287

A High-Resolution Eletrostatic Lens used as an Analyser of Electron Velocities—A. N. Kabanov and V. I. Milyutin. (*Radiotekh. Elektron.*, vol. 4, pp. 109–119; January, 1959.) Description of the design and input circuit of a single cylindrical es lens operating as a velocity analyzer with a resolving power of 60,000:1.

621.384.8:621.385.833 288

Construction of an Electrostatic Velocity Filter. Use in Electron Microdiffraction—R. Beaufils. (*Compt. rend. Acad. Sci., Paris*, vol. 248, pp. 3145–3147; June 1, 1959.) The apparatus, which is used in obtaining electron-diffraction diagrams for alloys, eliminates from a beam all electrons suffering an energy loss >4 ev.

621.385.833 289

An Electron Microscope of Universal Applicability for Electron Diffraction—H. Bethge. (*Optik*, vol. 16, pp. 33–42; January, 1959.) The instrument described incorporates three es lenses and one intermediate magnetic lens. Accessories for electron-diffraction investigations are described *ibid.*, pp. 43–49 (Bethge and Brauer).

621.385.833 290

An Electron-Lens System Excited by Permanent Magnets with a New Astigmatism Compensator—H. Kimura and S. Katagiri. (*Optik*, vol. 16, pp. 50–55; January, 1959. In English.)

621.385.833 291

The Combined Effect of Phase and Amplitude Contrast in Electron-Microscope Images—F. Lenz and W. Scheffels. (*Z. Naturforsch.*, vol. 13a, pp. 226–230; March, 1958.) The effect of defocusing on contrast is investigated.

621.385.833:535.767 292

Some Remarks on the Accuracy Obtainable in Electron Stereomicroscopy—R. I. Garrod and J. F. Nankivell. (*Optik*, vol. 16, pp. 27–29; January, 1959. In English.) The uncertainty in the calibration of the stereo-angle is not likely to be a major source of error, contrary to the suggestion of Helmcke and Orthmann (1183 of 1956). See also *Brit. J. Appl. Phys.*, vol. 9, pp. 214–218; June, 1958.

621.398 293

Variable Audio-Frequency Tele-voltmeter—H. R. Harant. (*Proc. IRE (Australia)*, vol. 20, pp. 338–343; June, 1959.) A time-division multiplex telemetry system is described for monitoring up to 22 voltages at a remote installation.

621.398:621.816 294

Amplitude-Modulation Radio-Telemetry of Nerve Action Potentials—R. M. Morell. (*Nature*, vol. 184, pp. 1129–1131; October 10, 1959.) Description of a telemetry system in which a pulse is transmitted to a specimen at a distant point and the response to the stimulus is transmitted to the point of origin.

621.398:621.3.066 295

Electromechanical Switches for Telemetering Systems—A. S. Kramer. (*Electronics*, vol. 32, pp. 54–55; October 2, 1959.) A table of specifications, performance data and applications is given.

621.398:621.318.57 296

Electronic Commutators in Multiplex Telemetering—A. S. Kramer. (*Electronics*, vol. 32, pp. 76–77; September 25, 1959.) A table of characteristics and suggested applications of some commutators for use with time-division multiplex is given.

621.398:621.396.934 297

Missile-to-Ground Telemetry of Variable Data—K. Zeilinger. (*Elektron. Rundschau*, vol. 12, pp. 345–346; October, 1958.) Details are given of a French telemetry system. A 2.5-watt airborne transmitter of length 19.5 cm and diameter 10 cm provides five FM channels, one of which has 15 switched signal inputs, which modulate the amplitude of a 90-mc carrier. Methods of data recording and evaluation are also described.

621.398:621.397.9:629.19 298

System Design Criteria for Space Television—A. J. Viterbi. (*J. Brit. IRE*, vol. 19, pp. 561–570; September, 1959.) The theory and design of a very-narrow-band telemetry system is described for relaying to the earth the images of planets recorded by a space vehicle. The main feature is the phase-locked-loop discriminator which enables very-narrow-band signals to be separated from noise. For a typical mission to Venus the received power would be about 1.6×10^{-18} watts.

PROPAGATION OF WAVES

621.391.812.6 299

Simple Methods for Computing Tropospheric and Ionospheric Refractive Effects on

Radio Waves—S. Weisbrod and L. J. Anderson. (PROC. IRE, vol. 47, pp. 1770–1777; October, 1959.) "The paper describes a simple and accurate method for computing ionospheric and tropospheric bending. The only assumptions made are that the refractive gradient is radial and that the refractive index profile can be approximated by a finite number of linear segments whose thickness is small compared with the earth's radius. These assumptions are readily justifiable in all practical cases. Since there are no limitations on the angle of elevation and the shape of the refractive index profile, the method has a wide application and it is extended to cover other refractive effects such as retardation, Doppler error and Faraday rotation."

621.391.812.62 300
Radio-Wave Scattering by Tropospheric Irregularities—A. D. Wheelon. (*J. Res. Nat. Bur. Stand.*, vol. 63D, pp. 205–233; September/October, 1959.) A review of theoretical work, published and unpublished, on radio-wave scattering by turbulent irregularities. 81 references.

621.391.812.62.029.64 301
Tests Conducted over Highly Reflective Terrain at 4000, 6000 and 11000 Mc/s—A. Oxehufwud. (*Commun. and Electronics*, pp. 265–270; July, 1959.) A report of aerial-height/path-loss investigations over four highly reflective paths.

621.391.812.621 302
Synoptic Study of the Vertical Distribution of the Radio Refractive Index—B. R. Bean, L. P. Riggs and J. D. Horn. (*J. Res. Nat. Bur. Stand.*, vol. 63D, pp. 249–254; September/October, 1959.) An exponential correction applied to the refractive-index height distribution facilitates the analysis of air-mass characteristics.

621.391.812.63 303
The Propagation of Fading Waves—R. P. Mercier. (*Phil. Mag.*, vol. 4, pp. 763–776; June, 1959.) A scalar wave with random variations of amplitude and phase across the wave front is assumed as a simple model of a radio wave after it has left the ionosphere. The fluctuating in-phase and quadrature components are assumed to have a Gaussian probability distribution which is described in terms of two parameters: the first measures the extent to which the signal is randomly phased and the second the change in phase of the modulation on the signal. Records of daytime fading on 16 kc analyzed on this basis show that the modulation is highly correlated at the ionosphere and that it is generally phase modulation.

621.391.812.63 304
Some Problems of Radio Wave Scattering in the Ionosphere—V. D. Gusev. (*Radiotekh. Elektron.*, vol. 4, pp. 12–16; January, 1959.) Investigation of the part played by inhomogeneous waves in the angular spectrum of a scattered field when the ionosphere is illuminated by plane and diverging waves. A space-time correlation function is derived

621.391.812.63 305
Correlation of Waves of Different Frequency after Passage through a Layer of a Statistically Inhomogeneous Medium—M. F. Bakhareva. (*Radiotekh. Elektron.*, vol. 4, pp. 88–96; January, 1959.) Correlation coefficients are obtained for the amplitude and phase fluctuations of two waves of different frequency traversing a medium with large random inhomogeneities of refractive index. A comparison is made with experimental data obtained by frequency-scatter sounding of the ionosphere. Values obtained for the magnitude of inhomogeneities in the F and E layers coincide with values found by correlation at various points.

621.391.812.63 306
The Relations between Field Strength and the Limits of the Transmission-Frequency Range (LUF, MUF)—B. Beckmann. (*Nachrtech. Z.*, vol. 11, pp. 523–528; October, 1958.) A single formula is derived for calculating field strength in the frequency range from LUF to MUF using LUF, MUF and FOT (OWF) data. Satisfactory agreement with measured field-strength values is obtained.

621.391.812.63:551.510.535 307
The D Region of the Ionosphere—B. Bjelland, O. Holt, B. Landmark and F. Lied. (*Nature*, vol. 184, suppl. no. 13, pp. 973–974; September 26, 1959.) Preliminary results are given of observations at Kjeller and Tromsö, Norway, of ionospheric cross-modulation and partial reflections from the D region.

621.391.812.63.029.45 308
A Study of VLF Field-Strength Data both Old and New—J. R. Wait. (*Geofis. pura e appl.*, vol. 41, pp. 73–85; September–December, 1958. In English.) Attenuation rates are derived from VLF data obtained in 1922/1923 by Round *et al.* and from recent measurements. For middle latitudes daytime rates of less that 2 db per 1000 km path length are found. These accord with values derived from "spherics" waveforms and are compatible with mode theory (see, *e.g.*, 2869 of 1958). Over 40 references.

621.391.812.63.029.62:523.75 309
The S.I.D. Effect on the VHF Scatter Propagation associated with the Great Solar Outburst of July 29, 1958—T. Obayashi. (*Rept. Ionosphere Research Japan*, vol. 12, pp. 336–338; September, 1958.) The fade-out of a 49.68-mc scatter-propagation signal coincident with solar flare is considered in relation to an enhancement of the type observed earlier by Bailey *et al.* (243 of 1956.)

621.391.812.7 310
Observation of Multipath Propagation over the Short-Wave Transmission Path Osaka–Frankfurt-on-Main—B. Beckmann and K. Vogt. (*Nachrtech. Z.*, vol. 11, pp. 519–523; October, 1958.) Analysis and discussion of results obtained during reception of pulse transmissions between Osaka and London at 14 and 19 mc. Observations were made in the forward and backward directions and include back scatter reception of 19.56-mc transmissions from London.

621.391.812.8 311
Errors in Ionospheric Forecasting—C. M. Minnis and G. H. Bazzard. (*Electronic Radio Eng.*, vol. 36, pp. 380–383; October, 1959.) Errors due to incorrect estimation of solar activity, and consequently the vertical-incidence critical frequency, are analyzed. It is concluded that a typical value for the standard deviation of the error in forecasting f_0F_2 is 15 per cent, and n forecasting f_2E, 5.5 per cent.

621.391.826.2 312
Study at 1046 Megacycles per Second of the Reflection Coefficient of Irregular Terrain at Grazing Angles—R. E. McGavin and L. J. Maloney. (*J. Res. Nat. Bur. Stand.*, vol. 63D, pp. 235–248; September/October, 1959.) The reflected signal is considered to be made up of a specularly reflected component and a Rayleigh-distributed component, and the contributions of these components are examined as a function of terminal height.

RECEPTION

621.391.81.029.62/.64 313
On the Graphical Method of Calculation of the Field Strength for Effective Earth Radii other than 4/3 Times the Actual Radius and for any Antenna Heights and Frequencies—K. Tao and K. Sawaji. (*J. Radio Research Labs, Japan*, vol. 6, pp. 311–372; April, 1959.) Field-strength curves for two ground constants, frequencies from 30–10,000 mc, and antenna heights up to 20,000 meters have been worked out by a graphical method which is simpler than that proposed by CCIR. 48 graphs are reproduced.

621.391.812.63:621.396.666 314
Reception of Space-Diversity Transmitters—J. W. Koch. (*Wireless World*, vol. 65, pp. 512–514; November, 1959.) Transmissions on 9.5 mc from widely spaced and closely spaced transmitters in England have been received at Boulder, U.S.A. Results show that the resultant field at the receiver has a Rayleigh distribution; there is no diversity gain.

621.391.82 315
Radio Interference: Part 6—The Control of Radio Interference—C. W. Sowton. (*P.O. Elec. Engrg. J.*, vol. 52, pt. 1, pp. 43–46; April, 1959.) The preparation of specifications and codes of practice is surveyed and details of U.K. regulations are given.
Part 5: 954 of 1959 (Sowton and Britton).

621.396.62:621.376.332 316
FM Receiver using New Dynamic Limiter—J. G. Spencer. (*Wireless World*, vol. 65, pp. 492–498; November, 1959.) The receiver described incorporates a recently developed limiter and discriminator circuit [1379 of 1958 (Head and Mayo)].

STATIONS AND COMMUNICATION SYSTEMS

621.376.5 317
Investigations of Pulse Modulation Methods—H. Hönicke. (*NachrTech.*, vol. 8, nos. 10 and 11, pp. 456–460 and 501–510, October, 1958; and vol. 9, pp. 29–35; January, 1959.) The frequency spectra of PAM, PPHM, and PWM pulse trains for various sampling methods are calculated using Fourier transformation, and formulas giving spectral components are tabulated. Modulator circuits shown were used for the experimental verification of results. Modulation and demodulation techniques are described and the practical limitations of sampling theorems based on an ideal low-pass filter are discussed with reference to measurements.

621.39:621.372.8 318
Waveguide as a Long-Distance Communication Medium—Karbowiak. (See 20.)

621.395.4+621.397.13]:621.315.212 319
Multichannel Systems along Coaxial Cables—J. Bauer. (*Tech. Mitt. PTT*, vol. 36, pp. 423–435; November 1, 1958. In German and French.) Expanded version of 2958 of 1958.

621.396:523.1 320
Searching for Interstellar Communications—G. Cocconi and P. Morrison. (*Nature*, vol. 184, pp. 844–846; September 19, 1959.) Discussion of the possible frequency, transmitted power and form of signals originating in an interstellar communication system.

621.396:629.19 321
Exotic Radio Communications—J. R. Pierce. (*Bell Lab. Record*, vol. 37, pp. 323–329; September, 1959.) Possible communication systems of the future, using earth satellites as passive and active reflectors, are discussed.

621.396.4:621.394.4 322
Voice-Frequency Telegraphy System Type FM-WTK 3/6 for Short-Wave Telephone Links—H. J. Neumann. (*Nachrtech. Z.*, vol. 11, pp. 510–514; October, 1958.)

621.396.43:523.5 323
Methods and Equipment for Meteor Scatter Propagation—E. Roessler. (*Nachrtech. Z.*, vol. 11, pp. 497–503; October, 1958.) A table comparing existing scatter links is included. See also 4198 of 1959 (Grosskopf).

SUBSIDIARY APPARATUS

621-526 324
A Digital Remote Position Control—K. G. Hilton. (*Electronic Engng.*, vol. 31, pp. 512–519; September, 1959.) A description of a servo shaft-position control system using digital techniques throughout. The logical circuit arrangements and methods of stabilizing are discussed, together with the design procedure.

621.311.61.078:621.375.4 325
Inverse Feedback Stabilizes Dry-Cell Current Sources—G. E. Fasching. (*Electronics*, vol. 32, p. 78; October 9, 1959.) A transistor emitter-follower circuit enables constant heavy currents to be drawn from dry cells despite variations in cell voltage.

621.311.62:621.382.2 326
Power Supply Design using Silicon Diodes—H. A. Kampf. (*Electronics*, vol. 32, pp. 60–62; October 2, 1959.)

621.311.62:621.382.3 327
Constant-Current-Coupled Transistor Power Supply—E. Gordy and P. Hasenpusch. (*Electronics*, vol. 32, pp. 60–61; October 9, 1959.) By feeding a constant current through a fixed resistor across the supply output, an unattenuated error voltage can be applied to the error-correcting amplifier of a series-regulated power supply.

621.311.62.078.3:621.382.3 328
Designing Highly Stable Transistor Power Supplies—E. Baldinger and W. Czaja. (*Electronics*, vol. 32, pp. 70–73; September 25, 1959.) Design techniques are summarized and a circuit is described with over-all stability $\pm 250\,\mu$v and $<40\,\mu$v/h.

621.314.5:621.318.57 329
Transistors and Saturable-Core Transformers as Square-Wave Oscillators—G. C. Fleming. (*Electronic Engng.*, vol. 31, pp. 543–545; September, 1959.) "The use of transistors as switches for the dc supply to saturable core transformers is described and it is shown that by this means small and efficient convertors and invertors can be constructed. The common base, common emitter and common collector configurations are considered and methods of obtaining a multi-phase output are described."

621.316.72.078 330
A Method of Reducing the Time Lag of Transducers which have an Exponential Response—L. Whitlow and M. J. Porter. (*Electronic Engng.*, vol. 31, pp. 536–542; September, 1959.) The response of a transducer such as a thermocouple is corrected for phase and amplitude by adding its output voltage to its amplified derivative. Details of a drift-corrected dc amplifier and highly stable power supply are given.

621.316.722 331
The Stabilization of DC Voltages by Switched Transistors—G. Meyer-Brötz. (*Elektron. Rundschau*, vol. 12, pp. 342–344; October, 1958.) Stabilizing circuits are discussed in which transistors function as continuous-control devices or as switches driven by a Schmitt trigger circuit. Comparison is also made with a transistor-switched rectifier circuit.

621.316.722.078 332
Method of Amplitude Control of AC Signals—J. B. Cornwall. (*J. Sci. Instr.*, vol. 36, pp. 395–396; September, 1959.) "A circuit for controlling the rms value of an ac signal is analyzed and practical results are discussed. The speed of response is such that for rates of change of 2.5 per cent per second the output is controlled continuously within 1 per cent. An alternative arrangement for maintaining, at a preset level, the peak value of repetitive pulses is also given."

621.316.722.1:621.383.2 333
Zener Diodes as Reference Sources in Transistor Regulated Power Supplies—R. E. Aitchison. (*Proc. IRE* (*Australia*), vol. 20, pp. 350–351; June, 1959.) A summary of the relevant properties of Zener diodes including a figure of merit representing the maximum value by which supply variations may be reduced. Methods for controlling the over-all temperature coefficient are considered.

621.352 334
Ammonia-Vapour-Activated Batteries—H. S. Gleason, J. M. Freund, L. J. Minnick and W. F. Meyers. (*J. Electrochem. Soc.*, vol. 106, pp. 157–160; March, 1959.)

TELEVISION AND PHOTOTELEGRAPHY

621.397.132 335
NTSC Colour-Television Signals—J. Davidse. (*Electronic Radio Eng.*, vol. 36, pp. 370–376; October, 1959.) A consideration of some statistical properties of NTSC color television signals obtained from normal picture material. Measurement equipment is described.

621.397.132 336
Propagation Tests of Colour Television in Band I with the Modified NTSC System—K. Bernath. (*Tech. Mitt. PTT*, vol. 36, pp. 413–423; November 1, 1958. In German and French.) Subjective assessments of picture quality of 625-line test transmissions were made by several observers at various localities within 60 km of the transmitter. Conditions of observation and reception and an analysis of the assessments are tabulated.

621.397.132:621.391.83 337
Gradation Correction in Colour Television—J. Kaashoek. (*Nachrtech. Z.*, vol. 11, pp. 515–518; October, 1958.) A circuit is described for obtaining variable gamma correction which depends on luminance and is free from other color distortion. The gamma range covered is 0.4–1 and the correction can be made color-dependent.

621.397.62:621.398 338
The Recording of TV Viewing and Radio Listening Statistics—E. W. P. Harris and G. D. Robinson. (*Brit. Commun. Electronics*, vol. 6, pp. 510–514; July, 1959.) General description of an automatic system in which information regarding the receiver switching is relayed by land-lines to a central station where it is recorded on perforated tape and then made immediately available for visual assessment or for data processing using punched cards.

621.397.74 339
Communications in Independent Television—L. F. Mathews. (*J. Brit. IRE*, vol. 19, pp. 545–552; September, 1959.) The provision of radio and cable links for the interchange of television programs between different transmitters, for outside broadcasts and for control and monitoring services is described. A new vision and sound monitoring link between London and Birmingham operates at 7304 and 7404 mc; associated 460-mc equipment provides an engineers' speech channel and an automatic alarm system.

621.397.9:621.039 340
The Use of Television for the Microscopical Examination of Radioactive Metals—E. C. Sykes. (*J. Brit. IRE*, vol. 19, pp. 555–560; September, 1959.) Measurement of microstructural features can be made from the monitor screen.

621.397.9:621.398:629.19 341
System Design Criteria for Space Television—Viterbi. (See 298.)

TUBES AND THERMIONICS

621.382.2/.3 342
The Characteristics and the Noise of Silicon *p-n* Diodes and Silicon Transistors—B. Schneider and M. J. O. Strutt. (*Arch. elektr. Übertragung*, vol. 12, pp. 429–440; October, 1958.) Carrier recombination and generation is considered as a cause of the differences between the characteristics of Si and Ge diodes. Characteristic curves for Si diodes are derived taking account of recombination and diffusion. A method of noise measurement in the forward direction is described which gives results in agreement with the calculated values of differential admittance and noise. Noise-figure formulas are also derived for Si transistors allowing for recombination in the emitter depletion layer.

621.382.2 343
Zener Diode Characteristics—M. R. Nicholls. (*Electronic Engng.*, vol. 31, p. 559; September, 1959.) Measurements on Zener diodes show that the V/I relation is exponential for currents below the "constant-voltage values." This region may be useful for conversion of linear to logarithmic functions.

621.382.2:621.374.4.029.65 344
Improved Diode for the Harmonic Generation of Millimetre and Submillimetre Waves—R. S. Ohl, P. P. Budenstein and C. A. Burrus. (*Rev. Sci. Instr.*, vol. 30, pp. 765–774; September, 1959.) The performance and stability of Si diodes can be greatly improved by bombarding the Si surface with positive ions. The methods of bombardment are described and also the method of mounting the Si, the construction of two waveguide circuits for harmonic generation and the optimum working conditions. A comparison is made between measured and calculated HF output.

621.382.2:621.372.622 345
Delay Distortion in Crystal Mixers—T. Kawahashi and T. Uchida. (IRE TRANS. ON MICROWAVE THEORY AND TECHNIQUES, vol. MTT-7, pp. 247–256; April, 1959. Abstract, PROC. IRE, vol. 47, p. 1286; July, 1959.)

621.382.2:621.376.233 346
The Germanium Diode in Demodulator Circuits—J. Meinhardt. (*Nachrtech.*, vol. 8, pp. 489–495; November, 1958.) The design of demodulator circuits is discussed on the basis of two-pole theory and a special analysis of the diode characteristic.

621.382.22 347
Investigation of the Impedances of Germanium Diodes and Diode Circuits—W. Drechsel. (*NachrTech.*, vol. 8, pp. 482–488; November, 1958.) Measurements on point-contact diodes are discussed. The results provide an indication of the performance characteristics of diode rectifier circuits.

621.382.3:538.63 348
Transistors in Magnetic Fields—P. C. Trivedi and G. P. Srivastava. (*Electronic Radio Eng.*, vol. 36, pp. 368–370; October, 1959.) Changes in the value of α' of *p-n-p* alloy junction AF transistors have been investigated experimentally. The results show a decrease of about 10 per cent with an increase of transverse field of approximately 8 kg. Longitudinal fields do not show a marked effect in AF transistors but an increase in current gain has been observed in RF transistors.

621.382.3.012.8 349
Transistor "h" Parameters—R. Hutchins and J. D. Martin. (*Electronic Radio Eng.*, vol. 36, pp. 383–387; October, 1959.) Modifications to a Boothroyd-Almond bridge (214 of 1955), which permit the measurement of complex hybrid parameters, are shown to facilitate the derivation of corresponding equivalent circuits.

621.385.032.212.3 350
The Magnesium Oxide Cold Cathode and its Application in Vacuum Tubes—A. M. Skellett, B. G. Firth and D. W. Mayer. (PROC. IRE, vol. 47, pp. 1704–1712; October, 1959.) The preparation of the cathode and its operation are described and details of surface potential, emission and other measurements are given. Its application in a pentode valve is discussed.

621.385.032.213.13 351
Current Fluctuations in the Oxide Cathode—M. Chisholm and L. Jacob. (*Nature*, vol. 184, suppl. no. 14, pp. 1058–1059; October 3, 1959.) Slow, marked fluctuations in both the conduction and emission currents were observed for certain values of anode potential. Over the temperature range explored, a threshold at 1100°K was indicated.

621.385.032.213.13:621.327.5 352
Cathode Emission Measurements in Low-Pressure Discharges—A. D. Forster-Brown and M. A. Cayless. (*Brit. J. Appl. Phys.*, vol. 10, pp. 409–411; September, 1959.) A probe method is used to measure zero-field emission. Good agreement is obtained with earlier methods [*e.g.*, 649 of 1958 (Cayless)].

621.385.032.213.63:537.226 353
New Properties of Electron Emission of Systems containing Thin Dielectric Layers—M. I. Elinson and A. G. Zhdan. (*Radiotekh. Electron.*, vol. 4, pp. 135–137; January, 1959.) An investigation is reported of the emission characteristics of a W-SiO_2-SiO_2C system. A layer of quartz is deposited from the vapor phase onto a tungsten point fixed to a curved base. Carbon is introduced into the quartz layer by thermal diffusion and electrical contact is made between the tungsten and the external layer. A stable field emission is observed. Breakdown occurs at 5–10 kv. After breakdown the emitter acquires a typical "crater" shape and anomalous emission is observed. Lowering the temperature from 650°C to room temperature increases the emission current. Possible explanations of the phenomena are noted and the constant-current voltage/temperature characteristic for an experimental diode is shown.

621.385.032.26 354
Nonlaminar Flow in Magnetically Focused Electron Beams from Magnetically Shielded Guns—T. W. Johnston. (*J. Appl. Phys.*, vol. 30, pp. 1456–1457; September, 1959.) An experimental confirmation of theory.

621.385.032.269.1 355
Trajectory Plotting in Electron Guns—G. D. Archard. (*Proc. Phys. Soc.*, vol. 74, pp. 177–182; August 1, 1959.) "A method of representing space charge on a resistance network analog by means of leak resistances is described and applied to the determination of trajectories in several conventional and unconventional electron guns."

621.385.1 356
Planar Diode Flow and the Langmuir Limit—H. Moss. (*J. Electronics Control*, vol. 6, pp. 403–414; May, 1959.) A treatment based on simple electron ballistics is given, and the results are discussed in relation to those of Langmuir's classical work.

621.385.1:537.533 357
Application of the Relaxation Method to the Solution of Space-Charge Problems—P. A. Lindsay. (*J. Electronics Control*, vol. 6, pp. 415–431; May, 1959.)

621.385.1:621.391.822.33 358
On the Problem of the Flicker Noise Spectrum—A. N. Malakhov. (*Radiotekh. Electron.*, vol. 4, pp. 54–62; January, 1959.) A brief survey of experimental and theoretical results on the problem of flicker noise in various systems. Possible methods of eliminating or reducing this noise are discussed. 41 references.

621.385.3:621.317.723 359
The Development of a New Type of Electrometer Valve—E. A. Frommhold. (*Nachr-Tech.*, vol. 8, pp. 461–466; October, 1958.) Design and constructional problems relating to electrometer and galvanometer tubes are discussed and two new tubes are described and compared with existing types.

621.385.6 360
Defocusing of a Plane Cycloidal Electron Beam Influenced by a Space-Charge Force—K. Ya. Lizhdvoĭ. (*Radiotekh. Elektron.*, vol. 4, pp. 120–125; January, 1959.) Investigation of the traveling of a plane electron beam in crossed electric and magnetic fields. An expression is found for the estimation of the surface charge acting on the outer electrons of the beam in the direction of the magnetic field. Conditions are determined under which it is necessary to compensate the space charge in order to prevent a large divergence in the beam.

621.385.6:621.375.9:621.372.44 361
The Quadrupole Amplifier, a Low-Noise Parametric Device—R. Adler, G. Hrbek and G. Wade. (PROC. IRE, vol. 47, pp. 1713–1723; October, 1959.) Unusually low noise combined with high stable gain is achieved by the action of a transverse quadrupole field upon a fast cyclotron wave. A description of the device and an analysis of its amplification process are given and experimental tubes operating in frequency bands between 400 and 800 mc are described.

621.385.6:621.375.9:621.372.44 362
Use of the Principles of Conservation of Energy and Momentum in connection with the Operation of Wave-Type Parametric Amplifiers—Pierce. (See 89.)

621.385.62 363
Harmonic Current Growth in Velocity-Modulated Electron Beams—T. B. Mihran. (*J. Appl. Phys.*, vol. 30, pp. 1346–1350; September, 1959.) Growth was discovered in the results of a series of disk-electron calculations on bunching in klystrons, and second-harmonic growth was observed experimentally. A physical explanation is given.

621.385.63 364
Interaction of a Modulated Electron Beam with a Travelling Electromagnetic Wave—V. N. Shevchik and I. P. Oleĭnikova. (*Radiotekh. Elektron.*, vol. 4, pp. 128–130; January, 1959.) A brief mathematical analysis.

621.385.63 365
Travelling-Wave Valves—C. H. Dix. (*Wireless World*, vol. 65, pp. 476–481; November, 1959.) Interaction processes between electrons and fields in the two main types of traveling-wave tube are discussed.

621.387:621.362 366
Thermoelectric Properties of the Plasma Diode—H. W. Lewis and J. R. Reitz. (*J. Appl. Phys.*, vol. 30, pp. 1439–1445; September, 1959.) The thermoelectric properties of a gas-filled diode with a high density of positive ions are discussed in detail and the results of the analysis are compared with experimental data.

This common game is a sequential machine. Its inputs are the possible moves at a given state. Its state is the arrangement of numbers at a given time.

States in a Sequential Machine

A "sequential machine" is any device producing prescribed sequences of outputs in response to given sequences of inputs. The theoretical problem of designing a machine, satisfying certain specifications with the fewest possible number of states, is now under study by IBM scientists.

The operation of a sequential machine is not necessarily completely specified. Some states may have no specified transitions for certain inputs, and some states may have no assigned outputs. For this general case, a technique has been developed for reducing a given machine to an equivalent machine with a minimum number of states. The procedure is to construct a state diagram of the machine which describes input and output sequences. Then through the use of a transition-matrix representation, a minimum-state diagram is obtained, which is equivalent to the original machine in the sense that it will produce the same sequences of outputs for the given sequence of inputs.

Earlier reduction procedures have been applicable only to state diagrams having known transitions for each input at each state. The extension of the procedure is important since many practical sequential machines (such as computers) require a specified operation for only a certain set of sequences of inputs.

IBM® RESEARCH

Investigate the many career opportunities available in exciting new fields at IBM.
International Business Machines Corporation, Dept. 645N, 590 Madison Avenue, New York 22, New York

From the home of *Planned Pioneering*

ALL NEW!

Ready for you at the

IRE Show*

Booths 3608-3610

439 RECORDING OSCILLOGRAPH . . . ALL NEW inside and out — utility engineered features: 14 channels; data numbering; weight 15 lbs.; rugged advanced design.

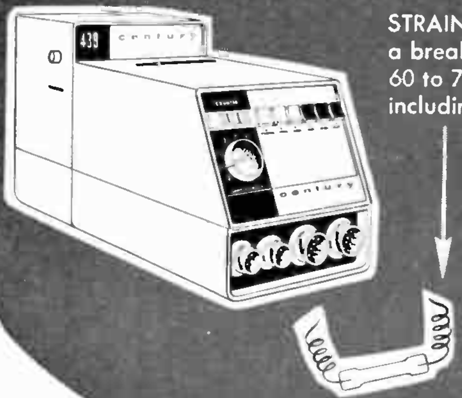

STRAINISTOR — First commercially available new Strainistor is a break-thru in ultra-sensitive strain sensing elements. Sensitivity 60 to 70 times greater than those of any other commercial units, including wire and foil units.

450 PORTABLE RECORDER NEW AND NEEDED! A utility engineered, reasonably priced null-balanced portable recorder with SELF CONTAINED POWER. Lightweight, adjustable speeds, accuracy sensitivity, and other features usually only available in external powered models.

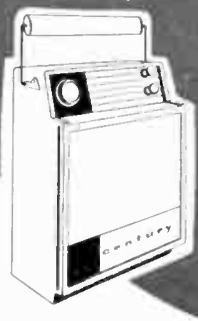

20-E QUICK-VIEW COLORBAR VISUAL MONITOR A new visual monitor with EEZE-READING bold bright colorbars and simple operational hook-up. Ideal for observation of strain gage network alignment; magnetic tape editing; jet engine function analysis, etc.

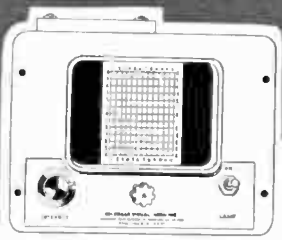

* *Units Available for delivery now*

Century OF TULSA

century
ELECTRONICS and INSTRUMENTS, INC.

The home of Planned Pioneering
TWX - TU 1407 Phone LU 4-7111
P. O. Box 6216, Pine Station, Tulsa 10, Oklahoma

SERVICED BY
Systems Engineering Offices of Airsupply-Aero Engineering Division
THE GARRETT CORPORATION . . . In all principal cities . . .

Opportunities available for Electronic Engineers in research and development. Contact Personnel Manager.

Kodak reports on:

a simple-minded stunt with a little honest fudging . . . a little something for the taxpayers . . . what the big wheels do

A tough window for the infrared

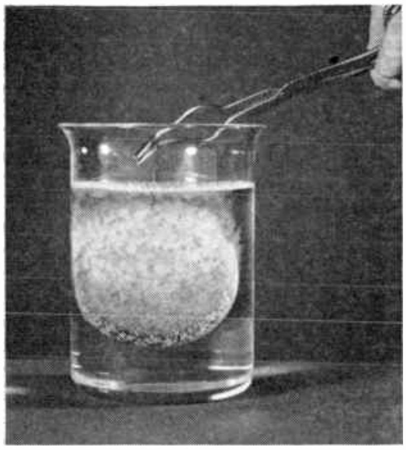

Here represented is a nice piece of infrared technology. We take pride in it, even though they tell us it will never replace the foot-soldier.

Our simple-minded stunt photo demonstrates that a 3-inch flat of the new *Kodak Irtran Optics, Type AB-1* can be fused so securely into a stainless steel mounting that plunging it at 200°C into tap water generates steam but does no harm.

We have developed this *Irtran* material for transmitting in structurally adequate thickness more than 90% of impinging energy from 3 to 6μ. Not only does it withstand thermal shock, weathering, humidity, and abrasion, but, defeating the emissivity of "hot-windows," it retains its high transmittance at 800°C and, possessing a refractive index less than 1.4, requires no coating to cut reflection losses.

The only fudging was a bit of detergent in the water. We justify this on the grounds that dividing the steam among a cloud of bubbles made the test more severe by increasing the cooling rate.

For the dope on what we can make in Kodak Irtran *lenses, domes, prisms, flats, and substrates for interference filters, write Eastman Kodak Company, Special Products Division, Rochester 4, N. Y.*

Microelectronics

The theme of microelectronics is that if you want environment-immune, highly "intelligent" circuitry that can handle problems of logic and fit into a tenth of a cubic inch of space or so, you quit at an early stage of the design thinking of transistors, diodes, capacitors, resistors, and such. Instead you think of the circuit as one or more plates half a millimeter thick and fabricated as intricately as necessary out of various conductive, semi-conductive, and dielectric materials disposed among the three dimensions of each plate.

The technique uses *Kodak High Resolution Plates* on which the geometry of the various sub-circuits is photographed from drawings at great reduction. These then become the masks under which are exposed to ultraviolet light the circuit substrate plates that have been coated with *Kodak Photo Resist*. Where the mask passes u-v, subsequent processing removes the resist and lays open the substrate for either removal of material or insertion of other materials by evaporation, printing, electro-deposition, or chemical deposition.

Send to Eastman Kodak Company, Special Sensitized Products Division, Rochester 4, N. Y., for a reprint of "The DOFL Microelectronics Program." Thus we nudge you toward great undertakings.

A kind word for triacetate tape

The time has come for a few carefully framed remarks from us about recording tape, a product which we do not offer in the United States, even though Kodak Pathé has done well with tape in France for about a decade. In this country we do make base for magnetic tape. This we sell to several competent organizations who practice their respective rival methods of depositing iron oxide on it.

Our base is cellulose triacetate, the same as in Kodak Aerographic Films for precision mapping from aloft. We

cast it from solution on the nigh miraculously smooth peripheries of 18-foot wheels like this one. In the 330° of rotation allotted for preliminary evaporation of the solvents before stripping off as sheet, the thickness—along with any thickness errors—shrinks by 4/5. This situation favors the maintenance of thickness with great uniformity. Except for infrequent replating, these prodigious wheels have been rotating with stately unbroken angular momentum night and day, winter and summer, weekends and workdays for a full generation of mortal man.

Not only do our tape-making customers rival each other in excellence of deposition, but our cellulose triacetate has a rival of its own in polyethylene terephthalate, which is known as polyester. Because of the slightly higher price of polyester tape, it has often been assumed on all counts superior. This misconception hurts us.* The price difference at least partially stems from the higher salable yield that the tape manufacturer gets from cellulose triacetate. He has to reject less tape for deformation or "skew" and has the inherent thickness uniformity of the solvent-evaporation method to thank.

Though most of the tape being bought today is our beloved cellulose triacetate, there is a place for polyester. That we admit. It's very good for humidity amplitude and devilishly strong.

Cellulose triacetate, on the other hand, has only 15% ultimate residual elongation, not 45%. It does not go on stretching and stretching when overloaded by apparatus design that leans too heavily on strength of the tape base. In many applications a stretch of large and unknown magnitude could have a sneaky effect on the results.

One other factor puts cellulose triacetate high with the man to whom the word "dropout" is an expression of horror. A dropout is caused by an inhomogeneity. Our cellulose triacetate, by the nature of its manufacture, is not likely to contribute inhomogeneity. Believe us.

Don't write to us about the foregoing unless you just happen to be in a mood for correspondence. All we ask is that you bear our assertions in mind when the occasion arises to specify magnetic recording tape.

*Another thing that disturbs us is inclusion of cellulose triacetate under the generic term "acetate." Fortunately, cellulose *diacetate* is fast disappearing from the tape market.

This is another advertisement where Eastman Kodak Company probes at random for mutual interests and occasionally a little revenue from those whose work has something to do with science

Kodak
TRADE MARK

AN IMPORTANT ANNOUNCEMENT TO ALL IRE MEMBERS AND SUBSCRIBERS

The IRE Professional Group on Antennas and Propagation has just published the "Proceedings of the URSI International Symposium on Electromagnetic Theory," held at the University of Toronto, Canada, on June 15-20, 1959, as a special supplement to Volume AP-7 (1959) of the IRE TRANSACTIONS on Antennas and Propagation.

Those who registered at the Toronto Symposium will automatically receive one copy as a part of their symposium registration fee. PGAP members and others may obtain a copy by ordering at the rates indicated below. There will be no free distribution because of the special nature and large size of the supplement.

This imposing 400-page volume, comprising invited papers by 54 of the world's leading authorities, promises to be one of the outstanding reference works in its field. The subjects covered include Diffraction and Scattering Theory, Radio Telescopes, Surface Waves, Boundary Value Problems, Propagation of Waves, and Antennas. The complete program may be found on page 18A of the June, 1959 issue of the PROCEEDINGS OF THE IRE.

IRE members and subscribers are urged to order their copies now by returning the form below to the IRE, accompanied by remittance made payable to The Institute of Radio Engineers.

The Institute of Radio Engineers, Inc.
1 East 79 Street, New York 21, N.Y.

ORDER FORM FOR PGAP TORONTO SYMPOSIUM PROCEEDINGS

No. of Copies	Price per Copy		Amount Paid
	PGAP Members	$ 8.00	$
	Other IRE Members	$12.00	$
	Libraries	$12.00	$
	Nonmembers	$16.00	$
	TOTAL REMITTANCE $		

ORDERED BY (Please Print): ____________________

SHIPPING ADDRESS: ____________________

____

NEWS New Products

These manufacturers have invited PROCEEDINGS readers to write for literature and further technical information. Please mention your IRE affiliation.

(Continued from page 98A)

Delay Lines

By using a new principle in delay network design, a new series of delay lines with ratio of rise time to total delay less than 0.02 has been achieved by **Ad-Yu Electronics Lab., Inc.**, 249–259 Terhune Ave., Passaic, N. J. Besides the feature of producing very fast rise time, the attenuation can be minimized to be less than 0.02 db per 10-microsecond delay. Two or more units of Type 10T series can be connected in tandem for longer delay whenever their impedances are identical. In this case, the time delay will be equal to the sum of the delay of each unit and the rise time will be approximately equal to the square root of the sum of the squares of the rise time of each unit.

The features of this delay line series can be summarized as follows: (1) The ratio of rise time to total delay can be made less than 0.02. (2) The distortion is generally less than 2%. (3) The attenuation can be made less than 0.2 db per microsecond delay. (4) Physical size can be made less than 2 cubic inches per microsecond delay. (5) The temperature coefficient is less than 50 parts per million per degree Centigrade. (6) All types of this series can also be made to meet existent MIL specifications. The characteristic impedance ranges from 50 ohms to 1000 ohms. The time delay per 10 sections ranges from 0.25 microsecond to 5 microseconds. The accuracy of delay is less than ±1.5%.

New Test Instrument Firm

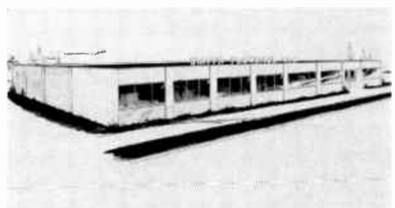

R. E. Florence, Vice President and General Manager of **Smith-Florence Inc.**, announces organization of a new electronics manufacturing corporation. The new firm is located in the Commodore Industrial Park, the address is 4226-36 23rd Avenue West, Seattle, Wash. President of the new company is Orville Smith, former

(Continued on page 108A)

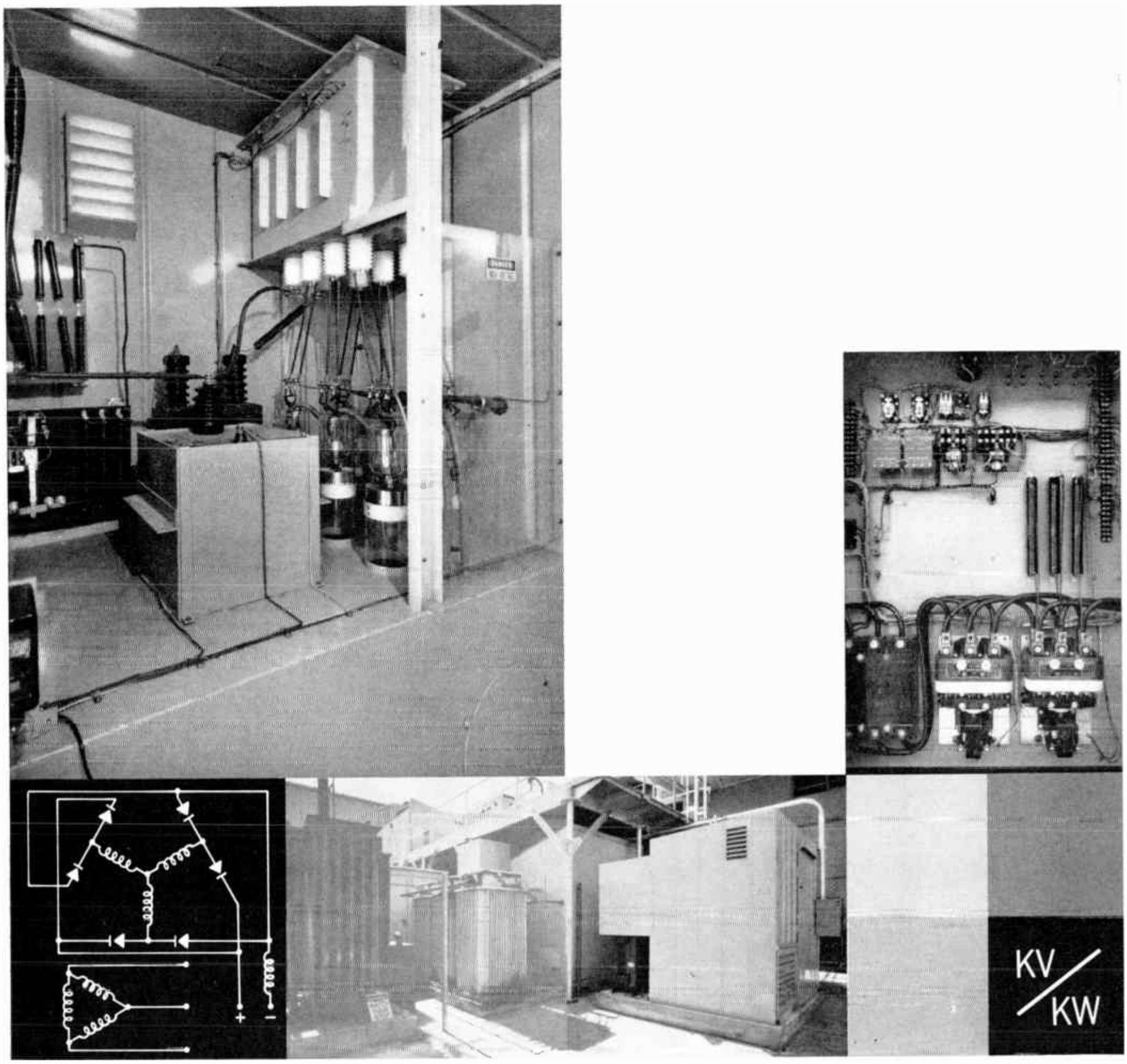

High voltages at high power. Tricky business — but a specialty of the Carad Corporation. Take this 30 kv, 3.3 ampere DC power supply, for instance. Carad designed and built this one in 70 days for Eitel-McCullough, Inc. It supplies beam voltage for production testing of high-power klystrons — 80 to 100 hours a week. One important characteristic is its ability to withstand severe load arcing — and protect the klystron being tested. This Carad supply will clear itself in 30 to 50 milliseconds and includes special reactors to limit current surges. For custom systems involving high-voltage supplies, pulsers, modulators or special transformers, investigate Carad's unusual capabilities.

CARAD CORPORATION

2850 Bay Road • Redwood City • California

DESIGNERS AND MANUFACTURERS OF
SYSTEMS AND PULSE COMPONENTS

NEWS New Products

These manufacturers have invited PROCEEDINGS readers to write for literature and further technical information. Please mention your IRE affiliation.

(Continued from page 106A)

President of Stetson-Ross Machine Tool Corporation of Seattle. The new firm will specialize in the manufacture of precision industrial and laboratory electronic test instruments for the military and commercial markets.

Anti-Coincidence Preamplifier

This firm also announces their completely transistorized Model 501 Anticoincidence Preamplifier. This instrument is designed particularly for low-level Beta work. Any existing scaler may now be converted to a low-level anti-coincidence counter. The Model 501 is used with a geiger tube detector and cosmic ray umbrella type detector, such as the new Amperex 18515 or 18517, to reduce the background count from 22 counts per minute to approximately 1 or 2 counts per minute. With this system there is no further need for the large, heavy 3000# lead shield for background protection. Any impulses from the umbrella or guard tube gate the detector circuitry so that background count will not appear at the scaler output. Voltage dividers are provided for the independent adjustment of the high voltage for guard and detector. Input impedance is 0.5 megohm. Sensitivity is from 0.1 volt to 20 volts. Resolving time is 400 microseconds. The Model 501 provides a 20 volt negative going pulse 20 microseconds wide to the scaler. The scaler used with this instrument may be switched to read guard tube output, detector output (without anti-coincidence) and 60 cps test signal. A test position on the Model 501 is provided which puts a 60 cps square wave into both the detector and guard circuits to test the anticoincident circuitry.

Dielectric Test Set

Designed by **Peschel Electronics, Inc.**, R.F.D. #1, Towners, Patterson, N. Y., for testing samples of magnet wire (twist test) in accordance with Military and Commercial Standards, Model P5 AC-T features a transparent test cage mounted on the front panel to receive the specimen pieces of magnet wire twisted in accordance with test requirements. A microswitch interlock on this test cage door prevents the application of high-voltage if the door is left open. Ends of the magnet wire slip into miniature mercury cups to facilitate contact with the high-voltage without the necessity of scraping insulation from the fine magnet wire.

Other features include continuously adjustable testing voltage from zero to 5,000 volts rms, a dual scale KV meter for accurate setting of test voltage, a push button high voltage "ON" control actuating a holding type contactor, plus usual safety and convenience controls. A fault relay deenergizes the high voltage and a reset push button must be operated again to obtain high voltage, providing that test cage door is closed. These controls and the interlock make it impossible to touch any high voltage circuits. Panel and metal cabinet are at ground potential to insure safety.

Though used mainly by manufacturers of magnet wire, the unit may be used as a standard hipot tester by plugging test leads into high voltage jacks at the rear of the unit.

The 0-5 KV rms test set is optionally available with other output ranges.

(Continued on page 110A)

NEWS New Products

These manufacturers have invited PROCEEDINGS readers to write for literature and further technical information. Please mention your IRE affiliation.

(Continued from page 108A)

PRD Sold To Harris-Intertype

Harris-Intertype Corp., Cleveland 13, Ohio, announced that it has completed an agreement for the acquisition of Polytechnic Research and Development Company from the Polytechnic Institute of Brooklyn.

"PRD," as Polytechnic Research and Development is generally known, is one of the nation's leading producers of microwave test equipment for advanced work in the communications field, both commercial and defense, including space and missile programs.

George S. Dively, chairman and president of Harris-Intertype, said purchase of the Brooklyn company will be largely for cash, although the price was not disclosed. The transaction is expected to be completed within a few weeks.

Dr. Ernst Weber, president of Polytechnic Institute of Brooklyn, is also president of PRD. An international authority on microwave electronics, he is the 1959 president of the Institute of Radio Engineers.

According to Dively, present plans are to continue the operation of PRD by the present organization as a decentralized subsidiary of Harris-Intertype. Both Dively and Weber said they hope to maintain the traditionally close relationship between PRD and Polytechnic Institute of Brooklyn.

Harris Now 20% in Electronics

In making the announcement Dively said, "This is another major move in the electronics phase of our growth and diversification program. The first step, other than the increasing application of electronics to printing equipment, was our purchase two years ago of the Gates Radio Company, Quincy, Illinois. Adding PRD sales of over $5 million per year to those of Gates brings Harris-Intertype's electronic business up to about 20% of its total sales."

North American Moves To New Plant

North American Electronics, Inc., Lynn, Mass., announces the removal of its plant and offices from Broad Street to the former General Electric Building on Linden St., in the same city.

John O. Cimaglia, president of N.A.E., declared today that this was the first step in the company's expansion program, designed to greatly enlarge production facilities to meet increased demand for the semiconductor products which they make.

In making the move, N.A.E. will quadruple its old plant size to 26,000 square feet. Along with this increase in

(Continued on page 114A)

Available now—ceramic "extras" in more than 40 tube types

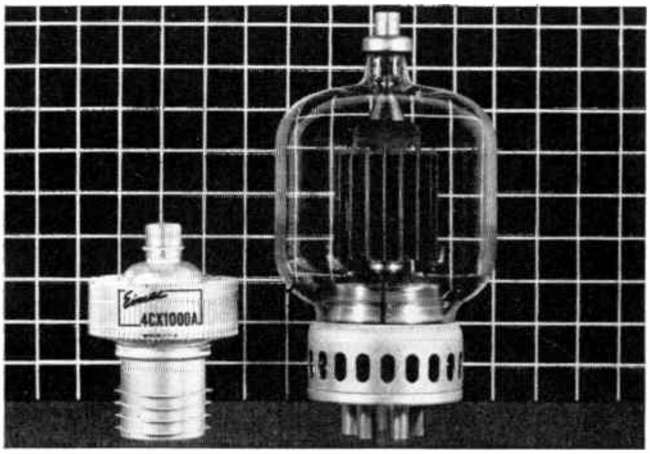

SMALLER SIZE

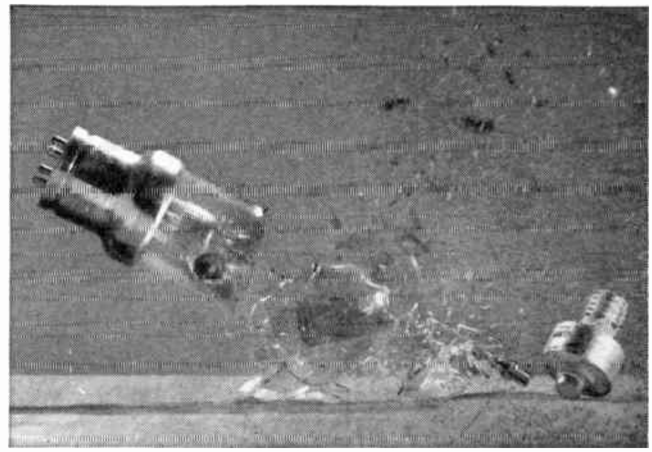
IMPACT SURVIVAL

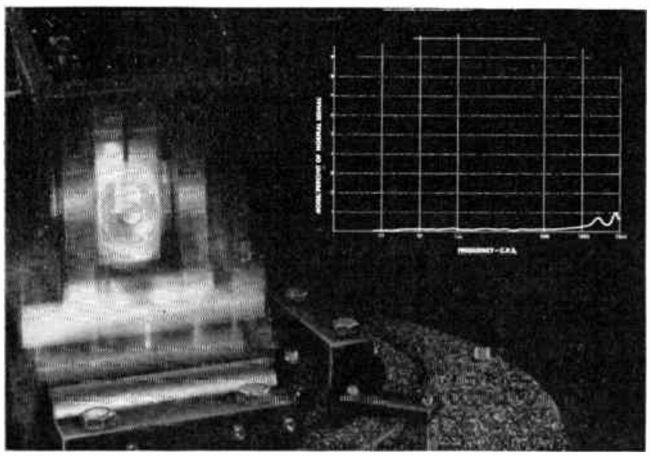
VIBRATION SURVIVAL

EXACT DIMENSIONAL UNIFORMITY

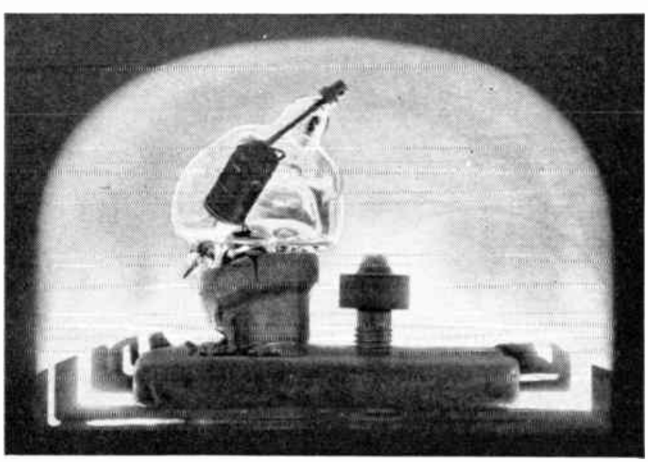
EXTREME HEAT SURVIVAL

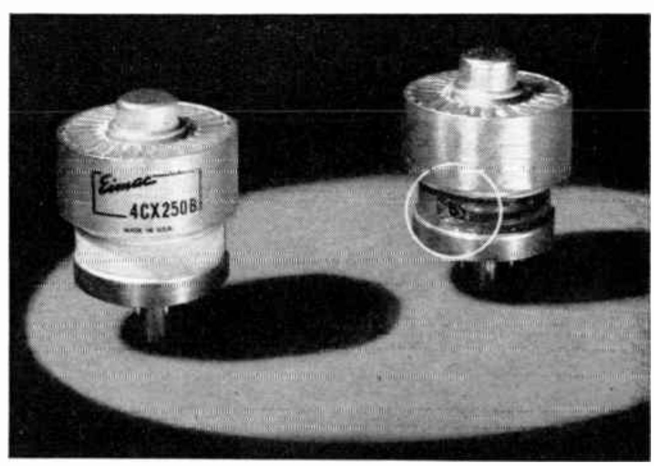

LOWER DIELECTRIC LOSS

Superior performing Eimac ceramic negative-grid tubes and klystrons are available now for modern equipments.

EITEL-McCULLOUGH, INC.
SAN CARLOS, CALIFORNIA
Eimac First with ceramic tubes that can take it

Cable address
EIMAC
San Carlos

Type R Unit Enables Tektronix Oscilloscopes

to measure

transistor high-frequency characteristics

by the pulse-response method

TYPE R TRANSISTOR-RISETIME PLUG-IN UNIT CHARACTERISTICS

Collector Supply 1 to 15 v continuously adjustable, positive or negative. Current capability—400 ma.

Mercury-Switch Pulse Generator Risetime less than 5 mμsec, amplitude 0.02 v to 10 v across 50 ohms, positive or negative. Overall risetime with Type 541A: 12 mμsec. Overall risetimes with other Tektronix Oscilloscopes—Types 543, 545A, 555: 12 mμsec—Type 551: 14 mμsec—Types 531A, 533, 535A: 23 mμsec.

Bias Supply +0.5 to −0.5 v and +5 v to −5 v, continuously variable.

Calibrated Vertical Deflection 0.5, 1, 2, 5, 10, 20, 50, and 100 ma/cm collector current.

Type R Transistor-Risetime Unit **$300**

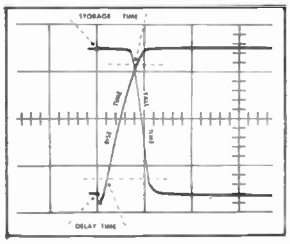

The Type R Unit can trigger the Oscilloscope sweep either on the start of the test pulse only, or on both the start and finish to display delay, rise, storage, and fall times simultaneously.

TYPE 541A CHARACTERISTICS

Vertical Response DC-to-30 MC passband, 12-mμsec risetime, 50-mv/cm deflection factor with Type K Plug-In Preamplifier.

Signal-Delay Permits observation of leading edge of signal that triggers the sweep.

Versatility—Other Plug-In Preamplifiers available for many specialized applications.

Sweep Range 0.1 μsec/cm to 5 sec/cm in 24 direct-reading steps. 5-x magnifier increases calibrated range to 0.02 μsec/cm. Continuously adjustable from 0.02 μsec/cm to 12 sec/cm.

Triggering Fully automatic, or amplitude-level selection with preset or manual stability control.

Accelerating Potential 10 kv for bright display with fast sweeps and low repetition rates.

Amplitude Calibrator 0.2 mv to 100 v in 18 steps. Square wave, frequency approximately 1 kc.

Regulation Electronically-regulated power supply.

Type 541A, without plug-in units **$1200**

Type K Plug-In Preamplifier **$135**

Prices f.o.b. factory.

The Type R Transistor-Risetime Unit, when plugged into a Tektronix Oscilloscope, supplies a fast-rising pulse and the required supply and bias voltages for measurement of transistor rise, fall, delay, and storage times. The Type R Unit can be used with all Tektronix Type 530 Series, Type 540 Series, and Type 550 Series Oscilloscopes.

When the Type R Unit is used with the Tektronix Type 541A Oscilloscope, risetime of the combination is 12 mμsec. The Type 541A is a fast-rise general-purpose oscilloscope that adapts to many specialized applications through its plug-in vertical preamplifier feature. Nine plug-in preamplifiers are presently available, others will be announced in the near future.

Please call your Tektronix Field Engineer for complete details. If desired, he can arrange a demonstration in your own application.

ENGINEERS—interested in furthering the advancement of the oscilloscope? We have openings for men with creative ability in circuit and instrument design, cathode-ray tube design, and semiconductor research. Please write Richard Ropiequet, V.P., Eng.

Tektronix, Inc.

P. O. Box 831 • Portland 7, Oregon

Phone CYpress 2-2611 • TWX-PD 311 • Cable: TEKTRONIX

TEKTRONIX FIELD OFFICES: Albertson, L. I., N.Y. • Albuquerque, N. M. • Annandale, Va. Atlanta, Ga. • Buffalo, N.Y. • Cleveland, Ohio • Dallas, Tex. • Dayton, Ohio • Denver, Colo. Endwell, N.Y. • Greensboro, N. C. • Houston, Tex. • Lathrup Village, Mich. • Lexington, Mass. East Los Angeles, Calif. • West Los Angeles, Calif. • Minneapolis, Minn. • Mission, Kan. • Orlando, Fla. • Palo Alto, Calif. • Park Ridge, Ill. • Philadelphia, Pa. • San Diego, Calif. • St. Petersburg, Fla. Scottsdale, Ariz. • Stamford, Conn. • Syracuse, N.Y. • Towson, Md. • Union, N. J. • Willowdale, Ont.

TEKTRONIX ENGINEERING REPRESENTATIVES: Hawthorne Electronics; Portland, Oregon, Seattle, Washington.

Tektronix is represented in 20 overseas countries by qualified engineering organizations.

NEWS New Products

(*Continued from page 110A*)

space, the company will increase the number of its employees accordingly.

The move represents not only an increase in space and facilities, but also an addition to its present product line. To its line of silicon diodes and cartridge rectifiers, N.A.E. will add a new line of transistors.

Formed two years ago in December, North American Electronics, has already seen considerable expansion in that period. Other officers in the company include: Arthur Bruno, vice president and chief engineer; Felix Piech, treasurer; Dr. Walter Henry, clerk.

Preset Counters

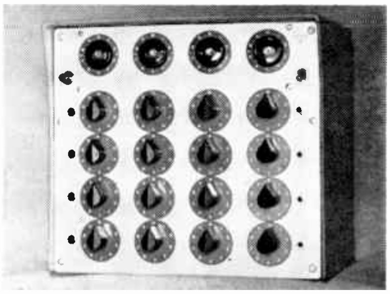

The 2000 Series Preset Counters are available from **Oxford Engineering Co.,** 47A River St., Wellesley Hills 81, Mass., in 3 to 6 digits, and from 1 to 6 preset banks. The Model 2044, 4-digit and 4-bank counter is shown. Although, initially, this series is designed for toroidal winding machines, other variations will soon be available. Some features include: all electronic circuitry, completely transistorized, solid state power supply, plug-in output relay, cold-cathode counting tube elements, reinforced fiberglas cabinet, low power drain, less than 10 watts at 115 volts ac.

Toroidal Inductors

Type TQA precision inductors manufactured by **United Transformer Corp.,** 150 Varick St., New York 13, N. Y., provide a solution to stable oscillators for frequencies from 400 cycles to 75 **kc.**

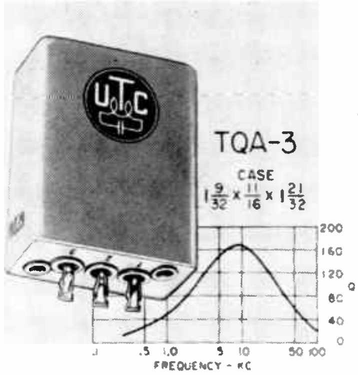

(*Continued on page 118A*)

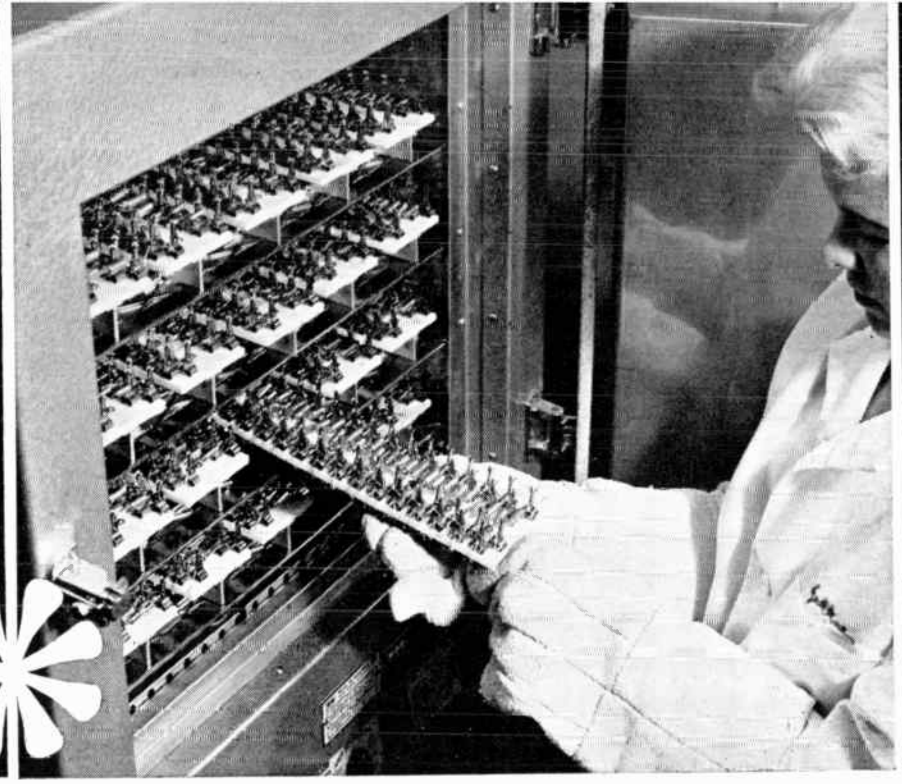

tan-TI-cap† CAPACITOR STABILITY ASSURED BY 250-HOUR PERFORMANCE LOAD TEST

...expanded TI line of type SCM solid tantalum capacitors meets MIL specs

ACTUAL SIZE

Another assurance to you of Texas Instruments capacitor reliability — 250-hour performance load test on a sample basis of *all* lots of the Type SCM series.

Your margin of design safety is greater with *tan-TI-cap* capacitors. Type SCM capacitors are *100% tested* for capacity, dc leakage and dissipation factor, and are aged under load at elevated temperature. SCM units in all 203 standard ratings (6 - 35 volts, 1 - 330 μfd.) meet and exceed the electrical and mechanical requirements of MIL-C-55057 (Sig. C) and/or MIL-C-21720A (NAVY) specifications for solid tantalum capacitors.

Contact your nearest authorized TI distributor or TI sales office today for your immediate and future delivery requirements.

† trademark of Texas Instruments Incorporated

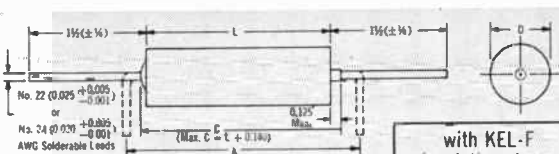

						with KEL-F insulating sleeve			with Mylar insulating sleeve**		
case size	D +0.010 −0.005	L ±0.031	*A ±0.031	wire size AWG	avg. wt. gms.	D +0.020 −0.010	L ±0.062	avg. wt. gms.	D ±0.010	L ±0.031	avg. wt. gms.
F	0.125	0.250	0.482	24	0.4	0.162	0.337	0.5	0.135	0.322	0.4
B	0.175	0.438	0.688	24	1.1	0.210	0.525	1.3	0.185	0.510	1.2
G	0.279	0.650	0.888	22	2.7	0.315	0,735	3.1	0.289	0.722	2.8
H	0.341	0.750	0.988	22	3.3	0.377	0.835	3.9	0.351	0.822	3.4

* Dimension "A" determined by suspending a one-pound weight from one lead and rotating the case from the vertical position to the horizontal position, and then repeating the procedure for the other lead.

** Meets all requirements of MIL-C-55057 and MIL-C-21720A, including dimensions.

All lots of Type SCM *tan-TI-cap* capacitors are tested for performance stability at rated temperature and voltage prior to release for shipment. Performed on a lot-sample basis, the test is run for 250 hours or until performance stability is established by successive time interval measurements of the principal parameters of each test capacitor.

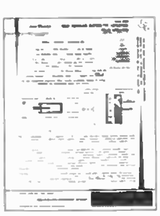

Write to your nearest TI sales office on your company letterhead for Bulletin DL-C 1173 which gives detailed specifications on the complete SCM series.

TEXAS INSTRUMENTS
INCORPORATED
SEMICONDUCTOR-COMPONENTS DIVISION
13500 N. CENTRAL EXPRESSWAY
POST OFFICE BOX 312 · DALLAS, TEXAS

NEWS New Products

These manufacturers have invited PROCEEDINGS readers to write for literature and further technical information. Please mention your IRE affiliation.

(*Continued from page 114A*)

These toroid inductors are center tapped for oscillator circuits and employ an extremely stabilized core for maximum temperature stability. TQA units are available as stock items in nineteen inductance values ranging from 7 mhy to 22 henries, laboratory adjusted to 1% accuracy. Maximum Q is approximately 160 at 7.5 kc ranging down to 20 at 400 cps and to approximately 30 at 75 kc for low inductance values. Hum pickup is extremely low due to a uniform toroid winding plus a high permeability outer case, providing 80 db at coupling attenuation.

TQA units are hermetically sealed to MIL-T-27A specifications and carry MIL identification TF4RX20YY. The case is $\frac{11}{16}\times1\frac{9}{32}\times1\frac{21}{32}$ inches; weight four ounces.

Spectrum Analyzer

The Type 190 Spectrum Analyzer was developed by **Ferranti Electric Inc., Electronics Division,** 95 Madison Ave., Hempstead, L. I., N. Y., originally as part of the Type 123 Noise Measuring Equipment. The latter instrument measures AM and FM noise in a narrow band and is specially suited to the requirements for noise measurement encountered in CW Doppler radar systems.

The Type 190 is useful to engineers working on other parts of such systems who do not need the RF head.

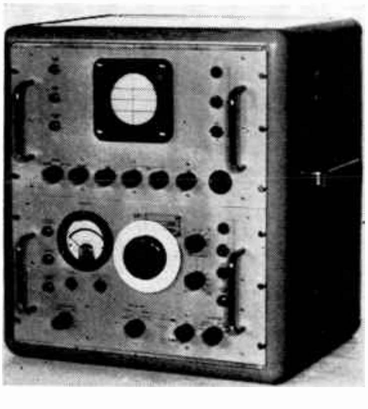

Frequency Range: The equipment measures power level in a selected bandwidth in the range 500 cps to 90 kc (a version with an upper frequency limit of 145 kc is under development).

Bandwidth: 70 cps or 1 kc by switch selection.

Presentation: Automatic using a swept oscilloscope or manual for accurate power measurements using a thermal meter once the frequencies of interest have been determined.

Sensitivity: The instrument can handle signals from 0.1 volt to 1 microvolt (100 db range).

Accuracy: ±2 db from 500 cps to 90 kc.

(*Continued on page 129A*)

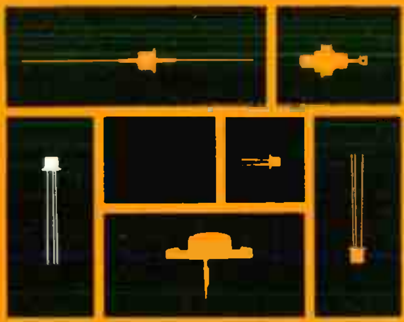

NEW MOTOROLA "MEG-A-LIFE" INDUSTRIAL ALLOY TRANSISTORS

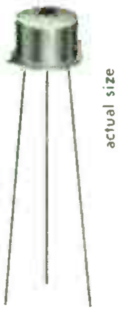

Motorola types 2N650A, 2N651A and 2N652A are the first to be offered under the Motorola "Meg A-Life" brand. Units are designed to provide extremely reliable amplifier and switching service in the audio frequency range.

- Meet or exceed mechanical and environmental requirements of MIL-S-19500 • PC = 200 mw
- Operating and storage temperature: to 100°C
- BVCBO = 45 volts • BVCER (R = 10K) = 30 volts

Type Number	h_{fe} (VCE = 6V, IE = 1 ma) MIN.	MAX.
2N652A	100	225
2N651A	50	120
2N650A	30	70

MOTOROLA announces a NEW QUALITY ASSURANCE PROGRAM "MEG-A-LIFE" offering ADVANCE CERTIFICATION of COMPONENT RELIABILITY

This new Motorola "Meg-A-Life" quality-assurance program provides users of semiconductor devices with:

1. Written certification of reliability with orders of 100 units or more.
2. Established specifications as severe as those required for military units.
3. Close quality control tolerances, with minimum and maximum parameters, AQL and inspection levels completely specified.

Under this new Motorola program, each production lot of a "Meg-A-Life" branded device is subjected to complete electrical, mechanical, environmental and life tests identical to those required for Military approved units. The purchaser receives written certification that units passed the specified tests and a copy of the actual test results is made available.

All tests and sampling are made in accordance with military specifications . . . representing the most adverse conditions under which the devices would be used. The Motorola "Meg-A-Life" certificate provides the industrial user with an assurance of reliability never before possible and makes possible the elimination of duplicate testing.

The first available Motorola "Meg-A-Life" devices are the 2N650A, 2N651A and 2N652A Industrial Alloy Transistors. Other Motorola semiconductors will be announced under the "Meg-A-Life" brand.

FOR COMPLETE INFORMATION and specifications on "Meg-A-Life" Industrial Alloy Transistors, contact your Motorola Semiconductor District Office:

RIDGEFIELD, NEW JERSEY
540 Bergen Boulevard
WHitney 5 7500
from New York WI 7 2980

DETROIT 27, MICHIGAN
13131 Lyndon Avenue
BRoadway 3 7171

CHICAGO 39, ILLINOIS
5234 West Diversey Avenue
AVenue 2 4300

MINNEAPOLIS 27, MINNESOTA
7731 6th Avenue
Liberty 5 2198

HOLLYWOOD 28, CALIFORNIA
1741 Ivar Avenue
HOllywood 2 0821

IN CANADA WRITE
MOTOROLA, Inc.
Semiconductor Products Division
4545 West Augusta Boulevard
Chicago 51 Illinois

OUTSIDE USA & CANADA WRITE
MOTOROLA INTERNATIONAL, S. A.
4545 West Augusta Boulevard
Chicago 51 Illinois

Semiconductor Division
MOTOROLA
5005 EAST McDOWELL ROAD • PHOENIX, ARIZONA

Positions Wanted

By Armed Forces Veterans

In order to give a reasonably equal opportunity to all applicants and to avoid overcrowding of the corresponding column, the following rules have been adopted:

The IRE publishes free of charge notices of positions wanted by IRE members who are now in the Service or have received an honorable discharge. Such notices should not have more than five lines. They may be inserted only after a lapse of one month or more following a previous insertion and the maximum number of insertions is three per year. The IRE necessarily reserves the right to decline any announcement without assignment of reason.

Address replies to box number indicated, c/o IRE, 1 East 79th St., New York 21, N.Y.

SENIOR ENGINEER—CHIEF

Age 43; broad electronic experience with vacuum tube and transistor circuitry, analog computers, gyro systems, power supplies, miniaturization and printed circuitry. Senior Member IRE. Tau Beta Pi, Eta Kappa Nu. Will relocate for an outstanding opportunity. Box 2051 W.

ENGINEERING TEACHER

B.S. and M.S. in E.E. 2 years industrial research, 2 years applicable military, and 4 years full-time teaching on the faculty of a major east coast university. Desires position of permanence with good family living conditions. Summer income opportunity desirable. Available June 1960. Box 2052 W.

ELECTRICAL ENGINEER

B.S. in physics, graduate work in E.E.; 7½ years experience in electronics of which 3½ years is in commercial data processing. Have published articles and hold patents in electronics. Desires overseas position. Box 2053 W.

ENGINEER

BSEE., extensive antenna and R.F. experience, design and project supervision. Broad background includes sales and engineering management, contract negotiations. Desires position as General Manager of antenna company, or participant in ownership management of antenna consulting firm or small growing company. Box 2054 W.

COMPONENTS ENGINEER

E.E. degree. 10 years solid experience in electromechanical components—development, evaluation, application and standardization. Desires a challenging, responsible position in a supervisory capacity, New York, Long Island area preferred. Box 2055 W.

ELECTRONIC FIELD ENGINEER

Graduate engineer, BSEE., several years experience, age 32, fair health, seeking position as electronic engineer—sales engineer, field engineer, coordinator customers' technical requirements either commercial or military customers, or supervisor equipment installation and installation check-out. Preparation with company training course desirable. Box 2056 W.

(Continued on page 123A)

RESEARCH AT COLLINS

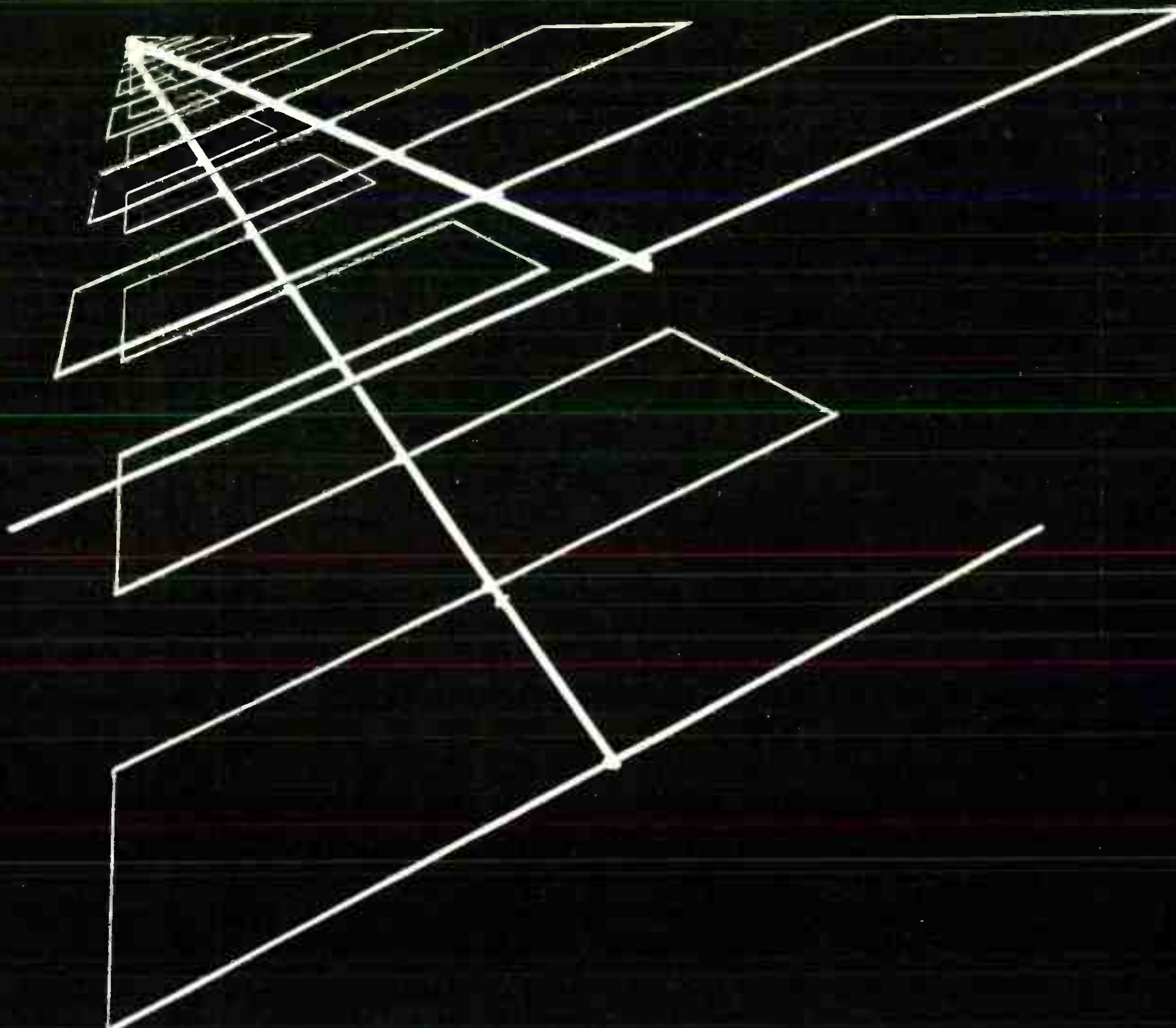

THE UNUSUAL SHAPE OF PROGRESS

Yesterday's basic and applied research in antennas has become today's technology in broadband antenna design at Collins Radio Company. Pictured here is a Collins Logarithmic Periodic Antenna. It performs functions previously requiring a large number of antennas. The Logarithmic Periodic concept is based on a structural geometry in which the electrical characteristics repeat periodically as the log of the frequency. Since only minor changes occur over each period, the characteristics are essentially constant over the entire frequency range.

Collins Radio Company Research Laboratories direct far ranging programs in circuits, advanced systems, antennas and propagation, mechanical sciences, and mathematics toward advancing scientific knowledge and developing new technologies. Collins provides freedom of activity in basic research for the physicist and engineer capable of looking beyond the apparent limits of today's science. In applying the new concepts thus created, Collins has attained an enviable position of leadership in electronics. Unique professional opportunities are now being offered. Your inquiry is invited.

COLLINS

COLLINS RADIO COMPANY • CEDAR RAPIDS, IOWA • DALLAS, TEXAS • BURBANK, CALIFORNIA

CAREER OPPORTUNITIES AT TI

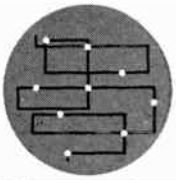

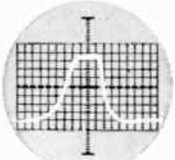

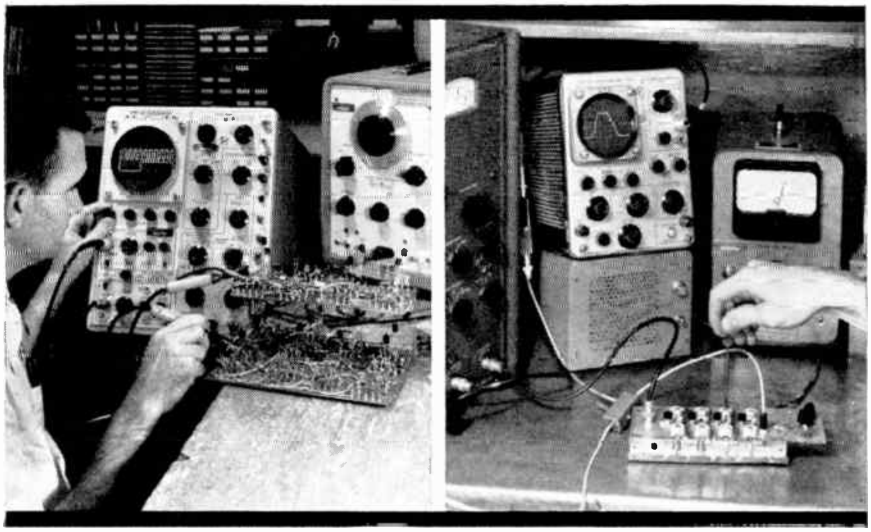

CIRCUIT DEVELOPMENT ENGINEER

your future: a challenging opportunity with an industry leader

At Texas Instruments, your future is filled with specific, stimulating growth assignments in evaluating and characterizing transistors and special semiconductor devices. You'll participate in such transistorization projects as:

- AM, FM, and TV receivers
- audio and video, i-f and r-f amplifiers
- hi-fi and electronic organs
- nonlinear and switching circuits
- computer system logic
- servo and power amplifiers

With TI . . . receive liberal company-paid benefits, including profit sharing *(over last several years, an average of more than 12% of base salary)* . . . enjoy premium living in a moderate climate with excellent neighborhoods, schools and shopping facilities . . . work in a plant selected as one of the 10 outstanding U. S. industrial buildings of 1958.

Interviews will be held in your area soon. If you have an Electrical Engineering degree and/or knowledge of transistor circuitry, please send a resume to:

C. A. Besio, Dept. 200-PI

For immediate Eastern appointment, contact
W. T. Hudson
Dept. 200-E-PI
1141 E. Jersey St.
Elizabeth, N. J.

TEXAS INSTRUMENTS
INCORPORATED
SEMICONDUCTOR - COMPONENTS DIVISION
POST OFFICE BOX 312 • DALLAS, TEXAS

grow with kollsman!

Opportunities in

GROUND SUPPORT EQUIPMENT

PROJECT ENGINEERS—EE & ME

Experience in ground support equipment built to military specifications.

ENGINEERS—EE

Some experience desired in ground support equipment.

SEMI-CONDUCTOR ACTIVITIES

PHYSICISTS or CHEMISTS

Significant educational and experience background in solid state physics. For participation in the following areas of research and development.

- Photoelectrics
- Magnetics (ferrites, magnetic films, etc.)
- Dielectrics
- Semiconductor Materials (as applied to diodes, transistors & Hall-effect devices)
- Microminiaturization

Kollsman is seeking a limited group of exceptional men to participate in its continuing growth in the field of automatic navigation and flight instrumentation. These openings offer unusual opportunity with an organization intimate enough to allow individual recognition, yet large enough to assure stability.

Please send resumes to T. A. DeLuca

kollsman
INSTRUMENT CORP.

Subsidiary of Standard Coil Products Co., Inc.

80-08 45th Avenue,
Elmhurst, New York

Positions Wanted

By Armed Forces Veterans

(Continued from page 120A)

ENGINEERING MANAGER—TECHNICAL REPRESENTATIVE

Retiring Navy Captain. Engineering Duty Officer. Senior Member IRE. Desires to locate in Southern California. Graduated Naval Academy 1926. 3 years sea duty, 12 years civilian electronics engineer. Returned to active duty 1941. 9 years technical administrator in Naval laboratories; 4 years comptroller in Naval Shipyard with collateral duty as Project Officer for electronic data processing. Available late spring 1960. Box 2057 W.

MARKETING DIRECTOR—SALES MANAGER

Desires to relocate. Connecticut preferred. Excellent background in building and managing electronic sales organizations. Experienced in directing all phases of marketing activities. Age 37, married. Resume furnished on request. Box 2061 W.

UNIVERSITY ADMINISTRATOR

11 years college administration and teaching experience, plus industrial research, electronic design and development Currently conducting year's research in industry. Have directed grant programs, technical adult education, research, taught undergraduate and graduate. BS. and MS. in E.E. Married. Age 36. Excellent references. Interested in challenging college position. Prefer Rocky Mountain area. Box 2062 W.

ELECTRICAL PATENT POSITION

BEE. Polytechnic Institute of Brooklyn 1958. Coast Guard officer desires position in Patent branch of organization located near a law school. Patent, law school and engineering experience. Box 2063 W.

Positions Open

The following positions of interest to IRE members have been reported as open. Apply in writing, addressing reply to company mentioned or to Box No. ....

The Institute reserves the right to refuse any announcement without giving a reason for the refusal.

Proceedings of the IRE
1 East 79th St., New York 21, N.Y.

DIRECTOR OF ELECTRONICS

Director of electronics R and D with aeronautical applications. Suburban location near New York City. Salary $30,000 plus. Doctor's degree desirable. Box 1098.

ENGINEERS

The Pratt & Whitney Aircraft Division of United Aircraft Corp., East Hartford, Conn. has openings for graduate engineers in the areas of Propulsion Systems Performance Analysis, Heat Transfer Research, Ultra High Temperature Materials, Dynamics, Vibrations, Structures Re-

(Continued on page 124A)

Positions Open

(Continued from page 123A)

search, Experimental Testing, Technical Report Writing and Propulsion System Control Engineering. Many of these openings are in our advanced Development Groups where we are presently conducting studies in solid and liquid propellants, ion propulsion, arc jet, plasma jet, and other advanced forms of propulsion. Openings are available at both the Conn. and Florida facilities. For more information, contact Mr. Henry M. Heldmann, Employment Office.

INSTRUCTOR OR ASSISTANT PROFESSORS

Retirement of a staff member creates a vacancy in the Electrical Technology Dept. for February 1960. Teaching area is mainly in electronics at the technican level. Minimum requirements are BEE. or B.S. in E.E. and 2 years of industrial experience. Starting salary $5000 to $7000. Opportunity for an additional $2000 through evening and summer teaching. Excellent pension system and other fringe benefits. Write to Prof. J. De France, Dept. of Elec. Tech., New York City Community College, 300 Pearl St., Brooklyn 1, New York.

DEVELOPMENT ENGINEER

Development Engineer to head a small development group in the field of small electronic components. Degree or its equivalent, and experience in this field required. Write Philadelphia Plant Employment, International Resistance Co., 401 North Broad St., Philadelphia 8, Pa.

PROFESSORS

Rank of Assistant Professor or Associate Professor, depending on qualifications. Salary $5500 to $8500 for session, 10 months nominal. 9 months actual. Start February or September 1960. Duties will include offering graduate courses and helping to develop research facilities. Opportunities for curriculum experimentation. Various sources of additional income available. Substantial allowance for relocation. Exceptionally good retirement plan. Fully accredited Electrical Engineering Dept. in medium sized university (700 undergraduate students in engineering) located in a very pleasant uncrowded city of 350,000. Address resume to Dean Otto Zmeskal, College of Engineering, University of Toledo, Toledo 6, Ohio.

NEW OPPORTUNITIES IN

LOW-NOISE AMPLIFIERS SEMICONDUCTOR DEVICES
ELECTRON-BEAM DYNAMICS MICROWAVE CIRCUITS
TV AND RADIO RECEIVER DESIGN ENGINEERS

AT ZENITH

Chicago, Ill., and Menlo Park, Calif.

The continuing expansion program at Zenith has created new opportunities for engineers with experience in the above fields

The fast-wave **electron-beam parametric amplifier,** conceived at Zenith, has opened up challenging new fields for research and development activity from UHF to SHF bands. Broad company interests in the microwave-tube area provide fertile atmosphere for original ideas and individual initiative.

An expanding research program in new fields centered around **compound semiconductors** provides opportunities for individuals with backgrounds in the solid-state art. Development of special devices for highly specific purposes, in collaboration with applications engineers, represents another area of active interest in the semiconductor field.

Positions are now available in the Research Department at Chicago; some openings are available in the San Francisco Bay Area. Congenial small-group atmosphere prevails, with all the advantages of a large, progressive company.

Interested applicants please contact:

DR. ALEXANDER ELLETT
Zenith Radio Corporation
6001 Dickens Avenue
Chicago 39, Illinois

BErkshire 7-7500

TECHNICAL SALES ENGINEER

Knowledge of Government operations and experience in microwave tube field desired. Retired service personnel would be considered. Good position in growing company. Please call or write American Radio Company, Inc., 445 Park Ave., New York 22, N.Y. Pl-3-5046.

PRODUCTION FOREMAN

Production Foreman—Electronic Transformer: 5 years (+) experience in coil winding business. Familiar with general machineshop equipment and vacuum potting techniques. New company. Excellent opportunity. Sunny San Diego. Apply Atlas Transformer Co., 1839 Moore St., San Diego 1, Calif.

ASSOCIATE PROFESSOR

Electrical Engineering faculty being expanded in rapidly growing department, graduating first class in 1960. Current positions available to rank of Associate Professor and to 9 months salary of $6000, depending upon education and experience. Background emphasis preferably upon electronics and advanced circuit theory. Opportunity for research and other industrial programs in the area. Send full background to Chairman, Electrical Engineering, University of Bridgeport, Bridgeport, Conn.

ENGINEERS

ASSISTANT DIRECTOR RESEARCH & DEVELOPMENT: E.E. graduate with an advanced degree, who has history in electronics, audio, transducers, pulse circuitry and electromechanical devices. Supervisory experience desired in organizing and planning R&D programs.

CHIEF RESEARCH ENGINEER: Electronic engineering graduate trained in audio, video and transistor circuits. Supervisory experience in R&D planning.

SENIOR MECHANICAL ENGINEER: Experienced in product design & development of small mechanisms, precision and electromechanical devices, speed reduction systems.

SENIOR & JUNIOR ELECTRONIC ENGINEERS will find ample opportunities and challenges in Gray Manufacturing Co., 16 Arbor St., Hartford, Conn.

ASSISTANT PROFESSOR

Assistant Professor of Electrical Engineering, University of North Dakota, Grand Forks, North Dakota. Position open September 1960. Must have M.S. degree and some experience in teaching or industry. Will teach electronic and circuitry courses to undergraduates primarily, with some graduate teaching available, if desired. Submit resume to Chairman, Electrical Engineering Dept.

(Continued on page 126A)

Positions Open

(Continued from page 124A)

ASSISTANT & ASSOCIATE PROFESSORS

Assistant & Associate Professors, Ph.D., 200 graduate students. Ideal dry mountain climate. Income $10,000 up with research. Chairman, E.E. Dept., University of New Mexico, Albuquerque, New Mexico.

ASSISTANT & ASSOCIATE PROFESSORS

Applications are invited for Assistant & Associate Professors of E.E. Candidates should be well qualified academically and should have some research experience, preferably in Control Systems, Solid-state devices, Microwaves, Telecommunications. Salary scales are competitive with industrial and research establishments. Additional stipends are offered for summer research work. Address applications to Chairman, Dept. of E.E., McMaster University, Hamilton, Ontario, Canada.

STAFF ENGINEER

A high level staff engineering position is available for an experienced engineer who desires a position without line responsibilities. The position requires ability to study systems and circuits proposed and under development with a view to steering engineering effort along productive paths. A superior educational background and considerable experience are required in carrier telephone, electronic switching, microwave systems, and related circuitry. Salary open. Northern California area. All replies will be kept confidential. Reply to Box 2008.

ELECTRONICS INSTRUCTOR

Post High School Institution—Degree required—Permanent, hospitalization and non-contributory pension system provided. Start February 1, 1960. Write giving complete resume and salary required to New York Trade School, 304-326 East 67 St., New York 21, N. Y. Att: Director, Electronic Training.

MICROWAVE SPECIALIST

Microwave physicist needed for applying microwave techniques to the study of plasma flows and ionized regions around high speed models and in shock tubes. Measurements and study of the radio-frequency energy emitted by the passage of high-speed models and of the transmission and reflection characteristics of the wake are required in order to evaluate the effects of these characteristics and also as an aid to further the knowledge of flow phenomena at extreme speeds. Applicant should have advanced degree with a good background in microwave propagation and field theory as well as ability to work with microwave hardware. He should be capable of taking the initiative in the application of microwave techniques and in the interpretation of results. Write Personnel Officer, NASA, Ames Research Center, Moffett Field, Calif.

ELECTRONIC ENGINEER

Young Electronic Engineer, experienced in circuit design, to work as assistant to one of the outstanding engineers in the country in the design and development of precision analog equipment. This is once-in-a-career opportunity for the right individual to learn from one who has, over the past 15 years, established a proven record of accomplishment in the analog field. Apply Milgo Electronic Corp., 7620 N.W. 36th Ave., Miami 47, Florida.

(Continued on page 128A)

General Motors pledges

AC QUESTMANSHIP

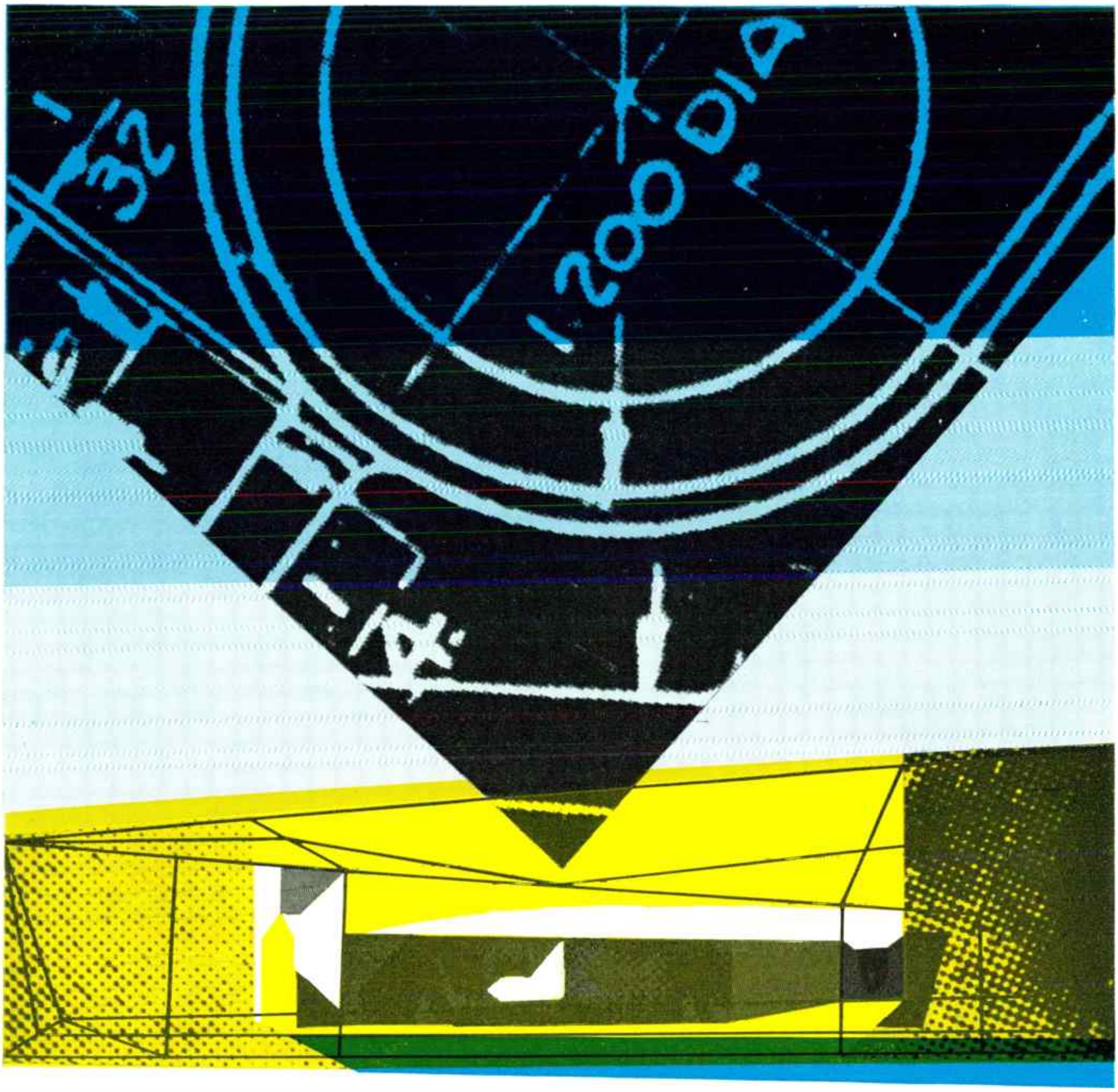

AC Seeks and Solves the Significant—Since GM has pledged its resources to this nation's defense, AC plans to forge to the forefront in the international race for technological superiority. The resolution of scientific problems even more complex than AChiever inertial guidance—that's what AC now has on its agenda / This is AC QUESTMANSHIP. It's an exciting creative quest for new ideas, methods, components and systems . . . to promote AC's many projects in guidance, navigation, control and detection / Questmanship is readily apparent in AC Manufacturing, headed by Mr. Roy McCullough, AC Works Manager. His group "offers an outstanding challenge to engineers capable of understanding the most advanced scientific concepts . . . and developing the techniques and tools to implement those concepts on a production basis" / There may be a position for you on our specially selected staff . . . if you have a B.S., M.S. or Ph.D. in the electronics, scientific, electrical or mechanical fields, plus related experience. If you are a "seeker and solver," you should write AC's Director of Scientific and Professional Employment, Mr. Robert Allen, Oak Creek Plant, Box 746, South Milwaukee, Wisconsin.

GUIDANCE / NAVIGATION / CONTROL / DETECTION / AC SPARK PLUG *The Electronics Division of General Motors*

ELECTRONIC ENGINEERS

STAVID

offers all 3 most important position considerations:

CAREER OPPORTUNITIES based on solid, long-term growth . . .
TOP EARNINGS fully commensurate with experience . . .
CHALLENGING ASSIGNMENTS made possible by project diversification.

STAVID has immediate openings in career opportunities in airborne, shipboard and ground-based systems and equipment. Degree or graduate degrees, Electrical or Mechanical Engineering, Physics or Math. Positions available at all levels in research, design, development and field service engineering.

WEAPONS SYSTEMS

- Feasibility Studies
- Advanced Designs
- Countermeasures
- Systems Analysis
- Missile Guidance
- Bombing & Navigation
- Logic Design
- Data Transmission
- Display Development
- Missile Detection
- Applied Mathematics

RADAR SYSTEMS

- High-Power Modulation
- UHF & VHF Development
- Antennas
- Receivers & Transmitters
- Transistor Applications
- Microwave Development
- Digital Techniques
- Electro-Mechanical Packaging
- Pulse Circuit Techniques
- Telemetry
- I.F. & Video Circuitry
- Environmental Testing

STAVID's facilities in Plainfield, New Jersey, at the foothills of the Watchung Mountains, are near excellent schools, modern shopping facilities and ample housing accommodations. With New York City just 45 minutes away, and the New Jersey shore within one hour's drive, the Plainfield area provides an ideal environment for work, recreation and comfortable suburban living.

For complete details, please send detailed resume to:

J. R. CLOVIS, Personnel Department IR-2

Lockheed Electronics Company

Stavid Division

U.S. HIGHWAY 22 PLAINFIELD, N. J. PLAINFIELD 7-1600

Positions Open

(Continued from page 126A)

STAFF OPENINGS—ELECTRICAL ENGINEERING DEPT.

Staff openings for September 1960 in Electrical Engineering Dept. Mostly undergraduate instruction. Attractive salary, living conditions. Recreation center of the West. Correspondence invited. I. J. Sandorf, Chairman, Dept. of E.E., University of Nevada, Reno, Nevada.

PROFESSOR

The University of Alaska has an opening for an Assistant Professor of Electrical Engineering —to teach and do research on the ionosphere, the aurora, or on problems in communications or power in the North. Industrial experience or advanced degree required. Write Airmail to Dept. of E.E., University of Alaska, Box 497, College, Alaska.

RESEARCH ENGINEER

Engineering or Physics degree. 5-10 years experience in inertial guidance systems and/or components. Aid in developing concepts of advanced guidance systems and in promulgating written and verbal communications on the subject to other groups in allied fields. Send resume to G. A. Nesbet, Litton Industries, Beverly Hills, Calif.

RESEARCH SCIENTIST

Physics degree, advanced preferable. Experienced in thermodynamics, cyrogenics, vacuum technology, optics. Aid in developing space stimulation techniques. Send resume to G. A. Nesbet, Litton Industries, Beverly Hills, Calif.

SCIENCE AND ENGINEERING

Opportunities at Robert College, Istanbul, Turkey for qualified men in civil engineering or mathematics, interested in combining teaching and the development of limited research and consulting activities with the opportunity to live in a vital part of the world: strengthening staff, modernizing undergraduate curricula, beginning graduate programs in engineering, developing undergraduate and later graduate programs in sciences, constructing new science and engineering building to prepare engineers for the industrial and technical development of Turkey and the Middle East. Address inquiries to Dean Howard P. Hall, School of Engineering, or Prof. Frank Potts, Acting Dean, School of Sciences, Robert College, Bebek, Post Box 8, Istanbul, Turkey, with copy to Near East College Assoc., 40 Worth St., Room 521, New York 13, N. Y.

ENGINEERING EDITOR

Young engineer with an interest in technical publications work has an excellent opportunity for a permanent position on the IRE headquarters staff as assistant to the Managing Editor. Send resume to E. K. Gannett, Managing Editor, Institute of Radio Engineers, 1 East 79 Street, New York 21, N.Y.

1960 Radio Engineering Show
March 21-24, 1960
New York Coliseum

These manufacturers have invited PROCEEDINGS readers to write for literature and further technical information. Please mention your IRE affiliation.

(Continued from page 118A)

Silicon Alloy Transistors

A new line of silicon alloy transistors for military and industrial electronic applications has been introduced by **National Semiconductor Corp.,** Danbury, Conn.

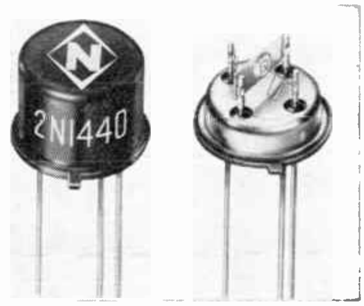

Designated by type numbers 2N1440, 2N1441, and 2N1442, these transistors are specifically designed for small signal applications, such as audio, servo and dc amplifiers. Low noise and high gain amplification characteristics at low collector currents are said to make these transistors suited for front end applications.

Unique features claimed for these units include: highest device dissipation at elevated temperatures (100 mw at 125°C in free air); highest junction and operating temperatures; and, guaranteed maximum current gain and maximum collector cutoff current at 150°C.

For increased mechanical strength, wafer mounting tabs are welded on both ends to supports. The firm states further that these transistors exceed the requirements of military specification MIL-T-19500 A.

Rack-And-Panel Connectors

The Series 8007, Varicon connector with screw actuating device (to provide positive lock against vibration plus easy engagement and disengagement) is available with 75, 100 and 130 contacts. Series 8008, without screw actuating device, available with 80, 95, 110, 125 and 140 contacts. Both Series are available with or without cover from **Elco Corp.,** "M" St. below Erie Ave., Philadelphia 24, Pa.

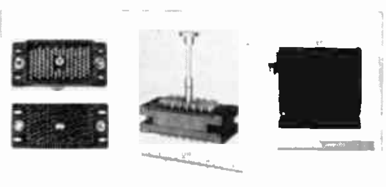

Contacts and contact rows are at 0.150" spacing; contacts are of standard, phosphor bronze, nickel plated, gold glashed. Insulators are glass-filled diallyl

(Continued on page 130A)

NEWS New Products

These manufacturers have invited PROCEEDINGS readers to write for literature and further technical information. Please mention your IRE affiliation.

(Continued from page 129A)

phthalate. Female insulator has Varicon contact recessed in holes below insulator surface; male insulator has forked contact exposed, with collar molded around contact pattern for positive protection of contact against damage. Collar also is designed for mating in only one possible position.

Both Series have male guide pin and female guide socket to align connectors properly during engagement and disengagement. Each pin and socket, in addition, is designed to permit 6 mounting and therefore 36 polarizing positions; with a theoretical possibility of over 100 polarizing variations. Polarization may be changed, if necessary, even after connector is mounted to chassis, by use of a small special tool.

Screw actuating device is permanently assembled to the insulator at the factory. Removal of knob is all that is required to assemble cover. Metal inserts are riveted to insulator center to act as guide or nut; nylon washers are inserted between moving parts to reduce friction and avoid metal wear. This design allows the use of screw actuating device with or without cover. Both cover and/or device can be factory assembled to the male or female member of the connector.

Audio Transmission Test

A test set for checking the characteristics of transmission lines and other voice band equipment has just been announced by the **Hallamore Electronics Co., a Division of the Siegler Corp.,** 714 N. Brookhurst St., Anaheim, Calif.

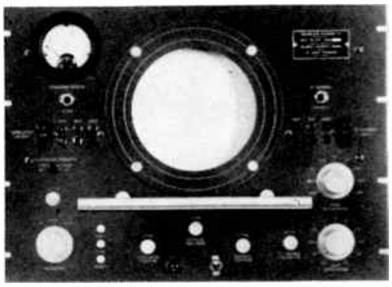

The test set, model TMS-0100, utilizes swept-band techniques to reduce the time needed to check-out a transmission network over the 200 to 400 cycle band.

The TMS-0100 employs a swept-frequency generator to provide a sinusoidal wave of adjustable constant amplitude at all frequencies in the voice-band, a measuring system to compare network input and output regardless of the absolute power level, and a cathode ray tube to display a visual form, the information necessary to evaluate network characteristics.

The entire unit is housed in a single 19″ chassis for rack-mounting or in a portable cabinet. The controls and the 7″ CRT face are located on the front pane. A CRT

(Continued on page 132A)

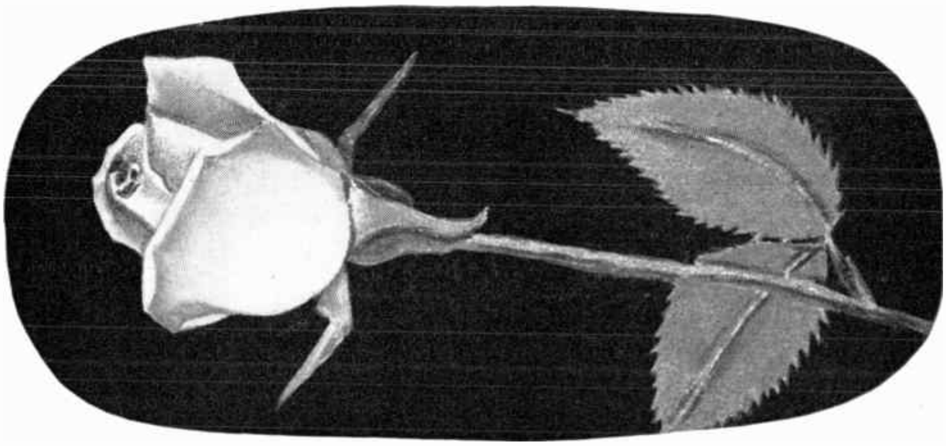

At Bendix York, we have a number of immediate openings for Electronic Engineers and Physicists.

There are many worthwhile advantages awaiting the Professional Engineer who chooses to advance his career with us at Bendix York.

A white rose . . .

The white rose is a symbol at Bendix York . . . a symbol with two meanings. Both of vital importance to *your* future.

First, the white rose is the official flower of York, Pennsylvania. It is a symbol of the good life in our dynamic community, located in the heart of the scenic Pennsylvania Dutch region. It is a wholesome, happy area with excellent schools, delightful recreational opportunities and many cultural advantages. Here—away from high-pressure, high-cost, big-city living—you will enjoy the fuller, more rewarding life that you want for yourself and for your family.

Second, the white rose is a symbol of perfection . . . the perfection for which we strive at Bendix York—perfection in the engineering and scientific pioneering and development in missile electronics that is our principal objective.

We offer a small Division's assurance of individual recognition and advancement, and yet you have the security and employee benefits of a large corporation.

We would like to have the opportunity to tell you more about Bendix York. We invite you to contact us—by dropping us a post card, by giving us a call or, if you will, by sending us a brief resume. Address Professional Employment: Dept. P

Bendix
AVIATION CORPORATION

YORK DIVISION

York, Pennsylvania
Phone: York 47-1951

NEWS New Products

These manufacturers have invited PROCEEDINGS readers to write for literature and further technical information. Please mention your IRE affiliation.

(Continued from page 130A)

with P7 phosphor and an amber filter is used to increase and accentuate persistance time and to reduce blue phosphor response.

Typical of the capabilities of the TMS-0100 test set is its use in checking the insertion gain or loss of transmission circuits in service. By using two independent signal channels, one operating with the sweep generator to establish an input power reference level and the other detecting changes in output, two distinct traces are produced on the tube. These traces represent the input reference and the voltage appearing across the load. Frequency is located on the horizontal axis and can be established by built-in markers appearing as pulses at 1000 cps intervals. The vertical deflection shows signal amplitude. The departure from coincidence of the two trace lines at any frequency is a measurement of network gain or loss. Coincidence may be established by the regulation of attenuators graduated in decibels from which the gain or loss is read directly. Instruments located at widely separated points may be synchronized for end-to-end circuit measurements.

In addition this model will also provide a whole-band display of relative input impedance and the transmission-frequency output characteristics of negative-impedance repeaters, equalizer networks and hybrid networks, where proper operation depends on incircuit adjustment.

Time Delay Relays

Wheaton Engineering Corp., 920 Manchester Rd., Box 191, Wheaton, Ill., announces the most recent addition to it's growing family of time delay relays.

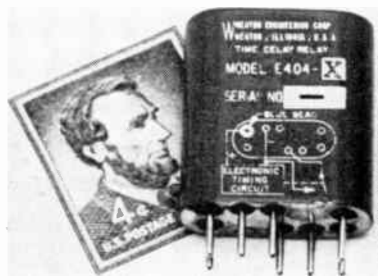

Weighing ½ an ounce and of crystal can size, Model E404 will fit into many systems previously impossible due to size limitations.

The input stage performs one or more of the following functions: rectification and filtering on ac timers; overvoltage and transient suppression on input power surges; voltage regulation. The timing stage is a conventional RC integrator. To secure a high degree of timing accuracy

(Continued on page 134A)

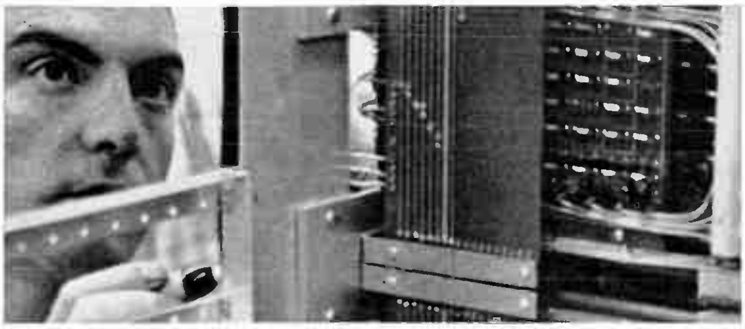

UNUSUAL ENGINEERING SUCCESS can be achieved in the creative climate at Martin Orlando. Talented young engineers and scientists carry big assignments in challenging electronics and missile programs. New projects and an expanding engineering department present rewarding opportunities to men who can manage and staff important new assignments.

WORK WHERE YOU WANT TO LIVE Engineers have discovered the fun of fishing, water skiing, boating, and swimming in the 54 lakes inside Orlando's city limits. They cook out more, spend more time with their families out-of-doors, and play more golf every month of the year than ever before.

FOR OUR FREE BOOKLET, write Mr. John F. Wallace, Director of Employment, The Martin Company, Orlando 21, Florida

SKILLED ENGINEERS, scientists, and production men moved into a new facility in Orlando, Florida, just two years ago. Working in the stimulating environment of a new $21-million plant, these men have written a most unusual growth record for five major electronic and missile projects and several advanced research programs at Martin Orlando. The professional advancement of the men who manage and staff ambitious new programs has kept pace with this rapid progress. Investigate new programs in Communications, Guidance and Control, Reliability and Quality, Radar Systems and Operations Analysis. You may move into a ground-floor position by sending your resume now.

MARTIN
ORLANDO

DURING IRE, VISIT MARTIN ORLANDO
AT WALDORF-ASTORIA

NEWS New Products

These manufacturers have invited PROCEEDINGS readers to write for literature and further technical information. Please mention your IRE affiliation.

(Continued from page 132A)

throughout temperature range, four different means of compensation are utilized. Each means is tailored to specific time delay intervals and temperature ranges. Also since each timer has an internally regulated voltage source for the timing network, the change in timing with changes in input voltage is negligible.

The transistorized sensing stage is adjusted to trigger at a preselected value of charge on the timing capacitor. In all these electronic timers the output function occurs at less than 1 RC leading to simplicity of detection and ensuring timing precision because of the steep slope of the charging curve below 1 RC.

When the transistorized sensing stage triggers on, another separate transistor is driven by the output of the sensing stage.

The unit is now available in prototype and production quantities.

Tunnel Diodes For Experimentation

Because of its electrical properties, the tunnel diode manufactured by the **Radio Corporation of America, 30 Rockefeller Plaza, New York 20, N. Y.**, is extremely useful as a high-frequency oscillator, low-noise amplifier, high-speed switch, self-excited converter and clipper, and in communications and storage devices. All of these functions can be handled with low power and low heat dissipation. The negative resistance characteristic of the tunnel diode—the simultaneous increase in voltage with decrease in current—permits the units to supply energy rather than dissipate it through a large portion of its cycle. The instantaneous transfer of charge carriers which gives rise to this characteristic is called the tunnel effect.

RCA's initial sample types include twelve tunnel diodes designed for operation up to 1,000 mc with power consumption ranging from 0.75 milliwatt to 3 milliwatts. Nominal peak currents (tunnel currents) range from 1.8 milliamperes to 6.8 milliamperes. For maximum usefulness of the negative resistance characteristic, the ratio of peak current to minimum current is maintained in excess of 4.5 to 1.

This mesa device consists of a p-n junction 1/1000 of an inch in diameter and 80 angstroms in width (about 1/150 the wave-length of visible light). This unit is mounted in a new miniature, low inductance ceramic case specially designed for ultra-high-frequency applications. The package, developed at RCA's Laboratories by Dr. Charles Mueller, has an inductance of 0.4 millimicrohenry, which is believed to be lower than that of any available semiconductor case.

(Continued on page 137A)

ARE YOUR TALENTS BEING RECOGNIZED?

Hughes-Fullerton's unique, new
Professional Capabilities Register
insures recognition of all your abilities

Creating a new world with ELECTRONICS

HUGHES

FULLERTON-RESEARCH & DEVELOPMENT

Please turn the page for information on the new Hughes-Fullerton Professional Register

First Class
Permit No. 358
Fullerton, Calif.

BUSINESS REPLY MAIL
No postage necessary if mailed in the United States

POSTAGE WILL BE PAID BY

HUGHES-FULLERTON RESEARCH & DEVELOPMENT
Hughes Aircraft Company
Building 600, Room: B-149
Fullerton, Orange County, California

Attention: Manager, Professional Placement I.R.E.

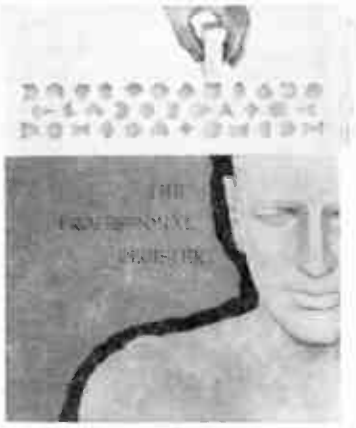

If you would like to know more about Hughes-Fullerton and participate in the new Professional Capabilities Register, please return this post-paid card, today.

PROFESSIONAL REGISTER EMPLOYMENT INQUIRY *(Strictly Confidential)*

Please complete this card, fold, staple and mail. The information you give constitutes the first phase of the Professional Register Program and will enable our professional staff to make a preliminary evaluation of your abilities. All inquiries will be answered immediately. When you complete the Program, the inventory of your talents and capabilities will be recorded on over 20 electronic data-cards available for instant use in guiding your future progress at HUGHES-FULLERTON.

Name__________

Address__________

City______ State______ Telephone______

Education:	BS	MS	PhD	Date (s):		BS	MS	PhD	Date (s):
EE	☐	☐	☐	____	Physics	☐	☐	☐	____
ME	☐	☐	☐	____	Other:____	☐	☐	☐	____
Mathematics	☐	☐	☐	____	____	☐	☐	☐	____

School (Highest Degree)__________

FOLD

AREAS OF PROFESSIONAL EXPERIENCE:
(please check boxes)

- ☐ Computers
- ☐ Electron Tubes
- ☐ Electronic Circuitry
- ☐ Telemetry
- ☐ Circuit Theory
- ☐ Radar
- ☐ Power Generation
- ☐ Power Transmission
- ☐ Servomechanisms
- ☐ Microwaves
- ☐ Solid State Physics
- ☐ Electromechanical Systems
- ☐ Other:____

FUNCTIONS PERFORMED:
(please check boxes)

- ☐ Research
- ☐ Development/Design
- ☐ Technical Writing
- ☐ Project Management/Supervision
- ☐ Administrative Staff Support
- ☐ Systems Analysis
- ☐ Testing/Process Control
- ☐ Product Engineering
- ☐ Field Engineering
- ☐ Operations Research
- ☐ General Engineering
- ☐ Systems Engineering
- ☐ Other:____

Are your talents being recognized?

Most engineers have had to face an unpleasant fact. Often an employer will hire from outside to fill a supervisory post. Entirely qualified men "inside" are passed over. The problem is generally one of communication. The employer simply does not have adequate knowledge of his employees' abilities and promise.

Hughes-Fullerton's new Professional Capabilities Register reflects the complete engineering-orientation of this fastest-growing Hughes activity. (From 800 to nearly 6,000 people since 1957. Planned, *scheduled* growth.)

The Register makes instantly available a complete record of every individual's abilities, interests and accomplishments. Previously hidden talents can now be put to use. Often these can mean the difference when reassignments or promotions are being made. Your potentials become a very real resource of Hughes-Fullerton Research and Development Staff.

Areas covered in the Register range from language skills through patents to books and articles published. It includes teaching experience, professional affiliations. All data is kept up-to-date and handled by automatic data processing equipment for utmost efficiency.

Hughes-Fullerton's philosophy of giving precedence to the needs of engineers has worked well. Hughes-Fullerton was first with three-dimension radar...a major breakthrough in the state of the art. Other vital areas of interest include advanced data processing and electronic display systems.

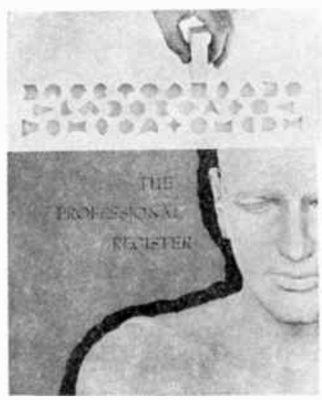

These are a few reasons why you should investigate Hughes-Fullerton. Openings exist at several experience levels for a variety of engineering specialties. For full information fill out the post card and mail it today!

Creating a new world with ELECTRONICS

HUGHES

FULLERTON RESEARCH & DEVELOPMENT
FULLERTON, ORANGE COUNTY, CALIF.

These manufacturers have invited PROCEEDINGS readers to write for literature and further technical information. Please mention your IRE affiliation.

(*Continued from page 134A*)

Digital Process Controllers

A new series of transistorized add-subtract digital process controllers has been developed by the **Dynapar Corp.**, 7312 N. Ridgeway Ave., Skokie, Ill., for a wide range of industrial bi-directional measurement and control applications.

These include: automatic machine or material positioning, measuring or cutting-to-length, coilwinding, pulse-tachometry—wherever precise forward and backward motion or up-and-down quantities must be measured to control other equipment. The controllers provide direct-reading numerical display of the measurement, and have provision to actuate various control functions on production equipment when a preset number (or series of numbers) is reached.

Controllers accept input pulses from two lines—one for addition, one for subtraction. Modified units accept inputs from one line if the add and subtract pulses are opposite in polarity. The units operate at rates up to 20,000 counts per second and higher. The positive and negative counts are displayed on the panel by either illuminated numerical tubes (Nixies), or glow counter tube decades; remote or printed readout also available.

Optional features: Dual or multiple preset numbers to actuate a series of control functions; binary outputs; simultaneous add and subtract; counting through zero; explosion-proof design.

Input sensitivity: One volt RMS at 1 ma. Unitized plug-in transistorized circuitry is unaffected by wear. Controllers are housed in dust-tight all-steel enclosures with pull-out chassis design.

Alumina Powder For Potting

A basically new approach in the protection of electronic components was revealed today by L. W. Kirkwood and R. S. Key of **Bell Telephone Laboratories**, 463 West St., New York 14, N. Y. They described how alumina powder (aluminum oxide) can be used successfully to insulate, or "pot" transformers and other electrical components within hermetically sealed cans. A paper describing the development was presented at the National Conference

(*Continued on page 138A*)

NEWS New Products

(Continued from page 137A)

on Application of Electrical Insulation in Washington, D. C. The first use of alumina in this application was made by H. S. Feder, also of Bell Laboratories.

Alumina powder does not show the disadvantage of melting at low temperatures. Its melting point is over 1500°C (2700°F), well above the operating temperatures of any electrical apparatus. It does not expand or contract to any noticeable extent under wide fluctuations of temperature, so no strains are imposed on the component. Also, it doesn't need to be cured or vulcanized for use, as some of the plastic potting compounds do, and thus no strains develop from these processes.

The powder possesses another advantage over asphalts, epoxy resins, and other similar potting compounds, in that it maintains its dry, granular form in use. The electrical component can be removed for inspection or repairs at will, simply by breaking the seal on the can and pouring out the powder.

Alumina is completely inert. Thus, there is no fire hazard, either during potting operations or in use, in contrast to inflammable asphalts or resins. Since alumina is stable to such high temperature, it can be used as a single potting compound to cover the gamut of temperature ranges.

The preferred physical form of the alumina is spherical. In this shape, the granules pack well, but do not have the abrasive characteristics of more irregular shapes. Material of this type is readily available at prices competitive with conventional materials.

The test program on alumina potting compounds was performed on typical, medium-sized electronic power transformers, which were impregnated with a polymerizing varnish before potting and encasing.

Audio Response Plotter

The Audio Response Plotter, Model ARP-2, which provides permanent pen-written frequency response curves of any audio-range equipment, is described and illustrated in a bulletin which outlines the product's applications, features, and includes a block diagram. Applications include: electrical response curves of amplifiers, broadcasting equipment, hearing aids filters, networks, equalizers, and transformers; acoustical response curves of room acoustics, Hi-Fi installations, microphones, speakers, earphones, phonograph cartridges, and recording systems; vibration analysis equipment. The manufacturer is **Southwestern Industrial Electronics Co.**, a division of Dresser Industries, Inc., 10201 Westheimer Rd., P. O. Box 22187, Houston 27, Texas.

Gridded TW Tube

A new one-kilowatt traveling wave tube combining a periodic focused permanent magnet (PPM) with a gridded gun is being produced by **Hughes Products, Electron Tube Div.**, International Airport Station, Los Angeles 45, Calif.

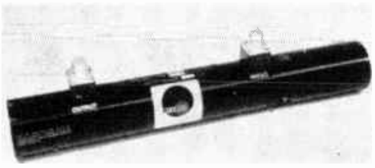

The tube, which operates in the S-band from 2.0 to 4.0 kmc, will be particularly useful to radar systems builders and users.

Combination of permanent magnet focusing with a gridded gun produces a traveling wave amplifier exhibiting full one-kilowatt power output characteristics with low power consumption.

Use of a control grid, however, enables the tube to operate with a very fast response time with much lower power consumption and simpler modulation problems.

Traveling wave tubes with gridded guns at this power level have been available but only with solenoid focusing, according to the firm. Permanent magnet focusing offers such advantages as light weight, no solenoid power supply needed, low heat generation and better reliability.

Known as the MAS-1E traveling wave amplifier, the new tube is the result of solution of certain technical problems by the company's research and development laboratories.

One of its primary uses is as a final output tube. If still more power is required it can be used to drive other high powered traveling wave tubes of klystrons. Its peak output is in excess of kw at only 0.5 watt input. By cascading two tubes an output of 1 kw can be obtained with less than 0.5 mw of drive.

Complete specifications can be obtained from the firm.

Motor-Generator Bulletin

A two-page technical bulletin just published by the **Holtzer-Cabot Motor Div., National Pneumatic Co., Inc.**, 125 Amory St., Boston 19, Mass., provides detailed performance data and design specifications on the new RBG-2407 miniature motor-generator unit. The unit consists of a low-inertia control motor (geared or direct output) and a 10v/1000 rpm ac drag-cup rate generator and is designed for precision instrument applications requiring a compact and commercially priced device.

(Continued on page 140A)

NEWS New Products

These manufacturers have invited PROCEEDINGS readers to write for literature and further technical information. Please mention your IRE affiliation.

(Continued from page 139A)

Bulletin MO-3.14 includes motor speed-torque and speed-voltage curves, complete dimensions, and electrical characteristics of the rate generator and combined unit.

A copy of Bulletin MO-3.14 may be obtained by writing to the firm.

Small Oscilloscope CR Tube

An improved three-inch rectangular faceplate cathode-ray tube for oscilloscope applications use is announced by the **Electronic Tube Division of Allen B. Du Mont Laboratories, Inc.,** 750 Bloomfield Ave., Clifton, N. J. Registered as type 3BDP, the new tube is an improved replacement for type 3SP.

Significant new features of the Du Mont 3BDP are a precision pressed faceplate to minimize parallax errors and a new gun structure for greater rigidity and improved electrical stability.

Actual face-plate measurements are $3 \times 1\frac{1}{2}$ inches, and the overall length is $9\frac{1}{4}$ inches. Focus and deflection are electrostatic.

Complete specifications on the 3BDP are available from the Electronic Tube Sales Department at the firm.

Small-Size 335-Watt Transformer

Arnold Magnetics Corp., 4613 W. Jefferson Blvd., Los Angeles, Calif., announces the addition of a 335-watt transformer to its line of small-size, high-temperature power transformers.

Unit operates over a wide temperature range of $-55°C$ to $+130°C$, and is designed to meet MIL-T 27A, Class "S." It occupies a chassis mounting space of $1\frac{9}{16} \times 3''$, and is $3\frac{5}{16}''$ high. The small size is made possible by a new design employing high-temperature wire wound in shallow coils which are widely distributed. This results in a short thermal path, thereby minimizing hot spot temperatures. Rating curves are given for 25, 75 and 100°C ambient temperatures.

A primary voltage of 115 volts, 400 cps, is standard, with secondary voltages available from 5 to 2000 volts. Breakdown voltage: 3000 VRMS, windings to case. Life expectancy: 10,000 hours under conditions specified in MIL-T-27A. Regulation: 5% maximum, at full ratings.

Designated "Thin Tran" Series 883, this transformer is fully encapsulated and hermetically sealed to meet the environmental requirements of MIL-E-5272B. Unit weighs 2.3 pounds, providing a power-to-weight ratio of 140 watts/pound. Complete information will be sent on request to the firm.

Pulse Mixer

A new pulse mixer, logically similar to their pulse gate, is now available from **Harvey-Wells Electronics, Inc.,** East Natick, Industrial Park, East Natick, Mass.

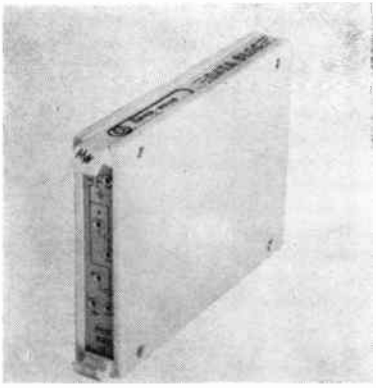

The unit consists of two gating transistors with a common output pulse transformer. It differs from the pulse gate in that two pulse rates can be mixed and amplified.

Electrical specifications of the unit are: input/output, negative four-volt 1/10 microsecond pulses; supply voltages and currents, negative 15-volts, 30 milliamperes; plus 10-volts, 0.3 milliamperes; and clamp voltage negative four-volts at plus 20 milliamperes. Detailed product and application data is available from the Research and Development Div.

Photoelectric Shaft Position Encoder

The new Type RD-17 DIGISYN, a product of **Wayne-George Corp.,** 588 Commonwealth Ave., Boston 15, Mass., is a highly precise, photoelectric, shaft-position encoder. It gives angular position data in 17-digit cyclic binary code with ±one-

(Continued on page 142A)

These manufacturers have invited PROCEEDINGS readers to write for literature and further technical information. Please mention your IRE affiliation.

(Continued from page 141A)

digit accuracy. This is better than ±10 seconds of arc. The 17-digit accuracy for 1 shaft revolution is obtained in unambiguous form without the use of gears. The 26 lb., 10-inch diameter unit includes power supplies, amplifiers and control electronics. It may be used wherever it is necessary to read a shaft position in digital form, either for recording on magnetic or punched tape, or for application to a digital computer. Typical applications include tracking, servo, machine control and navigation systems.

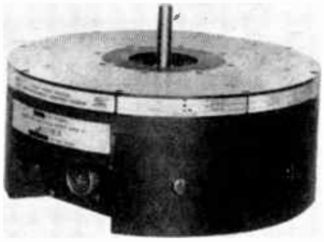

The Type RD-17 DIGISYN consists of a glass disc coded by an array of opaque and transparent segments, a flash lamp to illuminate a radius of the code disc, a multi-element photo sensitive light detector, 17 transistorized amplifier channels and all power supplies and control electronics. The unit operates from 115 V 60 cycle or 400 cycle primary power. Designed to meet applicable portions of MIL-E-4158B, all circuits feature solid state components. Modular, plug-in, electronic assemblies are easily replaced.

Alarm/Control System

Designed primarily for utilities, pipelines, railroads and similar companies which monitor and control unattended locations remotely from a central control point, a new Alarm/Control system has been placed on the market by **General Electric Co., Communication Products Dept.**, Lynchburg, Virginia.

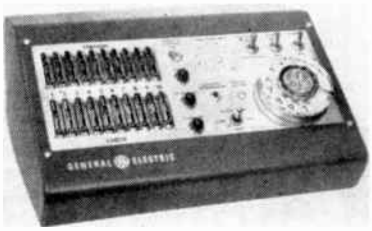

The new equipment may be used with various types of transmission media, such as microwave, carrier current, or wire lines. The control signals employed are in the

(Continued on page 144A)

NEWS New Products

These manufacturers have invited PROCEEDINGS readers to write for literature and further technical information. Please mention your IRE affiliation.

(*Continued from page 142A*)

form of tones which provide communication between the control point and remote locations. They may be used to check a single location or as many as 100 different points.

Ten functions may be checked at each point. The signals will indicate whether a certain prescheduled action is taking place at a remote location or whether faults have occurred.

At the control terminal, a small console is mounted on the operator's desk and a cable connects this with rack-mounted tone equipment. The console has a bank of 10 indicator lamps to show the stations being selected and a second bank to show whether any faults are present. A dial is employed to select and check the desired station and to operate remotely-controlled equipment at unattended distant points.

At the unattended station, the tone equipment is mounted in standard relay racks and requires two panels $3\frac{1}{2}$ inches deep. One panel has switching equipment for remote selection and the second contains the tone receiver and power supply.

Peak Responding Voltmeter

A new peak responding Voltmeter, Model 305A, is announced by **Ballantine Laboratories,** Boonton, N. J. The new instrument measures peak or peak-to-peak values of any repetitive waveforms—distorted or undistorted sine-waves, or pulses. Its operating mode can be selected to respond to a peak-to-peak and positive or negative peak of the waveform.

The dc component of the waveform is not measured by the instrument.

The frequency range when measuring sinewaves extends from 5 cps to 500 kc., but distorted waveforms with harmonics extending up to 2 mc, however, can also be measured. Pulses with duration from 0.5 μsec to 5 milliseconds and with a repetition rate from 5 to 500,000 pps can also be measured.

The accuracy is 2 to 5% depending on the waveform measured. The precision of the reading is better than 0.5% at any part of the scale.

The Model 305A can be used as a wide-band amplifier with a gain of 86 db and a source impedance of approximately 3 ohms in series with 0.22 μf. The maximum output voltage from amplifier is 150 volts pp. The amplifier output is intended to be used for waveform monitoring only into loads above 30,000 ohms and below 10 $\mu\mu$f.

The instrument has a magnetically regulated power transformer in addition to an electronically regulated power supply.

Miniaturized Digital Readout

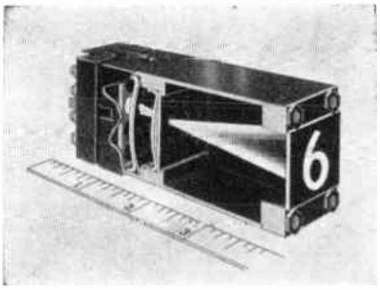

A miniaturized digital readout, named Series 120ooo, is announced by **Industrial Electronic Engineers, Inc.,** 5528 Vineland Ave., North Hollywood, Calif. It is the latest model of a complete line of rear-projection type digital readouts manufactured by this company.

It is designed for use with digital computers, control equipment, instruments, production and inventory controls, and other electronic or electrical test equipment.

The principle of operation is rearprojection. When one of the twelve lamps at the rear of the unit is lighted, the lamp projects the corresponding digit on the condensing lens through a projection lens onto the viewing screen at the front of the unit.

The light source comes from sub-miniature lamps, either No. 327, 328, or 330. Voltage is from 6 volts to 28 volts. An outstanding feature is the quick disconnect at the rear for lamp replacement.

The size of the character displayed on the viewing screen is $\frac{5}{8}''$ high. The case is aluminum and it may be mounted on one-inch centers. It weighs approximately four ounces.

Dimensions—$3\frac{7}{8}''$ long overall, 1" wide, and $1\frac{5}{16}''$ high. Other specifications include single-plane in-line presentation, no moving parts, low unit cost, long operating life, and rear wiring for easy installation.

The miniaturized digital readout is priced at $35.00 each. Quantity prices are available upon request. It is available from stock in single units or in assemblies.

Printed Circuit Connector Catalog

A new 36-page catalog section, featuring a large variety of printed connectors offered to the industry, is being released by

(Continued on page 146A)

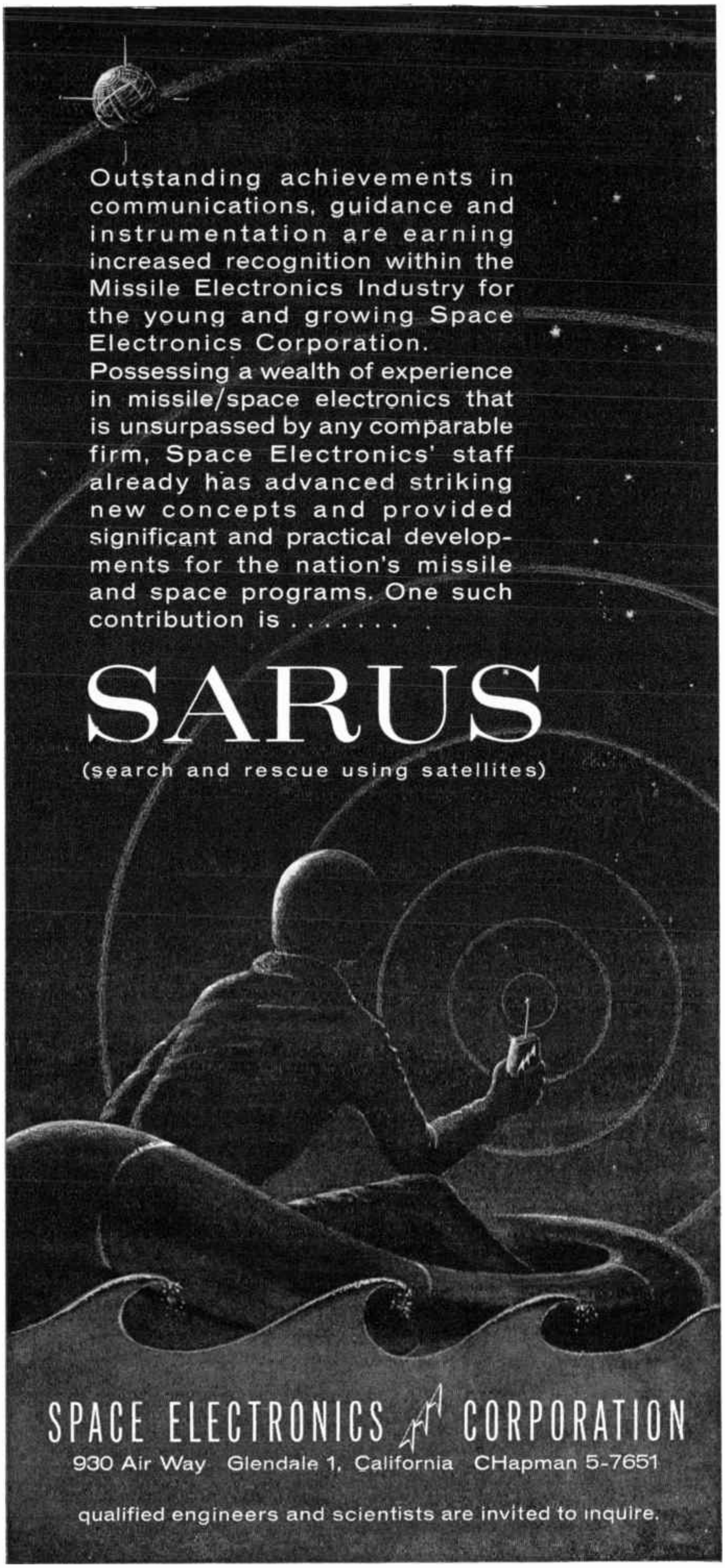

NEWS New Products

These manufacturers have invited PROCEEDINGS readers to write for literature and further technical information. Please mention your IRE affiliation.

(Continued from page 145A)

H. H. Buggie Division, Burndy Corp., Toledo 1, Ohio.

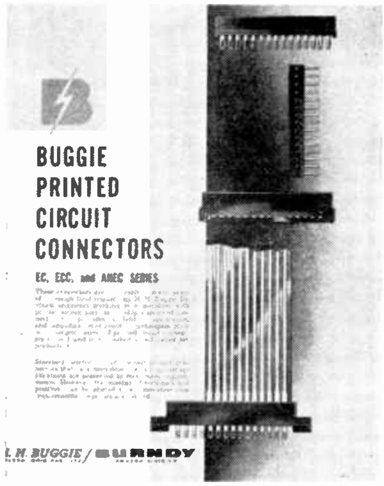

In addition to many standard card receptacles, terminal strips, contact strips, and miniature series EC coaxial connectors, twelve pages are used to illustrate and provide design and engineering data on printed circuit connectors that have been designed by the company engineers for special applications. The catalog section is the first to feature special male and female connectors and card receptacles.

Standard types are available with 10, 15, 18, and 22 contacts, while the special series features designs with 4 to 46 contacts in number. General specifications include details of construction and description of materials and terminations.

The catalog section has been prepared for the electronics design and specifications engineer in need of a thorough reference on printed circuit connectors. It is available by making requests on company letterhead.

Time Delay Relay

The new STR Series relay available from **Curtiss-Wright Corporation, Electronics Division, Components Department,**

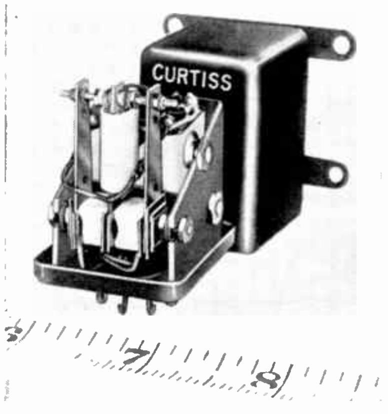

(Continued on page 148A)

These manufacturers have invited PROCEEDINGS readers to write for literature and further technical information. Please mention your IRE affiliation.

(Continued from page 146A)

620 Passaic Ave., West Caldwell, N. J., provides a combination of features to meet airborne and missile application requirements. The STR relay provides: Instantaneous resetting, Isolated load contacts, Preset T/D 20 180 seconds, miniature size, Voltage compensation, Ambient temperature compensation, Meets shock and vibration environments, Single Pole Double Throw Contacts, and is Hermetically sealed.

The STR relay will reset the instant it is deenergized, providing the same time delay period for each succeeding cycle. This operational advantage has been achieved by employing a special thermal element in conjunction with a pair of magnetic relays. This component combination utilizes the heating and cooling intervals to obtain the total time delay period.

Voltage compensation is provided for operation on 22 to 32 volts dc. Temperature compensation is over the range of $-65°C$ to $+125°C$. The unit may be operated under high shock and vibration.

Power drain less than 3 watts after the timing period: 10 watts during timing. Contact rating 2 amperes at 28 volts dc resistive load Approximate dimensions $1\frac{5}{8}'' \times \frac{13}{16}'' \times 1\frac{1}{2}''$ with bracket or stud mounting.

Miniature Switch

A new miniature rotary switch ($1\frac{5}{8}''$ body diameter) designed for low power selector switching applications has been developed by **Trolex Corp.**, McHenry, Ill., a subsidiary of Chicago Telephone Supply Corp. Uniformity and reliability is attained by new automated manufacturing processes. Permanently positioned terminals are molded into housing and cannot turn or twist out of place. The design prevents solder from running down into cir-

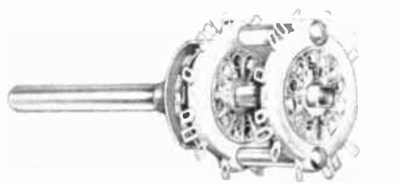

cuit elements during soldering. Molded glass alkyd housing exceeds MIL standards, has high mechanical strength, low toxicity and nondrift characteristics. Type 212 is not subject to breakage during ordinary handling nor accidental dropping. Wafers can be stacked directly on top of each other with no spacers required. Laminated coin silver contacts provide reliable contact life for a minimum of 100,000 cycles thru 12 positions without appreciable increase in contact resistance. Trolex standard layouts handle most circuits; are quickly adapted to more complex circuits. Flexible tooling provides countless contact arrangements without special tooling. (Now in production for delivery approximately 3 to 4 weeks from receipt of order. Price based upon quantity and design requirement.)

Synchro Brochure

A reference data brochure on Size 8 Synchro Components is now available from **Induction Motors of California**, 6058 Walker Ave., Maywood, Calif. The brochure will be of particular value for the application of synchros in the design of control systems, computers, fire control mechanics, missile settings and many other applications.

The new brochure contains general electrical specifications for torque receivers, torque transmitters, control transformers, resolver transmitters, vector resolvers, linear transformers, and control differentials. The design options and mechanical characteristics are also listed.

The synchros are manufactured in general accordance with MIL-S-20708, ARP-461, MIL-E-5272 and MIL-E-5400.

Copies of the new brochure, Bulletin 204, as well as information on size 11 synchros, step-servo motors, and solenoids, may be obtained by writing direct to the firm.

Micro-Microammeter

The Model 414, an economical instrument for measuring dc currents from 10^{-2} to 10^{-11} amperes, is available from **Keithley Instruments, Inc.**, 12415 Euclid Ave., Cleveland 6, Ohio. It is priced at $280.00 and is specifically designed for production tests, monitoring installations, and laboratory measurements of micro-

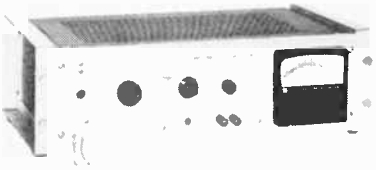

currents. Its large, mirror-scale presents 17 ranges in overlapping 1X and 3X steps. Accuracy is within 3% of full scale down to 10 milli-microamperes. Additional features include: a five-volt output at up to one milliampere, output noise less than 1% peak to peak of full scale, a 0.2 second response speed, and optional contact meter variations.

Details about the Model 414 Micro-microammeter are available in Keithley Engineering Notes, Vol. 7 No. 5.

Pot Cores

Ferroxcube Corporation of America, Saugerties, N. Y., a producer of magnetic ceramics, has expanded its facilities to meet the growing demand for its miniature type 332P pot cores and assure users of

(Continued on page 150A)

NEWS New Products

(Continued from page 149A)

production quantities on short notice. These $\frac{3}{4}''$ diameter pot cores, now widely used for pulse transformers and kindred

applications, meet the assembly and mounting requirements of all component manufacturers and are available in several varieties, including one which has a hole in its center post to accept a No. 1 screw. Samples, in sufficient quantities to enable research and development engineers to conduct investigations in the light of their own specific application requirements, will be furnished promptly on request.

Waveguide Switches

New E-plane waveguide switches manufactured by **DeMornay-Bonardi**, 780 S. Arroyo Parkway, Pasadena, Calif., are used to transfer the connection between waveguides. Transfer may be direct, or by remote control.

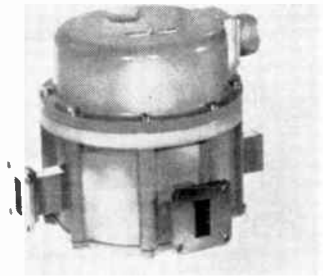

Two switch types are supplied, one is a 2-way exchange, which switches a common waveguide to either adjacent waveguide. Disconnected waveguide is terminated in a matched load. The second is a 4-way exchange, which switches two pairs of waveguides. The switches are used in measurement set-ups, and in experimental and operational systems.

Each unit consists of a cylindrical housing, with waveguide flange connections brought out for the positions required. Switching is accomplished by a solenoid-operated rotor which connects any leg to either adjacent leg. Quarter wave chokes provide continuity between stationary waveguide and rotor.

Units are designed for high capacity, and high channel separation. Remote indication or interlock of other functions can be controlled through two micro-switches

(Continued on page 151A)

fmc FOOD MACHINERY AND CHEMICAL CORPORATION

SAN JOSE

Current Career Opportunities

In Commercial Products R&D

ELECTRONIC ENGINEERS PHYSICISTS

experienced in Industrial Electronics and Automation

Creative top level engineers and physicists are needed now to work on advanced assignments in the design of optimum systems using electronic and mechanical components.

FMC Central Engineering's current expansion into automatic measurement and control fields offers permanent career opportunities for technical accomplishment on important company-sponsored, long-range programs. Systems engineers, circuit designers and specialists needed to staff new million dollar laboratories.

With corporate headquarters in San Jose, California, FMC is highly diversifed in both machinery and chemicals, with 15 divisions operating throughout the U. S. and overseas.

BS required and advanced degrees desirable for these responsible positions. Experienced applicants or recent graduates should send complete resume:

Contact E. M. Card, Jr., or C. F. Duvall at FMC Central Engineering, P.O. Box 760, San Jose, Calif. Phone: CYpress 4-8124.

Putting Ideas to Work

Central Engineering Laboratories

fmc FOOD MACHINERY AND CHEMICAL CORPORATION

FOOD MACHINERY AND CHEMICAL CORPORATION

Look beyond the obvious . . .

. . . as you consider *your* future in the electronics industry. First, what is the obvious? It's obvious that you're in demand. You don't have to worry about getting your material wants satisfied.

But, when you look beyond the obvious, you realize that you want something more than simple "want satisfaction" out of your career. You want *pride*—pride in the importance of your personal, *individual* contribution.

At Melpar, where we are now working on 120 advanced defense and space exploration projects, we have significant opportunities for the professional engineer or scientist who wants to be proud of his contribution to advancing the state of electronic art.

Senior-level positions are available in the following areas at this time:

Reconnaissance Systems	Detection & Identification Systems
Airborne Equipment	Antenna & Radiation Systems
Ground Data Handling Equipment	Physical Sciences Laboratory
Simulation & Training Systems	Production Engineering
Communication & Navigation Systems	Quality Control
Ground Support Equipment	Field Service Engineering

INTERVIEWS ARRANGED IN YOUR LOCALE

For details wire collect or write to:
Professional Employment Supervisor

MELPAR INC.

A SUBSIDIARY OF WESTINGHOUSE AIR BRAKE COMPANY

3322 Arlington Boulevard, Falls Church, Virginia
In Historic Fairfax County
10 miles from Washington, D. C.

season by season

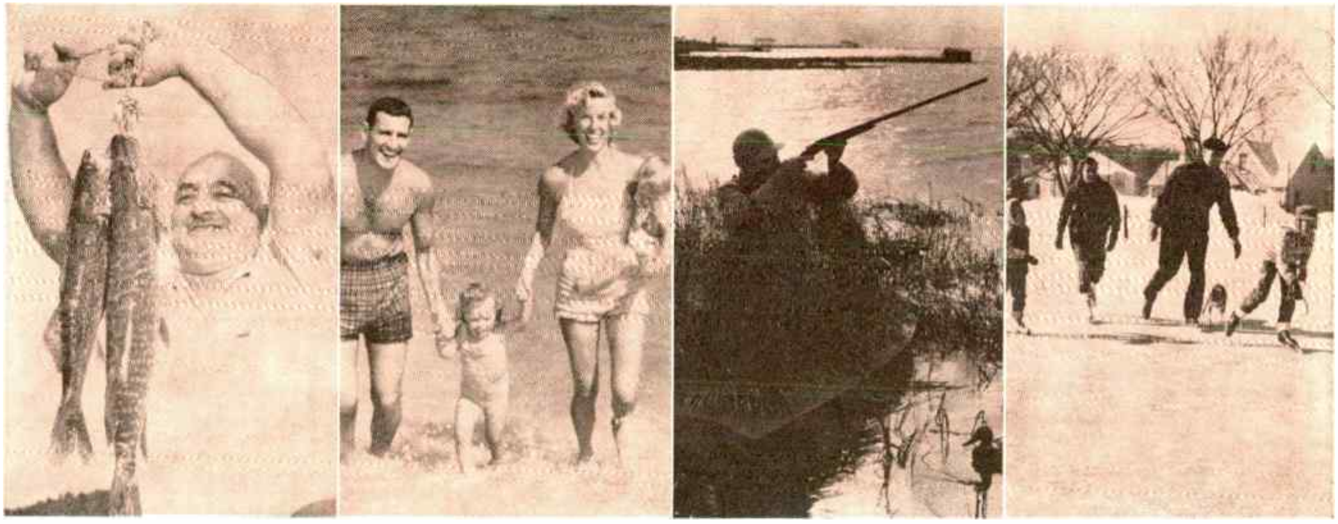

Honeywell engineers and their families experience wide variations in climate—and their activities vary as much as the climate. Some spend winter in hibernation-type activities such as reading by the fireplace. More enterprising souls enjoy outdoor activities like skating, skiing, ice fishing, ice boating, sleigh-riding. Griping about the weather seems to be a universal pastime, and Minnesotans are no exception. Yet, ask a Minnesotan who has moved away what he misses most—he'll tell you it's the seasonal changes. The foot-and-a-half snowfalls, the melting springs when everything begins to turn green again, the warm, pleasant summers, the colorful autumns. Such pronounced changes seem to stimulate mental as well as physical activities. It's a good place to live and a good place to raise a family. And it's part of the living that Honeywell engineers and their families enjoy.

For further information on working at Honeywell Aero—and living in Minneapolis, please send a resumé to Bruce Wood, Dept. 364A.

AERONAUTICAL DIVISION
1433 Stinson Blvd. N.E., Minneapolis 13, Minnesota

To explore professional opportunities in other Honeywell operations coast to coast, send your application in confidence to H. K. Eckstrom, Honeywell, Minneapolis 8, Minnesota.

These manufacturers have invited PROCEEDINGS readers to write for literature and further technical information. Please mention your IRE affiliation.

(Continued from page 150A)

which are in turn controlled by switch position. Remote control boxes are available for remote indication and control. The waveguide portion of the switch is supplied pressurized on request.

All units are plated nickel over silver over copper. Sizes range from 2.6 to 90 kmc. Deliveries: 2 weeks on most items from receipt of order. Prices: $591 to $919, depending on size.

Variable Delay Line Box

Valor Instruments Inc., 13214 Crenshaw Blvd., Gardena, Calif., has designed a new variable delay line box which delivers any delay up to 0.79 μsec with an accuracy of 0.8% of the maximum delay by means of binary switching. Reflections, ordinarily associated with variable delay lines, are eliminated because the unused portion of Model 443B3 is disconnected from the circuit by means of the switching.

Specifications: Rise time is 0.05, μsec for the maximum delay and decreases as lesser delays are used; Impedance: 100 ohms; Attenuation: 3.5%; Size: 3″×3″×5″.

Uses: The variable unit may be connected into a circuit to determine the specifications of the delay line that will provide optimum characteristics or, as a substitute until production prototype delay line is delivered.

Universal Joint

A new telescoping miniature universal joint has been designed by the **Falcon Machine & Tool Co.**, 209 Concord Turnpike,

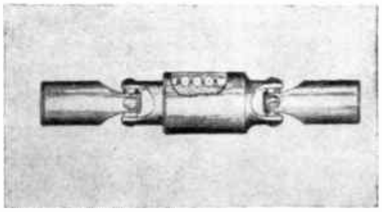

Cambridge Mass. This device allows greater freedom in the design of systems, such as magnetron and klystron drives, servodrives, and so forth, where the precise transmission of information is essential.

(Continued on page 156A)

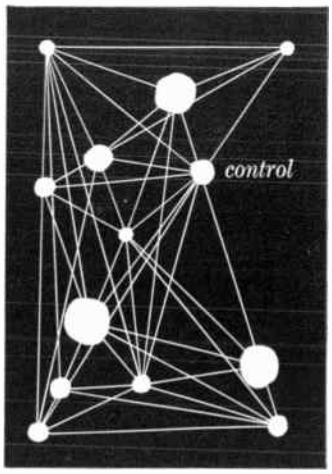

professional opportunities at Honeywell Aero

INERTIAL SYSTEM DEVELOPMENT

Systems Analyst—employs mathematical techniques such as operational calculus, matrix algebra, and difference equations to the solution of problems concerning performance characteristics of various system configurations including analysis for error introduced by sensors and computer, requirements for alignment, and optimization of the system configuration.

Digital System and Logic Designer—requires familiarity with capabilities of various digital computer configurations and ability to employ system and logic relations in specifying necessary configuration for solving inertial navigation problem.

Electronic and Mechanical Designers—engineers with background in transistor circuitry, inertial sensor development and evaluation, and precision mechanical equipment design are needed to perform component development and evaluation, and to design mounting and alignment equipment.

APPLIED RESEARCH

Programmer Analyst—mathematician with experience in the use of medium and large scale digital computers for analysis of scientific problems.

Human Factors Engineer—capable of analysis and direction of experiments in human motor skills, and application to man-machine systems involving automatic control techniques.

Systems Analyst—capable of conducting research studies involving new techniques of space navigation and guidance.

DESIGN AND DEVELOPMENT

Flight Control Systems—analytical, systems, and component engineers to work in areas such as advanced flight reference and guidance systems. Positions range from analyzing stability and control problems, systems engineering—through design, testing, and proof of electrical and mechanical equipment —including flight test and production test.

Advanced Gyro Design—Engineers with two and up to twenty years' experience in precision gyro and accelerometer development, servo techniques, digital techniques, solid state electronic development, advanced instrumentation and magnetic component design.

Electronic Circuit Designers—experienced in the areas of analog/digital computers, transistor circuits, servos, instrumentation, and/or gyro stabilization.

For the less experienced professional engineer, there are opportunities in the Evaluation Laboratory which lead to careers in any of the above fields.

To investigate any of the above professional opportunities at the Aeronautical Division, please write in confidence to Bruce Wood, Dept. 364C

To explore professional opportunities in other Honeywell operations coast to coast, send your application to H. K. Eckstrom, Honeywell, Minneapolis 8, Minnesota.

Honeywell H HONEYWELL
AERONAUTICAL DIVISION
1433 Stinson Blvd. NE, Minneapolis 13, Minnesota

NEWS New Products

These manufacturers have invited PROCEEDINGS readers to write for literature and further technical information. Please mention your IRE affiliation.

(Continued from page 154A)

Two preloaded ball splines provide lateral travel and a minimum amount of thrust on connected components. The two universal joints feature sealed-in lubrication of preloaded bearing surfaces between burnished sockets and precision balls giving continuous contact. This design assures zero backlash for the entire assembly.

Body components are type 303 stainless steel; balls are of type 440 stainless.

Standard assemblies have $\frac{1}{4}''$ lateral travel; greater travel available on special units. Standard joints are available in following sizes: $\frac{3}{16}''$ body with choice of $\frac{3}{32}''$ and $\frac{1}{8}''$ bores, $\frac{3}{32}''$ body with $\frac{3}{16}''$ bore, $\frac{3}{8}''$ body with $\frac{1}{4}''$ bore. Torque ratings for the three body sizes are 16, 64, and 256 inch ounces respectively.

Stepper Motor Catalog

Technical brochure, SP9-1, a 12 page booklet describing a new line of stepper motors and pulsed stepping devices produced by **The A. W. Haydon Co.**, 232 Elm St., Waterbury, Conn., has been published.

For each of the new units in this line—series 18100 motors, rotary stepping switches, pulse dividers, precision sequences, counters, interval timers and positioning devices—complete information is given. This includes product features, application and construction details.

Well illustrated, the booklet contains schematic drawings of application circuitry as well as pulse profiles. Copies of the two color brochure may be obtained by writing to the firm.

Snap-acting Switches

To satisfy a wide variety of assembly requirements, **Unimax Switch, Division, The W. L. Maxson Corp.**, Ives Road, Wallingford, Conn., now provides subminiature precision snap-acting switches with three kinds of solder-lug terminals, as well as snap-on terminals and terminals for printed-circuit wiring.

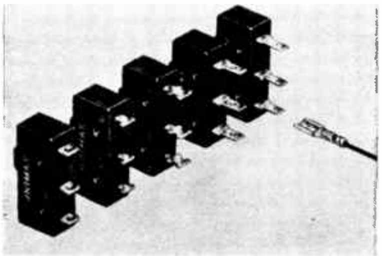

The solder-lug terminals include the short type with hole for wires up to #18, a single-turret lug, and a double-turret lug.

(Continued on page 158A)

NEWS New Products

These manufacturers have invited PROCEEDINGS readers to write for literature and further technical information. Please mention your IRE affiliation.

(Continued from page 156A)

The turret lugs are flat so that wires do not slip when wrapped around the terminal.

The snap-on terminals fit miniature AMP or Ark-Les Quick-Connect female terminals. The printed-circuit terminals are designed to fit $\frac{3}{32}$-inch slots in wiring boards and have holes to allow ready connection of component leads beneath the board.

A data sheet giving details of Unimax switches with all five terminal styles is available on request to the firm.

VSWR Amplifier

An improved version of the Narda VSWR Amplifier has been introduced by the **Narda Microwave Corp.**, 118 Herricks Rd., Mineola, N. Y. Designated Model 441B, the unit is transistorized and battery-operated and has built-in provision to show the state of battery charge. The amplifier's own meter is used to indicate this.

The Model 441B is supplied with nickel-cadmium batteries, providing complete independence from line voltage fluctuations. Batteries recharge automatically when unit is plugged in.

A special protective circuit permits switching and connect-disconnect with no danger of bolometer burnout. Provision is made for both crystals and high and low current bolometers. An expanded scale is claimed to offer the highest gain of all VSWR amplifiers on the market, and provides the same sensitivity at both expanded and normal stages (0.1 microvolts at 200 ohms for full scale).

The standard model is designed for operation (1,000 cps $\pm 1\%$ plug-in frequency networks are available for 315–4,000 cps and broad-band applications). Bandwidth is 25–30 cps; the range is 72 db (60 db in 10 db steps, 11 db continuous).

Attenuator accuracy is ± 0.2 db maximum cumulative. Meter linearity is 1% of full scale.

The Narda Model 441B is priced at $225 and is available from stock. Additional information is available from Narda representatives or by writing directly to the address shown above.

(Continued on page 162A)

Explorer VI
is a

space laboratory
orbiting
around
the
earth

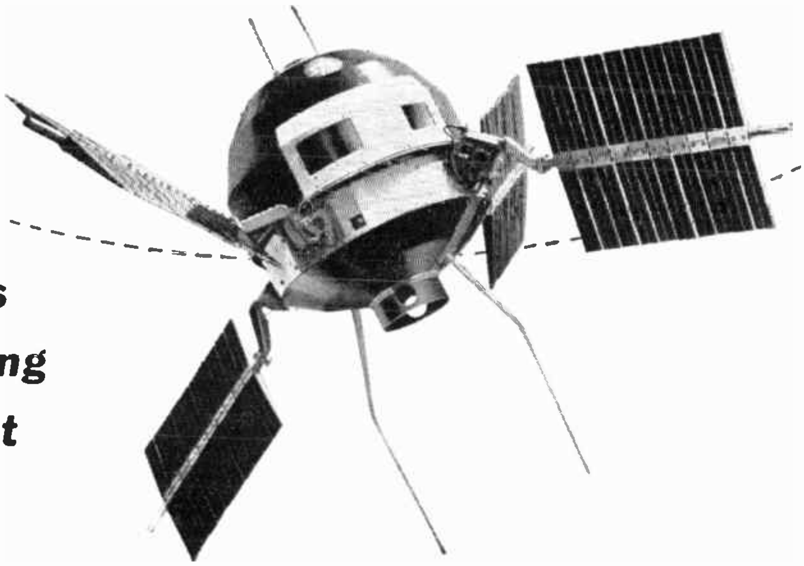

with
paddles
capturing
sunlight
for
power

The scientific data that will some day enable us to probe successfully to the very fringes of the universe is being recorded and transmitted at this moment by the space laboratory Explorer VI, a satellite now in orbit around the earth ● This project, carried out by Space Technology Laboratories for the National Aeronautics and Space Administration under the direction of the Air Force Ballistic Missile Division, will advance man's knowledge of: *The earth and the solar system . . . The magnetic field strengths in space . . . The cosmic ray intensities away from earth . . . and, The micrometeorite density encountered in inter-planetary travel* ● Explorer VI is the most sensitive and unique achievement ever launched into space. The 29" payload, STL designed and instrumented by STL in cooperation with the universities, will remain "vocal" for its anticipated one year life.

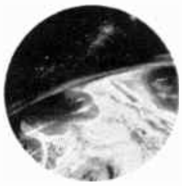

How? Because Explorer VI's 132 pounds of electronic components are powered by storage batteries kept charged by the impingement of solar radiation on 8,000 cells in the four sails or paddles equivalent to 12.2 square feet in area ● Many more of the scientific and technological miracles of Explorer VI will be reported to the world as it continues its epic flight. The STL technical staff brings to this space research the same talents which have provided systems engineering and over-all direction since 1954 to the Air Force Missile Programs including Atlas, Thor, Titan, Minuteman, and the Pioneer I space probe.

Important staff positions in connection with these activities are now available for scientists and engineers with outstanding capabilities in propulsion, electronics, thermodynamics, aerodynamics, structures, astrophysics, computer technology, and other related fields and disciplines.

Inquiries and resumes are invited.

Space Technology Laboratories, Inc.

P.O. Box 95004
Los Angeles 45, California

Take...

- forefront work essential to our National defense
- constant variety of interesting projects
- the academic atmosphere of a great University
- big Company orderliness plus small-group freedom
- inspirational elbow-rubbing with outstanding men
- a milieu free from dogma, time clocks, petty details
- "doing" as well as "thinking" projects
- stability, permanence, most fortunate living conditions
- leading institutions nearby for advanced degree work

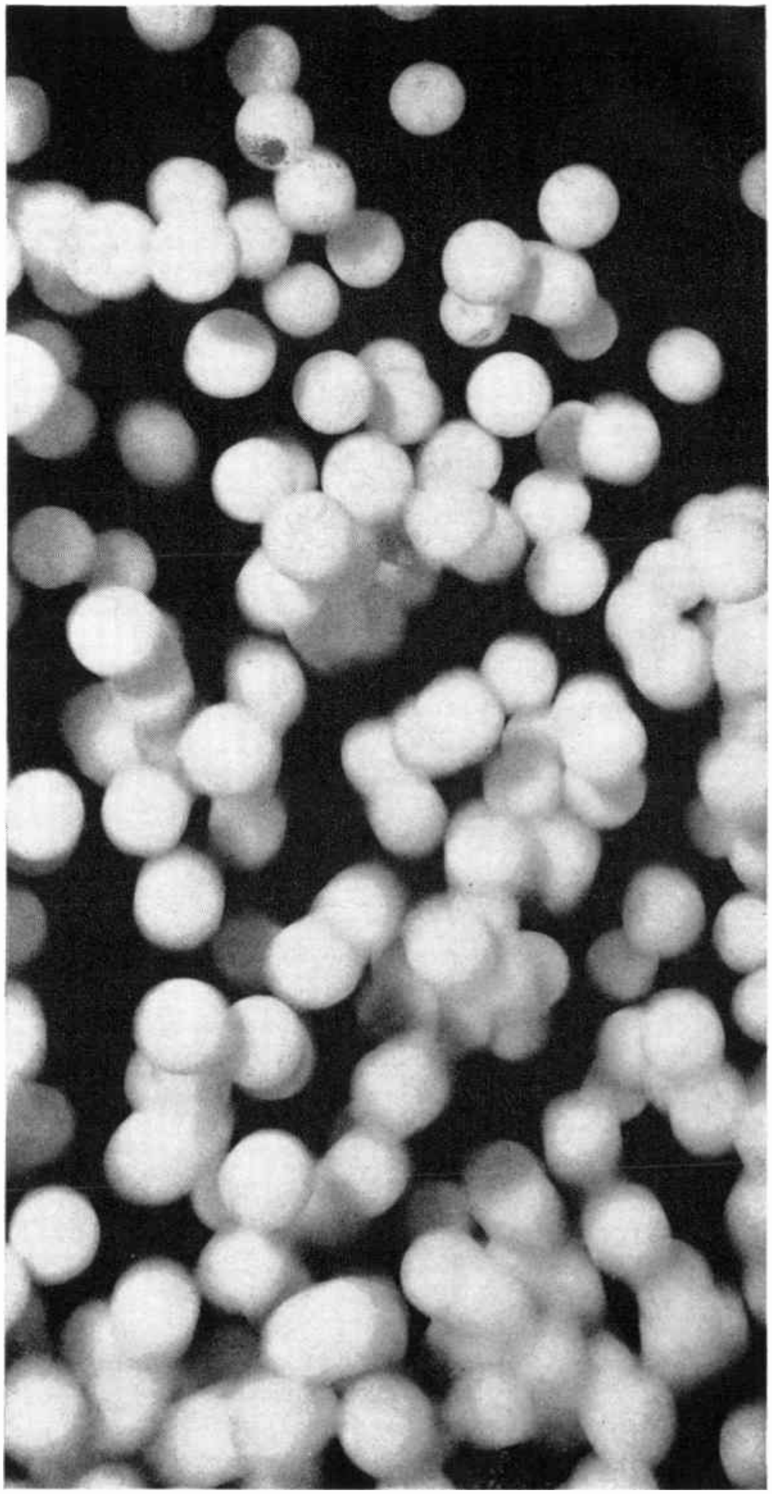
Large-scale dynamical model of gas in operation

blend—and see why so many leading engineers and scientists come to and remain at

SYLVANIA MOUNTAIN VIEW OPERATIONS

on the San Francisco Peninsula

SYLVANIA MOUNTAIN VIEW OPERATIONS

occupy large, established facilities 45 minutes south of San Francisco in the Stanford-Berkeley scientific complex. They include

ELECTRONIC DEFENSE LABORATORIES — renowned quick-reaction electronic warfare capability, R&D and fabrication being performed by the Systems Engineering Laboratory, Equipment Engineering Laboratory, Advanced Analysis Department and Equipment Fabrication Facility.

RECONNAISSANCE SYSTEMS LABORATORY — R&D on advanced ground and airborne reconnaissance systems involving antenna systems, receiving systems, data processing systems, related circuitry and hardware.

SPECIAL TUBE OPERATIONS — R&D and Product Engineering of microwave tubes and devices for missiles, radar, ECM, navigational devices. Includes the widely-known Microwave Physics Laboratory — research in plasma physics, ferromagnetic materials and gaseous electronics.

REWARDING ASSIGNMENTS NOW AT B.S., M.S., AND Ph.D. LEVELS IN

System Concept, Planning and Design . . . Receivers Transmitters . . . Digital Data Handling . . . Circuit Design Instrumentation . . . Product and Mechanical Engineering Electronic Packaging . . . Environmental Testing . . . System Integration and Evaluation . . . Theoretical and Experimental Physics . . . Microwave Tube Research, Development and Production . . . Solid State Physics . . . Sales Engineering . . . Engineering Writing

If your specialty appears above, your letter and resumé would be welcomed by Mr. Wayne Pearson at the address below. Why not write him tonight. Your answer will be prompt, complete and confidential.

SYLVANIA MOUNTAIN VIEW OPERATIONS

Box 188, Dept. B 2, Mountain View, California

SYLVANIA

Subsidiary of GENERAL TELEPHONE & ELECTRONICS

NEWS New Products

These manufacturers have invited PROCEEDINGS readers to write for literature and further technical information. Please mention your IRE affiliation.

(Continued from page 158A)

24-Channel Recorder

Designed primarily to measure environmental parameters, the ES-102, a product of **Santa Barbara Instrumentation Corp.**, 411 State St., Santa Barbara, Calif., can be used with any transducing element having contact closures as the output presentation. Digital accelerometers and temperature end-instruments are typical examples. Humidity, pressure, velocity, angular position, radiation level, and so forth, are other possible parameters. The ES-102 provides 24 channels for recording up to 20 events per second, and one time channel for correlation. Typical system

(Continued on page 164A)

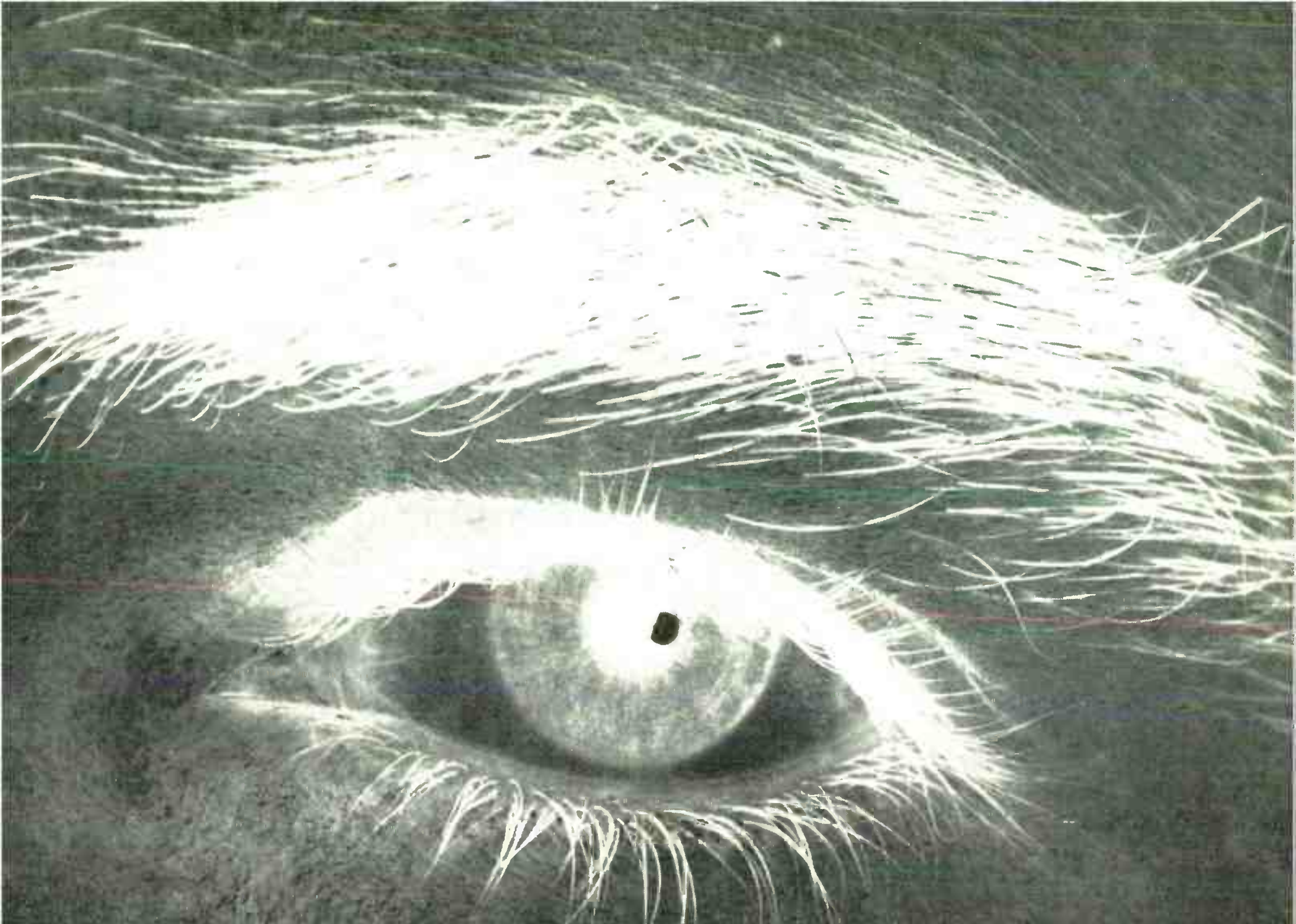

HOW FAR CAN A MAN SEE?

Optically as far as the first obstruction. For some, the same applies to mental vision. By seeing beyond the apparent obstacles, established theories or accepted principles, Fairchild Semiconductor Corporation has been able to achieve spectacular product innovations in transistors. Because of this faculty, the company has grown from an original nucleus of eight scientists to a complement of more than fourteen hundred in little more than two years.

From continuing research and development work through engineering, tooling, manufacturing and testing of products on the line, the success of Fairchild is built on the abilities of its men to see around the obstacles and move beyond. It has resulted in products more advanced than any others of their type and in a solid reputation for quality workmanship.

In a rapidly growing company with many challenging programs (e.g. current work on Esaki diodes and micro-logic circuits), there is a constant need for men who can see beyond the first obstacles. If yours is a relevant background and you find our approach attractive, we would like very much to hear from you.

FAIRCHILD
SEMICONDUCTOR CORPORATION

545 WHISMAN ROAD / MOUNTAIN VIEW, CALIFORNIA / YORKSHIRE 8-8161

NEWS New Products

These manufacturers have invited PROCEEDINGS readers to write for literature and further technical information. Please mention your IRE affiliation.

(Continued from page 162A)

applications are in monitoring large industrial control systems and transportation impact and temperature recorders. Large tape storage enables long unattended recording intervals. Data reduction is simplified and electomechanical counters can eliminate unnecessary reduction by providing quick access information. The ES-102 is available for purchase or for lease. Write for specifications.

DeMatteo General Sales Manager at Pyramid

The appointment of Mario A. DeMatteo as general sales manager of **Pyramid Electric Co.,** 507 26th St., Union City, N. J., was announced today. The electronics firm, with distributor sales and warehousing here, factories in Darlington, S. C. and Gastonia, N. C., manufactures capacitors and rectifiers.

For the past eight years DeMatteo was with Astron Corp. where he was assistant general sales manager, having moved up from distributor sales manager.

Prior to that he spent three years with Cornell-Dubilier Electric Corp. as manager of its distributor division.

DeMatteo attended Union Junior College, Cranford, N. J., The University of South Carolina, and Rutgers University.

Microwave Filter

A new 13-element low-pass filter that features a more compact design is now available from **Frequency Standards,** Asbury Park, N. J., according to Harry C. Dolan, General Sales Manager for the firm.

The filter, Model FS-23L, has 1 db down frequency of 2300 mc and a power

(Continued on page 166A)

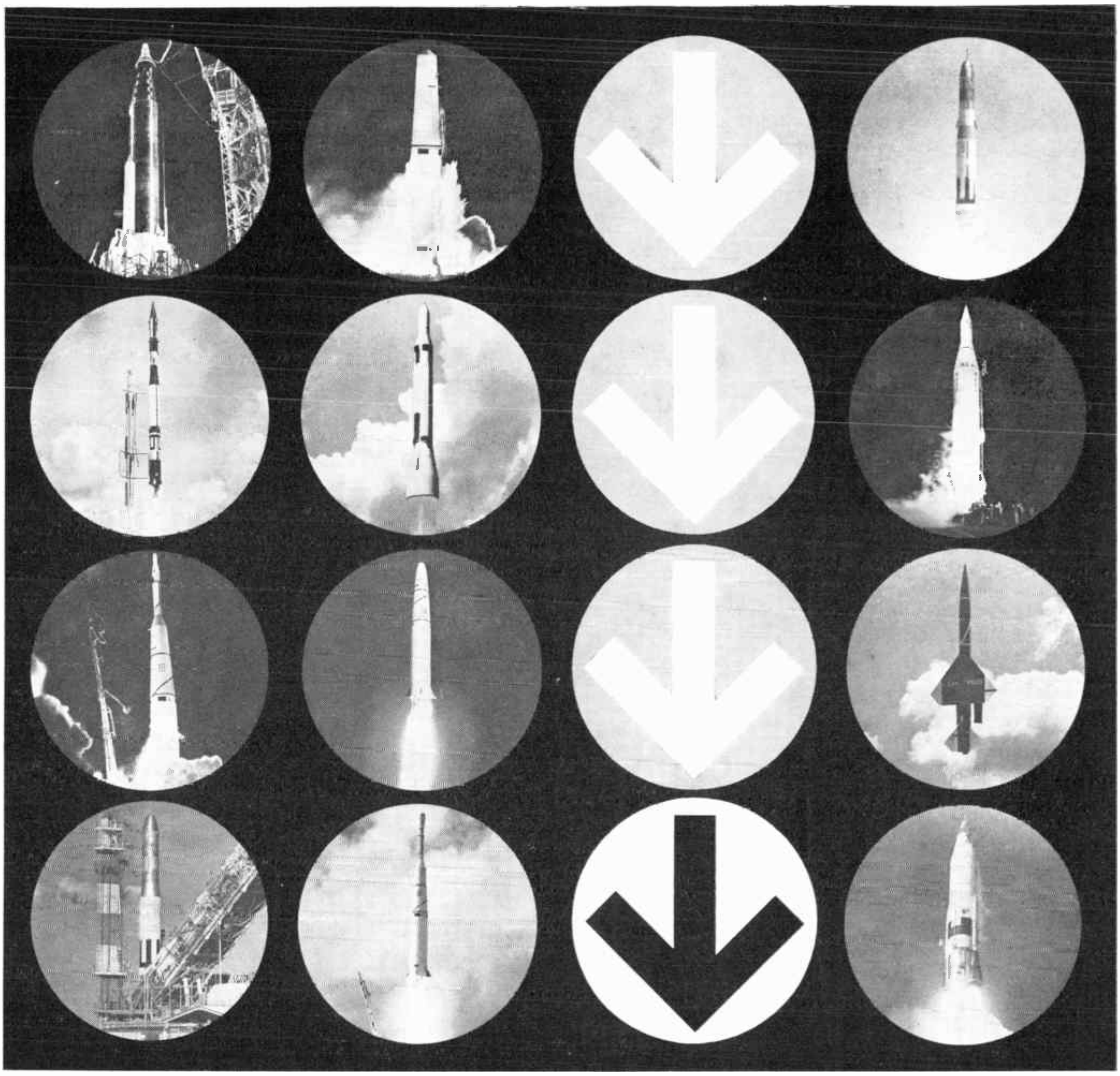

Engineers who seek professional achievement in missile ground support will find there are many missiles and many missile ground support opportunities at Cape Canaveral with Pan Am.

Investigate our career engineering openings by addressing your resume to Mr. J. B. Appledorn, Director of Technical Employment, Pan American World Airways, Inc., Patrick Air Force Base, Florida, Dept. C-14.

PAN AM

NEWS New Products

These manufacturers have invited PROCEEDINGS readers to write for literature and further technical information. Please mention your IRE affiliation.

(Continued from page 164A)

handling capacity up to 2 kw peak. The maximum insertion loss is 0.5 db in the pass-band; the input VSWR is 1.5:1 below the 0.1 db.

Write to the firm for additional information.

Differential DC Amplifier

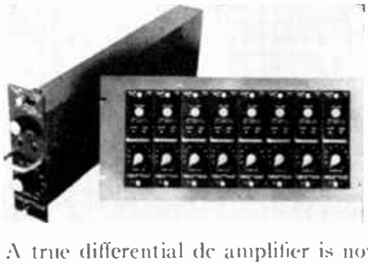

A true differential dc amplifier is now in production by the **Allegany Instrument Co.**, 1091 Wills Mountain, Cumberland, Md. Chopper stabilized, the Model 516 features low noise of 14 microvolts ms over the entire bandwidth of dc to 25 kc. An output of ±100 ma at 10 volts, with continuously variable gain to 1000X, makes the amplifier a flexible general-purpose instrument. It is available in individual case or eight to a 19" rack. For detailed information write to the firm.

Ferrite Phase Shifter

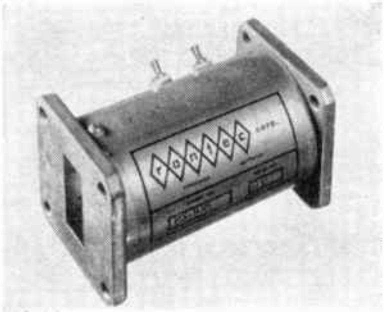

Rantec Corporation Model PX 105-Band temperature compensated ferrite phase shifter, a product of **Rantec Corp.**, Calabasas, Calif., produces ±90° of phase shift, maintaining absolute phase stability within ±15° over the temperature range −10°C to +100°C. Special matching techniques are utilized which maintain the input VSWR less than 1.15:1 for all control coil current ranges over the temperature range specified. Control coil impedance is 200 ohms and requires 100 ma current for maximum phase shift. The unit is rated at 2 kw peak, 2 watts average. Also available in other frequency bands.

Surge Test Adapter

The Model 142 Surge Test Adapter available from **Wallson Associates, Inc.**,

(Continued on page 168A)

SENIOR ENGINEERS & SCIENTISTS

General Electric's Missile & Space Vehicle Dept. Building New $14,000,000 Space Research Center

17 miles from Philadelphia, Near Valley Forge Park

Back in 1956 this General Electric organization outgrew its quarters in Schenectady, N. Y. and moved to Philadelphia. Since then its research and development staff has increased 5-fold. A new move is fast becoming imperative and will be met by the $14,000,000 Space Research Center now under construction on a 132 acres site near Valley Forge Park. This construction will feature unique facilities, to be utilized in a long-term program, to expand the activities in the realm of space research and the development of space vehicles and systems—areas in which MSVD has already contributed so many notable advances:

- the FIRST re-entry at ICBM range with both heatsink and ablation methods
- the FIRST recovery of payload from space
- the FIRST movies of earth from space
- the FIRST flight demonstration of effective space vehicle stabilization control and navigation (control systems of interplanetary capacity)
- the FIRST measurements in space of earth's magnetic field and infrared radiation
- the FIRST meteorological information from space
- the FIRST organic plastic ablation material for nose cone re-entry protection capable of withstanding temperatures from 5,000 to 13,000°F

Currently a broad diversity of programs are under way at MSVD, offering assignments of exceptional interest to engineers and scientists qualified to work with a research-oriented organization. Your inquiries are invited regarding the following areas: SYSTEMS ENGINEERING • AERODYNAMICS • THERMODYNAMICS • GUIDANCE & CONTROL • INSTRUMENTATION & COMMUNICATION • PLASMA PHYSICS • GAS DYNAMICS • AEROMEDICAL DESIGN ENGINEERING • ANTENNA & MICROWAVE DESIGN • SPACE MECHANICS • STRUCTURAL DESIGN • ENERGY CONVERSION • HUMAN FACTORS • ADVANCED POWER SYSTEMS • RELIABILITY ENGINEERING • PRODUCIBILITY ENGINEERING • ARMING AND FUZING SYSTEMS • APPLIED MATHEMATICS & COMPUTER PROGRAMMING

Write in confidence to: Mr. Thomas H. Sebring, Div. 53MB

Missile & Space Vehicle Department

GENERAL ELECTRIC

3198 Chestnut St., Philadelphia 4, Pa.

DIVERSITY OF ADVANCED PROGRAMS NOW UNDER WAY AT MSVD INCLUDE:

- Follow-on contracts for 2nd generation nose cones
- NERV (Nuclear Emulsion Recovery Vehicles) for NASA to study the Lower Van Allen radiation belts at altitudes from 200 to 1800 miles
- STEER—a communications satellite to provide global military radio communications.
- Satellite Aero-Medical Recovery Vehicle (SARV) for Discoverer
- Study programs in the area of accessory space power for a variety of missions, including chemical, nuclear and solar energy sources, electrolytic fuel cells and thermoelectric and thermionic converters
- Studies for three of the nation's space agencies to develop more accurate "space maps" than have hitherto existed to guide rockets and manned flights to the moon and planets.

A well qualified scientist or engineer is likely to find advanced work going on at MSVD on almost any field of space research of special interest to him.

A campus-like setting is planned for the new Space Research Center which General Electric's Missile and Space Vehicle Department is building close to historic Valley Forge Park. Situated at the junction of the Schuylkill Expressway and Pennsylvania Turnpike, the Center will be easily reached by engineers and scientists living in the Philadelphia area and in southern New Jersey.

NEWS New Products

These manufacturers have invited PROCEEDINGS readers to write for literature and further technical information. Please mention your IRE affiliation.

(Continued from page 166A)

912–914 Westfield Ave., Elizabeth, N. J., for use as an accessory with either the Wallson Type 138A or 141A Silicone Rectifier Test Sets. The adapter may also be used alone, and a permanent cabinet is provived for positioning when desired. The Type 142 supplies single ½-wave sinusoidal surge currents, adjustable between 5 and 75 amperes at a maximum repetition rate of 4 per minute. Provisions are made to monitor the output through a 50 mv shunt with an oscilloscope using the sync signal provided.

Specifications are: power input; 120 volts, 60 cps; overall size: 21¼" long, 8" high, 16" wide; weight 25 pounds; delivery, 4 weeks from stock; price, $700.00 rack mounting, $725.00 complete in self contained cabinet—F.O.B. Elizabeth, N. J.

Ceramic Triode

An improved, ruggedized version of the GL-6897 high mu, coplanar ceramic lighthouse triode has been announced by **General Electric Co.**, Schenectady 5, N. Y.

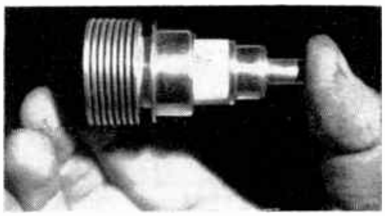

The new GL-6897, designed for reliable long life CW operation, has a typical power output of 20 watts at 1850 mc with 33 percent plate efficiency, plate current of 100 ma, plate voltage of 600 volts, and RF drive power of 2.5 watts.

It is shock tested to 400 g's, and can be purchased to specification MIL-E-1/1037A.

The GL-6897 is immediately available in production quantities for microwave frequency communications service applications in grounded-grid, power amplifier, oscillator or frequency multiplier circuits. In such service, it will operate at frequencies up to 2900 mc.

For further information contact the firm direct.

(Continued on page 171A)

New Programs at

CONVAIR - POMONA . . .

Creators and

prime contractor

of the Army's new

RED - EYE

Shoulder Fired

MISSILE

and developers of the Navy's

ADVANCED TERRIER

and TARTAR MISSILES

Refer to the reverse side of this page for additional information and positions.

Please fill out the convenient confidential inquiry card and mail to:

CONVAIR / POMONA

CONVAIR DIVISION OF

GENERAL DYNAMICS CORPORATION

POMONA, CALIFORNIA

FIRST CLASS
PERMIT NO. 484
POMONA, CALIF.

BUSINESS REPLY MAIL

NO POSTAGE STAMP NECESSARY IF MAILED IN THE UNITED STATES

POSTAGE WILL BE PAID BY

CONVAIR/POMONA ENGINEERING
POST OFFICE BOX 1011
POMONA, CALIFORNIA

PERSONAL AND CONFIDENTIAL
ATTENTION: MR. B. L. DIXON
DEPARTMENT: E.P.-320

SENIOR ENGINEERS AND SCIENTISTS . . .

who are interested in extending their career will find the New Programs offered by Convair-Pomona an excellent challenge.

Convair-Pomona is engineering the Red-Eye, shoulder-fired Missile, which American infantrymen will use against attacking aircraft. This is one of the most advanced projects in its field. Other programs on advanced Terrier and Tartar Missiles, along with still highly classified projects, provide excellent long-range positions.

In your association with Convair-Pomona you join a group of men who are leaders in their respective fields of scientific endeavor—men whose contributions to science are significant. You will find a warm friendly atmosphere—the type of atmosphere that is conducive to your best competitive effort—where every endeavor is made to insure that your salary is commensurate with that effort.

You will find a wide diversification of interesting, challenging assignments at Convair-Pomona. You will also find that our engineering department is one of the most modern and best equipped in the country.

The excellent location of this modern air-conditioned plant offers unsurpassed living conditions. Suburban Pomona is only thirty minutes from Los Angeles and Hollywood and in close proximity to many recreational centers; the mountains, the desert, the ocean and is within America's finest year-round living climate.

Assignments are available now for engineers and scientists with training and experience in one or more of the following specialties:

ELECTRONICS ENGINEERS • (Circuits-Analysis, Design, Development, Guidance and Control Systems, Systems Analysis, Component Evaluation, Test Equipment Development, Microwave and Antenna Development, Publications Engineering, Electronic Packaging, Test Engineering, Flight Analysis, Instrumentation, Radar Systems) PHYSICISTS • (Radio and Radar Systems, Physical Electronics, Solid State Physics, Magnetics, Optics, Microwave Electronics, Infrared Systems, Theoretical Physics) AERONAUTICAL ENGINEERS • (Aerodynamics, Structural Dynamics, Aeroelasticity, Aerothermodynamics) MECHANICAL ENGINEERS • (Applied Mechanics, Thermodynamics)

If you are a qualified engineer or scientist, we urge your prompt inquiry on the attached Professional Employment Inquiry form. Interviews in your area will be arranged for qualified applicants.

CONVAIR / POMONA

CONVAIR DIVISION OF

GENERAL DYNAMICS CORPORATION

POMONA, CALIFORNIA

PROFESSIONAL EMPLOYMENT INQUIRY

This card may be folded and sealed or stapled and mailed in complete confidence. It will enable the professional staff at Convair-Pomona to make a preliminary evaluation of your background. A personal interview can be arranged in your city by appointment. Every completed inquiry will be acknowledged.

PERSONAL INFORMATION (PLEASE PRINT)

NAME ______

STREET ADDRESS ______

CITY & STATE ______ TELEPHONE ______

EDUCATION:
COLLEGE GRADUATE: YES ☐ NO ☐ DEGREE: B.S. ☐ M.S. ☐ PH.D. ☐

MAJOR SUBJECT:
AERONAUTICAL ENGINEERING ☐ MECHANICAL ENGINEERING ☐
ELECTRICAL ENGINEERING ☐ PHYSICS ☐
ELECTRONIC ENGINEERING ☐

OTHER ______

FOLD

EXPERIENCE:

PRIMARY SPECIALTY ______

SECONDARY SPECIALTY ______

ADDITIONAL COMMENTS, IF ANY, CONCERNING YOUR JOB INTERESTS:

PLEASE SEND CONVAIR/POMONA ENGINEERING DEPARTMENT BROCHURE ☐

NEWS
New Products

These manufacturers have invited PROCEEDINGS readers to write for literature and further technical information. Please mention your IRE affiliation.

(*Continued from page 168A*)

Frequency Synthesizer

A new low frequency synthesizer, designated type XUB is now available from **Rohde & Schwarz (USA), Inc., 111 Lexington Ave., Passaic, N. J.**

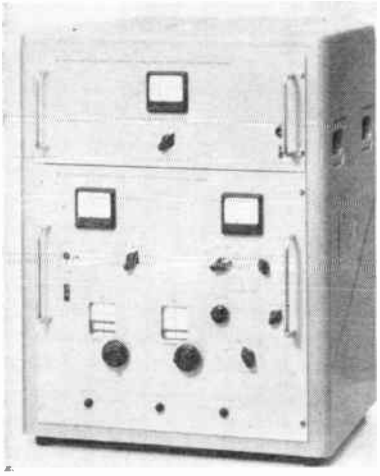

The new synthesizer can either be used alone or in combination with the synthesizer type XUA. Together, these two synthesizers cover the frequency range from 30 cps to 30 mc, with the XUB acting as vernier in crystal-locked steps of 10 cps and a continuously variable oscillator for the interval of 10 cps with a scale graduation of 10 millicycles per division. This combination XUA–XUB covers the entire frequency range up to 30 mc with the accuracy of the master crystal ($10^{-8} \pm 5$ millicycles.

Used alone, the XUB is a high class low frequency synthesizer ranging from dc to 100, 1,000 and 10,000 cps in 3 ranges with crystal locked steps of 1; 10; and 100 cps and maximum error of 0.5; 5; and 50 millicycles.

Output voltage is continuously variable from 3 millivolts to 3 volts, sinusoidal and spurious frequencies suppressed by more than 60 db. This instrument finds application in the calibration of direct reading frequency meters, in the investigation of mechanical resonant systems such as timing forks or resonant relays, in measuring low-frequency crystals and in control engineering.

Quartz Crystal Measurements

Reprints of a paper entitled "Measuring Instruments for Determination of Electrical Characteristics of Quartz Over the Range From 0 to 300 mc" by Herbert Flicker of Rohde & Schwarz, Munich, West Germany, are available from the Passaic, N. J. office by letterhead request.

The paper was recently delivered at the Symposium on Frequency Control, sponsored by the U. S. Signal Corps, R&D Laboratories, Fort Monmouth, N. J. It

(*Continued on page 172A*)

NEWS New Products

(Continued from page 171A)

covers instruments and techniques for the precise measurement of quartz crystal characteristics in accordance with the IRE standards.

Microwave Diodes

Latest addition to a line of miniaturized microwave diodes designed and produced by **Sylvania Electric Products Inc.**, Semiconductor Div., Woburn, Mass., for specialized applications in radar communications, missiles, satellites and other critical electronic equipment is a point contact microwave mixer for use in the Ku band frequency spectrum. Sylvania is a subsidiary of General Telephone & Electronics Corp.

In addition to meeting the electrical performance requirements of conventional ceramic or metal microwave diodes up to ten times their size, "Micro-Min" Type 1N918 diodes "are also their match in ruggedness and stability," he added.

The maximum conversion loss of the new silicon diode is less than 7.5 db whereas the output noise ratio does not exceed 2.5 times. Type 1N918 operates as a mixer at 16,000 mc.

The "Micro-Min" diodes are suited for the growing trend toward printed circuitry in microwave equipment. Hermetically sealed in minature glass envelopes, they form an integral part of microwave circuits in wave guide, coaxial line, microwave strip transmission line, or any other transmission line. They also employ greatly simplified holder compared with those required by their larger counterparts.

Tunnel Diodes

The **General Electric Co., Semiconductor Products Dept.**, Syracuse, N. Y., has made sample quantities of its second tunnel diode, a 1,000 megacycle device, available to electronic industry designers, it was disclosed here today.

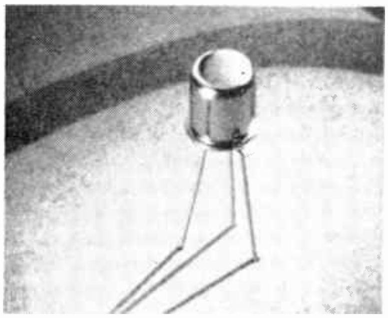

The newest tunnel diode is priced at sixty dollars and is immediately available in limited quantities.

Features of the new tunnel diode include a minimum peak to valley current ratio of 5 to 1, a typical peak point current

(Continued on page 174A)

ELECTRONICS ENGINEERS: YOU CAN KEEP IT ON COURSE

With The World Leader In Continuous Wave Doppler Navigation Systems

Twelve years of research and development in the field of continuous wave doppler has brought Ryan Electronics leadership in airborne electronics, ground velocity indicators and radar navigation systems.

This leadership has earned Ryan Electronics important multi-million dollar contracts for navigation systems for America's major military aircraft. In addition, systems utilizing Ryan-pioneered C-W doppler techniques are involved in some of the most advanced missiles in our nation's arsenal. These projects, plus advanced study in future space application of the same principle, call for a continually growing staff of electronics engineers of exceptional skill and ambition.

Expanded facilities of Ryan Electronics at San Diego and Torrance in Southern California provide the optimum for working, living, educating your children and pursuing your own advanced studies. For full particulars, send resume or write for brochure to Ryan Electronics. Department 5, 5650 Kearney Mesa Road, San Diego 11, California.

RYAN ELECTRONICS

DIVISION OF RYAN AERONAUTICAL COMPANY, TORRANCE, CALIFORNIA, SAN DIEGO, CALIFORNIA

NEWS New Products

These manufacturers have invited PROCEEDINGS readers to write for literature and further technical information. Please mention your IRE affiliation.

(Continued from page 172A)

rating of 1-milliampere, which is held to ±10% and a typical negative conductance of 0.065-mho.

Other characteristics are identical with the other germanium tunnel diode being offered by the company.

Both devices are hand-made laboratory samples and thus are higher priced than they will be when the mass production phase is reached.

Samples of the other G-E tunnel diode, which has a minimum peak to valley current ratio of 8 to 1, are priced at seventy-five dollars each. They were first made available to the industry last September.

Both tunnel diodes are packaged in the TO-18 standard transistor housing. Pins one and two are positive electrodes connected internally to reduce lead inductance. Pin three is the negative electrode and is connected to the case.

Both the ZJ-56 and the new ZJ-56A are rated for an operating junction temperature of minus 55°C to plus 100°C. They have typical peak point voltages of 55-millivolts and typical valley point voltages of 350-millivolts.

Operational Amplifiers

Combining the transistor's efficiency and reliability with the flexibility of operational amplifiers, the 1300 Series Amplifiers produced by **Burr-Brown Research Corp.**, Box 6444, Tucson, Arizona, are useful in many applications. Basic units are high gain differential dc amplifiers designed to be used with external feedback. Stable with any resistive feedback, the user may select the "closed-loop" performance best suited to his application. Typical applications include dc and ac amplifiers, integrators, current and voltage regulators, preamplifiers, selective filters, and many others.

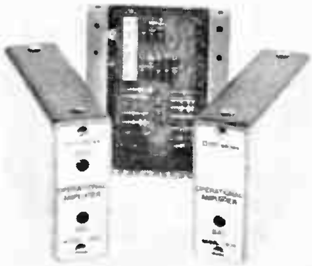

Typical units feature gains of 10,000 and input impedance of 100K. Outputs to ±10 volts at 200 ma are available. Both germanium and silicon units are packaged in a case measuring 1″×2½″. Prices range from $65 to $98 for germanium to $310 for silicon. Available from stock to 30 days.

(Continued on page 176A)

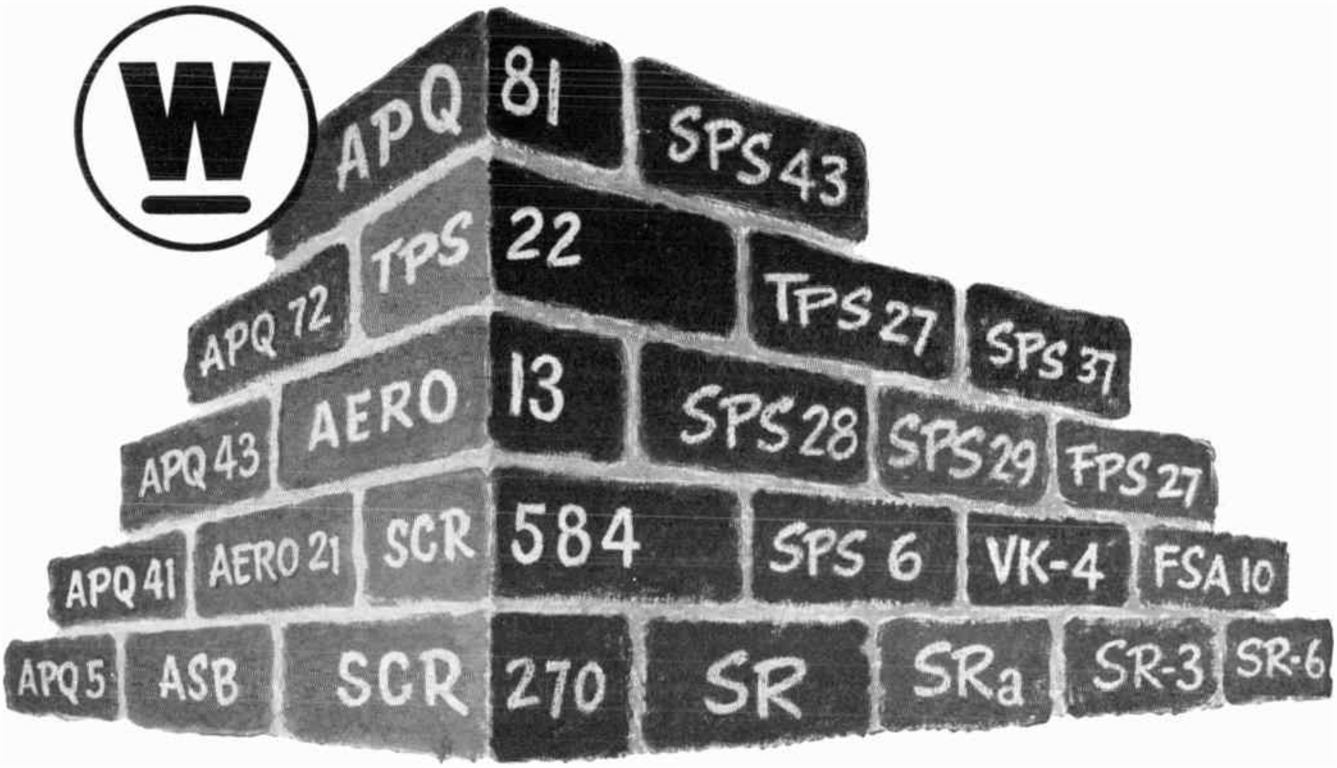

Build Your RADAR Career On This Solid Foundation!

The Weapons System Concept is one more step forward in a long series of "firsts" for the men who pioneered this field with the SCR-270, the first long range radar. In ground, shipboard and airborne radar, Westinghouse is the recognized leader in advanced programs and techniques. As Westinghouse builds new levels of accomplishment on this solid foundation, new career opportunities in radar development are created. Westinghouse-Baltimore invites inquiries from radar engineers with experience or interest in the following fields:

- **Operations Research and Analysis**
- **Systems Development and Evaluation**
- **Transmitter and Receiver System Development**
- **Advanced Antenna Systems**
- **Molecular Electronics**
- **System Synchronization**
- **Data Processing**
- **Liaison and Field Engineering**
- **Advanced Displays and Monitoring**
- **Network Synthesis**
- **Microwave Systems**
- **Systems Reliability Prediction**
- **Advanced Systems Automated Test**

SEND RESUME TO: Mr. A. M. Johnston, Dept. 231

Westinghouse

BALTIMORE

P. O. Box 746 **Baltimore 3, Maryland**

AIR ARM • ELECTRONICS • ORDNANCE

NEWS New Products

These manufacturers have invited PROCEEDINGS readers to write for literature and further technical information. Please mention your IRE affiliation.

(Continued from page 174A)

Metallized Paper-Plastic Capacitor

Cornell-Dubilier Electric Corp., affiliated with Federal Pacific Electric Co., Plainfield, N. J., announces miniature metallized paper-plastic film capacitors for military, industrial and other high-grade electronic equipment for operation from −55°C to +125°C without voltage derating.

Designed as Type MTWK, these capacitors are hermetically-sealed in tubular metal cases with glass-to-metal end seals and are available in various mounting styles for efficient chassis design.

Type MTWK capacitors are designed for use in power supply filter circuits, by-pass functions and where high insulation-resistance values are not essential, as well as applications in which occasional momentary voltage breakdowns can be tolerated.

Temperature characteristics of these capacitors, such as dissipation factor and capacitance change are comparable to those of standard paper-dielectric capacitors, but afford higher capacitance values than are generally obtainable with the same size paper-dielectric or metallized-paper types.

Available in three different internal circuit configuration, Type MTWK is supplied in 200, 400 and 600 volt sizes. Engineering Bulletin No. 185, showing specifications and availability of the MTWK capacitors, is available on request.

Flight Simulation Table

Micro Gee Products, Inc., 6319 West Slauson Ave., Culver City, Calif., announces the New Model 17A Two-Axis Flight Simulation Table which enables "flight testing" of complete missile or air-space craft stabilization and control systems on the ground, as contrasted to such programs where gyro and accelerometer dynamics are linearily simulated. One of these New Model 17A Tables has just been placed in operation on the Pacific Missile Range.

The Model 17A two-degrees-of-freedom table is also used for angularly displacing gyros and accelerometers, in pitch and roll, either statically or dynamically.

(Continued on page 180A)

SPECIAL TUBES FOR SPECIAL USES:

EMI

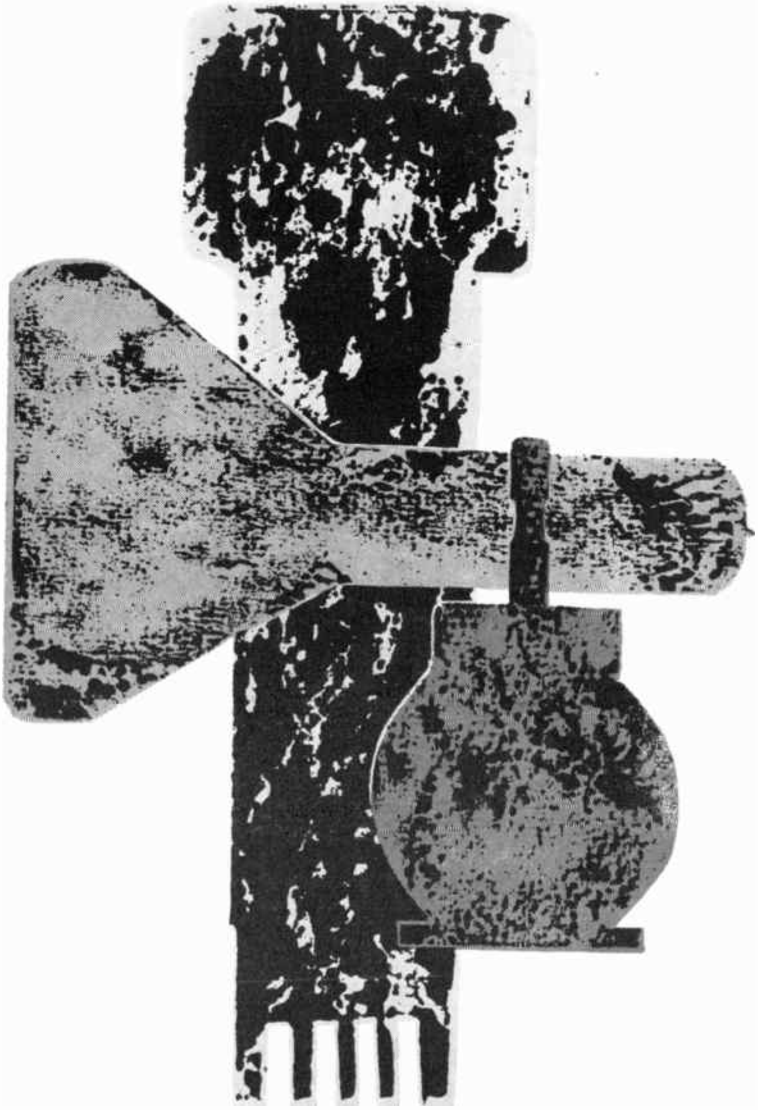

PHOTOMULTIPLIER TUBES / KLYSTRONS / MAGNETRONS
SPECIAL CATHODE RAY TUBES / TV CAMERA TUBES / STORAGE TUBES

E.M.I. Electronics Ltd. is one of the world's leading pioneers in the development of special high-performance tubes for military and commercial use. Through the Hoffman Electron Tube Corp., its United States Representative, a wide range of E.M.I. tubes are now available from inventory for such systems as missile and satellite tracking, ground mapping, weather radar, air traffic control, early warning, combat situation plotting by tactical television cameras, closed circuit television for industry, airborne radar, automatic landing, nuclear radiation scanning, and spectrophotometry ■ You can rely on E.M.I. for the highest standards of accuracy and reliability. Visit us at the IRE Show, Booth #1520 ■ Write for full technical information to:

HOFFMAN ELECTRON TUBE CORP.
804 NEWBRIDGE AVENUE / WESTBURY / NEW YORK

North Atlantic Series RB500 Ratio Boxes

Model RB-501
Rack mount

Measure A.C. Ratios From −0.011111 To +1.11111...with accuracy to 1 ppm

With any of North Atlantic's RB500 Ratio Boxes you can now measure voltage ratios about zero and unity—without disrupting test set-ups.

And—a complete range of models from low cost high-precision types to ultra-accurate ratio standards —in portable, bench, rack mount, binary and automatic stepping designs—lets you match the model to the job.

For example, characteristics covered by the RB500 Series include:

Frequency: 25 cps to 10 kc.
Accuracy: 10 ppm to 1.0 ppm
Input voltage: 0.35f to 1.0f
Input impedance: 60 k to 1 megohm
Effective series impedance: 9 ohms to 0.5 ohms
Long life, heavy duty switches

Name your ratio measurement and its probable there's a North Atlantic Ratio Box to meet them —precisely. Write for complete data in Bulletin IIE

Also from North Atlantic
...a complete line of complex voltage ratiometers...ratio test sets...phase angle voltmeters

NORTH ATLANTIC
industries, inc.
603 Main Street, Westbury, N.Y.
EDgewood 4-1122

satisfies more
application requirements...
faster, easier, at low cost

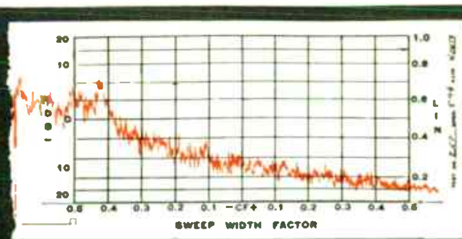

LF 2a plot of amplitude vs. frequency of noise in a 500cps wide segment. Db amplitude scale

Panoramic Subsonic Spectrum Analyzer

LF-2a

0.5 cps. to 2500 cps.

dependable CERTIFIED SPECIFICATIONS for accurate data

SUMMARY OF SPECIFICATIONS:

Frequency range: 0.5 cps to 2500 cps in two operating modes:
X1.0—Linear segments 500, 100 or 20 cps wide, centerable between 0 and 2250 cps
X0.1—Linear segments 50, 10 or 2 cps wide, centerable between 0 and 225 cps
Sensitivity: 10 mv to 100v for full scale deflection
Amplitude scales: Linear and 2 decade log
Chart size: 12" length, usable width 4½"
Resolution: 0.1 cps to 20 cps in 11 steps
Sweep Rate: One scan in 10 seconds, and 1, 2, 4, 8 or 16 minutes; also may be scanned in 1, 2, 4, 8, or 16 hours (optional)
Stability: better than 0.05 cps/hr. in X0.1 mode—0.5 cps/hr. in X1.0 mode
Input Impedance: 5 megohms
Frequency Markers: Self contained
Optional: LF-2aM, with automatic frequency advance after each scan interval provides unattended analysis from 0.5-2000 cps.

Write, wire or phone *today* for complete specifications, applications and price of the Panoramic Model LF-2a Subsonic Spectrum Analyzer.

Send for Panoramic's NEW CATALOG DIGEST and ask to be put on our regular mailing list for the PANORAMIC ANALYZER featuring application data.

EXCLUSIVE FEATURES:

- Adjustable scan widths—2 cps to 500 cps
- 10 second "quick look" on external scope
- Exceptional adjustable resolution (selectivity): 0.1 cps to 20 cps
- Low cost
- Easy to use

Unusually flexible and versatile, the economical Model LF-2a automatically separates and measures the frequency and amplitude of discrete or random signals between 0.5 and 2500 cps . . . and displays these data on either an integral chart recorder or external scope. More application requirements are satisfied by providing analyses of spectrum segments—as narrow as 2 cps, as wide as 500 cps—plotted over the *full* width of the calibrated 12" x 4½" chart record. A calibrated tuning control enables rapid selection of the center frequency of the spectrum portion of interest. Frequency selectivity—or resolution—is independently adjustable from 0.1 cps to 20 cps for more accurate detection and measurement of either closely spaced discrete signals or noise.

Scan intervals range from just 10 sec. for "quick look" location and evaluation of signals on an external scope, to 16 hours for thorough statistical analysis.

Among the LF-2a's many proven uses are: • Vibration and Acoustic Analysis • Random Waveform Studies • Spectral Power Density Analysis • Medical Investigations • Servo Analysis • General Low Frequency Waveform Studies

With optional auxiliary equipment, the LF-2a is used for Spectral Power Density Analysis and Frequency Response Curve Tracing. Adding the Panoramic LP-1a Sonic Analyzer extends the analysis range to 22.5 Kc.

the pioneer is the leader

Panoramic RADIO PRODUCTS, INC.

522 So. Fulton Ave., Mount Vernon, New York
Phone OWens 9-4600 Cables: Panoramic, Mount Vernon, N. Y. State

NEWS New Products

(Continued from page 176A)

The smooth operation, due to specially designed, driven pendulum mechanisms, also enables use of the table as an oscillating table to determine the threshold characteristics of high performance gyros and accelerometers.

Features of the table include extended angular travel over prior models and the ability to handle a 25-pound load. The natural frequency of each axis is in excess of 15 cps. Adjustable damping is provided and the threshold of each axis is less than 0.005°.

The table will follow signals such as those from an analog computer, a low frequency function generator, a tape recorder, or a digital-to-analog converter.

(Continued on page 182A)

ARNOLD:
WIDEST SELECTION OF MO-PERMALLOY POWDER CORES FOR YOUR REQUIREMENTS

For greater design flexibility, Arnold leads the way in offering you a full range of Molybdenum Permalloy powder cores . . . 25 different sizes, from the smallest to the largest on the market, from 0.260" to 5.218" OD.

In addition to pioneering the development of the cheerio-size cores, Arnold is the exclusive producer of the largest 125 Mu core commercially available. A huge 2000-ton press is required for its manufacture, and insures its uniform physical and magnetic properties. This big core is also available in three other standard permeabilities: 60, 26 and 14 Mu.

A new high-permeability core of 147 Mu is available in most sizes. These cores are specifically designed for low-frequency applications where the use of 125 Mu cores does not result in sufficient Q or inductance per turn. They are primarily intended for applications at frequencies below 2000 cps.

Most sizes of Arnold M-PP cores can be furnished with a controlled temperature coefficient of inductance in the range of 30 to 130° F. Many can be supplied temperature stabilized over the MIL-T-27 wide-range specification of −55 to +85°C . . . another special Arnold feature.

Graded cores are available upon special request. All popular sizes of Arnold M-PP cores are produced to a standard inductance tolerance of + or −8%, and many of these sizes are available for immediate delivery from strategically located warehouses.

Let us supply *your* requirements for Mo-Permalloy powder cores (*Bulletin PC-104C*). Other Arnold products include the most extensive line of tape-wound cores, iron powder cores, permanent magnets and special magnetic materials in the industry. • Contact ***The Arnold Engineering Co., Main Office and Plant, Marengo, Illinois.***

ADDRESS DEPT. P-02

ARNOLD
SPECIALISTS in MAGNETIC MATERIALS

BRANCH OFFICES and REPRESENTATIVES in PRINCIPAL CITIES • *Find them FAST in the YELLOW PAGES*

1187

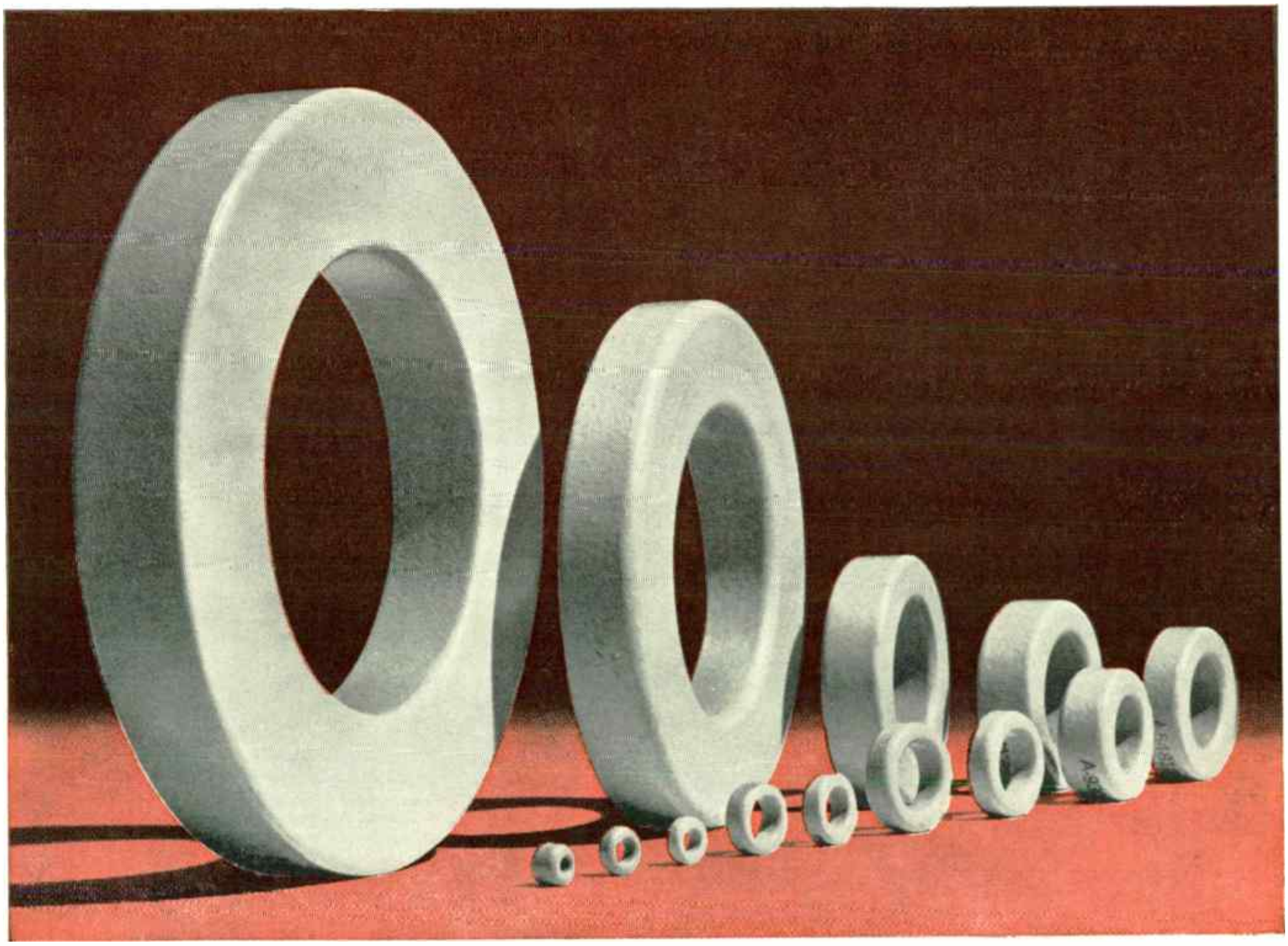

NEWS New Products

These manufacturers have invited PROCEEDINGS readers to write for literature and further technical information. Please mention your IRE affiliation.

(Continued from page 180A)

General Radio Traveling Exhibit

An innovation in exhibits—a traveling instrument display-demonstration vehicle—designed by the **General Radio Co.**, West Concord, Mass., was previewed on Friday, December 4, in the Garden City Hotel, Garden City, Long Island, New York.

Produced to bring a full complement of the latest developments in electronic measuring equipment directly to local government agencies, laboratories, industry and educational institutions, the car—a modified station wagon—carries over 1500 pounds of instruments mounted on six collapsible tables, which can be set up in an hour by a three-man team of engineers.

Equipment on display at the hotel included an inductance bridge (Type 1632-A), unit oscillator (Type 1210-C), unit amplifier (Type 1206-B), amplifier and null detector (Type 1231-B); also a graphic level recorder (Type 1521-A), random noise generator (Type 1390-B), sound and vibration analyzer (Type 1554-A and sound level meter (Type 1551-B). Other instruments displayed were a pulse, sweep and time-delay generator (Type 1391-B), time-delay generator (Type 1392-A), unit pulser (Type 1217-A) and unit pulse amplifier (Type 1219-A). A self-contained portable impedance bridge (Type 1650-A) featuring the Orthonull ganging device to facilitate low-Q balancing was also at the show. Additional items on display were components, accessories and coaxial fittings, plus a variety of Variac® autotransformers, three terminal capacitors and an adjustable regulated power supply.

The show will go on to Fort Monmouth, New York Naval Shipyard, Bell Telephone Labs, ITT Labs, and then proceed to Stamford, Conn., Elmsford, N. Y., and Somerville, N. J., for local plant-lab viewing.

Standard Seminar

Over 20 electrical-electronic standards' specialists from U. S. and Canadian government agencies recently met for a 3½-day General Radio seminar-workshop clinic on precision inductance and capacitance measurements at low frequencies.

Held at the plant in West Concord, Mass., the meeting was attended by engineers from the National Bureau of Standards and the Canadian National Research Council; also top technical personnel from the primary standards laboratories of the Signal Corps, Frankfort Arsenal, Aberdeen Proving Ground, Redstone Arsenal, Bureau of Ships, Royal Canadian Navy, U. S. Air Force, BuAir, and BuOrd-Bureau of Ships.

The symposium, featuring ten lectures and six-workshop sessions, was conducted by I. G. Easton, R. A. Soderman, P. K. McElroy, J. F. Hersh, H. P. Hall, R. A. Boole, D. H. Chute, J. F. Eberle and C. L. Woodford of General Radio.

Another highlight of the meeting was a plant tour and a question answer program-evaluation and future-trends session.

(Continued on page 186A)

1960
1961
1962
1963
1964
IF YOU INSTALL LAMBDA POWER SUPPLIES NOW, YOU KNOW THEY'LL STILL PERFORM TO GUARANTEE IN 1965

BECAUSE ONLY LAMBDA GIVES YOU A 5-YEAR GUARANTEE!

Each Lambda Power Supply carries a written guarantee that warrants full performance to specified ratings for five full years.

Lambda, alone, offers this unprecedented guarantee because Lambda specializes in the design and manufacture of just one product – power supplies.

Each unit is built from the ground up to rigid quality standards in a modern, completely integrated plant. Nothing is overlooked to provide you with the finest performance. When you buy a Lambda Power Supply, you are assured of a unit that is conservatively rated – a unit designed to provide continuous-duty service at all specified loads and ratings.

Lambda power supplies are available in a wide range of rack, portable and bench models for laboratory and production service. Of particular interest to electronic designers are:

L-T Transistor-Regulated Series . . . . 0-1 and 0-2 AMP, 0-32 VDC
Com-Pak Tube Regulated Series . . . . 200-400-800-1500 MA
0-200, 125-325, 325-525 VDC

Write for free 32-page catalog for complete specifications, dimensions, performance ratings and prices on Lambda's full line of tube-regulated and transistorized power supplies.

LAMBDA ELECTRONICS CORP.
11-11 131 STREET • COLLEGE POINT 56, N. Y. • INDEPENDENCE 1-8500

Watch for Lambda's exciting new solid-state power supply developments.

IRE SHOW — Booths 2318-2320

from the USUAL.... ...

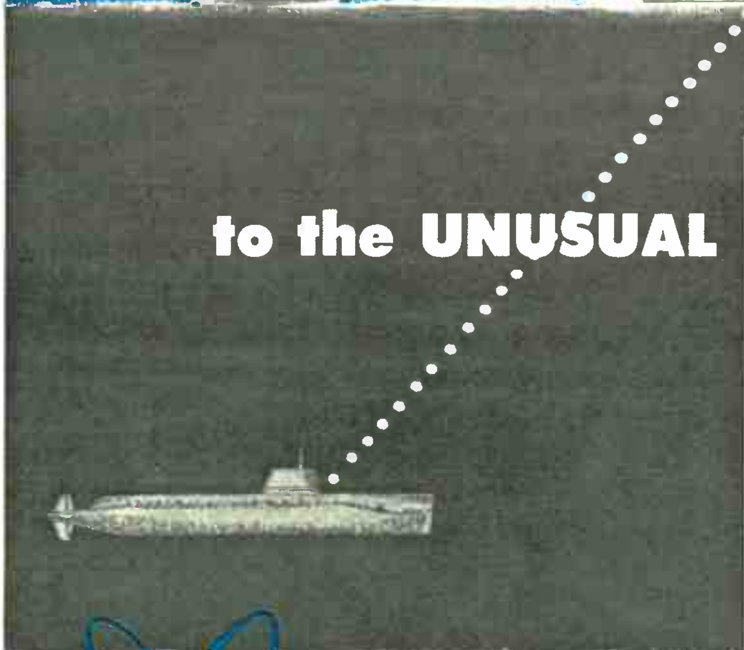

DELAY LINES

by C-A-C

In the C-A-C line of quality toroidal components, the design and manufacturer of delay lines has become a growing series of custom projects.

From simple types used in communication system to complexities such as this design for use in sonar gear, C-A-C's design engineering in lumped constant delay lines plays a big part in developing *the component* to meet your tighest requirements.

C-A-C®

Technical data sheets are available.

COMMUNICATION ACCESSORIES CO.

Lee's Summit, Missouri • Phone Kansas City, Broadway 1-1700

A Subsidiary of Collins Radio Company

C135

(Continued from page 182A)

New Plant

The Electrodynamic Instrument Corp., which has been operating at 2511 Robinhood and 2508 Tangley Rd., moved to a new plant on January 31, 1960.

The company's new location on which a long term lease has been negotiated is at 1841 Old Spanish Trail, Houston, Texas. EIC has been occupying three buildings in the Village totalling 8,000 square feet of space, but the newly renovated structure on OST will provide more than 17,500 square feet, President Joe Houghton stated.

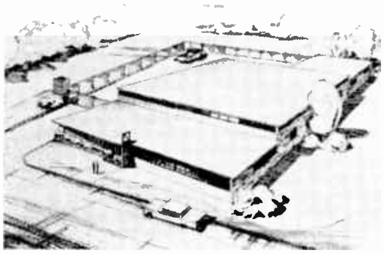

EIC came into existence just four years ago when Houghton and Paul E. Madeley, executive vice president, decided to leave their posts as design engineers with another local instrument manufacturer to launch their own company. EIC's extensive research and manufacturing programs extend into the fields of seismic tape recordings and data processing systems, well logging instrumentation, digital readout systems, precision transformers, portable and laboratory test equipment and transistorized power supplies.

Telemeter Discriminator

Deeco Instruments, Inc., 14737 Arminta St., Van Nuys, Calif., announces production of a new telemetering discriminator designated Model A115. It is a plug-in modular unit designed for rack mounting, four being accommodated on a standard 19″ rack panel.

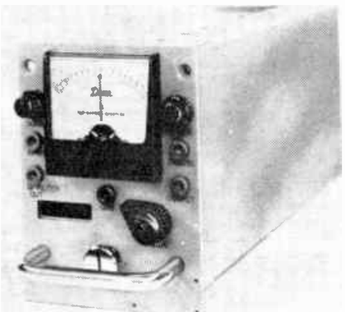

The basic chassis includes a limiter amplifier and driver amplifier with a front panel meter to read subcarrier deviation. A gain pot is incorporated to adjust the dc output level

Each chassis accepts a plug-in-sub-

(Continued on page 188A)

When Reliability is a must . . .
specify EMPIRE

NOISE AND FIELD INTENSITY METER
Model NF-108 • 14 KC to 1000 MC

Use of five quick-change tuning heads avoids costly repetition of components common to all frequency ranges. Built-in impulse generator serves as calibrator. Carrier and peak reading VTVM. Fully regulated power supply.

NOISE AND FIELD INTENSITY METER
Model NF-112 • 1 KMC to 10 KMC

Companion unit to NF-105. Four interchangeable tuning heads. Excellent shielding effectiveness. Calibration by means of built-in impulse generator. Compact. Simple to operate.

BROADBAND POWER DENSITY METER
Model NF-157
200 MC to 10 KMC

Personnel safety indicator. Average power from 1 mw/cm² to 1 w/cm². Complete with 3 pick-up probes. Portable. Self contained.

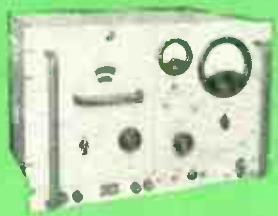

AM MODULATION METER
Model MM-120 • 15 KC to 1000 MC

Indicates modulation percentage of signal generators and transmitters. RF sensitivity 0.01 volts. Two plug-in tuning units.

BROADBAND COAXIAL ATTENUATORS
DC to 4 KMC

Pads, 6 and 12 position step attenuators (manually and motor operated). attenuator panels. 1 watt to 4 watts. Also 50 watt power attenuators. Large range of values. Low VSWR, high accuracy. Long term stability. Conservative power ratings.

NOISE AND FIELD INTENSITY METER
Model NF-205 • 14 KC to 1000 MC

Modified version of Model NF-105.

BROADBAND CRYSTAL MIXER
Model CM-107 • 225 MC to 5000 MC

Eight fixed tuned models. Low noise figure. Laboratory or production applications. Versatile.

BROADBAND POWER DIVIDER
Model PD-99 • 500 MC to 10 KMC

Five models permit lossless, accurate division of RF power. Many special versions available.

VARIABLE FREQUENCY POWER SUPPLIES
Models VP-100, VP-410, VP-1000
100 VA, 400 VA, 1000 VA

Low distortion. Excellent regulation. Quick recovery. Wide frequency range.

IMPULSE GENERATORS
Models IG-102, IG-115, IG-118
20 KC to 10 KMC

Generate high output level of impulse noise over wide frequency range. For receiver gain calibration, noise susceptibility investigations.

BROADBAND COAXIAL STUB TUNERS
200 MC to 10 KMC

Single, double and triple stub tuners of rugged construction. Locking nuts insure stable operation.

COAXIAL TERMINATION
Model TE-80 • DC to 10 KMC

Low VSWR throughout. Type "N" connector. Many special versions available.

edp

EMPIRE DEVICES PRODUCTS CORP.

AMSTERDAM, NEW YORK

VICTOR 2-8400

MANUFACTURERS OF:

FIELD INTENSITY METERS • DISTORTION ANALYZERS • IMPULSE GENERATORS • COAXIAL ATTENUATORS • CRYSTAL MIXERS

NEWS New Products

These manufacturers have invited PROCEEDINGS readers to write for literature and further technical information. Please mention your IRE affiliation.

(Continued from page 186A)

chassis containing the band pass filter, discriminator and low pass filter. 18 plug-in channel selectors provide standard telemetry channels 1 through 18.

Linearity is within 1% of bandwidth, and sensitivity is 50 mv to 10 V.

Complete technical data is available from the firm.

Rectifier

PEK Labs, Inc., 4024 Transport St., Palo Alto, Calif., announces the availability of the PEK 5973 high voltage rectifier or surge limiting diode.

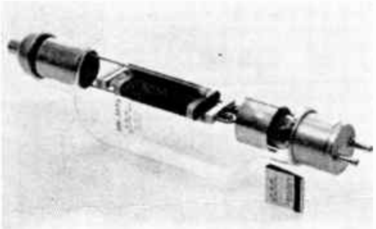

Rated at 75 kb peak inverse voltage and 800 watts average plate dissipation the 5973 is suited to applications where low

(Continued on page 191A)

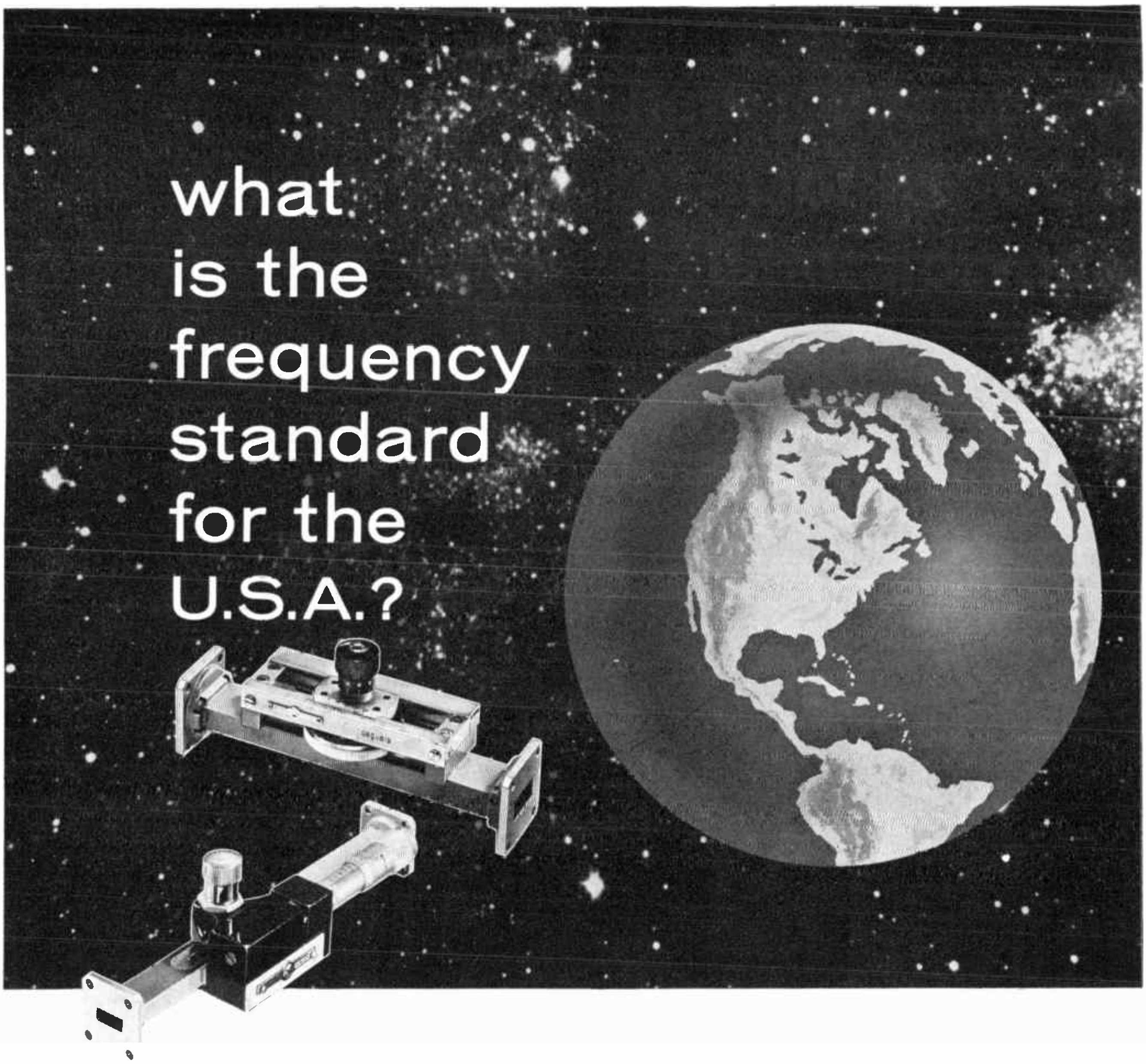

ANSWER: By act of Congress, the U.S. Bureau of Standards determines the primary standard, based on the revolution of the earth. All DeMornay-Bonardi microwave instruments are calibrated at frequencies which are verified by our secondary standard, which, in turn, is periodically calibrated, point for point, by the U.S. Bureau of Standards.

One way to properly match a microwave transmission line is by using a D-B Stub Tuner to reduce mismatch losses and utilize the total energy available.

D-B stub tuners in the 2.6 to 18 KMC range have a new scale and vernier that gives precise resettability in longitudinal travel. A new micrometer scale on the probe measures penetration with very high accuracy.

Probe wobble is eliminated, and no resonances can occur under any conditions. You can correct VSWR as high as 20:1 with amazing accuracy (1.02). You can tune with precision . . . reset to original settings with certainty that phase and magnitude have been duplicated.

Ditto for higher frequencies. D-B tuners in the 18 to 90 KMC range are not simply scaled-down units—they're engineered for ultramicrowave® use. All the above features are available, plus micrometer positioning which provides readability to .0001″.

Write for data sheets—they detail all features, applications, dimensions, sizes. Bulletin DB-919.

DE MORNAY BONARDI®   780 SOUTH ARROYO PARKWAY • PASADENA, CALIFORNIA

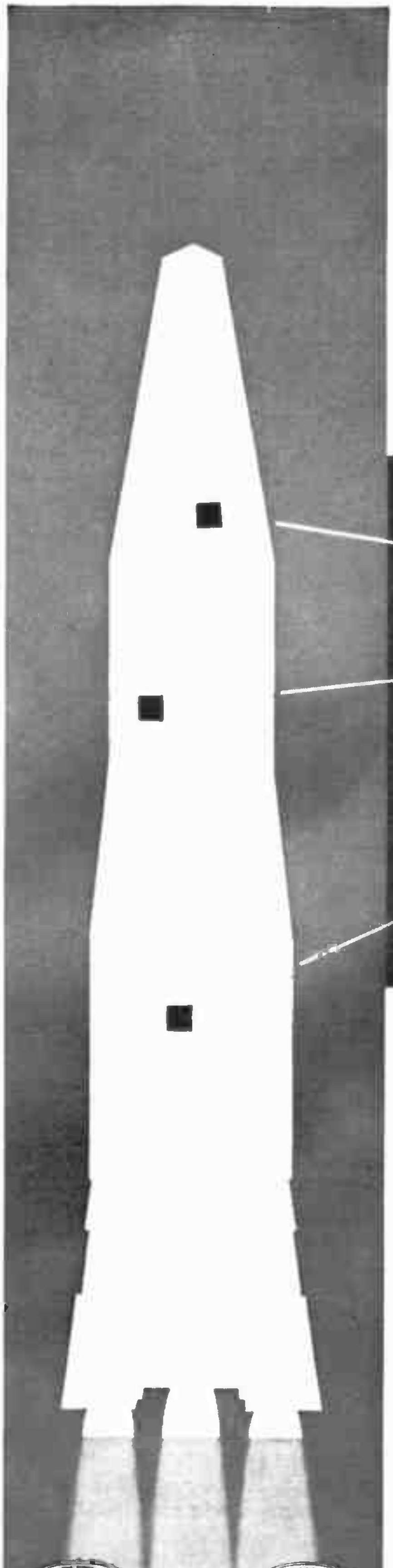

SUPRAMICA® 555 ceramoplastic

the world's most nearly perfect precision-moldable electronic insulation

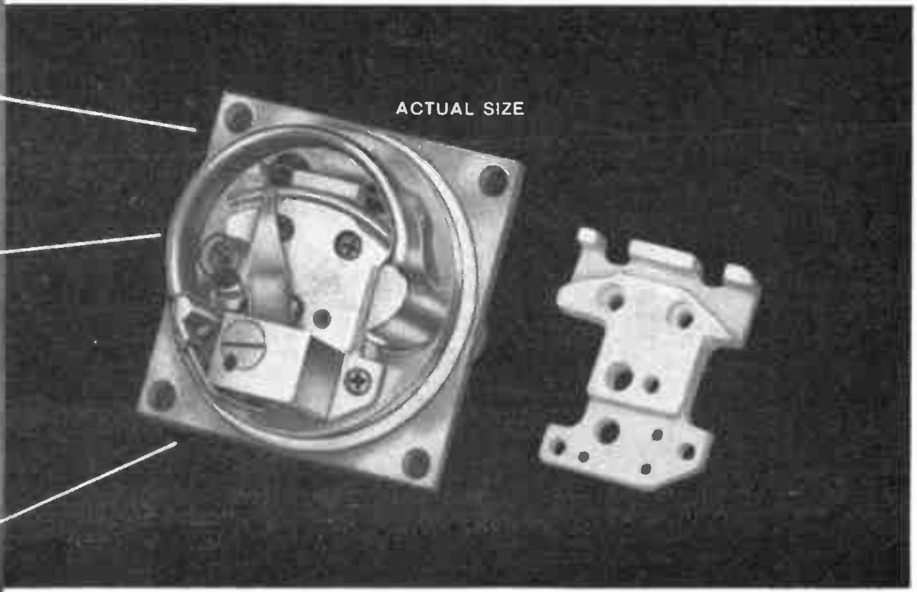

for total reliability... at high temperatures ...specified in BOURNS Inc. transducers

Why did BOURNS, INC. select SUPRAMICA 555 ceramoplastic as the insulating base for its ultra high-temperature differential pressure transducers?

BOURNS' engineers cite three reasons . . . each a contribution to the total reliability of these airborne telemetering devices. "First is temperature. The sensitive element of the mechanism must withstand high operating temperatures. Next, SUPRAMICA 555 offers a combination of excellent insulating characteristics, which are essential to the highly accurate functioning of the potentiometer. In addition, this ceramoplastic material is readily moldable into complex shapes, such as that required for this intricate part."

For other applications SUPRAMICA 555 is used under operating conditions as high as +700°F. . . . SUPRAMICA 555 is one of the many ceramoplastic and glass-bonded mica insulation materials produced by MYCALEX CORPORATION OF AMERICA, in precision-molded and machinable formulations. Whatever your insulation need there is a MYCALEX product to meet it—for example, SUPRAMICA 620 machinable ceramoplastic, which has a maximum operating temperature of +1550°F. Write today outlining your design problem for specific information.

General Offices and Plant: 126K Clifton Blvd., Clifton, N. J.
Executive Offices: 30 Rockefeller Plaza, New York 20, N. Y.

SYNTHAMICA® SYNTHETIC MICA · SUPRAMICA® CERAMOPLASTIC · SINCE 1919 MYCALEX®

MYCALEX
CORPORATION OF AMERICA

WORLD'S LARGEST MANUFACTURER OF GLASS-BONDED MICA AND CERAMOPLASTIC PRODUCTS

NEWS New Products

(Continued from page 188A)

tube drop is important such as in radar where it is used as a charging diode or limiter. It is also suitable for use in high voltage power supplies for dielectric or cable testing, or in air cleaners or precipitrons.

As a rectifier the 5973 will operate at an average of 1.25 amperes to 40 kv and one ampere to 75 kv. As a limiter, peak currents as high as 20 amperes at 75 kv apply.

Spectrum Analyzer

A telemetering analyzer with automatic optimum logarithmic display of subcarrier channels and simultaneous linear display of individual channels is now available in the Model TA-100L-120L, from **Probescope Co., Inc.**, 8 Sagamore Hill Drive, Port Washington, N. Y.

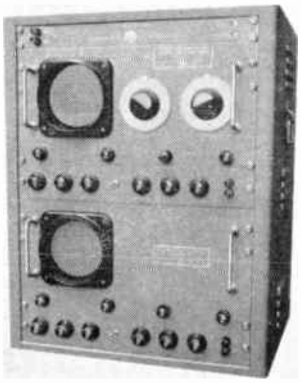

All FM/FM subcarrier channels will be linearly displayed along the horizontal axis of the log scan cathode-ray tube and at the same time individual portions of the spectrum can be analyzed on a second cathode ray tube. A searching marker is available to insure analyzer accuracy. As the linear analyzer is tuned thru the spectrum a marker signal will appear on the log display to pinpoint signals for detailed analysis.

Logarithmic and linear scanning analyzers are self contained and can be used and purchased separately.

Frequency ranges are 350 cps to 85 kc or 120 kc logarithmic display and 13 cps to 85 kc or 120 kc linear display. Sweep width, 150 cps to 22 kc.

Other features include: 60 mc dynamic range, 500 microvolt sensitivity and linear and logarithmic amplitude scale.

A 3 point marker and synchronous sweep generator attachments are also available.

Frequency Standards

The James Knights Co., Sandwich, Ill., announces new refinements in its JK-Sulzer FS-1100T frequency standards, including the newly available supplemental Frequency Divider to furnish subharmonic frequencies. All sub-harmonic frequencies, including the commonly used 1,000, 400, and 60 cps have the same order of stability, 5×10^{-10} per day or better, as the FS-1100T standard itself. Frequencies as low as 1 pulse per second are available. The new unit measures $3\frac{3}{16}$" W $\times 12\frac{1}{2}$" D $\times$ 6" H, and is available for table or rack mounting. It is designated the FS-1100TD.

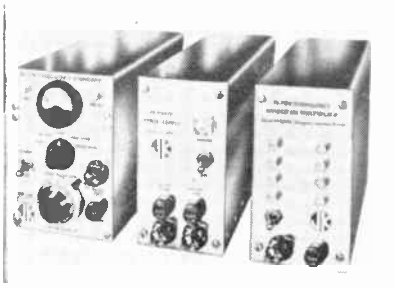

Normal ouputs for the FS-1100T frequency standard is 1.0 mc and 100 kc simultaneously with 1 volt available to 50 ohm loads. At these frequencies it offers a minimum stability of 5×10^{-10} per day after initial aging. Output frequencies in the 900–1300 kc range and 3.5 and 5.0 mc range are now available on special order. The FS-1100T is fully transistorized, with a double proportional control oven, representing an advanced stage of crystallography, electronic circuitry, thermal and mechanical design. It is a compact unit measuring $4\frac{3}{16}$" W $\times$ 12" D $\times$ 6" H, available for table or rack mounting. It is designed for 24–32 volt operation.

The FS-1100TP is a companion power

(Continued on page 194A)

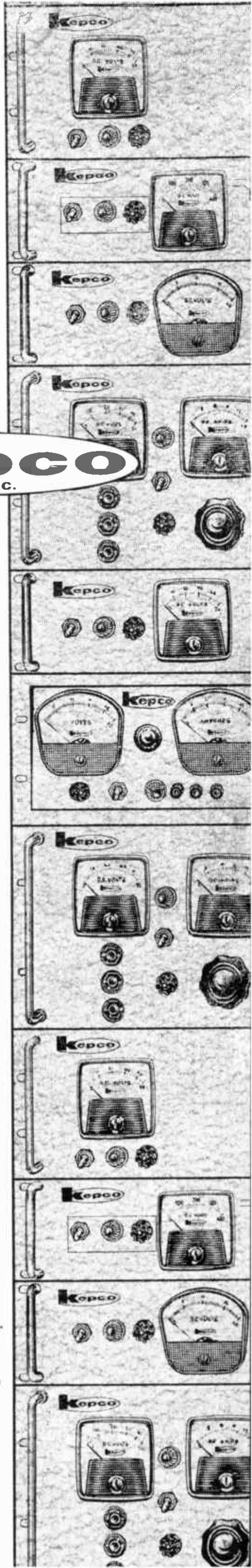

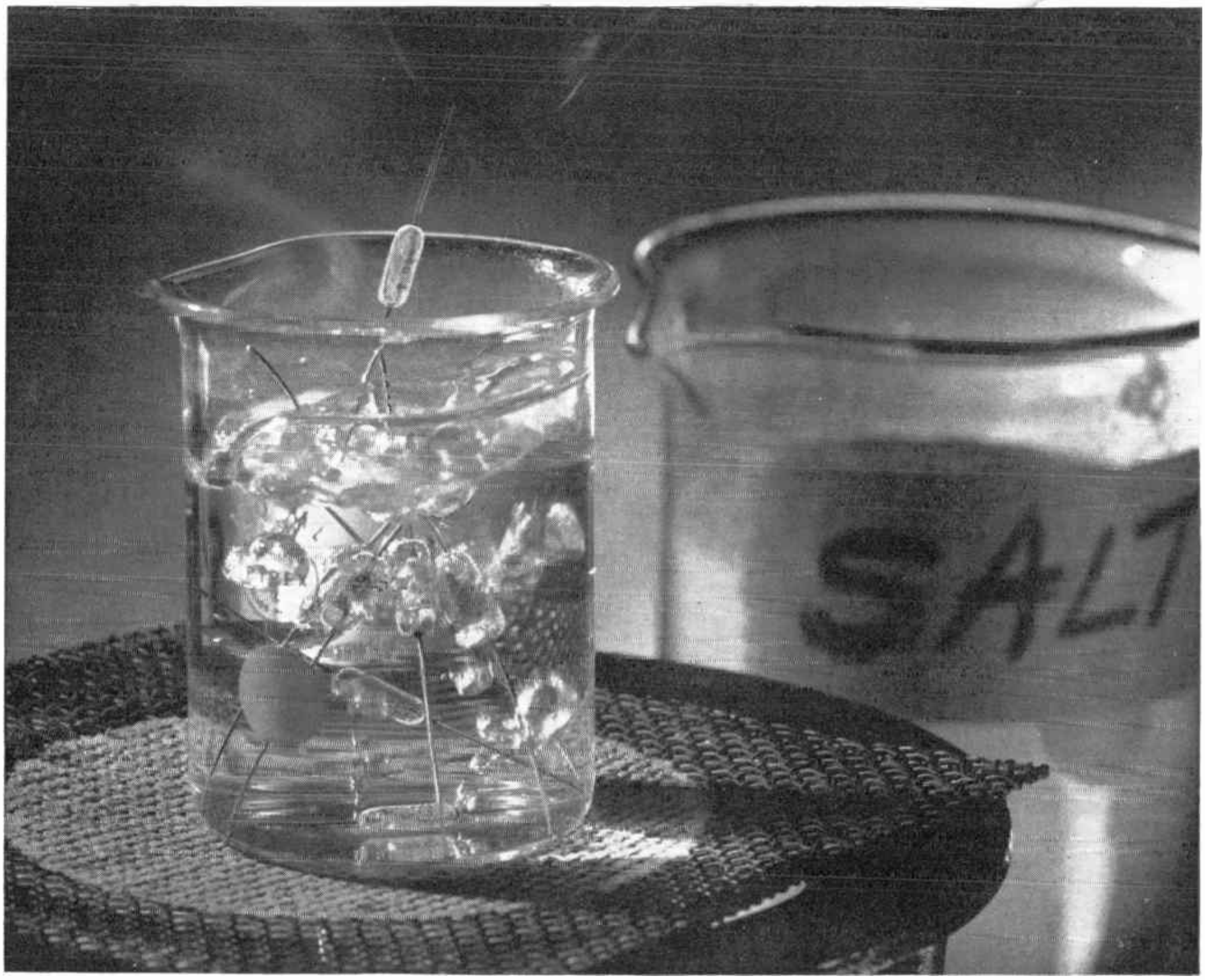

NEW FUSION-SEALED glass capacitors defy environmental stresses

Corning's NEW CYF Capacitors are guaranteed to be four times better than MIL specs require on moisture resistance.

Here are two new capacitors that are *practically indestructible* under severe environmental stresses.

For example the CYF's will withstand MIL-STD 202A moisture conditions for over 1000 hours with no signs of deterioration.

And you'll find that both the CYF-10's and CYF-15's do better on all counts for the specifications set forth in MIL-C-11272A.

To make the CYF's impervious to environmental stresses, we've completely encapsulated the glass dielectric element in a glass casing. This encapsulation is completely fusion-sealed against moisture, salt, corrosion and weathering.

Here's the basic availability picture:

At 125°C. you can get CYF-10's in 5-150 uuf @ 500 VDC and 160-240 uuf @ 300 VDC.

At 125°C. you can get CYF-15's in 160-510 uuf @ 500 VDC and 560-1200 uuf at 300 VDC.

If you need high reliability and miniaturization, the CYF's—the only FUSION-SEALED Capacitors available—are worth looking into. Stocked by Erie Distributor Organization for immediate delivery in small quantities. For details, write to **Corning Glass Works, 542** High Street, Bradford, Pa. Or contact our sales offices in New York, Chicago, or Los Angeles.

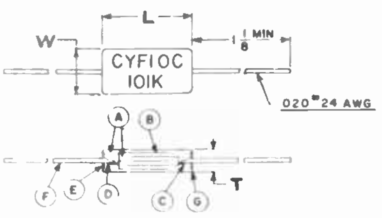

	CYF-10	CYF-15
L	$11/32 \pm 3/64$	$15/32 \pm 3/64$
W	$11/64 \pm 1/32$	$17/64 \pm 1/32$
T	$5/64 \pm 1/32$	$7/64 \pm 3/64$

- **A DIELECTRIC AND CASE**—Fused Structure of Same Glass Composition.
- **B FOIL PLATES**—Completely embedded in Glass.
- **C CONNECTION**—Welded for Reliability.
- **D TERMINAL SEAL**—True Glass-to-Metal Seal.
- **E WASHER**—Added Terminal Strength.
- **F TERMINALS**—Copper-clad nickel-iron, hot tinned.
- **G ROUNDED**—All Edges, for Maximum Strength.

CORNING ELECTRONIC COMPONENTS

NEWS New Products

These manufacturers have invited PROCEEDINGS readers to write for literature and further technical information. Please mention your IRE affiliation.

(Continued from page 191A)

supply unit operating on 115v ac. A feature of this power supply is the internal nickel-cadmium battery that will provide stand-by power for up to 12 hours operation in the event of power failure or to permit transport of an operating unit. This feature, for example, permits the frequency standard to be calibrated in Washington, D. C., then transported operating to any point in the country. The FS-1100TP measures $3\frac{3}{16}$" W×$12\frac{1}{2}$" D×6" H, and is available for table or rack mounting.

Plug-In Transistor Chopper Kit

The Solid State Electronics Co., 15321 Rayen St., Sepulveda, Calif., announces the availability of a new circuit designer's plug-in transistorized chopper kit which includes application notes. The kit is being introduced at a lower than standard price to acquaint circuit designers with new applications.

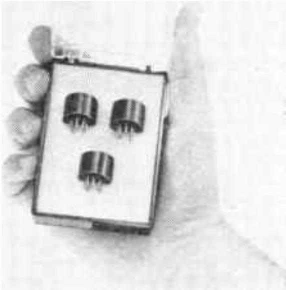

This kit contains three choppers—Models 50P, 60P and 70P. These units are plug-in versions of the Models 50, 60 and 70 solder-in types. They provide for immediate insertion into a standard 7-pin miniature socket and are also directly solderable into a printed circuit board. These solid state choppers are designed to alternately connect and disconnect a load from a signal source. They may also be used as a demodulator to convert an ac signal to dc. They are capable of linearly switching or chopping voltages over a wide dynamic range which extends down to fraction of a millivolt and up to 10 volts. Unlike mechanical choppers which can only be designed to operate over a narrow and comparatively low frequency range due to mechanical limitations, these transistorized choppers are inertialess devices that can be driven from dc to hundreds of kilocycles.

The Models 50P and 60P are germanium units for operation from −55°C to +90°C, whereas the Model 70P utilizes silicon transistors exclusively for high temperature applications up to 150°C. Only carefully matched pairs of transistors are utilized.

NEW SILICON "PILL" VARACTOR

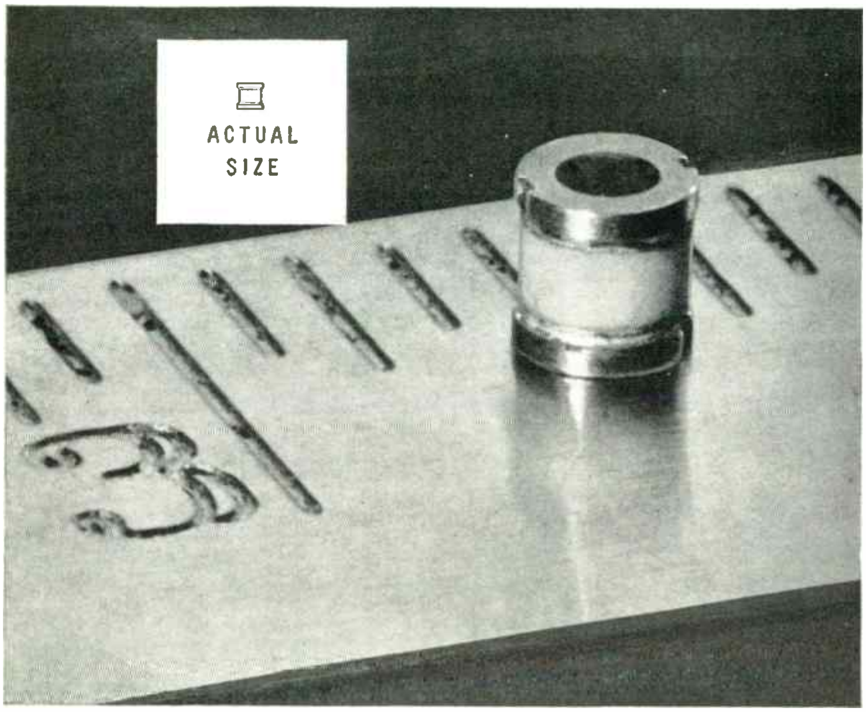

GREATLY REDUCES THE PACKAGE AS A FACTOR IN CIRCUIT DESIGN

specifically developed for:

- amplifiers at the higher microwave frequencies (1000 mc and above)
- travelling wave parametric amplifiers
- microwave computers as sub-harmonic generators
- amplifiers in which stray susceptance effects must be minimized
- applications of varactors to stripline circuits
- modulators for frequency synthesis

Experimental quantities are available with these nominal specifications

TYPE NUMBER	*CAPACITANCE TOLERANCE (Zero Bias)	TYPICAL Q AT −6 VOLTS
MA-4255X	0.5-1.4 $\mu\mu f$	60-80
MA-4256X	1.2-2.5 $\mu\mu f$	50
MA-4257X	2.5-4.0 $\mu\mu f$	30

*Package shunt capacitance ~ 0.2 $\mu\mu f$. Series lead inductance $<10^{-9}$ henries.

Write or call:

MICROWAVE ASSOCIATES INC.
BURLINGTON, MASSACHUSETTS
BRowning 2-3000 • TWX Burlington, Mass. 942.

Advertising Index

DISPLAY ADVERTISERS

Now from Weston—

a new package concept for AC-DC laboratory standards

time-saving, easy-to-operate calibration consoles—accurate within .05% in D.C. .1% in A.C.

There's remarkable simplicity and precision in these Weston AC and DC Calibration Consoles – design simplicity that is readily apparent in clean, uncluttered panels . . . operating simplicity that now enables one operator to perform the work in 1/3 the time previously required by two skilled operators . . . with the precision of Weston engineering and craftsmanship that assures ultimate accuracy. Highly stable and readily adjustable, these consoles are truly value-packed.

Unique switching networks automatically divide scales into any number of equal parts regardless of range. It's no longer necessary to calibrate each checkpoint or set up extra equipment to obtain required outputs. Operation is reduced to four or five simple steps.

These consoles typify Weston leadership in long-term reliability and stability. All are supplied in blue-gray cabinets or ready for mounting in standard 19" rack panels. Also available: an oil bath which accommodates up to 12 Weston Normal Standard Cells . . . maintains temperatures within .01C. Removable racks also fit baths at U.S. Bureau of Standards.

For full information, contact your local Weston representative . . . or write to Daystrom-Weston Sales Division, Newark 12, N. J. In Canada: Daystrom Ltd., 840 Caledonia Rd., Toronto 19, Ont. Export: Daystrom Int'l., 100 Empire St., Newark 12, N. J.

A DAYSTROM UNIT

WESTON

Instruments

WORLD LEADER IN MEASUREMENT AND CONTROL

See these calibrators at the Daystrom Exhibit at the IRE Show

READ PHASE NULL VOLTS DIRECTLY

MODEL 301 Broadband Phase Angle Voltmeter is designed for laboratory use, features 10 cps to 100 kc operation, 12 voltage ranges covering 1 mv to 300 volts.

NORTH ATLANTIC PHASE ANGLE VOLTMETERS

For Production Line, Laboratory, Ground Checkout

Now, combined in one compact package, all the functions required for precise measurement of voltage, phase angle, quadrature, impedance and power factor. Measurement of AC signals which previously required extensive equipment—or which could not be made at all—can be accomplished simply and accurately in the laboratory, on the production line or in the field. For broadband or single frequency operation.

READ DIRECTLY
- **Total Voltage**
- **Phase Angle**
- **In-phase Voltage**
- **Quadrature Voltage**
- **Null**

Specifications: Abridged specifications of the Model 301 Broadband Phase Angle Voltmeter are shown below. Specifications of other models on request.

- Frequency range 10 cps to 100 kc
- 1 mv to 300 volts full scale
- Accuracy 1/2° absolute; special technique .01°
- 0—360° phase angle without ambiguity
- Nulling sensitivity 5 microvolts
- Signal and/or reference isolation
- Optional filters plug in from front
- Bench or rack mounting

Model 202. For production line or checkout applications. Characteristics similar to Model 301 but designed for single frequency operation.

Model 401 AC To DC Phase Sensitive Converter permits conventional DC instrumentation to be used for AC measurements. Single- or double-ended DC output proportional to rms, fundamental, in-phase or quadrature component of AC signal.

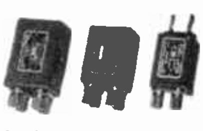

Plug-In Accessories for Phase Angle Voltmeters include reference isolation, resistance summing, and bridging transformer modules for eliminating ground loops and adapting voltmeter to ratiometer applications.

TECHNICAL DATA

Write for detailed specifications and application information

NORTH ATLANTIC
industries, inc.
603 Main Street, Westbury, New York
EDgewood 4-1122

Advertising Index

PROFESSIONAL CONSULTING SERVICES

Advertising rates

Professional Consulting Service Cards.

1 insertion	$ 25.00
12 insertions	$180.00

50% discount to IRE members on 3 or more consecutive insertions.

In IRE DIRECTORY $25.00 flat rate.
1 inch only, no cuts or display type.

New rate effective January 1961
1 insertion $30.00
12 insertions $240.00
50% discount to IRE members on 3 or more consecutive insertions.
In IRE DIRECTORY $30.00 flat rate

Advertising restricted to professional engineering and consulting services by individuals only. No product may be offered for sale, and firm names may not be mentioned in cards.

Transistor Circuits
ALBERT J. BARACKET
MS IN EE & Staff
Development, and design of transistorized and standard regulated power supplies; broadcast and closed circuit TV camera and synchronizing circuitry both military and commercial.
36 Commerce Road — Cedar Grove, N.J.
CEnter 9-6100

W. J. BROWN
& Staff
Fel.AIEE., M.IEE., Sen.Mem.IRE.
INTERNATIONAL CONSULTANTS
35 Years Executive Electrical Engineering Experience in U.K. and U.S.A.
71 Gurley Rd., Stamford, Conn., U.S.A.
Cables—Browninter — Stamford, Conn.

MARKET DEVELOPMENT*
A. D. Ehrenfried and associates
Technical product planning—product and market evaluation—market development programs—all by graduate engineers.
*Ref.: IRE/PGEM paper
Concord, Massachusetts — EMerson 9-5500

M. D. ERCOLINO
Antenna Laboratories and Engineering Staff
Consultation and Development
Antennas, Systems, Baluns, Rotators, Rotatable Antenna Masts
Asbury Park, N.J. — PRospect 5-7252

CLYDE E. HALLMARK
and associates
Specializing in Instrumentation—Automatic Control—Television—General Electronics—Semiconductor & Magnetics Application—Systems Research—Project Evaluation.
ENGINEERING SERVICE—CONTRACT R&D
New Haven — Indiana

LEONARD R. KAHN
Consultant in Communications and Electronics
Single-Sideband and Frequency-Shift Systems
Diversity Reception - Stereophonic Systems
Television Systems
81 South Bergen Place, Freeport, L.I., N.Y.
FReeport 9-8800

J. A. Matthews — J. B. Minter
Consulting Engineers for
Professional Sound Recording, Disk mastering, Tape Editing, Dubbing, etc.
106 Main St. — Denville, New Jersey
OAkwood 7-0290

Telecommunications Consulting Engineers
"Worldwide Experience"
V. J. Nexon — S. K. Wolf — M. Westheimer
WIRE, CARRIER, RADIO, MICROWAVE, TROPO SCATTER
Feasibility Studies, Terrain Surveys, System Design, Job Supervision, Government Proposals, Market Research, Product Planning.
1475 Broadway, New York 36, N.Y., BRyant 9-8517

E. M. OSTLUND & associates
Electronic Engineers
Radio—Microwave—Carrier—Communication—Control—Systems and Equipment
Consulting—Research—Development
ANDOVER, NEW JERSEY
Tel: PArkway 9-6635 — P.E.N.J.

NATHAN GRIER PARKE
and staff
Consulting Applied Mathematicians
Research • Analysis • Computation
Bedford Road • Carlisle, Massachusetts
Telephone EMerson 9-3818

PAUL ROSENBERG
& associates
Established 1945
Consultation, Research & Development in Applied Physics
100 Stevens Ave., Mt. Vernon, New York
MOunt Vernon 7-8040 Cable: PHYSICIST

MYRON M. ROSENTHAL
& staff
Microwave & Electronic Systems
19 Brookline Dr., North Massapequa, N.Y.
PErshing 5-2501

HAROLD A. WHEELER
Laboratories and Engineering Staff
Consultation — Research — Development
Microwaves — UHF — VHF — VLF
Antennas and Components
HUnter 2-7876 — Great Neck, N. Y.
Antenna Laboratory: — Smithtown, N. Y.

A COMPLETE LIST

of exhibitors at the 1960 Radio Engineering Show, together with a complete program of technical papers and social events for the annual IRE International Convention, will be featured in next month's issue, to give you plenty of advance planning time before you come to the show. Complete product descriptions and photographs will make this an "exhibit in print" for those IRE members who will be unable to attend.

IMPULSE

A DIGEST OF NEW DEVELOPMENTS IN ELECTRONICS AND AUTOMATION

PUBLISHED BY ROME CABLE DIV. OF ALCOA, ROME, N. Y.

PIONEERS IN INSTRUMENTATION CABLE ENGINEERING

INSTANT MAIL. Not long ago, one of the wire services carried a story that should gladden the heart of letter writers from coast to coast. The big news is the use of microwave radio or coaxial cables for speeding letters to their destination. Naturally, much researching, development and experimental work are yet to be done before facsimile mail will be unveiled by Uncle Sam. However, as of December 1, a commercial service linking Washington, New York, Chicago, Los Angeles and San Francisco has been in operation. So *instant mail* joins the many other wonders and conveniences of the electronic world.

UHF GIVES WEATHER REPORT. High in the sky, all over the world, helium-filled balloons carry radio-sonde transmitters which telemeter changes in air pressure, humidity and temperature. All three measurements are converted into radio signals . . . and measuring and reporting goes on and on until the balloons burst at 20,000 feet. The UHF signals are picked up by a ground antenna and fed to an FM receiver which has a tapper bar that records on special graph paper. If your work involves telemetering, data recording, circuit-control testing, or computers, you probably will want a copy of Bulletin RCD-400. It covers the cable you can get from Rome for such purposes. Write to Rome Cable Corp., Dept. 1220, Rome, New York. Or contact the Rome representative in your area.

NAME THE TONE. Any tone imaginable can now be generated electronically with an electronic music synthesizer recently installed at Columbia University. The synthesizer produces musical sounds in response to code signals fed into the system on perforated tape. It will be used in a program of composition and research in electronic music, conducted by Columbia and Princeton Universities under a grant of the Rockefeller Foundation.

WHO PAYS FOR WHAT? New ground rules have been handed down for electronic contractors handling defense work. The new way to figure who pays for what goes into effect July 1, 1960, and covers both negotiated and fixed-price contracts. All the details are wrapped up in "Revision No. 50 Armed Services Procurement Regulation." You can get the whole story by sending 35 cents for each copy you want to the Government Printing Office, Washington 25, D. C.

CABLEMAN'S CORNER. To help you in replacing or reordering cable, it has become standard practice for most cable manufacturers to identify their cable in one of several ways. These include the stamping of solid conductors, the inclusion of marker threads or tapes within the cable structure, and surface printing or molding the insulations or jackets. Of these methods, the use of marker threads or tapes is the most popular. Manufacturers of Underwriters-labeled products are assigned specific colors for their marker threads, and most manufacturers extend the use of these same threads in other cable products whenever it is practical. Other information appearing on marker tapes often includes unit length markings and the date that the cable was manufactured.

These news items represent a digest of information found in many of the publications and periodicals of the electronics industry or related industries. They appear in brief here for easy and concentrated reading. Further information on each can be found in the original source material. Sources will be forwarded on request. ⑮

Advertising Index

LOW LEVEL INPUT AMPLIFICATION

- *1,000,000:1 rejection ratio at 60 cps*
- *floating input*
- *isolated output*

IN 2 NEW SANBORN CHOPPER AMPLIFIERS

INDIVIDUAL SET-UPS

portable, self-contained unit amplifier

The Model 350-1500 Low Level Amplifier provides extremely versatile measurement of low level signals through use of two interchangeable plug-in circuits — one for thermocouple applications, another for DC strain gage work (other plug-ins now in development). Floating input and isolated output make the 350-1500 useful when signal measurements are made in the presence of large ground loop voltages. The 10-1/2" high x 4-3/16" wide 350-1500 may be used individually with its own power supply to drive a 'scope, meter, optical element, etc. or as a preamplifier in 6- or 8-channel 350 series recording systems.

MULTI-CHANNEL INSTALLATIONS

8-unit 7" high modules for "850" series direct writers

Compact Model 850-1500A Low Level Preamplifiers are economical, space-saving units for large installations such as aircraft and missile development and test facilities where many recording channels are used to monitor strain gage and thermocouple outputs. Required 440 cps chopper drive voltages can be supplied for up to 16 channels with the *Model 850-1900 MOPA.*

SPECIFICATIONS

	350-1500	850-1500A
Sensitivity	20 uv input for 1 volt output, or 10 chart div. with Sanborn recorder; X1 to X2000 attenuator	100 uv input for 1 volt output, or 10 chart div. with Sanborn recorder; X1 to X200 attenuator
Input	Floating, can be grounded	
Input Impedance	100,000 ohms	200,000 ohms
Output	Floating or grounded (independent of input)	
Output Impedance	350 ohms	
Output Capabilities	±2.5 volts across 1000 ohm load	
Bandwidth	DC – 100 cps (3db)	
Linearity	±0.1% of full scale	
Common Mode Performance	120 db for 60 cps and 160 db for DC with 5000 ohms unbalance in source	
Noise	2 uv peak-to-peak over a 0 to 100 cps bandwidth	
Drift	±2 uv for 24 hours	
Gain Stability	±0.1% for 24 hours	

(specifications subject to change without notice)

Complete specifications and application data are available from Sanborn Sales-Engineering Representatives in principal cities throughout the United States, Canada, and foreign countries.

SANBORN COMPANY

INDUSTRIAL DIVISION

175 Wyman Street, Waltham 54, Mass.

Advertising Index

CDE *Consistently Dependable Capacitors*

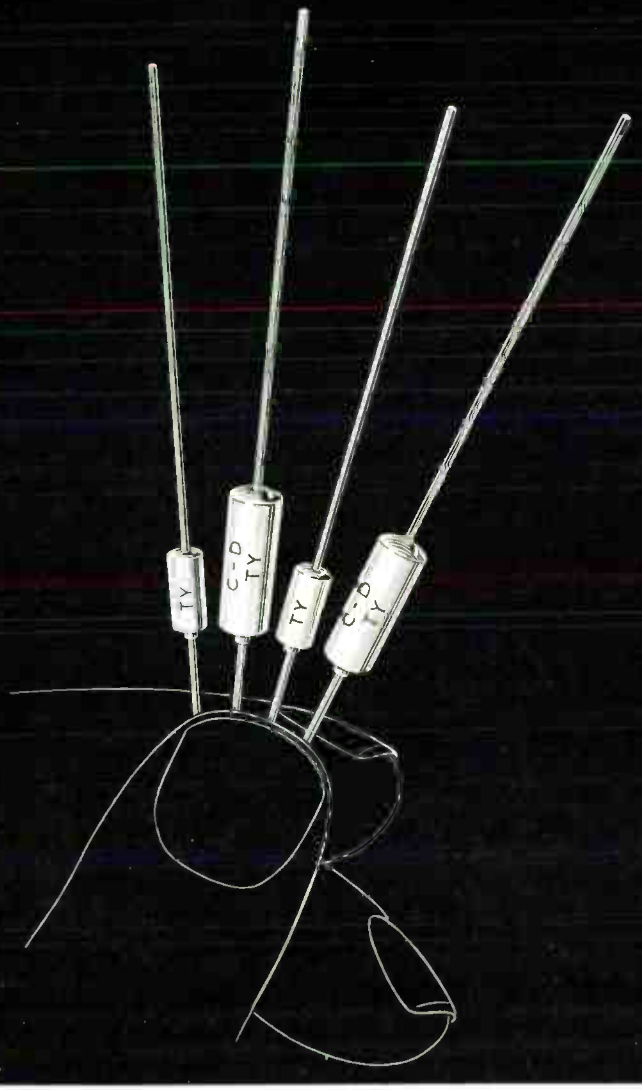

SOLITAN®

Cornell-Dubilier's truly dry tantalum capacitors for transistorized circuits

Subminiature Solitan capacitors — truly dry, solid-state electrolytic capacitors by Cornell-Dubilier — are specifically designed for transistorized applications in computer and military circuits. Immediately available in production quantities, Solitan capacitors offer these outstanding advantages: wide useful temperature characteristics; remarkable stability of capacitance with time and temperature; freedom from corrosion and service aging; unusual resistance to shock and vibration; indefinite shelf life; low dc leakage; low dissipation factor. For engineering assistance and complete data on C-D Solitan tantalum capacitors, write for Bulletin 537 to Cornell-Dubilier Electric Corporation, South Plainfield, New Jersey. *Manufacturers of consistently dependable capacitors, filters and networks for electronics, thermonucleonics, broadcasting and utility use for 50 years.*

SPECIFICATIONS AND FEATURES

• Ratings up to 6.0 mfd. at 35 volts DC Working, or 60.0 mfd. at 6 volts. • Wider useful temperature characteristics within range of —80 C to +85 C. • Freedom from corrosion and leakage. • Extremely small size. • Remarkable stability of capacitance with time and temperature. • Metal cased, hermetically sealed.

CDE CORNELL-DUBILIER ELECTRIC CORPORATION

AFFILIATED WITH FEDERAL PACIFIC ELECTRIC COMPANY

AUTOMATIC RECORDING of FREQUENCY RESPONSE

. . . for Study of Filters, Networks, Amplifiers, Equalizers, Loudspeakers, Microphones, and Transducers of All Types.

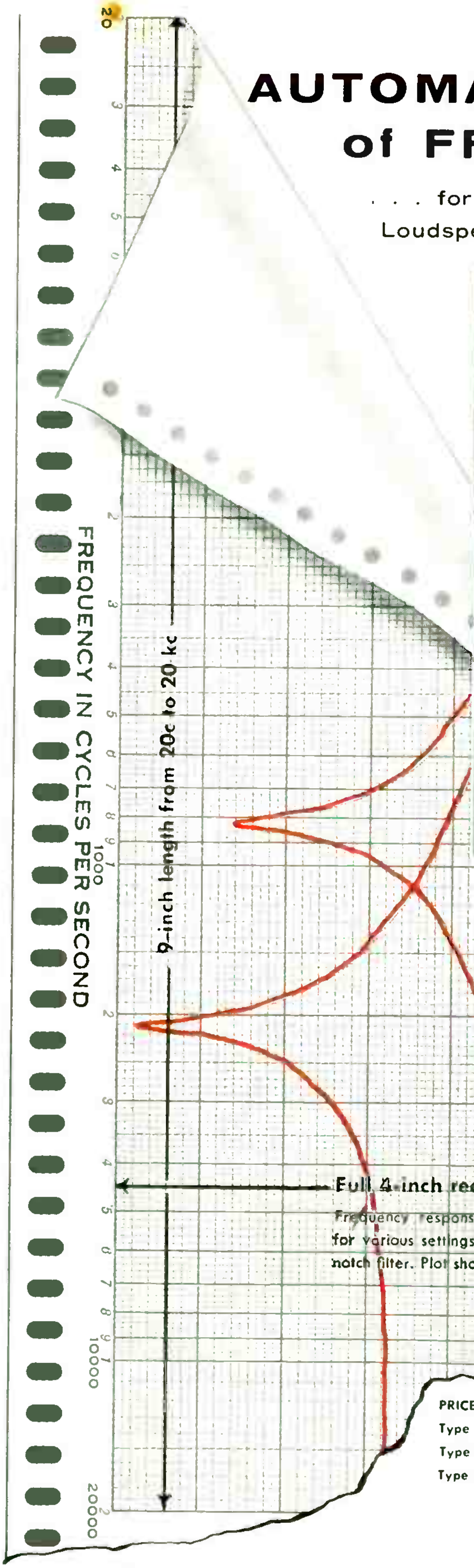

Frequency response recording for various settings of an adjustable notch filter. Plot shown actual size.

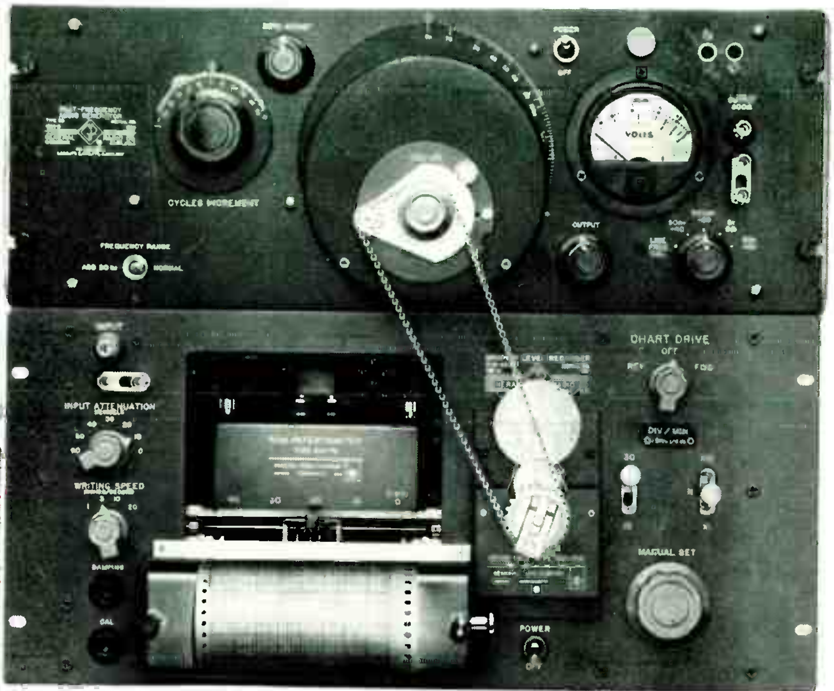

Audio generator and level recorder couple mechanically for graphic recording in db on a truly logarithmic frequency scale.

SYSTEM SPECIFICATIONS

Frequency Range: Generator, 20c to 20 kc on logarithmic scale, 20 kc to 40 kc. Recorder, traces rms level from 20c to 200 kc.

Generator Output: flat within ±0.25 db from 20c to 20 kc. Output is adjustable from 5 mv to 50v open-circuit. Harmonic distortion is less than 0.25% from 100c to 10 kc, 0.5% below 100c, 1% above 10 kc.

Recorder Sensitivity: 1 mv, maximum (corresponds to 0 db). Can be varied from 1 mv to 1v in 10 steps with input attenuator.

Recorder Range: 40-db full scale, with plug-in potentiometer supplied; 20-db and 80-db pots also available.

Pen Writing Speed: 20 in/sec maximum with 40-db Pot (200 db/sec) with less than 1-db overshoot. Slower speeds (1, 3, or 10 in/sec) selected by panel switch to provide mechanical filtering of rapidly fluctuating levels.

Paper Speeds: 2.5, 7.5, 25, and 75 in/min. Optional slow-speed motor available for speeds from 2.5 to 75 in/hr.

Recorder Accuracy: Static accuracy better than 0.4% of full scale. Fast servo system with low overshoot provides excellent dynamic accuracy.

Write For Complete Information

PRICES: Type 1304-B Beat-Frequency Generator	$625
Type 1521-A Graphic Level Recorder (with 40-db pot)	$995
Type 1521-P10 Drive Unit	$ 72
Type 1521-P11 Link Unit	$ 18
Complete System	$1710

Chart paper only $2.30 per 100-ft roll

GENERAL RADIO COMPANY

Since 1915 — Manufacturers of Electronic Apparatus for Science and Industry

WEST CONCORD, MASSACHUSETTS

NEW YORK AREA: Tel. N. Y. WOrth 4-2722, N. J. WHitney 3-3140 CHICAGO: Tel. VIllage 8-9400
PHILADELPHIA: Tel. HAncock 4-7419 WASHINGTON, D. C.: Tel. JUniper 5-1088
SAN FRANCISCO: Tel. WHitecliff 8-8233 LOS ANGELES 38: Tel. HOllywood 9-6201
In CANADA, TORONTO: Tel. CHerry 6-2171

We introduced our first cathode-ray oscilloscope with a German-made tube in 1931, and in 1933 substituted a better tube manufactured by Westinghouse. We introduced the linear sweep circuit in 1932. That circuit is still used in today's scopes.